

# **Enzymatic synthesis of selected phenolic and vitamin glycosides**

**A thesis submitted to the  
University of Mysore**

**for the award of  
*Doctor of Philosophy*  
in**

**BIOTECHNOLOGY**

**By  
R. Sivakumar, M.Pharm.,**

Fermentation Technology and Bioengineering Department  
Central Food Technological Research Institute  
Council of Scientific and Industrial Research  
Mysore- 570020, INDIA

**June 2008**

**R. SIVAKUMAR, M.Pharm.,**  
Senior Research Fellow  
Fermentation Technology and Bioengineering  
Central Food Technological Research Institute  
Council of Scientific and Industrial Research  
Mysore – 570 020, India

---

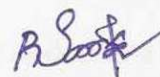
### **Declaration**

I hereby declare that the thesis entitled, “**Enzymatic synthesis of selected phenolic and vitamin glycosides**” submitted for the degree of **Doctor of Philosophy in Biotechnology** to the **University of Mysore** is the result of the work carried out by me under the guidance of **Dr. S. Divakar** in the Department of Fermentation Technology and Bioengineering, Central Food Technological Research Institute, Mysore, India, during the period 2005-2008.

I further declare that the results of this work have not been submitted for the award of any other degree or fellowship.

Date: 30-06-08

Place: Mysore



(R. Sivakumar)

Website : <http://www.cftri.com>

Grams : FOODSEARCH, Mysore

☎ : 0821- 2514760 ; 2516802 ; 2514306 ; Fax : 0821 - 2517233



केन्द्रीय खाद्य प्रौद्योगिक अनुसंधान संस्थान, मैसूर - 570 020, भारत  
Central Food Technological Research Institute  
Mysore - 570 020, India

*cftri*

Dr. S. Divakar  
Fermentation Technology and Bioengineering  
E-mail: [divakar643@gmail.com](mailto:divakar643@gmail.com)

### Certificate

I hereby declare that the thesis entitled, **“Enzymatic synthesis of selected phenolic and vitamin glycosides”** submitted by **Mr. R. Sivakumar** for the degree of **Doctor of Philosophy in Biotechnology** to the **University of Mysore** is the result of the work carried out by him under my guidance in the Department of Fermentation Technology and Bioengineering, Central Food Technological Research Institute, Mysore, India, during the period April 2005 – June 2008.

Date: 30-6-2008  
Place: Mysore

*S Divakar*  
(S. Divakar)

Guide and Supervisor

ePrints@CFTRI



*Dedicated to my beloved parents*



## Acknowledgements

I express my deep sense of gratitude to **Dr. S. Divakar**, Head, Central Food Technological Research Institute, Mysore for his guidance, invaluable suggestions and constant encouragement throughout the course of my Ph.D work.

I would like to acknowledge my gratitude to Mr. B. Manohar, Scientist, Food Engineering Department, CFTRI for his kind help in my work.

I express my sincere thanks to my colleagues Dr. K. Lohith, Dr. G. R. Vijayakumar, Mr. B. R. Somashekar, Mr. T. Ponrasu and Mr. R. Einstein Charles for scientific inputs and being there for me whenever in need.

I am thankful to all the students and staff of FTBE and other departments of the Institute for their timely help during my course of work.

I express my sincere thanks to all the staff of Central Instrumentation Facilities and Service Departments for their technical help in analyzing my samples.

My sincere gratitude to NMR Research Centre, Indian Institute of Science, Bangalore and NMR facility centre, CFTRI for recording NMR spectra presented in this work.

I thank Director Dr. V. Prakash, for providing me an opportunity to carry out my research work at the Central Food Technological Research Institute, Mysore.

My special thanks to all the scientific and non-scientific staff of CFTRI, Mysore and those who have directly or indirectly helped me in carrying out this work.

My special gratitude to my parents, brother, sisters and relatives for their constant encouragement and support.

Last but not least, I am grateful to the Council of Scientific and Industrial Research, India for providing the Senior Research fellowship.

*R. Sivakumar*

## List of Patent and Publications

### Patent

1. **Sivakumar, R.**, Vijayakumar, G. R., Manohar, B., Divakar, S., 2005. An enzymatic process for the preparation of vanillin glycosides. Indian Patent, 284/NF/2006

### Papers

1. **R. Sivakumar** and S. Divakar. Glycosylation of vanillin by amyloglucosidase in organic media. *Tetrahedron letters*, 2006, 47, 695-699.
2. **R. Sivakumar**, G. R. Vijayakumar, B. Manohar and S. Divakar. Competitive substrate inhibition of amyloglucosidase from *Rhizopus mold* by vanillin and curcumin in respective glycosylation reactions. *Biocatalysis and Biotransformation*, 2006, 24(4), 299-305
3. K. Lohith, G.R. Vijayakumar, B.R. Somashekar, **R. Sivakumar** and S. Divakar. Glycosides and amino acyl esters of carbohydrates as potent inhibitors of Angiotensin Converting Enzyme. *European Journal of Medicinal Chemistry*, 2006, 41, 1059-1072
4. **R. Sivakumar**, B. Manohar and S. Divakar. Synthesis of vanillyl-maltoside using glucosidases by response surface methodology. *European Food Research and Technology*. 2007, 226, 255-263
5. **R. Sivakumar** and S. Divakar. Syntheses of N-vanillyl-nonanamide glycosides using amyloglucosidase from *Rhizopus mold* and  $\beta$ -glucosidase from sweet almond. *Biotechnology letters*. 2007, 29, 1537-1548
6. T. Ponrasu, R. Einstein Charles, **R. Sivakumar** and S. Divakar. Glucosidase catalysed synthesis of  $\alpha$ -tocopheryl glycosides. *Biotechnology Letters*. 2008, 30, 1431-1439
7. R. Einstein Charles, T. Ponrasu, **R. Sivakumar** and S. Divakar. Angiotensin converting enzyme inhibitory and antioxidant activities of selected enzymatically synthesised phenolic and vitamin glycosides. *Biotechnology and Applied Biochemistry*. 2008. DOI: 10.1042/BA 20080041.

## **Abstract**

In the present work amyloglucosidase from *Rhizopus* mold and  $\beta$ -glucosidase isolated from sweet almond were employed to synthesize few selected phenolic and vitamin glycosides. The phenols employed possess a hydroxyl group at the 4<sup>th</sup> position of phenyl ring along with another hydroxyl or -OCH<sub>3</sub> group at the 3<sup>rd</sup> position besides possessing a -CH=CH-, -CH<sub>2</sub> or -CHO group *para* to the 4<sup>th</sup> -OH like vanillin **1**, N-vanillyl-nonanamide **2**, curcumin **3**, DL-dopa **4** and dopamine **5**. The vitamins employed are riboflavin **43** (vitamin B2), ergocalciferol **44** (vitamin D2) and  $\alpha$ -tocopherol **45** (vitamin E). All these vitamins possess OH groups in their structure in the form of ribitol OH in riboflavin **43**, acyclic OH in ergocalciferol **44** and phenolic OH in  $\alpha$ -tocopherol **45**. The thesis consists of six chapters with conclusions and a summary.

**Chapter 1** – Introduction

**Chapter 2** – Materials and Methods

**Chapter 3** – Enzymatic syntheses of vanillin, N-vanillyl-nonanamide, curcumin, DL-dopa and dopamine glycosides

**Chapter 4** – Enzymatic syntheses of riboflavin, ergocalciferol and  $\alpha$ -tocopherol glycosides

**Chapter 5** – Competitive inhibition of amyloglucosidase by vanillin in the glucosylation of vanillin

**Chapter 6** – Evaluation of antioxidant and angiotensin converting enzyme inhibition activity of the synthesized phenolic and vitamin glycosides

Conclusions

Summary

The results from these investigations are presented in detail.

Chapter **ONE** deals with literature reports on biotransformations, glycosidases, their sources, structural features of glucoamylase and  $\beta$ -glucosidase, glycosylation methods, glycosylation mechanism and information on related enzymatically synthesized glycosides. A detailed report on investigations of some important factors that influence the glycosidase catalyzed reactions in organic solvents like nature of substrate, nature of solvent, thermal stability, role of water, kinetic studies of glycosidase catalyzed reactions and immobilization are presented. Besides, advantages of carrying out glycosylation using reverse micelles, super critical carbon di-oxide, microwave and response surface methodology (RSM) have been discussed. This chapter ends with a brief scope of the present investigation.

Chapter **TWO** describes materials and methods employed in the present work. Enzyme and chemicals employed and their sources are mentioned. Glycosylation procedure encompassing the related analytical and assay procedures are described and the newer methods wherever necessary have been described in detail.

Chapter **THREE** describes amyloglucosidase from *Rhizopus* mold and  $\beta$ -glucosidase from sweet almond (native/immobilized) catalysed syntheses of selected phenolic glycosides of vanillin **1**, N-vanillyl-nonanamide **2**, curcumin **3**, DL-dopa **4** and dopamine **5** with D-glucose **6**, D-galactose **7**, D-mannose **8**, D-fructose **9**, D-arabinose **10**, D-ribose **11**, maltose **12**, sucrose **13**, lactose **14**, D-sorbitol **15** and D-mannitol **16** by reflux method in di-isopropyl ether solvent at 68 °C. Reaction parameters were optimized in terms of incubation period, pH, buffer, enzyme and substrate concentrations for the synthesis of respective glucosides. Maximum conversion yields obtained for amyloglucosidase catalyses were: 4-*O*-(D-glucopyranosyl)vanillin **17a-c** - 53%, 4-*O*-(D-glucopyranosyl)N-vanillyl-nonanamide **24a-c** - 56%, DL-dopa-D-glucoside **34a-d** - 62% and dopamine-D-glucoside **40a-c** - 58%. Similarly, maximum glucosides obtained for  $\beta$ -

glucosidase catalyses were: 4-*O*-( $\beta$ -D-glucopyranosyl)vanillin **17b** - 10%, 4-*O*-(D-glucopyranosyl)N-vanillyl-nonanamide **24c** - 35%, 1,7-*O*-(bis- $\beta$ -D-glucopyranosyl)curcumin **30** - 44%, DL-dopa-D-glucoside **34b,c** - 33% and dopamine-D-glucoside **40b** - 65%. Solubility in water of 4-*O*-(D-glucopyranosyl)vanillin, 4-*O*-(D-glucopyranosyl)N-vanillyl-nonanamide and 1,7-*O*-(bis- $\beta$ -D-glucopyranosyl)curcumin were found to be 35.2 g/L, 7.7 g/L and 14 g/L respectively.

Under the optimized conditions determined, glycosides of vanillin **1**, N-vanillyl-nonanamide **2**, curcumin **3**, DL-dopa **4** and dopamine **5** were synthesized with various carbohydrates molecules. Product glycosides were isolated through column chromatography and characterized by measuring melting point and optical rotation besides subjecting them to a detailed spectroscopic investigation by UV, IR, Mass and 2D HSQCT NMR. Phenols underwent glycosylation mostly and in few cases arylation also with the respective carbohydrates indicated: vanillin **1** – D-glucose **6**, D-galactose **7**, D-mannose **8**, maltose **12**, sucrose **13**, lactose **14** and D-sorbitol **15** with conversion yields for amyloglucosidase catalyses in the 13-53% range and for  $\beta$ -glucosidase in the 6-25% range; N-vanillyl-nonanamide **2** – D-glucose **6**, D-galactose **7**, D-mannose **8**, D-ribose **11**, maltose **12** and lactose **14** with conversion yields for amyloglucosidase catalyses in the 9-56% range and for  $\beta$ -glucosidase in the 9-35% range; curcumin **3** – D-glucose **6**, D-galactose **7**, D-mannose **8** and lactose **14** with conversion yields for  $\beta$ -glucosidase in the 12-44% range; DL-dopa **4** – D-glucose **6**, D-galactose **7**, D-mannose **8**, D-sorbitol **15** and D-mannitol **16** with conversion yields for amyloglucosidase catalyses in the 12-62% range and for  $\beta$ -glucosidase in the 17-33% range and dopamine **5** – D-glucose **6**, D-galactose **7** and D-mannose **8** with conversion yields for amyloglucosidase catalyses in the 32-58% range and for  $\beta$ -glucosidase in the 28-65% range. About 61 individual glycosides were synthesized enzymatically using both the glucosidases, of

which 45 are being reported for the first time. Two-Dimensional NMR studies confirmed the linking between phenolic OH of aglycon and C1 and/or C1-*O*-/C6-*O*- position of the carbohydrate molecules.

$\beta$ -Glucosidase exclusively yielded  $\beta$ -glycosides and in very few cases C6-*O*-arylated products. However, amyloglucosidase on the other hand showed both C1 $\alpha$  and C1 $\beta$ -glycosylated and/or C1-*O*-/C6-*O*-arylated products. In most cases C1 glycosylated products were detected. Only few carbohydrate molecules showed C1-*O*-/C6-*O*-arylation. D-Sorbitol **15** and D-mannitol **16** gave arylated products by reacting only to the primary OH groups. No reaction occurred at the secondary hydroxyl groups of the carbohydrate molecules. Also, only mono glycosylated or mono arylated products were detected. No carbohydrate molecule gave bis products. Both amyloglucosidase and  $\beta$ -glucosidase did not catalyze the reaction with D-fructose **9** and D-arabinose **10**. Among the phenols employed only curcumin **3** showed bis glycosylated products. Phenolic OH at the 4<sup>th</sup> position readily reacted with the carbohydrate molecules employed and wherever possible DL-dopa **4** and dopamine **5** underwent reaction at the 3<sup>rd</sup> phenolic OH also. Thus water insoluble N-vanillyl-nonanamide **2**, curcumin **3** and less water soluble vanillin **1** were converted to more water soluble glycosides.

Amyloglucosidase from *Rhizopus* mold and  $\beta$ -glucosidase from sweet almond, catalysed synthesis of 4-*O*-( $\alpha$ -D-glucopyranosyl-(1'→4)D-glucopyranosyl)vanillin was optimized using response surface methodology. A Central Composite Rotatable Design involving 32 experiments of five variables: glucosidases 10-50% w/w of maltose, vanillin 0.5-2.5 mmol, incubation period 24-120 h, buffer concentration 0.04 mM-0.2 mM (0.4-2 mL) and pH 4-8 were employed. Saddle shaped surface plots for both the enzymes exhibited total reversal of the maltosylation behaviour at a critical cross-over point corresponding to 30% (w/w maltose) enzyme concentration, pH 6 and a buffer

concentration of 0.125 mM (1.25 mL) implying that a critical enzyme to buffer concentration and pH dictate the extent of vanillin maltosylation.

Chapter **FOUR** describes amyloglucosidase and  $\beta$ -glucosidase catalysed syntheses of glycosides of riboflavin **43** (vitamin B2), ergocalciferol **44** (vitamin D2) and  $\alpha$ -tocopherol **45** (vitamin E). Since ergocalciferol **44** and  $\alpha$ -tocopherol **45** are light and air sensitive, the reaction was carried out in an amber coloured 150 mL round bottomed flask under nitrogen atmosphere. Work-up and isolation of the compound was also carried out in dark. Reaction parameters were optimized in terms of incubation period, pH, buffer, enzyme and substrate concentrations for the syntheses of glycosides of riboflavin **43**, ergocalciferol **44** and  $\alpha$ -tocopherol **45**. Maximum conversion yields for the glycosides obtained for amyloglucosidase catalyses were: 5-*O*-(D-glucopyranosyl) riboflavin **46a-c** - 25% and 20-*O*-(D-glucopyranosyl)ergocalciferol **53a-c** - 42%. With  $\beta$ -glucosidase the maximum glycoside yields were: 5-*O*-( $\beta$ -D-glucopyranosyl)riboflavin **46b** - 24% and 6-*O*-( $\beta$ -D-glucopyranosyl) $\alpha$ -tocopherol **54** - 23%. Water solubility of 5-*O*-(D-glucopyranosyl) riboflavin, 20-*O*-(D-glucopyranosyl)ergocalciferol and 6-*O*-( $\beta$ -D-glucopyranosyl) $\alpha$ -tocopherol were determined to be 8.2 g/L, 6.4 g/L and 25.9 g/L respectively.

Under the optimized conditions, glycosides of riboflavin **43**, ergocalciferol **44** and  $\alpha$ -tocopherol **45** with various carbohydrates like D-glucose **6**, D-galactose **7**, D-mannose **8**, D-ribose **11**, maltose **12**, sucrose **13** and lactose **14** were synthesised. Vitamins underwent glycosylation/arylation with the respective carbohydrates indicated: riboflavin **43** – D-glucose **6**, D-galactose **7**, D-mannose **8**, D-ribose **11**, maltose **12**, sucrose **13** and lactose **14** with conversion yields for amyloglucosidase catalyses in the 5-40% range and for  $\beta$ -glucosidase in the 7-24% range; ergocalciferol **44** reacted only with D-glucose **6** to give a conversion yield of 42% for amyloglucosidase catalyses and  $\alpha$ -



tocopherol **45** – D-glucose **6**, D-galactose **7** and D-mannose **8** with conversion yields for  $\beta$ -glucosidase catalyses in the 11-23% range. Out of 21 individual glycosides prepared, 15 glycosides are reported for the first time. Here also the glycosides were isolated by column chromatography and characterized by measuring melting point and optical rotation and by recording UV, IR, Mass and 2D HSQCT spectra. Two-Dimensional NMR studies confirmed the linking between primary/acyclic/phenolic OH of the aglycon and the C1 and/or C1-*O*-/C6-*O*- position of the carbohydrate molecules.

$\beta$ -Glucosidase exclusively yielded  $\beta$ -glycosides only and no C6-*O*-arylated products were detected. However, amyloglucosidase on the other hand showed both C1 $\alpha$  and C1 $\beta$ -glycosylated and/or C1-*O*-/C6-*O*-arylated products. Here also, no reaction occurred at the secondary hydroxyl groups of the carbohydrate molecules. Also, only mono glycosylated or mono arylated products were detected. Both amyloglucosidase and  $\beta$ -glucosidase did not catalyze the reaction with D-fructose **9**, D-arabinose **10**, D-Sorbitol **15** and D-mannitol **16**. Among the vitamins employed ergocalciferol **44** showed glycosylation/arylation only with D-glucose **6**. Thus the water insoluble ergocalciferol **44** and  $\alpha$ -tocopherol **45** and less water soluble riboflavin **43** were converted to more water soluble glycosides thereby improving their potential bioavailability and pharmacological properties.

Chapter **FIVE** describes kinetic study of the glycosylation reaction between vanillin **1** and D-glucose **6** catalyzed by amyloglucosidase from *Rhizopus* mold leading to the synthesis of 4-*O*-(D-glucopyranosyl)vanillin **17a-c** in detail. Initial reaction rates were determined from kinetic runs involving different concentrations of vanillin **1** 5 mM to 0.1 M and D-glucose **6** 5 mM to 0.1 M. Graphical double reciprocal plots showed that kinetics of the amyloglucosidase catalyzed reaction followed Ping-Pong Bi-Bi mechanism where competitive substrate inhibition by vanillin **1** led to dead-end

amyloglucosidase-vanillin complexes at higher concentrations of vanillin **1**. An attempt to obtain best fit of this kinetic model through computer simulation yielded in good approximation, the values of four important kinetic parameters:  $k_{cat} = 35.0 \pm 3.2 \cdot 10^{-5} \text{M/h.mg}$ ,  $K_i = 10.5 \pm 1.1 \text{ mM}$ ,  $K_{m \text{ D-glucose}} = 60.0 \pm 6.2 \text{ mM}$ ,  $K_{m \text{ vanillin}} = 50.0 \pm 4.8 \text{ mM}$ .

Chapter **SIX** describes evaluation of antioxidant and angiotensin converting enzyme inhibition activity of the enzymatically synthesized phenolic and vitamin glycosides. About 39 enzymatically prepared phenolic and vitamin glycosides were subjected to antioxidant activities and 48 glycosides were tested for angiotensin converting enzyme (ACE) inhibition activity. Both phenolic and vitamin glycosides exhibited  $IC_{50}$  values for antioxidant activities in the  $0.5 \pm 0.03 \text{ mM}$  to  $2.66 \pm 0.13 \text{ mM}$  range and ACE inhibition in the  $0.56 \pm 0.03 \text{ mM}$  to  $3.33 \pm 0.17 \text{ mM}$  range. Introduction of a carbohydrate molecule to the phenolic OH decreased the antioxidant activity. However, some of the glycosides still possessed substantial amount of antioxidant activities. Also, comparable ACE inhibition values only were observed between free phenol/vitamin and the respective glycosides. Best  $IC_{50}$  values ( $\leq 0.75 \text{ mM}$ ) observed for antioxidant activity are for: 4-*O*-( $\alpha$ -D-glucopyranosyl-(1'→4) $\beta$ -D-glucopyranosyl)N-vanillyl-nonanamide **28d** -  $0.75 \pm 0.04 \text{ mM}$ , 1,7-*O*-(bis-D-mannopyranosyl)curcumin **32a,b** -  $0.75 \pm 0.04 \text{ mM}$ , 6-*O*-(D-galactopyranosyl) $\alpha$ -tocopherol **55a,b** -  $0.72 \pm 0.04 \text{ mM}$  and 6-*O*-(D-mannopyranosyl) $\alpha$ -tocopherol **56a,b** -  $0.5 \pm 0.03 \text{ mM}$ . Similarly, best ACE inhibitory activities for the glycosides ( $< 0.75 \text{ mM}$ ) detected were: 4-*O*-( $\beta$ -D-glucopyranosyl)vanillin **17b** -  $0.61 \pm 0.03 \text{ mM}$ , 4-*O*-(D-galactopyranosyl)vanillin **18a,b** -  $0.61 \pm 0.03 \text{ mM}$ , 1,7-*O*-(bis- $\beta$ -D-galactopyranosyl-(1'→4)D-glucopyranosyl) curcumin **33a,b** -  $0.67 \pm 0.03 \text{ mM}$  and DL-3-hydroxy-4-*O*-(6-D-sorbitol)phenylalanine **38** -  $0.56 \pm$

0.03 mM. Among the glycosides tested, phenolic glycosides showed better antioxidant and ACE activities than the vitamin glycosides.

Thus the present investigation has brought out clearly the glycosylation potentialities of amyloglucosidase from *Rhizopus* mold and  $\beta$ -glucosidase from sweet almond in the reaction between selected phenols/vitamins with structurally diverse carbohydrate molecules employed.

ePrints@CFTRI

---

## CONTENTS

**Page  
No.**

---

### **Chapter 1**

#### **Introduction**

1.1 Biotransformations	1
1.2 Glycosidases	2
1.2.1 Amylolytic enzymes	2
1.2.1.1 Glucoamylase	3
1.2.1.2 Sources of glucoamylase	4
1.2.1.3 Structural features of glucoamylase	7
1.2.2 $\beta$ -Glucosidase	9
1.2.2.1 Sources of $\beta$ -glucosidase	10
1.2.2.2 Structural features of $\beta$ -glucosidase	11
1.3 Glycosylation	14
1.3.1 Glycosylation mechanism	16
1.3.2 Advantages of enzymatic glycosylation over chemical methods	19
1.4 Glycosides	20
1.4.1 Properties of glycosides	20
1.4.2 Uses of glycosides	21
1.5 Enzyme catalysis in organic solvents	33
1.5.1 Important factors influencing glycosylation in organic solvents	33
1.5.1.1 Nature of substrate	33
1.5.1.2 Nature of solvent	36
1.5.1.3 Thermal stability	38
1.5.1.4 Water activity	41
1.5.1.5 Kinetics	43
1.5.1.6 Immobilization	44
1.6 Strategies employed in glycosylation	48
1.6.1 Glycosylation in reverse micelles	48
1.6.2 Glycosylation in supercritical carbon dioxide	49
1.6.3 Microwave-assisted glycosylation reactions	50
1.6.4 Response Surface Methodology in glycosylation	52
1.7 Scope of the present work	53

### **Chapter 2**

#### **Materials and Methods**

2.1 Materials	55
2.1.1 Glycosidases	55
2.1.1.1 Amyloglucosidase	55
2.1.1.2 $\beta$ -Glucosidase	55
2.1.2 Phenols/Vitamins	55
2.1.3 Carbohydrates	55
2.1.4 Solvents	56
2.1.5 Other chemicals	56
2.2 Methods	57
2.2.1 Enzyme activity assay for amyloglucosidase	57
2.2.1.1 Calibration	57
2.2.1.2 Activity assay	57
2.2.2 Protein estimation	58
2.2.3 Extraction of $\beta$ -glucosidase	59
2.2.4 Immobilization of $\beta$ -glucosidase	60

---

2.2.4.1 Activity assay	60
2.2.5 Preparation of buffers	61
2.2.6 Glycosylation procedure	61
2.2.7 Analysis	62
2.2.7.1 High Performance Liquid Chromatography	62
2.2.7.2 Thin Layer Chromatography	62
2.2.8 Separation of glycosides	62
2.2.9 Spectral characterization	63
2.2.9.1 UV-Visible spectroscopy	63
2.2.9.2 Infrared spectroscopy	63
2.2.9.3 Mass spectroscopy	63
2.2.9.4 Polarimetry	63
2.2.9.5 Melting point	64
2.2.9.6 NMR	64
<sup>1</sup> H NMR	64
<sup>13</sup> C NMR	65
2D-HSQCT	65
2.2.10 Antioxidant activity by DPPH method	65
2.2.11 Extraction of angiotensin converting enzyme (ACE) from pig lung	66
2.2.12 Angiotensin converting enzyme (ACE) inhibition assay	66
2.2.13 Protease activity	67
2.2.14 Lipase activity	68
2.2.15 Gel electrophoresis of glycosidases and ACE	69
<b>Chapter 3</b>	
<b>Enzymatic syntheses of vanillin, N-vanillyl-nonanamide, curcumin, DL-dopa and dopamine glycosides</b>	
Introduction	72
Present work	73
3.1 Syntheses of vanillyl glycosides	75
3.1.1 Synthesis of 4- <i>O</i> -(D-glucopyranosyl)vanillin using amyloglucosidase	76
3.1.1.1 Effect of incubation period	76
3.1.1.2 Effect of pH	77
3.1.1.3 Effect of buffer concentration	77
3.1.1.4 Effect of amyloglucosidase concentration	77
3.1.1.5 Effect of vanillin concentration	77
3.1.1.6 Solubility of 4- <i>O</i> -(D-glucopyranosyl)vanillin	79
3.1.2 Syntheses of vanillyl glycosides of other carbohydrates using amyloglucosidase	79
3.1.3 Syntheses of vanillyl glycosides of other carbohydrates using $\beta$ -glucosidase	79
3.1.4 Spectral characterization	79
3.1.4.1 4- <i>O</i> -(D-Glucopyranosyl)vanillin <b>17a-c</b>	81
3.1.4.2 4- <i>O</i> -(D-Galactopyranosyl)vanillin <b>18a,b</b>	82
3.1.4.3 4- <i>O</i> -(D-Mannopyranosyl)vanillin <b>19a,b</b>	83
3.1.4.4 4- <i>O</i> -( $\alpha$ -D-Glucopyranosyl-(1'→4)D-glucopyranosyl)vanillin <b>20a-d</b>	83
3.1.4.5 4- <i>O</i> -(D-Fructofuranosyl-(2→1') $\alpha$ -D-glucopyranosyl)vanillin <b>21a,b</b>	84
3.1.4.6 4- <i>O</i> -( $\beta$ -D-Galactopyranosyl-(1'→4) $\beta$ -D-glucopyranosyl)vanillin <b>22</b>	85
3.1.4.7 4- <i>O</i> -(D-sorbitol)vanillin <b>23a-c</b>	85
3.1.5 Discussion	87

3.1.6	Synthesis of 4- <i>O</i> -( $\alpha$ -D-glucopyranosyl-(1'→4)D-glucopyranosyl)vanillin using glucosidases by response surface methodology	92
3.1.6.1	Glycosylation	94
3.1.6.2	Response Surface Methodology	94
3.1.6.3	Amyloglucosidase catalysed synthesis of 4- <i>O</i> -( $\alpha$ -D-glucopyranosyl-(1'→4)D-glucopyranosyl)vanillin	97
3.1.6.4	$\beta$ -Glucosidase catalysed synthesis of 4- <i>O</i> -( $\alpha$ -D-glucopyranosyl-(1'→4) $\beta$ -D-glucopyranosyl)vanillin	101
3.2	Syntheses of N-vanillyl-nonanamide glycosides	104
3.2.1	Synthesis of 4- <i>O</i> -(D-glucopyranosyl)N-vanillyl-nonanamide using amyloglucosidase	106
3.2.1.1	Effect of incubation period	107
3.2.1.2	Effect of pH	107
3.2.1.3	Effect of buffer concentration	107
3.2.1.4	Effect of amyloglucosidase concentration	107
3.2.1.5	Effect of N-vanillyl-nonanamide concentration	109
3.2.1.6	Solubility of 4- <i>O</i> -(D-glucopyranosyl)N-vanillyl-nonanamide	109
3.2.2	Syntheses of N-vanillyl-nonanamide glycosides of other carbohydrates using amyloglucosidase and $\beta$ -glucosidase	109
3.2.3	Spectral characterization	110
3.2.3.1	4- <i>O</i> -(D-Glucopyranosyl)N-vanillyl-nonanamide <b>24a-c</b>	110
3.2.3.2	4- <i>O</i> -(D-Galactopyranosyl)N-vanillyl-nonanamide <b>25a,b</b>	111
3.2.3.3	4- <i>O</i> -( $\beta$ -D-Mannopyranosyl)N-vanillyl-nonanamide <b>26</b>	112
3.2.3.4	4- <i>O</i> -(D-Ribofuranosyl)N-vanillyl-nonanamide <b>27a,b</b>	113
3.2.3.5	4- <i>O</i> -( $\alpha$ -D-Glucopyranosyl-(1'→4)D-glucopyranosyl)N-vanillyl-nonanamide <b>28a-d</b>	114
3.2.3.6	4- <i>O</i> -( $\beta$ -D-Galactopyranosyl-(1'→4) $\beta$ -D-glucopyranosyl)N-vanillyl-nonanamide <b>29</b>	115
3.2.4	Discussion	117
3.3	Syntheses of curcuminyl-bis-glycosides	120
3.3.1	Synthesis of 1,7- <i>O</i> -(bis- $\beta$ -D-glucopyranosyl)curcumin using $\beta$ -glucosidase	122
3.3.1.1	Effect of incubation period	122
3.3.1.2	Effect of pH	122
3.3.1.3	Effect of buffer concentration	123
3.3.1.4	Effect of $\beta$ -glucosidase concentration	123
3.3.1.5	Effect of curcumin concentration	123
3.3.1.6	Solubility of 1,7- <i>O</i> -(bis- $\beta$ -D-glucopyranosyl)curcumin	123
3.3.2	Syntheses of curcuminyl-bis-glycosides of other carbohydrates using $\beta$ -glucosidase	125
3.3.3	Spectral characterization	125
3.3.3.1	1,7- <i>O</i> -(Bis- $\beta$ -D-glucopyranosyl)curcumin <b>30</b>	125
3.3.3.2	1,7- <i>O</i> -(Bis-D-galactopyranosyl)curcumin <b>31a,b</b>	126
3.3.3.3	1,7- <i>O</i> -(Bis-D-mannopyranosyl)curcumin <b>32a,b</b>	127
3.3.3.4	1,7- <i>O</i> -(Bis- $\beta$ -D-galactopyranosyl-(1'→4)D-glucopyranosyl)curcumin <b>33a,b</b>	127
3.3.4	Discussion	129
3.4	Syntheses of DL-dopa glycosides	131
3.4.1	Synthesis of DL-dopa-D-glucoside using amyloglucosidase	133

3.4.1.1 Effect of incubation period	134
3.4.1.2 Effect of pH	134
3.4.1.3 Effect of buffer concentration	134
3.4.1.4 Effect of amyloglucosidase concentration	134
3.4.1.5 Effect of DL-dopa concentration	136
3.4.2 Syntheses of DL-dopa glycosides of other carbohydrates using amyloglucosidase	136
3.4.3 Syntheses of DL-dopa glycosides of other carbohydrates using $\beta$ -glucosidase	136
3.4.4 Spectral characterization	137
3.4.4.1 DL-Dopa-D-glucoside <b>34a-d</b>	137
3.4.4.2 DL-Dopa-D-galactoside <b>35a-e</b>	138
3.4.4.3 DL-3-Hydroxy-4- <i>O</i> -( $\beta$ -D-mannopyranosyl)phenylalanine <b>36</b>	139
3.4.4.4 DL-3-Hydroxy-4- <i>O</i> -( $\beta$ -D-galactopyranosyl-(1'→4) $\beta$ -D-glucopyranosyl)phenylalanine <b>37</b>	140
3.4.4.5 DL-3-Hydroxy-4- <i>O</i> -(6-D-sorbitol)phenylalanine <b>38</b>	140
3.4.4.6 DL-3-Hydroxy-4- <i>O</i> -(1-D-mannitol)phenylalanine <b>39a,b</b>	141
3.4.5 Discussion	142
3.5 Syntheses of dopamine glycosides	146
3.5.1 Amyloglucosidase catalysed glucosylation of dopamine	148
3.5.1.1 Effect of incubation period	148
3.5.1.2 Effect of pH	148
3.5.1.3 Effect of buffer concentration	148
3.5.1.4 Effect of enzyme concentration	148
3.5.1.5 Effect of dopamine concentration	149
3.5.2 Immobilized $\beta$ -glucosidase catalysed glucosylation of dopamine	150
3.5.2.1 Effect of incubation period	150
3.5.2.2 Effect of pH	150
3.5.2.3 Effect of buffer concentration	150
3.5.2.4 Effect of enzyme concentration	151
3.5.2.5 Effect of dopamine concentration	152
3.5.3 Syntheses of dopamine glycosides of various carbohydrates using amyloglucosidase	152
3.5.4 Syntheses of dopamine glycosides of various carbohydrates using imm. $\beta$ -glucosidase	152
3.5.5 Spectral characterization	153
3.5.5.1 Dopamine-D-glucoside <b>40a-c</b>	153
3.5.5.2 Dopamine-D-galactoside <b>41a-d</b>	154
3.5.5.3 Dopamine-D-mannoside <b>42a-c</b>	155
3.5.6 Discussion	157
3.6 General discussion	160
3.7 Experimental	166
3.7.1 Glycosylation procedures	166
3.7.2 Response surface methodology	166
3.7.3 High Performance Liquid Chromatography	166
3.7.4 Size exclusion chromatography	167
3.7.5 Solubility	167
3.7.6 Spectral characterization	167



3.7.6.1 UV-visible spectroscopy	167
3.7.6.2 IR spectroscopy	168
3.7.6.3 Mass spectroscopy	168
3.7.6.4 Polarimetry	168
3.7.6.5 Melting point	168
3.7.6.6 <sup>1</sup> H NMR	168
3.7.6.7 <sup>13</sup> C NMR	169
3.7.6.8 2D HSQCT NMR	169
<b>Chapter 4</b>	
<b>Enzymatic syntheses of riboflavin, ergocalciferol and α-tocopherol glycosides</b>	
Introduction	170
Present work	171
4.1 Syntheses of riboflavinyl glycosides	172
4.1.1 Synthesis of 5- <i>O</i> -(D-glucopyranosyl)riboflavin using amyloglucosidase	175
4.1.1.1 Effect of incubation period	175
4.1.1.2 Effect of pH	175
4.1.1.3 Effect of buffer concentration	176
4.1.1.4 Effect of enzyme concentration	177
4.1.1.5 Effect of substrate concentration	177
4.1.2 Synthesis of 5- <i>O</i> -(β-D-glucopyranosyl)riboflavin using β-glucosidase	177
4.1.2.1 Effect of incubation period	177
4.1.2.2 Effect of pH	178
4.1.2.3 Effect of buffer concentration	178
4.1.2.4 Effect of enzyme concentration	178
4.1.2.5 Effect of substrate concentration	178
4.1.3 Solubility of 5- <i>O</i> -(D-glucopyranosyl)riboflavin	178
4.1.4 Syntheses of riboflavinyl glycosides of other carbohydrates using amyloglucosidase	180
4.1.5 Syntheses of riboflavinyl glycosides of other carbohydrates using β-glucosidase	180
4.1.6 Spectral characterization	180
4.1.6.1 5- <i>O</i> -(D-Glucopyranosyl)riboflavin <b>46a-c</b>	181
4.1.6.2 5- <i>O</i> -(D-Galactopyranosyl)riboflavin <b>47a,b</b>	182
4.1.6.3 5- <i>O</i> -(D-Mannopyranosyl)riboflavin <b>48a,b</b>	183
4.1.6.4 5- <i>O</i> -(D-Ribofuranosyl)riboflavin <b>49a,b</b>	184
4.1.6.5 5- <i>O</i> -(α-D-Glucopyranosyl-(1'→4)D-glucopyranosyl)riboflavin <b>50a-c</b>	184
4.1.6.6 5- <i>O</i> -(1-D-Fructofuranosyl-(2→1')α-D-glucopyranosyl)riboflavin <b>51</b>	185
4.1.6.7 5- <i>O</i> -(β-D-Galactopyranosyl-(1'→4)β-D-glucopyranosyl)riboflavin <b>52</b>	186
4.1.7 Discussion	187
4.2 Syntheses of ergocalciferol glycosides	193
4.2.1 Synthesis of 20- <i>O</i> -(D-glucopyranosyl)ergocalciferol using amyloglucosidase	195
4.2.1.1 Effect of pH	195
4.2.1.2 Effect of buffer concentration	195
4.2.1.3 Effect of amyloglucosidase concentration	195
4.2.2 Solubility of 20- <i>O</i> -(D-glucopyranosyl)ergocalciferol	196
4.2.3 Spectral characterization	196
4.2.3.1 20- <i>O</i> -(D-Glucopyranosyl)ergocalciferol <b>53a-c</b>	197
4.2.4 Discussion	198

4.3 Syntheses of $\alpha$ -tocopheryl glycosides	199
4.3.1 Synthesis of 6- <i>O</i> -( $\beta$ -D-glucopyranosyl) $\alpha$ -tocopherol using $\beta$ -glucosidase	202
4.3.1.1 Effect of incubation period	202
4.3.1.2 Effect of pH	202
4.3.1.3 Effect of buffer concentration	202
4.3.1.4 Effect of enzyme concentration	204
4.3.1.5 Effect of $\alpha$ -tocopherol concentration	204
4.3.2 Solubility of 6- <i>O</i> -(D-glucopyranosyl) $\alpha$ -tocopherol	204
4.3.3 Syntheses of $\alpha$ -tocopheryl glycosides of other carbohydrates using $\beta$ -glucosidase	204
4.3.4 Spectral characterization	205
4.3.4.1 6- <i>O</i> -( $\beta$ -D-Glucopyranosyl) $\alpha$ -tocopherol <b>54</b>	205
4.3.4.2 6- <i>O</i> -(D-Galactopyranosyl) $\alpha$ -tocopherol <b>55a,b</b>	206
4.3.4.3 6- <i>O</i> -(D-Mannopyranosyl) $\alpha$ -tocopherol <b>56a,b</b>	207
4.3.5 Discussion	208
4.4 General discussion	211
4.5 Experimental	213
4.5.1 Glycosylation procedures	213
<b>Chapter 5</b>	
<b>Competitive inhibition of amyloglucosidase by vanillin in the glycosylation of vanillin</b>	
Introduction	214
Present work	215
5.1 Kinetic experiments on amyloglucosidase catalyzed synthesis of 4- <i>O</i> -(D-glucopyranosyl)vanillin	215
5.2 Discussion	219
5.3 Experimental	221
5.3.1 Kinetic experiments	221
<b>Chapter 6</b>	
<b>Evaluation of antioxidant and angiotensin converting enzyme inhibition activity of the synthesized phenolic and vitamin glycosides</b>	
Introduction	222
Present work	224
6.1 Antioxidant activity	225
6.2 Angiotensin converting enzyme inhibitory activity	228
6.3 Discussion	229
6.4 Experimental	232
6.4.1 Glycosylation procedure	232
6.4.2 Antioxidant activity by DPPH method	232
6.4.3 Extraction of ACE from pig lung	232
6.4.4 Angiotensin converting enzyme (ACE) inhibition assay	233
6.4.5 Protease and lipase assay	234
<b>Conclusions</b>	235
<b>Summary</b>	242
<b>References</b>	246
<b>Publications</b>	

## LIST OF TABLES

Table No.	Title	Page No.
Table 1.1	Glycosides prepared through enzymatic glycosylation	22
Table 1.2	Vitamin glycosides prepared through enzymatic glycosylation	29
Table 2.1	Chemicals and their companies of procurement.	56
Table 2.2	Activity assay for amyloglucosidase, $\beta$ -glucosidase and immobilized $\beta$ -glucosidase	58
Table 3.1	Optimization of reaction conditions for the synthesis of 4- <i>O</i> -(D-glucopyranosyl)vanillin	78
Table 3.2	NMR data for free carbohydrate molecules employed in the present work	80
Table 3.3	Syntheses of vanillyl glycosides using amyloglucosidase and $\beta$ -glucosidase	89
Table 3.4	Coded values of the variables and their corresponding actual values used in the design of experiments	95
Table 3.5	Experimental design with experimental and predictive yields of maltosylation based on response surface methodology	96
Table 3.6	Amyloglucosidase catalysed reaction: Analysis of variance ( <i>ANOVA</i> ) of the response surface model along with coefficients of the response equation	98
Table 3.7	Validation data for the amyloglucosidase catalysed reactions at selected random conditions	100
Table 3.8	$\beta$ -Glucosidase catalysed reaction: Analysis of variance ( <i>ANOVA</i> ) of the response surface model along with coefficients of the response equation	102
Table 3.9	Validation data for the $\beta$ -glucosidase catalysed reactions at selected random conditions	104
Table 3.10	Optimization of reaction conditions for the synthesis of 4- <i>O</i> -(D-glucopyranosyl) <i>N</i> -vanillyl-nonanamide	108
Table 3.11	Syntheses of <i>N</i> -vanillyl-nonanamide glycosides	118
Table 3.12	Optimization of reaction conditions for the synthesis of 1,7- <i>O</i> -(bis- $\beta$ -D-glucopyranosyl)curcumin using $\beta$ -glucosidase	124
Table 3.13	Syntheses of curcuminyl-bis-glycosides using $\beta$ -glucosidase	130

Table 3.14	Optimization of reaction conditions for the synthesis of DL-dopa-D-glucoside using amyloglucosidase	135
Table 3.15	Syntheses of DL-3,4-dihydroxyphenylalanine (DL-dopa) glycosides using amyloglucosidase and $\beta$ -glucosidase	143
Table 3.16	Optimization of reaction conditions for the synthesis of dopamine-D-glucoside using amyloglucosidase	149
Table 3.17	Optimization of reaction conditions for the synthesis of 3-hydroxy-4- <i>O</i> -( $\beta$ -D-glucopyranosyl)phenylethylamine using imm. $\beta$ -glucosidase	151
Table 3.18	Syntheses of dopamine glycosides using amyloglucosidase and imm. $\beta$ -glucosidase	158
Table 4.1	Optimization of reaction conditions for the synthesis of 5- <i>O</i> -(D-glucopyranosyl)riboflavin using amyloglucosidase	176
Table 4.2	Optimization of reaction conditions for the synthesis of 5- <i>O</i> -( $\beta$ -D-glucopyranosyl)riboflavin using $\beta$ -glucosidase	179
Table 4.3	Syntheses of riboflavinyl glycosides using amyloglucosidase and $\beta$ -glucosidase	189
Table 4.4	Optimization of reaction conditions for the synthesis of 20- <i>O</i> -(D-glucopyranosyl)ergocalciferol using amyloglucosidase	196
Table 4.5	Synthesis of 20- <i>O</i> -(D-glucopyranosyl)ergocalciferol using amyloglucosidase	199
Table 4.6	Optimization of reaction conditions for the synthesis of 6- <i>O</i> -( $\beta$ -D-glucopyranosyl) $\alpha$ -tocopherol using $\beta$ -glucosidase	203
Table 4.7	Syntheses of $\alpha$ -tocopheryl glycosides using $\beta$ -glucosidase	209
Table 5.1	Kinetic parameters for the synthesis of 4- <i>O</i> -(D-glucopyranosyl)vanillin	218
Table 5.2	Experimental and predicted initial rate values for the synthesis of 4- <i>O</i> -(D-glucopyranosyl)vanillin	219
Table 6.1	Antioxidant and angiotensin converting enzyme inhibitory activities of various phenolic and vitamin glycosides	225
Table 6.2	Inhibition of protease in ACE by glycoside	228

## LIST OF FIGURES

Number	Captions
Fig. 2.1	Calibration plot for D-glucose
Fig. 2.2	Calibration curve for the estimation of protein by Lowry's method
Fig. 2.3	Calibration plot for the determination of p-nitrophenol concentration by $\beta$ -glucosidase activity
Fig. 2.4	Calibration plot for hippuric acid estimation by the spectrophotometric method.
Fig. 2.5	Log $M_r$ versus $R_f$ plot
Fig. 2.6	SDS-PAGE
Fig. 3.1	HPLC chromatogram for the reaction mixture of D-glucose and 4- <i>O</i> -(D-glucopyranosyl)vanillin
Fig. 3.2	(A) Reaction profile for 4- <i>O</i> -(D-glucopyranosyl)vanillin synthesis by the reflux method and (B) Effect of amyloglucosidase concentration for 4- <i>O</i> -(D-glucopyranosyl) vanillin synthesis
Fig. 3.3	Ultraviolet-visible spectra of (A) Vanillin <b>1</b> and (B) 4- <i>O</i> -(D-glucopyranosyl) vanillin <b>17a-c</b>
Fig. 3.4	4- <i>O</i> -(D-Glucopyranosyl)vanillin <b>17a-c</b> (A) IR spectrum and (B) Mass spectrum.
Fig. 3.5	(A) 2D-HSQCT spectrum showing the C2-C6 region of 4- <i>O</i> -(D-glucopyranosyl)vanillin <b>17a-c</b> and (B) Anomeric region of the same compound
Fig. 3.6	4- <i>O</i> -( $\beta$ -D-glucopyranosyl)vanillin <b>17b</b> (A) Mass spectrum and (B) 2D-HSQCT spectrum showing the C1-C6 region
Fig. 3.7	4- <i>O</i> -(D-Galactopyranosyl)vanillin <b>18a,b</b> (A) IR spectrum and (B) 2D-HSQCT spectrum showing the C1-C6 region
Fig. 3.8	4- <i>O</i> -(D-Mannopyranosyl)vanillin <b>18a,b</b> (A) Mass spectrum and (B) 2D-HSQCT spectrum showing the C1-C6 region
Fig. 3.9	4- <i>O</i> -( $\alpha$ -D-Glucopyranosyl-(1'→4)D-glucopyranosyl)vanillin <b>20a,c,d</b> (A) IR spectrum and (B) 2D-HSQCT spectrum showing the C1-C6' region
Fig. 3.10	4- <i>O</i> -( $\alpha$ -D-Glucopyranosyl-(1'→4) $\beta$ -D-glucopyranosyl)vanillin <b>20b</b> (A) Mass spectrum and (B) 2D-HSQCT spectrum showing the C1-C6' region
Fig. 3.11	4- <i>O</i> -(D-Fructofuranosyl-(2→1') $\alpha$ -D-glucopyranosyl)vanillin <b>21a,b</b> (A) IR spectrum, (B) 2D-HSQCT spectrum showing the C1-C6' region and (C) Anomeric region
Fig. 3.12	4- <i>O</i> -( $\beta$ -D-Glucopyranosyl-(1'→4) $\beta$ -D-glucopyranosyl)vanillin <b>22</b> (A) Mass spectrum and (B) 2D-HSQCT spectrum showing the C1-C6' region
Fig. 3.13	4- <i>O</i> -(D-Sorbitol)vanillin <b>23a-c</b> (A) IR spectrum, (B) Mass spectrum and (C) 2D-HSQCT spectrum showing the C1-C6 region
Fig. 3.14	Three-dimensional surface plots showing the effect of variables in the amyloglucosidase catalysed reaction (A) Amyloglucosidase and buffer concentrations on the extent of maltosylation yield and (B) Amyloglucosidase and incubation period on the extent of maltosylation yield

- 
- Fig. 3.15 Three-dimensional surface plots showing the effect of variables in the amyloglucosidase catalysed reaction (A) Vanillin and incubation period on the extent of maltosylation yield and (B) Amyloglucosidase concentrations and pH on the extent of maltosylation yield
- Fig. 3.16 Three-dimensional surface plots showing the effect of variables in the  $\beta$ -glucosidase catalysed reaction (A) Vanillin and  $\beta$ -glucosidase concentrations on the extent of maltosylation yield and (B)  $\beta$ -Glucosidase concentration and buffer concentration on the extent of maltosylation yield
- Fig. 3.17 Three-dimensional surface plots showing the effect of variables in the  $\beta$ -glucosidase catalysed reaction (A) Incubation period and pH on the extent of maltosylation yield and (B)  $\beta$ -Glucosidase concentration and incubation period on the extent of maltosylation yield
- Fig. 3.18 Three-dimensional surface plots showing the effect of variables in the  $\beta$ -glucosidase catalysed reaction:  $\beta$ -Glucosidase concentration and pH on the extent of maltosylation yield
- Fig. 3.19 HPLC chromatogram for the reaction mixture of D-glucose and 4-*O*-(D-glucopyranosyl)N-vanillyl-nonanamide
- Fig. 3.20 (A) Reaction profile on 4-*O*-(D-glucopyranosyl)N-vanillyl-nanamide synthesis and (B) Effect of buffer concentration on 4-*O*-(D-glucopyranosyl)N-vanillyl-nanamide synthesis
- Fig. 3.21 Ultraviolet-visible spectra of (A) N-Vanillyl-nonanamide **2** and (B) 4-*O*-(D-Glucopyranosyl)N-vanillyl-nonanamide **24a,b**
- Fig. 3.22 4-*O*-(D-Glucopyranosyl)N-vanillyl-nonanamide **24a,b** (A) IR spectrum, (B) Mass spectrum and (C) 2D-HSQCT spectrum showing the C1-C6 region
- Fig. 3.23 4-*O*-( $\beta$ -D-Glucopyranosyl)N-vanillyl-nonanamide **24c** (A) Mass spectrum and (B) 2D-HSQCT spectrum showing the C1-C6 region
- Fig. 3.24 4-*O*-(D-Galactopyranosyl)N-vanillyl-nonanamide **25a,b** (A) IR spectrum and (B) 2D-HSQCT spectrum showing the C1-C6 region
- Fig. 3.25 4-*O*-( $\beta$ -D-Galactopyranosyl)N-vanillyl-nonanamide **25b** (A) Mass spectrum and (B) 2D-HSQCT spectrum showing the C1-C6 region
- Fig. 3.26 4-*O*-( $\beta$ -D-Mannopyranosyl)N-vanillyl-nonanamide **26** (A) IR spectrum and (B) 2D-HSQCT spectrum showing the C1-C6 region
- Fig. 3.27 4-*O*-(D-Ribofuranosyl)N-vanillyl-nonanamide **27a,b** (A) IR spectrum and (B) 2D-HSQCT spectrum showing the C1-C5 region
- Fig. 3.28 4-*O*-( $\alpha$ -D-Glucopyranosyl-(1'→4)D-glucopyranosyl)N-vanillyl-nonanamide **28a-c** (A) Mass spectrum and (B) 2D-HSQCT spectrum showing the C1-C6' region
- Fig. 3.29 4-*O*-( $\alpha$ -D-Glucopyranosyl-(1'→4) $\beta$ -D-glucopyranosyl)N-vanillyl-nonanamide **28d** (A) IR spectrum and (B) 2D-HSQCT spectrum showing the C1-C6' region
-

- 
- Fig. 3.30 4-*O*-( $\beta$ -D-Galactopyranosyl-(1'→4) $\beta$ -D-glucopyranosyl)N-vanillyl-nona  
namide **29** (A) IR spectrum and (B) 2D-HSQCT spectrum showing the C1-  
C6' region
- Fig. 3.31 HPLC chromatogram for the reaction mixture of D-glucose and 1,7-*O*-(bis- $\beta$ -  
D-glucopyranosyl)curcumin
- Fig. 3.32 (A) Reaction profile for 1,7-*O*-(bis- $\beta$ -D-glucopyranosyl)curcumin synthesis  
and (B) Effect of curcumin concentration for 1,7-*O*-(bis- $\beta$ -D-  
glucopyranosyl)curcumin synthesis
- Fig. 3.33 Ultraviolet-visible spectra of (A) Curcumin **3** and (B) 1,7-*O*-(Bis- $\beta$ -D-  
glucopyranosyl)curcumin **30**
- Fig. 3.34 1,7-*O*-(Bis- $\beta$ -D-glucopyranosyl)curcumin **30** (A) IR spectrum and (B) 2D-  
HSQCT spectrum showing the C1-C6 region
- Fig. 3.35 1,7-*O*-(Bis-D-galactopyranosyl)curcumin **31a,b** (A) IR spectrum and (B) 2D-  
HSQCT spectrum showing the C1-C6 region
- Fig. 3.36 1,7-*O*-(Bis-D-mannopyranosyl)curcumin **32a,b** (A) Mass spectrum, (B) 2D-  
HSQCT spectrum (anomeric region) and (C) 2D-HSQCT spectrum showing  
the C2-C6 region
- Fig. 3.37 1,7-*O*-(Bis- $\beta$ -D-galactopyranosyl-(1'→4)D-glucopyranosyl)curcumin **33a,b**  
(A) Mass spectrum and (B) 2D-HSQCT spectrum showing the C1-C6' region
- Fig. 3.38 HPLC chromatogram for the reaction mixture of D-glucose and DL-dopa-D-  
glucoside
- Fig. 3.39 (A) Reaction profile for DL-dopa-D-glucoside synthesis and (B) Effect of pH  
for DL-dopa-D-glucoside synthesis
- Fig. 3.40 Ultraviolet-visible spectra of (A) DL-Dopa **4** and (B) DL-Dopa-D-glucoside **34a-d**
- Fig.3.41 DL-Dopa-D-glucoside **34a-d** (A) IR spectrum, (B) Mass spectrum and (C)  
2D-HSQCT spectrum showing the C1-C6 region
- Fig. 3.42 DL-3-Hydroxy-4-*O*-(D-glucopyranosyl)phenylalanine **34b,c** (A) Mass  
spectrum and (B) 2D-HSQCT spectrum showing the C1-C6 region
- Fig. 3.43 DL-Dopa-D-galactoside **35a-e** (A) Mass spectrum and (B) 2D-HSQCT  
spectrum showing the C1-C6 region
- Fig. 3.44 DL-3-Hydroxy-4-*O*-( $\beta$ -D-mannopyranosyl)phenylalanine **36** (A) IR spectrum  
and (B) 2D-HSQCT spectrum showing the C1-C6 region
- Fig. 3.45 DL-3-Hydroxy-4-*O*-( $\beta$ -D-galactopyranosyl-(1'→4) $\beta$ -D-glucopyranosyl)  
phenylalanine **37** (A) IR spectrum and (B) 2D-HSQCT spectrum showing the  
C1-C6' region
- Fig. 3.46 DL-3-Hydroxy-4-*O*-(6-D-sorbitol)phenylalanine **38** (A) Mass spectrum and  
(B) 2D-HSQCT spectrum showing the C1-C6 region
- Fig. 3.47 DL-Dopa-D-mannitol **39a,b** (A) IR spectrum and (B) 2D-HSQCT spectrum  
showing the C1-C6 region
- Fig. 3.48 HPLC chromatogram for the reaction mixture of D-glucose and dopamine-D-  
glucoside
-



- 
- Fig. 3.49 (A) Reaction profile for dopamine-D-glucoside synthesis and (B) Effect of buffer concentration for dopamine-D-glucoside synthesis
- Fig. 3.50 (A) Reaction profile for 3-hydroxy-4-*O*-( $\beta$ -D-glucopyranosyl) phenylethylamine synthesis and (B) Effect of buffer concentration for 3-hydroxy-4-*O*-( $\beta$ -D-glucopyranosyl) phenylethylamine synthesis
- Fig. 3.51 Ultraviolet-visible spectra of (A) Dopamine and (B) Dopamine-D-glucoside **40a-c**
- Fig. 3.52 Dopamine-D-glucoside **40a-c** (A) IR spectrum, (B) Mass spectrum and (C) 2D-HSQCT spectrum showing the C1-C6 region
- Fig. 3.53 3-Hydroxy-4-*O*-( $\beta$ -D-glucopyranosyl)phenylethylamine **40b** (A) IR spectrum and (B) 2D-HSQCT spectrum showing the C1-C6 region
- Fig. 3.54 Dopamine-D-galactoside **41a-d** (A) Mass spectrum and (B) 2D-HSQCT spectrum showing the C1-C6 region
- Fig. 3.55 Dopamine-D-mannoside **42a-c** (A) IR spectrum and (B) 2D-HSQCT spectrum showing the C1-C6 region
- Fig. 4.1 HPLC chromatogram for the reaction mixture of 5-*O*-(D-glucopyranosyl)riboflavin
- Fig. 4.2 (A) Reaction profile for 5-*O*-(D-glucopyranosyl)riboflavin synthesis and (B) Effect of buffer concentration for 5-*O*-(D-glucopyranosyl)riboflavin synthesis
- Fig. 4.3 (A) Reaction profile for 5-*O*-( $\beta$ -D-glucopyranosyl)riboflavin synthesis and (B) Effect of riboflavin concentration for 5-*O*-( $\beta$ -D-glucopyranosyl)riboflavin synthesis
- Fig. 4.4 Ultraviolet-visible spectra of (A) Riboflavin **43** and (B) 5-*O*-(D-Glucopyranosyl)riboflavin **46a-c**
- Fig. 4.5 5-*O*-(D-Glucopyranosyl)riboflavin **46a-c**: (A) IR spectrum, (B) Mass spectrum and (C) 2D-HSQCT spectrum showing the C1-C6 region
- Fig. 4.6 5-*O*-( $\beta$ -D-Glucopyranosyl)riboflavin **46b**: (A) IR spectrum and (B) 2D-HSQCT spectrum showing the C1-C6 region
- Fig. 4.7 5-*O*-(D-Galactopyranosyl)riboflavin **47a,b**: (A) IR spectrum and (B) 2D-HSQCT spectrum showing the C1-C6 region
- Fig. 4.8 5-*O*-(D-Mannopyranosyl)riboflavin **48a,b**: (A) Mass spectrum, (B) 2D-HSQCT spectrum showing the C2-C6 region and (C) Anomeric region of the same compound
- Fig. 4.9 5-*O*-(D-Ribofuranosyl)riboflavin **49a,b**: (A) IR spectrum, (B) 2D-HSQCT spectrum showing the C2-C5 region and (C) Anomeric region of the same compound
- Fig. 4.10 5-*O*-( $\alpha$ -D-Glucopyranosyl-(1'→4)D-glucopyranosyl)riboflavin **50a-c**: (A) IR spectrum and (B) 2D-HSQCT spectrum showing the C1-C6' region
- Fig. 4.11 5-*O*-(1-D-Fructofuranosyl-(2→1') $\alpha$ -D-glucopyranosyl)riboflavin **51**: (A) Mass spectrum and (B) 2D-HSQCT spectrum showing the C1-C6' region
-

- 
- Fig. 4.12 5-*O*-( $\beta$ -D-Galactopyranosyl-(1'→4) $\beta$ -D-glucopyranosyl)riboflavin **52**: (A) IR spectrum, (B) 2D-HSQCT spectrum showing the C2-C6' region and (C) Anomeric region of the same compound
- Fig. 4.13 HPLC chromatogram for the reaction mixture of 20-*O*-(D-glucopyranosyl)ergocalciferol
- Fig. 4.14 (A) Effect of pH for 20-*O*-(D-glucopyranosyl)ergocalciferol synthesis and (B) Effect of enzyme concentration for 20-*O*-(D-glucopyranosyl)ergocalciferol synthesis
- Fig. 4.15 Ultraviolet-visible spectra of (A) Ergocalciferol **44** and (B) 20-*O*-(D-Glucopyranosyl) ergocalciferol **53a-c**
- Fig. 4.16 20-*O*-(D-Glucopyranosyl)ergocalciferol **53a-c**: (A) IR spectrum, (B) Mass spectrum and (C) 2D-HSQCT spectrum showing the C1-C6 region
- Fig. 4.17 HPLC chromatogram for the reaction mixture of 6-*O*-( $\beta$ -D-glucopyranosyl) $\alpha$ -tocopherol
- Fig. 4.18 (A) Reaction profile for 6-*O*-( $\beta$ -D-glucopyranosyl) $\alpha$ -tocopherol synthesis and (B) Effect of buffer concentration for 6-*O*-( $\beta$ -D-glucopyranosyl) $\alpha$ -tocopherol synthesis
- Fig. 4.19 Ultraviolet-visible spectra of (A)  $\alpha$ -Tocopherol **45** and (B) 6-*O*-( $\beta$ -D-Glucopyranosyl) $\alpha$ -tocopherol **54**
- Fig. 4.20 6-*O*-( $\beta$ -D-Glucopyranosyl) $\alpha$ -tocopherol **54**: (A) IR spectrum, (B) Mass spectrum and (C) 2D-HSQCT spectrum showing the C1-C6 region
- Fig. 4.21 6-*O*-(D-Galactopyranosyl) $\alpha$ -tocopherol **55a,b**: (A) IR spectrum, (B) 2D-HSQCT full spectrum and (C) Anomeric region of the same compound
- Fig. 4.22 6-*O*-(D-Mannopyranosyl) $\alpha$ -tocopherol **56a,b**: (A) IR spectrum and (B) 2D-HSQCT spectrum showing the C1-C6 region
- Fig. 5.1 Initial rate (*v*) plot
- Fig. 5.2 Double reciprocal plot: 1/*v* versus 1/[vanillin]
- Fig. 5.3 Double reciprocal plot: 1/*v* versus 1/[D-glucose]
- Fig. 5.4 Replot of Slope
- Fig. 6.1 Antioxidant inhibition plot for Butylated Hydroxy Anisole (BHA)
- Fig. 6.2 Antioxidant activity plot for phenolic glycosides
- Fig. 6.3 Antioxidant activity plot for phenolic and vitamin glycosides
- Fig. 6.4 ACE inhibition plot for enalapril
- Fig. 6.5 ACE inhibition plots for phenolic glycosides
- Fig. 6.6 ACE inhibition plots for phenolic and vitamin glycosides
- Fig. 6.7 ACE inhibition plots: (A) 20-*O*-(D-glucopyranosyl)ergocalciferol **53a-c**, (B) 6-*O*-( $\beta$ -D-glucopyranosyl) $\alpha$ -tocopherol **54** and (C) 6-*O*-(D-mannopyranosyl) $\alpha$ -tocopherol **56a,b**
-

## LIST OF SCHEMES

<b>Scheme No.</b>	<b>Title</b>	<b>Page No.</b>
Scheme 1.1	Reactions catalyze by glycosidases	16
Scheme 1.2A	Nucleophilic double displacement mechanism	18
Scheme 1.2B	Oxocarbenium ion intermediate mechanism	19
Scheme 3.1	Syntheses of vanillyl glycosides	76
Scheme 3.2	Syntheses of N-vanillyl-nonanamide glycosides	106
Scheme 3.3	Syntheses of curcuminyl-bis-glycosides	122
Scheme 3.4	Syntheses of DL-dopa glycosides	133
Scheme 3.5	Syntheses of dopamine glycosides	147
Scheme 4.1	Syntheses of riboflavinyl glycosides	174
Scheme 4.2	Synthesis of 20- <i>O</i> -(D-glucopyranosyl)ergocalciferol	194
Scheme 4.3	Syntheses of $\alpha$ -tocopheryl glycosides	201
Scheme 5.1	Ping-Pong Bi-Bi model with competitive substrate inhibition	217
Scheme 6.1	Role of angiotensin converting enzyme (ACE) in regulating blood pressure	223

## LIST OF ABBREVIATIONS AND SYMBOLS

A	Absorbance
ANOVA	Analysis of variance
ACE	Angiotensin Converting Enzyme
Å	Angstrom
bp	Boiling point
BSA	Bovine serum albumin
<sup>13</sup> C	Carbon-13
cm	Centimeter
CCRD	Central Composite Rotatable Design
δ	Chemical shift value
J	Coupling constant
CMC	Critical Micellar Concentration
°C	Degree centigrade
DMSO-d <sub>6</sub>	Deuteriated Dimethyl sulfoxide
eV	Electronvolt
E/S	Enzyme by substrate ratio
EC	Enzyme commission
eq	Equivalents
g	Gram
Hz	Hertz
HSQCT	Heteronuclear Single Quantum Coherence Transfer
HPLC	High Performance Liquid Chromatography
h	Hour
IR	Infra red
K <sub>i</sub>	Inhibitor constant
v	Initial velocity
IUPAC	International union of pure and applied chemistry
kDa	Kilo Dalton
kV	Kilovolts
MS	Mass spectroscopy
v <sub>max</sub>	Maximum velocity
MHz	Mega hertz
mp	Melting point
K <sub>M</sub>	Michelis Menton constant
μg	Microgram
μL	Microlitre
mg	Milligram
mL	Milliliter
mm	Millimeter
mmol	Millimole
min	Minute
ε	Molar extinction coefficient
M	Molarity
mol	Mole

[M] <sup>+</sup>	Molecular ion
nm	Nanometer
N	Normality
NMR	Nuclear Magnetic Resonance
[α]	Optical rotation
ppm	Parts per million
%	Percentage
π	Pi
PAGE	Polyacrylamide gel electrophoresis
KBr	Potassium bromide
<sup>1</sup> H	Proton
RSM	Response Surface Methodology
RT	Retention time
rpm	Round per minute
sec	Seconds
σ	Sigma
SDS	Sodium dodecyl sulphate
SCCO <sub>2</sub>	Super critical carbon dioxide
SCF	Super critical fluid
TMS	Tetra methyl silane
TLC	Thin layer chromatography
2D	Two-Dimensional
UV	Ultra violet
v/v	Volume by volume
v/w	Volume by weight
a <sub>w</sub>	Water activity
cm <sup>-1</sup>	Wave per centimeter
w/w	Weight by weight
w/v	Weight by volume

ePrints@CFTRI

***Chapter 1***  
***Introduction***

## 1.1 Biotransformations

Enzymes are biocatalysts used increasingly in industrial synthetic chemistry in recent times, particularly in cases, where chemical routes are difficult to implement (Johannes and Zhao 2006; Schoemaker *et al.* 2003). Oxido-reductases, hydrolases (lipases, esterases, glycosidases, transglycosidases, peptidases, acylases, amidases, epoxide hydrolases, nitrilases and hydantoinases), lyases and isomerases have been used in organic synthesis to a great extent (Nakamura and Matsuda 2002; Faber 2004). The conversion of substrate to product occurs at active site on an enzyme molecule. Presently, chiral compounds are the most important building blocks in chemical and pharmaceutical industries used for the production of flavours, agrochemicals and drugs (Daubmann *et al.* 2006). Interest for creating stereogenic centers by applying biocatalytic methods are on the rise (Davis and Boyer 2001; Honda *et al.* 2006; Fellunga *et al.* 2007; Szymanski *et al.* 2007; Arrigo *et al.* 2007; Lukowska and Plenkiewicz 2007; Zheng *et al.* 2007; Omori *et al.* 2007). Enzymes are powerful tools in the synthesis and modification of carbohydrate molecules, used either alone or as whole cells (Goldberg *et al.* 2007a; 2007b).

Carbohydrates in the form of oligo- and polysaccharides are universally found in nature and possess highly diverse biological functions. These compounds are obtained from simple carbohydrates by glycosyltransferases and are degraded by glycoside hydrolases and polysaccharide lyases. These type of enzymes known as carbohydrate active enzymes are key enzymes for clean processing of abundant and useful renewable resources (Laine 1994). They are essential for biochemical studies in glycobiology as potential drugs due to their biocompatibility, structure forming capacity and environmentally benign properties (Allison and Grande 2006; Volpi 2006; Yip *et al.* 2006; Prabakaran and Mano 2006).



## 1.2 Glycosidases

Glycosyl transferases, transglycosidases and phosphorylases are the enzymes responsible for glycosyl bond formation (Faijes and Planas 2007). However, the enzymes like esterases, epimerases and sulfotransferases modify the carbohydrate structures to produce functional biomolecules (Whitelock and Iozzo 2005; Lerouxel *et al.* 2006).

Among the enzymes, glycosidases and transglycosidases play an important role in organic synthesis of glycosides. They are widely distributed in nature, belonging to the group of carbohydrate processing enzymes, widely employed in the regio and stereoselective glycosylation reactions. Glycosidases are enzymes that catalyze the hydrolysis of glycosidic bonds in simple glycosides, oligosaccharides and polysaccharides, as well as in complex carbohydrates such as glycoproteins and glycolipids, with the liberation of monosaccharides and oligosaccharides of lower molecular weight than the native substrate. Payen and Persoz (1833) were probably the first to recognize this enzyme in 1833 and they named it as “diastase” (now known as amylase). The phenomenon of hydrolysis was investigated by Liebig and Wohler in 1837 and Robiquet in 1838 on amygdalin (an aromatic glycoside) by bitter almonds and named the active principle as “emulsions”. Subsequently, a detailed study on glycosidases was carried out by many eminent chemists and biochemists (Fischer 1894).

### 1.2.1 Amylolytic enzymes

Starch degrading enzymes have been broadly classified into two groups - endo-acting enzymes or endohydrolases and exo-acting enzymes or exohydrolases (Berfoldo and Antranikian 2001).  $\alpha$ -Amylase ( $\alpha$ -1,4-glucan-4-glucanohydrolase, EC 3.2.1.1) is an endo-acting enzyme, which is widely distributed in plant mammalia tissues and microorganisms (Maheswar Rao and Satyanarayana 2007). The wide spread occurrence of  $\alpha$ -amylases in various organisms and the consumption of their substrates for food

reserves and energy sources have led to intense interest in their biomedical properties and to major biotechnological applications in industry (Vander Maarel *et al.* 2002; Bestoldo *et al.* 1999). They catalyse the hydrolysis of  $\alpha$ -1 $\rightarrow$ 4 glucosidic linkages of polysaccharides such as starch, glycogen or their degradation products (Tripathi *et al.* 2007). The structure consists of a single polypeptide chain folded into three domains (A, B and C). The catalytic domain 'A' consists of  $(\beta/\alpha)_8$  barrel, domain 'B' is probably responsible for differences in substrate specificity and stability among the  $\alpha$ -amylase (Svensson 1994) and domain 'C' constitutes the C-terminal part of the sequence (Nielsen *et al.* 2004).

Exo acting starch hydrolases include  $\beta$ -amylase, glucoamylase,  $\alpha$ -glucosidase and isoamylase. These enzymes attack the substrate from the nonreducing end, producing oligosaccharides.  $\beta$ -Amylase (1,4- $\alpha$ -D-glucan maltohydrolase, EC 3.2.1.2) is an exo-acting enzyme which catalyzes the hydrolysis of 1,4- $\alpha$ -glycosidic linkages in starch, glycogen and related polysaccharides and oligosaccharides to remove successive  $\beta$ -maltose units from the non-reducing end of the chains.  $\alpha$ -Glucosidase (EC 3.2.1.20) attacks  $\alpha$ -1,4 linkages of oligosaccharides and liberates glucose with  $\alpha$ -anomeric configuration. Isoamylase (Glycogen 6-glucoanohydrase) is a debranching enzyme specific for  $\alpha$ -1,6 linkages in polysaccharides, such as amylopectin, glycogen and  $\beta$ -limit dextrin.

#### **1.2.1.1 Glucoamylase**

Glucoamylase [ $\alpha$ -(1,4)-D-glucan glucohydrolase, EC 3.2.1.3] is a fungal enzyme also known as amyloglucosidase, maltase, saccharogenic amylase and  $\gamma$ -amylase belonging to an important group of starch degrading enzymes (Riaz *et al.* 2007). They catalyze the hydrolysis of  $\alpha$ -1,4 and  $\alpha$ -1,6 glycosidic linkages from the non-reducing end

of starch and related oligosaccharides, the  $\alpha$ -1,6 activity rate is only 0.2% of that of  $\alpha$ -1,4 (Meages 1989; Jafari-Aghdam *et al.* 2005) with the inversion of anomeric configuration to produce  $\beta$ -glucose (Norouzian 2006; Thorsen 2006). However, the size of the substrate and the position of the  $\alpha$ -1,6 linkages play a significant role in the hydrolytic process. Reverse reactions involving synthesis of saccharides and glycosides from D-glucose occur with a very high glucoamylase concentration, prolonged incubation periods and high concentration of substrates. Moreover, these are extensively used in the production of different antibiotics and amino acids in brewing, textile, food, paper and pharmaceutical industries (Mamo and Gessesse 1999; Marlida *et al.* 2000; Sanjay and Sugunan 2005). Thermostability and near neutral pH activity are some of the properties which can largely benefit the starch industry and therefore have been the areas of great interest in glucoamylase research (Ford 1999; Vieille and Zeikus 2001). *Rhizopus oryzae* was reported as being capable of simultaneously saccharifying and fermenting cornstarch and other cereals to L-lactic acid (Yu and Hang 1991; Suntornsuk and Hang 1994).

#### **1.2.1.2 Sources of glucoamylases**

A diverse group of microorganisms including bacteria, yeast and moulds are known to produce glucoamylases (Bhatti *et al.* 2007a). Filamentous fungi are better suited for commercial purposes because of their ability to secrete larger quantities of extracellular proteins (Kumar and Satyanarayana 2007a). Thermophilic fungi (*Thermomucor indicae-seudaticae*, *Scytalidium thennophilum*) have emerged as potential sources of thermostable glucoamylases (Kaur and Satyanarayana 2004; Cereia *et al.* 2006; Kumar and Satyanarayana 2005; 2007b). Microbial stains of *Aspergillus* and *Rhizopus* sp. are mainly used for the commercial production of glucoamylase (Pandey 1995; Panday *et al.* 2000). Filamentous fungi such as *Aspergillus niger* have a high

capacity secretory system and therefore widely used for the industrial production of native and heterologous protein (Guillemette *et al.* 2007), which exists in two forms, GA1 and GA2 having molecular weights of 96 and 74 kDa respectively (Mislovicova 2006). Amylolytic yeasts like *Arxula adenivorans*, *Lipomyces*, *Saccharomycopsis*, *Schwanniomyces*, *Candida japonica* and *Filobasidium capsuligenum* possess the potential to convert starchy biomass to single-cell proteins and the enzymes produced are also well characterized (Chi *et al.* 2001; Gupta *et al.* 2003).

Fungal glucoamylases are usually glycoproteins. *A. niger* produces an extracellular glucoamylase existing in two forms (Pazur *et al.* 1971), known to be glucoamylase I (99 kDa) and glucoamylase II (112 kDa). These forms differ in their carbohydrate content, as well as pH and temperature stabilities and optima for activity (Ramasesh *et al.* 1982). Gucoamylase from *Aspergillus terreus* strains were also examined to make it suitable for production of D-glucose and corn syrups (Ghosh *et al.* 1990; Ali and Hossain 1991). There were several reports on purification and characterization of glucoamylase from *A. niger* strains (Williamson *et al.* 1992; Stoffer *et al.* 1993). A fungal glucoamylase was produced from *Saccharomyces cerevisiae* through the expression of heterologous genes in the yeast and the expression is influenced by many factors such as strength of the promoter, mRNA stability and translation efficiency (Ekino *et al.* 2002).

*Rhizopus* sp. produced a glucoamylase capable of releasing glucose from starch with 100% efficiency (Yu and Hang 1991). Three forms of glucoamylase were isolated (Takahashi *et al.* 1985) from *Rhizopus* sp., GA-I (74 kDa), GA-II (58.6 kDa) and GA-III (61.4 kDa). Glucoamylases from other mold strains are *Humicola lanuginosa* (Taylor *et al.* 1978; Riaz *et al.* 2007), *Thermomyces lanuginosa* (Haasum *et al.* 1991; Thorsen *et al.* 2006), *Myrothecium* sp. M1 (Malek and Hossain 1994), *Acremonium* sp. (Marlida *et al.*

2000), brown-rot basidiomycete *Fomitopsis palustris* (Yoon *et al.* 2006) and from marine yeast *Aureobasidium pullulans* N13d (Li and Chi 2007). A phyto pathogenic fungus *Colletotrichum gloeosporioides* also produces a glucoamylase (Krause *et al.* 1991).

The enzymes produced by *Saccharomycopsis fibuligera* comprise a significant group of yeast glucoamylase. They are about 60-64 kDa large extracellular glycoprotein enzymes (Hostinova *et al.* 1991). There are several well reviewed reports on the production of yeast glucoamylases (Saha and Zeikus 1989; Pretorius *et al.* 1991). Glucoamylase has been identified in *Saccharomyces cerevisiae* (Pugh *et al.* 1989), *Saccharomyces cerevisiae* var. *diastolicus* (Kleinman *et al.* 1988; Pretorius *et al.* 1991), *S. fibuligera* (Itoh *et al.* 1989), *Schwanniomyces castelli* (Sills *et al.* 1984), *Schwanniomyces occidentalis* (Gellissen *et al.* 1991), *Pichia burlonii* and *Talaromyces* sp. Glucoamylase from a diastatic strain of *S. cerevisiae* was purified chromatographically and characterized (Kleinman *et al.* 1988).

Bacterial glucoamylase from gram positive bacteria DSM 5853 (Candussio *et al.* 1990), *Clostridium acetobutylicum* ATCC 824 (Nolling *et al.* 2001), *Clostridium thermosaccharolyticum* (Ganghofner *et al.* 1998) have also been reported. *Lactobacillus amylovorus* ATCC 33621 is an active amyolytic bacterial strain producing a cell-bound glucoamylase (EC 3.2.1.3, James and Lee 1995; James *et al.* 1997). Bacterial glucoamylases have also been identified from aerobic strains such as *Bacillus stearothermophilus* (Srivastava 1984), *Flavobacterium* sp. (Bender 1981), *Halobacterium sodamense* (Chaga *et al.* 1993) and *Arthrobacter globiformis* I42 (Okada and Unno 1989). Anaerobic strains include *Clostridium thermohydrosulfuricum* (Hyun and Zeikus 1985), *Clostridium* sp. G0005 (Ohinishi *et al.* 1991), *Clostridium acetobutylicum* (Chojacki and Blaschek, 1986; Soni *et al.* 1992), *Clostridium*

*thermosaccharolyticum* (Specka *et al.* 1991) and the microaerophile, *Lactobacillus amylovorus* (James and Lee 1995).

### 1.2.1.3 Structural features of glucoamylase

Glucoamylase family consists of a starch binding domains attached to each other by means of an *O*-glycosylation linker (Saver *et al.* 2000; Coutinho and Reilly 1997; Horvathova *et al.* 2001). Structures of a family of 21 carbohydrate binding modules from starch binding domain of *Rhizopus oryzae* glucoamylase determined by NMR spectroscopy explains ligand binding sites and structural features of this glucoamylases (Liu *et al.* 2007). The enzyme contains a very specific carbohydrate region consisting of 30 chains in the form of di- or trisaccharides (Wang *et al.* 1996). Also, it contains three domains (Svennson *et al.* 1983): N-terminal catalytic domain (residues 1 to 470, 55 kDa), a short bulky linker (residues 471 to 508, 13 kDa) which is heavily *O*-glycosylated at the abundant serine and threonine residues and C-terminal granular starch binding domain (residues 509 to 616, 12 kDa). The bulky linker joins the two main domains giving the enzyme an overall dumb-bell shape (Kvamer *et al.* 1993). Starch binding domain glucoamylase I from *A. niger* shows a well defined  $\beta$ -sheet structure consisting of one parallel and six antiparallel pairs of  $\beta$ -strands which forms an open sided  $\beta$ -barrel (Sorimachi *et al.* 1996). Three forms of glucoamylase were isolated from *Rhizopus* sp., Glu1, Glu2 and Glu3. Various forms of glucoamylases are thought to be the result of several mechanisms: mRNA modifications, limited proteolysis, variation in carbohydrate content or the presence of several structural genes (Pretorius *et al.* 1991; Takahashi *et al.* 1985; Vihinen and Mantsala 1989).

The catalytic domain of glucoamylase from *A. niger* was purified and characterized from glucoamylases G1 and G2 using subtilisin for crystallization studies (Stoffer *et al.* 1993). Functionally important carboxyl groups in glucoamylase from *A.*

*niger* and *A. awamori* were identified using a differential labeling approach and it was concluded that both the sp. have three groups Asp176, Glu179 and Glu180 in the catalytical active site (Svensson *et al.* 1990; Sierks *et al.* 1990).

A subsite theory for analyzing the substrate affinities of glucoamylases was also developed (Hiromi 1970; Hiromi *et al.* 1973). The structure of different glucoamylases showed a common subsite arrangement, seven in total and the catalytic site was located between subsites 1 and 2 (Ohinishi 1990; Fagerstrom 1991; Ermer *et al.* 1993). Subsite 2 has the highest affinity for oligomeric substrates and glucose, followed by decreasing affinity towards subsites 3 to 7 (Fagerstrom 1991). Complexes of glucoamylase from *A. awamori* with acarbose and D-gluco-dihydroacarbose indicate hydrogen bonds between carbohydrate OH groups and Arg54, Asp55, Leu177, Try178, Glu180 and Arg305 involved in binding at subsites 1, 2 and an array of outer subsites leading into these inner ones (Aleshin *et al.* 1994; Stoffer *et al.* 1995). The geometry of the general acid and base catalysis of Glu179 (Sierks *et al.* 1990; Aleshin *et al.* 1992) and Glu400, is excellent for the glucoside bond cleavage and assistance in the nucleophilic attack of water at the anomeric center of the carbohydrate (Harris *et al.* 1993; Frandsen *et al.* 1994). Based on chemical modification studies on *A. niger* glucoamylase, tryptophan (Trp120) residues have been proposed to be essential for enzymatic activity (Rao *et al.* 1981; Clarks and Svensson 1984). The active site of *A. niger* glucoamylase is very much identical to that of the *Rhizopus oryzae* (Stoffer *et al.* 1995). In the active site of *R. oryzae*, the amino acid residues Arg191, Asp192, Leu312, Trp313, glu314, Glu315 and Arg443 are responsible for substrate binding through hydrogen bonds where as Glu314 and Glu544 are for glucosidic bond cleavage (Ashikari *et al.* 1986; Sierks *et al.* 1990; Aleshin *et al.* 1992).

The glucoamylase from thermophilic fungus *T. lanuginosus* has a molecular weight of 66 kDa and the protein sequence comprises 617 amino acid residues showing

60% identity with that of *Talaromyces emersonii*. Also, isoelectric point, pH and temperature optimum are 3.8-4.0, 5.0 and 70°C respectively (Thorsen *et al.* 2006). Aleshin *et al.* (1992) produced a crystal structure of proteolysed form of glucoamylase I from *A. awamori* var X100 determined to a resolution of 2.2 Å, containing the complete catalytic domain plus the N-terminal half of the *O*-glycosylated domain (residue 1-471) being referred to as glucoamylase II. Amino acid sequence of three glucoamylases from *Rhizopus*, *Aspergillus* and *Saccharomyces* were compared and the sequence studies suggested that glucoamylases from *Rhizopus* and *Aspergillus* are highly homologous in the nucleotide as well as the amino acid sequence and are more closely related among the three (Tanaka *et al.* 1986). The catalytic site in glucoamylase is believed to consist of two carboxyl groups (Hiromi *et al.* 1966a; 1966b). In accordance with a commonly accepted mechanism for carbohydrases (Braun *et al.* 1977; Masumura *et al.* 1984; Post and Karplus 1986) one of these acts as a general acid protonating the glucosidic oxygen, while the other is present in the ionized carboxylate form, stabilizing the substrate intermediary oxonium ion (Rantwijk *et al.* 1999). Itoh *et al.* (1989) concluded that in *S. fibuligera* glucoamylase, Ala81, Asp89, Trp94, Arg96, Arg97 and Trp166 were required for catalytic activity, among which Ala81, Asp89 however being not essential for catalytic activity played a role in thermal stability.

### 1.2.2 $\beta$ -Glucosidase

$\beta$ -Glucosidase (EC 3.2.1.21) is also known as amygdalase,  $\beta$ -D-glucoside glucohydrolase, cellobiase and gentobiase. It exhibits wide substrate specificity and is capable of cleaving  $\beta$ -glucosidic linkages of conjugated glucosides and disaccharides (Dale *et al.* 1986). It plays a major role in the carbohydrate metabolism in many organisms by acting on  $\beta$ -glycosidic linkages containing  $\beta$ -D-1,4 glycosidic bonds. It shows hydrolytic activity towards  $\alpha$ -galactoside,  $\beta$ -D-xyloside and  $\beta$ -L-arabinoside as



well as  $\alpha$ -D-mannoside but it is inert toward  $\alpha$ -glucoside. Also,  $\beta$ -glucosidase is able to hydrolyse cellulo-oligosaccharides and cellobiose into glucose (Ortega *et al.* 2001) and glycosidic anthocyanin (Hang 1995).  $\beta$ -Glucosidase is used in the synthesis of glycoconjugates by reversing the normal hydrolytic reaction (Hirofumi *et al.* 1991; Basso *et al.* 2002; Hui-Lei *et al.* 2007). These enzymes are classified under three glycoside hydrolase (GH) families: GH 1, 3 and 9 according to the classification by Coutinho and Henrissat (1999). Both GH 1 and 3 are families with a retaining mechanism dominated by enzyme acting on oligosaccharide substrates, while family 9 exhibits an inverting mechanism, mostly that of endoglucanases (Coutinho and Henrissat 1999).

#### 1.2.2.1 Sources of $\beta$ -glucosidase

$\beta$ -Glucosidase is an exo type glycoside hydrolase that cleaves  $\beta$ -glycosidic bonds which is present in bacteria and fungi involved in the metabolism of cellulose and other carbohydrates.  $\beta$ -Glucosidase from sweet almond is the most widely used and characterized representative and is the commercially available one (Hestrin *et al.* 1955; Basso *et al.* 2002; Kouptsova *et al.* 2001; Andersson and Adlercrevtz 2001; Thanukrishnan *et al.* 2004). Recently Hui-Lei *et al.* (2007) found  $\beta$ -glucosidase from apple seed to be a novel catalyst for the synthesis of *O*-glycosides. Almond  $\beta$ -glucosidase has been widely employed for the synthesis of alkyl and phenolic glycosides (Ljunger *et al.* 1994; Crout and Vic 1998; Vic *et al.* 1995; Ducret *et al.* 2002a). Two intracellular  $\beta$ -glucosidase (BGL1A and BGL1B) belonging to glycoside hydrolase (family 1) from white-rot fungus *Phanerochaete chrysosporium* (Nijikken *et al.* 2007; Bhatia *et al.* 2002) and an extracellular  $\beta$ -glucosidase from *Daldinia eschscholzii* with a molecular weight of 64.2 kDa were purified (Karnchanatat *et al.* 2007). A number of thermostable glycosidases have been identified and characterized in recent years, which

have already been used in the synthesis of glycosides. A novel variant of *Thermotoga neapolitana*  $\beta$ -glucosidase B is an efficient catalyst for the synthesis of alkyl glycosides by trans-glycosylation (Turner *et al.* 2007). The most remarkable one among these newcomers is the  $\beta$ -glucosidase from the hyperthermophilic archeon *Pyrococcus furiosus* (Kengen *et al.* 1993; Hansson 2001). The organism is relatively easy to grow and its  $\beta$ -glucosidase is stable for an unprecedented 85 h at 100°C. The enzyme has been cloned and over-expressed in *Escheria Coli* (Voorhorst *et al.* 1995).

Fungal sources of  $\beta$ -glucosidase from *Humicola grisea*, *Hypocrea jecorina* (Takashima *et al.* 1999) and *Streptomyces* sp. QM-B814 (Vallimitjana *et al.* 2001) belong to family 1 class of  $\beta$ -glucosidase. A few thermostable sources of  $\beta$ -glucosidase were also identified as *Talaromyces emersonii* (Collins *et al.* 2007) and *Thermoascus aurantiacus* (Hong 2007). The edible straw mushroom, *Volvariella volvacea* mycelial extract contains a  $\beta$ -glucosidase with a molecular weight of 95 kDa (Ding 2007). *Aspergillus*  $\beta$ -glucosidase is active at low pH values and effectively hydrolyzes a wide range of substrates including glucosides of geraniol and linalool (Shoseyov *et al.* 1990; Wei *et al.* 2007). Also, bacterial sources of  $\beta$ -glucosidase from *Bacillus circulans* (Hakulinen *et al.* 2000), *Bacillus polymyxa* (Sanz-Aparicio *et al.* 1998) and *Sulfolobus solfataricus* (Aguilar *et al.* 1997) have also been reported.

#### 1.2.2.2 Structural features of $\beta$ -glucosidase

All  $\beta$ -glycosidases from family 1 share the same tertiary  $\alpha$  ( $\beta/\alpha$ )<sub>8</sub> barrel structure (Coutinho and Henrissat 1999). The active site of  $\beta$ -glycosidase is located in the C-terminal portion of the  $\beta$ -barrel and is surrounded by loops connecting the  $\alpha$ -helix to the  $\beta$ -strands (Marana 2006).  $\beta$ -Glucosidase from *Streptomyces* sp., a family 1 glycosyl hydrolase, has a broad substrate specificity and a non-nucleophilic mutant E383A has

proven to be an efficient glycosynthase enzyme (Faijes *et al.* 2006). On the basis of sequence alignment, site-directed mutagenesis and chemical free experiments, it was concluded that Glu383 is the catalytic nucleophile of the  $\beta$ -glucosidase from *Streptomyces* sp. (Vallmitjana *et al.* 2001). The overall structure of family 1 glucosyl hydrolases is uniform, especially the regions around the catalytic site residues Glu166 (acid/base), nucleophilic Glu355 strictly conserved along with Arg77, His121, Asn165, Asn294, Tyr296 and Trp402. The presence of Cys169 located in the close vicinity of the acid/base catalyst Glu166 constitutes the strongly responsible pKa for the active pH range (Hakulinen *et al.* 2000). The carboxylate group of Glu352 is pointing to the anomeric carbohydrate C1 atom in a position consistent with its role in the nucleophilic attack (Sanz-Aparicio *et al.* 1998). Tyr296 is also important for catalysis as it is hydrogen bonded to Glu352 in the native enzyme contributing to stabilization of the oxocarbenium species (Wang *et al.* 1995). Replacement of the other residues by 'Pro' at suitable positions can enhance the protein thermostability and can thermodynamically stabilize the  $\alpha$ -helix (Yun *et al.* 1991). High content of 'Pro' residues rendered restricted flexibility of loops and increased number of ion pairs. A high percentage of 'Arg' occurrence resulted in reduction in thermolabile residues (Wang *et al.* 2003). Thermodynamically favorable interactions with the relatively rigid active site of  $\beta$ -1,4 glycosidase is necessary to bind, distort and subsequently hydrolyse glycoside substrates (Poon *et al.* 2007).

On the basis of the sequence of the peptide derived from a trapped glycosyl-enzyme intermediate, the sweet almond  $\beta$ -glucosidase has been assigned to glycosidase family 1, with its active site nucleophile contained within the sequence Ile-Thr-Glu-Asn-Gly (He and Withers 1997). It is known to hydrolyze glycosides resulting in the net retention of anomeric configuration (Eveleigh and Perlin 1969; Czjzek *et al.* 2000). It

follows the standard mechanism of such retaining glycosidases, in which the substrate binds to an active site containing a pair of carboxylic acids (McCarter and Withers 1994; Sinnott 1990).

The primary structures of maize and sorghum  $\beta$ -glucosidases possess highly conserved peptide motifs TENEP and ITENG, which contains the two glutamic acids (Glu191 and Glu406) involved as the general acid/base catalyst and the nucleophile, respectively in all family of 1  $\beta$ -glucosidases (San-Aparicio *et al.* 1998; Czjzek *et al.* 2000). In the glycosylation step, the nucleophile Glu406 attacks the anomeric carbon C-1 of the substrate and forms a covalent glycosyl-enzyme intermediate with concomitant release of the aglycon after protonation of the glucosidic oxygen by the acid catalyst Glu191 (Withers *et al.* 1990). In the next step (deglycosylation), Glu191 acts as a base with a water molecule performing as the nucleophile attacks the covalent glycosyl-enzyme, releasing the glucose and regenerating the nucleophilic Glu406. In maize  $\beta$ -glucosidase isozyme Glu1, these two catalytic glutamic acids are positioned within the active site at expected distances ( $\sim 5.5$  Å) for this mechanism (Czjzek *et al.* 2001). Verdoucq *et al.* (2003) studied the structural data from cocrystals of enzyme substrate and enzyme aglycon complexes of maize  $\beta$ -glucosidase isozyme Glu1 (ZmGlu1) and has shown that five amino acid residues - Phe198, Phe205, Try378, Phe466 and Ala467, are located in the aglycon-binding site of ZmGlu1.

$\beta$ -Glucosidase (CelB) from the hyperthermophilic archaean *Pyrococcus furiosus*, a family 1 glycosyl hydrolase, shows a homo-tetramer configuration, with subunits having a typical  $(\beta\alpha)_8$ -barrel fold. The 3D model of the *Pyrococcus furiosus*  $\beta$ -glucosidase was compared with the previously determined 6-phospho- $\beta$ -glycosidase (LacG) from the mesophyllic bacterium *Lactococcus lactis* (Kaper *et al.* 2000). The positions of the active site residues in LacG and CelB are very well conserved and the conserved residues

involved in substrate binding are Asn17, Arg77, His150, Asn206, Tyr307 and Trp410 (Wiesmann *et al.* 1997). Glu207 and Glu372 in CelB are the equivalents of the catalytic glutamate residues in LacG. The average distance between the oxygen atoms of these glutamate carboxylic acids is 4.3 Å ( $\pm 1$  Å) in CelB, which is in the range of the general observed distance in retaining glycosyl hydrolases,  $\sim 5$  Å (McCarter and Withers 1994).

Guinea pig liver Cytosolic  $\beta$ -glucosidase (CBG) follows a two-step catalytic mechanism with the formation of a covalent enzyme- carbohydrate intermediate and that CBG transfers carbohydrate residues to primary hydroxyl and equatorial but not axial C-4 hydroxyl of aldopyranosyl carbohydrates (Hays *et al.* 1998). Also results have shown that the specificity of CBG for transglycosylation reactions is different from its specificity for hydrolytic reactions (Hays *et al.* 1998). From the inhibitor stoichiometry and reactivation studies, it was shown that the catalytic mechanism of CBG involves a covalent enzyme- carbohydrate intermediate. From its aminoacid sequence, CBG is predicted to have a single active site nucleophile, specifically the glutamate residue in the sequence TITENG (Hays *et al.* 1996).

### 1.3 Glycosylation

Glycosylation is the process or result of addition of carbohydrate molecules to proteins, aglycons and lipids. It is an enzyme directed site specific process as opposed to the non-enzymatic chemical glycation. Enzyme catalysed synthesis of glycosides can be achieved (Kadi and Crouzet 2008) through reverse hydrolysis (thermodynamically controlled) or transglycosylation (kinetically controlled). Because of multiple hydroxyl groups of similar reactivity, controlled glycosylation remains a challenge to organic chemists. Well elaborated and still widely employed classical chemical approaches inevitably require quite a number of protection, activation, coupling and deprotection steps (Akita *et al.* 1999; Konstantinovic *et al.* 2001). In contrast, glycosidases and

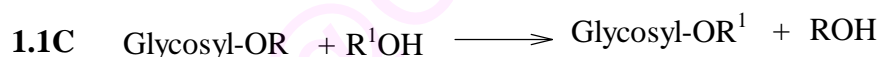
transglycosidases offer one step synthesis under mild conditions in a regio and stereoselective manner (Vic and Thomas 1992; Vijayakumar and Divakar 2007; Vijayakumar *et al.* 2007). Enzyme-catalyzed glycosylation involves a glycosidase or a glycosyl transferase catalyzed glycoside bond formation. A carbohydrate nucleotide donor and acceptor are incubated with the appropriate glycosidase or glycosyl transferase that catalyzes the efficient and selective transfer of the glycosyl residue to the acceptor. A great number of reports using glycosyltransferases are now available but these enzymes are often difficult to obtain (Auge *et al.* 1990). In contrast, the glycosidase approach uses simpler glycosyl donors, which can be a free monosaccharide itself. This method has the advantage of using relatively simple glycosyl donors and readily available commercial enzymes. Its main disadvantage is that regioselectivity may not be observed in all the cases (Trincone *et al.* 2003).

Glycosidases catalyze the reaction by hydrolysis, reverse hydrolysis and transglycosylation (Scheme 1.1) depending upon the media employed. In aqueous media, when there is large excess of water, hydrolysis of glycoside or oligosaccharide or polysaccharide is the dominant reaction (Scheme 1.1A). In case of reverse hydrolysis and transglycosylation reactions, synthesis of glycosides using glycosidases or transglycosidases depends on the nature of the glycosyl donor and the nature of the medium.

The reverse hydrolytic approach is an equilibrium controlled synthesis where the equilibrium is shifted towards synthesis (Panintrarux *et al.* 1995; Vic *et al.* 1997; Rantwijk *et al.* 1999; Biely 2003) involving a carbohydrate and an alcohol (Scheme 1.1B). This can be achieved by reducing the water activity and by increasing the substrate concentrations so that the substrate itself acts as a solvent media (Vic and Crout 1995). This method is widely employed for the enzymatic synthesis of alkyl glycosides and phenolic glycosides

is an organic solvent or co-solvent (Vic and Crout 1995; Vic *et al.* 1997; Ducret *et al.* 2002b; Vijayakumar and Divakar 2005).

The transglycosylation method is a kinetically controlled synthesis where the enzyme catalyzes the transfer of a glycosyl residue from a glycosyl donor to the glycosyl acceptor (Scheme 1.1C). The reaction yield depends on the rate of product synthesis relative to the rate of hydrolysis. An efficient acceptor used in a high concentration should favor the synthesis (Ismail *et al.* 1999a; Rantwijk *et al.* 1999; Eneyskaya *et al.* 2003; Jiang *et al.* 2004; Tsuruhami *et al.* 2005).



(Glycosyl = Carbohydrate moiety, ROH and R<sup>1</sup>OH = alcohol)

**Scheme 1.1** Reactions catalyze by glycosidases

### 1.3.1 Glycosylation mechanism

During glycosidase catalysis, there are two possible stereochemical outcomes for the hydrolysis of a glycosidic bond - inversion and retention of anomeric configuration. Both the mechanisms involve oxocarbenium ion through transition states and a pair of carboxylic acids at the active site. In inverting glycosidase, the reaction occurs via single displacement mechanism wherein one carboxylic group acts as a general base and the other as a general acid. In the retaining enzyme, the reaction proceeds via double displacement mechanism (McCarter and Withers 1994; Wang *et al.* 1994). Site-directed mutagenesis continues to play a significant role in understanding mechanisms and an important role in the generation of enzymes with new specificities and possibly even new mechanisms (Fajjes and Planas 2007).

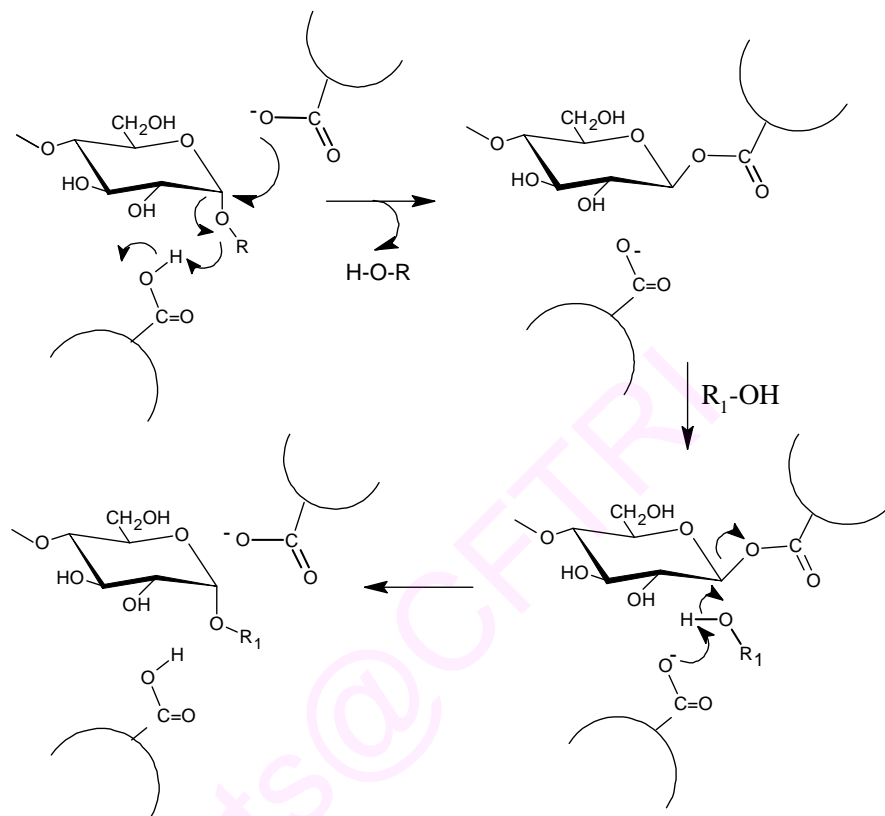
In general, every hydrolysis of a glycosidic linkage by glycosidase is a reaction in which the product retains ( $\alpha \rightarrow \alpha$  or  $\beta \rightarrow \beta$ ) or inverts ( $\alpha \rightarrow \beta$  or  $\beta \rightarrow \alpha$ ) the anomeric configuration of the substrate (Chiba 1997). In the normal hydrolytic reaction, the leaving group is a carbohydrate molecule and the nucleophile (glycosyl acceptor) is water (Scheme 1.1A). However, an alcohol or a monosaccharide can also act as glycosyl acceptor (glycosylation). In reverse hydrolysis, the condensation of a monosaccharide and alcohol with water as the leaving group (Scheme 1.1B, Rantwijk *et al.* 1999). A recent review by Zechel and Withers (2001) focuses on the recent developments in the understanding of nucleophilic and general acid-base catalysis in glycosidase-catalyzed reactions. Even the mechanism of well-studied glycosidases and the functional significance of their interactions with the substrates is not fully understood (Vasella *et al.* 2002). Two significant models, such as nucleophilic displacement mechanism (Scheme 1.2A) and an oxo-carbenium ion intermediate mechanism (Scheme 1.2B) were suggested for the hydrolytic reaction where glycosyl acceptor is water (Chiba 1997). Oxocarbenium ions are postulated to be the common intermediates in most of the glycosylation procedures (Morales-Serna *et al.* 2007).

### 1.3.1.1 Nucleophilic double displacement mechanism

The double displacement mechanism was found to be applicable to the enzymes, which retain the anomeric configuration of the substrate (Scheme 1.2A). The two catalytic ionisable groups, a carboxyl  $-\text{COOH}$  and a carboxylate,  $-\text{COO}^-$ , cleave the glycosidic linkage cooperatively by direct electrophilic and nucleophilic attacks against the glycosyl oxygen and anomeric carbon atoms respectively, resulting in a covalent glucosyl-enzyme complex through a single displacement. Subsequently glucosyl-acetal bond is attacked with the hydroxyl group of the water (alcohol hydroxyl group in glycosylation) by retaining the anomeric configuration of the product by the double



displacement. The double displacement mechanism is adequate for explaining the reaction, where the anomeric configuration of the substrates is retained (Chiba 1997).

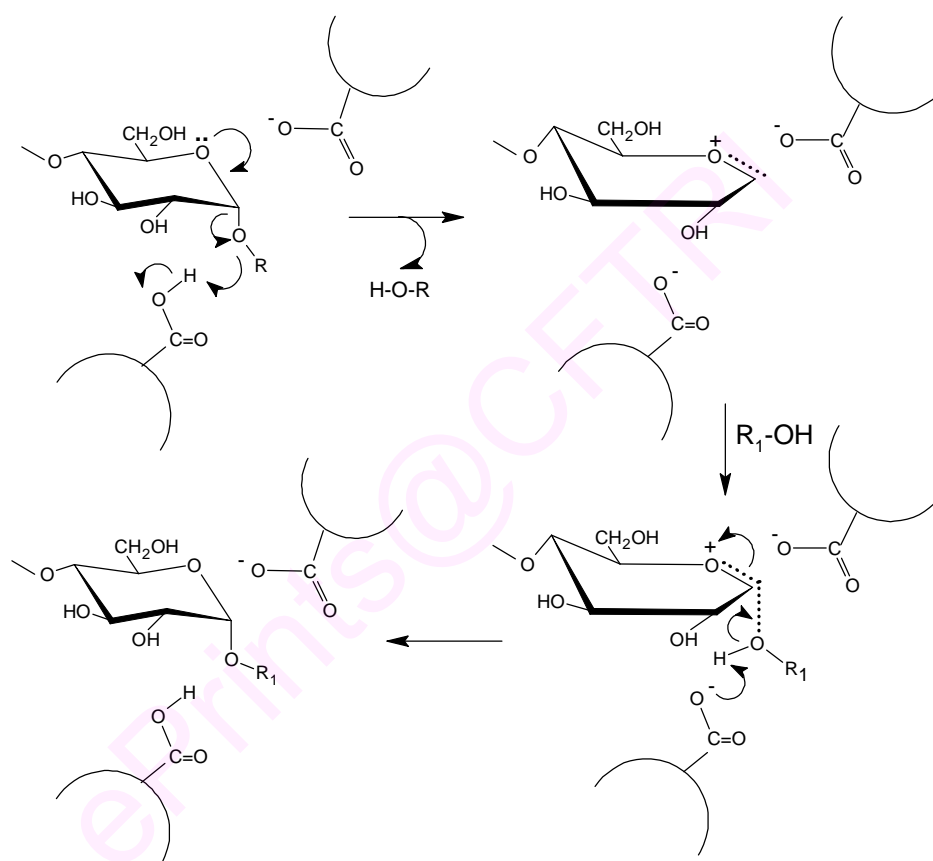


**Scheme 1.2A** Nucleophilic double displacement mechanism

### 1.3.1.2 Oxocarbenium ion intermediate mechanism

In the oxo-carbenium intermediate mechanism, the two catalytic groups of the carboxyl and carboxylate ion participate cooperatively in the departure of the leaving group by a proton transfer to the anomeric oxygen atom (Scheme 1.2B). An enzyme bound oxonium ion intermediate has been detected by NMR (Withers and Street 1988). The second carboxylate, which is deprotonated in the resting state, stabilizes the oxonium ion intermediate. In the next step, a nucleophile adds to the same face of the glycosyl-enzyme intermediate from which the leaving group was expelled, resulting in the net retention of the anomeric configuration at the anomeric center. The addition of the nucleophile is assisted by the first carboxylate which in this step reverts to carboxylic

acid. The oxo-carbenium intermediate mechanism has been applied to interpret the catalytic mechanism of many carbohydrate degrading enzymes. This mechanism is applicable to both 'retaining' and 'inverting enzymes'. Mutagenesis and X-ray structural studies have confirmed that the mechanism of retaining glycosidases is similar (Sinnot 1990; Jacobson *et al.* 1994; Jacobson *et al.* 1995).



**Scheme 1.2B:** Oxocarbenium ion intermediate mechanism

### 1.3.2 Advantages of enzymatic glycosylation over chemical methods

There are many advantages of using glycosidases (Takayama *et al.* 1997)

1. High regio and stereoselectivity.
2. Mild reaction conditions and biocompatibility
3. To replace wasteful or expensive chemical procedure with more efficient semi-natural processes.

4. Improved product-yield and better product quality
5. Use of non-polar solvents which imparts stability to glycosidases, renders insolubility of the enzyme, solubility of alcohols and products in organic solvents and easy product workout procedures
6. No protection, activation and deprotection required
7. Less environmental pollution

## 1.4 GLYCOSIDES

Glycosides are asymmetric mixed acetals formed by reaction of the anomeric carbon atom of intermolecular hemiacetal or pyranose or furanose form of the aldohexose or aldopentose or ketohexose with a hydroxyl group furnished by an alcohol. Glycosides are widely distributed in nature and can be found in nearly every living organism (Roode *et al.* 2003).

### 1.4.1 Properties of glycosides (Stanek *et al.* 1963)

1. Glycosides are readily soluble in water and crystallize easily.
2. Their aqueous solutions, if not attacked by microorganisms, are stable, do not exhibit mutarotation and are non-reducing.
3. The circumstance that water insoluble substances are rendered soluble by their linkage to carbohydrate is of great importance for the detoxification of many phenolic compounds which has application in industries and pharmaceuticals.
4. In contrast to free carbohydrate, the glycosides are not sweet (apart from a few exceptions such as methyl  $\alpha$ -D-glucopyranoside). They taste more or less bitter.
5. Glycosides are split by acids even at low concentrations. The rate of hydrolysis depends on the anomeric configuration, nature of aglycon, type of carbohydrate and cyclic arrangement.

6. Unsubstituted glycosides are less sensitive to oxidative agents than free carbohydrate.
7. The glycosides are also cleaved by the action of enzymes, which are generally termed glycosidases. The reaction is a reversible one and under suitable conditions they may also be used for the synthesis of glycosides from free carbohydrate components and aglycons.

#### **1.4.2 Uses of glycosides**

Glycosides exhibit a wide variety of applications (Table 1.1). Carbohydrate connected to long alkyl chains as aglycons yield glycosides with good surfactant and emulsifying properties and therefore used in detergents (Katsumi *et al.* 2004; Larsson *et al.* 2005) and cosmetics (Luther *et al.* 1999). Glycosides with terpenes are claimed to possess antifungal and antimicrobial activities (Zhou 2000). Glycosides of flavour and fragrances are used in perfumery (Watanabe *et al.* 1993; Odoux *et al.* 2003). In plants, glycosides are believed to play an important role in accumulation, storage and transport of hydrophobic substances. Cyanogenic glycosides play a role in plant defense mechanism. Table 1.1 lists some of the important alkyl, phenolic, flavonoid, terpinyl, sweetner and medicinal glycosides and Table 1.2 lists some important vitamin glycosides.

**Table 1.1** Glycosides prepared through enzymatic glycosylation

<b>Name of the compound</b>	<b>Source of enzyme</b>	<b>Applications</b>	<b>References</b>
A. Surfactant glycosides			
<b>Alkyl-<math>\beta</math>-D-glucopyranoside</b>	$\beta$ -Glucosidase	Non ionic surfactant	Turner <i>et al.</i> 2007, Smaali <i>et al.</i> 2007
<b>Hexyl-<math>\beta</math>-xyloside, hexyl-<math>\beta</math>-xylobioside, hexyl-<math>\beta</math>-xylotrioside</b>	Xylosidase/xylanase	Surfactant	Tramice <i>et al.</i> 2007
$\beta$ -D-Glycopyranosides of n-heptanol, n-octanol, 2-phenyl hexanol, 3-phenyl propanol, 4-phenyl butanol, 5-phenyl petanol, 6-phenyl hexanol, 2-pyridine methanol, isobutanol, isopentanol, p-methoxy cinamyl alcohol, isopropanol, cyclohexanol, 1-phenyl ethanol, 1,5-pentanediol, 1,6-hexanediol, 1,7-heptanediol, 1,8-octanediol, 1,9-nonanediol, salicyl alcohol and 4-nitrophenol.	Almond $\beta$ -glucosidase	As non ionic surfactants in detergents and cosmetics	Katusumi <i>et al.</i> 2004
$\beta$ -D-Glucopyranosides of propanol, hexanol and octanol.	Raw almond meal	In detergents and cosmetics	Chahid <i>et al.</i> 1992
$\alpha/\beta$ -Glucopyranosides of ethanol, 1-propanol, 2-propanol, 2-methyl 2-propanol,	Glucoamylase and $\beta$ -glucosidase	In detergents and cosmetics	Laroute and Willemot 1992a

---

1-butanol, 2-butanol, 1-pentanol, 1-hexanol, 1,3-butanediol, 1,4-butanediol, 2,3-butanediol, 1,2-pentanediol, 1,5-pentanediol	Almond $\beta$ -glucosidase	Used in the synthesis of glycopolymers, as temporary anomeric protected derivatives in carbohydrate chemistry	Vic and Crout 1995
Allyl and benzyl $\beta$ -D-glucopyranoside, allyl- $\beta$ -D-galactopyranoside.			
n-Octyl glucoside, n-octyl galactoside	$\beta$ -Galactosidase from <i>A. oryzae</i> , almond meal	In detergents and cosmetics	Chahid <i>et al.</i> 1994
n-Octyl- $\beta$ -D-glucoside, 2-hydroxy benzyl glucopyranoside.	Almond $\beta$ -glucosidase	In detergents and cosmetics	Vic <i>et al.</i> 1997
n-Octyl- $\beta$ -D-glucoside, n-octyl- $\beta$ -D-xylobioside, n-octyl- $\beta$ -D-xyloside	Xylanase from <i>Aureobasidium pullulans</i>	As biological detergents and emulsifying agents in cosmetics	Nakamura <i>et al.</i> 2000
Hexyl- $\beta$ -D-glucoside, heptyl- $\beta$ -D-glucoside, octyl- $\beta$ -D-glucoside, octyl- $\beta$ -D-galactoside, hexyl- $\beta$ -D-galactoside, hexyl- $\beta$ -D-fucoside, octyl- $\beta$ -D-fucoside, heptyl- $\beta$ -D-galactoside, heptyl- $\beta$ -D-fucoside,	Almond $\beta$ -glucosidase	Non-ionic surfactant in cosmetics, pharmaceuticals, kitchen detergents	Kobayashi <i>et al.</i> 2000

---

Methyl glucoside	$\alpha$ -amylase	Biodegradable surfactant	Larsson <i>et al.</i> 2005
n-Octyl-D-glucoside, n-octyl-D-maltoside, n-octyl-D-sucroside	Amyloglucosidase	Biodegradable surfactant	Vijayakumar <i>et al.</i> 2007
<b>B. Phenolic glycosides</b>			
Eugenol-5-O- $\beta$ -(6'-galloyl)glucopyranoside)	<i>Melaleuca ericifolia</i>	Antibacterial	Hussein <i>et al.</i> 2007
Eugenol- $\alpha$ -glucoside	$\alpha$ -Glucosyltransfer enzyme of <i>Xanthomonas campestris</i> WU-9701	As a prodrug of a hair restorer, as a derivative of spices	Sato <i>et al.</i> 2003
Eugenol- $\beta$ -glucoside	Biotransformation by cultured cells of <i>Eucalyptus perriniana</i>	As a prodrug of a hair restorer	Orihara <i>et al.</i> 1992
Eugenyl- $\alpha$ -D-glucoside, eugenyl- $\alpha$ -D-mannoside, eugenyl-maltoside, eugenyl-sucrose, eugenyl-mannitol	Amyloglucosidase, almond $\beta$ -glucosidase	Antioxidant	Vijayakumar and Divakar 2007
Vanillin- $\beta$ -D-monoglucopyranoside	Cell suspension culture of <i>Coffea arabica</i>	As a food additive flavor	Kometani <i>et al.</i> 1993b, Odoux <i>et al.</i> 2003
Capsaicin- $\beta$ -D-glucopyranoside	Cells suspension culture of <i>Coffea arabica</i> Cultured cells of <i>Phytolacca americana</i>	Food ingredient and pharmacological applications	Kometani <i>et al.</i> 1993a Hamada <i>et al.</i> 2003

Capsaicin-4- <i>O</i> -(6- <i>O</i> - $\beta$ -D-xylopyranosyl)- $\beta$ -D-glucopyranoside, capsaicin-4- <i>O</i> -(6- <i>O</i> - $\alpha$ -L-arabinopyranosyl)- $\beta$ -D-glucopyranoside, 8-nordihydrocapsaicin-4- <i>O</i> -(6- <i>O</i> - $\beta$ -D-xylopyranosyl)- $\beta$ -D-glucopyranoside, 8-nordihydrocapsaicin-4- <i>O</i> -(6- <i>O</i> - $\alpha$ -L-arabinopyranosyl)- $\beta$ -D-glucopyranoside,	Cultured cells of <i>Catharanthus roseus</i>	Food, spices and medicines		Shimoda <i>et al.</i> 2007
$\alpha$ -Salicin, $\alpha$ -isosalicin, $\beta$ -salicin	<i>Bacillus macerans</i> cyclodextrin glucanyl transferase and <i>Leuconostoc mesenteroides</i> B-742CB dextranase	Anti-inflammatory, analgesic and antipyretic prodrug		Yoon <i>et al.</i> 2004
Curcumin glucosides, Curcumin-4'-4''- <i>O</i> - $\beta$ -D-digentiobioside	Cell suspension cultures of <i>Catharanthus roseus</i>	Food colorant, anticancer	antioxidant,	Kaminaga <i>et al.</i> 2003
Curcuminyl-bis- $\alpha$ -D-glucoside, curcuminyl-bis- $\alpha$ -D-mannoside, curcuminyl-bis-maltoside, curcuminyl-bis-sucrose, curcuminyl-bis-mannitol	Amyloglucosidase	Food colorant, antioxidant		Vijayakumar and Divakar 2007
Echinacoside, acetoside, 2'-acetyl acetoside, cistanoside A, cistanoside B	Plant cell culture of <i>Cistanche deserticola</i>	Antinociception, anti-inflammatory, sedation		Ouyang <i>et al.</i> 2005



Elymoclavine- <i>O</i> - $\beta$ -D-fructofuranoside	Saprophytic culture of <i>Claviceps</i> sp.	In the treatment orthostatic circulary disturbances, hyperprolactinemia, antibacterial and cytostatic effects and hypolipemic activty	Ken and Cvak 1999
2-Hydroxybenzyl- $\beta$ -D-galactopyranoside, 3-hydroxy benzyl- $\beta$ -D-galactopyranoside, 4-hydroxybenzyl- $\beta$ -D-galactopyranoside, 3-aminobenzyl- $\beta$ -D-galactopyranoside, 3-(hydroxymethyl)-aminobenzyl- $\beta$ -D-galactopyranoside, [3-(2-methoxy)-2-hydroxy propanol]- $\beta$ -D-galactopyranoside, [3-(4-chloro phenoxy)-2-hydroxypropanol]- $\beta$ -D-galacto pyranoside, 3-methoxybenzyl- $\beta$ -D-galacto pyranoside, 1-phenylethyl- $\beta$ -D-galactopyranoside,	$\beta$ -galactosidase from <i>Kluyveromyces lactis</i>	Therapeutic agent	Bridiau <i>et al.</i> 2006
<b>C. Flavonoid glycosides</b>	<i>Trifolium repens</i> L	UV-B radiation protection	Hofman <i>et al.</i> 2000
Quercetin-3- <i>O</i> - $\beta$ -D-xylopyranosyl (1 $\rightarrow$ 2)- $\beta$ D-galactopyranoside, kaempferol-3- <i>O</i> - $\beta$ -D-xylopyranosyl (1 $\rightarrow$ 2)- $\beta$ -D-galactopyranoside			

Quercetin-3- <i>O</i> - $\alpha$ -D-glucopyranoside, quercetin - 4- <i>O</i> - $\alpha$ -D-glucopyranoside	Glucansucrase from <i>Leuconostoc mesenteroides</i>	Antioxidant	Moon <i>et al.</i> 2007
Silybin A 3- <i>O</i> - $\beta$ -D-glucopyranoside, silybin A 7- <i>O</i> - $\beta$ -D-galactopyranoside, silybin B 3- <i>O</i> - $\beta$ -D-glucopyranoside, silybin B 7- <i>O</i> - $\beta$ -D-galactopyranoside	Culture broth of <i>Trichoderma koningii</i>	Hepatoprotectant and an antidote in mushroom poisoning	Kim <i>et al.</i> 2006
Neohesperidin- $\beta$ -D-glucoside, naringin- $\beta$ -D-glucoside	Cyclodextrin glucanotransferase	Sweet in taste	Kometani <i>et al.</i> 1996
<b>D. Sweetener glycosides</b>			
Stevioside	Cell free extract of <i>Gibberella fujikuroi</i>	Natural sweetener	Oliveira <i>et al.</i> 2007; Brandle and Telmer 2007
Stevioside, steviobioside, rebaudioside A, rebaudioside B	Leaves of <i>Stevia rebaudiana</i>	As natural sweeteners, utilized in beverages	Kohda <i>et al.</i> 1976
Steviol-13- <i>O</i> -glucopyranoside, stevio-bioside, stevioside and rebaudioside	Soluble extracts of stevia	As natural food sweeteners	Shibata <i>et al.</i> 1991
<b>E. Terpinyl glycosides</b>			
Amarantholidosides IV, V, VI and VII	<i>Amaranthus retroflexus</i>	Pesticide, autotoxic effects	Fiorentino <i>et al.</i> 2006
Geraniol- $\beta$ -glucoside, nerol- $\beta$ -glucoside, citroniol- $\beta$ -glucoside	$\beta$ -Glucosidase from <i>A. niger</i> , <i>Trichoderma reesei</i> , <i>Candida molischiana</i> and almond	Good bioavailability, antifungal and antimicrobial activity	Gunata <i>et al.</i> 1994

Geraniol $\beta$ -galactoside, nerol $\beta$ -galactoside, citroniol $\beta$ -galactoside	<i>A. oryzae</i> $\beta$ -Galactosidase	Good bioavailability, antifungal and antimicrobial activity	Donho <i>et al.</i> 1996
<b>F. Glycosides in medicine</b>			
Enedyne antibiotics-calicheamycin	Cultivation broth of <i>Micromonospora echinospora</i>	Antitumor agents	Lee <i>et al.</i> 1987; Golik <i>et al.</i> 1987
Esperamycins	<i>Actinomadura verrucosospora</i>	Antitumor activity	Long <i>et al.</i> 1989
<b>G. Steroidal glycosides</b>			
$\beta$ -D-Glucopyranosyl-(1 $\rightarrow$ 2)- <i>O</i> -[ $\beta$ -D-xylopyranosyl-(1 $\rightarrow$ 3)]- <i>O</i> - $\beta$ -D-glucopyranosyl-(1 $\rightarrow$ 4)-D-galactopyranosyl (lycotetraosyl)	<i>Solanum</i> sp.	Antitumour	Ikeda <i>et al.</i> 2006
Eryloside A, eryloside K, eryloside L	Marine sponge of <i>Erylus lendenfeldi</i>	Anticancer, antifungal, anticoagulative agent	Sandler <i>et al.</i> 2005
Glycosides of diosgenin, solasodine, solasonine	<i>Solanum</i> sp.	Anticarcinogenic activity	Nakamura <i>et al.</i> 1996

**Table 1.2** Vitamin glycosides prepared through enzymatic glycosylation

Name of the compound	Source of enzyme	Applications	References
<b>A. Vitamin A glycosides</b>			
<i>t</i> -Retinoyl $\beta$ -glucuronides	Rat bile	Less cytotoxicity and teratogenicity	Nath and Olsen 1967
Retinyl- $\beta$ -glucoside	Glucoserebrosidase-mediated transglycosylation	Less cytotoxicity	Gregory 1998
Retinol monophosphate galactoside	Crude cell fraction from mouse mastocytoma tissue	Less cytotoxicity	Helting and Peterson 1972; Peterson <i>et al.</i> 1976
<b>B. Vitamin D glycosides</b>			
1- $\alpha$ -Hydroxyvitamin-D <sub>3</sub> -3- $\beta$ -D-glucopyranoside, 1- $\alpha$ -hydroxyvitamin-D <sub>3</sub> -3- $\beta$ -D-cellobioside	<i>Trisetum flavescens</i> $\beta$ -glucosidase	Calcium supplement	Rambeck <i>et al.</i> 1984
3- $\beta$ - <i>O</i> -Glucopyranosyl-5 $\alpha$ , 6 $\beta$ -dihydroxyergosta-7,22-diene	<i>Hericum erinacens</i>	Gastric ulcer and chronic gastritis	Takaishi <i>et al.</i> 1991
Ergosta-7, 22-dien-3 $\beta$ - <i>O</i> -glucopyranoside	<i>Tylopilus neofelleus</i>	Rickets	Takaishi <i>et al.</i> 1989
<b>C. Vitamin E glycosides</b>			
Neurosporaxanthin - $\beta$ -D-glucopyranoside	Cultured cells of <i>Fusarium</i> sp.	Stabilizing the membranes, Antioxidant	Sakaki <i>et al.</i> 2002

2,5,7,8-tetramethyl-2-(4-methylpentyl)-chroman-6-yl- $\beta$ -D-glucopyranoside, 2,5,7,8-tetramethyl-2-(4,8-dimethylnonyl)-chroman-6-yl- $\beta$ -D-glucopyranoside	Cultured plant cells of <i>Phytolacca americana</i> and <i>Catharanthus roseus</i>	Antioxidant	Shimoda <i>et al.</i> 2006
2,2,5,7,8-pentamethyl-6-chroman-6-yl-6-O- $\beta$ -D-glucopyranosyl- $\beta$ -D-glucopyranoside	Cultured plant cells of <i>Phytolacca americana</i> , <i>Catharanthus roseus</i> and <i>Eucalyptus perriniana</i>	Antioxidant	Kondo <i>et al.</i> 2006
2-( $\alpha$ -D-glucopyranosyl)methyl-2,5,7,8-tetramethyl chroman-6-ol	$\alpha$ -glucosidase	Therapeutic agent for acute lung injury and mortality, Protect against aspirin induced gastric mucosal injury	Ochiai <i>et al.</i> 2002, Isozaki <i>et al.</i> 2005, Murasae <i>et al.</i> 1997
<b>D. Vitamin B<sub>1</sub> glycosides</b>			
5'-O-( $\beta$ -D-galactopyranosyl)thiamin	<i>A. oryzae</i> $\beta$ -galactosidase	Pleasant taste and odor, good bioavailability. More stable towards oxidative stress and UV irradiation	Suzuki and Uchida 1994
5'-O-( $\alpha$ -D-glucopyranosyl)thiamin	Cyclomaltodextrin glucanotransferase from <i>Bacillus stearothersophilus</i>	Excellent nutritional efficiencies, more stable against UV and light,	Uchida and Suzuki 1998

Thiamine- $\beta$ -D-2-deoxy-2-acetylglucopyranoside	<i>A. oryzae</i> $\beta$ -N-acetylhexosaminidase	Pleasant odour and taste	Kren <i>et al.</i> 1998
<b>E. Vitamin B<sub>2</sub> glycosides</b>			
Riboflavin-5'- $\alpha$ -D-glucoside	Liver $\alpha$ -transglucosidase	More solubility and bioavailability.	Joseph and McCormick 1995
5'-D-Riboflavin-5'- $\alpha$ -D-glucopyranoside	Transglucosidase from plant grains	More bioavailability.	Suzuki and Uchida 1969
Riboflavin- $\alpha$ -D-glucoside	$\alpha$ -glucosidase from pig liver	More bioavailability.	Uchida and Suzuki 1974
5'-O-( $\alpha$ -D-glucopyranosyl)-pyridoxine	Transglucosidase from <i>Micrococcus</i> sp.	Excellent nutritional efficiency, more heat and UV stability	Kawai <i>et al.</i> 1971a Kawai <i>et al.</i> 1971b Tsuge <i>et al.</i> 1996
<b>F. Vitamin B<sub>6</sub> glycosides</b>			
Pyridoxine-5'- $\beta$ -D-glucoside, pyridoxine-4' and 5'-olligosaccharides, 5'-O-(6-O-(5-hydroxydioxindole-3-acetyl)- $\beta$ -cellobiosyl)-pyridoxine, pyridoxine-5'-( $\beta$ -D-glucosyl-6-malonyl ester), pyridoxine-5'-( $\beta$ -D-glucosyl-6-hydroxymethylglutaryl ester).	$\beta$ -glucosidase	Excellent nutritional efficiency, more heat and UV stability.	Gregory 1998

---

**G. Vitamin C glycosides**

2-*O*-( $\alpha$ -D-Glucopyranosyl)ascorbic acid, 2-*O*-( $\beta$ -D-glucopyranosyl)ascorbic acid, 2-*O*-( $\beta$ -D-galactopyranosyl)ascorbic acid, 3-*O*-( $\beta$ -D-glucopyranosyl)ascorbic acid

*Lycium* fruit

Cosmetics, quasi-drugs and food additive Toyoda-Ono *et al.* 2004

2-*O*- $\alpha$ -Glucopyranosyl-L-ascorbic acid

Cyclomaltodextrin glucanotransferase from *Bacillus stearothermophilus*

More stable towards oxidative stress and UV irradiation, skin-whitening, agent in cosmetics. Kumano *et al.* 1998; Aga *et al.* 1991

**H. Other vitamin glycosides**

4-Oxonicotinamide-1-(1'- $\beta$ -D-ribofuranoside)

*Rothmannia longiflora* salib

Anti-diarrhoeal, analgesic Bringmann *et al.* 1999

4'-*O*-( $\beta$ -Glucopyranosyl)-D-(R)-pantothenic acid

Tomato juice

Growth factor of malo-lactic acid fermentation bacteria. Kren and Martinkova 2001

---

## 1.5 Enzyme catalysis in organic solvents

Organic synthesis is being carried out in organic media through enzyme catalysis (Laane *et al.* 1987; Vulfson 1990; Oshima *et al.* 2007). Biocatalysts have been successfully employed to catalyze a number of transformations and chiral resolution of biological and industrially important compounds (De Santis and Davis 2006; Effenberger and Syed 1998). In the last two decades the use of organic solvents in enzyme catalysed reactions has dramatically increased (Gorman and Dordick 1992). Employing biocatalysts in organic phase follows solid-liquid system (Therisod and Klivanov 1987), liquid-liquid system (Cantarella and Alfani 1991) and microemulsion system (Luthi and Luisi 1984). It is well documented that enzymes catalysis in this non-natural media over that in natural aqueous-environment offers prevention of autolysis, hydrolysis and increased thermostability (Fitzpatrick 1993; Griebenow and Klivanov 1995). Physical properties of enzyme effected by various solvents are generally attributed to alteration of various non-covalent interactions in the protein, solvation, ionic, dipolar, hydrogen bonding and hydrophobic interactions. The conformation of the enzyme in organic media is based on the ratio between hydrophobic and hydrophilic region on its surface (Carra and Privalov 1996; Rehan and Younus 2006).

### 1.5.1 Important factors influencing glycosylation in organic solvents

A few important factors that govern the glycosidase catalysed reactions in organic solvents like nature of substrate, solvent, thermal stability, role of water, kinetics and immobilization are discussed below.

#### 1.5.1.1 Nature of substrate

Glycoside synthesis and affinity of the enzyme towards substrate depends upon the nature of substrate as well as substrate concentration. The effect of initial D-glucose concentration on the glucoside yield in the glycosylation of alkanols using glucoamylase



from *Rhizopus oryzae* and  $\beta$ -glucosidase from almonds (Laroute and Willemot 1992a) showed a difference in behaviour between these two enzymes. By increasing the D-glucose concentration, the glucoside yields with glucoamylase decreased very rapidly whereas with  $\beta$ -glucosidase the yields were constant and finally fell low drastically. The formation of oligosaccharides (side products) depends upon the substrate concentration employed (Laroute and Willemot 1992a). Substrate study provides useful information on optimum substrate concentrations for carbohydrates and aglycons to be employed. Glycoside yield can be increased by increasing the concentration of the acceptor alcohol, provided that concentration is not sufficient enough to reduce enzyme stability or carbohydrate solubility or enzyme activity through inhibition (Stevensson *et al.* 1993). Effect of lactose and substrate alcohols varied to investigate the effects on the galactoside yields (Stevensson *et al.* 1993) showed that the galactoside yields distinctly increased with increase in concentrations of both the substrates.

In some of the glycosylation reactions, acceptor alcohols employed acts as both substrate and reaction media (Laroute and Willemot 1992a; Ljunger *et al.* 1994; Vic and Crout 1995; Vic *et al.* 1997; Crout and Vic 1998). The effect of D-glucose concentration on the synthesis of allyl  $\beta$ -glucopyranoside catalyzed by  $\beta$ -D-glucosidase showed that higher concentrations of D-glucose gave lower yields (Vic and Crout 1995). Glycosidases like  $\alpha$ -glucoamylase,  $\beta$ -glucosidase and galctosidases accept broad range of alcohols and very hydrophobic compounds as their substrates for glycosylation (Vic *et al.* 1997; Kosary *et al.* 1998; Kurashima *et al.* 2004).

The high specificity of enzymes, which means a strict limitation of the action of each enzyme to one substrate or to a very small number of closely related substances, is one of their most striking characteristics. In case of glycosidases, the interchange of hydrogen and hydroxyl on any single carbon atom of a glycoside substrate is sufficient to

prevent the action of the corresponding enzyme. For example,  $\beta$ -glucosidase does not act on  $\beta$ -mannosides nor does it act on  $\alpha$ -D-glucosides and probably not on  $\beta$ -galactosides. In case of the epimers involving carbon atoms 1, 2 and 4 of the aldohexoses ring, separate enzymes exist for each structure and the corresponding specific enzymes are  $\alpha$  and  $\beta$ -glucosidases  $\alpha$  and  $\beta$ -mannosidases and  $\alpha$  and  $\beta$ -galactosidases (Brown *et al.* 1997; Fujimoto *et al.* 1997; Woudenberg-van *et al.* 1998; Kim *et al.* 2003). Substrate specificity of a *Spodoptera frugiperda*  $\beta$ -glycosidase (Sfbetagly50) using site directed mutagenesis and bioenergetic analysis was investigated (Marana *et al.* 2004). It showed that replacement of Glu451 with glutamine increased the preference of Sfbetagly50 for glucosides in comparison to galactosides, whereas replacing Glu451 with serine had the opposite effect (Marana *et al.* 2004). In contrast, the replacement of Glu451 with aspartate did not change Sfbetagly50 specificity. The groups involved in catalysis of this enzyme were Glu187 (proton donor) and Glu399 nucleophile (Marana *et al.* 2001). A subsite model proposed by Hiromi (1970) was applied to various hydrolases including glucoamylase (Natarajan and Sierks 1997). The substrate specificity of pig intestinal glucoamylase-maltase was investigated (Gunther and Heymann 1998). Various substrates with  $\alpha$ -1,4-glycosidic bonds (maltose, oligosaccharides) were hydrolyzed with high maximal reaction velocities, whereas  $\alpha$ -1,  $\beta$ -2 glycosidic bond of the disaccharide sucrose was not hydrolyzed (Gunther and Heymann 1998).  $\beta$ -Glucosidase fixes one molecule of D-glucose on 1,2 pentanediol at position 1 or 2 with glucoamylase and two glucosides were formed with alcohol 1, 3 butanediol (Laroute and Willemot 1992a). Thus the authors demonstrated that the behaviour of these two enzymes were different so for as affinity and substrate specificity were concerned. Cytosolic  $\beta$ -glucosidase from mammalian liver is known for its broad specificity, which hydrolyses  $\beta$ -D-

galactopyranosides,  $\beta$ -D-fucopyranosides,  $\beta$ -D-xylopyranosides and  $\alpha$ -L-arabinosides in addition to  $\beta$ -glucopyranosides.

### 1.5.1.2 Nature of solvent

The mechanism of enzyme inactivation in organic media is still unclear (Castillo *et al.* 2005). Enzyme loses most of its initial activity after only few hours of exposure to organic solvents and that the inactivation was independent of the reaction temperature, solvent and enzyme hydration (Martinez *et al.* 2002). It was suggested that the enzyme inactivation probably does not involve structural changes because cross-linked enzyme crystals have been shown to be structurally defined in organic solvents (Fitzpatrick *et al.* 1993). In an organic solvent protein molecules are surrounded by a thin layer of hydration and the solvent molecule tend to displace the water molecules both from the hydration shell and from the interior of the protein, thereby distorting the interactions responsible for maintaining the native conformation of the enzymes (Simon *et al.* 2007). Some enzymes do not display any significant structural change during inactivation and local active site effects might be responsible for the loss in activity (Yang *et al.* 2004). When water and organic solvents are in equimolar ratio, the cross-linked crystals of glucoamylase exhibited high activity in water immiscible solvents than in water-miscible solvents (Abraham *et al.* 2004). Biotransformations can be performed on a preparative scale in nonaqueous solvents for most of the organic compounds (Vic and Crout 1995; Vic *et al.* 1997). In case of hydrolases, organic solvents shift the equilibrium towards synthesis (Vulfson *et al.* 1990; Vic *et al.* 1997; Crout and Vic 1998). In organic media, enzymatic thermostability could be increased (Zaks and Klivanov 1984) and enzyme specificity could be changed (Rubio *et al.* 1991). Moreover, since enzymes are not soluble in organic solvents, they can be easily removed and reused. Organic solvents also affect the binding of substrates to the active site by altering the apparent  $K_m$  values and

controlling the enantio selectivity of the enzymatic synthesis (Margolin *et al.* 1987; Sakurai *et al.* 1988). Also, organic solvents employed influence reaction rate, maximum velocity ( $V_{\max}$ ) or specific activity ( $K_{\text{cat}}$ ), substrate affinity ( $K_M$ ) and specificity ( $K_{\text{cat}}/K_M$ ) constants (Zaks and Klibanov 1986).

Water-organic solvent systems can be distinguished as homogeneous water-water soluble organic solvent liquid system and two-liquid water-water immiscible organic solvent (Antonini *et al.* 1981; Butler 1979). In the latter case, the free or immobilized biocatalysts are present in the aqueous phase, whereas the main part of the substrate and product are contained in the organic phase (Vulfson *et al.* 1990). High concentrations of poorly water-soluble substrates and/or products are possible in organic solvent containing media. The chance of microbial contamination is reduced. Further more, reaction equilibria may be shifted favorably and substrate and/or product hydrolysis can be largely prevented. Substrate or product inhibition may be reduced as a consequence of a lower inhibitor concentration in the aqueous environment of the enzyme and recovery of product and biocatalyst is facilitated (Vic *et al.* 1997).

To establish a correlation between the nature of solvent and the observed enzyme behaviour (stability or initial reaction rate), the most commonly used parameters are dielectric constant ( $\epsilon$ ), dipole moment ( $\mu$ ), Hildebrand solubility parameter ( $\delta$ ) and the logarithm of the partition coefficient ( $\log P$ ) in a standard octanol-water two-phase system (Weast 1983). The partition co-efficient is the ratio of concentrations of the substrates between the two solutions. The  $\log P$  value of a solvent could be defined as the logarithmic value of the partition co-efficient of the solvent in n-octanol/water two phase system. Brink and Tramper (1985) explained the influence of many water immiscible solvents on biocatalysis by employing the Hildebrand parameter ( $\delta$ ), as a measure of solvent polarity. The enhanced reaction rates could be expected when the polarity of the

organic solvents was low ( $\delta \approx 8$ ) and its molecular weight  $> 150$ . But later, it was demonstrated that  $\delta$  was a poor measure of solvent polarity. Laane *et al.* (1987) quantified solvent polarity on the basis of log P values. Generally, biocatalysis is low in solvents of log P  $< 2$ , is moderate in solvents with a log P value between 2 and 4 and high in non-polar solvents of log P  $> 4$ .

Physicochemical properties of solvent and enzyme stability was also studied for the synthesis of 2-hydroxybenzyl- $\beta$ -D-glucopyranoside (Vic *et al.* 1997), who used the Hildebrand solubility parameter which gives a measure of the overall cohesive energy density of a solution and Hansen parameters ( $\delta$ ) that distinguishes between the different types of interactions in a solution. Laroute and Willemot (1992b) tested the harmfulness of 66 solvents for two glycosidases (glucoamylase from *Rhizopus oryzae* and  $\beta$ -glucosidase from *A. flavus*) to allow for a first choice before considering the feasibility of reversing hydrolytic reactions. Biocatalysts were placed in the anhydrous organic solvents at 24 °C and residual activities were checked. They found that most of the ethers, alcohols and esters are not harmful and enzymes retained 65 to 100% of their initial activity after 24h of incubation. However, still no correlation was found between enzymatic stability and hydrophobicity of the organic medium except for the Hansen parameters and log P.

### 1.5.1.3 Thermal stability

Catalytic efficiency of the glycosidases is most commonly affected by the reaction temperature in the media. Glucoamylase from *A. niger* cross-linked with glutaraldehyde via lysine residues were shown to retain 98.6% activity at 70°C for 1 h (Abraham *et al.* 2004). Glucoamylase from *Humicola* sp. was stable over a pH of 3.5-5.9 with a pH optimum of 4.7 and a temperature optimum of 55°C (Riaz *et al.* 2007). Also, thermophilic fungus *Thermomyces lanuginosus* showed a temperature optimum of 70°C

(Thorsen *et al.* 2006).  $\alpha$ -Amylase showed optimum activities at pH 6.5 and high activity at temperatures between 60 and 80°C (Almeida *et al.* 2007). Almond  $\beta$ -D-glucosidase stability was carried out (Vic *et al.* 1997) by suspending a known amount of enzyme in 9:1 (v/v) and 3:7 (v/v) solvent-water mixture (acetone, acetonitrile, tert-butanol, DMF and DMSO) at 40°C for 24h and the hydrolytic activity against salicin was determined. Enzyme incubated in 9:1 (v/v) acetone, acetonitrile and tert-butanol mixture showed 75 to 90% of the hydrolytic activity, whereas the enzyme in 9:1 (v/v) DMF and DMSO lost almost completely its hydrolytic activity. For a 30% (v/v) of solvent, the effect on enzyme stability is exactly reversed. In acetone, acetonitrile and tert-butanol, the enzyme was rapidly inactivated. However, 66% and 97% of the initial activity was still present after 24 h of incubation in DMF and DMSO respectively. From this study, authors concluded that stability of the enzyme depends on the concentration of the solvent in the medium but the effect may be reversed depending on the nature of the solvent. Two  $\beta$ -glucosidases (isoenzyme 120 kDa) purified from apple seed displayed higher thermal stability than the commercially supplied  $\beta$ -glucosidase from almond in an aqueous environment (Hui-Lei *et al.* 2007). Thermostable  $\beta$ -glucosidase from *Geobacillus pallidus* exhibited an optimum temperature at 70°C which was greater than that observed for  $\beta$ -xylosidase from *Bacillus stearothermophilus* T-6 (Bravman *et al.* 2001). Also, the enzyme retained 68% of the initial activity after 42 h incubation at 60°C (Quintero *et al.* 2007). Thermal inactivation studies carried out by changing the temperature between 60 and 90°C for the free and an immobilized  $\beta$ -galactosidase from *Thermus* sp., showed that both the forms retained a certain activity between 60 and 70°C (Ladero *et al.* 2006)

Both glucoamylase from *Rhizopus oryzae* and  $\beta$ -glucosidase from *Aspergillus flavus*, showed thermal stability in a low water environment at a high temperature of 60 °C. The studies indicated that some solvents in which the enzymes retained 57 to 95% of

their residual activity at 24°C did not stabilize against thermal denaturation. The solvents with longer carbon chain lengths prevented thermal denaturation effectively (Laroute and Willemot 1992b). Stability of  $\beta$ -glucosidase from *Caldocellum Saccharolyticum* was studied in comparison to commercially available  $\beta$ -galactosidase from *A. oryzae* (Stevenson *et al.* 1996). The enzyme was incubated in 0, 2, 4, 5 and 6 M ethanol solutions at 65 °C and no reduction in activity was observed upto 6 h except with 6 M ethanol present. *A. oryzae* enzyme was denatured in 4 M ethanol at 45 °C and the enzyme form *Kluyveromyces fragilis* and *Kluyveromyces lactis* were inactivated in 3M ethanol at 40 °C (Stevenson *et al.* 1993). The stability of the immobilized  $\beta$ -glucosidase preparation was investigated by measuring the residual activity after incubation in octanol at 50 °C and  $a_w = 1.0$  (Ljunger *et al.* 1994). The remaining enzyme activity was determined after 6, 13 and 27 days and compared with the original activity at time zero. Due to stability of this enzyme, the conditions were employed for the repeated synthesis of octyl- $\beta$ -glucoside. Stability of glycosidases also enhanced due to substrates (Svendsen 2003). Thermal stability of glucoamylase was enhanced 2 fold in the presence of 0.5% starch (Gill and Kour 2004). *Talaromyces emersonii* glucoamylase showed significantly improved thermal stability with a half life of 48 h at 65 °C in 30% (w/v) D-glucose, compared to 10 h for *A. niger* glucoamylase (Nielsen *et al.* 2002). Compared to the native enzyme, temperature profile of immobilized glucoamylase was widened and the optimum pH also changed (Huo *et al.* 2004). Thermal stability of the enzyme can be modified by means of cloning and mutation (Nielsen *et al.* 2002; Allen *et al.* 2003). Mutation provides increased thermal stability, reduced isomaltose formation and increased pH optimum to the enzyme (Allen *et al.* 2003). Based on the results of molecular dynamic simulations, twelve mutations were constructed to improve the thermal stability of glucoamylase from *A. awamori* (Liu and Wang 2003). Glycation of

the enzyme also resulted in increase in thermal stability (Pornpong *et al.* 2005). The stability and kinetic parameters of glycosylated and the intact enzyme were compared. The glycosylated enzyme was more resistant to heat, but glycosylation did not affect the pH stability and the isoelectric value significantly (Pornpong *et al.* 2005).

#### 1.5.1.4 Water activity

Activity of the enzyme in organic media is strongly dependent on its hydration layer which is also essential for its conformational flexibility. Increased enzyme selectivity for alcohol was observed with increased water activity. One possibility is that the effect is linked with enzyme flexibility which is known to increase with increasing water activity in organic media. At low water activity, enzymes are rather rigid and under those conditions it is not unexpected that the enzyme favours the small natural nucleophile, water. At higher water activity, the increased flexibility might cause the enzymes to accept the larger alcohol nucleophiles (Hansson *et al.* 2001). Influence of water activity for the production of galactooligosaccharides (GOS) gradually grew as water activity increased in the reaction system and later their synthesis decreased as water activity increased further (Cruz-Guerrero *et al.* 2006).

For the synthesis of hexyl- $\beta$ -D-glucoside and hexyl- $\beta$ -D-galactoside,  $\beta$ -glucosidase from hyperthermophilic organisms such as *Sulfolobus solfataricus* and *Pyrococcus furiosus* did not show any catalytic activity below  $a_w = 0.6$ . However at higher water activity ( $a_w = 1.0$ ) both the enzymes showed very good activity (Hansson and Adlercreutz 2002). Higher reaction rates and yields were obtained using almond  $\beta$ -glucosidase in presence of water-miscible organic solvents with a water activity of 0.53 for the synthesis of octyl- $\beta$ -D-glucoside (Ducret *et al.* 2002a).

As the hydration level increases, the enzyme becomes more flexible and the activity increases. The hydration level requirement differs for each one of the enzymes



(Valivety *et al.* 1992). In order to achieve glycosylation using glycosidases instead of hydrolysis, the equilibrium position should be shifted (kinetically controlled reaction) which can be achieved by using predominantly organic media at a low water activity. One approach to shift the equilibrium position is to add a water-miscible solvent, which decreases the thermodynamic water activity and thereby favors synthesis. An alternative approach is to add a water immiscible solvent in which case, a hydrophobic product is extracted to the organic phase, so that its concentration in the aqueous phase is kept low and more product is synthesized. This approach has been applied successfully in the synthesis of alkyl glycoside in the two-phase system using hydrophobic alcohol as both substrate and organic phase. (Vulfson *et al.* 1990; Ljunger *et al.* 1994).

Almond  $\beta$ -glucosidase catalyzed synthesis of octyl- $\beta$ -glucoside showed that a water activity ( $a_w$ ) of at least 0.67 was required for the synthesis and the rate increased with increasing  $a_w$  (Ljunger *et al.* 1994). But the final yield decreased with increasing water activity. The best results were obtained using a high initial water activity which decreased during the course of the reaction. The condensation of glucose and allyl alcohol showed that the water concentration should be adjusted carefully to balance the enzyme activity against equilibrium yield to optimize the productivity (Vic and Crout 1995). Comparable minimum water procedures have been adopted in the glycosylation of butanol (Ismail and Ghoul 1996), 1,6-hexanediol as well as medium chain alcohols (Vic *et al.* 1996; Chahid *et al.* 1992) by many researchers in this field.

By analogy with the lipase-catalysed esterification of carbohydrates (Oosterom *et al.* 1996), it would seem advantageous to use an inert polar solvent to increase the solubility of the carbohydrate. Acetonitrile, acetone and tert-butyl alcohol (Vic and Crout 1994; Vic *et al.* 1995; Vic *et al.* 1997) containing 10% water ( $a_w \sim 0.8$ ) have been used for this purpose, but the reaction rates and the yields were generally lower than when the

acceptor alcohol was used as the solvent. As an alternative to the minimum water procedures, reactions have also been performed with aqueous glucose at  $a_w \sim 1$ . Such an approach has the advantage of optimum enzyme activity (Ljunger *et al.* 1994) but its efficiency in terms of equilibrium yield depends upon the extraction of the product into the organic phase. Compared to lipases, glucosidases require higher water activity for glycosylation reaction. However, unlike in case of lipases, a systematic study on water activity on glucosidase action is yet to be done.

#### 1.5.1.5 Kinetics

Kinetics of enzyme catalyzed reactions help in not only quantifying a reaction but also bring out some intricate details of enzyme inhibition and mechanism which have quite a lot of bearing on the industrial application of glucosidases. The kinetic study of glucoamylase catalyzed hydrolysis of starch granules from six different sources (rice, wheat, maize, cassava, sweet potato and potato) was studied, where  $K_o$  (catalytic constant of the adsorbed enzyme) is largely influenced by the type of starch granules. The relation between  $K_o$  value and crystalline structure of starch granules suggested that  $K_o$  values increases as the crystalline structure become dense (Tatsumi *et al.* 2007). Glucoamylase catalysed hydrolysis of raw starch suspension discussed by the rate equations from a three-step mechanism, consists of adsorption of the free enzyme on to the surface of the substrate, reaction of the adsorbed enzyme with the substrate and liberation of the product (Tatsumi and Katano 2005).

Kinetics of the maltose hydrolysis by free and immobilized (in polyacrylamide gel) glucoamylase was investigated by constructing a mathematical model (Yankov *et al.* 1997). Kinetic parameters determined by Michaelis-Menten equation for both free and immobilized enzyme resulted in a good correlation between calculated and experimental data. Statistical analysis for the kinetic model developed for the saccharification of

potato starch with glucoamylase showed that the Michaelis-Menten equation could be used as a simulation model, the Line weaver-Burk and Wilkinson methods could be used for mathematical regression and the final proposed kinetic model explained the enzyme behaviour clearly (Zhang *et al.* 1998). In the kinetics of almond  $\beta$ -glucosidase catalyzed hexyl-glucoside synthesis, the kinetic constants  $V_{\max}$ ,  $K_m$  (glycosyl donor) and  $V_{\max} / K_m$  were all influenced by the water activity and they all increased in value with increasing water activity (Andersson and Adlercreutz 2001). Alcoholysis and reverse hydrolysis reactions performed enzymatically with a hyperthermophilic  $\beta$ -glucosidase and lactose or glucose used as substrate to produce heptyl- $\beta$ -galactoside and/or heptyl- $\beta$ -glucoside in one phase water saturated 1-heptanol system followed Michaelis-Menten kinetics where conversions were limited by a strong product inhibition and the formation of oligosaccharides (Mariano *et al.* 2000). Thermostable  $\beta$ -glycosidase of *Thermus thermophilus*, addition of D-glucose to reaction mixtures of enzyme and glycosyl donors ( $\beta$ -D-glucoside,  $\beta$ -D-galactoside and  $\beta$ -D-fucosides), resulted in an inhibition or activation depending upon both the substrate concentration and temperature. Enzyme displaying non-Michaelian kinetic behavior within the range of 25-80°C, might be due to inactivation below 60°C and activation above 60°C in presence of high substrate concentrations (Fourage *et al.* 2000).

#### **1.5.1.6 Immobilization**

Immobilized enzymes have been widely used in food, fine chemicals and pharmaceutical industries because they provide many advantages over free enzymes including repeated or continuous reuse, easy separation of the product from the reaction media, easy recovery of the enzyme and improvement in stability (Torres *et al.* 2004; Yavuz *et al.* 2002). The most important factors influencing immobilization processes are carrier properties (material, particle diameter, pore size, available anchor groups and

their amount), enzyme stability and immobilization conditions: pH, ionic strength, protein concentration and carrier activators (Eupergit *et al.* 2000). Immobilization of glucoamylase on many supports include ceramic membrane (Ida *et al.* 2000), polymer microspheres (Oh and Kim 2000), magnetic supports (Bahar and Celebi 1998) through wide variety of methods such as adsorption, entrapment, cross-link and covalent attachment (Marin-Zamoraa *et al.* 2006; Rebros *et al.* 2006; Cao *et al.* 2000).

Non-covalent immobilization techniques such as metal-chelated adsorption (Sari *et al.* 2006) has been successful in a few enzymes including  $\alpha$ -amylase (Kara *et al.* 2005) and invertase (Osman *et al.* 2005). Purified glucoamylase from *Arachniotus citrinus* was immobilized on polyacrylamide gel where immobilization decreased the entropy and enthalpy of deactivation and made the immobilized glucoamylase thermodynamically more stable (Perveen *et al.* 2006). Also, *A. niger* glucoamylase was immobilized on montmorillonite clay (K-10) through adsorption and covalent binding which increased the affinity towards substrate (Sanjay and Sugunan 2005). Eventhough recent research on glucoamylase immobilization was mainly focused on entrapment of the cross-linked enzyme and covalent binding on many matrices, structurally had drawbacks (Bai *et al.* 2006). To resolve these drawbacks, glucoamylase was chelated to nonporous micron-sized magnetic poly(vinyl acetate-divinylbenzene-g-glycidyl methacrylate-iminodiaceticacid-Cu<sup>2+</sup>—PVA-DVB-g-GMA-IDA-Cu<sup>2+</sup>) particles which exhibited excellent reusability (Wang *et al.* 2007). Thermal stability of glucoamylase have been improved through covalent immobilization on the cellulose-based carrier Granocel (Bryjak *et al.* 2007). Glucoamylase from *Fusarium solani* was chemically modified by cross-linking with aniline hydrochloride in presence of 1-ethyl-3-(3-dimethyl aminopropyl)carbodiimide with enhancing effects on temperature, pH optima and pKa values of active site residues (Bhatti *et al.* 2007b). Chitosan-clay is cross linked with

glutaraldehyde to immobilize  $\beta$ -glucosidase to improve activity and stability of the enzyme (Chang and Juang 2007).

The free enzyme is immobilized by trapping it in an inert matrix such that the immobilized enzyme retains its catalytic properties for a much longer time than the free enzyme and hence can be used continuously for many more synthesis (Huo *et al.* 2004). Many types of immobilization impart greater stability to the enzyme making them more useful over wider pH ranges and at higher temperatures (Chang and Juang 2005). Immobilized enzyme appears to be less susceptible to the normal activators and inhibitors that affect the soluble enzyme (Barolini *et al.* 2004).

Immobilized glucoamylase possesses excellent storage and working stability. Immobilization of glucoamylase can be performed on to polyvinyl alcohol complex gel (Jianping *et al.* 2003), chitosan-clay composite (Chang and Juang 2005) and plastic material (Roig *et al.* 1995). Thermal and pH stabilities of free and immobilized  $\alpha$ -amylase,  $\beta$ -amylase and glucoamylases were compared after immobilization with chitosan-clay (cross-linked with glutaraldehyde). It was shown that the relative activities of immobilized enzymes are higher than free enzymes over broader pH and temperature ranges for starch hydrolytic reaction (Chang and Juang 2005). Glucoamylase from *A. niger* was immobilized through ionic adsorption onto DEAE-agarose, Q1A-Sepabeads and Sepabeads EC-EP3 supports (Torres *et al.* 2004) coated with polyethyleneimine (PEI) with marginal improvement in thermal stability due to this immobilization. Huo *et al.* (2004) reported, glucoamylase immobilization onto novel porous polymer supports, which led to enhanced temperature profile of the immobilized glucoamylase and altered optimum pH. Optimum substrate concentration of the immobilized glucoamylase was higher than that of the native enzyme. After storage for 23 days, the immobilized glucoamylase still maintained about 84% of its initial activity, whereas the native

enzyme only maintained about 58% of the initial activity. Moreover, after using repeatedly seven times, the immobilized enzyme maintained about 85% of its initial activity. Glucoamylase from *A. niger* was immobilized on cationic nonporous glass beads by electrostatic adsorption followed by cross linking with glutaraldehyde (Wasserman *et al.* 1982) and the immobilized glucoamylase showed decreased stability upon heating, compared to the soluble enzyme.

Properties of thermostable  $\beta$ -glucosidase from *Sulfolobus shibatae* immobilized on silica gel by cross linking with transglutaminase is more stable for the hydrolysis of lactose during milk and whey processing. Due to high thermal stability, the immobilized enzyme can be used at high temperatures, which restrict microbial growth during operating time of continuous flow reactors (Synowiecki and Wolosowska 2006). Kosary *et al.* (1998) studied  $\alpha$ - and  $\beta$ -glucosidases catalyzed *O*-glycosylation activity with D-glucose as substrate and with different alcohols by reverse hydrolytic processes. With native glucosidases, upscaling resulted in low yields due to heterogeneity of the reaction mixtures and the aggregation of undissolved enzymes in organic media. Immobilization of the enzymes on a modified polyacrylamide-type bead support (Acrylex C-100) increased enzyme stability resulting in higher yields necessary to perform glucosylations on a larger scale (Kosary *et al.* 1998). In this report, immobilized glucosidases retained 55–80% of their original activity depending on the water content and the type of alcohol after 72 h incubation. The enzymatic synthesis of alkyl- $\beta$ -glucosides by water-immiscible alcohols studied using immobilized  $\beta$ -glycosidase gave a higher conversion yield than the native enzyme (Papanikolaou 2001).

Gargouri *et al.* (2004) reported the production of  $\beta$ -xylosidase and  $\beta$ -glucosidase from *Sclerotinia sclerotiorum* and evaluation of physico-chemical characteristics of its immobilization on supports for use in continuous reactors. The majority of the

immobilized preparations were unable to catalyze the synthesis of alkyl-glycosides. Immobilized  $\beta$ -glycosidase systems using ion exchange resins were found to increase the enzyme stabilities when tested for hydrolysis but did not increase the synthetic efficiency. This may be due to the unfavorable conformation of the immobilized enzyme for synthetic reaction (Gargouri *et al.* 2004).

## **1.6 Strategies employed in glycosylation**

The advantages of carrying out glycosylation using reverse micelles, super critical carbon di-oxide, microwave and response surface methodology are discussed below.

### **1.6.1 Glycosylation in reverse micelles**

Water in oil microemulsions with reverse micelles provides an interesting alternative to normal organic solvents in enzyme catalysis with hydrophobic substrates. Reverse micelles are useful microreactors because they can host proteins like enzymes (Luisi *et al.* 1998). Catalytic reactions with water–oil substrates can occur at the large internal water-oil interface inside the microemulsion (Eriksson *et al.* 2004). A salient feature in all the enzymes in which thermostability has been documented is that thermostability decreases as the water content in the system increases. In this media, both the activity and stability of biomolecules can be controlled by the concentration of water (Srivastava and Strasser 2001; Orlich and Schomacker 2002). In reverse micelles, it has been possible to probe the relation between the solvent and enzyme kinetics, as well as some of the factors that affect the enzyme thermostability and catalysis (Srivastava and Strasser 2001). The overall activity of amyloglucosidase entrapped into reverse micelles of Triton-X-100-xylene-hexanol was lower, than in aqueous systems, but showed higher stability upto 50°C (Shah *et al.* 2000). Synthetic applications of enzymes entrapped in reverse micelles and organo-gels were discussed elaborately by Fadnavis and Deshpande

(2002). Study of  $\beta$ -1,4-glucosidase in water/phosphatidylcholine/heptane-butanol reverse micelles was reported (Miao and Yao 1999). The activity and kinetics of  $\beta$ -1,4-glucosidase in hydrolysis of salicin showed that Michaelis-Menton kinetics was followed.  $V_{\max}$  was found to be 11.8 times larger than that in aqueous media and  $K_m$  was only 1/25 of that in aqueous media. There are reports on the synthesis of alkyl glycosides and oligosaccharides (galacto-oligosaccharides) in reverse micelles by using glycosidases and higher yields were reported compared to aqueous media (Chen *et al.* 2001; 2003; Kouptsova *et al.* 2001). Transgalactosylation reaction of the enzyme  $\beta$ -galactosidase was strongly dependent on the molar ratio of water to surfactant ( $W_o$ ) of Aerosol-OT (AOT)/isooctane reverse micelles (Chen *et al.* 2001). Synthesis of alkyl glycosides in AOT reverse micelles system showed (Kouptsova *et al.* 2001) that the direction of the reaction depended on the pH of the aqueous solution solubilized in reverse micelles.

### 1.6.2 Glycosylation in supercritical carbon dioxide

Current research has provided insight into the advantages and possibilities of using supercritical carbon dioxide (SCCO<sub>2</sub>) in biochemical processes (Dijkstra *et al.* 2007). The main advantages of SCCO<sub>2</sub> include increased catalytic activities as a result of improved mass transfer, higher selectivities and strongly reduced organic waste streams (De Simone 2002; Beckmann 2003; Rezaci *et al.* 2007).

Carbon dioxide was chosen as the super critical fluid (SCF) for the following reasons: (1) CO<sub>2</sub> becomes a SCF above 31°C and 73.8 atm, which are easily accomplished conditions with gentle heating from ambient temperature and a commercial liquid chromatography pump, (2) the solvent properties of SCCO<sub>2</sub> can be continuously varied by changing the pressure or temperature and (3) CO<sub>2</sub> is nontoxic and the medium is easily removed by decompression to atmospheric pressure (Mori and



Okahata 1998; 2000). Several reviews describe the variety of organic reactions including chemical (hydrogenation, hydroformylation, photorection, halogenation, Diels Alder cycloaddition, oxidation, coupling reaction, Pauson-Khand reaction, olefin methathese, Friedel-Craft alkylation, asymmetric reaction) and enzymatic reactions carried out in supercritical fluids (Mori and Okahata 2000; Oakes *et al.* 2001; Mori and Okahata 2002; Matsuda *et al.* 2002). Enzyme stability can be improved by SCCO<sub>2</sub> pretreatment. The application of supercritical fluids in the control of enzyme reactions, with emphasis on the use of supercritical fluoroform in the regulation of  $\beta$ -D-galactosidase mediated transglycosylation and oxidation has been discussed (Mori and Okahata 2003). SCCO<sub>2</sub> pretreated  $\alpha$ -amylase retained 41% activity based on the original activity, whereas, the non-treated  $\alpha$ -amylase completely lost its activity in an hour in water (Liu and Chang 2000). n-Octyl- $\beta$ -D-xylotrioside and xylobioside synthesis were significantly increased in supercritical CO<sub>2</sub> and fluoroform (CHF<sub>3</sub>) fluids mediated one-step reaction of xylan and n-octanol using the acetone powder (acetone-dried cells) of *A. pullulans* as the enzyme source of xylanase (Nakamura *et al.* 2000; Matsumura *et al.* 1999). A lipid-coated  $\beta$ -galactosidase catalyzed transgalactosylation reactions carried out in SCCO<sub>2</sub> resulted in good conversion yields up to 72%, whereas, native  $\beta$ -galactosidase hardly catalyzed the transgalactosylation in SCCO<sub>2</sub> due to its insolubility and instability in SCCO<sub>2</sub> (Mori and Okahata 1998).

### 1.6.3 Microwave-assisted glycosylation reactions

Ultrasonification and microwave assistance are two emerging approaches for enhancing reaction rates in low water media. Microwave irradiation is becoming an increasingly popular method of heating which replaces the classical one because it proves to be a clean, cheap and convenient method. Often, it affords higher yields and shorter reaction times (De Oliveira *et al.* 2002). A new trend in organic synthesis by

utilizing microwave irradiation and enzyme catalysis has evolved (Cai *et al.* 2003), called Microwave Irradiation Enzyme Coupling Catalysis (MIECC). This technique can be divided into two categories, such as enzyme synthesis under microwave irradiation in non/micro-aqueous media (wet method) and without media (dry method). Microwave irradiation of a mixture of tri-*O*-acetyl-D-glucal and an appropriate alcohol in the presence of Montmorillonite K-10 catalyst, provided unsaturated glycosides in much shorter time and in yields comparable to conventional heating (De Oliveira *et al.* 2002). Glucose and dodecanol were reacted in the presence of dodecyl-benzenesulfonic acid under microwave irradiation to yield dodecanol glucoside with a degree of oligomerization of 1.43 (Rhode *et al.* 1999). A three step microwave assisted solvent-free synthesis of decyl D-glucopyranoside with 1-decanol was established for D-glucose and extended to D-galactose, D-mannose and N-(2,2,2 trichloroethoxy-carbonylamino)-D-glucosamine with 70% average overall yield for the three steps such as peracetylation, glycosylation and saponification (Limousin *et al.* 1997). In the synthesis of alkyl glycosides under microwave assistance using catalytic amount of acid, the ratio of the  $\alpha/\beta$ -anomers was influenced by the reaction conditions (Nuchter *et al.* 2001). The effect of microwave irradiation on a thermostable  $\beta$ -galactosidase from *Bacillus acidocaldarius* enzyme was experimentally tested, showing that residual activity depends on enzyme concentration, microwave power level and exposure time (La Cara *et al.* 1999). The selectivity for galacto-oligosaccharides synthesis can be increased by 217-fold under microwave irradiation using immobilized  $\beta$ -glucosidase from *Kluyveromyces lactis* with added co-solvents such as hexanol (Maugard *et al.* 2003). Reduced hydrolysis product and increased rates of conversion have been reported in transglycosylation reactions to simple alcohols catalyzed by other thermophilic  $\beta$ -galactosidases in microwave irradiated dry media (Gelo-Pujic *et al.* 1997).

#### 1.6.4 Response surface methodology (RSM) in glycosylation

Response surface methodology (RSM) is a technique used in the experimental study of relationship between response variables and many input variables. The techniques have been used to answer the key question of what values of the input variables will yield a maximum. RSM has been widely used in various disciplines such as food, chemical and in biological processes (Linder *et al.* 1995; Bandaru *et al.* 2006; Ratnam *et al.* 2005; Ambati and Ayyanna 2001; Chen *et al.* 1997).

In recent years, this methodology has been applied to some glycosylation reactions as well. The objective of these studies is to evaluate the optimum conditions within the parameters employed to achieve a maximum conversion yield. Enzymatic synthesis of butyl glucoside by  $\beta$ -glucosidase from sweet almonds was optimized by response surface methodology (Ismail *et al.* 1998). The empirical models were developed to describe relationship between the operating variables - temperature, water/butanol volume ratio, glucose concentration, enzyme concentration and responses - butyl glucoside concentration. The statistical analysis indicated that the four factors have significant effects on the butyl glucoside synthesis. Ismail *et al.* (1998) found good agreement between predicted and experimental data. Optimization was also carried out for the synthesis of butyl galactoside by  $\beta$ -galactosidase from *A. oryzae* by using RSM (Ismail *et al.* 1999b). In this work, they performed a transglycosylation reaction using lactose as a glycosyl donor. n-Octyl glucoside was produced and optimized by using this method by employing Doehlert's matrix design (Chahid *et al.* 1994). The three parameters employed were amount of acetate buffer, octanol and lactose and the products obtained were octyl glycosides (octyl galactoside and octyl glucoside).

Usefulness of several statistical designs in experimental optimization including Box-Behnken, Central Composite Rotatable and Plackett-Burman designs in enzyme

catalysed glycosylation reactions have been carried out (Vijayakumar *et al.* 2005; Vijayakumar *et al.* 2006). Analyses of several response surface plots obtained by employing statistical designs in glycosidase catalysed reactions have indicated that such plots could explain the glycosylation behaviour in the presence of different kinds of substrates and reaction conditions.

### 1.7 Scope of the present work

Many enzymatic transformations in organic solvents have found their way into flavor, fragrance, pesticides, pharmaceutical and polymer industries. Enzymatic synthesis definitely has an important role to play in the development of novel efficient asymmetric processes. Carbohydrate containing natural products is an important biological substance, which plays a significant role in molecular recognition for the transmission of biological information. Many glycosides are used in broad range of applications as food colorants and flavoring agents (Sakata *et al.* 1998), sweeteners (Shibata *et al.* 1991; Oliveira *et al.* 2007), antioxidants, anti-inflammatory (Gomes *et al.* 2002; Moon *et al.* 2007), antitumor (Kaljuzhin and Shkalev 2000; Ikeda *et al.* 2006), antibiotics (Ikeda and Umezawa 1999), antifungal (Tapavicza *et al.* 2000), antimicrobial (Zhou 2000) and cardiac related drugs (Ooi *et al.* 1985). Glycosylation renders lipophilic compounds more water soluble and thereby increase bioavailability of biologically active compounds besides imparting stability to the aglycon (Kren and Martinkova 2001). So, efficient methods for the syntheses of biologically active glycoconjugates are of increasing interest.

Usefulness of glycosylation is explored in this present work leading to the syntheses of few phenolic and vitamin glycosides. Thus the present investigation attempts to explore the potentialities of amyloglucosidase from *Rhizopus mold* and  $\beta$ -glucosidase from sweet almond in effecting glycosylation of a wide variety of glycosyl

acceptors including few selected phenols like vanillin, N-vanillyl-nonanamide, curcumin, L-dopa, dopamine and vitamins like riboflavin, ergocalciferol and  $\alpha$ -tocopherol. Of these many phenols and vitamins are either less soluble in water (vanillin 2 g/L, riboflavin 0.2 g/L) or insoluble in water at all (N-vanillyl-nonanamide, curcumin, ergocalciferol and  $\alpha$ -tocopherol) or susceptible to heat, light and oxidation (DL-dopa, dopamine). Also, the phenols employed vanillin, N-vanillyl-nonanamide, curcumin, DL-dopa and dopamine possess structural similarity by having hydroxyl group at the 4<sup>th</sup> position and hydroxyl or methoxy group at 3<sup>rd</sup> position besides having a CH= or CH<sub>2</sub> carbon *para* to the 4<sup>th</sup> OH position.

Amyloglucosidase from *Rhizopus* sp. and  $\beta$ -glucosidase from sweet almond catalyzed synthesis of above mentioned phenols and vitamins were carried out in diisopropyl ether solvent in an experimental setup where larger concentration of substrates can be employed with lesser concentration of enzyme to get better conversion. The carbohydrate molecules employed for the glycoside preparations were D-glucose, D-galactose, D-mannose, D-fructose, D-arabinose, D-ribose, maltose, sucrose, lactose, D-mannitol and D-sorbitol. The glycosylating reactions were investigated in detail in terms of incubation period, pH and buffer concentration, enzyme concentration, substrate concentration, regio and stereo selectivity, response surface methodology and kinetics. Glycosides prepared were analysed by HPLC, separated through size exclusion chromatography and characterized spectroscopically to determine their nature and proportions. The glycosides were tested for angiotensin-converting enzyme inhibition and antioxidant activities. The salient features of these investigations are described in detail in the ensuing chapters.

ePrints@CFTRI

***Chapter 2***  
***Materials and Methods***

## 2.1 Materials

### 2.1.1 Glycosidases

Amyloglucosidase from *Rhizopus* mold and  $\beta$ -glucosidase isolated from sweet almonds were employed for the present work.

#### 2.1.1.1 Amyloglucosidase

Amyloglucosidase (3.2.1.3) from *Rhizopus* mold a fungal source, with an activity of 22,570 units/g of solid, purchased from Sigma Chemical Co., St. Louis, MO, USA was employed for the glycosylation work. One unit liberates 1.0 mg of glucose from starch in 3 min at pH 4.5 at 55 °C. This enzyme was used for the synthesis of glycosides of phenols - vanillin, N-vanillyl-nonamide, L-dopa, dopamine and vitamins - riboflavin, ergocalciferol and  $\alpha$ -tocopherol.

#### 2.1.1.2 $\beta$ -Glucosidase

$\beta$ -Glucosidase was isolated from sweet almonds and the crude enzyme was employed. This enzyme was used for the synthesis of glycosides of phenols - vanillin, N-vanillyl-nonamide, curcumin, L-dopa and vitamins - riboflavin and  $\alpha$ -tocopherol. The isolated  $\beta$ -glucosidase was also immobilized on calcium alginate and was employed for the synthesis of dopamine glycosides.

### 2.1.2 Phenols/vitamins

Vanillin procured from Sisco Research Laboratories Pvt. Ltd, curcumin (>95% purity) from Flavors and Essences Pvt. Ltd. India, N-vanillyl-nonamide, dopamine and ergocalciferol from Sigma Chemical Co., St. Louis, MO, USA and DL-dopa, riboflavin,  $\alpha$ -tocopherol from Hi-Media Ind. Ltd. were employed.

### 2.1.3 Carbohydrates

D-Glucose and sucrose purchased from SD fine chemicals (Ind.) Ltd.; D-galactose and D-fructose from Hi-Media Ind. Ltd.; D-mannose, D-arabinose, D-ribose, D-sorbitol

and D-mannitol from Loba Chemie Pvt. India Ltd.; maltose from Sigma Chemical Co., St. Louis, MO, USA and lactose from Sisco Research Laboratories Pvt. Ltd. India, were employed in the glycosylation reactions.

#### 2.1.4 Solvents

Chloroform, di-isopropyl ether, diethyl ether, dimethyl sulphoxide (DMSO), ethyl acetate, petroleum ether (60-80 °C) were purchased from SD fine Chemicals (Ind.) Ltd. All the solvents were distilled once before use. HPLC grade acetonitrile was purchased from Qualigens Fine Chemicals Ltd. and was used as such.

#### 2.1.5 Other chemicals

The following chemicals and their sources are shown in Table 2.1

**Table 2.1** Chemicals and their companies of procurement.

Chemicals	Company
Sodium acetate ( $\text{CH}_3\text{COONa}$ ), di-sodium hydrogen phosphate ( $\text{Na}_2\text{HPO}_4$ )	Ranboxy Laboratories Ltd. India.
Di-sodium tetra borate ( $\text{Na}_2\text{B}_4\text{O}_7 \cdot 10 \text{H}_2\text{O}$ ), sodium chloride ( $\text{NaCl}$ ), sodium hydroxide ( $\text{NaOH}$ ), sodium sulphite ( $\text{Na}_2\text{SO}_3$ ), sodium sulphate anhydrous ( $\text{Na}_2\text{SO}_4$ ), zinc sulphate ( $\text{ZnSO}_4$ ), calcium chloride ( $\text{CaCl}_2$ ), hydrochloric acid ( $\text{HCl}$ ), sulphuric acid ( $\text{H}_2\text{SO}_4$ ), iodine resublimed ( $\text{I}_2$ ), sodium potassium tartarate (Rochelle salt), di-nitrosalicylic acid, silica gel and ammonium per sulphate.	SD fine Chemicals (Ind.) Ltd.
1-Naphthol, hippuric acid, Coomassie brilliant blue R 250, $\beta$ -mercaptoethanol, bromophenol, trichloro acetic acid, sodium benzoate, sodium dodecyl sulfate, gum acacia and triton X-100	LOBA Chemie Pvt. Ltd. India.
Hippuryl-L-histidyl-L-leucine acetate, 2,2-diphenyl-1-picrylhydrazyl (DPPH), butylated hydroxyanisole (BHA), bovine serum albumin (BSA), Sephadex G-15	Sigma Chemical Co., St. Louis, MO, USA.



and Sephadex G-25, acrylamide, tributyrin, sodium alginate and bis-acrylamide

Potassium bromide (KBr), Folin-Cicolteau reagent and HEPES buffer (N-[2-hydroxyethyl] piperazine-N'-[2-ethanesulphonic acid]) Sisco Research Laboratories Pvt. Ltd. India.

---

## 2.2 Methods

### 2.2.1 Enzyme activity assay for amyloglucosidase

Enzyme activity for amyloglucosidase was determined using Sumner and Sisler (1944) method. Activity was expressed in terms of micromoles ( $\mu\text{mol}$ ) of glucose released per min per mg of enzyme employed. Specific activity was expressed as  $\mu\text{mol}$  of glucose released per min per mg of protein present in the enzyme (Table 2.2).

#### 2.2.1.1 Calibration

A stock solution was prepared by dissolving 25 mg of D-glucose in 25 mL of distilled water. A series of aliquots of 0.1 to 1.5 mL were pipetted out into appropriate volumes of 0.2 M sodium acetate buffer pH 4.2 such that, the final volume was 3.0 mL. To this 3.0 mL of di-nitro salicylic acid (DNS) reagent (Sumner and Sisler 1944) containing 1% di-nitro salicylic acid, 0.2% phenol, 0.05% sodium sulphite and 1% NaOH was added and the reaction mixture was incubated on a boiling water bath for 5 min with shaking. Then the reaction mixture was cooled under running tap water. Absorbance of each solution was determined on a Shimadzu UV-1601 Spectrophotometer at 575 nm. A calibration plot was constructed for the concentration of glucose in the range 0.1 mg to 1.5 mg (Fig. 2.1).

#### 2.2.1.2 Activity assay

A stock solution of 4% starch was prepared by dissolving 4 g of potato starch in 100 mL 0.2 M acetate buffer pH 4.2. Enzyme amyloglucosidase (1 mg) was added separately into 5.0 mL of stock solution and incubated at 60 °C on a Heto-Holten

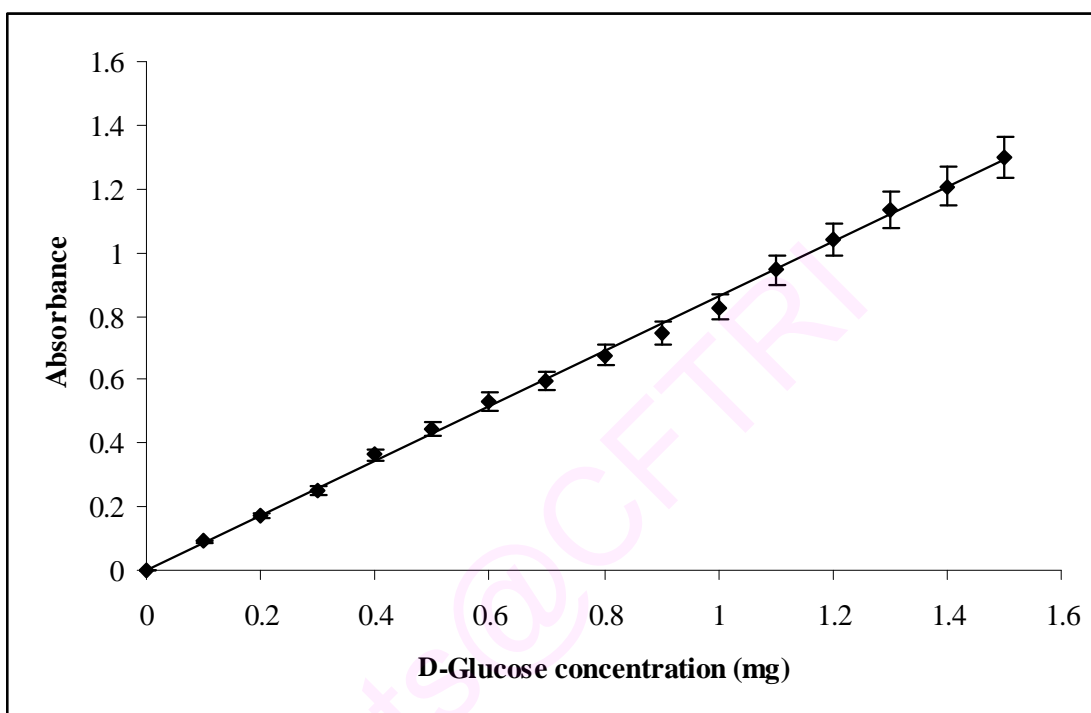


**Fig. 2.1** Calibration plot for D-glucose. A stock solution of 25 mg/25 mL D-glucose solution was used for considering 0.1 to 1.5 mL aliquots. Absorbance was measured at 575 nm.

shaking water bath for 60 min at 200 rpm. The reaction was arrested by adding 0.8 mL 4 N NaOH. A duplicate was also performed. Pipetted out 0.1 mL of this solution and made up to 3.0 mL using 0.2 M acetate buffer pH 4.2. Further 3 mL of DNS reagent was added and boiled for 5 min on a water bath and cooled. Absorbance values were measured at 575 nm using a Shimadzu UV-1601 Spectrophotometer and the amount of glucose present was determined from the calibration plot. The activity of each enzyme was evaluated and shown in Table 2.2.

**Table 2.2** Activity assay for amyloglucosidase,  $\beta$ -glucosidase and immobilized  $\beta$ -glucosidase

Enzyme	Protein content <sup>a</sup> (%)	Unit activity mol/min/mg of enzyme	Specific activity mol/min/mg of protein
Amyloglucosidase <sup>b</sup>	46.2	$11.2 \times 10^{-6}$	$24.3 \times 10^{-6}$
$\beta$ -Glucosidase <sup>c</sup>	76.9	$3.12 \times 10^{-3}$	$4.06 \times 10^{-3}$
Immobilized $\beta$ -glucosidase <sup>c</sup>	4.2	$0.084 \times 10^{-3}$	$1.99 \times 10^{-3}$

<sup>a</sup>Protein estimation by Lowry's method. <sup>b</sup>Activity assay by Sumner and Sisler method. <sup>c</sup>Activity assay by Colowick and Kaplan (1976).

### 2.2.2 Protein estimation

Protein content of amyloglucosidase,  $\beta$ -glucosidase (isolated from sweet almonds) and immobilized  $\beta$ -glucosidase were determined by using Lowry's method (Lowry *et al.* 1951). In order to leach out the protein from the immobilized matrix or carrier, 25 mg of enzyme (amyloglucosidase,  $\beta$ -glucosidase and immobilized  $\beta$ -glucosidase) in 50 mL, 0.5 M NaCl was stirred at 4 °C for 12 h and from this, known volumes of the samples were taken for protein estimation.

Solution **A** – 1% of copper sulphate in water, solution **B** – 1% of sodium potassium tartarate in water and solution **C** – 2% of sodium carbonate solution in 0.1 N NaOH were prepared. Working solution **I** was prepared by mixing one part each of solution **A** and **B** and 98 parts of **C**. A 1:1 diluted solution of commercially available

Folin-Cicolteau reagent with distilled water served as working solution **II**. To the protein sample in 1 mL water, 5 mL of working solution **I** was added and incubated for 10 min at room temperature. A 0.5 mL of working solution **II** was then added followed by incubation at room temperature for 30 min and the absorbance was measured at 660 nm using a Shimadzu UV – 1601 spectrophotometer. Calibration plot for protein concentration was prepared by employing bovine serum albumin (BSA) in the concentration range 0-100 µg in 6.5 mL of the sample (Fig. 2.2). Using this calibration plot, protein content of the glycosidases was determined and the values are shown in Table 2.2.

### 2.2.3 Extraction of $\beta$ -glucosidase

About 1 kg of finely powdered defatted sweet almond powder was dispersed in a solution of 50 g of  $\text{ZnSO}_4 \cdot 7\text{H}_2\text{O}$  in 4 L of water and left standing at 0 °C for 4 to 5 h (Hestrin *et al.* 1955). The cold solution was then filtered through cloth and well pressed on the filter. To the filtrate was cautiously added, a solution of 1.4 g tannin (0.28%) in 500 mL water. A precipitate consisting mostly of impurities was removed by centrifugation and discarded. The bulk of the enzyme was then precipitated slowly by adding 500 mL of 3% tannin solution (15 g/500 mL) in water. The precipitate was removed by centrifugation, freed from tannin by repeatedly dispersing it in acetone and centrifuging it to get crude powder. The crude powder was dialyzed using 3.5 kDa membrane and finally lyophilized to get a dry powder.

$\beta$ -Glucosidase, 10.3 g, was obtained from 1 Kg of almond powder. Protein content determined by Lowry's method was found to be 76.9% and activity determined by Colowick and Kaplan (1976) method was found to be 3.12 mmol/min/mg of enzyme (Table 2.2).

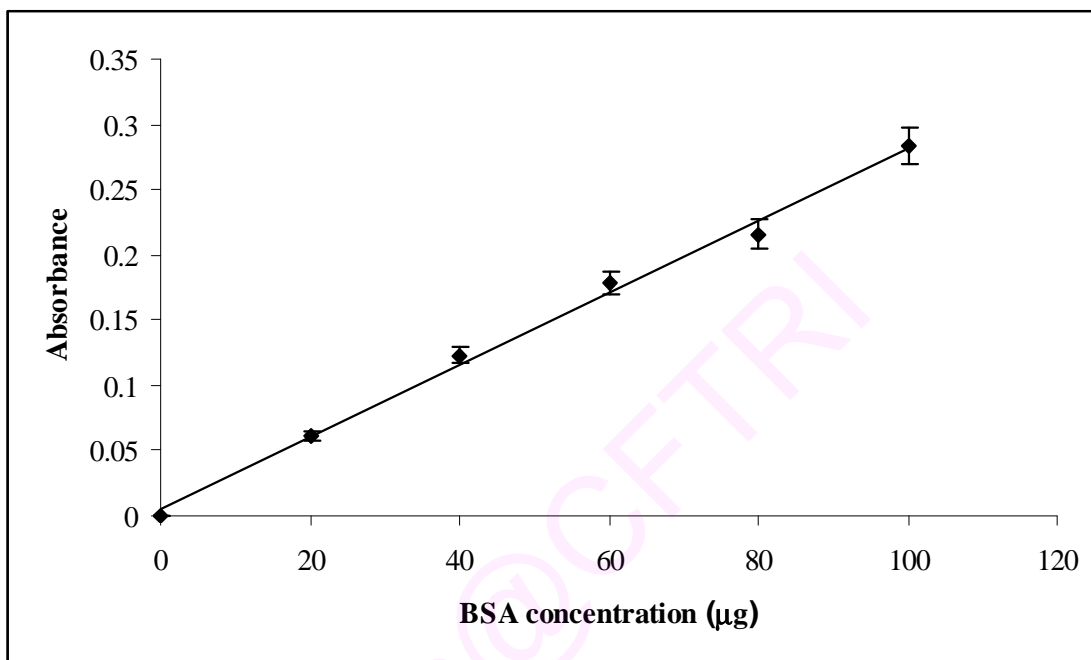


**Fig. 2.2** Calibration curve for the estimation of protein by Lowry's method. A stock solution of 1mg / 10 mL BSA solution was prepared. From the stock solution 0.1 - 1.0 mL solutions were pipetted out and the total volume was made upto 1.0 mL with distilled water. This was then treated with solutions described in Section 2.2.2. Absorbance was measured at 660 nm.

## 2.2.4 Immobilization of $\beta$ -glucosidase

Immobilization of the isolated  $\beta$ -glucosidase was carried out according to the method described by Won *et al.*, (2005) by entrapping  $\beta$ -glucosidase on calcium-alginate beads. A 200 ml of 1 g  $\beta$ -glucosidase solution was mixed with 800 ml of 1 % sodium alginate. The mixture was stirred thoroughly to ensure complete mixing. Mixed solution was then drawn with a syringe into 1 L of 50 mM  $\text{CaCl}_2$  solution through a needle of 0.5 mm diameter. The beads formed were allowed to harden for 30 minutes. The  $\text{CaCl}_2$  solution was separated from beads by filtration. They were then washed twice with 50 mM Tris-HCl buffer (pH 7.2). Calcium alginate beads obtained were lyophilized. A yield of 3.92 g immobilized  $\beta$ -glucosidase was obtained.

The protein content determined by Lowry method (Section 2.2.2) was found to be 4.2% and activity determined by Colowick and Kaplan (1976) method was found to be 0.084 mmol/min/mg of enzyme (Table 2.2).

### 2.2.4.1 Activity assay

$\beta$ -Glucosidase (EC 3.2.1.21) and immobilized  $\beta$ -glucosidase was assayed by the method of Colowick and Kaplan (1976). A volume of 10 mL, 25 mM p-nitrophenyl- $\beta$ -D-glucopyranoside was prepared in 50 mM sodium acetate buffer, pH 5.5. A known amount of the enzyme was added into 0.25 mL of the freshly prepared p-nitrophenyl- $\beta$ -D-glucopyranoside solution and incubated at 30 °C for a definite intervals. To follow the course of the reaction, aliquots of the reaction mixture were treated with 0.7 mL of sodium carbonate (200 mM) and the p-nitrophenol concentration was determined from a calibration plot from the absorbance measured using a Shimadzu UV – 1601 spectrophotometer at 420 nm (Table 2.2). A calibration plot was constructed by employing p-nitrophenol in the 0 to 45  $\mu\text{g}$  concentration range (Fig. 2.3).

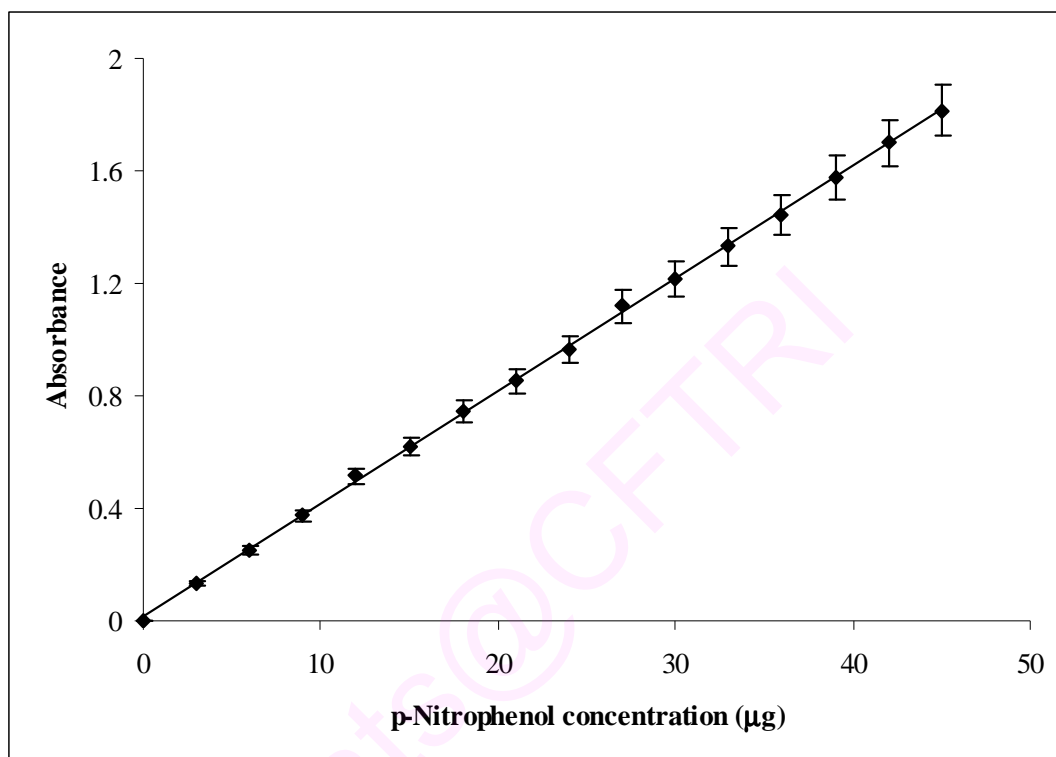


**Fig. 2.3** Calibration plot for the determination of p-nitrophenol concentration by  $\beta$ -glucosidase activity. A stock solution of 3 mg/ 10 mL p-nitrophenol concentration was prepared from which different aliquots of concentrations 0 to 45  $\mu$ g were pipetted out and made up to 2.5 mL. Absorbance was measured at 420 nm.

### 2.2.5 Preparation of buffers

A buffer concentration of 10 mM  $\text{CH}_3\text{COONa}$  for pH 4.0 and 5.0,  $\text{Na}_2\text{HPO}_4$  for pH 6.0 and 7.0 and  $\text{Na}_2\text{B}_4\text{O}_7 \cdot 10\text{H}_2\text{O}$  for pH 8.0 buffers were prepared by dissolving appropriate quantities of the respective buffer salts in distilled water and the pH was adjusted by adding 0.1 M of HCl or NaOH. A Control Dynamics pH meter model APX175E/C, India was employed for measuring the pH of the solutions.

### 2.2.6 Glycosylation procedure

Reflux method was employed for the preparation of all the glycosides described in the present work. In the reflux method, the carbohydrate and phenol/vitamin of known concentrations were taken along with appropriate quantities of amyloglucosidase,  $\beta$ -glucosidase and immobilized  $\beta$ -glucosidase (% w/w carbohydrate) in a 150 mL two-necked flat-bottomed flask. A known concentration of buffer of 0.01M (pH 4.0 to 8.0) was added and then refluxed in 100 mL di-isopropyl ether with stirring for a specified period of incubation, usually 72 h unless otherwise specified. The product workup for vanillyl and N-vanillyl-nonanamide glycosides involved extracting the reaction mixture with chloroform to remove unreacted vanillin and N-vanillyl-nonanamide. In case of curcuminyl and riboflavinyl glycosides the reaction mixture were extracted using 20-30 mL of water and further filtered through Whatmann filter paper No.1 to remove the unreacted curcumin and riboflavin. The filtrate and the extracted reaction mixture (in case of vanillyl and N-vanillyl-nonanamide) were evaporated to dryness to get the unreacted carbohydrate and the product glycoside. For ergocalciferol and  $\alpha$ -tocopherol glycosides, the reaction mixture was extracted with hexane to remove unreacted ergocalciferol and  $\alpha$ -tocopherol. The reaction mixtures containing unreacted carbohydrate and the product glycosides were analyzed by HPLC.



## 2.2.7 Analysis

### 2.2.7.1 High Performance Liquid Chromatography

The reaction mixtures were analyzed by high performance liquid chromatography (HPLC) on a Shimadzu LC 8A instrument using a  $\mu$ -Bondapak amino-propyl column (10  $\mu$ m particle size, 300 mm  $\times$  3.9 mm) and acetonitrile: water in 70:30 v/v (unless otherwise mentioned in specific cases) as the mobile phase at a flow rate of 1mL/min and detected using refractive index detector. Retention times for carbohydrates were in the range 4.9 to 11.5 min and for glycosides 7.5 to 17.9 min range. Conversion yields were determined from HPLC peak areas of the glycoside and free carbohydrates and percentage conversions were expressed with respect to the carbohydrate concentration employed. Error measurements in HPLC yields will be  $\pm$  5-10%.

### 2.2.7.2 Thin Layer Chromatography

A chloroform:methanol:water:pyridine (65:30:4:1v/v) solvent system was used as a mobile phase for TLC on plates coated with 40% silica gel. The spots were detected by spraying a solution containing 1.6 g of  $\alpha$ -naphthol dissolved in 50 mL of ethanol, 5 mL of water and 6.5 mL of 18 M of sulfuric acid and heating at 100 °C in an oven for 5 min (Ismail *et al.* 1998).

## 2.2.8 Separation of glycosides

Synthesized glycosides were separated from the reaction mixture by column chromatography. Sephadex G15 and Sephadex G25 column materials were employed. A sample concentration of 100 to 200 mg was loaded on to the column (100x 1cm) and eluted with water at a flow rate of 2 mL/h. Various fractions were collected and the separation was monitored by thin layer chromatography (TLC). Product glycoside fractions were pooled, evaporated on a water bath and subjected to characterization. Although chromatographic separation resulted in separating glycosides from unreacted

carbohydrate molecules, further separation of the individual glycosides was not possible with Sephadex G15 or any other column material employed because of similar polarity of the glycosides in the product mixture.

### **2.2.9 Spectral characterization**

#### **2.2.9.1 UV-Visible spectroscopy**

Ultraviolet-Visible spectra were recorded on a Shimadzu UV-1601 spectrophotometer. Known concentration of the sample dissolved in the indicated solvent was used for recording the spectra.

#### **2.2.9.2 Infrared spectroscopy**

Infrared spectra were recorded on a Nicolet-FTIR spectrophotometer. Isolated solid glycoside samples (5-8 mg) were prepared as a KBr pellet and employed for spectral recording. Liquid alcohol standards were employed as such between salt plates to obtain the IR spectra.

#### **2.2.9.3 Mass spectroscopy**

Mass spectra were obtained using a Q-TOF Waters Ultima instrument - Q-ToF GAA 082, Waters corporation, Manchester, UK, fitted with an electron spray ionization (ESI) source. A software version 4.0 was used for data acquisition. A positive ion mode using a spray voltage at 3.5 kV and a source temperature of 80 °C was employed for recording the spectra. Mass spectra were recorded under electron impact ionization at 70 eV electron energy. Samples were prepared in the concentration range of 0.5-1.0 mg/mL in distilled water and injected by flow injection analysis at a flow rate of 10 µL/min. The recorded mass of the sample were in the range of 100-1500.

#### **2.2.9.4 Polarimetry**

Optical rotations of the isolated glycosides were recorded on a Perkin-Elmner 243 Polarimeter. Sodium lamp at 599 nm was used as the light source. Sample

concentration of 0.5 to 1% in H<sub>2</sub>O was used for the rotation measurements and specific rotations were calculated using the equation.

$$[\alpha]_D^{25^\circ\text{C}} = \frac{[\alpha]_{\text{obs}} \times 100}{C \times l}$$

where,  $[\alpha]_D$  is the specific rotation in degrees at 25 °C,  $[\alpha]_{\text{obs}}$  is the observed rotation, C is the concentration of the sample in percentage and l is the path length in dm.

#### 2.2.9.5 Melting point

Melting point of the glycosides was determined by capillary method. A thin walled capillary tube 10-15 cm long of about 1 mm inside diameter sealed at one end containing the sample was employed. The sample capillary was pressed gently into the sample several times and then pushed to the bottom of the tube by repeatedly dropping onto a table through a glass tube of 1m in length. The sample capillary was tightly packed to a depth of 2-3 mm. The capillary, containing the sample was pressed on to a thermometer and then suspended into paraffin is heated slowly and evenly with the help of burner flame. A narrow temperature range over which the sample was observed to melt was taken as the melting point.

#### 2.2.9.6 NMR

##### <sup>1</sup>H NMR

<sup>1</sup>H spectra were recorded on a Bruker DRX 500 MHz NMR spectrometer (500.13MHz). Proton pulse width was 12.25 μs. Sample concentration of about 40 mg of the sample dissolved in DMSO-*d*<sub>6</sub> was used for recording the spectra at 35 °C. About 100-200 scans were accumulated to get a good spectrum. The region between 0-10 ppm was recorded for all the samples. Chemical shift values were expressed in ppm relative to internal tetra-methyl silane (TMS) as the standard.

## **<sup>13</sup>C NMR**

<sup>13</sup>C NMR spectra were recorded on a Bruker DRX 500 MHz NMR spectrometer (125MHz). Carbon 90° pulse widths was 10.5 μs. Sample concentration of about 40 mg dissolved in DMSO-*d*<sub>6</sub> was used for recording the spectra at 35 °C. About 500 to 2000 scans were accumulated for each spectrum in the 0-200 ppm region. Chemical shift values were expressed in ppm relative to internal tetramethyl silane (TMS) as the standard.

## **2D-HSQCT**

Two-dimensional Heteronuclear Single Quantum Coherence Transfer Spectra (2D HSQCT) were recorded on a Bruker DRX 500 MHz NMR spectrometer. A sample concentration of about 40 mg in DMSO-*d*<sub>6</sub> was used for recording the spectrum. Spectra were recorded in magnitude mode with the sinusoidal shape *Z* gradients of strength 25.7, 15.42 and 20.56 G/cm in the ratio of 5:3:4 applied for a duration of 1 ms each with a gradient recovery delay of 100 μs to defocus unwanted coherences. Then it was incremented in 256 steps. The size of the computer memory used to accumulate the 2D data was 4K. The spectra were processed using unshifted and  $\pi/4$  shifted sine bell window function in *F*<sub>1</sub> and *F*<sub>2</sub> dimensions respectively.

### **2.2.10 Antioxidant activity by DPPH method**

Antioxidant activity of the glycosides were determined by DPPH (2,2-Diphenyl-1-picrylhydrazyl) radical scavenging method (Moon and Terao 1998). Absorbance of a solution in duplicate, containing 0.1 mL of test sample (5-10 mM), 1.0 mL of DPPH (0.36 mM in ethanol) was measured with the final volume made upto 2.0 mL with 0.1 M Tris-HCl buffer (pH 7.4). After incubation at room temperature for 20 minutes in dark, absorbance was measured at 517 nm on a UV-Visible Shimadzu, UV 1601 spectrophotometer. Decrease in absorbance compared to DPPH itself was a measure of

the radical scavenging ability of the test sample. Butylated hydroxyanisole (BHA, 5.55 mM) was used as a positive control. Error in the measurements will be  $\pm 5\%$ . IC<sub>50</sub> value was expressed as the amount of the glycoside required to reduce 50% of the absorbance value of DPPH. Antioxidant activities for the phenolic and vitamin glycosides were in the range of  $0.5 \pm 0.03$  mM to  $2.66 \pm 0.13$  mM.

#### **2.2.11 Extraction of angiotensin converting enzyme (ACE) from pig lung**

ACE was extracted from pig lung (Sanchez *et al.* 2003). A 250 g of pig lung was minced and homogenized using a blender with 10 mM pH 7.0 HEPES buffer containing 0.4 M NaCl at a volume ratio of 5:1 (v/w of pig lung). The temperature was maintained at 4 °C throughout the procedure. The homogenate was centrifuged at 9000 g for 60 min. The supernatant was discarded and the precipitate was washed twice with 200 mL of 10 mM pH 7.0 HEPES buffer containing 0.4 M NaCl. The final precipitate was resuspended in 200 mL of pH 7.0, 10 mM HEPES buffer containing 0.4 M NaCl, 10  $\mu$ M ZnCl<sub>2</sub> and 0.5% (w/v) triton X-100 and stirred over night. The solution was centrifuged to remove the pellet. The supernatant was dialyzed against water using a dialysis bag of molecular weight cut off 10 kDa and later lyophilized. A 14 g of crude ACE was obtained from 250 g of pig lung.

#### **2.2.12. Angiotensin converting enzyme (ACE) inhibition assay**

ACE inhibition assay for the glycosides prepared were performed by the Cushman and Cheung (1971) method. Aliquots of glycoside solutions in the concentration range 0.2 to 1.8 mM (0.1 mL to 0.8 mL of 2.0 mM stock solution) were taken and to this 0.1 mL of ACE solution (0.1% in 0.1 M phosphate buffer, pH 8.3 containing 0.3 M NaCl) was added. To this solution further 0.1 mL of 2.5 mM hippuryl-L-histidyl-L-leucine (HHL) was also added and the total volume made upto 1.25 mL with phosphate buffer (0.1 M pH 8.3 containing 0.3 M NaCl). The solution was incubated on

a Heto-Holten shaking water bath for 30 min at 37 °C. Blanks were performed without the enzyme by taking only the glycoside solution (0.1 to 0.8 mL) along with 0.1 mL of 5.0 mM HHL. The total volume was made up to 1.25 mL with the same buffer. The reaction was terminated by adding 0.25 mL of 1 M HCl. Hippuric acid formed in the reaction was extracted with 1.5 mL of ethyl acetate. One mL of ethyl acetate layer was evaporated to dryness and treated with equal amount of distilled water and the absorbance was measured at 228 nm for hippuric acid. Hippuric acid formed in 1.5 mL of ethyl acetate was determined from a calibration curve using standard 0-280 nmol hippuric acid solution in 1 mL of distilled water (Fig. 2.4). Specific activity was expressed as  $\mu\text{mol}$  of hippuric acid formed per min per mg of enzyme protein.

$$\text{Specific activity} = \frac{A_{\text{ts}} - A_{\text{blank}}}{T \times S \times E}$$

$A_{\text{ts}}$  = absorbance of test solution,  $A_{\text{blank}}$  = absorbance of blank solution, T = incubation period in min, S = slope value of the calibration plot, E = amount of the enzyme in mg protein.

Percentage inhibition was expressed as the ratio of the specific activity of ACE in the presence of the inhibitor to that in its absence, the latter being considered as 100%.  $\text{IC}_{50}$  value was expressed as the concentration of the inhibitor required for 50% reduction in ACE specific activity. Molecular weights of the glycosides employed in the calculations are weighted averages of molecular weights of glycosides estimated by NMR spectroscopy.

### 2.2.13 Protease activity

Hydrolyzing activity of the protease in ACE was carried out using bovine hemoglobin as substrate (Dubey and Jagannadham 2003). To 0.5 mL of enzyme solution, 0.5 mL of 0.6% (w/v) substrate was added and the reaction was allowed to proceed for

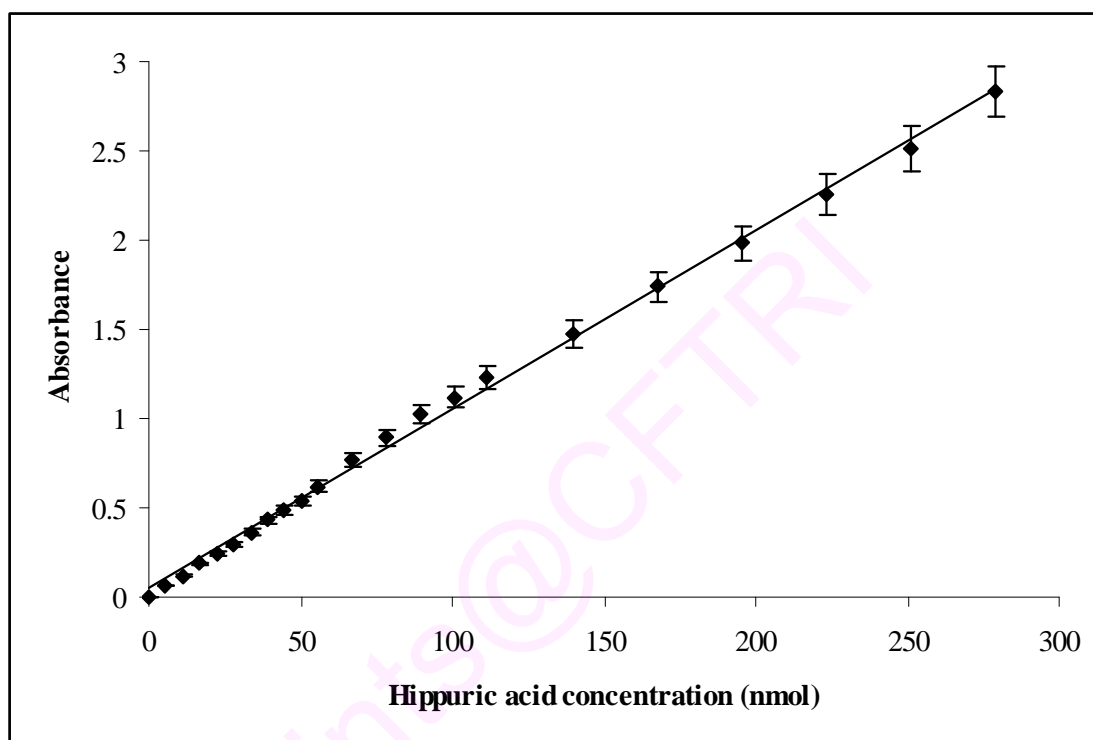


**Fig. 2.4** Calibration plot for hippuric acid estimation by the spectrophotometric method. A stock solution of  $5.58 \times 10^{-6}$  mol hippuric acid in water was prepared from which different aliquots of concentrations 0 to 280 nmol were pipetted out and made up to 1.0 mL. Absorbance was measured at 228 nm

30 min at 37 °C. The reaction was terminated by the addition of 0.5 mL of 10% trichloro acetic acid and allowed to stand for 10 min. The resulting precipitate was removed by centrifugation at 20000 g for 15 min. A 0.5 mL of supernatant was taken and mixed with equal volume of 0.5 M NaOH and the color developed was measured by absorbance at 440 nm. A control assay without the enzyme was carried out and used as a blank. Inhibitory activity was measured out by adding 0.5 mL of inhibitor solution to 0.5 mL of enzyme solution. To this was added 0.5 mL of hemoglobin solution and incubated at 37 °C for 30 min.

One unit of enzyme activity was expressed as the amount of enzyme under given assay conditions required to increase one unit absorbance at 440 nm per min digestion. Number of units of activity per milligram of protein was considered as the specific activity of the enzyme.

$$\text{Activity} = \frac{A_{\text{sample}} - A_{\text{blank}}}{T \times E}$$

$A_{\text{sample}}$  = Sample absorbance at 440 nm,  $A_{\text{blank}}$  = Blank absorbance at 440 nm, T = Time in min, E = mg enzyme protein

#### 2.2.14 Lipase activity

Lipase activity was determined by the tributyrin method (Vorderwulbecke *et al.* 1992). A stock solution containing 10 mL of tributyrin, 90 mL of 0.01 M pH 7.0 sodium phosphate buffer, 0.2 g sodium benzoate, 0.5 g of gum acacia and 50 µL 10% SDS was prepared. It was emulsified by stirring and the pH was adjusted to 7.0 with concentrated NaOH. From this stock solution, 4 mL was pipetted out into stoppered conical flasks (S), containing 8 mL, 0.01 M pH 7.0 sodium phosphate buffer to obtain a solution with a final concentration of 0.113 M tributyrin. Known quantities of enzyme (5 –15 mg) were



added to this solution and incubated at 37 °C in a Heto-Holten shaker water bath for different intervals of time. After incubation, the pH of the reaction mixture in the flask was titrated to 9.5 with standard 0.04 N NaOH. A blank (B) was also performed without adding enzyme. The hydrolytic activity was evaluated by using the following equation.

$$\text{Hydrolytic activity} = \frac{(S-B) \times N}{1000 \times E \times T} \quad \mu \text{ mol}/(\text{min.mg of enzyme preparation or protein})$$

Where, (S-B) = difference in volume of NaOH in mL between sample (S) and blank (B), N= normality of NaOH, E = amount of enzyme preparation or protein taken in mg and T= incubation period in min.

#### 2.2.15 Gel electrophoresis of glycosidases and ACE

Sodium dodecyl sulphate-polyacrylamide gel electrophoresis (SDS-PAGE) was carried out to check the purity of glycosidases and ACE employed in the present work. SDS-PAGE was carried out according to the method described by Lamelli (1970) in a discontinuous buffer system.

The following reagents were prepared.

- A. Acrylamide (29.2 g) and bis-acrylamide (0.8 g) were dissolved in 100 mL water filtered and stored in a dark brown bottle at 4 °C (amounting to 30% acrylamide solution).
- B. Separating gel buffer (18.1 g) was dissolved in water and the pH of the solution was adjusted to 8.8 with HCl. Then the solution was made upto 100 mL and stored at 4 °C.
- C. Stocking gel buffer – Tris-HCl (3.0 g) was dissolved in water, pH of the solution was adjusted to 6.8 with HCl (6.0 N) and made upto 100 mL in water.
- D. Sodium dodecyl sulphate (SDS), 10 g was dissolved in 100 mL water

- E. Ammonium persulphate was freshly prepared by dissolving 50 mg in 0.5 mL of distilled water.
- F. Tank buffer – Tris-HCl (0.3 g), glycine (1.44 g) and SDS (0.15 g) were dissolved in 150 mL of water.
- G. Staining solution – A 0.2 g of Coomassie brilliant blue R 250 was dissolved in a mixture of methanol: acetic acid : water (25: 15: 60 v/v/v). The reagent was filtered and stored in room temperature.
- H. Destaining solution – methanol: acetic acid: water (25: 15: 60 v/v/v).
- I. Sample buffer was prepared in solution C diluted to 1:4 containing 4% w/v SDS, 10% v/v  $\beta$ -mercaptoethanol, 20% v/v glycerol and 0.1% bromophenol blue.

Preparation of separating gel (10% T, 2.7% C) – A 2.6 mL of A, 2.0 mL of B, 3.31 mL of distilled water, 0.05 mL of D and 0.03 mL of solution E were mixed and then degassed and poured between the assembled glass plates sealed with agar (2% w/v). The gels were layered with 0.5 mL of distilled water and allowed to polymerize at room temperature for 30 min.

A stock solution (5% T, 2.7% C) was prepared by mixing the solutions of 0.83 mL of A, 1.25 mL of C, 3.0 mL of distilled water, 0.05 mL of solution D, 0.01 mL of TEMED and 0.03 mL of E and poured above the polymerized gel. The gel thus prepared were of the size 10.5 x 9.0 cm and thickness 0.8 mm.

Glycosidase and ACE samples were prepared by dissolving 25 mg of protein in solution 'I' (50  $\mu$ L). The samples were heated in a boiling water bath for 10 min, after which the samples were loaded onto the wells immersed in solution F (tank buffer) and were run at a constant voltage of 40 Volts until the tracking dye, bromophenol blue was just (0.5 cm) above the lower end of the gel. Medium range protein markers phosphorylase (97.4 kDa), bovine serum albumin (66.3 kDa), ovalbumin (43.0 kDa) and

carbonic anhydrase (29.0 kDa) were used. The markers were supplied as a solution having each protein at a concentration of 0.5 to 0.8 mg/mL. The markers were 1:1 diluted with solution I and boiled prior to use. Later, the gel was stained for protein with reagent 'G' for 6 h at room temperature followed by destaining in reagent H.

A plot was constructed by plotting  $R_f$  values of molecular marker on X-axis and  $\log M_r$  values of each molecular marker on Y-axis (Fig 2.5). From this plot molecular weight of the unknown protein was determined. Enzyme amyloglucosidase from *Rhizopus* sp. (obtained from Sigma),  $\beta$ -glucosidase, isolated from sweet almonds and molecular weight markers were subjected to SDS-PAGE and stained with Coomassie brilliant blue R 250 (Fig. 2.6A). Lane 1 contained amyloglucosidase, showing molecular masses 72.4 kDa, 60.3 kDa, 58.6 kDa along with other protein contaminants having molecular masses 43.6 kDa, 39.8 kDa and 31.6 kDa. Molecular masses 72.4 kDa, 60.3 kDa and 58.6 kDa showed good correspondence to the GA-I (72.4 kDa), GA-II (58.6 kDa) and GA-III (61.4 kDa) reported by Takahashi *et al.* (1985).

Lane 2 contained  $\beta$ -glucosidase isolated from sweet almonds showing a single band of molecular mass 64.6 kDa, which is in good correspondence with the one active component of molecular mass 66.5 kDa reported by Helferich and Kleinschmidt (1965).

ACE showed a molecular mass 152 kDa corresponding to 150 kDa reported by Lee *et al.* (1971) along with the other protein contaminations (Fig. 2.6 B, Lane 1).

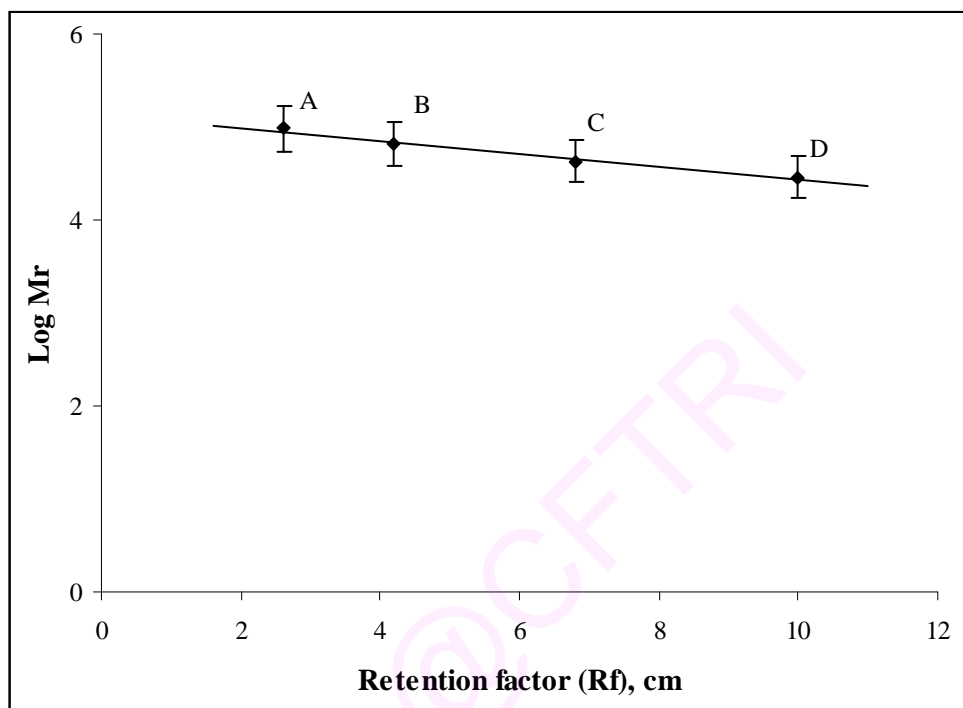


**Fig. 2.5** Log  $M_r$  versus  $R_f$  plot . (A) Phosphorylase (97.4 kDa), (B) BSA (66.3 kDa), (C) Ovalbumin (43.0 kDa), (D) Carbonic anhydrase (29.0 kDa).

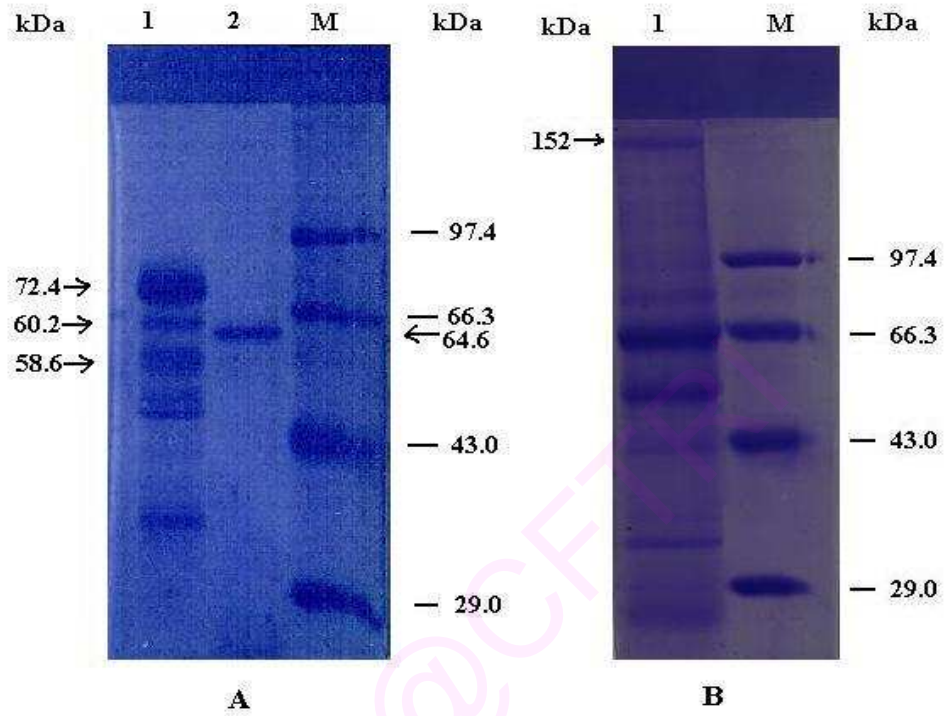


**Fig. 2.6** SDS-PAGE (A) Lane 1 for amyloglucosidase from *Rhizopus* sp. (from Sigma), Lane 2 for  $\beta$ -glucosidase isolated from sweet almond, Lane M for M<sub>r</sub> standard proteins: Phosphorylase (97.4 kDa), BSA (66.3 kDa), Ovalbumin (43.0 kDa) and Carbonic anhydrase (29.0 kDa), (B) Lane 1 for ACE isolated from pig lung.

ePrints@CFTRI

### ***Chapter 3***

***Enzymatic syntheses of vanillin, N-vanillyl-nonanamide, curcumin, DL-dopa and dopamine glycosides***

## Introduction

Glycosylation of phenols in a regioselective manner involving carbohydrates is a quite challenging synthetic task because of several hydroxyl groups in these molecules (Haines 1976). Glycosyl transfer reactions for the synthesis of glycosides can be carried out under thermodynamically or kinetically controlled conditions (Ichikawa *et al.* 1992; Rantwijk *et al.* 1999). Reverse hydrolytic method is thermodynamically controlled (Chahid *et al.* 1992; Ismail and Ghoul 1996; Vic *et al.* 1996; Ljunger *et al.* 1994) and transglycosylation is a kinetically controlled reaction wherein glycoside (for example disaccharide) is used as a glycosyl donor (Stevenson *et al.* 1993; Ismail *et al.* 1999a). The process of glycosylation can be effected under non-aqueous, solvent free conditions, high substrate, high temperature and moderate to high water activity to yield glycosides (Gygax *et al.* 1991; Laroute and Willemot 1992a; Vic and Thomas 1992; Shin *et al.* 2000; Vijayakumar and Divakar 2005; Vijayakumar *et al.* 2007).

Synthesis of glycosides has generated much interest because of their broad range of applications in food and pharmaceutical industries (Matsumura *et al.* 1990; Balzar 1991). Many phenols exhibit pharmacological properties. For example vanillin, primarily a flavor, possesses antimicrobial (Lopez-Malo *et al.* 1998), anticarcinogenic (Stephan and Peter 2003), antioxidant (Burri *et al.* 1983), antifungal (Fitzgerald *et al.* 2005) and antimutagenic (Kometani *et al.* 1993b) activities. Capsaicin, a fat soluble and an irritant principle of hot pepper, exhibits extensive role in energy metabolism (Henry and Emery 1986). N-Vanillyl-nonanamide, a synthetic analogue of capsaicin also possesses similar pharmacological properties like natural capsaicin. Curcumin, a yellow pigment of turmeric from *Curcuma longa*, is primarily used as a food colorant which possesses potent anti-oxidative, anti-inflammatory and anti-leishmanial (Gomes *et al.* 2002) activities (Hergenhahn *et al.* 2002; Kaminaga *et al.* 2003; Mohri *et al.* 2003). DL-Dopa

(DL-3,4-dihydroxyphenylalanine) and dopamine (3,4-dihydroxyphenylethylamine) potent neurotransmitters, are used in Parkinson's disease (Bonina *et al.* 2003). Also, glycosyl derivatives of dopamine and DL-dopa are synthesized to overcome the problem of blood-brain barrier flow permeability of dopamine and low bioavailability of its precursor, L-dopa.

Biological activities are primarily due to aglycon of the glycosides. However, their extensive uses in pharmacological application are restricted by their low water solubility, cell permeability, irritability and low bio-availability. All these properties can be improved by glycosylation, which enhances all these characteristics (Suzuki *et al.* 1996; Seung-Heon *et al.* 2004; Kren 2001).

Hence, glycosylation of the above mentioned aglycons vanillin, N-vanillyl-nonanamide, curcumin, DL-dopa, dopamine are investigated in the present work. All these phenols possess a common structural motif. They are all 3,4-dihydroxy phenyl derivatives, with a substituent *para* to the hydroxyl group at position 4 of the phenyl ring. The groups *para* to the phenolic OH at the 4<sup>th</sup> position are CHO or –CH=CH– or –CH<sub>2</sub>. The present work has extensively investigated the efficiency of glycosylation of these aglycons by amyloglucosidase and  $\beta$ -glucosidase. The results are presented below.

### **Present work**

The present chapter describes optimization and syntheses of selected phenolic glycosides of vanillin **1**, N-vanillyl-nonanamide **2**, curcumin **3**, DL-dopa **4** and dopamine **5** by reflux method using amyloglucosidase from *Rhizopus* mold and  $\beta$ -glucosidase from sweet almond in di-isopropyl ether solvent. The carbohydrate molecules employed for the glycoside preparations are: aldohexoses - D-glucose **6**, D-galactose **7**, D-mannose **8**, ketohexose - D-fructose **9**, aldopentoses - D-arabinose **10**, D-ribose **11**, disaccharides - maltose **12**, sucrose **13**, lactose **14**, sugar alcohols - D-sorbitol **15** and D-mannitol **16**.



Glycosylation reaction was conducted in the presence of a buffer employing acetate buffer (0.01 M) for pH 4 and 5, phosphate buffer (0.01 M) for pH 6 and 7 and borate buffer (0.01 M) for pH 8. The reactions were investigated in terms of incubation period, pH, buffer, enzyme and substrate concentrations, regio and stereo selectivity. All the experiments were performed in duplicate. Unless otherwise stated the glycosides prepared were analyzed by HPLC on an aminopropyl column (300 mm × 3.9 mm) eluted with 80:20 (v/v) acetonitrile:water at a flow rate of 1 mL/h and monitored using a RI detector. Conversion yields were determined from HPLC peak areas of the glycoside and free carbohydrate and expressed with respect to free carbohydrate concentration. Error based on HPLC measurements are of the order of  $\pm 10\%$ . Glycosides were subjected to column chromatography using Sephadex G25/G15/G10 columns (100 × 1 cm), eluting with water at 1 mL/h rate. Although the glycosides were separated from unreacted carbohydrates by these procedures, individual glycosides could not be isolated in pure forms due to similar polarity of these molecules.

The isolated glycosides were subjected to measurement of melting point and optical rotation and were also characterized by recording UV, IR, Mass and 2D Heteronuclear Single Quantum Coherence Transfer (HSQCT) spectra. Unless otherwise mentioned, in the 2D NMR data of the present work, only resolvable signals are shown. Some of the assignments are interchangeable. Non-reducing end carbohydrate units are primed. Glycosides are surfactant molecules, which form micelles above certain critical micellar concentrations (CMC). Since the concentrations employed for 2D HSQCT spectral measurements are very much higher than their respective CMCs, the proton NMR signals were unusually broad such that, in spite of recording the spectra at 35 °C, the individual coupling constant values could not be determined precisely.

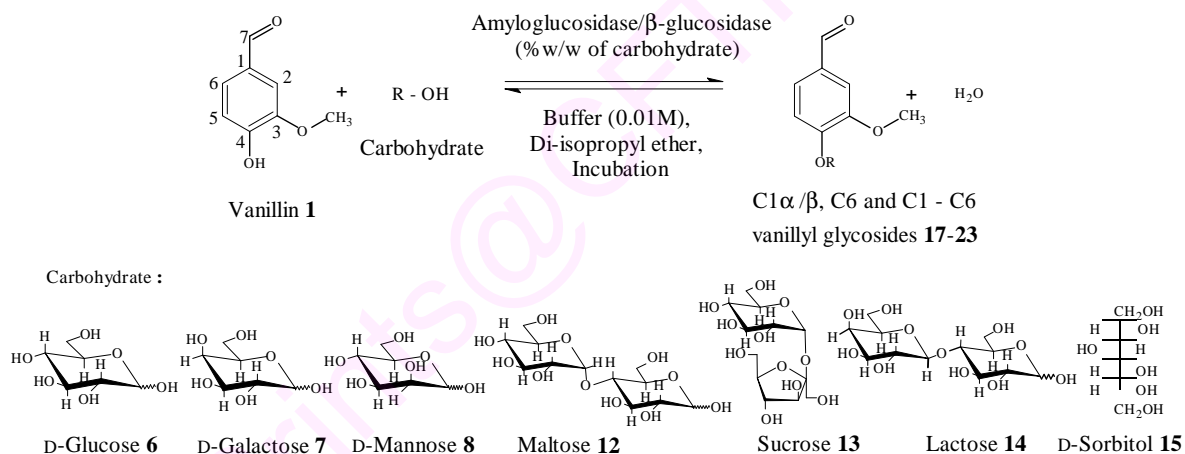
### 3.1 Syntheses of vanillyl glycosides

Vanillin **1** (4-hydroxy-3-methoxybenzaldehyde) is used as an additive in food and beverages (60%), considerable amounts as flavour and fragrances (20–25%) and 5–10% as an intermediate for pharmaceuticals (Walton *et al.* 2003). It possesses a wide range of pharmacological activities such as antimicrobial (Lopez-Malo *et al.* 1998), anticarcinogenic (Stephan and Peter 2003), antioxidant (Burri *et al.* 1983), antifungal (Fitzgerald *et al.* 2005) and antimutagenic (Kometani *et al.* 1993b). The solubility of vanillin in water varies from 3 g/L at 4.4 °C to 62.5 g/L at 80 °C (The Merck Index 2006). Thus the solubility and bioavailability of vanillin **1** limits its pharmacological applications. Glycosylation is a useful tool to improve the water solubility and bioavailability (Kometani *et al.* 1993a; Tietze *et al.* 2003) of vanillin **1**.

Preparation of vanillyl glycosides has been reported by cell suspension cultures (Tietze *et al.* 2003), plant cell tissue cultures, organ cultures (Sommer *et al.* 1997) and chemical methods (Reichel and Sckickle 1943). However, preparation by enzymatic methods have not been previously reported. The present work describes an enzymatic method using amyloglucosidase from a *Rhizopus* mold and  $\beta$ -glucosidase from sweet almond for the preparation of vanillyl glycosides in a non-polar solvent.

Synthesis of 4-*O*-(D-glucopyranosyl)vanillin was studied in detail. A typical synthesis involved reacting vanillin **1** (0.5-2.5 mmol) and D-glucose **6** (1 mmol) at reflux with stirring in 100 mL of di-isopropyl ether in the presence of 10-75% (w/w D-glucose) amyloglucosidase/ $\beta$ -glucosidase and 0.02-0.12 mM (0.2-1.2 mL) of 10 mM of pH 4-8 buffer for a period of 72 h (Scheme 3.1). Workup involved distilling off the solvent and maintaining the reaction mixture at boiling water temperature for 5-10 min to denature the enzyme. The residue was repeatedly extracted with chloroform to remove unreacted vanillin **1**, the dried residue consisting of 4-*O*-(D-glucopyranosyl)vanillin and unreacted

D-glucose **6**, was subjected to HPLC (Fig. 3.1) and the conversion yields were determined from HPLC peak areas. Other procedures are as described on page 74. HPLC analysis showed the following retention times: D-glucose-5.4 min, 4-*O*-(D-glucopyranosyl)vanillin-7.8 min, D-galactose-5.3 min, 4-*O*-(D-galactopyranosyl)vanillin-7.5 min, D-mannose-4.9 min, 4-*O*-(D-mannopyranosyl)vanillin -7.8 min, maltose-11.5 min, 4-*O*-( $\alpha$ -D-glucopyranosyl-(1'→4)D-glucopyranosyl)vanillin -17.1 min, sucrose-9.8 min, 4-*O*-(D-fructofuranosyl-(2→1') $\alpha$ -D-glucopyranosyl)vanillin -14.3 min, lactose-9.9 min, 4-*O*-( $\beta$ -D-galactopyranosyl-(1'→4) $\beta$ -D-glucopyranosyl) vanillin-11.2 min, D-sorbitol-6.7 min and 4-*O*-(D-sorbitol)vanillin-10.1 min.



**Scheme 3.1** Syntheses of vanillyl glycosides

### 3.1.1 Synthesis of 4-*O*-(D-glucopyranosyl)vanillin using amyloglucosidase

Optimum conditions for the synthesis of 4-*O*-(D-glucopyranosyl)vanillin using amyloglucosidase was studied in detail in terms of incubation period, pH, buffer, enzyme and vanillin concentration.

#### 3.1.1.1 Effect of incubation period

At a fixed vanillin (1 mmol) and D-glucose (1 mmol) concentrations increasing the incubation period from 3 h to 72 h, increased the conversion yield to 53%. Further increase in incubation period decreased (96 h, yield-46%) the conversion. This could be

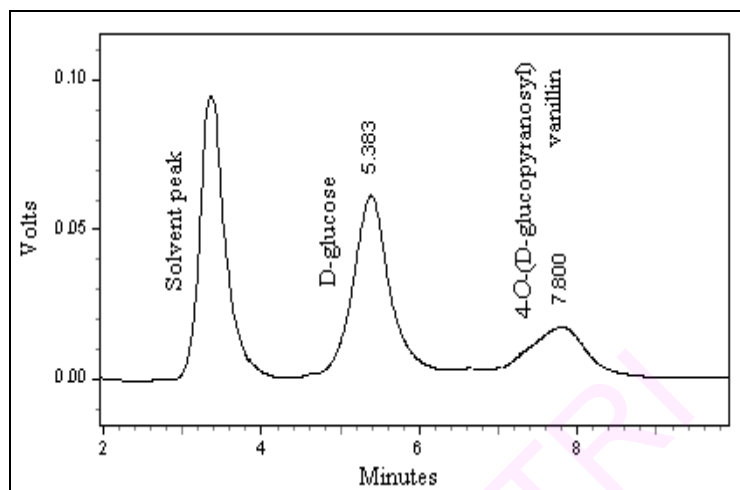


**Fig. 3.1** HPLC chromatogram for the reaction mixture of D-glucose and 4-*O*-(D-glucopyranosyl)vanillin. HPLC conditions: Aminopropyl column (10  $\mu$ m, 300 mm  $\times$  3.9 mm), solvent-CH<sub>3</sub>CN: H<sub>2</sub>O (80:20 v/v), Flow rate-1 mL/min, RI detector. Retention times: D-glucose-5.4 min and 4-*O*-(D-glucopyranosyl)vanillin -7.8 min.

due to denaturation of the enzyme owing to prolonged incubation (Fig. 3.2A, Table 3.1) at the reflux temperature of di-isopropyl ether at 68 °C.

#### **3.1.1.2 Effect of pH**

The reaction was carried out at various pH values from 4 to 8 at a fixed buffer concentration of 0.1 mM (1 mL) with 40% (w/w D-glucose) amyloglucosidase. Acetate buffer for pH 4 and 5, phosphate buffer for pH 6 and 7 and borate buffer for pH 8 was employed. A maximum conversion of 51% yield was obtained at pH 4 (Table 3.1). Further increase in pH decreased the conversion yield drastically (pH 8, yield-17%).

#### **3.1.1.3 Effect of buffer concentration**

In presence of pH 4 acetate buffer, increasing the buffer concentration from 0.02 mM (0.2 mL of 10 mM buffer) to 0.12 mM (1.2 mL) increased the conversion yield to a maximum of 51% at 0.1 mM (1 mL). Further increase in buffer concentration decreased the conversion yield which could be due to hydrolysis of the product (Table 3.1) formed.

#### **3.1.1.4 Effect of amyloglucosidase concentration**

Effect of increasing amyloglucosidase concentration on the glucoside synthesis was studied by varying the amyloglucosidase concentration from 10 to 75% (w/w D-glucose) of enzyme (Fig. 3.2B, Table 3.1). At lower enzyme concentration (10% w/w D-glucose) the conversion yield was 17%. Increasing the enzyme concentration increased the glucosylation yield attained maximum yield of 53% at 40% (w/w D-glucose) enzyme concentration. At higher concentration of 75% (w/w D-glucose) the enzyme showed lesser conversion (yield-31%).

#### **3.1.1.5 Effect of vanillin concentration**

Under the above determined optimized conditions of pH 4 (0.01 M) acetate buffer, 0.1 mM (1 mL) of buffer and 40% (w/w D-glucose) amyloglucosidase concentration, vanillin concentration was varied from 0.5 mmol to 2.5 mmol (Table 3.1).

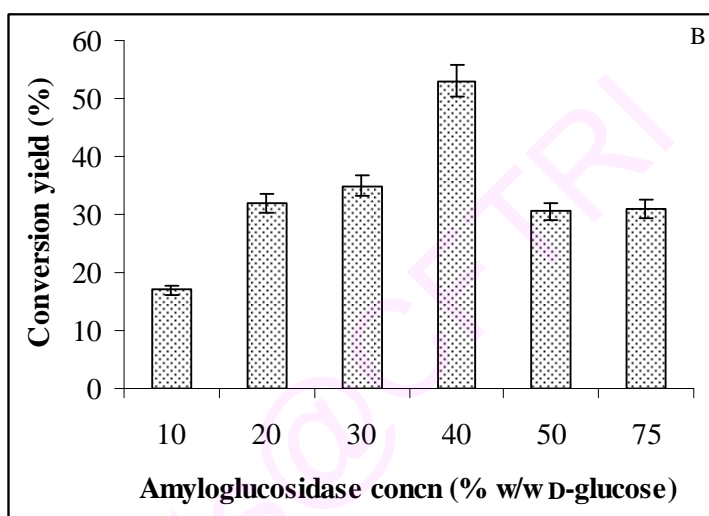
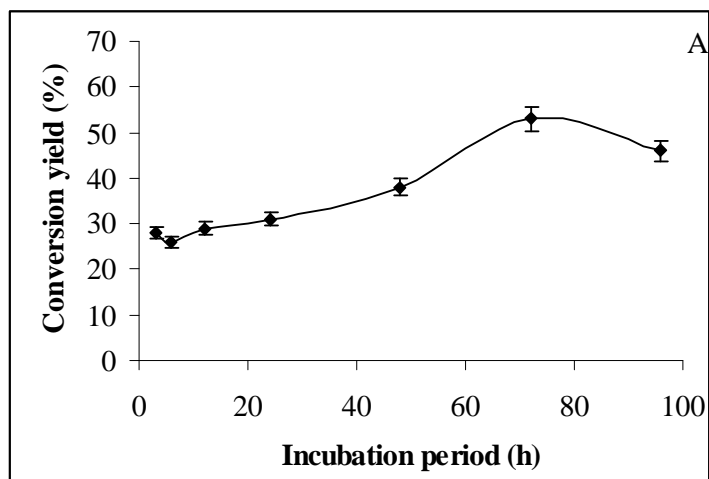


**Fig. 3.2 (A)** Reaction profile for 4-*O*-(D-glucopyranosyl)vanillin synthesis by the reflux method. Conversion yields were from HPLC with respect to 1 mmol of D-glucose. Reaction conditions: D-glucose-1 mmol, vanillin-1 mmol, amyloglucosidase-40% (w/w D-glucose), 0.1 mM pH 4 acetate buffer, solvent-di-isopropyl ether and temperature-68 °C and **(B)** Effect of amyloglucosidase concentration for 4-*O*-(D-glucopyranosyl) vanillin synthesis. Reaction conditions: D-glucose-1 mmol, vanillin-1 mmol, 0.1 mM pH 4 acetate buffer, solvent-di-isopropyl ether, temperature-68 °C and incubation period – 72 h

The conversion yield reached a maximum of 53% at 1 mmol. It decreased slightly (46%) at a higher vanillin concentration of 2.5 mmol.

**Table 3.1** Optimization of reaction conditions for the synthesis of 4-*O*-(D-glucopyranosyl)vanillin

Reaction conditions	Variable parameter <sup>b</sup>	Yield (%) <sup>c</sup>
	Incubation period (h)	
Vanillin – 1 mmol	3	28
D-glucose – 1 mmol	6	26
pH – 4	12	29
Buffer concentration – 0.1 mM (1 mL)	24	31
Enzyme – 40% w/w D-glucose	48	38
	72	53
	96	46
	pH (0.01M)	
Vanillin – 1 mmol <sup>a</sup>	4	51
D-glucose – 1 mmol	5	28
Enzyme – 40% w/w D-glucose	6	22
Buffer concentration – 0.1 mM (1 mL)	7	18
Incubation period – 72 h	8	17
	Buffer concentration (mM)	
Vanillin – 1 mmol	0.02	13
D-glucose – 1 mmol	0.04	46
Enzyme – 40% w/w D-glucose	0.06	48
pH – 4	0.08	50
Incubation period – 72 h	0.1	51
	0.12	42
	Enzyme concentration (% w/w D-glucose)	
Vanillin – 1 mmol	10	17
D-glucose – 1 mmol	20	32
pH – 4	30	35
Buffer concentration – 0.1 mM (1 mL)	40	53
Incubation period – 72 h	50	30
	75	31
	Vanillin (mmol)	
pH – 4	0.5	49
Buffer concentration – 0.1 mM (1 mL)	1	53
D-glucose – 1 mmol	1.5	47
Enzyme – 40% w/w D-glucose	2	48
Incubation period – 72 h	2.5	46

<sup>a</sup>Initial reaction conditions. <sup>b</sup>Other variables are the same as under reaction conditions, except the specified ones. <sup>c</sup>HPLC yields expressed with respect to 1 mmol D-glucose employed.

### 3.1.1.6 Solubility of 4-*O*-(D-glucopyranosyl)vanillin

Determination of water solubility of 4-*O*-(D-glucopyranosyl)vanillin showed that it is soluble to the extent of 35.2 g/L (Section 3.7.5). Hence, 4-*O*-(D-glucopyranosyl)vanillin was found to be more soluble than vanillin (2 g/L) at 25 °C in water.

### 3.1.2 Syntheses of vanillyl glycosides of other carbohydrates using amyloglucosidase

Syntheses of vanillyl glycosides involved refluxing vanillin **1** (1 mmol) and carbohydrate (D-glucose **6**, D-galactose **7**, D-mannose **8**, maltose **12**, sucrose **13**, D-sorbitol **15**, 1 mmol) with stirring in 100 mL of di-isopropyl ether in the presence of 40% (w/w carbohydrate) amyloglucosidase and 0.1 mM (1 mL of 10 mM buffer) of pH 4 acetate buffer for a period of 72 h (Scheme 3.1). All the other workup, analysis and isolation as described on page 74.

### 3.1.3 Syntheses of vanillyl glycosides of other carbohydrates using $\alpha$ -glucosidase

Syntheses of vanillyl glycosides using  $\beta$ -glucosidase was carried out. A typical reaction involved refluxing vanillin **1** (1 mmol) and carbohydrate (D-glucose **6**, D-galactose **7**, D-mannose **8**, maltose **12**, lactose **14**, 0.5 mmol) with stirring in 100 mL of di-isopropyl ether in the presence of 50% (w/w carbohydrate)  $\beta$ -glucosidase and 0.17 mM (1.7 mL) of 10 mM pH 4.2 acetate buffer for a period of 24 h (Scheme 3.1). Other procedural conditions described on page 74 was followed for workup and isolation of the glycosides.

### 3.1.4 Spectral characterization

Vanillyl glycosides besides measuring melting point and optical rotation were also characterized by recording UV, IR, Mass and 2D-HSQCT spectra. NMR data of the free carbohydrates employed are shown in Table 3.2.



Table 3.2 NMR data for free carbohydrate molecules employed in the present work<sup>a</sup>

Carbohydrate	Chemical shift values in ppm (J Hz)											
	<sup>1</sup> H <sup>13</sup> C	<sup>1</sup> H <sup>13</sup> C	<sup>1</sup> H <sup>13</sup> C	<sup>1</sup> H <sup>13</sup> C	<sup>1</sup> H <sup>13</sup> C	<sup>1</sup> H <sup>13</sup> C	<sup>1</sup> H <sup>13</sup> C	<sup>1</sup> H <sup>13</sup> C	<sup>1</sup> H <sup>13</sup> C	<sup>1</sup> H <sup>13</sup> C	<sup>1</sup> H <sup>13</sup> C	<sup>1</sup> H <sup>13</sup> C
	H-1 C1	H-2 C2	H-3 C3	H-4 C4	H-5 C5	H-6 C6	H-1'' C1''	H-2'' C2''	H-3'' C3''	H-4'' C4''	H-5'' C5''	H-6'' C6''
D-Glucose α	4.95 92.3	3.14 72.5 (6.2)	3.44 73.2 (5.01)	3.07 70.7 (5.01)	3.58 72.0 (6.49)	3.53 61.4 (11.3, 6.5)						
	4.30 97.0 (6.2)	2.92 75.0 (6.2)	3.06 76.9 (5.01)	- -	3.45 76.9 (4.14, 1.3)	3.62 61.6 (11.3, 6.5)						
D-Galactose α	4.14 92.7	3.50 68.4 (6.2)	3.59 69.0 (5.01)	3.70 70.0 (5.0, 4.14)	3.35 70.5 (4.14, 1.3)	3.31 60.7 (1.3, 11.3)						
	4.83 97.6 (6.2)	--	3.15 73.7 (5.01)	3.10 72.3 (5.0, 4.14)	3.25 74.8 (4.14, 1.3)	3.32 60.8 (1.3, 11.3)						
D-Mannose α	4.89 94.0	3.54 71.3 (6.2)	3.55 70.0 (6.2, 5.0)	3.36 67.4 (5.0, 4.14)	3.50 73.0 (4.14, 1.3)	3.63 61.5 (1.3, 11.3)						
	4.54 93.9 (6.2)	3.32 71.5	3.26 73.7 (6.2, 5.0)	3.37 67.0 (5.0, 4.14)	3.02 77.0 (4.14, 1.3)	3.46 61.4 (1.3, 11.3)						
D-Fructose β	3.80 63.9 (12.23)	- 97.5	3.56 67.9 (5.8)	3.64 69.9 (5.8, 4.07)	3.57 68.7 (5.8, 4.07)	3.50 62.6 (2.4, 12.0)						
D-Ribose α	4.75 93.2 (5.1)	3.23 70.6 (5.1, 5.0)	3.33 68.8 (5.0, 4.97)	3.71 66.7 (4.97, 2.4)	3.51 62.8 (2.4, 12.0)							
	4.31 94.0 (2.6)	3.31 71.5 (2.6, 4.7)	3.38 68.0 (4.7, 4.97)	3.54 67.5 (4.97, 2.4)	3.29 62.8 (2.4, 12.0)							
D-Arabinose α	4.92 92.3 (1.7)	4.32 - (1.7, 5.8)	4.6 - (5.8, 4.07)	4.08 - (4.07, 2.4)	3.73 60.4 (2.4, 12.0)							
	4.33 96.2 (4.5)	3.65 69.1 (4.5, 7.2)	4.02 68.9 (7.2, 4.07)	3.37 67.1 (4.07, 2.4)	3.64 60.7 (2.4, 12.0)							
Lactose α	4.90 91.9 (6.2)	3.70 69.8 (6.2)	3.54 71.4 (6.2, 5.0)	3.27 80.8 (5.0, 4.14)	3.55 72.1 (4.14, 1.3)	3.64 60.5 (1.3, 11.3)	4.19 103.7 (6.2)	3.30 70.7 (6.2)	3.18 73.2 (6.2, 5.0)	3.62 68.2 (5.0, 4.14)	2.93 75.4 (4.14, 1.3)	3.52 60.9 (1.3, 11.3)
	4.34 96.3	3.31 74.2 (6.2)	3.53 74.7 (6.2, 5.0)	3.28 81.1 (5.0, 4.14)	3.44 74.9 (4.14, 1.3)	3.72 60.6 (1.3, 11.3)						
Maltose α	4.80 92.0 (6.2)	2.85 73.9 (6.2)	3.29 76.4 (6.2, 5.0)	3.15 69.7 (5.0, 4.14)	3.30 73.3 (4.14, 1.3)	3.50 60.8 (1.3, 11.3)	4.90 100.3 (6.2)	2.94 72.0 (6.2)	3.10 73.0 (6.2, 5.0)	3.51 69.5 (5.0, 4.14)	3.62 72.7 (4.14, 1.3)	3.60 60.2 (1.3, 11.3)
	4.20 96.9	3.10 74.3 (6.2)	3.31 76.0 (6.2, 5.0)	3.19 79.4 (5.0, 4.14)	3.38 76.4 (4.14, 1.3)	3.34 60.9 (1.3, 11.3)						
Sucrose Glc α Fru β							5.18 91.7 (6.2)	3.65 72.7 (6.2)	3.20 71.5 (6.2, 5.0)	3.11 69.8 (5.0, 4.14)	3.47 72.8 (4.14, 1.3)	3.54 60.5 (1.3, 11.3)
	3.41 62.0 (12.23)	- 103.9	3.78 77.1 (5.8)	3.88 74.1 (5.8, 4.07)	3.41 82.4 (4.07, 2.4)	3.55 62.0 (2.4, 12.0)						
D-Sorbitol	3.41 62.5 (12.0, 7.3)	3.54 73.6 (7.3, 4.3)	3.68 68.9 (4.3)	3.39 72.2 (4.3)	3.48 71.4 (4.3, 7.3)	3.56 63.3 (7.3, 12.0)						
D-mannitol	3.40 63.7 (12.0, 7.3)	3.47 71.2 (7.3, 4.3)	3.54 69.6 (4.3)	3.54 69.6 (4.3)	3.47 71.2 (4.3)	3.61 63.7 (7.3, 12.0)						

<sup>a</sup> Assignments were based on Book and Pedersen 1983; Book *et al.* 1983

**Vanillin 1:** Solid; mp 81 °C, UV (H<sub>2</sub>O,  $\lambda_{\max}$ ): 195 nm ( $\sigma \rightarrow \sigma^*$ ,  $\epsilon_{195} - 2145 \text{ M}^{-1}$ ), 228.5 nm ( $\sigma \rightarrow \pi^*$ ,  $\epsilon_{228.5} - 711 \text{ M}^{-1}$ ), 272 nm ( $\pi \rightarrow \pi^*$ ,  $\epsilon_{272} - 480 \text{ M}^{-1}$ ), 325.5 nm ( $n \rightarrow \pi^*$ ,  $\epsilon_{325.5} - 221 \text{ M}^{-1}$ ), 340 nm ( $n \rightarrow \pi^*$  extended conjugation,  $\epsilon_{340} - 175 \text{ M}^{-1}$ ), IR (stretching frequency,  $\text{cm}^{-1}$ ): 3458 (OH), 1626 (aromatic C=C), MS ( $m/z$ ) 152.1 [M]<sup>+</sup>, 2D-HSQCT (DMSO-*d*<sub>6</sub>) <sup>1</sup>H NMR  $\delta_{\text{ppm}}$  (500.13 MHz): 7.40 (H-2), 6.92 (H-5), 7.35 (H-6), 3.83 (OCH<sub>3</sub>), 9.71 (CHO), <sup>13</sup>C NMR  $\delta_{\text{ppm}}$ : (125 MHz): 129.3 (C1), 111.5 (C2), 148.3 (C3), 153.5 (C4), 116.2 (C5), 126.9 (C6), 56.4 (OCH<sub>3</sub>), 191.2 (CHO). Ultraviolet-visible spectra is shown in Fig 3.3A.

**3.1.4.1 4-O-(D-Glucopyranosyl)vanillin 17a-c:** Solid; UV (H<sub>2</sub>O,  $\lambda_{\max}$ ): 195.5 nm ( $\sigma \rightarrow \sigma^*$ ,  $\epsilon_{195.5} - 2241 \text{ M}^{-1}$ ), 223 nm ( $\sigma \rightarrow \pi^*$ ,  $\epsilon_{223} - 978 \text{ M}^{-1}$ ), 279.5 nm ( $n \rightarrow \pi^*$ ,  $\epsilon_{279.5} - 291 \text{ M}^{-1}$ ), IR (stretching frequency,  $\text{cm}^{-1}$ ): 3358 (OH), 1260 (glycosidic aryl alkyl C–O–C asymmetric), 1030 (glycosidic aryl alkyl C–O–C symmetric), 1408 (C=C), 1636 (CO), 2933 (CH), MS ( $m/z$ ) 316.31 [M+2]<sup>+</sup>, 2D-HSQCT (DMSO-*d*<sub>6</sub>) **C1 $\alpha$ -glucoside 17a:** <sup>1</sup>H NMR  $\delta_{\text{ppm}}$  (500.13 MHz) **Glu:** 4.65 (H-1 $\alpha$ , d, J = 4.5 Hz), 3.23 (H-2 $\alpha$ ), 3.42 (H-3 $\alpha$ ), 3.78 (H-4 $\alpha$ ), 3.15 (H-5 $\alpha$ ), 3.60 (H-6 $\alpha$ ), **Van:** 6.59 (H-2), 6.20 (H-5), 3.73 (OCH<sub>3</sub>), <sup>13</sup>C NMR  $\delta_{\text{ppm}}$  (125 MHz) **Glu:** 99.2 (C1 $\alpha$ ), 72.3 (C2 $\alpha$ ), 73.5 (C3 $\alpha$ ), 70.2 (C4 $\alpha$ ), 72.5 (C5 $\alpha$ ), 60.5 (C6 $\alpha$ ), **Van:** 111.4 (C2), 114.5 (C5), **C1 $\beta$ -glucoside 17b:** Solid; mp 91 °C, UV (H<sub>2</sub>O,  $\lambda_{\max}$ ): 196.5 nm ( $\sigma \rightarrow \sigma^*$ ,  $\epsilon_{196.5} - 2641 \text{ M}^{-1}$ ), 278.5 nm ( $\pi \rightarrow \pi^*$ ,  $\epsilon_{278.5} - 365 \text{ M}^{-1}$ ), IR (stretching frequency,  $\text{cm}^{-1}$ ): 3360 (OH), 1262 (glycosidic aryl alkyl C–O–C asymmetric), 1031 (glycosidic aryl alkyl C–O–C symmetric), 1417 (C=C), 1630 (CO), 2931 (CH), optical rotation (*c* 1, H<sub>2</sub>O):  $[\alpha]_{\text{D}}$  at 25 °C = +62.8, MS ( $m/z$ ) 316.31 [M+2]<sup>+</sup>, 2D-HSQCT (DMSO-*d*<sub>6</sub>) <sup>1</sup>H NMR  $\delta_{\text{ppm}}$  **Glu:** 4.25 (H-1 $\beta$ , d, J = 6.2 Hz), 2.98 (H-2 $\beta$ ), 3.12 (H-3 $\beta$ ), 3.60 (H-4 $\beta$ ), 3.68 (H-6 $\beta$ ), **Van:** 7.42 (H-2), 7.25 (H-5), 6.86 (H-6), 3.71 (OCH<sub>3</sub>), <sup>13</sup>C NMR  $\delta_{\text{ppm}}$  **Glu:** 101.5 (C1 $\beta$ ), 74.6 (C2 $\beta$ ), 76.1 (C3 $\beta$ ), 72 (C4 $\beta$ ), 60.8 (C6 $\beta$ ),

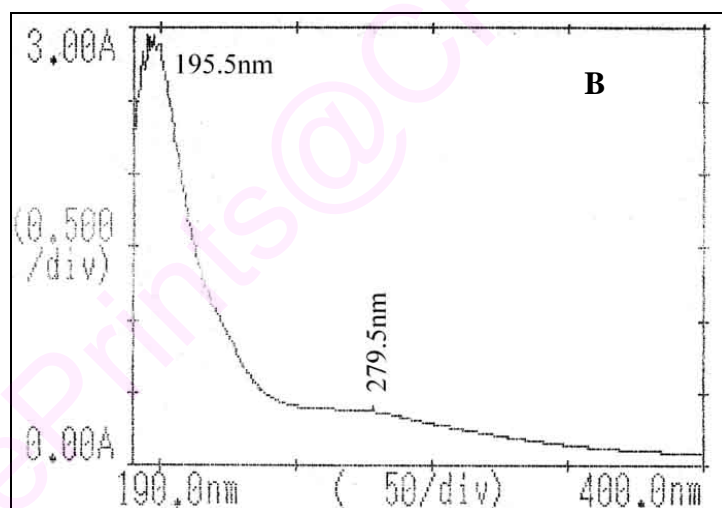
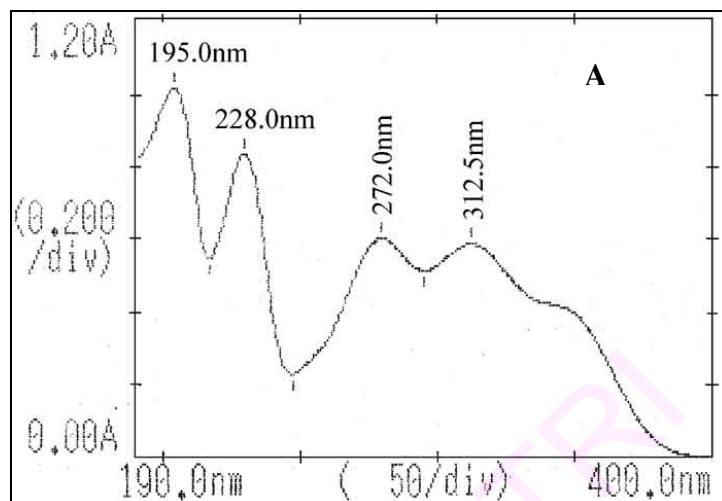
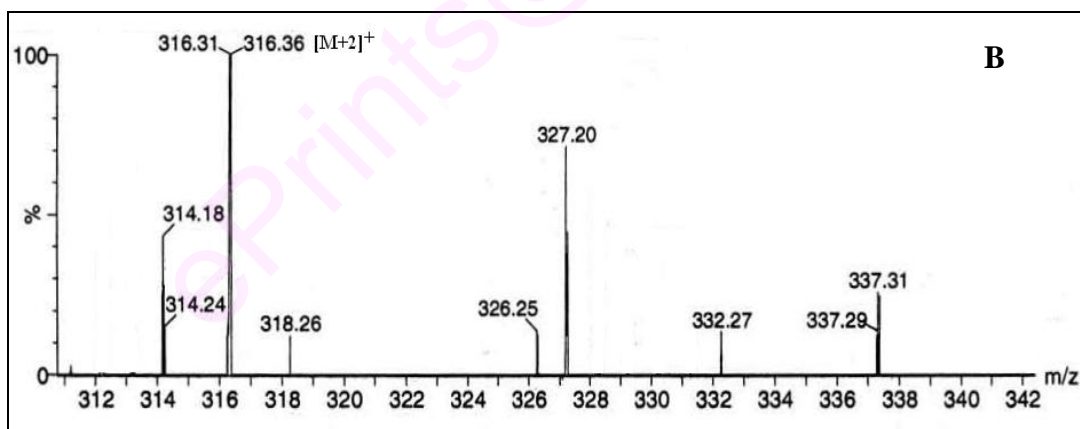
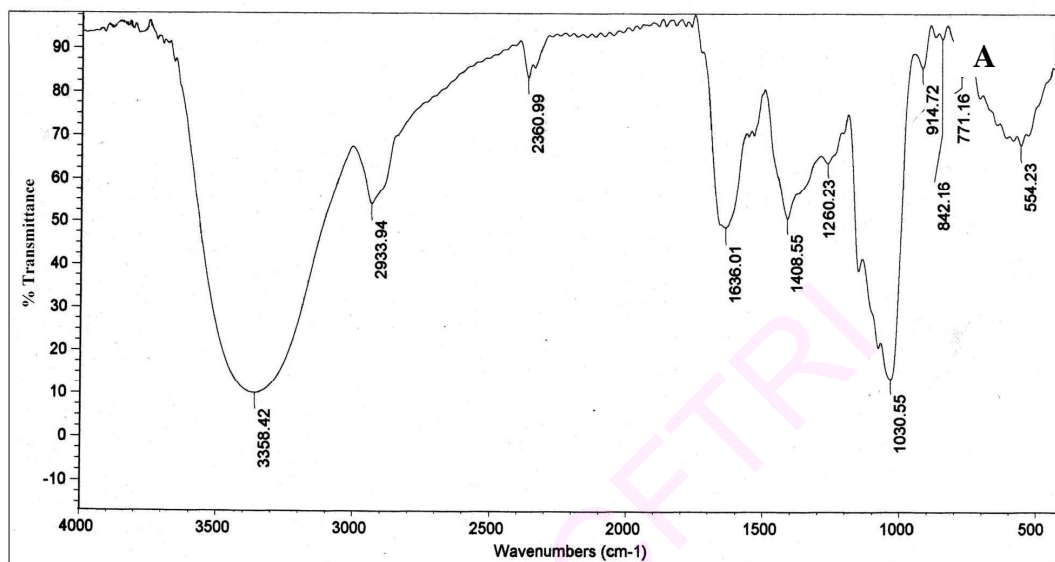


Fig. 3.3 Ultraviolet-visible spectra of (A) Vanillin **1** and (B) 4-O-(D-glucopyranosyl)vanillin **17a-c**



**Fig. 3.4** 4-*O*-(D-Glucopyranosyl)vanillin **17a-c** (A) IR spectrum and (B) Mass spectrum.

**Van:** 113.5 (C2), 149.4 (C3), 151.2 (C4), 115.3 (C5), 123.7 (C6), 55.1 (OCH<sub>3</sub>), 191 (CHO), **C6-O-arylated 17c:** <sup>1</sup>H NMR: 4.91 (H-1 $\alpha$ ), 3.23 (H-2 $\alpha$ ), 3.20 (H-3 $\alpha$ ), 3.62 (H-4 $\alpha$ ), 3.23 (H-5 $\alpha$ ), 3.55 (H-6 $\alpha$ ), <sup>13</sup>C NMR: 92.7 (C1 $\alpha$ ), 72.3 (C2 $\alpha$ ), 72.6 (C3 $\alpha$ ), 70.2 (C4 $\alpha$ ), 75.2 (C5 $\alpha$ ), 68 (C6 $\alpha$ ).

Ultraviolet-visible, IR, mass and 2D-HSQCT NMR spectra for 4-*O*-(D-glucopyranosyl)vanillin **17a-c** for amyloglucosidase catalysed products were shown in Figures 3.3B, 3.4A, 3.4B and 3.5 respectively. Mass and 2D-HSQCT NMR spectra for 4-*O*-( $\beta$ -D-glucopyranosyl)vanillin **17b** for  $\beta$ -glucosidase catalysed product are shown in Figures 3.6A and 3.6B respectively.

**3.1.4.2 4-O-(D-Galactopyranosyl)vanillin 18a,b:** Solid, mp 89 °C, UV (H<sub>2</sub>O,  $\lambda_{\max}$ ): 198 nm ( $\sigma \rightarrow \sigma^*$ ,  $\epsilon_{198} - 2909 \text{ M}^{-1}$ ), 224.5 nm ( $\sigma \rightarrow \pi^*$ ,  $\epsilon_{224.5} - 1104 \text{ M}^{-1}$ ), 281 nm ( $\pi \rightarrow \pi^*$ ,  $\epsilon_{281} - 518 \text{ M}^{-1}$ ), IR (stretching frequency, cm<sup>-1</sup>): 3271 (OH), 1262 (glycosidic aryl alkyl C–O–C asymmetric), 1032 (glycosidic aryl alkyl C–O–C symmetric), 1407 (C=C), 1665 (CO), optical rotation (*c* 1, H<sub>2</sub>O),  $[\alpha]_{\text{D}}$  at 25 °C = +8.82, MS (*m/z*) 314.18 [M]<sup>+</sup>, 2D-HSQCT (DMSO-*d*<sub>6</sub>): **C1 $\alpha$ -galactoside 18a:** <sup>1</sup>H NMR  $\delta_{\text{ppm}}$  **Gal:** 5.10 (H-1 $\alpha$ , d, *J* = 2.2 Hz), 3.62 (H-2 $\alpha$ ), 3.75 (H-3 $\alpha$ ), 3.48 (H-4 $\alpha$ ), 3.58 (H-5 $\alpha$ ), 3.45 (H-6 $\alpha$ ), **Van:** 7.38 (H-2), 6.90 (H-5), 7.33 (H-6), 3.86 (OCH<sub>3</sub>), 9.74 (CHO), <sup>13</sup>C NMR  $\delta_{\text{ppm}}$  **Gal:** 95.8 (C1 $\alpha$ ), 69.4 (C2 $\alpha$ ), 71 (C3 $\alpha$ ), 70.8 (C4 $\alpha$ ), 69.9 (C5 $\alpha$ ), 62 (C6 $\alpha$ ), 129.2 (C1), 111.3 (C2), 148.6 (C3), 153.5 (C4), 115.9 (C5), 126.4 (C6), 56.1 (OCH<sub>3</sub>), 191.4 (CHO), **C1 $\beta$ -galactoside 18b** <sup>1</sup>H NMR  $\delta_{\text{ppm}}$  **Gal:** 4.95 (H-1 $\beta$ , d, *J* = 7.8 Hz), 3.21 (H-2 $\beta$ ), 3.36 (H-3 $\beta$ ), <sup>13</sup>C NMR  $\delta_{\text{ppm}}$  **Gal:** 102.1 (C1 $\beta$ ), 72 (C2 $\beta$ ), 75 (C3 $\beta$ ).

Infra-red and 2D-HSQCT NMR spectra for 4-*O*-(D-galactopyranosyl)vanillin **18a,b** are shown in Figures 3.7A and 3.7B respectively.

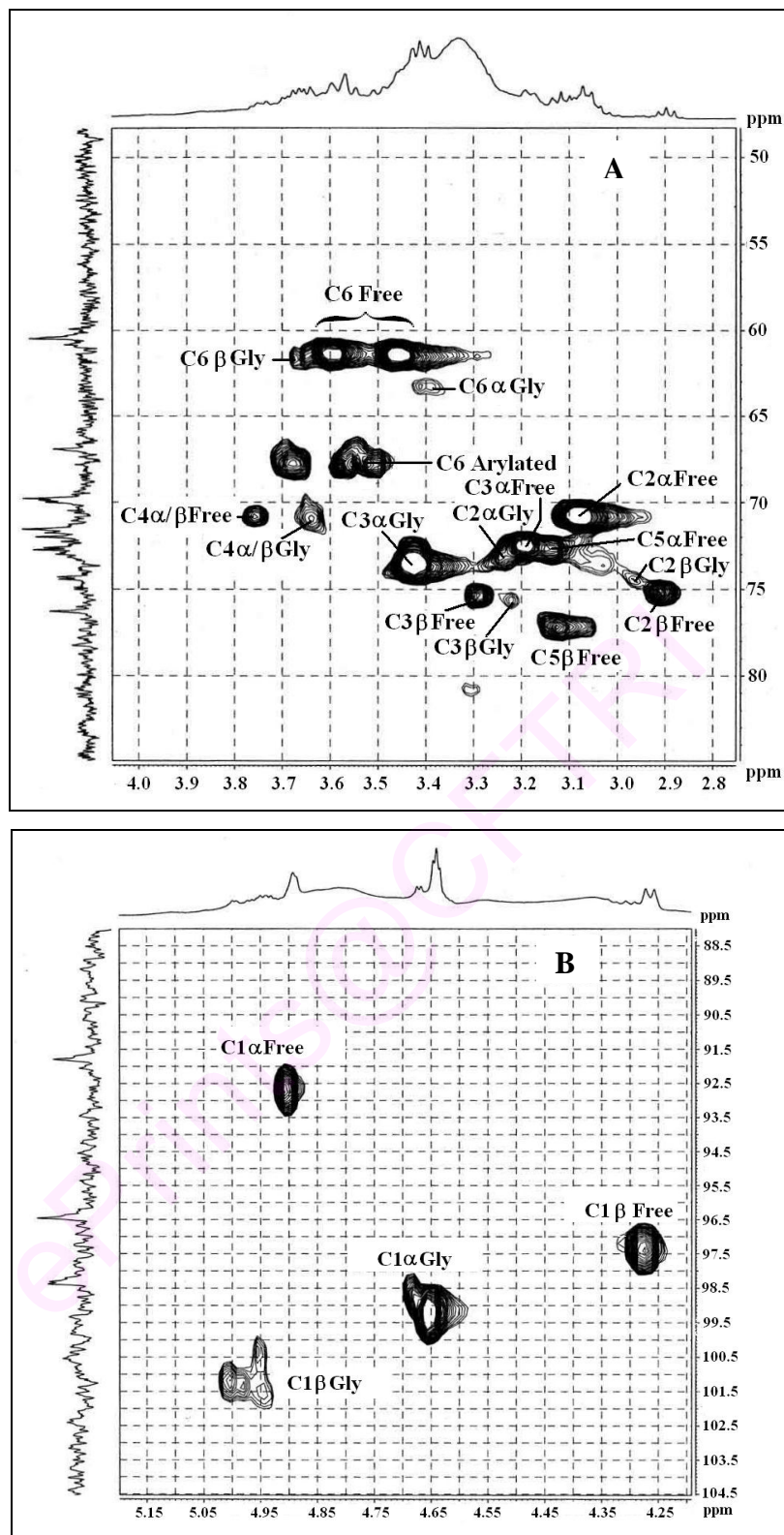


**Fig. 3.5** (A) 2D-HSQC spectrum showing the C2-C6 region of 4-*O*-(D-glucopyranosyl)vanillin **17a-c** and (B) Anomeric region of the same compound. Some of the assignments in 'A' could be interchangeable.

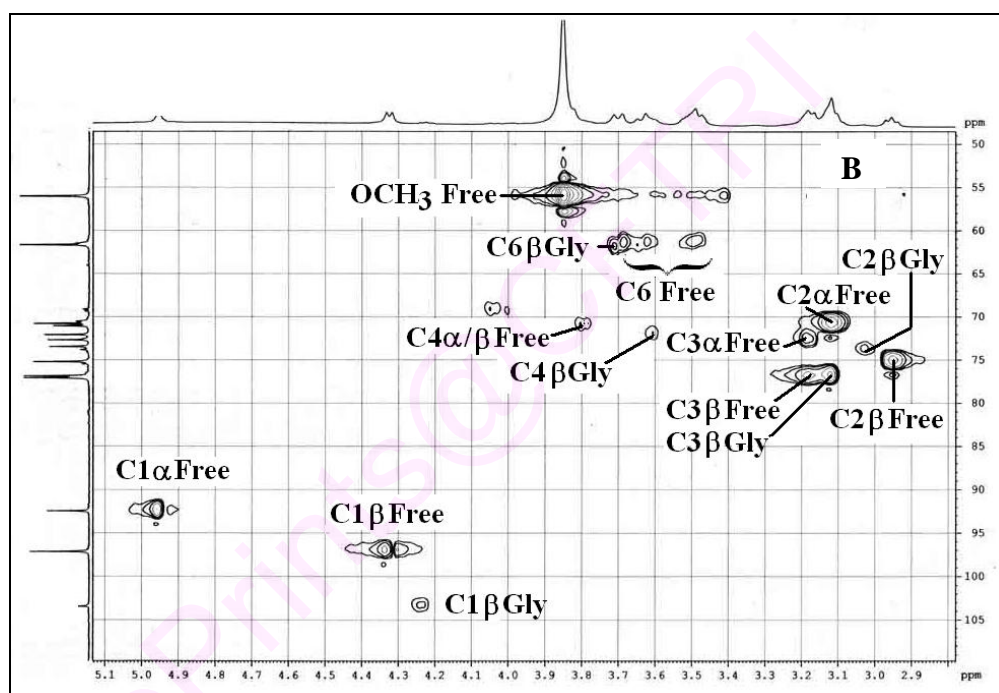
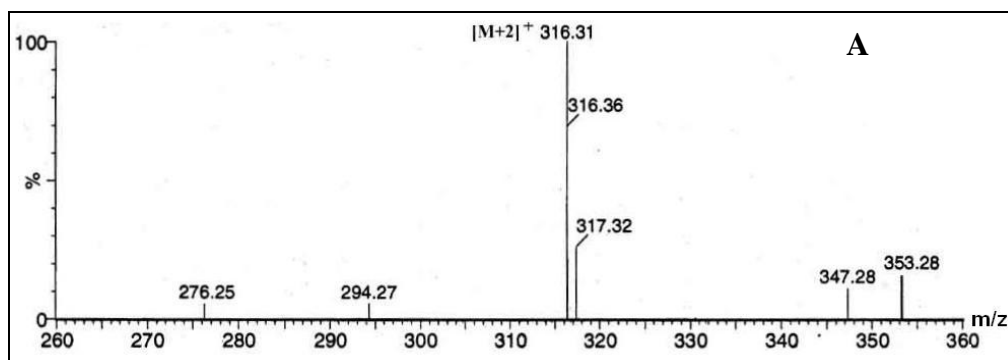


**Fig. 3.6** 4-*O*-( $\beta$ -D-glucopyranosyl)vanillin **17b** (A) Mass spectrum and (B) 2D-HSQC spectrum showing the C1-C6 region. Some of the assignments are interchangeable.



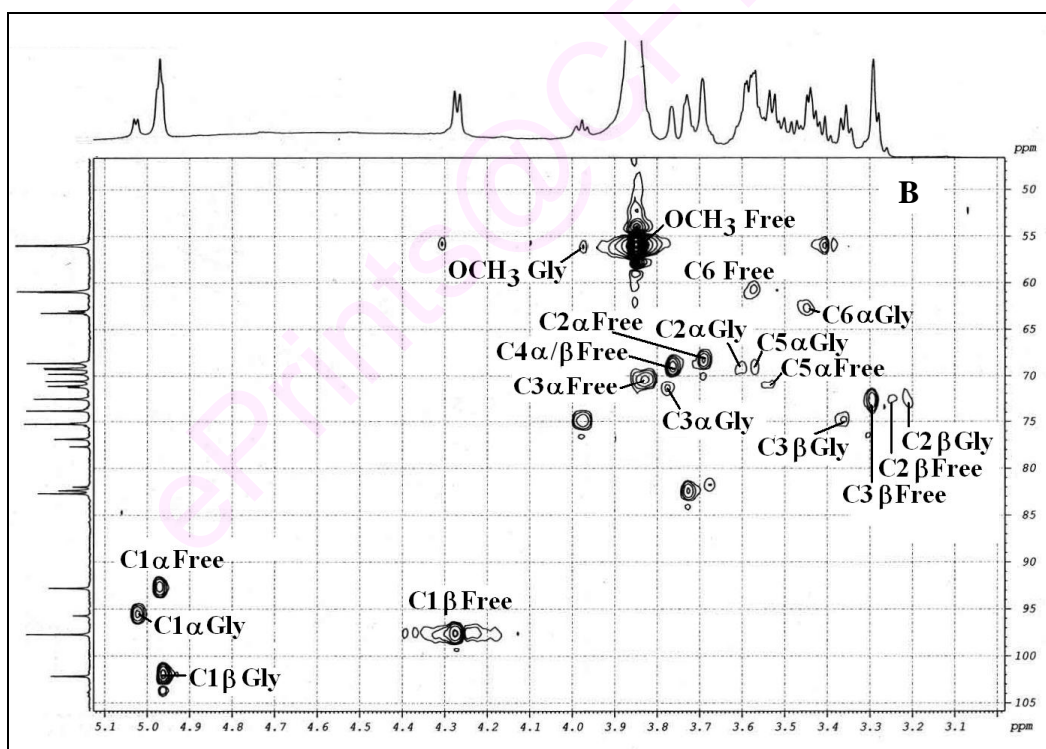
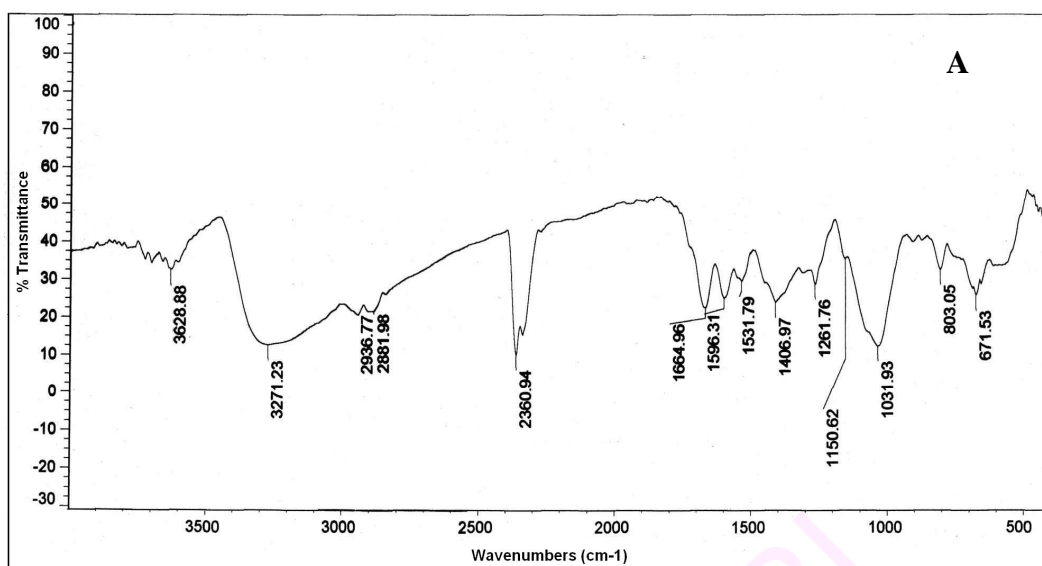


**Fig. 3.7** 4-*O*-(D-Galactopyranosyl)vanillin **18a,b** (A) IR spectrum and (B) 2D-HSQC spectrum showing the C1-C6 region. Some of the assignments are interchangeable.



**3.1.4.3 4-*O*-(D-Mannopyranosyl)vanillin 19a,b:** Solid; mp 93 °C, UV (H<sub>2</sub>O,  $\lambda_{\max}$ ): 198.5 nm ( $\sigma \rightarrow \sigma^*$ ,  $\epsilon_{198.5} = 3402 \text{ M}^{-1}$ ), 224 nm ( $\sigma \rightarrow \pi^*$ ,  $\epsilon_{224} = 1325 \text{ M}^{-1}$ ), 278 nm ( $\pi \rightarrow \pi^*$ ,  $\epsilon_{278} = 284 \text{ M}^{-1}$ ), IR (stretching frequency,  $\text{cm}^{-1}$ ): 3365 (OH), 1249 (glycosidic aryl alkyl C–O–C asymmetric), 1030 (glycosidic aryl alkyl C–O–C symmetric), 1406 (C=C), 1651 (CO), 2940 (CH), optical rotation ( $c$  1, H<sub>2</sub>O):  $[\alpha]_{\text{D}}$  at 25 °C = -3.6, MS ( $m/z$ ) 314.22  $[\text{M}]^+$ , 2D-HSQCT (DMSO- $d_6$ ) **C1 $\alpha$ -mannoside 19a:**  $^1\text{H}$  NMR  $\delta_{\text{ppm}}$  (500.13 MHz) **Man:** 4.99 (H-1 $\alpha$ , d,  $J = 1.98 \text{ Hz}$ ), 3.38 (H-2 $\alpha$ ), 3.56 (H-3 $\alpha$ ), 3.45 (H-4 $\alpha$ ), 3.96 (H-5 $\alpha$ ), 3.50 (H-6 $\alpha$ ), **Van:** 7.40 (H-2), 6.90 (H-5),  $^{13}\text{C}$  NMR (DMSO- $d_6$ ) **Man:** 100.8 (C1 $\alpha$ ), 70.5 (C2 $\alpha$ ), 71.3 (C3 $\alpha$ ), 67.1 (C4 $\alpha$ ), 73.8 (C5 $\alpha$ ), 61.3 (C6 $\alpha$ ), **Van:** 109.4 (C2), 114.7 (C5), 121.9 (C6), **C1 $\beta$ -mannoside 19b:**  $^1\text{H}$  NMR  $\delta_{\text{ppm}}$  **Man:** 4.90 (H-1 $\beta$ , d,  $J = 3.42 \text{ Hz}$ ), 3.40 (H-2 $\beta$ ), 3.43 (H-4 $\beta$ ), 3.11 (H-5 $\beta$ ), 3.53 (H-6 $\alpha$ ),  $^{13}\text{C}$  NMR  $\delta_{\text{ppm}}$  **Man:** 102 (C-1 $\beta$ ), 71.6 (C-2 $\beta$ ), 67.4 (C-4 $\beta$ ), 75.8 (C-5 $\beta$ ), 62.7 (C-6 $\beta$ ).

Mass and 2D-HSQCT NMR spectra for 4-*O*-(D-mannopyranosyl)vanillin **19a,b** are shown in Figures 3.8A and 3.8B respectively.

**3.1.4.4 4-*O*-( $\alpha$ -D-Glucopyranosyl-(1 $\rightarrow$ 4)D-glucopyranosyl)vanillin 20a-d:** Solid; UV (H<sub>2</sub>O,  $\lambda_{\max}$ ): 194.5 nm ( $\sigma \rightarrow \sigma^*$ ,  $\epsilon_{194.5} = 4782 \text{ M}^{-1}$ ), 224.5 nm ( $\sigma \rightarrow \pi^*$ ,  $\epsilon_{224.5} = 1389 \text{ M}^{-1}$ ), 278.5 nm ( $\pi \rightarrow \pi^*$ ,  $\epsilon_{278.5} = 328 \text{ M}^{-1}$ ), IR (stretching frequency,  $\text{cm}^{-1}$ ): 3361 (OH), 1266 (glycosidic aryl alkyl C–O–C asymmetric), 1024 (glycosidic aryl alkyl C–O–C symmetric), 1413 (C=C), 1651 (CO), 2930 (CH), 1205 (OCH<sub>3</sub>), MS ( $m/z$ ) 478  $[\text{M}+2]^+$ , 2D-HSQCT (DMSO- $d_6$ ) **C1 $\alpha$ -maltoside 20a:**  $^1\text{H}$  NMR  $\delta_{\text{ppm}}$  (500.13 MHz) **Malt:** 4.68 (H-1 $\alpha$ , d,  $J = 2.56 \text{ Hz}$ ), 3.10 (H-2 $\alpha$ ), 3.20 (H-3 $\alpha$ ), 3.30 (H-4 $\alpha$ ), 3.72 (H-5 $\alpha$ ), 3.48 (H-6 $\alpha$ ), 4.94 (H-1' $\alpha$ ), 3.25 (H-2'), 2.88 (H-3'), 3.65 (H-4'), 3.60 (H-6'), **Van:** 6.26 (H-2), 6.62 (H-5), 7.18 (H-6), 3.73 (OCH<sub>3</sub>),  $^{13}\text{C}$  NMR  $\delta_{\text{ppm}}$  (125 MHz) **Malt:** 98.2 (C1 $\alpha$ ), 70.1 (C2 $\alpha$ ), 75.1 (C3 $\alpha$ ), 79.1 (C4 $\alpha$ ), 69.8 (C5 $\alpha$ ), 60.8 (C6 $\alpha$ ), 100.3 (C1' $\alpha$ ), 73.8 (C2'), 74.5

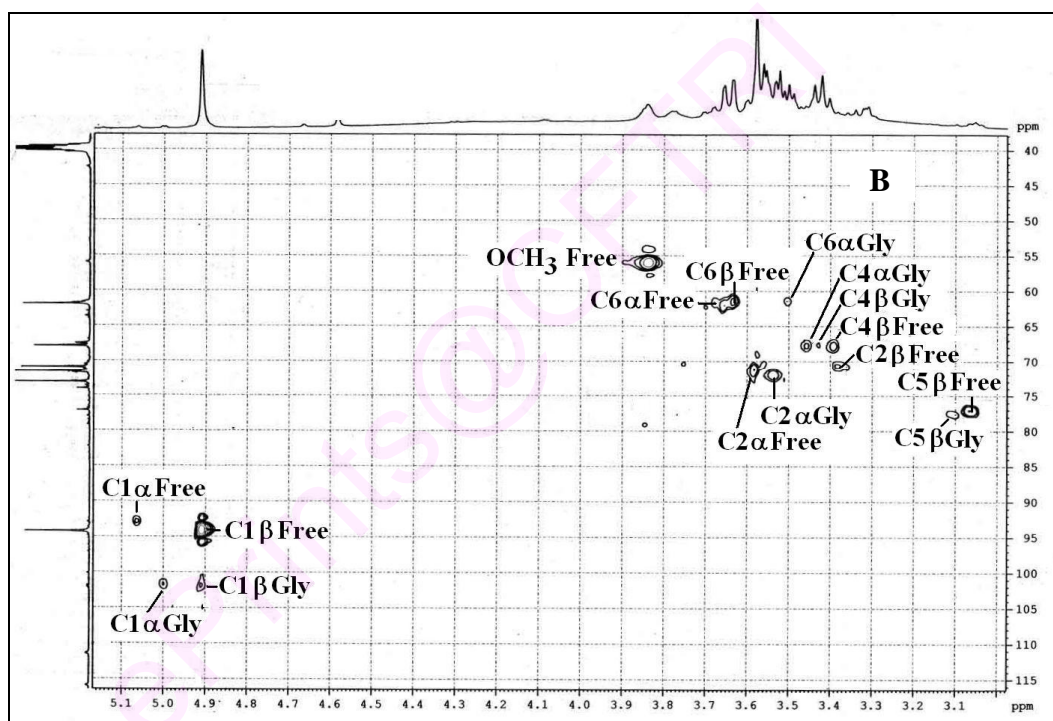
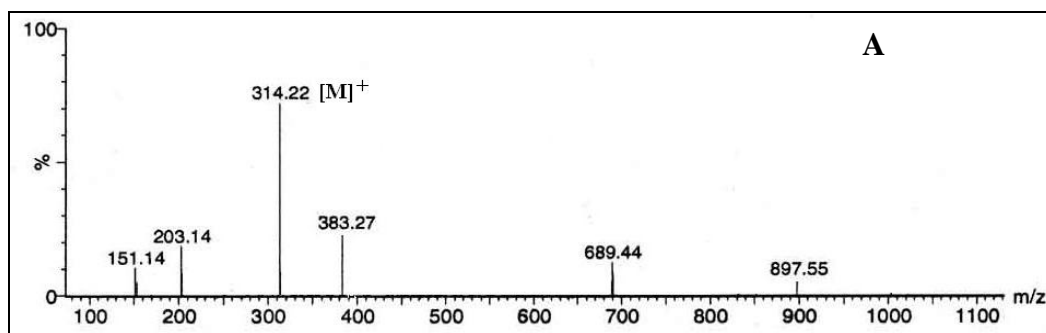


**Fig. 3.8** 4-*O*-(D-Mannopyranosyl)vanillin **18a,b** (A) Mass spectrum and (B) 2D-HSQC spectrum showing the C1-C6 region. Some of the assignments are interchangeable

(C3'), 70 (C4'), 60.8 (C6'), **Van**: 130 (C1), 109.5 (C2), 114.2 (C5), 126.8 (C6), **C1 $\beta$ -maltoside 20b**: Solid; mp. 102 °C, UV (H<sub>2</sub>O,  $\lambda_{\max}$ ): 195.5 nm ( $\sigma \rightarrow \sigma^*$ ,  $\epsilon_{195.5}$  - 3962 M<sup>-1</sup>), 225 nm ( $\sigma \rightarrow \pi^*$ ,  $\epsilon_{225}$  - 986 M<sup>-1</sup>), 279 nm ( $\pi \rightarrow \pi^*$ ,  $\epsilon_{279}$  - 417 M<sup>-1</sup>), IR (stretching frequency, cm<sup>-1</sup>): 3360 (OH), 1260 (glycosidic aryl alkyl C–O–C asymmetric), 1029 (glycosidic aryl alkyl C–O–C symmetric), 1422 (C=C), 1661 (CO), 2935 (CH), MS (*m/z*) 477 [M+1]<sup>+</sup>, optical rotation (*c* 1, H<sub>2</sub>O): [ $\alpha$ ]<sub>D</sub> at 25 °C = +92, 2D-HSQCT (DMSO-*d*<sub>6</sub>) <sup>1</sup>H NMR  $\delta_{\text{ppm}}$  (500.13 MHz) **Malt**: 4.25 (H-1 $\beta$ , d, *J* = 7.56 Hz), 3.24 (H-5 $\beta$ ), 3.52 (H-6a), 4.94 (H-1' $\alpha$ ), 3.25 (H-2'), 3.02 (H-3'), 3.64 (H-4'), 3.62 (H-5'), 3.54 (H-6'), **Van**: 7.97 (H-2), 7.18 (H-6), 3.71 (OCH<sub>3</sub>), <sup>13</sup>C NMR  $\delta_{\text{ppm}}$  (125 MHz) **Malt**: 100.5 (C1 $\beta$ ), 75.3 (C5 $\beta$ ), 61.3 (C6 $\beta$ ), 100.8 (C1' $\alpha$ ), 70.7 (C2'), 75 (C3'), 73.1 (C4'), 70.4 (C5'), 60.9 (C6'), **Van**: 129 (C1), 109.5 (C2), 126 (C6), 169.6 (CHO), **C6-O-arylated 20c**: <sup>1</sup>H NMR  $\delta_{\text{ppm}}$  **Malt**: 4.88 (H-1 $\alpha$ ), 3.54 (H-6 $\alpha$ ), 4.94 (H-1' $\alpha$ ), <sup>13</sup>C NMR  $\delta_{\text{ppm}}$  **Malt**: 92.4 (C1 $\alpha$ ), 67.2 (C6 $\alpha$ ), 100.3 (C1' $\alpha$ ). **C6'-O-arylated 20d**: <sup>1</sup>H NMR  $\delta_{\text{ppm}}$  **Malt**: 4.88 (H-1 $\alpha$ ), 4.94 (H-1' $\alpha$ ), 3.69 (H-6'), <sup>13</sup>C NMR  $\delta_{\text{ppm}}$  **Malt**: 92.4 (C1 $\alpha$ ), 100.3 (C1' $\alpha$ ), 66.1 (C6').

Infra-red and 2D-HSQCT NMR spectra for 4-*O*-( $\alpha$ -D-glucopyranosyl-(1'→4)D-glucopyranosyl)vanillin **20a,c,d** for amyloglucosidase catalysed products were shown in Figures 3.9A and 3.9B respectively. Mass and 2D-HSQCT NMR spectra for 4-*O*-( $\alpha$ -D-glucopyranosyl-(1'→4) $\beta$ -D-glucopyranosyl)vanillin **20b** for  $\beta$ -glucosidase catalysed product are shown in Figures 3.10A and 3.10B respectively.

**3.1.4.5 4-*O*-(D-Fructofuranosyl-(2→1') $\alpha$ -D-glucopyranosyl)vanillin 21a,b**: Solid; UV (H<sub>2</sub>O,  $\lambda_{\max}$ ): 194 nm ( $\sigma \rightarrow \sigma^*$ ,  $\epsilon_{194}$  - 6820 M<sup>-1</sup>), 278.5 nm ( $\pi \rightarrow \pi^*$ ,  $\epsilon_{278.5}$  - 423 M<sup>-1</sup>), IR (stretching frequency, cm<sup>-1</sup>): 3375 (OH), 1254 (glycosidic aryl alkyl C–O–C asymmetric), 1027 (glycosidic aryl alkyl C–O–C symmetric), 1408 (C=C), 1650 (CO), 2937 (CH), 1211 (OCH<sub>3</sub>), MS (*m/z*) 476 [M]<sup>+</sup>, 2D-HSQCT (DMSO-*d*<sub>6</sub>): **C1-O-arylated**

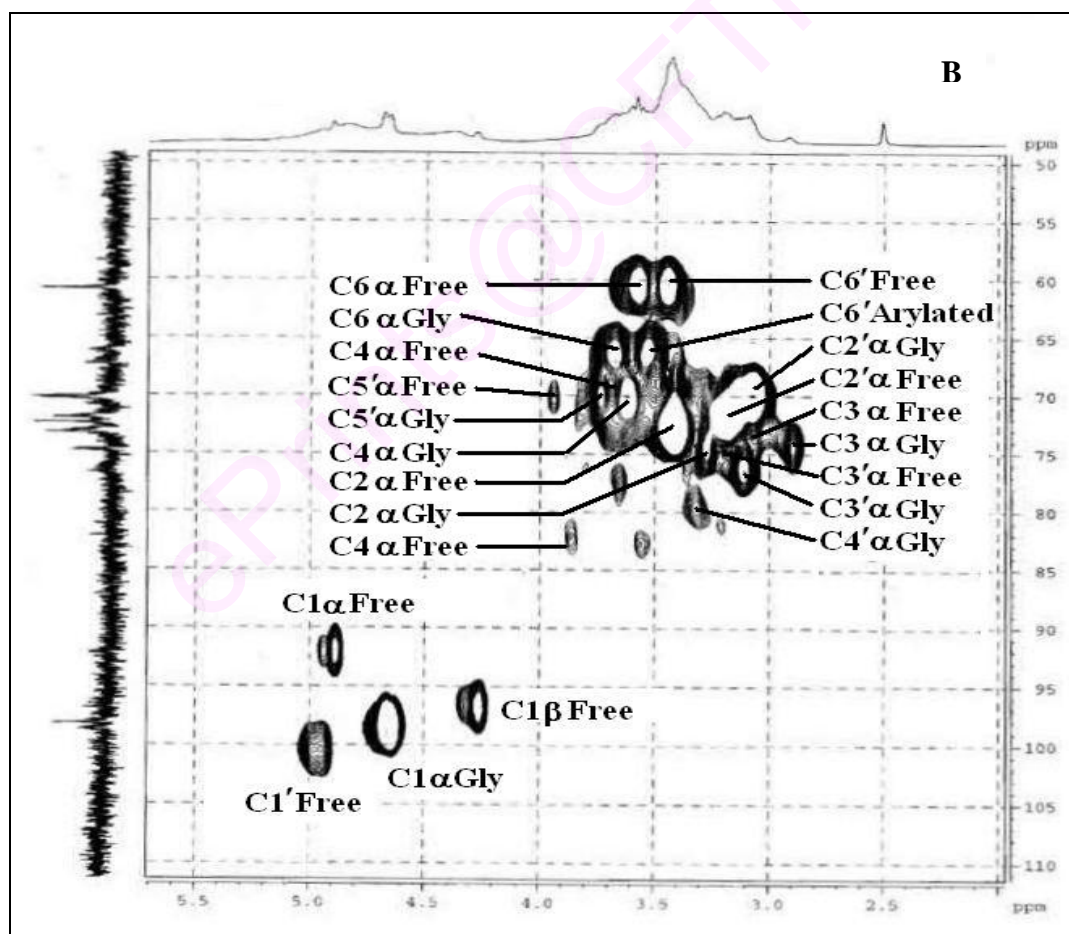
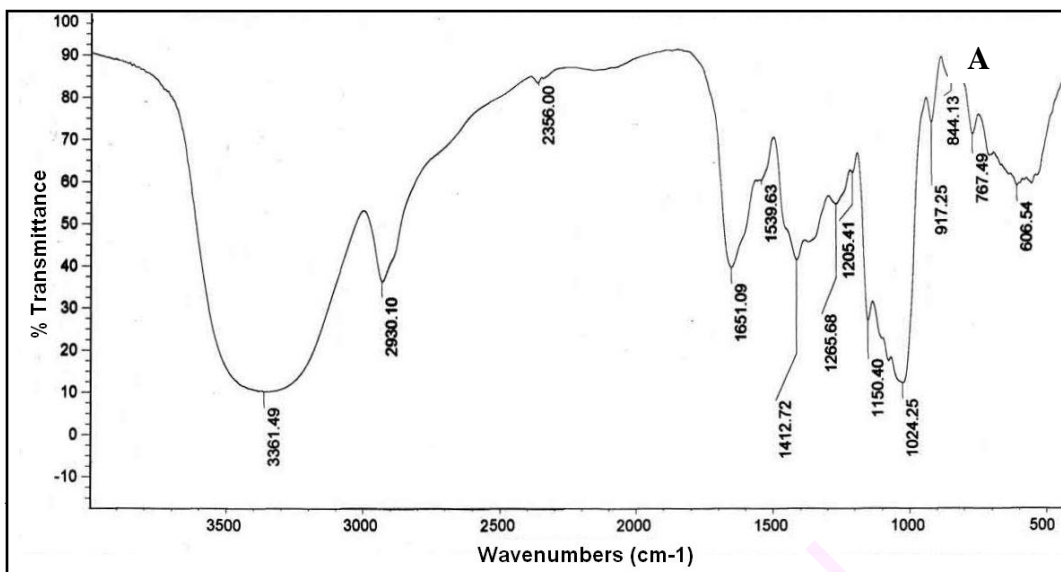


**Fig. 3.9** 4-*O*-( $\alpha$ -D-Glucopyranosyl-(1' $\rightarrow$ 4)D-glucopyranosyl)vanillin **20a,c,d** (A) IR spectrum and (B) 2D-HSQC spectrum showing the C1-C6' region. Some of the assignments are interchangeable.

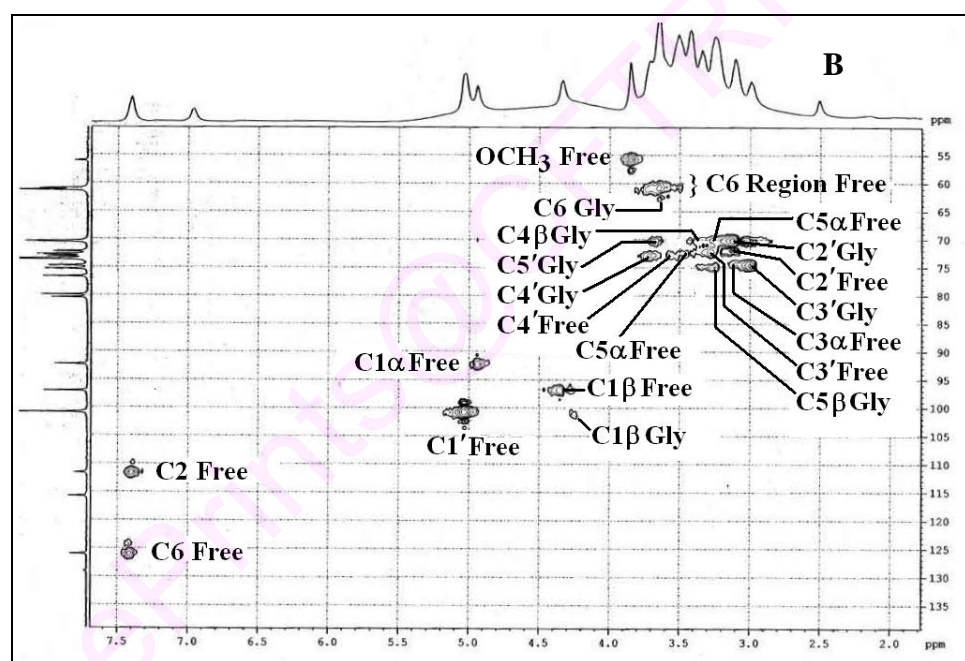
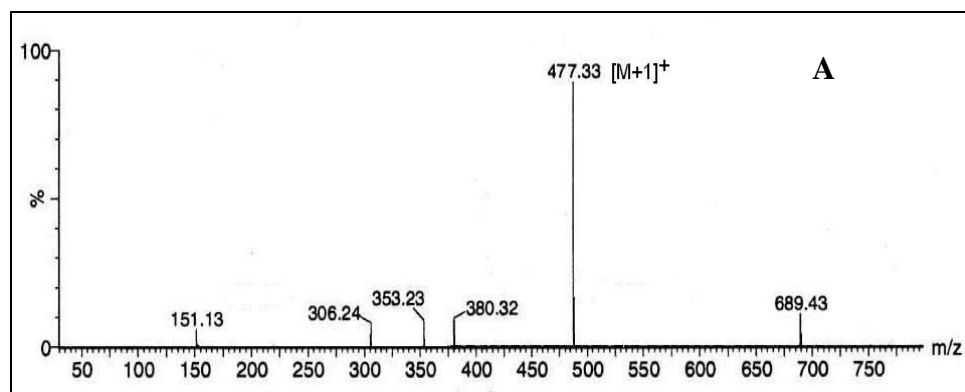


**Fig. 3.10** 4-*O*-( $\alpha$ -D-Glucopyranosyl-(1' $\rightarrow$ 4) $\beta$ -D-glucopyranosyl)vanillin **20b** (A) Mass spectrum and (B) 2D-HSQC spectrum showing the C1-C6' region. Some of the assignments are interchangeable

**21a:**  $^1\text{H}$  NMR  $\delta_{\text{ppm}}$  (500.13 MHz) **Sucr:** 3.49 (H-1), 3.88 (H-3), 3.89 (H-4), 3.86 (H-5), 3.40 (H-6), 4.72 (H-1' $\alpha$ ), 3.68 (H-2'), 3.46 (H-3'), 3.62 (H-4'), 3.65 (H-5'), 3.59 (H-6'), **Van:** 7.22 (H-2), 6.60 (H-5), 8.35 (H-6),  $^{13}\text{C}$  NMR  $\delta_{\text{ppm}}$  (125 MHz) **Sucr:** 66 (C1), 70.8 (C3), 80.9 (C4), 81.5 (C5), 62.2 (C6), 98.5 (C1' $\alpha$ ), 71 (C2'), 72.2 (C3'), 69.8 (C4'), 72.1 (C5'), 60.5 (C6'), **Van:** 112.8 (C5), 126.3 (C6), **C6'-O-arylated 21b:**  $^1\text{H}$  NMR  $\delta_{\text{ppm}}$  **Sucr:** 3.48 (H-1), 3.67 (H-3), 3.57 (H-5), 3.46 (H-6), 4.63 (H-1' $\alpha$ ), 3.08 (H-2'), 3.42 (H-3'), 3.72 (H-6'),  $^{13}\text{C}$  NMR  $\delta_{\text{ppm}}$  **Sucr:** 62.3 (C1), 76.5 (C3), 82.2 (C5), 60.5 (C6), 98.6 (C1' $\alpha$ ), 69.9 (C2'), 72.3 (C3'), 66.1 (C6').

Figure 3.11A shows IR spectrum and Figures 3.11B and 3.11C show 2D-HSQCT NMR spectra for 4-*O*-(D-fructofuranosyl-(2 $\rightarrow$ 1') $\alpha$ -D-glucopyranosyl) vanillin **21a,b**.

**3.1.4.6 4-O-( $\beta$ -D-Galactopyranosyl-(1 $\rightarrow$ 4) $\beta$ -D-glucopyranosyl)vanillin 22:** Solid, mp. 119°C, UV (H<sub>2</sub>O  $\lambda_{\text{max}}$ ): 194.5 nm ( $\sigma \rightarrow \sigma^*$ ,  $\epsilon_{194.5} = 8230 \text{ M}^{-1}$ ), 222 nm ( $\sigma \rightarrow \pi^*$ ,  $\epsilon_{222} = 1347 \text{ M}^{-1}$ ), 283.5 nm ( $\pi \rightarrow \pi^*$ ,  $\epsilon_{283.5} = 349 \text{ M}^{-1}$ ), IR (stretching frequency,  $\text{cm}^{-1}$ ): 3350 (OH), 1256 (glycosidic aryl alkyl C-O-C asymmetrical), 1040 (glycosidic aryl alkyl C-O-C symmetrical), 1416 (C=C), 1669 (CO), 2928 (CH), optical rotation (*c* 0.5, H<sub>2</sub>O):  $[\alpha]_{\text{D}}$  at 25 °C = +3.4, MS (*m/z*) = 499.3  $[\text{M}+\text{Na}]^+$ , 2D-HSQCT (DMSO-*d*<sub>6</sub>):  $^1\text{H}$  NMR  $\delta_{\text{ppm}}$  (500.13 MHz) **Lact:** 4.96 (H-1 $\beta$ , d, *J* = 6.4 Hz), 3.15 (H-2 $\beta$ ), 3.44 (H-3 $\beta$ ), 3.48 (H-6a), 4.16 (H-1 $\beta'$ ), 3.81 (H-4'), 3.05 (H-5'), **Van:** 7.41 (H-2), 6.96 (H-6), 3.70 (OCH<sub>3</sub>), 9.75 (CHO),  $^{13}\text{C}$  NMR  $\delta_{\text{ppm}}$ : (125 MHz) **Lact:** 101.5 (C1 $\beta$ ), 76.5 (C2 $\beta$ ), 70.8 (C3 $\beta$ ), 62 (C6 $\beta$ ), 104 (C1 $\beta'$ ), 68.2 (C4'), 74.5 (C5'), **Van:** 111.6 (C2), 153.3 (C4), 129 (C6), 56 (OCH<sub>3</sub>), 190.9 (CHO).

Mass and 2D-HSQCT NMR spectra for 4-*O*-( $\beta$ -D-galactopyranosyl-(1' $\rightarrow$ 4) $\beta$ -D-glucopyranosyl)vanillin **22** are shown in Figures 3.12A and 3.12B respectively.

**3.1.4.7 4-O-(D-sorbitol)vanillin 23a-c:** Solid; UV (H<sub>2</sub>O,  $\lambda_{\text{max}}$ ): 193.5 nm ( $\sigma \rightarrow \sigma^*$ ,  $\epsilon_{193.5} = 2940 \text{ M}^{-1}$ ), 273 nm ( $\pi \rightarrow \pi^*$ ,  $\epsilon_{273} = 289 \text{ M}^{-1}$ ), IR (stretching frequency,  $\text{cm}^{-1}$ ): 3387 (OH),



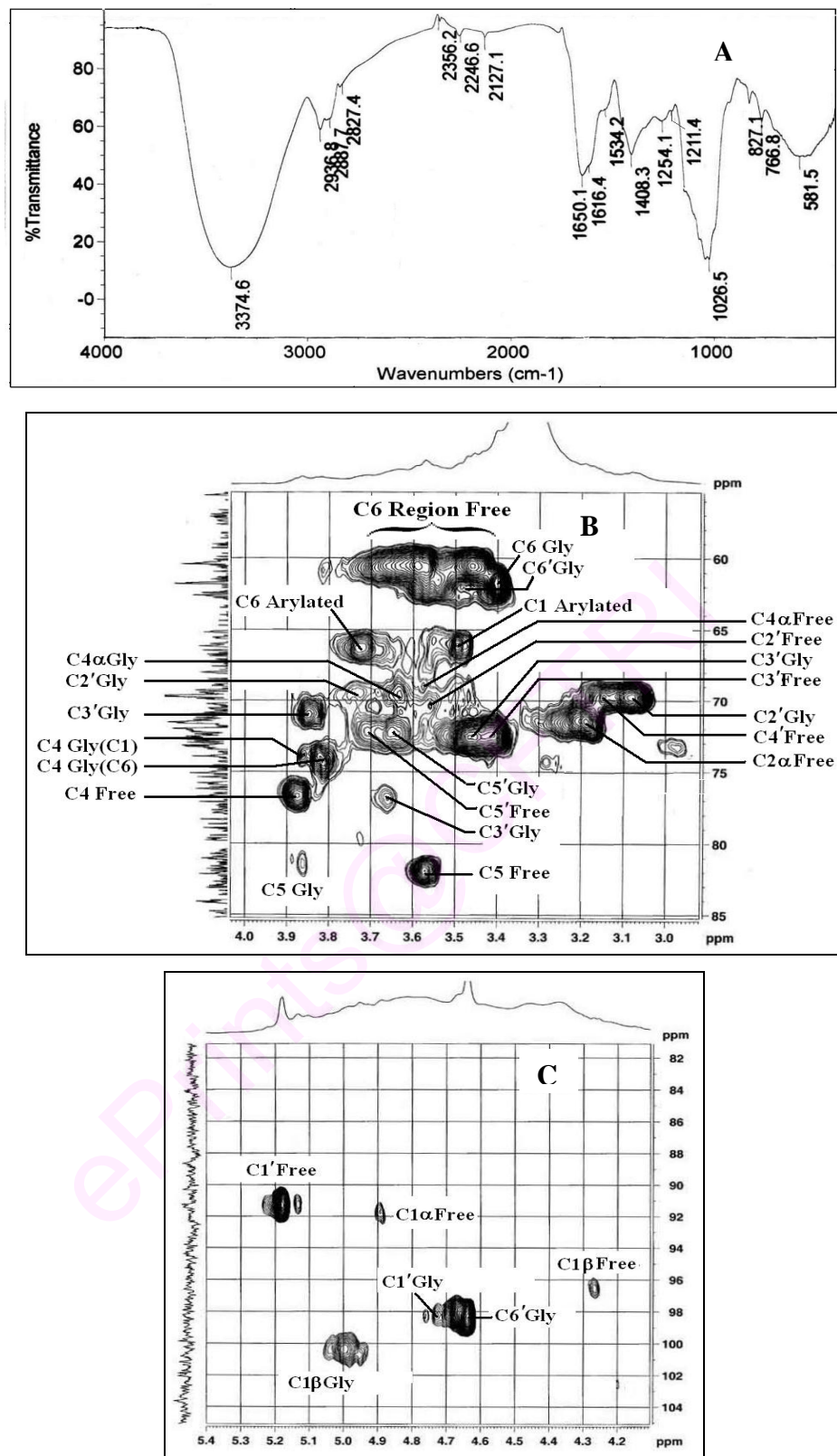


**Fig. 3.11** 4-*O*-(D-Fructofuranosyl-(2→1')-α-D-glucopyranosyl)vanillin **21a,b** (A) IR spectrum, (B) 2D-HSQC spectrum showing the C1-C6' region and (C) Anomeric region. Some of the assignments are interchangeable.

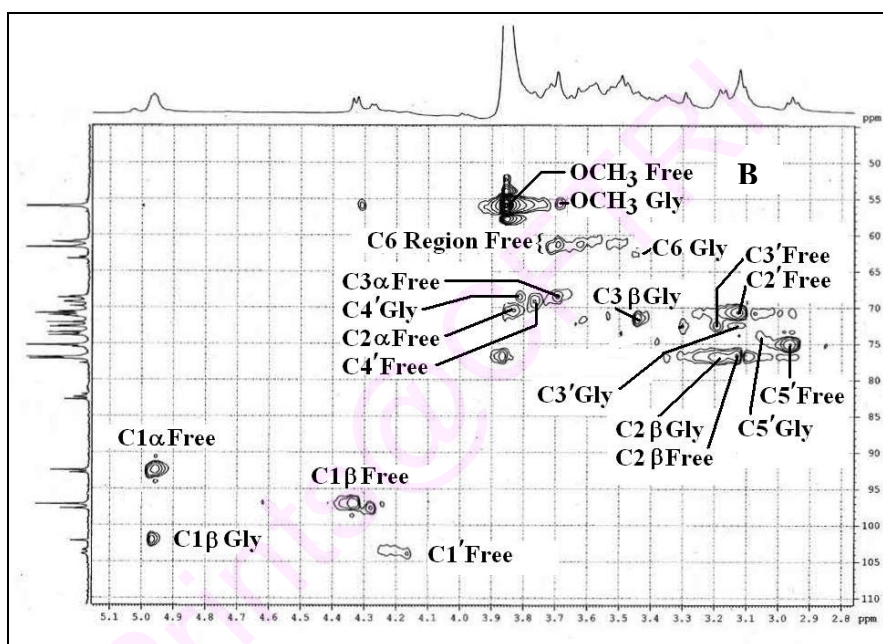
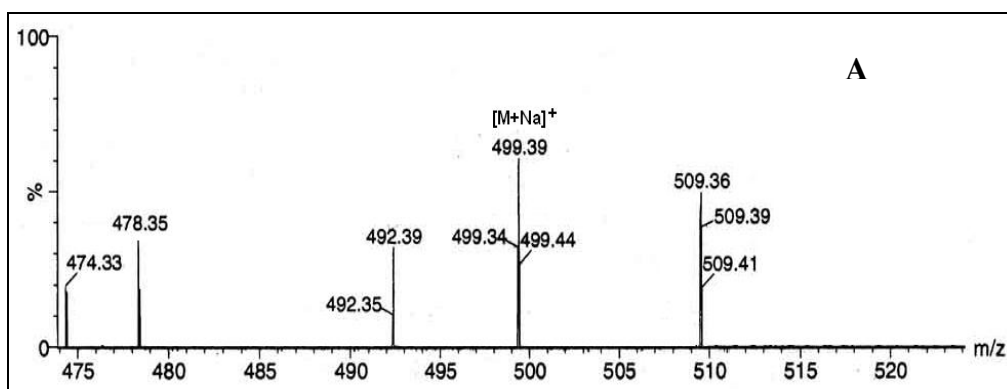


**Fig. 3.12** 4-*O*-( $\beta$ -D-Glucopyranosyl-(1'→4) $\beta$ -D-glucopyranosyl)vanillin **22**  
**(A)** Mass spectrum and **(B)** 2D-HSQC spectrum showing the C1-C6' region. Some of the assignments are interchangeable



1260 (glycosidic aryl alkyl C–O–C asymmetric), 1039 (glycosidic aryl alkyl C–O–C symmetric), 1409 (C=C), 2943 (CH), MS: ( $m/z$ ) mono-arylated 339.2  $[M+Na]^+$ , di-arylated 473.4  $[M+Na]^+$ ; 2D-HSQCT (DMSO- $d_6$ ): **C1-O-arylated 23a**:  $^1H$  NMR  $\delta_{ppm}$  (500.13 MHz) **Sorb**: 3.65 (H-1), 3.37 (H-2), 3.48 (H-3), 3.57 (H-4), 3.54 (H-5), 3.58 (H-6), **Van**: 7.40 (H-2), 7.20 (H-5), 7.58 (H-6), 3.81 (OCH<sub>3</sub>), 9.75 (CHO),  $^{13}C$  NMR (125 MHz)  $\delta_{ppm}$  **Sorb**: 67.2 (C1), 70.5 (C2), 74.1 (C3), 71.2 (C4), 69 (C5), 62.9 (C6), **Van**: 130.5 (C1), 111.2 (C2), 153.8 (C4), 111.1 (C5), 124.5 (C6), 55.9 (OCH<sub>3</sub>), 191.5 (CHO), **C6-O-arylated 23b**:  $^1H$  NMR  $\delta_{ppm}$  **Sorb**: 3.55 (H-1), 3.54 (H-2), 3.44 (H-3), 3.68 (H-4), 3.46 (H-5), 3.58 (H-6), **Van**: 6.88 (H-2), 6.85 (H-5), 7.39 (H-6),  $^{13}C$  NMR  $\delta_{ppm}$  **Sorb**: 63.2 (C1), 70.8 (C2), 72.5 (C3), 73.1 (C4), 68.2 (C5), 66.2 (C6), **Van**: 129.1 (C1), 110.8 (C2), 153.8 (C4), 111.4 (C5), 126.1 (C6), **C1–C6 di-O-arylated 23c**:  $^1H$  NMR  $\delta_{ppm}$  **Sorb**: 3.46 (H-1), 3.35 (H-2), 3.36 (H-3), 3.54 (H-4), 3.65 (H-6), **Van**: 6.65, 6.68 (H-5), 6.69, 6.84 (H-6),  $^{13}C$  NMR  $\delta_{ppm}$  **Sorb**: 66.5 (C1), 67 (C2), 73.5 (C3), 76.1 (C4), 65.5 (C6), **Van**: 129.1, 130.5 (C1), 111.3, 111.7 (C2), 153.5, 153.5 (C4), 115.3, 115.9 (C5), 119.8, 120.3 (C6).

Infra-red, mass and 2D-HSQCT NMR spectra for 4-*O*-(D-sorbitol)vanillin **23a-c** are shown in Figures 3.13A, 3.13B and 3.13C respectively.

UV spectra of vanillyl glycosides, showed shifts in  $\sigma \rightarrow \sigma^*$  band in the 193.5 – 198.5 nm (195 nm for free vanillin) range,  $\sigma \rightarrow \pi^*$  band in the 222 – 224.5 nm (228.5 nm for free vanillin) range,  $\pi \rightarrow \pi^*$  band in the 273 - 283.5 nm (272 nm for free vanillin) range, IR C-O-C asymmetrical stretching frequencies in the 1249 - 1265  $cm^{-1}$  range and symmetrical stretching frequencies in the 1024 - 1038  $cm^{-1}$  range indicating that vanillin had undergone glycosylation. From 2D HSQCT spectra of the vanillyl glycosides, the following glycoside formation were confirmed from their respective chemical shift values: from D-glucose **6** C1 $\alpha$  glucoside **17a** to C1 $\alpha$  at 99.2 ppm and H-1 $\alpha$  at 4.65 ppm,

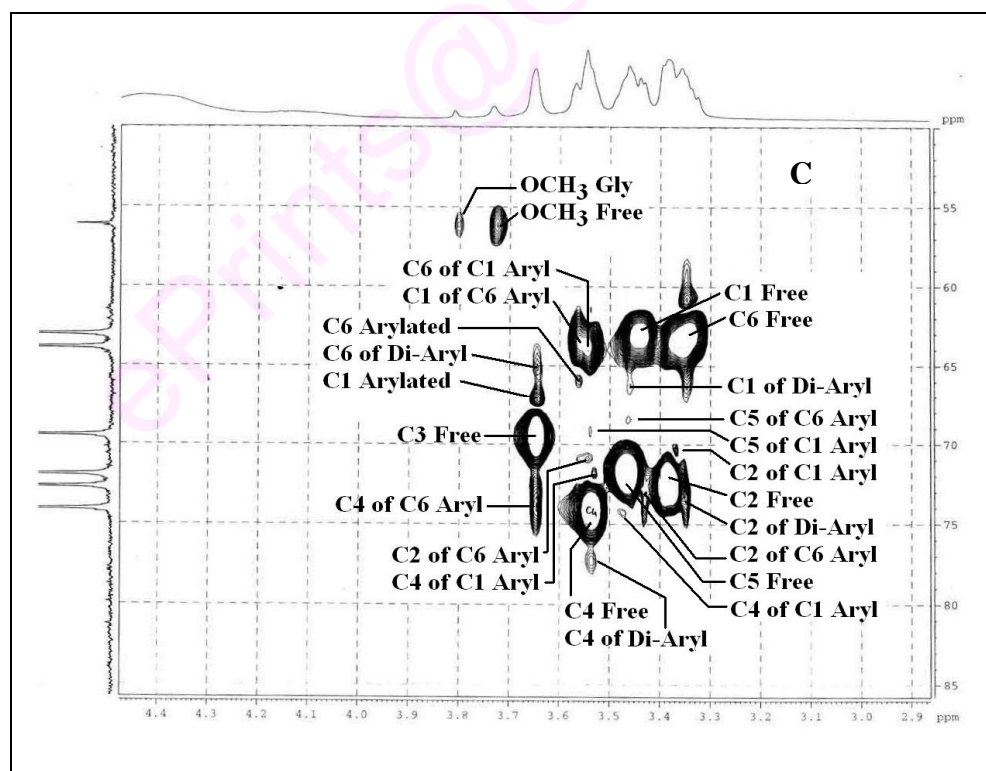
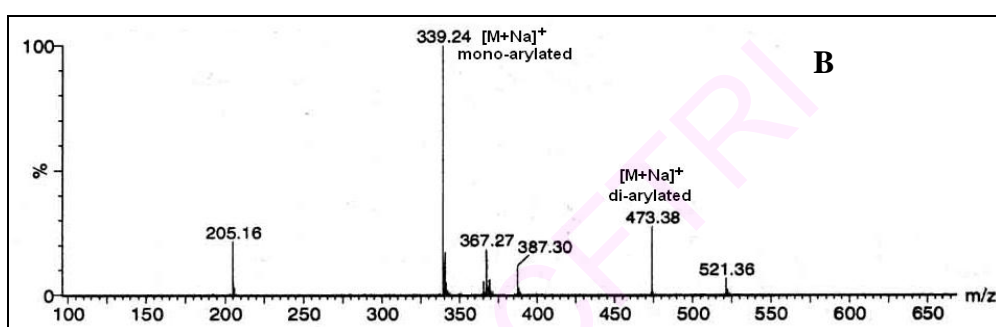
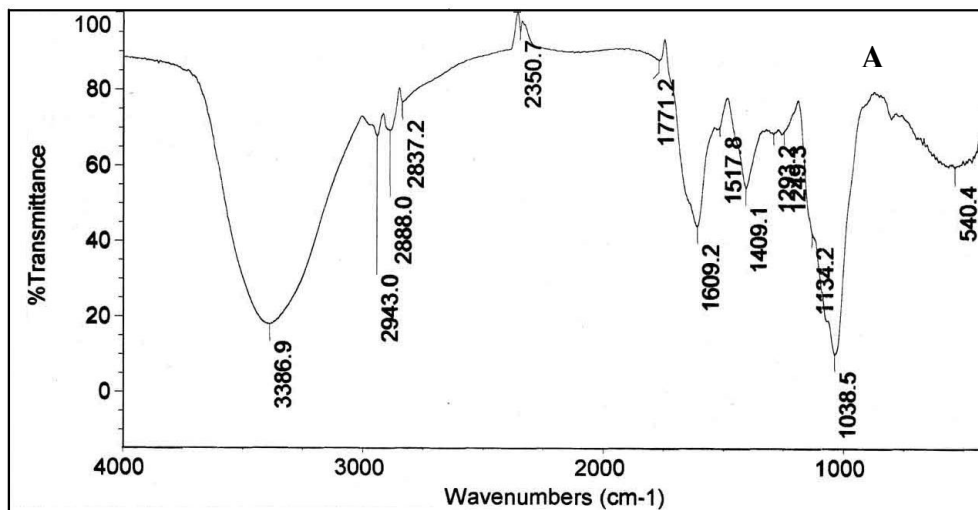


**Fig. 3.13** 4-*O*-(*D*-Sorbitol)vanillin **23a-c** (A) IR spectrum, (B) Mass spectrum and (C) 2D-HSQC spectrum showing the C1-C6 region. Some of the assignments are interchangeable

C1 $\beta$  glucoside **17b** to C1 $\beta$  at 101.5 ppm and H-1 $\beta$  at 4.94 ppm and C6-*O*-arylated **17c** to C6 at 68 ppm and H-6a at 3.55 ppm; from D-galactose **7** C1 $\alpha$  galactoside **18a** to C1 $\alpha$  at 95.8 ppm and H-1 $\alpha$  at 5.10 ppm and C1 $\beta$  galactoside **18b** to C1 $\beta$  at 102.1 ppm and H-1 $\beta$  at 4.95 ppm; from D-mannose **8** C1 $\alpha$  mannoside **19a** to C1 $\alpha$  at 100.8 ppm and H-1 $\alpha$  at 4.99 ppm and C1 $\beta$  mannoside **19b** to C1 $\beta$  at 102 ppm and H-1 $\beta$  at 4.90 ppm; from maltose **12** C1 $\alpha$  maltoside **20a** to C1 $\alpha$  at 98.2 ppm and H-1 $\alpha$  at 4.68 ppm, C1 $\beta$  maltoside **20b** to C1 $\beta$  at 100.5 ppm and H-1 $\beta$  at 4.25 ppm, C6-*O*-arylated **20c** to C6 at 67.2 ppm and H-6a at 3.54 ppm and C6'-*O*-arylated **20d** to C6' at 66.1 ppm and H-6'a at 3.69 ppm; from sucrose **13** C1-*O*-arylated **21a** to C1 at 66 ppm and H-1 at 3.49 ppm and C6-*O*-arylated **21b** to C6 at 66.1 ppm and H-6 at 3.72 ppm; from lactose **14** C1 $\beta$  lactoside **22** to C1 $\beta$  at 101.5 ppm and H-1 $\beta$  at 4.96 ppm; from D-sorbitol **15** C1-*O*-arylated **23a** to C1 at 67.2 ppm and H-1 at 3.65 ppm, C6-*O*-arylated **23b** to C6 at 66.2 ppm and H-6 at 3.58 ppm and C1,C6-*O*-arylated **23c** to C1 at 66.5 ppm and H-1 at 3.46 ppm and C6 at 65.5 ppm and H-6 at 3.65 ppm. Also NMR data clearly showed that hydrolysis of sucrose to glucose and fructose had occurred along with the transglucosylated product to C1 $\beta$  at 101.5 and H-1 at 4.94 ppm, besides C6-*O*-arylated at 68 ppm and H-6 at 3.55 ppm. Mass spectra also confirmed the formation of the above mentioned glycosides.

### 3.1.5 Discussion

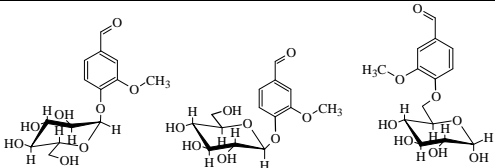
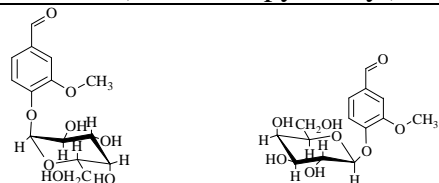
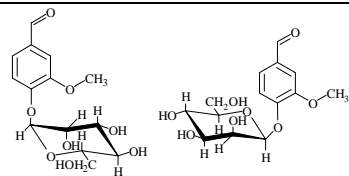
The nature and proportions of vanillyl glycosides formed are shown in Table 3.3. Among the carbohydrates **6-16** employed amyloglucosidase gave rise to six glycosides: 4-*O*-(D-glucopyranosyl)vanillin **17a-c**, 4-*O*-( $\alpha$ -D-galactopyranosyl)vanillin **18a**, 4-*O*-( $\alpha$ -D-mannopyranosyl)vanillin **19a**, 4-*O*-( $\alpha$ -D-glucopyranosyl-(1'→4)D-glucopyranosyl)vanillin **20a,c,d**, 4-*O*-(D-fructofuranosyl-(2→1') $\alpha$ -D-glucopyranosyl)vanillin **21a,b** and

4-*O*-(D-sorbitol)vanillin **23a-c**.  $\beta$ -Glucosidase gave rise to five glycosides: 4-*O*-( $\beta$ -D-glucopyranosyl)vanillin **17b**, 4-*O*-(D-galactopyranosyl)vanillin **18a,b**, 4-*O*-(D-mannopyranosyl)vanillin **19a,b**, 4-*O*-( $\alpha$ -D-glucopyranosyl-(1'→4) $\beta$ -D-glucopyranosyl)vanillin **20b** and 4-*O*-( $\beta$ -D-galactopyranosyl-(1'→4) $\beta$ -D-glucopyranosyl)vanillin **22**.

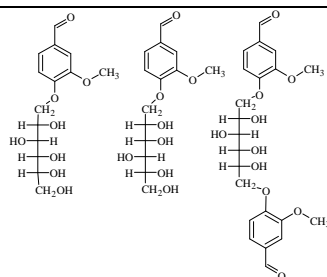
D-Glucose **6** employed was an  $\alpha,\beta$  anomeric mixture (40:60), the glycosides formed showed predominant proportions of the  $\alpha$  anomer (>80%), indicating the potential for 'inverting' amyloglucosidase (from *Rhizopus* mold) to convert the majority of  $\beta$ -D-glucose into its respective  $\alpha$ -D-glucoside. In hydrolysis, amyloglucosidase hydrolyses  $\alpha$ -1,4 linked glucose units in amylose to give  $\beta$ -glucose.

A maximum yield of 53% was obtained for a mixture of three mono-glucosides of 4-*O*-(D-glucopyranosyl)vanillin **17a-c** (Table 3.3). Also, amyloglucosidase catalysis gave C1  $\alpha$  and  $\beta$  glycosides along with arylated derivatives in many cases except D-galactose **7** and D-mannose **8** (Table 3.3). However,  $\beta$ -glucosidase catalysis gave exclusively C1 $\beta$  glycosides with the exception of D-galactose **7** and D-mannose **8**, indicating its capability to exhibit excellent regioselectivity in this glycosylation with the carbohydrate molecules D-glucose **6**, maltose **12** and lactose **14** (Table 3.3). In case of  $\beta$ -glucosidase, it significantly altered the anomeric composition of D-galactose **7** - 23%  $\alpha$ -D-galactoside and 77%  $\beta$ -D-galactoside compared to the 92:8  $\alpha$ :  $\beta$  anomeric composition of D-galactose employed and D-mannose **8** - 44%  $\alpha$ -D-mannoside and 56%  $\beta$ -D-mannoside compared to the 27:73  $\alpha$ :  $\beta$  anomeric composition of D-mannose employed. Among the carbohydrates employed sucrose **13** and D-sorbitol **15** gave C1-*O*- and C6-*O*-arylated products with vanillin **1**.

**Table 3.3** Syntheses of vanillyl glycosides using amyloglucosidase and  $\beta$ -glucosidase.

Glycosides	Amyloglucosidase catalysis <sup>a</sup>		$\beta$ -Glucosidase catalysis <sup>b</sup>	
	Product (% proportion) <sup>c</sup>	Yields (%) <sup>d</sup>	Product (% proportion) <sup>c</sup>	Yields (%) <sup>d</sup>
 <p><b>17a</b> 4-<i>O</i>-(<math>\alpha</math>-D-Glucopyranosyl)vanillin  <b>17b</b> 4-<i>O</i>-(<math>\beta</math>-D-Glucopyranosyl)vanillin  <b>17c</b> 4-<i>O</i>-(6-D-Glucopyranosyl)vanillin</p>	C1 $\alpha$ glucoside (52), C1 $\beta$ glucoside (17), C6- <i>O</i> -arylated (31)	53	C1 $\beta$ glucoside	10
 <p><b>18a</b> 4-<i>O</i>-(<math>\alpha</math>-D-Galactopyranosyl)vanillin  <b>18b</b> 4-<i>O</i>-(<math>\beta</math>-D-Galactopyranosyl)vanillin</p>	C1 $\alpha$ galactoside	18	C1 $\alpha$ galactoside (23), C1 $\beta$ galactoside (77)	6
 <p><b>19a</b> 4-<i>O</i>-(<math>\alpha</math>-D-Mannopyranosyl)vanillin  <b>19b</b> 4-<i>O</i>-(<math>\beta</math>-D-Mannopyranosyl)vanillin</p>	C1 $\alpha$ mannoside	13	C1 $\alpha$ mannoside (44), C1 $\beta$ mannoside (56)	13

	<b>20a</b> 4- <i>O</i> -( $\alpha$ -D-Glucopyranosyl-(1'→4) $\alpha$ -D-glucopyranosyl)vanillin	C1 $\alpha$ maltoside (42), C6- <i>O</i> -arylated (30), C6'- <i>O</i> -arylated (28)	29	C1 $\beta$ maltoside	8
<b>20b</b> 4- <i>O</i> -( $\alpha$ -D-Glucopyranosyl-(1'→4) $\beta$ -D-glucopyranosyl)vanillin					
	<b>20c</b> 4- <i>O</i> -( $\alpha$ -D-Glucopyranosyl-(1'→4)6-D-glucopyranosyl)vanillin <b>20d</b> 4- <i>O</i> -( $\alpha$ -D-Glucopyranosyl-(1'→4)6'-D-glucopyranosyl)vanillin				
	<b>21a</b> 4- <i>O</i> -(1-D-Fructofuranosyl-(2→1') $\alpha$ -D-glucopyranosyl)vanillin <b>21b</b> 4- <i>O</i> -(6'-D-Fructofuranosyl-(2→1') $\alpha$ -D-glucopyranosyl)vanillin	C1- <i>O</i> -arylated (39), C6'- <i>O</i> -arylated (61)	23	-	-
	<b>22</b> 4- <i>O</i> -( $\beta$ -D-Galactopyranosyl-(1'→4) $\beta$ -D-glucopyranosyl)vanillin	-	-	C1 $\beta$ lactoside	25



**23a** 4-*O*-(1-D-Sorbitol)vanillin

**23b** 4-*O*-(6-D-Sorbitol)vanillin

**23c** 1,6-*O*-(Bis-4-*O*-vanillin)D-sorbitol

C1-*O*-arylated (13),  
C6-*O*-arylated (25),  
C1,6 di-*O*-arylated (62) 13 - -

<sup>a</sup>Vanillin and carbohydrate – 1 mmol each; amyloglucosidase concentration 40% w/w of carbohydrate; solvent – di-isopropyl ether; buffer – 0.1 mM (1 mL) pH 4 acetate buffer; incubation period – 72 h. <sup>b</sup>Vanillin – 1 mmol and carbohydrate – 0.5 mmol;  $\beta$ -glucosidase concentration 50% w/w of carbohydrate; solvent – di-isopropyl ether; buffer – 0.17 mM (1.7 mL) pH 4.2 acetate buffer; incubation period – 24 h. <sup>c</sup>Conversion yields were from HPLC with respect to free carbohydrate. Error in yield measurements is  $\pm 10\%$ . <sup>d</sup>The product proportions were determined from the area of respective <sup>1</sup>H/<sup>13</sup>C signals.

In case of sucrose **13** the C6-*O*-arylated product proportion was more compared to the C1-*O*-arylated product, which could be due to the steric hindrance offered by the C2 position of the fructose moiety when it is transferred to such phenolic nucleophiles. The hydrolysis of the disaccharides, maltose **12**, sucrose **13** and lactose **14** during the course of the reaction has been observed and only in case of sucrose **13** the resultant glucose formed, underwent transglycosylation to yield C1 $\beta$  glucosylated and C6-*O*-arylated products with vanillin **1**. In general  $\beta$ -glucosidase gave low conversions compared to amyloglucosidase. Also, while  $\beta$ -glucosidase catalysed reaction with lactose **14**, amyloglucosidase did not. Even the presence of an hydrophobic aldehydic group in vanillin did not pose much of a steric hindrance when the carbohydrate molecules were transferred to its phenolic OH group. Both amyloglucosidase and  $\beta$ -glucosidase did not catalyse D-fructose **9**, D-arabinose **10**, D-ribose **11** and D-mannitol **16**. Vanillin **1** could be a better inhibitor to these enzymes compared to these carbohydrate molecules, binding strongly to the enzyme, thereby blocking the facile transfer of the carbohydrate molecule to the nucleophilic phenolic OH of vanillin **1**.

About 17 individual glycosides were synthesized enzymatically using both the glucosidases, of which 14 are being reported for the first time. The new glycosides reported are: 4-*O*-(D-galactopyranosyl)vanillin **18a,b**, 4-*O*-(D-mannopyranosyl)vanillin **19a,b**, 4-*O*-( $\alpha$ -D-glucopyranosyl-(1'→4)D-glucopyranosyl)vanillin **20a-d**, 4-*O*-(D-fructofuranosyl-(2→1') $\alpha$ -D-glucopyranosyl)vanillin **21a,b**, 4-*O*-( $\beta$ -D-galactopyranosyl-(1'→4) $\beta$ -D-glucopyranosyl)vanillin **22** and 4-*O*-(D-sorbitol)vanillin **23a-c**.

### 3.1.6 Synthesis of 4-*O*-( $\alpha$ -D-glucopyranosyl-(1'→4)D-glucopyranosyl)vanillin using glucosidases by response surface methodology

Hydrolytic enzymes have been used to catalyze reverse reactions that are impossible to carry out under aqueous conditions because of kinetic or thermodynamic



restrictions (Zaks and Klibanov 1985; Coulon *et al.* 1996). Glucosidases exhibit potential use in the synthesis of glycosides (Ismail *et al.* 1999b). Reverse hydrolytic method can be an attractive approach for the synthesis of glycosides as it results in a cost-effective and simple procedure making it acceptable for industrial scale-up (David and Gabin 1998). Recent developments in molecular glycobiology has shown better understanding of the aglycon and glycoside activities and made it possible to develop new and more active compounds (Kren and Martinkova 2001).

Response Surface Methodology has been successfully applied in many areas such as food, chemicals, or biological processes (Manohar and Divakar 2002; Gunawan *et al.* 2005; Huang and Akoh 1996; Shieh *et al.* 1995; Chen *et al.* 1997). Almond  $\beta$ -glucosidase catalysed synthesis of hexyl glycoside was carried out by Andersson and Adlercreutz (Andersson and Adlercreutz 2001) and butyl glucoside by Ismail *et al.* (Ismail *et al.* 1998). Amyloglucosidase requires some amount of water to be present in the form of buffer salts to exhibit its optimum activity and this can be achieved by adding buffer of certain volume, salt concentration and pH (Chahid *et al.* 1992; Vic *et al.* 1997). Chahid *et al.* (Chahid *et al.* 1994) synthesized a mixture of octyl glucoside and octyl galactoside with lactose and n-octanol using  $\beta$ -galactosidase through a transglycosylation reaction. In our earlier work, Central Composite Rotatable Design was successfully employed for the optimization of parameters for the amyloglucosidase catalysed synthesis of n-octyl-D-glucoside at shake flask method (Vijayakumar *et al.* 2005) and curcumin-bis- $\alpha$ -D-glucoside by reflux method (Vijayakumar *et al.* 2006).

The present work involves synthesis of 4-O-( $\alpha$ -D-glucopyranosyl-(1'→4)D-glucopyranosyl)vanillin using amyloglucosidase from *Rhizopus* mold and  $\beta$ -glucosidase from sweet almond to deduce the optimum reaction conditions through Response Surface Methodology. A Central Composite Rotatable Design (CCRD) was employed with five

parameters, namely, enzyme concentration, vanillin concentration, incubation period, buffer volume and pH with both the enzymes. The results of this investigation are presented in detail here.

### 3.1.6.1 Glycosylation

A typical synthesis involved refluxing vanillin **1** (0.5-2.5 mmol) and maltose **12** (0.5 mmol) with stirring in 100 mL of di-isopropyl ether in presence of 10–50% (w/w of maltose) amyloglucosidase/ $\beta$ -glucosidase and 0.04 mM (0.4 mL) - 0.2 mM (2 mL) of 10 mM pH 4 – 8 buffer (CH<sub>3</sub>COONa buffer for pH 4 and pH 5, Na<sub>2</sub>HPO<sub>4</sub> for pH 6 and pH 7 and Na<sub>2</sub>B<sub>4</sub>O<sub>7</sub> .10 H<sub>2</sub>O for pH 8 were used) for a period of 24-120 h (Scheme 3.1). The solvent was distilled off and the reaction mixture was held on a boiling water bath for 5-10 min to denature the enzyme. The reaction mixture was dissolved in 20-30 mL water and the unreacted vanillin **1** was removed by repeated extraction with chloroform. The aqueous portion was subjected to flash evaporation to obtain the unreacted maltose **12** and the product maltoside as a solid. The workup analysis and isolation are as described on page 74.

### 3.1.6.2 Response Surface Methodology

A five variable parametric study was employed for the CCRD analysis (Montgomery 1991). The five variables employed were glucosidase concentration, vanillin concentration, incubation period, buffer volume and pH in case of both the glucosidases. The experimental design included 32 experiments of five variables at five levels (-2, -1, 0, +1, +2). Table 3.4 shows the coded and actual levels of the variables employed in the design matrix. Actual set of experiments undertaken as per CCRD with coded values and the maltosylation yields obtained are given in Table 3.5. A second order polynomial equation was developed to study the effect of the variables on the

maltoside yields. The equation indicates the effect of variables in terms of linear, quadratic and cross product terms. The general equation is of the form,

$$Y = A_0 + \sum_{i=1}^N A_i X_i + \sum_{i=1}^N A_{ii} X_i^2 + \sum_{i=1}^{N-1} \sum_{j=i+1}^N A_{ij} X_i X_j \dots\dots\dots(1)$$

where Y is the maltosylation yield (%),  $A_0$  = constant term,  $X_i$  are the variables,  $A_i$  are the coefficients of the linear terms,  $A_{ii}$  are the coefficients of the quadratic terms,  $A_{ij}$  are the coefficients of the cross product terms and N is the number of variables.

**Table 3.4** Coded values of the variables and their corresponding actual values used in the design of experiments.

Variables	-2	-1	0	1	2
Amyloglucosidase/ $\beta$ -glucosidase (% w/w maltose)	10	20	30	40	50
Vanillin (mmol)	0.5	1	1.5	2	2.5
Incubation Period (h)	24	48	72	96	120
Buffer Volume (mL)	0.4	0.8	1.2	1.6	2
pH (0.01M)	4	5	6	7	8

Coefficients of the equation were determined by employing Microsoft Excel software, version 5. Analysis of variance (ANOVA) for the final predictive equation was also done using Microsoft Excel software. ANOVA is required to test the significance and adequacy of the model. The response surface equation was optimized for maximum yield in the range of process variables using a Multiple Regression Software (Wessa 2006).

Our preliminary study on the synthesis of vanillyl glucoside has shown that amyloglucosidase, vanillin and buffer concentrations along with buffer pH and incubation period have profound influence on the extent of glycosylation and formation of product glycosides. Hence, these parameters were employed in the present RSM study of 4-*O*-( $\alpha$ -D-glucopyranosyl-(1'→4)D-glucopyranosyl)vanillin (**20a-d**) synthesis by both the glucosidases.

**Table 3.5** Experimental design with experimental and predictive yields of maltosylation based on response surface methodology<sup>a</sup>.

Expt. No.	Glucosidase (% w/w maltose)	Vanillin (mmol)	Incubation Period (h)	Buffer Volume (mL)	PH (0.01M)	Amyloglucosidase		β-Glucosidase	
						Experimental	Predicted	Experimental	Predicted
						yield (%)	yield (%)	yield (%)	yield (%)
1	20	1	48	0.8	7	13.6	13.2	24.3	23.8
2	20	1	48	1.6	5	16.7	27.6	15.6	13.5
3	20	1	96	0.8	5	21.8	27.2	20.1	12.8
4	20	1	96	1.6	7	7.92	1.5	12.4	12.6
5	20	2	48	0.8	5	19.1	21.7	37.7	30.1
6	20	2	48	1.6	7	17.4	25.7	21.8	22.9
7	20	2	96	0.8	7	17.3	14.6	30.6	29.2
8	20	2	96	1.6	5	12.2	0	13.1	11.9
9	40	1	48	0.8	5	11.9	8.6	21.9	17.5
10	40	1	48	1.6	7	59.6	43.4	7.6	14.5
11	40	1	96	0.8	7	15.8	22.5	15.2	13.8
12	40	1	96	1.6	5	9.2	0	24.4	24.1
13	40	2	48	0.8	7	19.2	17	19.3	15.2
14	40	2	48	1.6	5	8.8	23.1	37.7	32.5
15	40	2	96	0.8	5	13.7	10.1	29.5	24.9
16	40	2	96	1.6	7	23.9	15.2	32.4	28.7
17	10	1.5	72	1.2	6	27.5	16.7	16.7	19.5
18	50	1.5	72	1.2	6	14.6	18.6	20.9	23.2
19	30	0.5	72	1.2	6	16.8	19.7	22.8	16.1
20	30	2.5	72	1.2	6	16.4	15.6	25.7	31.8
21	30	1.5	24	1.2	6	68.1	40.8	23.6	22.8
22	30	1.5	120	1.2	6	12.8	18.1	17.4	19.8
23	30	1.5	72	0.4	6	14.8	17.7	10.6	22.2
24	30	1.5	72	2	6	9.7	17.6	19.5	20.5
25	30	1.5	72	1.2	4	10.1	0	15.7	16.3
26	30	1.5	72	1.2	8	10.7	7.3	28.1	14.7
27	30	1.5	72	1.2	6	13.4	17.7	17.6	21.3
28	30	1.5	72	1.2	6	12.9	17.7	15.8	21.3
29	30	1.5	72	1.2	6	11.5	17.7	18.1	21.3
30	30	1.5	72	1.2	6	13.3	17.7	14.2	21.3
31	30	1.5	72	1.2	6	11.8	17.7	17.9	21.3
32	30	1.5	72	1.2	6	12.5	17.7	16.2	21.3

<sup>a</sup>Conversion yields obtained from HPLC with respect to 0.5mmol of maltose. Error in yield measurement will be  $\pm 10\%$ .

This applies to all the yields given in the subsequent tables also.

### 3.1.6.3 Amyloglucosidase catalysed synthesis of 4-O-( $\alpha$ -D-glucopyranosyl-(1'→4)D-glucopyranosyl)vanillin

The data obtained using amyloglucosidase were fitted to a second-order polynomial equation and the predictive equation obtained with coefficients exhibited a  $R^2$  value of 0.81 (Table 3.6). Only few terms were found to be significant at 90% level and a reduced equation obtained with the significant terms is given below,

$$Y = - 3.7258 X_1 + 25.3461 X_5 + 0.0051 X_3X_3 - 3.7238 X_5X_5 + 0.6985 X_1X_4 + 0.4896 X_1X_5 - 0.0281X_2X_3 - 0.7730 X_3X_4 + 5.7750 X_4X_5 \dots\dots\dots(2)$$

Where  $X_1$  – enzyme concentration;  $X_2$  – vanillin concentration;  $X_3$  – incubation period;  $X_4$  – buffer volume;  $X_5$  – pH; Y – yield. Table 3.6 shows the predicted yields obtained by using the reduced equation.

Surface plots were generated using the above reduced equation by varying any two of the variables maintaining the other three variables at their '0' coded values. The surface plots containing iso-maltosidic regions clearly brought out the maltosylation behaviour of the enzymes under diverse reaction conditions. All the experiments with respect to both the enzymes were carried out at a constant maltose concentration of 0.5 mmol.

Figure 3.14A shows the effect of amyloglucosidase and buffer concentration on the extent of maltosylation at 1.5 mmol vanillin, pH 6 and 72 h incubation period. At a buffer concentration of 0.05 mM (0.5 mL), increase in amyloglucosidase concentration from 10% to 50% (w/w maltose) decreased the maltosylation yield. However, at higher buffer concentrations beyond 0.125 mM (1.25 mL), the maltosylation yield increased with increase in amyloglucosidase concentration. A critical enzyme to buffer concentration could be dictating the extent of maltosylation, as there is a cross-over point

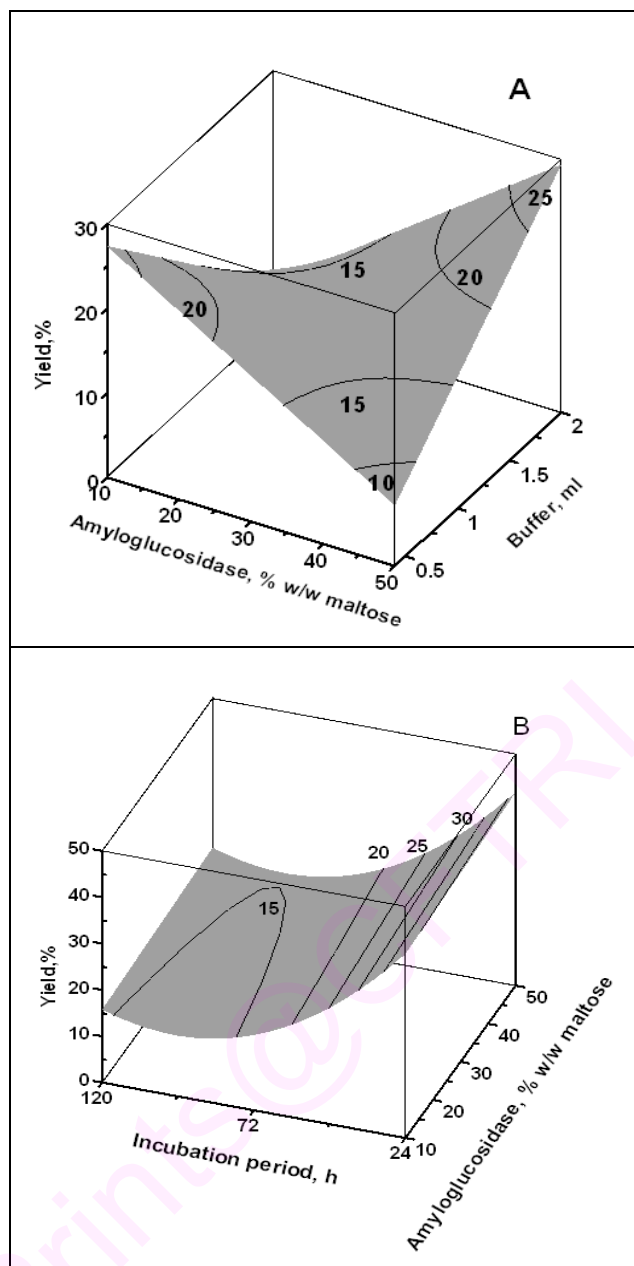


**Fig. 3.14** Three-dimensional surface plots showing the effect of variables in the amyloglucosidase catalysed reaction: **(A)** Amyloglucosidase and buffer concentrations on the extent of maltosylation yield (pH - 6, vanillin - 1.5 mmol, incubation period - 72 h) and **(B)** Amyloglucosidase and incubation period on the extent of maltosylation yield (pH - 6, buffer concentration - 0.125mM - 1.25 mL, vanillin concentration -1.5 mmol).

clearly depicting the reversal of the maltosylation behaviour at 30% (w/w maltose) amyloglucosidase concentration and a buffer volume of 0.125 mM (1.25 mL).

**Table 3.6** Amyloglucosidase catalysed reaction: Analysis of variance (ANOVA) of the response surface model along with coefficients of the response equation<sup>a</sup>.

Regression statistics					
Multiple R		0.897			
R <sup>2</sup>		0.806			
Standard error		9.158			
Observations		32			
ANOVA					
	Degrees of freedom	Sum of squares	Mean sum of squares	F ratio	Significance F
Regression	19	4169	119	2.616	0.05
Residual	12	1006	84		
Total	31	5176			
Coefficients	Values of coefficients	Standard error	t-Stat	1-tail p-value	
A <sub>1</sub>	-4.4337	2.0975	-2.1137	0.0281*	
A <sub>2</sub>	4.3254	41.9500	0.1033	0.4597	
A <sub>3</sub>	-1.0538	0.8739	-1.2058	0.1255	
A <sub>4</sub>	-70.8690	80.0240	-0.8856	0.1966	
A <sub>5</sub>	53.3690	34.1840	1.5612	0.0722*	
A <sub>11</sub>	0.0217	0.0171	1.2648	0.1149	
A <sub>22</sub>	4.2387	6.8691	0.6171	0.2743	
A <sub>33</sub>	0.0122	0.0029	4.0891	0.0007*	
A <sub>44</sub>	10.2940	26.0570	0.3951	0.3499	
A <sub>55</sub>	-5.7506	3.6490	-1.5759	0.0705*	
A <sub>12</sub>	-0.4610	0.4579	-1.0067	0.1669	
A <sub>13</sub>	-0.0076	0.0095	-0.8003	0.2195	
A <sub>14</sub>	0.9137	0.5724	1.5962	0.0682*	
A <sub>15</sub>	0.5530	0.2289	2.4151	0.0163*	
A <sub>23</sub>	0.2588	0.1908	1.3561	0.1000*	
A <sub>24</sub>	-11.6630	11.4490	-1.0186	0.1642	
A <sub>25</sub>	-1.6650	4.5794	-0.3635	0.3612	
A <sub>34</sub>	-0.3521	0.2385	-1.4762	0.0828*	
A <sub>35</sub>	-0.1179	0.0954	-1.2359	0.1201	
A <sub>45</sub>	10.1890	4.9573	2.0553	0.0311*	

<sup>a</sup>Significant at 90% confidence level for the original equation. Regression statistics and ANOVA shown are for the original equation. Significant term indicated by \* are for the reduced equation after further regression of the original. Reduced model exhibits an overall significance of  $F = 0.05$ .

Effect of amyloglucosidase concentration and incubation period at 1.5 mmol vanillin, pH 6 and 0.125 mM (1.25 mL) buffer concentration is shown in Figure 3.14B. With increase in incubation period from 24-120 h, maltosylation yield decreases. At all

the other incubation periods, increase in amyloglucosidase concentration from 10-50% (w/w maltose) showed a very slight increase in the maltosylation yields.

Effect of vanillin and buffer concentration on maltosylation at 30% (w/w maltose) amyloglucosidase concentration, pH 6 and 72 h incubation period showed that at all the buffer concentrations in the range 0.05 mM (0.5 mL) to 0.2 mM (2 mL) increase in vanillin concentration brought out a marginal decrease in the maltosylation yield (Data not shown). Similar marginal increase in yields were observed with increase in buffer concentrations at all the vanillin concentrations in the range 0.5 - 2.5 mmol.

Effect of vanillin and incubation period on the maltosylation yield at 30% (w/w maltose) amyloglucosidase, pH 6 and 0.125 mM (1.25 mL) buffer concentration is shown in Figure 3.15A. With increase in incubation period, the maltosylation yield decreases at all the vanillin concentrations in the range 0.5 - 2.5 mmol. This decrease in yield is quite steep upto 84 h and thereafter gradual. However, at all the incubation periods in the range 24 h to 120 h, increase in vanillin concentration causes a marginal decrease in yields indicating that vanillin could be mildly inhibitory to amyloglucosidase.

Effect of vanillin and pH on the extent of maltosylation at 30% (w/w maltose) amyloglucosidase concentration, 0.125 mM (1.25 mL) buffer concentration and 72 h incubation period was also studied. The surface plot shows a pH optimum at pH 6 for this reaction at all the vanillin concentrations in the 0.5 - 2.5 mmol range (Data not shown). At all the pH values in the 4 - 8 range, increase in vanillin causes only a marginal decrease in the maltosylation yields. Observation of pH optima at 6 clearly indicates that the enzyme functions efficiently at pH 6, exhibiting maximum catalytic activity at this pH. At pH values other than 6, the yields are invariably low. Similar plots



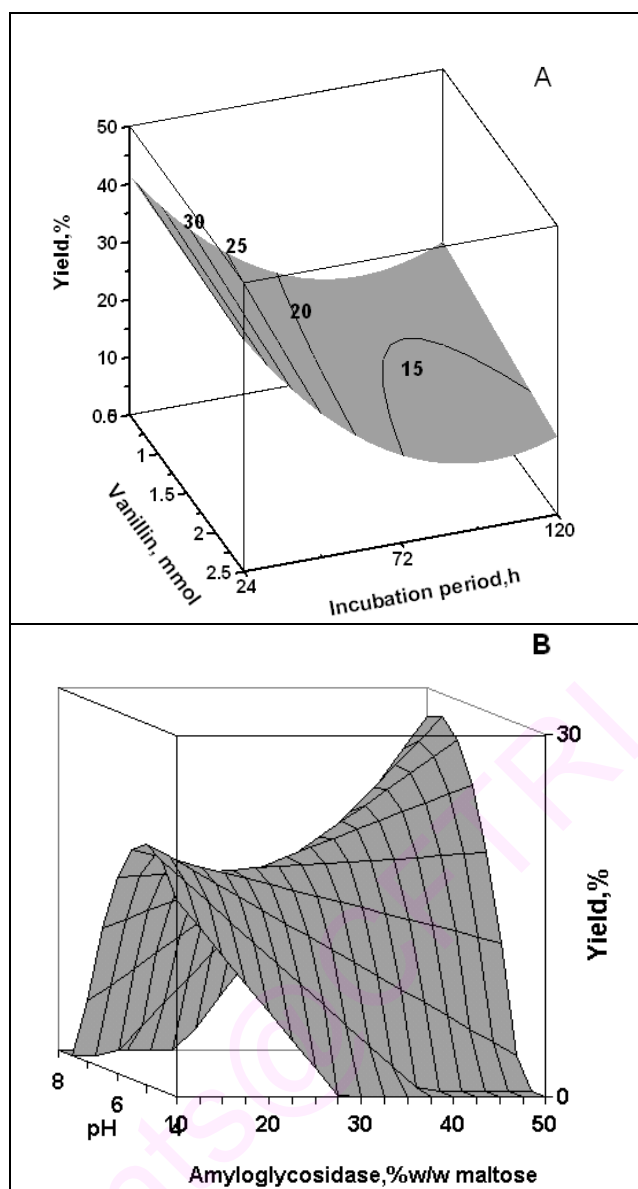


**Fig. 3.15** Three-dimensional surface plots showing the effect of variables in the amyloglycosidase catalysed reaction: **(A)** Vanillin and incubation period on the extent of maltosylation yield (pH - 6, buffer concentration - 0.125 mM - 1.25 mL, amyloglycosidase - 30% w/w maltose) and **(B)** Amyloglycosidase concentrations and pH on the extent of maltosylation yield (vanillin concentration - 1.5 mmol, buffer concentration - 0.125 mM - 1.25 mL, incubation period - 72 h).

were obtained for the effect of enzyme and pH also (Data not shown), emphasizing that pH 6 is the optimum pH for this reaction.

Effect of amyloglucosidase concentration and pH on the extent of maltosylation at 0.125 mM (1.25 mL) buffer, 1.5 mmol vanillin and 72 h incubation period is shown in Figure 3.15B. An optimum pH of 6 observed at 10% (w/w maltose) amyloglucosidase concentration is maintained throughout upto 50% (w/w maltose) amyloglucosidase concentration with an increasing extent of conversion from 10 to 50% (w/w maltose) enzyme concentration. However, a cross over point exhibiting reversal in the maltosylation yields is observed around pH 6 and 30% (w/w maltose) amyloglucosidase concentration. Above pH 6 and above 30% (w/w maltose) amyloglucosidase, the yield increases with enzyme concentration and pH. The extent of conversion is lesser below 30% (w/w maltose) enzyme and pH 6.

**Table 3.7** Validation data for the amyloglucosidase catalysed reactions at selected random conditions<sup>a</sup>

Expt. no.	Amyloglucosidase (% w/w maltose)	Vanillin (mmol)	Incubation period (h)	Buffer Volume (mL)	pH	Predicted yield (%)	Experimental yield (%)
1	30	1.5	72	1.2	6	17.6	10.7
2	15	2	72	1.2	6	15.9	22.1
3	30	1	24	1.2	6	41.1	49.6
4	30	0.5	72	2	6	19.6	29.7
5	30	1.5	72	0.8	6	17.7	11.6
6	45	1.5	48	1.2	6	27	30.2
7	30	2	72	1.2	6	16.6	13.9
8	30	1.5	48	1.2	7	24.8	22.1
9	30	1.5	36	1.6	6	43.9	38.7
10	20	1.5	24	1.2	6	40.3	42.3

<sup>a</sup>Conversion yields obtained from HPLC with respect to 0.5 mmol of maltose.

Maximum yield predicted based on the response model is 43.9% for the amyloglucosidase catalysed reaction under the following conditions: amyloglucosidase-30% (w/w of maltose), vanillin-1 mmol, buffer concentration-0.125 mM (1.25 mL) pH-6

and incubation period 24 h. The experiments conducted at the above optimum conditions resulted in 49.4% yield. Further validation of the response model was carried out at certain selected random process conditions and the experimental yields are shown in Table 3.7. There appears to be a good correspondence between predicted and experimental yields at yields less than 40% and the correspondence appears to deviate a little at higher predictive yields.

#### 3.1.6.4 $\beta$ -Glucosidase catalysed synthesis of 4-O-( $\alpha$ -D-glucopyranosyl-(1'→4) $\beta$ -D-glucopyranosyl)vanillin

The data obtained using  $\beta$ -glucosidase were fitted to a second-order polynomial equation and the final predictive equation was obtained with coefficients exhibiting a  $R^2$  value of 0.69 (Table 3.8).

Here also, as in amyloglucosidase catalysed reaction, only few terms were found to be significant at 90% level and the reduced equation obtained with significant terms is given below,

$$Y = -0.7408 X_3 - 30.6961 X_4 + 20.7320 X_5 + 2.6099 X_2 X_2 - 1.4606 X_5 X_5 + 0.0092 X_1 X_3 + 0.9891 X_1 X_4 - 0.2937 X_1 X_5 + 0.0720 X_3 X_5 \quad \dots\dots\dots(3)$$

Where  $X_1$  – enzyme concentration;  $X_2$  – vanillin concentration;  $X_3$  – incubation period;  $X_4$  – buffer volume;  $X_5$  – pH; Y – yield. Table 3.8 shows the predicted yields obtained by using the reduced equation. Average Absolute deviation between the experimental and predicted yields using this model is 22.3 %.

Figure 3.16A. shows the effect of  $\beta$ -glucosidase and vanillin concentrations on the maltoside yield at pH 6, 0.125 mM (1.25 mL) buffer concentration and 72 h incubation period. At all the  $\beta$ -glucosidase (10-50% w/w maltose) concentrations, the maltosylation yield increases with increase in vanillin concentration. However, increase in  $\beta$ -glucosidase concentration, exhibited very little enhancement in yield. Maximum

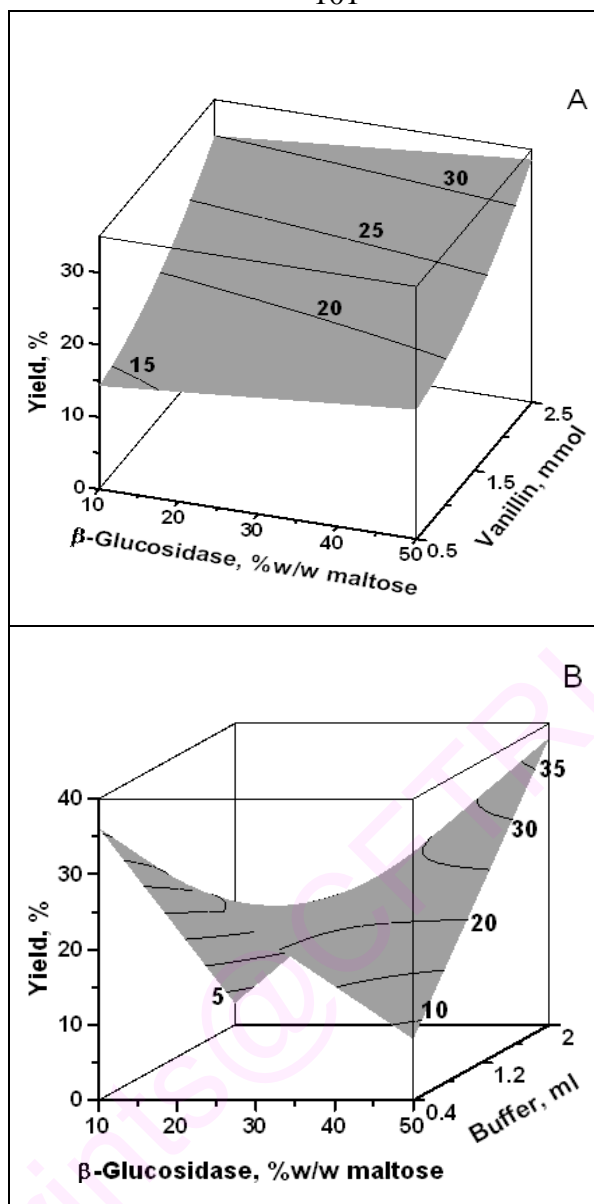


**Fig. 3.16** Three-dimensional surface plots showing the effect of variables in the  $\beta$ -glucosidase catalysed reaction: (A) Vanillin and  $\beta$ -glucosidase concentrations on the extent of maltosylation yield (pH - 6, buffer concentration - 0.125 mM - 1.25 mL, incubation period - 72 h) and (B)  $\beta$ -Glucosidase concentration and buffer concentration on the extent of maltosylation yield (pH - 6, incubation period - 72 h, vanillin concentration - 1.5 mmol).

yield is depicted at 50% (w/w maltose)  $\beta$ -glucosidase concentration and 2 - 2.5 mmol of vanillin.

**Table 3.8**  $\beta$ -Glucosidase catalysed reaction: Analysis of variance (ANOVA) of the response surface model along with coefficients of the response equation<sup>a</sup>.

Regression statistics					
Multiple <i>R</i>	0.833				
<i>R</i> <sup>2</sup>	0.693				
Standard error	6.527				
Observations	32				
ANOVA					
	Degrees of freedom	Sum of squares	Mean sum of squares	<i>F</i> ratio	Significance <i>F</i>
Regression	19	1159	61	1.54	0.12
Residual	12	475	39.6		
Total	31	1635			
Coefficients	Values of coefficients	Standard error	<i>t</i> -Stat	1-tail p-value	
A <sub>1</sub>	-0.6963	1.4696	-0.4738	0.3221	
A <sub>2</sub>	-20.6340	29.5690	-0.6978	0.2492	
A <sub>3</sub>	-1.0839	0.6123	-1.7701	0.0510*	
A <sub>4</sub>	-75.1470	52.1920	-1.4398	0.0877*	
A <sub>5</sub>	41.9310	22.9610	1.8262	0.0463*	
A <sub>11</sub>	0.0051	0.0122	0.4210	0.3406	
A <sub>22</sub>	7.1131	4.9755	1.4296	0.0891*	
A <sub>33</sub>	0.0016	0.0021	0.7693	0.2283	
A <sub>44</sub>	18.7010	15.2140	1.2292	0.1212	
A <sub>55</sub>	-3.3568	2.4792	-1.3540	0.1003*	
A <sub>12</sub>	0.2116	0.3260	0.6489	0.2643	
A <sub>13</sub>	0.0094	0.0068	1.3851	0.0956*	
A <sub>14</sub>	0.9988	0.4075	2.4510	0.0153*	
A <sub>15</sub>	-0.2859	0.1625	-1.7602	0.0519*	
A <sub>23</sub>	-0.0816	0.1358	-0.6010	0.2795	
A <sub>24</sub>	2.2890	8.1504	0.2809	0.3918	
A <sub>25</sub>	0.5562	3.2490	0.1712	0.4334	
A <sub>34</sub>	0.0347	0.1698	0.2042	0.4208	
A <sub>35</sub>	0.1022	0.0677	1.5101	0.0784*	
A <sub>45</sub>	-1.3355	3.4806	-0.3837	0.3539	

<sup>a</sup>Significant at 90% confidence level for the original equation. Regression statistics and ANOVA shown are for the original equation. Significant term indicated by \* are for the reduced equation after further regression of the original. Reduced model exhibits overall significance of *F* = 0.05.

Effect of  $\beta$ -glucosidase and buffer concentration at pH 6, 1.5 mmol vanillin and 72 h incubation period on the maltosylation yield is shown in Figure 3.16B. In the saddle shaped surface obtained, a cross over point indicating reversal in the maltosylation behaviour is observed at 30% (w/w maltose)  $\beta$ -glucosidase concentration and 0.125 mM

(1.25 mL) buffer concentration. Upto 30% (from 10% w/w maltose)  $\beta$ -glucosidase and 0.125 mM to 0.04 mM (1.25 mL to 0.4 mL) buffer concentration, the maltosylation yield decreases with increase in enzyme concentration. Above this crossover values in both the variables, the yield increases. Here also, a critical  $\beta$ -glucosidase to buffer concentration appears to influence the extent of maltosylation.

The surface plot showing the effect of pH and incubation period at 30% (w/w maltose), 0.125 mM (1.25 mL) buffer concentration and 1.5 mmol vanillin (Fig. 3.17A), shows a saddle-shaped surface, exhibiting an optimum pH of 6. At pH 6 the highest maltosylation yield (28%) is observed. The yield increases from 24 h incubation period to 120 h incubation at pH 6. At other pH values, the yield decreases with increasing incubation periods indicating clearly that the enzyme exhibits maximum stability and activity at pH 6.

Similarly, the effect of  $\beta$ -glucosidase and incubation period (Fig. 3.17B), at 1.5 mmol vanillin, pH 6 and 0.125 mM (1.25 mL) buffer concentration, showed the maximum yield at 50% (w/w maltose)  $\beta$ -glucosidase concentration and 120 h incubation period. Here also, the saddle-shaped curve exhibits a reversal in the maltosylation behaviour (crossover point) at 30% (w/w maltose)  $\beta$ -glucosidase concentration and 84 h incubation period. This also clearly indicates that the maltosylation behaviour is favourably affected around 30% (w/w maltose)  $\beta$ -glucosidase concentration and 84 h incubation period.

Effect of  $\beta$ -glucosidase and pH at 0.125 mM (1.25 mL) buffer concentration, 72 h incubation period and 1.5 mmol vanillin is shown in Figure 3.18. In the saddle-shaped surface plot obtained, the reversal behaviour is observed at pH 6 and 30% (w/w maltose)  $\beta$ -glucosidase concentration besides exhibiting maximum yield at pH 6 at all the  $\beta$ -glucosidase concentrations.

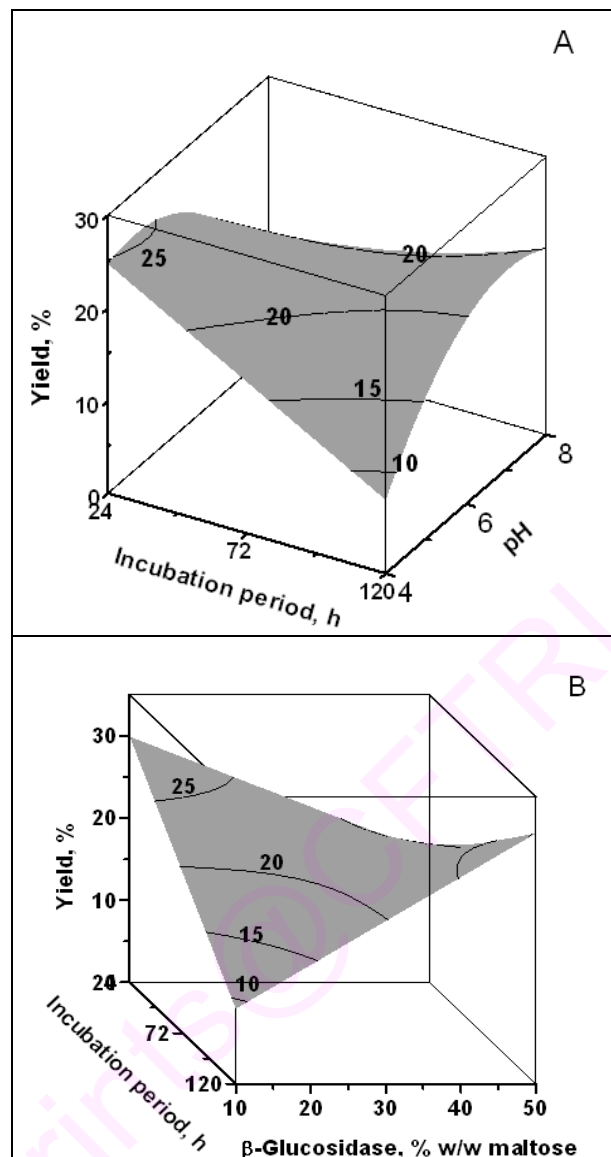


**Fig. 3.17** Three-dimensional surface plots showing the effect of variables in the  $\beta$ -glucosidase catalysed reaction: (A) Incubation period and pH on the extent of maltosylation yield (vanillin concentration - 1.5 mmol,  $\beta$ -glucosidase concentration - 30% w/w maltose, buffer concentration - 0.125 mM - 1.25 mL) and (B)  $\beta$ -Glucosidase concentration and incubation period on the extent of maltosylation yield (vanillin concentration - 1.5 mmol, buffer concentration - 0.125 mM - 1.25 mL pH - 6)

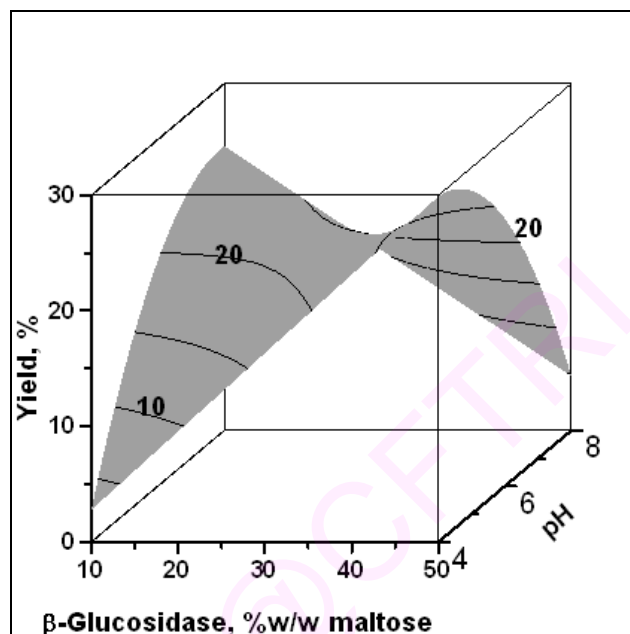


**Fig. 3.18** Three-dimensional surface plots showing the effect of variables in the  $\beta$ -glucosidase catalysed reaction:  $\beta$ -Glucosidase concentration and pH on the extent of maltosylation yield (buffer concentration- 0.125 mM - 1.25 mL, vanillin concentration - 1.5 mmol, incubation period – 72 h).



The maximum yield predicted based on the response model is 33.6% for the  $\beta$ -glucosidase catalysed reaction under the conditions:  $\beta$ -glucosidase-50% (w/w of maltose), vanillin-2.5 mmol, buffer concentration-0.125 mM (1.25 mL) pH-6 and 72 h incubation period. The experiment conducted at the above optimum conditions gave 27.1% yield. Validation experiments performed at certain random selected conditions also showed good correspondence between experimental and predicted yields (Table 3.9).

**Table 3.9** Validation data for the  $\beta$ -glucosidase catalysed reactions at selected random conditions<sup>a</sup>

Expt. no.	$\beta$ -Glucosidase (% w/w maltose)	Vanillin (mmol)	Incubation period (h)	Buffer Volume (mL)	pH	Predicted yield (%)	Experimental yield (%)
1	50	2.5	72	1.2	6	33.6	27.1
2	10	0.5	72	1.2	6	14.3	22.5
3	30	1.5	72	1.2	6	21.3	18.7
4	40	1.5	72	1.5	6	22.3	20.6
5	25	1.5	80	1.2	6	20.2	17.5
6	45	1.5	100	1.2	6	25.7	21.3
7	35	1.5	72	1.2	6	21.8	15.7
8	30	1.5	48	0.6	6	22.7	27.6
9	30	1.5	108	1.2	7	20.9	15.5
10	30	1.5	72	0.5	6	22.1	24.7

<sup>a</sup>Conversion yields obtained from HPLC with respect to 0.5mmol of maltose.

Hence, the present RSM study has clearly showed the usefulness of CCRD technique in clearly bringing out the most salient features of this maltosylation reaction.

### 3.2 Syntheses of N-vanillyl-nonanamide glycosides

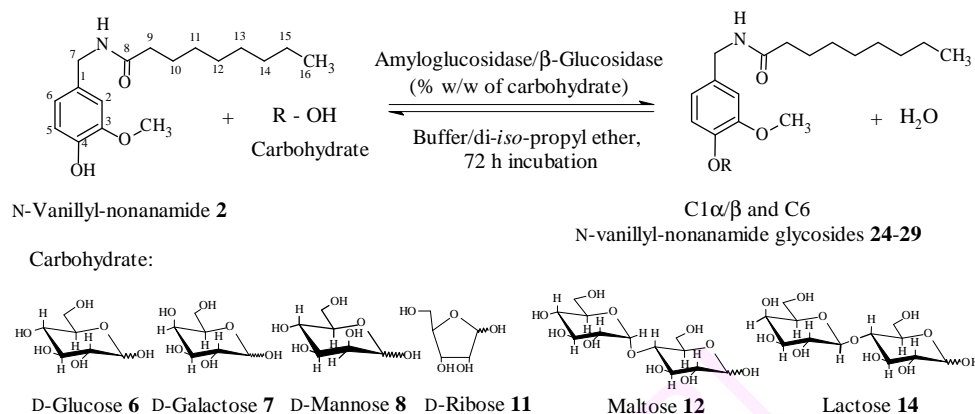
Capsaicin  $\{(E)\text{-N-}[(4\text{-hydroxy-3-methoxyphenyl)methyl]\text{-8-methyl-6-nonemide}\}$ , (Ohnuki *et al.* 2001), a fat-soluble phenolic compound present as the major pungent principle in fruits of *Capsicum* species, can also be used as a hypoglycemic (Lan *et al.* 2004), mutagenic and carcinogenic agent (Gannett *et al.* 1988), as a topical analgesic in pharmaceutical preparations (Rashid *et al.* 2003), antioxidant (Lee *et al.* 1995), anti-

inflammatory (Heyes *et al.* 2004) and antifungal agent (Bhabadesh *et al.* 1996). It also can increase catecholamine secretion and suppress body fat accumulation (Watanabae *et al.* 1994), inhibit NADH oxidase in plasma membranes (Morre *et al.* 1995) and reduce the peri-renal adipose tissue weight and serum triacyl glycerol by enhancing energy metabolism through a  $\beta$ -adrenergic action (Kawada *et al.* 1986). N-Vanillyl-nonanamide **2** {N-[(4-hydroxy-3-methoxy-phenyl)methyl]nonanamide}, a synthetic substitute of capsaicin, exhibits hypotensive and antinociceptive effects as that of natural capsaicin (Chen *et al.* 1992). Capsaicin (Iorizzi *et al.* 2001) has also been converted into its corresponding glucoside by cell suspension cultures (Kometani *et al.* 1993a; Hamada *et al.* 2003) and chemical methods (Hamada *et al.* 2001). Capsaicin and usage of its derivatives have been limited due to its low water solubility and high pungency.

Glycosylation, besides being an important method for the structural modification of compounds with useful biological activities, also allows the conversion of a water-insoluble component into water-soluble one, thereby improving its pharmacological applications (Suzuki *et al.* 1996; Vijayakumar and Divakar 2005). The present work describes syntheses of N-vanillyl-nonanamide glycosides using amyloglucosidase from *Rhizopus* mold and  $\beta$ -glucosidase isolated from sweet almond (Hestrin *et al.* 1955) in a non-polar solvent (Scheme 3.2).

Synthesis of 4-*O*-(D-glucopyranosyl)N-vanillyl-nonanamide was studied in detail. A typical reaction involved refluxing N-vanillyl-nonanamide **2** (0.2-1 mmol) with D-glucose **6** (0.5 mmol) in 100 mL di-isopropyl ether in presence of amyloglucosidase (10 to 75% w/w of D-glucose **6**) and 0.03 mM – 0.25 mM (0.3-2.5 mL of 0.01 M) pH 4-8 buffer for an incubation period of 72 h (Scheme 3.2). The solvent was evaporated, the enzyme denatured at 100 °C for 5-10 min and the residue containing unreacted D-glucose **6** along with the product 4-*O*-(D-glucopyranosyl)N-vanillyl-nonanamide were dissolved

in 20-30 mL water. After extracting with chloroform to remove unreacted N-vanillyl-nonanamide **2**, the aqueous layer containing unreacted D-glucose **6** and 4-*O*-(D-glucopyranosyl)N-vanillyl-nonanamide was evaporated to dryness.



**Scheme 3.2** Syntheses of N-vanillyl-nonanamide glycosides

The products were monitored by HPLC on an aminopropyl column (250 mm × 4.6 mm), using acetonitrile:water (70:30 v/v) as a mobile phase and a refractive index detector (Fig. 3.19). Other procedures are as described on page 74. HPLC analysis showed the following retention times: D-glucose-6.9 min, 4-*O*-(D-glucopyranosyl)N-vanillyl-nonanamide-10.2 min, D-galactose-7.1 min, 4-*O*-(D-galactopyranosyl)N-vanillyl-nonanamide-11.3 min, D-mannose-6.7 min, 4-*O*-(β-D-mannopyranosyl)N-vanillyl-nonanamide-11.9 min, D-ribose-7.4 min, 4-*O*-(D-ribofuranosyl)N-vanillyl-nonanamide-10.9 min, maltose-11.5 min, 4-*O*-(α-D-glucopyranosyl-(1'→4)D-glucopyranosyl)N-vanillyl-nonanamide-15.2 min, lactose-9.3 min and 4-*O*-(β-D-galactopyranosyl-(1'→4)β-D-glucopyranosyl)N-vanillyl-nonanamide-17.9 min.

### 3.2.1 Synthesis of 4-*O*-(D-glucopyranosyl)N-vanillyl-nonanamide using amyloglucosidase

Glucosylation of N-vanillyl-nonanamide **2** with D-glucose **6** using amyloglucosidase was studied in detail (Table 3.10) in terms of incubation period, pH, buffer, enzyme and N-vanillyl-nonanamide concentration.

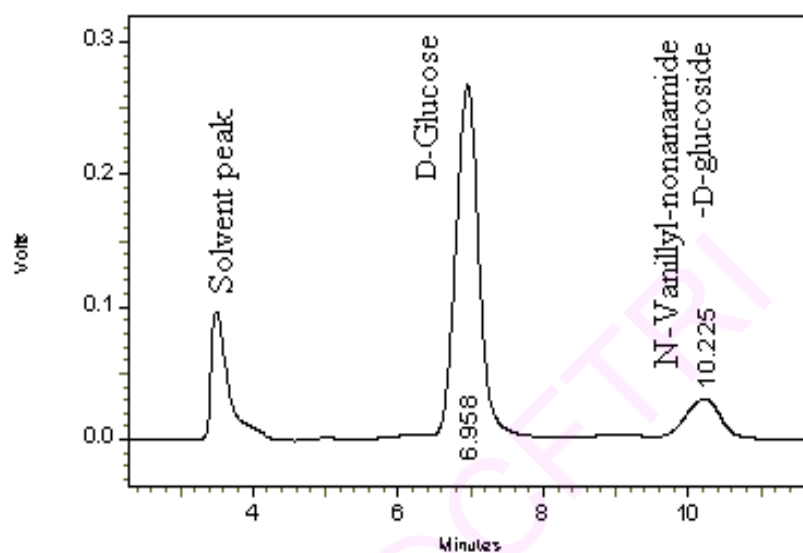


**Fig. 3.19** HPLC chromatogram for the reaction mixture of D-glucose and 4-*O*-(D-glucopyranosyl)N-vanillyl-nonanamide. HPLC conditions: Aminopropyl column (10  $\mu$ m, 250 mm  $\times$  4.6 mm), solvent-CH<sub>3</sub>CN: H<sub>2</sub>O (70:30 v/v), Flow rate-1 mL/min, RI detector. Retention times: D-glucose-7 min and 4-*O*-(D-glucopyranosyl)N-vanillyl-nonanamide -10.2 min.

### 3.2.1.1 Effect of incubation period

Effect of incubation period was carried out at fixed N-vanillyl-nonanamide (0.5 mmol) and D-glucose (0.5 mmol). Incubation increased the yield from 25% for 3 h to 56% at 72 h. Further increase in incubation period upto 120 h, decreased the glucosylation yield to 28% which could be due to partial hydrolysis of the glucosides formed (Fig. 3.20A, Table 3.10).

### 3.2.1.2 Effect of pH

In presence of 0.2 mM, pH 7 phosphate buffer (2 mL of 0.01 M buffer in 100 mL di-isopropyl ether solvent), glucosylation of N-vanillyl-nonanamide reached a maximum of 39% (Table 3.10).

### 3.2.1.3 Effect of buffer concentration

At pH 7, increase in buffer concentration from 0.03 to 0.25 mM (0.3-2.5 mL) showed increase in conversion with increase in buffer concentration to a maximum of 56% at 0.2 mM (2 mL) buffer and pH 7, thus showing that pH and buffer concentration had pronounced effect on the extent of glucosylation which could be due to stabilization of enzyme for maximum activity under these conditions (Fig. 3.20B, Table 3.10).

### 3.2.1.4 Effect of amyloglucosidase concentration

Effect of increasing enzyme concentration at fixed N-vanillyl-nonanamide and D-glucose (0.5 mmol) showed that at 10% (w/w D-glucose) amyloglucosidase concentration conversion yield was the lowest of 16% which this increased to a maximum yield of 56% at 40% (w/w D-glucose) enzyme concentration. Further increase to 50% (w/w D-glucose) decreased the conversion probably due to inhibition of the enzyme by N-vanillyl-nonanamide (Table 3.10).

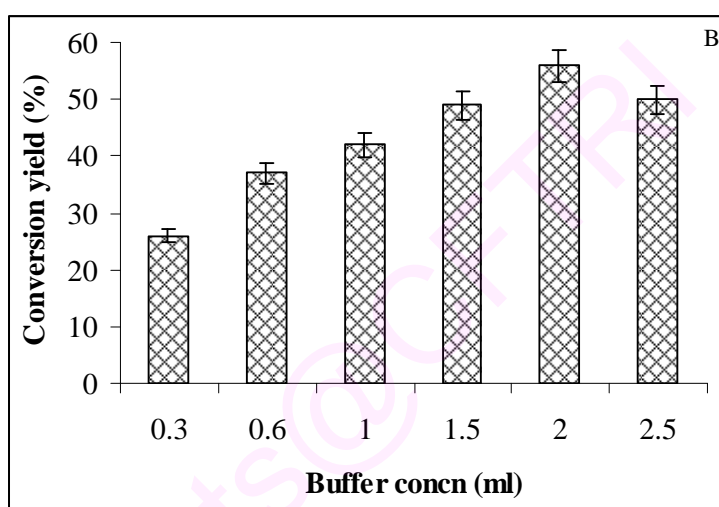
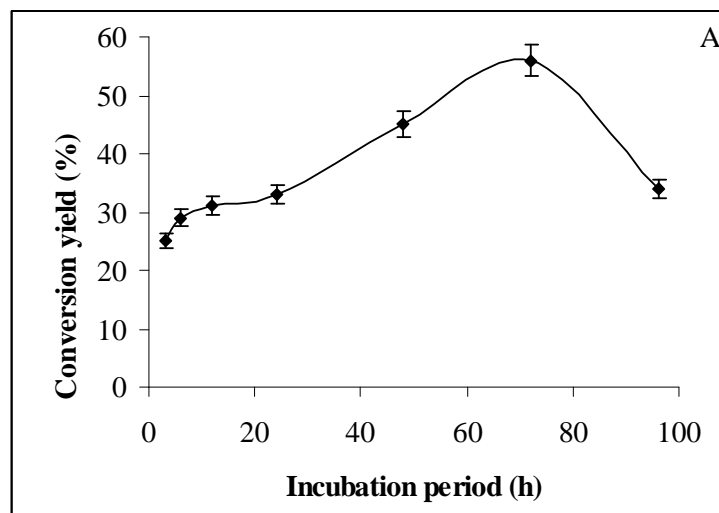


**Fig. 3.20** (A) Reaction profile on 4-*O*-(D-glucopyranosyl)N-vanillyl-nanamide synthesis by the reflux method. Conversion yields were from HPLC with respect to 0.5 mmol of D-glucose. Reaction conditions: N-vanillyl-nonanamide-0.5 mmol, D-glucose-0.5 mmol, amyloglucosidase-40% (w/w D-glucose), 0.2 mM (2 mL), pH 7 phosphate buffer, solvent-di-isopropyl ether and temperature-68 °C and (B) Effect of buffer concentration on 4-*O*-(D-glucopyranosyl)N-vanillyl-nanamide synthesis. Reaction conditions: N-vanillyl-nonanamide-0.5 mmol, D-glucose-0.5 mmol, amyloglucosidase-40% (w/w D-glucose), pH 7 phosphate buffer, solvent-di-isopropyl ether, temperature-68 °C and incubation period – 72 h

**Table 3.10** Optimization of reaction conditions for the synthesis of 4-*O*-(D-glucopyranosyl)N-vanillyl-nonanamide

Reaction conditions	Variable parameter <sup>b</sup>	Yield (%) <sup>c</sup>
Incubation period (h)		
N-vanillyl-nonanamide – 0.5 mmol	3	25
D-glucose – 0.5 mmol	6	29
pH – 7	12	31
Buffer concentration – 0.2 mM (2 mL)	24	33
Enzyme – 40% w/w D-glucose	48	45
	72	56
	96	34
	120	28
pH (0.01M)		
N-vanillyl-nonanamide – 0.5 mmol <sup>a</sup>	4	18
D-glucose – 0.5 mmol	5	18
Enzyme – 40% w/w D-glucose	6	25
Buffer – 0.1 mM (1 mL)	7	39
Incubation period – 72 h	8	19
Buffer concentration (mM)		
N-vanillyl-nonanamide – 0.5 mmol	0.03	26
D-glucose – 0.5 mmol	0.06	37
Enzyme – 40% w/w D-glucose	0.1	42
pH – 7	0.15	49
Incubation period – 72 h	0.2	56
	0.25	50
Enzyme concentration (% w/w D-glucose)		
N-vanillyl-nonanamide – 0.5 mmol	10	16
D-glucose – 0.5 mmol	20	24
pH – 7	30	39
Buffer concentration – 0.2 mM (2 mL)	40	56
Incubation period – 72 h	50	21
	75	10
N-vanillyl-nonanamide (mmol)		
pH – 7	0.2	12
Buffer concentration – 0.2 mM (2 mL)	0.4	14
D-glucose – 0.2 mmol	0.6	23
Enzyme – 40% w/w D-glucose	0.8	24
Incubation period – 72 h	1	23

<sup>a</sup>Initial reaction conditions. <sup>b</sup>Other variables are the same as under reaction conditions, except the specified ones. <sup>c</sup>HPLC yields expressed with respect to 0.5 mmol D-glucose employed except for the last experiment where N-vanillyl-nonanamide concentrations was varied with respect to only 0.2 mmol D-glucose.

### 3.2.1.5 Effect of N-vanillyl-nonanamide concentration

Effect of N-vanillyl-nonanamide concentration at a constant 0.2 mmol D-glucose (Table 3.10) exhibited increase in glucosylation from 0.2 mmol (12% yield) to 0.6 mmol (23%) and thereafter remained constant upto 1 mmol (23%). Saturation of 40% (w/w D-glucose) amyloglucosidase with N-vanillyl-nonanamide could result in such a constant yield beyond 0.6 mmol of N-vanillyl-nonanamide.

### 3.2.1.6 Solubility of 4-*O*-(D-glucopyranosyl)N-vanillyl-nonanamide

4-*O*-(D-Glucopyranosyl)N-vanillyl-nonanamide was found to be soluble in water to the extent of 7.7 g/L (Section 3.7.5). Thus the water insoluble and predominanatly fat soluble N-vanillyl-nonanamide has been rendered water soluble through this glycosylation reaction.

## 3.2.2 Syntheses of N-vanillyl-nonanamide glycosides of other carbohydrates using amyloglucosidase and $\beta$ -glucosidase

Syntheses of N-vanillyl-nonanamide glycosides involved refluxing N-vanillyl-nonanamide **2** (0.5 mmol) with carbohydrates (D-glucose **6**, D-galactose **7**, D-ribose **11**, maltose **12**, 0.5 mmol) in 100 mL di-isopropyl ether in presence of amyloglucosidase (40% w/w of carbohydrate) and 0.2 mM (2 mL) of 0.01 M pH 7 buffer for an incubation period of 72 h (Scheme 3.2). The work up procedure and isolation of the compounds were as described on page 74.

Similarly, syntheses of N-vanillyl-nonanamide glycosides using  $\beta$ -glucosidase involved refluxing N-vanillyl-nonanamide **2** (0.5 mmol) with carbohydrates (D-glucose **6**, D-galactose **7**, D-mannose **8**, D-ribose **11**, maltose **12**, lactose **14**, 0.5 mmol) in 100 mL di-isopropyl ether in presence of  $\beta$ -glucosidase (40% w/w of carbohydrate) and 0.2 mM (2 mL) of 0.01 M pH 7 buffer for an incubation period of 72 h (Scheme 3.2). The other details are as described in Section 3.2.



### 3.2.3 Spectral characterization

N-Vanillyl-nonanamide glycosides besides measuring melting point and optical rotation were also characterized by recording UV, IR, Mass and 2D-HSQCT spectra.

**N-Vanillyl-nonanamide 2 (VN):** Solid, mp 58 °C, UV (Ethanol,  $\lambda_{\max}$ ): 201.5 nm ( $\sigma \rightarrow \sigma^*$ ,  $\epsilon_{201.5} - 8488 \text{ M}^{-1}$ ), 225 nm ( $\sigma \rightarrow \pi^*$ ,  $\epsilon_{225} - 1874 \text{ M}^{-1}$ ), 279 nm ( $\pi \rightarrow \pi^*$ ,  $\epsilon_{279} - 739 \text{ M}^{-1}$ ), IR (stretching frequency,  $\text{cm}^{-1}$ ): 3310 (NH), 3292 (OH), 1432 (C=C), 1643 (CO), 2952 (CH), MS ( $m/z$ ) – 293.2  $[\text{M}]^+$ , 2D-HSQCT (DMSO- $d_6$ ):  $^1\text{H}$  NMR  $\delta_{\text{ppm}}$ : 6.88 (H-2), 6.73 (H-5), 7.03 (H-6), 4.16 (H-7), 2.18 (H-9), 1.46 (H-10), 1.33 (H-11), 1.34 (H-12), 1.18 (H-13), 1.18 (H-14), 1.18 (H-15), 0.92 (H-16), 3.83 (OCH<sub>3</sub>),  $^{13}\text{C}$  NMR  $\delta_{\text{ppm}}$  (125 MHz): 135.89 (C1), 110.5 (C2), 150.1 (C3), 146.5 (C4), 114.6 (C5), 124.4 (C6), 37.8 (C7), 176.4 (C8), 35.4 (C9), 25.3 (C10), 28.4 (C11), 28.6 (C12), 28.9 (C13), 31.5 (C14), 22.2 (C15), 13.9 (C16), 55.5 (OCH<sub>3</sub>). Ultraviolet-visible spectra is shown in Fig. 3.21A.

**3.2.3.1 4-O-(D-Glucopyranosyl)N-vanillyl-nonanamide 24a-c:** Solid, UV ( $\lambda_{\max}$ ): 196.5 nm ( $\sigma \rightarrow \sigma^*$ ,  $\epsilon_{196.5} - 3138 \text{ M}^{-1}$ ), 225.5 nm ( $\sigma \rightarrow \pi^*$ ,  $\epsilon_{225.5} - 1625 \text{ M}^{-1}$ ), 263 nm ( $\pi \rightarrow \pi^*$ ,  $\epsilon_{263} - 392 \text{ M}^{-1}$ ), IR (stretching frequency,  $\text{cm}^{-1}$ ): 3285 (OH), 1274 (glycosidic aryl alkyl C-O-C asymmetrical), 1032 (glycosidic aryl alkyl C-O-C symmetrical), 1429 (C=C), 1639 (CO), 2923 (CH), MS ( $m/z$ ) – 477.2  $[\text{M}+\text{Na}]^+$ , 2D-HSQCT (DMSO- $d_6$ ) **C1 $\alpha$ -glucoside 24a:**  $^1\text{H}$  NMR  $\delta_{\text{ppm}}$  **Glu:** 4.65 (H-1 $\alpha$ , d, J = 3.7 Hz), 3.17 (H-2 $\alpha$ ), 3.72 (H-3 $\alpha$ ), 3.65 (H-4 $\alpha$ ), 3.11 (H-5 $\alpha$ ), 3.41 (H-6a); **VN:** 6.66 (H-2), 6.59 (H-5), 6.77 (H-6), 2.06 (H-9), 1.48 (H-10), 1.33 (H-11), 1.34 (H-12), 1.21 (H-13), 1.21 (H-14), 1.21 (H-15), 0.83 (H-16), 3.71 (OCH<sub>3</sub>),  $^{13}\text{C}$  NMR  $\delta_{\text{ppm}}$  **Glu:** 98.7 (C1 $\alpha$ ), 75.2 (C2 $\alpha$ ), 71.9 (C3 $\alpha$ ), 70.2 (C4 $\alpha$ ), 72.5 (C5 $\alpha$ ), 60.8 (C6 $\alpha$ ); **VN:** 130.5 (C1), 111.7 (C2), 147.5 (C3), 145.3 (C4), 115.2 (C5), 119.7 (C6), 172.1 (C8), 35.4 (C9), 25.3 (C10), 28.7 (C11), 28.6 (C13), 31.1 (C14), 21.9 (C15), 14.1 (C16), 55.6 (OCH<sub>3</sub>). **C6-O-arylated 24b:**  $^1\text{H}$  NMR **Glu:** 3.63 (H-6a),  $^{13}\text{C}$  NMR **Glu:** 67.2 (C6 $\alpha$ ). **C1 $\beta$ -glucoside 24c:** Solid, mp 107 °C, UV (H<sub>2</sub>O  $\lambda_{\max}$ ): 203.5 nm

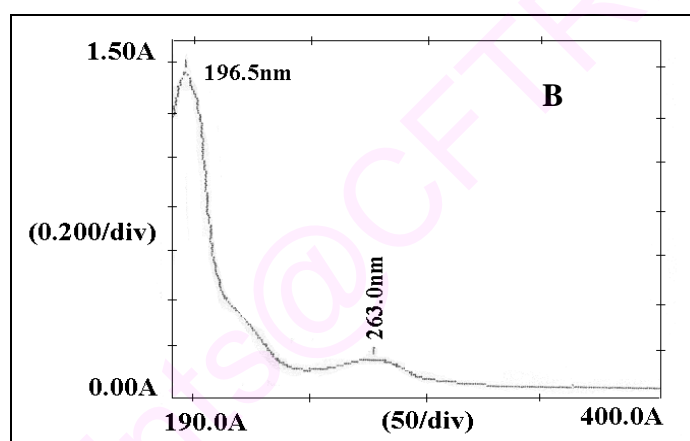
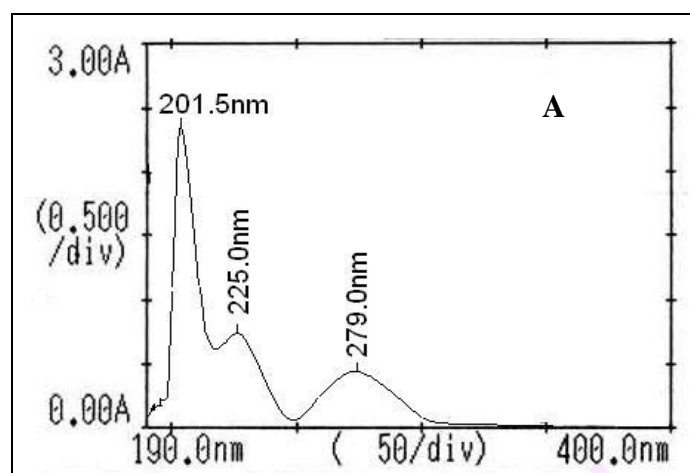


**Fig. 3.21** Ultraviolet-visible spectra of (A) N-Vanillyl-nonanamide **2** and (B) 4-O-(D-Glucopyranosyl)N-vanillyl-nonanamide **24a,b**

( $\sigma \rightarrow \sigma^*$ ,  $\epsilon_{203.5} - 7458 \text{ M}^{-1}$ ), 226.5 nm ( $\sigma \rightarrow \pi^*$ ,  $\epsilon_{226.5} - 2648 \text{ M}^{-1}$ ), 276 nm ( $\pi \rightarrow \pi^*$ ,  $\epsilon_{276} - 850 \text{ M}^{-1}$ ), IR (stretching frequency,  $\text{cm}^{-1}$ ): 3280 (OH), 1279 (glycosidic aryl alkyl C-O-C asymmetrical), 1038 (glycosidic aryl alkyl C-O-C symmetrical), 1425 (C=C), 1645 (CO), 2925 (CH), optical rotation ( $c$  0.5,  $\text{H}_2\text{O}$ ):  $[\alpha]_{\text{D}}$  at 25 °C = -23.8, MS ( $m/z$ ) - 456.3  $[\text{M}+1]^+$ , 2D-HSQCT (DMSO- $d_6$ ):  $^1\text{H}$  NMR  $\delta_{\text{ppm}}$  **Glu**: 4.15 (H-1 $\beta$ , d,  $J = 6.6 \text{ Hz}$ ), 2.92 (H-2 $\beta$ ), 3.12 (H-3 $\beta$ ), 3.66 (H-4 $\beta$ ), 3.51 (H-5 $\beta$ ), 3.40 (H-6a); **VN**: 6.77 (H-2), 6.61 (H-5), 6.85 (H-6), 2.08 (H-9), 1.49 (H-10), 1.35 (H-11), 1.33a (H-12), 1.21 (H-13), 1.21 (H-14), 1.21 (H-15), 0.84 (H-16), 3.69 (OCH<sub>3</sub>),  $^{13}\text{C}$  NMR  $\delta_{\text{ppm}}$  **Glu**: 103.1 (C1 $\beta$ ), 72.8 (C2 $\beta$ ), 76.4 (C3 $\beta$ ), 70 (C4 $\beta$ ), 73.8 (C5 $\beta$ ), 61.2 (C6 $\beta$ ); **VN**: 130.2 (C1), 108.8 (C2), 148.3 (C3), 146 (C4), 41.8 (C7), 172.2 (C8), 36.1 (C9), 25.2 (C10), 28.5 (C11), 28.6 (C12), 28.5 (C13), 31.1 (C14), 21.9 (C15), 14 (C16), 52.5 (OCH<sub>3</sub>).

Ultraviolet-visible, IR, mass and 2D-HSQCT NMR spectra for 4-*O*-(D-glucopyranosyl)N-vanillyl-nonanamide **24a,b** for amyloglucosidase catalysed products were shown in Figures 3.21B, 3.22A, 3.22B and 3.22C respectively. Mass and 2D-HSQCT NMR spectra for 4-*O*-( $\beta$ -D-glucopyranosyl)N-vanillyl-nonanamide **24c** for  $\beta$ -glucosidase catalysed product are shown in Figures 3.23A and 3.23B respectively.

**3.2.3.2 4-*O*-(D-Galactopyranosyl)N-vanillyl-nonanamide 25a,b**: Solid, UV ( $\text{H}_2\text{O}$   $\lambda_{\text{max}}$ ): 195.5 nm ( $\sigma \rightarrow \sigma^*$ ,  $\epsilon_{195.5} - 3911 \text{ M}^{-1}$ ), 226 nm ( $\sigma \rightarrow \pi^*$ ,  $\epsilon_{226} - 947 \text{ M}^{-1}$ ), 273 nm ( $\pi \rightarrow \pi^*$ ,  $\epsilon_{273} - 742 \text{ M}^{-1}$ ), IR (stretching frequency,  $\text{cm}^{-1}$ ): 3381 (OH), 1277 (glycosidic aryl alkyl C-O-C asymmetrical), 1035 (glycosidic aryl alkyl C-O-C symmetrical), 1425 (C=C), 1640 (CO), 2926 (CH), 3305 (NH), MS ( $m/z$ ) - 452.3  $[\text{M}-2]^+$ , 2D-HSQCT (DMSO- $d_6$ ) **C1 $\alpha$ -galactoside 25a**:  $^1\text{H}$  NMR  $\delta_{\text{ppm}}$  **Gal**: 4.95 (H-1 $\alpha$ , d,  $J = 3.5 \text{ Hz}$ ), 3.65 (H-2 $\alpha$ ), 3.62 (H-3 $\alpha$ ), 3.62 (H-5 $\alpha$ ), 3.35 (H-6a); **VN**: 6.61 (H-2), 6.42 (H-5), 6.77 (H-6), 4.12 (H-7), 2.07 (H-9), 1.48 (H-10), 1.33 (H-11), 1.21 (H-13), 1.21 (H-14), 1.21 (H-15), 0.84 (H-16),

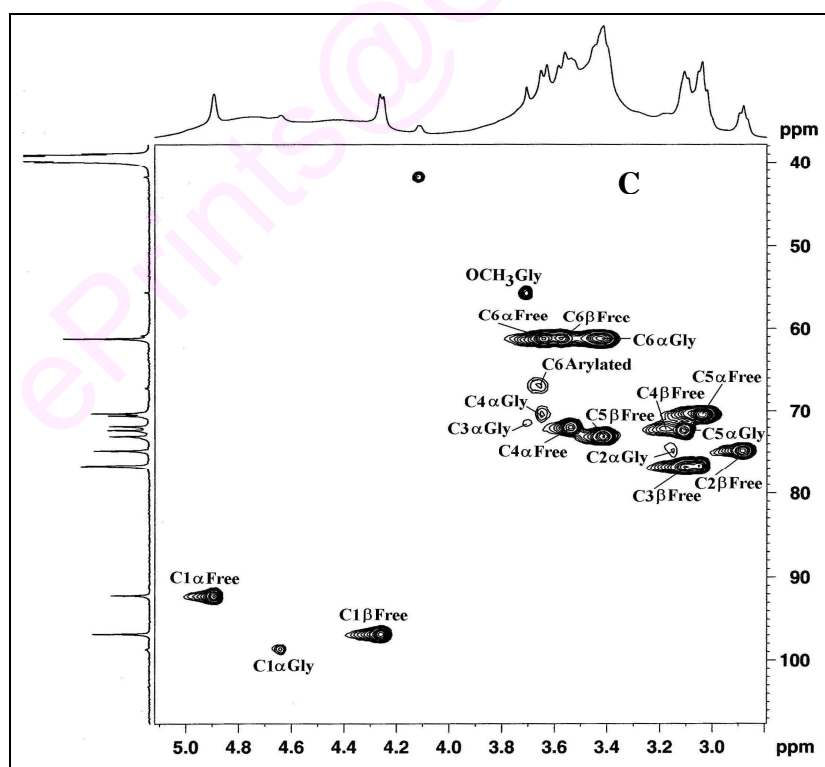
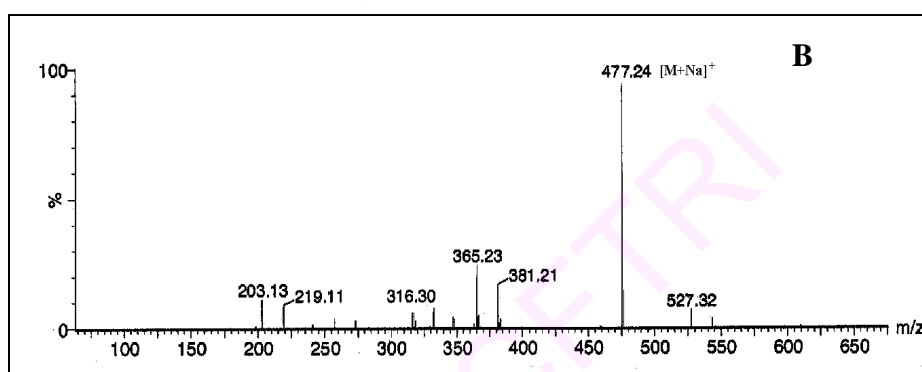
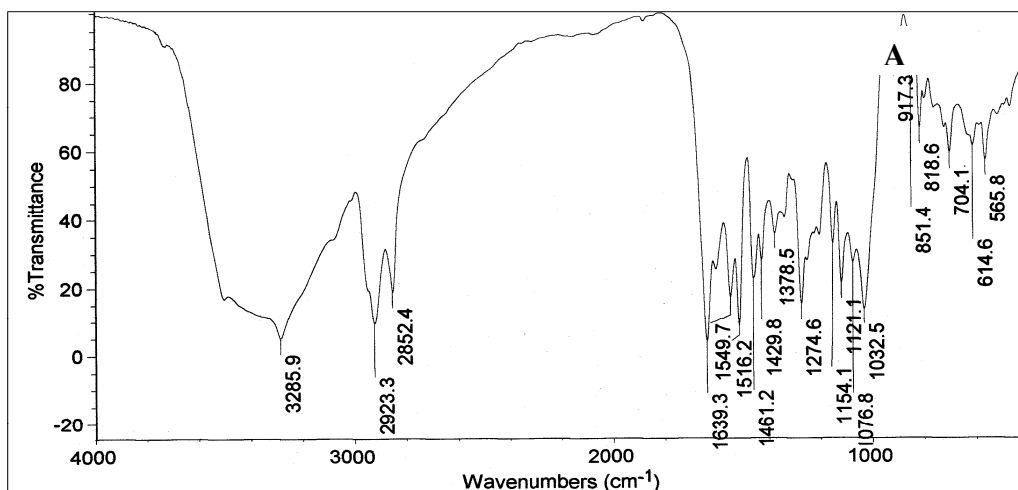


**Fig. 3.22** 4-*O*-(*D*-Glucopyranosyl)*N*-vanillyl-nonanamide **24a,b** (A) IR spectrum, (B) Mass spectrum and (C) 2D-HSQC spectrum showing the C1-C6 region. Some of the assignments are interchangeable.

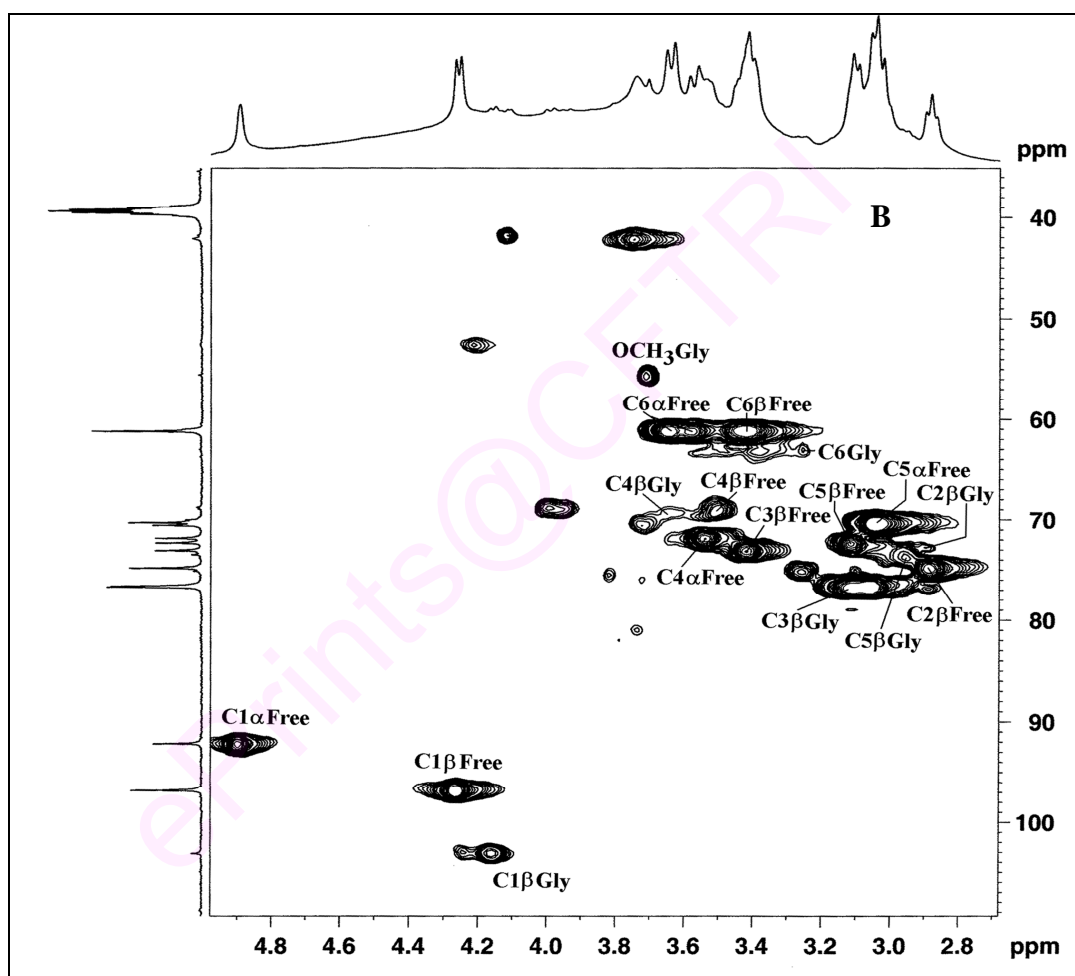
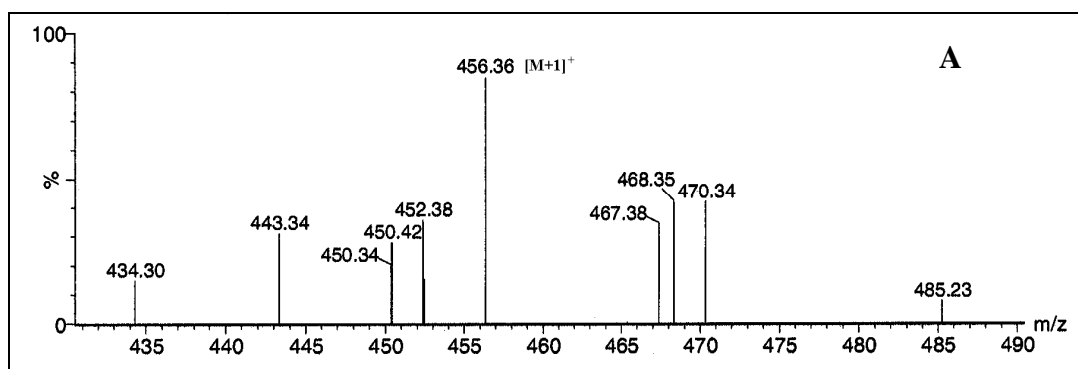


**Fig. 3.23** 4-*O*-( $\beta$ -D-Glucopyranosyl)N-vanillyl-nonanamide **24c** (A) Mass spectrum and (B) 2D-HSQC spectrum showing the C1-C6 region. Some of the assignments are interchangeable.

3.71 (OCH<sub>3</sub>), <sup>13</sup>C NMR δ<sub>ppm</sub> **Gal**: 95.3 (C1α), 68.8 (C2α), 68.9 (C3α), 70.9 (C5α), 62.8 (C6α); **VN**: 130.5 (C1), 111.7 (C2), 147.3 (C3), 145.3 (C4), 115.1 (C5), 119.6 (C6), 172.1 (C8), 35.3 (C9), 25.3 (C10), 28.5 (C11), 28.5 (C13), 31.2 (C14), 21.9 (C15), 14.1 (C16), 55.5 (OCH<sub>3</sub>). **C1β-galactoside 25b**: Solid, mp 115 °C, UV (H<sub>2</sub>O λ<sub>max</sub>): 192.5 nm (σ→σ\*, ε<sub>192.5</sub> – 2321 M<sup>-1</sup>), 226 nm (σ→π\*, ε<sub>226</sub> – 587 M<sup>-1</sup>), 276.5 nm (π→π\*, ε<sub>276.5</sub> – 312 M<sup>-1</sup>), IR (stretching frequency, cm<sup>-1</sup>): 3285 (OH), 1268 (glycosidic aryl alkyl C-O-C asymmetrical), 1035 (glycosidic aryl alkyl C-O-C symmetrical), 1438 (C=C), 1634 (CO), 2935 (CH), optical rotation (*c* 0.5, H<sub>2</sub>O): [α]<sub>D</sub> at 25 °C = -9.38, MS (*m/z*) – 455.3 [M]<sup>+</sup>, 2D-HSQCT (DMSO-*d*<sub>6</sub>): <sup>1</sup>H NMR δ<sub>ppm</sub> **Gal**: 4.90 (H-1β, d, *J* = 7.3 Hz), 3.40 (H-3β), 3.68 (H-5β), 3.38 (H-6a); **VN**: 6.64 (H-2), 6.55 (H-5), 6.75 (H-6), 2.06 (H-9), 1.48 (H-10), 1.10 (H-13), 1.10 (H-14), 1.10 (H-15), 0.82 (H-16), 3.71 (OCH<sub>3</sub>), <sup>13</sup>C NMR δ<sub>ppm</sub> **Gal**: 101.7 (C1β), 74.6 (C3β), 76.5 (C5β), 62.6 (C6β); **VN**: 130.6 (C1), 145.3 (C4), 115.5 (C5), 118.8 (C6), 41.7 (C7), 174.1 (C8), 37.9 (C9), 25.3 (C10), 28.7 (C11), 28.6 (C12), 28.5 (C13), 31.1 (C14), 22.1 (C15), 14.1 (C16), 55.5 (OCH<sub>3</sub>).

Infra-red and 2D-HSQCT NMR spectra for 4-*O*-(D-galactopyranosyl)N-vanillyl-nonanamide **25a,b** for amyloglucosidase catalysed products were shown in Figures 3.24A and 3.24B respectively. Mass and 2D-HSQCT NMR spectra for 4-*O*-(β-D-galactopyranosyl)N-vanillyl-nonanamide **25b** for β-glucosidase catalysed product are shown in Figures 3.25A and 3.25B respectively.

**3.2.3.3 4-*O*-(β-D-Mannopyranosyl)N-vanillyl-nonanamide 26**: Solid, mp 96 °C, UV (H<sub>2</sub>O λ<sub>max</sub>): 202 nm (σ→σ\*, ε<sub>202</sub> – 7314 M<sup>-1</sup>), 227 nm (σ→π\*, ε<sub>227</sub> – 2633 M<sup>-1</sup>), 273 nm (π→π\*, ε<sub>273</sub> – 969 M<sup>-1</sup>); IR (stretching frequency, cm<sup>-1</sup>): 3280 (OH), 1277 (glycosidic aryl alkyl C-O-C asymmetrical), 1030 (glycosidic aryl alkyl C-O-C symmetrical), 1432 (C=C), 1634 (CO), 2928 (CH), optical rotation (*c* 0.5, H<sub>2</sub>O): [α]<sub>D</sub> at 25 °C = -15, MS

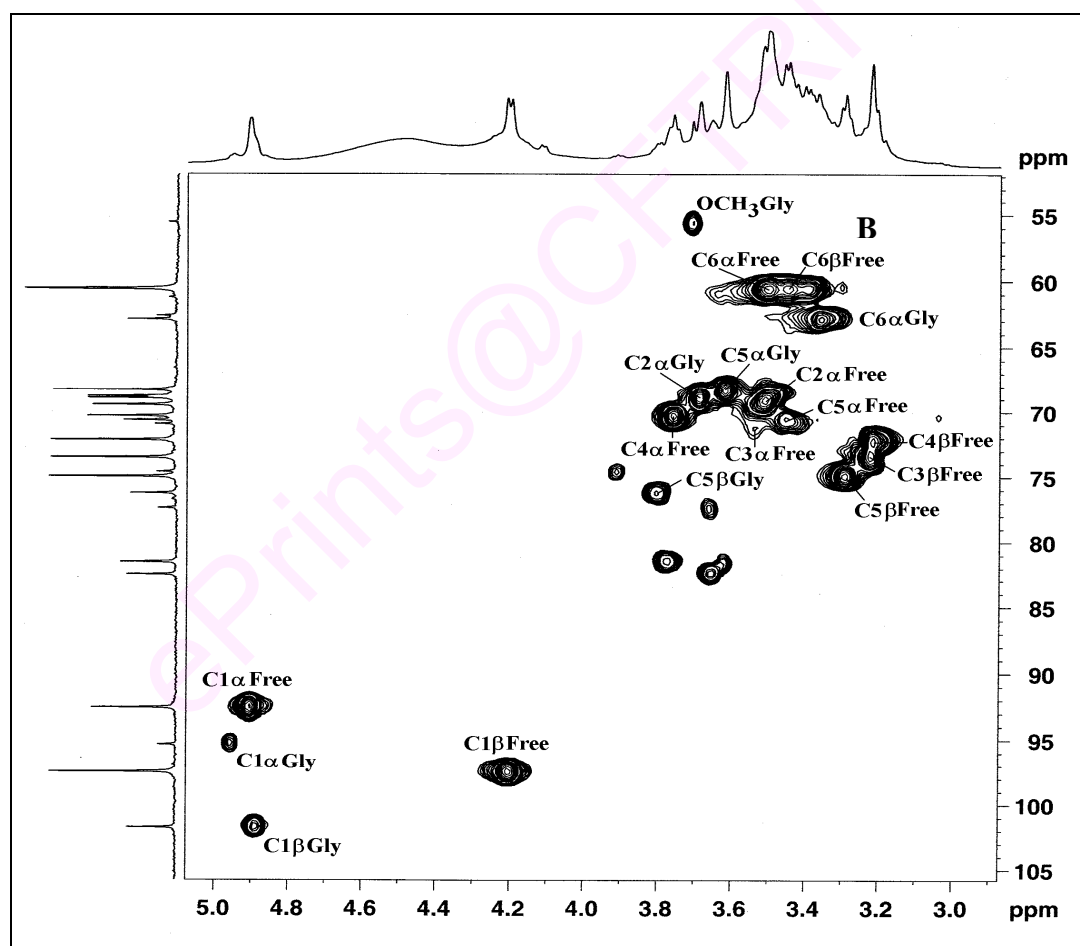
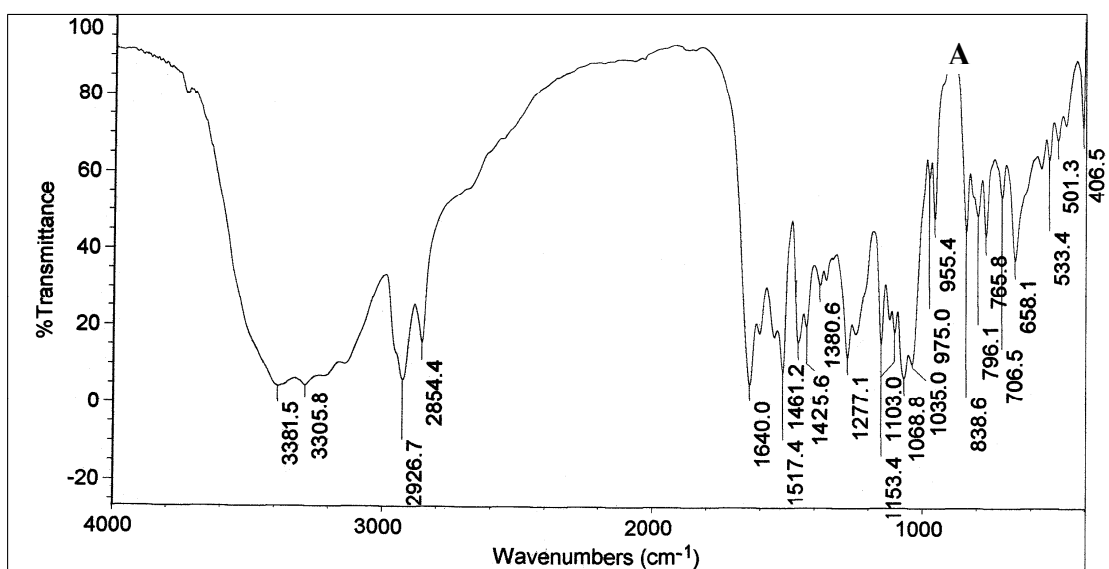


**Fig. 3.24** 4-*O*-(D-Galactopyranosyl)N-vanillyl-nonanamide **25a,b** (A) IR spectrum and (B) 2D-HSQC spectrum showing the C1-C6 region. Some of the assignments are interchangeable.

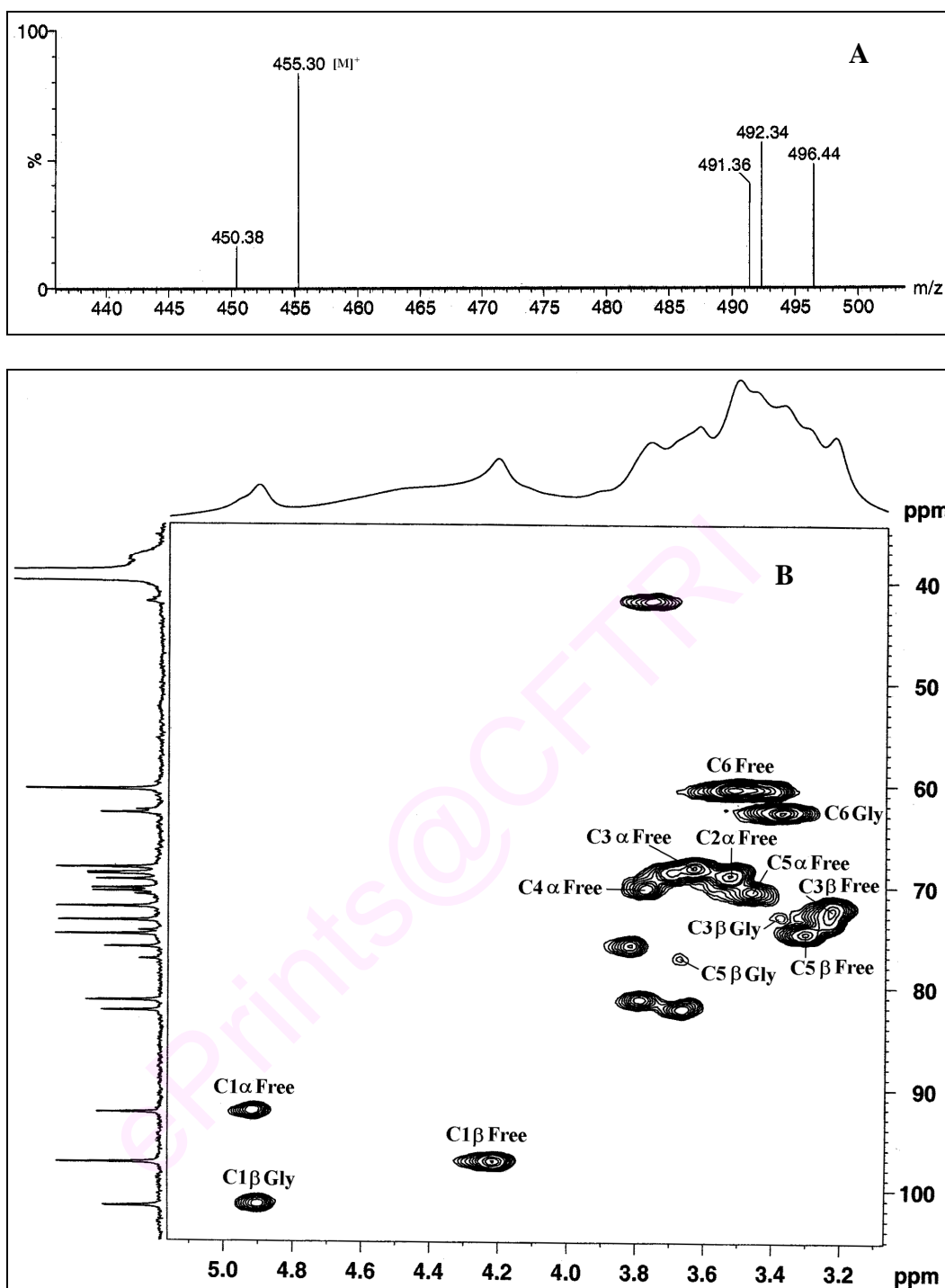


**Fig. 3.25** 4-*O*-(β-D-Galactopyranosyl)N-vanillyl-nonanamide **25b** (A) Mass spectrum and (B) 2D-HSQC spectrum showing the C1-C6 region. Some of the assignments are interchangeable.



( $m/z$ ) – 455.3 [M]<sup>+</sup>, 2D-HSQCT (DMSO- $d_6$ ): <sup>1</sup>H NMR  $\delta_{\text{ppm}}$  **Man**: 4.61 (H-1 $\beta$ , d, J = 3.1 Hz), 3.39 (H-2 $\beta$ ), 3.38 (H-3 $\beta$ ), 3.36 (H-4 $\beta$ ), 3.38a, 3.22b (H-6); **VN**: 6.64 (H-2), 6.55 (H-5), 6.75 (H-6), 2.06 (H-9), 1.48 (H-10), 1.10 (H-13), 1.10 (H-14), 1.10 (H-15), 0.82 (H-16), 3.71 (OCH<sub>3</sub>); <sup>13</sup>C NMR  $\delta_{\text{ppm}}$  **Man**: 101.6 (C1 $\beta$ ), 72.5 (C2 $\beta$ ), 73.3 (C3 $\beta$ ), 67.5 (C4 $\beta$ ), 62.1 (C6 $\beta$ ); **VN**: 130.6 (C1), 111.8 (C2), 147.5 (C3), 145.5 (C4), 115.3 (C5), 119.8 (C6), 41.9 (C7), 172.3 (C8), 35.5 (C9), 25.4 (C10), 28.7 (C11), 28.6 (C12), 28.6 (C13), 31.3 (C14), 22.1 (C15), 14.1 (C16), 55.6 (OCH<sub>3</sub>).

Infra-red and 2D-HSQCT NMR spectra for 4-*O*-( $\beta$ -D-mannopyranosyl)N-vanillyl-nonanamide **26** are shown in Figures 3.26A and 3.26B respectively.

**3.2.3.4 4-*O*-(D-Ribofuranosyl)N-vanillyl-nonanamide 27a,b**: Solid, UV (H<sub>2</sub>O  $\lambda_{\text{max}}$ ): 201.5 nm ( $\sigma \rightarrow \sigma^*$ ,  $\epsilon_{201.5} - 3429 \text{ M}^{-1}$ ), 268.5 nm ( $\pi \rightarrow \pi^*$ ,  $\epsilon_{268.5} - 1194 \text{ M}^{-1}$ ), IR (stretching frequency, cm<sup>-1</sup>): 3288 (OH), 1275 (glycosidic aryl alkyl C-O-C asymmetrical), 1034 (glycosidic aryl alkyl C-O-C symmetrical), 1429 (C=C), 1640 (CO), 2924 (CH), MS ( $m/z$ ) – 422.3 [M-2]<sup>+</sup>, 2D-HSQCT (DMSO- $d_6$ ) **C1 $\alpha$ -riboside 27a**: <sup>1</sup>H NMR  $\delta_{\text{ppm}}$  **Rib**: 5.25 (H-1 $\alpha$ , d, J = 3.5 Hz), 3.40 (H-2 $\alpha$ ), 3.50 (H-3 $\alpha$ ), 3.88 (H-4 $\alpha$ ), 3.61 (H-5a); **VN**: 6.27 (H-2), 6.14 (H-5), 6.78 (H-6), 4.12 (H-7), 2.12 (H-9), 1.48 (H-10), 1.32 (H-11), 1.21 (H-13), 1.21 (H-14), 1.21 (H-15), 0.83 (H-16), 3.70 (OCH<sub>3</sub>), <sup>13</sup>C NMR  $\delta_{\text{ppm}}$  **Rib**: 96.1 (C1 $\alpha$ ), 72.5 (C2 $\alpha$ ), 71 (C3 $\alpha$ ), 67.1 (C4 $\alpha$ ), 62.5 (C5 $\alpha$ ); **VN**: 130.5 (C1), 111.8 (C2), 147.5 (C3), 145.4 (C4), 115.1 (C5), 119.6 (C6), 41.8 (C7), 172.1 (C8), 35.3 (C9), 25.3 (C10), 28.5 (C11), 28.6 (C13), 31.2 (C14), 21.9 (C15), 14.2 (C16), 55.6 (OCH<sub>3</sub>), **C1 $\beta$ -riboside 27b**: <sup>1</sup>H NMR  $\delta_{\text{ppm}}$  **Rib**: 4.90 (H-1 $\beta$ , d, J = 6.3 Hz), 3.75 (H-4 $\beta$ ), 3.26 (H-5a); <sup>13</sup>C NMR  $\delta_{\text{ppm}}$  **Rib**: 101.4 (C1 $\beta$ ), 67.1 (C4 $\beta$ ), 62.9 (C5 $\beta$ ).

Infra-red and 2D-HSQCT NMR spectra for 4-*O*-(D-ribofuranosyl)N-vanillyl-nonanamide **27a,b** are shown in Figures 3.27A and 3.27B respectively.

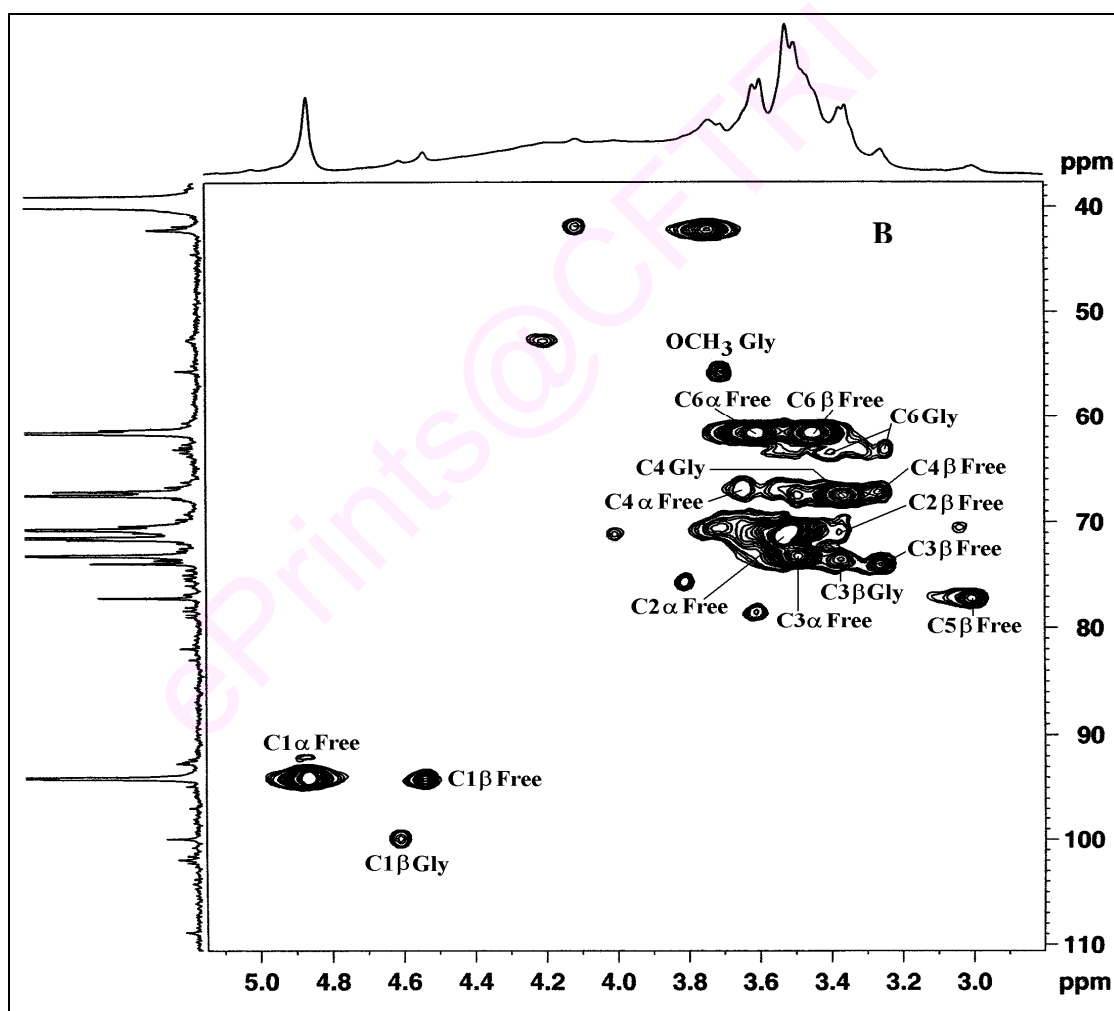
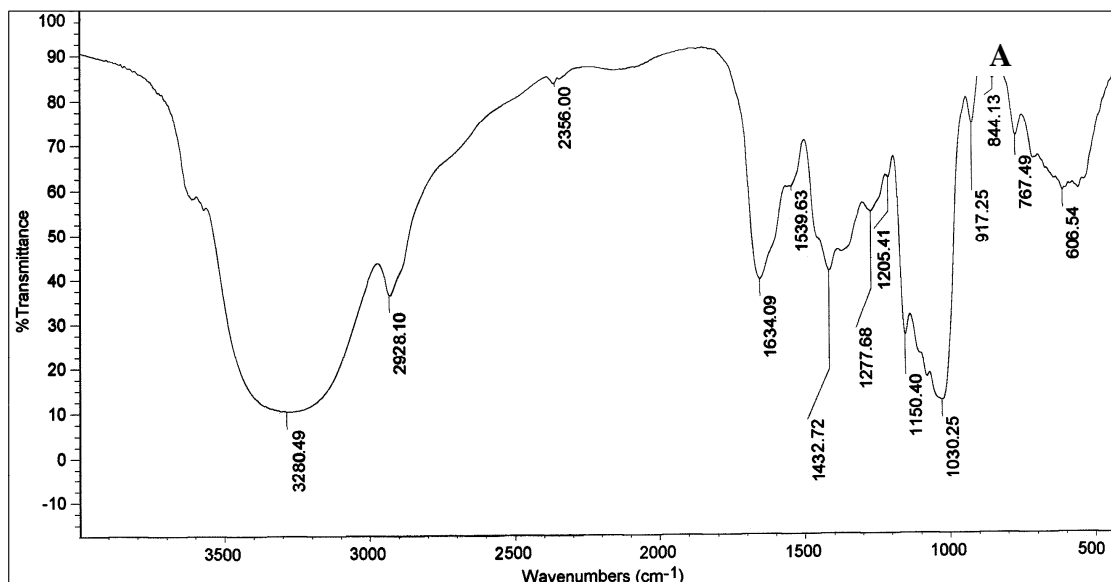


**Fig. 3.26** 4-*O*-( $\beta$ -D-Mannopyranosyl)*N*-vanillyl-nonanamide **26** (A) IR spectrum and (B) 2D-HSQC spectrum showing the C1-C6 region. Some of the assignments are interchangeable.

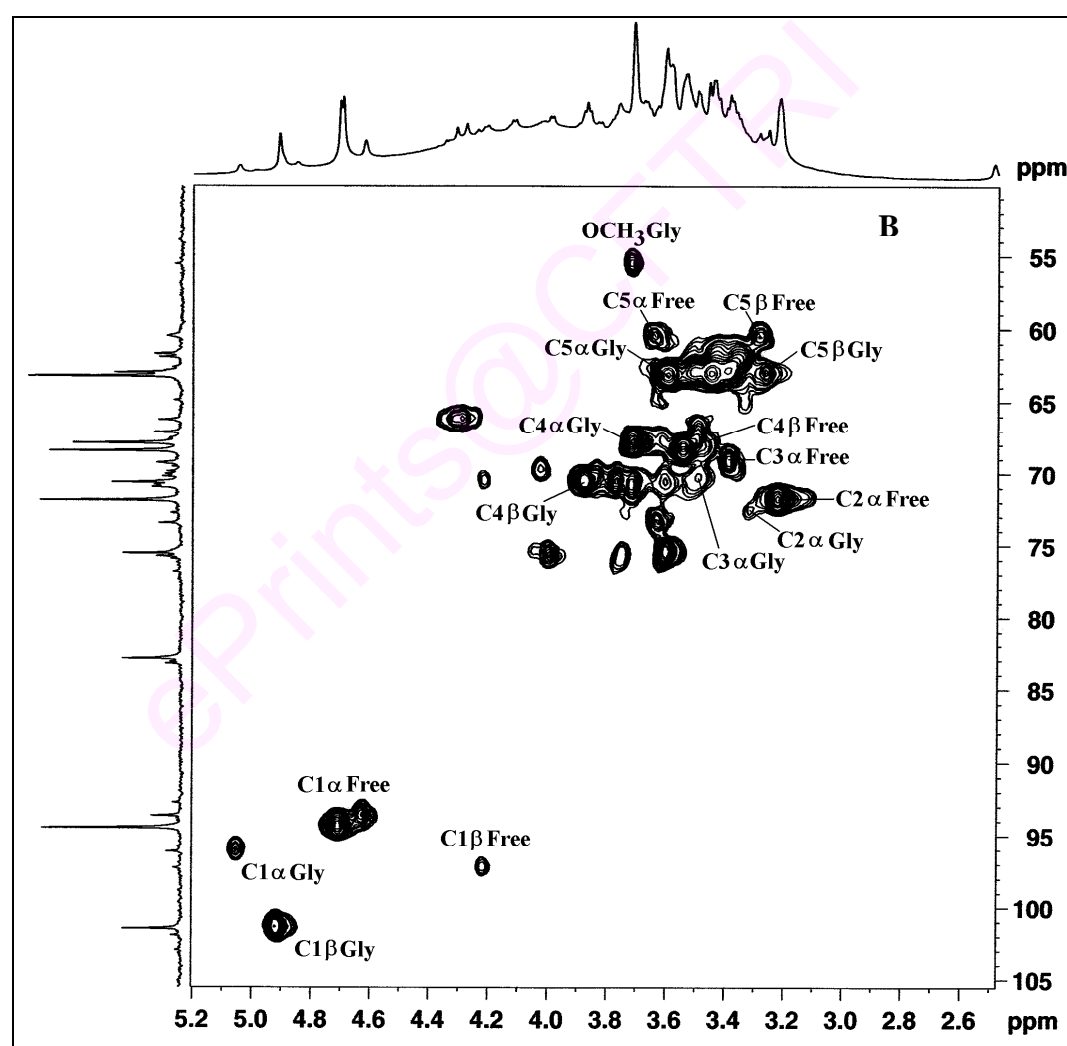
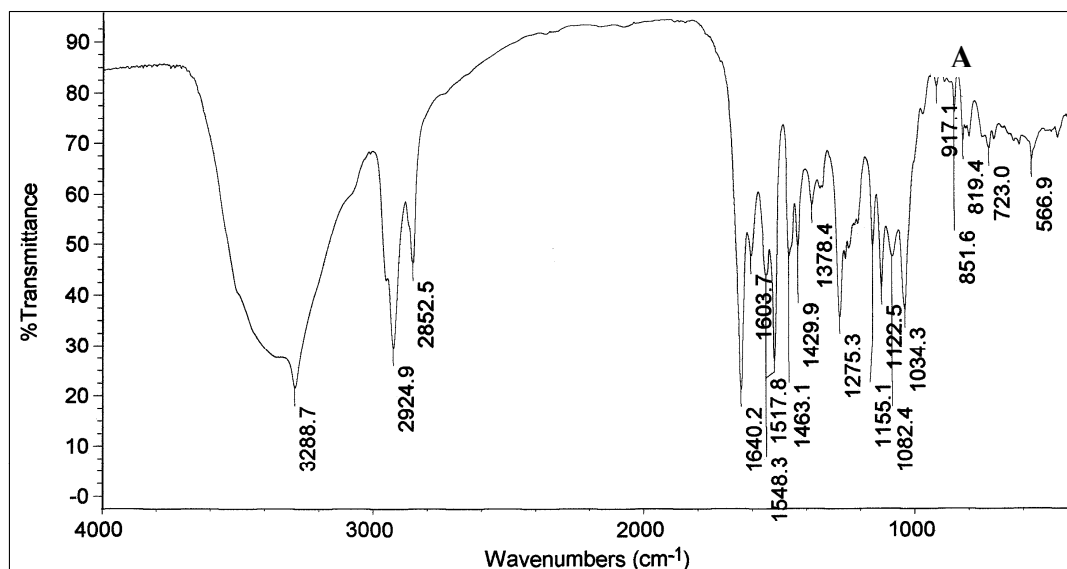


**Fig. 3.27** 4-*O*-(*D*-Ribofuranosyl)*N*-vanillyl-nonanamide **27a,b** (A) IR spectrum and (B) 2D-HSQC spectrum showing the C1-C5 region. Some of the assignments are interchangeable.

### 3.2.3.5 4-*O*-( $\alpha$ -D-Glucopyranosyl-(1'→4)D-glucopyranosyl)N-vanillyl-nonanamide

**28a-d:** Solid, UV (H<sub>2</sub>O  $\lambda_{\max}$ ): 198 nm ( $\sigma \rightarrow \sigma^*$ ,  $\epsilon_{198} = 6023 \text{ M}^{-1}$ ), 225 nm ( $\sigma \rightarrow \sigma^*$ ,  $\epsilon_{225} = 826 \text{ M}^{-1}$ ), 279.5 nm ( $\pi \rightarrow \pi^*$ ,  $\epsilon_{279.5} = 819 \text{ M}^{-1}$ ), IR (stretching frequency,  $\text{cm}^{-1}$ ): 3382 (OH), 1254 (glycosidic aryl alkyl C-O-C asymmetrical), 1027 (glycosidic aryl alkyl C-O-C symmetrical), 1405 (C=C), 1631 (CO), 2927 (CH), MS ( $m/z$ ) – 639.5 [M+Na]<sup>+</sup>, 2D-HSQCT (DMSO-*d*<sub>6</sub>) **C1 $\alpha$ -maltoside 28a:** <sup>1</sup>H NMR  $\delta_{\text{ppm}}$  **Malt:** 4.95 (H-1 $\alpha$ , d, J = 3.7 Hz), 3.10 (H-2 $\alpha$ ), 3.32 (H-4 $\alpha$ ), 3.26 (H-5 $\alpha$ ), 3.68 (H-6 $\alpha$ ), 4.63 (H-1' $\alpha$ ), 2.88 (H-3'), 3.65 (H-4'), 3.62 (H-5'), 3.55 (H-6'a); **VN:** 6.12 (H-2), 6.22 (H-5), 6.70 (H-6), 4.12 (H-7), 2.12 (H-9), 1.48 (H-10), 1.20 (H-13), 1.20 (H-14), 1.20 (H-15), 0.82 (H-16), 3.62 (OCH<sub>3</sub>), <sup>13</sup>C NMR  $\delta_{\text{ppm}}$  **Malt:** 100.5 (C1 $\alpha$ ), 72.8 (C2 $\alpha$ ), 79.2 (C4 $\alpha$ ), 74.5 (C5 $\alpha$ ), 61.2 (C6 $\alpha$ ), 98.1 (C1' $\alpha$ ), 74.9 (C3'), 72.8 (C4'), 70.1 (C5'), 61.3 (C6'); **VN:** 130.1 (C1), 110.7 (C2), 115.2 (C5), 119.6 (C6), 41.7 (C7), 172.1 (C8), 35.3 (C9), 25.3 (C10), 28.6 (C11), 28.5 (C12), 28.5 (C13), 31.1 (C14), 21.9 (C15), 14.1 (C16), 55.5 (OCH<sub>3</sub>). **C6-O-arylated 28b:** <sup>1</sup>H NMR **Glu:** 3.68 (H-6 $\alpha$ ), <sup>13</sup>C NMR **Glu:** 66.1 (C6 $\alpha$ ). **C6'-O-arylated 28c:** <sup>1</sup>H NMR **Glu:** 3.55 (H-6 $\alpha$ ), <sup>13</sup>C NMR **Glu:** 67.1 (C6'). **C1 $\beta$ -maltoside 28d:** Solid, mp 135 °C, UV (H<sub>2</sub>O  $\lambda_{\max}$ ): 199.5 nm ( $\sigma \rightarrow \sigma^*$ ,  $\epsilon_{199.5} = 9300 \text{ M}^{-1}$ ), 225 nm ( $\sigma \rightarrow \pi^*$ ,  $\epsilon_{225} = 2818 \text{ M}^{-1}$ ), 280.5 nm ( $\pi \rightarrow \pi^*$ ,  $\epsilon_{280.5} = 1347 \text{ M}^{-1}$ ), IR (stretching frequency,  $\text{cm}^{-1}$ ): 3345 (OH), 1249 (glycosidic aryl alkyl C-O-C asymmetrical), 1037 (glycosidic aryl alkyl C-O-C symmetrical), 1410 (C=C), 1662 (CO), 2917 (CH), optical rotation (*c* 0.5, H<sub>2</sub>O):  $[\alpha]_{\text{D}}$  at 25 °C = +7.3, MS ( $m/z$ ) – 615.4 [M-2]<sup>+</sup>, 2D-HSQCT (DMSO-*d*<sub>6</sub>): <sup>1</sup>H NMR  $\delta_{\text{ppm}}$  **Malt:** 4.88 (H-1 $\beta$ , d, J = 6.2 Hz), 3.20 (H-5 $\beta$ ), 3.42 (H-6 $\alpha$ ), 4.95 (H-1' $\alpha$ ), 3.05 (H-2'), 2.92 (H-3'), 3.65 (H-4'), 3.61 (H-5'), 3.55 (H-6'); **VN:** 6.65 (H-2), 6.60 (H-5), 6.80 (H-6), 4.12 (H-7), 2.07 (H-9), 1.21 (H-13), 1.21 (H-14), 1.21 (H-15), 0.83 (H-16), 3.70 (OCH<sub>3</sub>); <sup>13</sup>C NMR  $\delta_{\text{ppm}}$  **Malt:** 98.5 (C1 $\beta$ ), 75 (C5 $\beta$ ), 61.2 (C6 $\beta$ ), 100.7 (C1' $\alpha$ ), 74.1 (C2'), 74.2 (C3'), 73 (C4'), 70.2

(C5'), 60.8 (C6'); **VN**: 111.7 (C2), 145.3 (C4), 115.2 (C5), 119.6 (C6), 41.8 (C7), 172.1 (C8), 35.4 (C9), 25.3 (C10), 28.6 (C11), 28.5 (C13), 31.2 (C14), 21.9 (C15), 14.1 (C16), 55.6 (OCH<sub>3</sub>).

Mass and 2D-HSQCT NMR spectra for 4-*O*-( $\alpha$ -D-glucopyranosyl-(1'→4)-D-glucopyranosyl)N-vanillyl-nonanamide **28a-c** for amyloglucosidase catalysed products were shown in Figures 3.28A and 3.28B respectively. Infra-red and 2D-HSQCT NMR spectra for 4-*O*-( $\alpha$ -D-glucopyranosyl-(1'→4)- $\beta$ -D-glucopyranosyl)N-vanillyl-nonanamide **28d** for  $\beta$ -glucosidase catalysed product are shown in Figures 3.29A and 3.29B respectively.

### 3.2.3.6 4-*O*-( $\alpha$ -D-Galactopyranosyl-(1'→4)- $\beta$ -D-glucopyranosyl)N-vanillyl-nonanamide

**29**: Solid, mp 126°C, UV (H<sub>2</sub>O  $\lambda_{\max}$ ): 192.5 nm ( $\sigma \rightarrow \sigma^*$ ,  $\epsilon_{192.5} = 9823 \text{ M}^{-1}$ ), 222.5 nm ( $\sigma \rightarrow \pi^*$ ,  $\epsilon_{222.5} = 5334 \text{ M}^{-1}$ ), 252.5 nm ( $\pi \rightarrow \pi^*$ ,  $\epsilon_{252.5} = 4553 \text{ M}^{-1}$ ), 283.5 nm ( $\pi \rightarrow \pi^*$ ,  $\epsilon_{283.5} = 2877 \text{ M}^{-1}$ ), IR (stretching frequency, cm<sup>-1</sup>): 3345 (OH), 1273 (glycosidic aryl alkyl C-O-C asymmetrical), 1037 (glycosidic aryl alkyl C-O-C symmetrical), 1415 (C=C), 1662 (CO), 2918 (CH), optical rotation (*c* 0.5, H<sub>2</sub>O):  $[\alpha]_{\text{D}}^{25} = +16$ , MS (*m/z*) – 615.5 [M-2]<sup>+</sup>, 2D-HSQCT (DMSO-*d*<sub>6</sub>): <sup>1</sup>H NMR  $\delta_{\text{ppm}}$ : **Lact**: 4.80 (H-1 $\beta$ , d, *J* = 7.4 Hz), 3.15 (H-2 $\beta$ ), 3.45 (H-3 $\beta$ ), 3.48 (H-6a), 4.16 (H-1' $\beta$ ), 3.22 (H-3'), 3.81 (H-4'), 2.98 (H-5'), 3.36 (H-6'); **VN**: 6.76 (H-2), 6.65 (H-5), 6.80 (H-6), 4.10 (H-7), 2.09 (H-9), 1.21 (H-13), 1.21 (H-14), 1.21 (H-15), 0.84 (H-16), 3.65 (OCH<sub>3</sub>), <sup>13</sup>C NMR  $\delta_{\text{ppm}}$  **Lact**: 102.9 (C1 $\beta$ ), 76.5 (C2 $\beta$ ), 70.8 (C4 $\beta$ ), 60.6 (C6 $\beta$ ), 103.6 (C1' $\beta$ ), 73 (C3'), 68.2 (C4'), 73.5 (C5'), 62.6 (C6'); **VN**: 130.5 (C1), 111.7 (C2), 147.4 (C3), 130.5 (C4), 115.1 (C5), 119.7 (C6), 41.8 (C7), 172.5 (C8), 35.4 (C9), 25.2 (C10), 28.6 (C11), 28.5 (C12), 27.3 (C13), 31.1 (C14), 21.9 (C15), 14.2 (C16), 55.4 (OCH<sub>3</sub>).

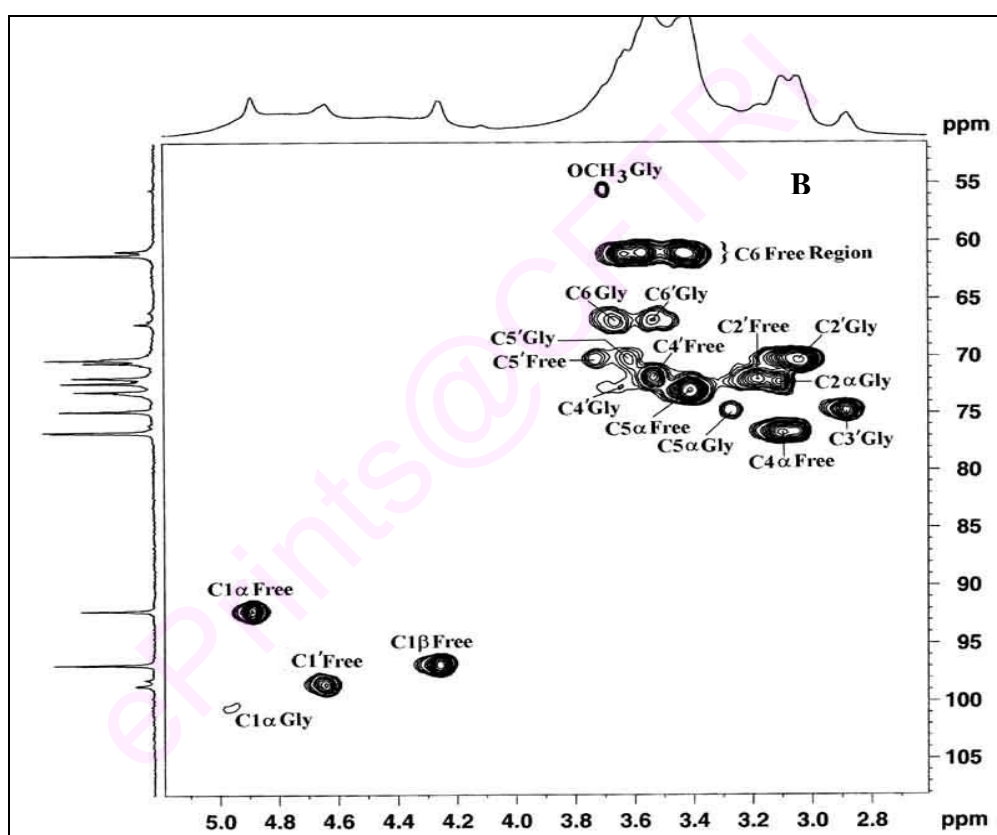
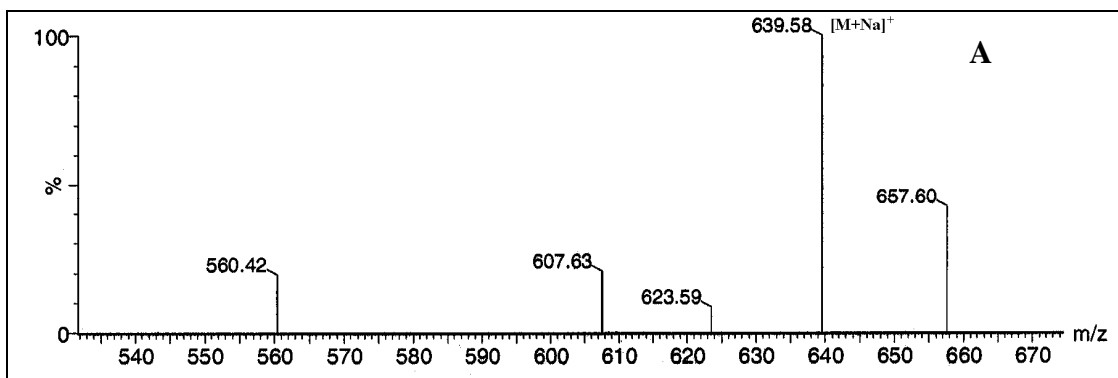


**Fig. 3.28** 4-*O*-( $\alpha$ -D-Glucopyranosyl-(1'→4)D-glucopyranosyl)N-vanillyl-nonanamide **28a-c** (A) Mass spectrum and (B) 2D-HSQC spectrum showing the C1-C6' region. Some of the assignments are interchangeable.

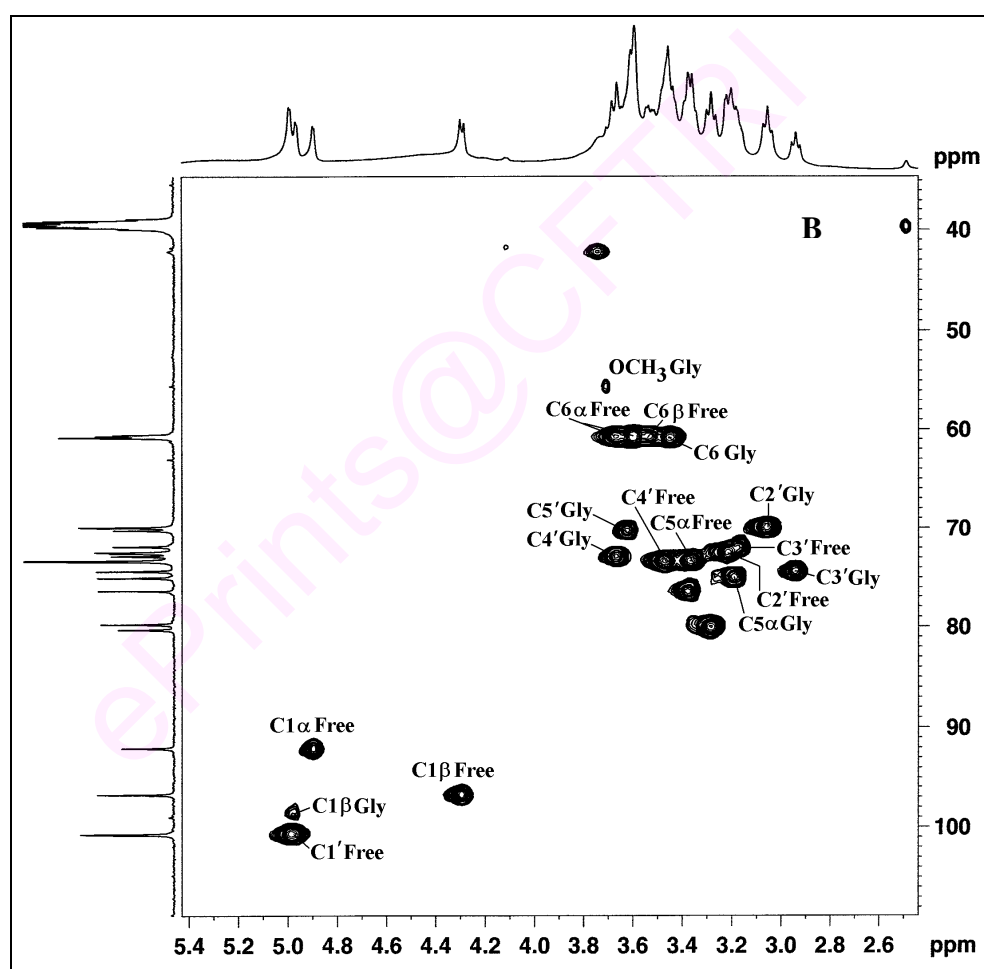
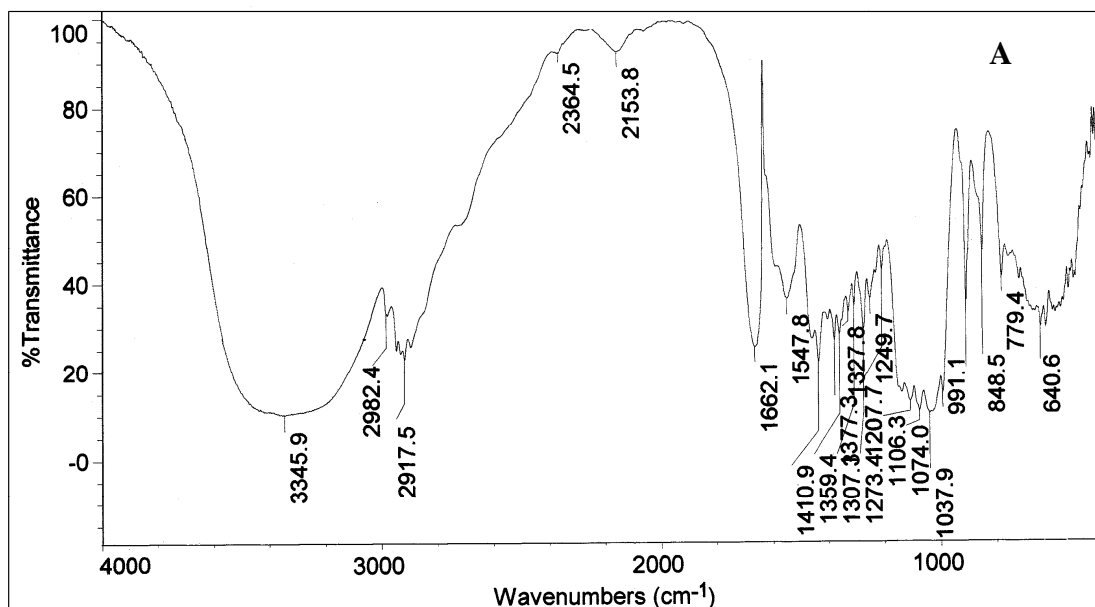


**Fig. 3.29** 4-*O*-( $\alpha$ -D-Glucopyranosyl-(1'→4) $\beta$ -D-glucopyranosyl)N-vanillyl-nonanamide **28d** (A) IR spectrum and (B) 2D-HSQC spectrum showing the C1-C6' region. Some of the assignments are interchangeable.

Infra-red and 2D-HSQCT NMR spectra for 4-*O*-( $\beta$ -D-galactopyranosyl-(1'→4) $\beta$ -D-glucopyranosyl)N-vanillyl-nonanamide **29** are shown in Figures 3.30A and 3.30B respectively.

UV spectra of N-vanillyl-nonanamide glycosides, showed shifts for  $\sigma \rightarrow \sigma^*$  band in the 192.5 – 203.5 nm (201.5 nm for free N-vanillyl-nonanamide) region,  $\sigma \rightarrow \pi^*$  band in the 225 – 227 nm (225 nm for free N-vanillyl-nonanamide) region and  $\pi \rightarrow \pi^*$  band in the 263 – 283.5 nm (279 nm for free N-vanillyl-nonanamide) region, IR C-O-C asymmetrical stretching frequencies in the 1254 - 1279  $\text{cm}^{-1}$  region and symmetrical stretching frequencies in the 1027 - 1038  $\text{cm}^{-1}$  region indicating that N-vanillyl-nonanamide had undergone glycosylation. From the 2D HSQCT spectra of the N-vanillyl-nonanamide glycosides, the following glycoside formation were confirmed from their respective chemical shift values: from D-glucose **6** C1 $\alpha$  glucoside **24a** to C1 $\alpha$  at 98.7 ppm and H-1 $\alpha$  at 4.65 ppm, C6-*O*-arylated **24b** to C6 at 67.2 ppm and H-6a at 3.63 ppm and C1 $\beta$  glucoside **24c** to C1 $\beta$  at 103.1 ppm and H-1 $\beta$  at 4.15 ppm; from D-galactose **7** C1 $\alpha$  galactoside **25a** to C1 $\alpha$  at 95.3 ppm and H-1 $\alpha$  at 4.95 ppm and C1 $\beta$  galactoside **25b** to C1 $\beta$  at 101.7 ppm and H-1 $\beta$  at 4.87 ppm; from D-mannose **8** C1 $\beta$  mannoside **26** to C1 $\beta$  at 101.6 ppm and H-1 $\beta$  at 4.61 ppm; from D-ribose **11** C1 $\alpha$  riboside **27a** to C1 $\alpha$  at 96.1 ppm and H-1 $\alpha$  at 5.25 ppm and C1 $\beta$  riboside **27b** to C1 $\beta$  at 101.4 ppm and H-1 $\beta$  at 4.90 ppm; from maltose **12** C1 $\alpha$  maltoside **28a** to C1 $\alpha$  at 100.5 ppm and H-1 $\alpha$  at 4.95 ppm, C6-*O*-arylated **28b** to C6 at 66.1 ppm and H-6a at 3.68 ppm and C6'-*O*-arylated **28c** to C6' at 67.1 ppm and H-6a' at 3.55 ppm and C1 $\beta$  maltoside **28d** to C1 $\beta$  at 98.5 ppm and H-1 $\beta$  at 4.88 ppm; from lactose **14** C1 $\beta$  lactoside **29** to C1 $\beta$  at 102.9 ppm and H-1 $\beta$  at 4.80 ppm. Mass spectra also confirmed the formation of the above mentioned glycosides.



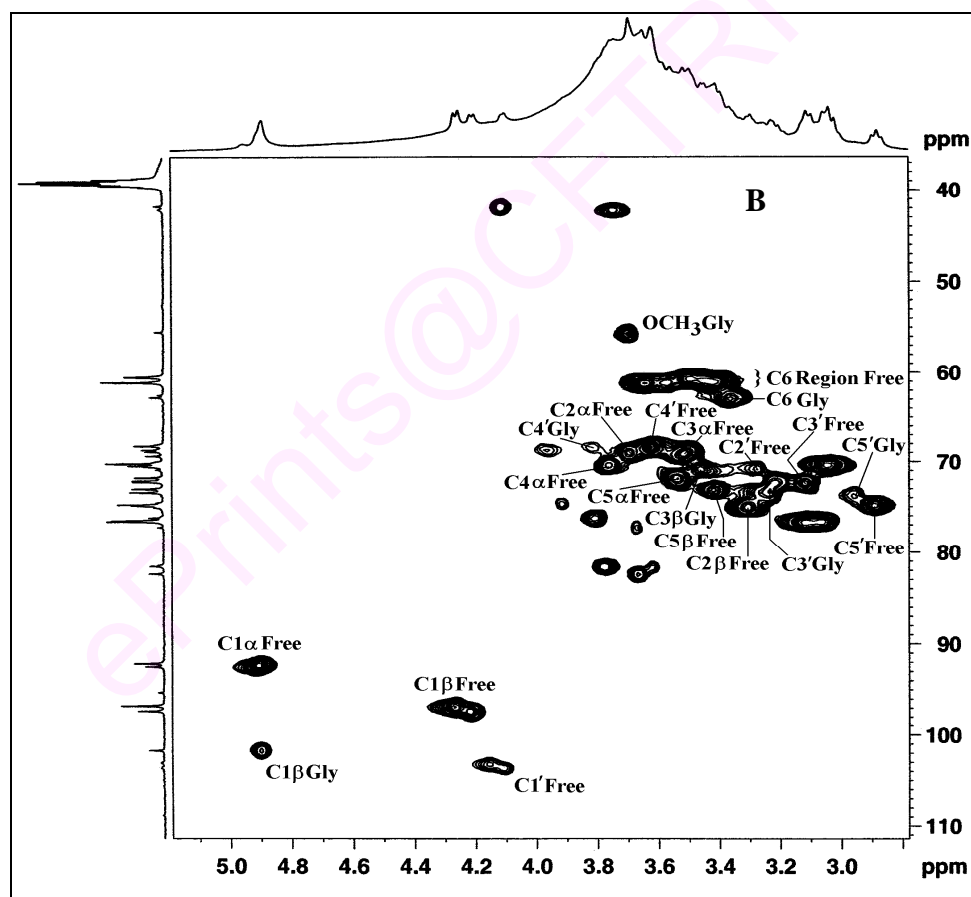
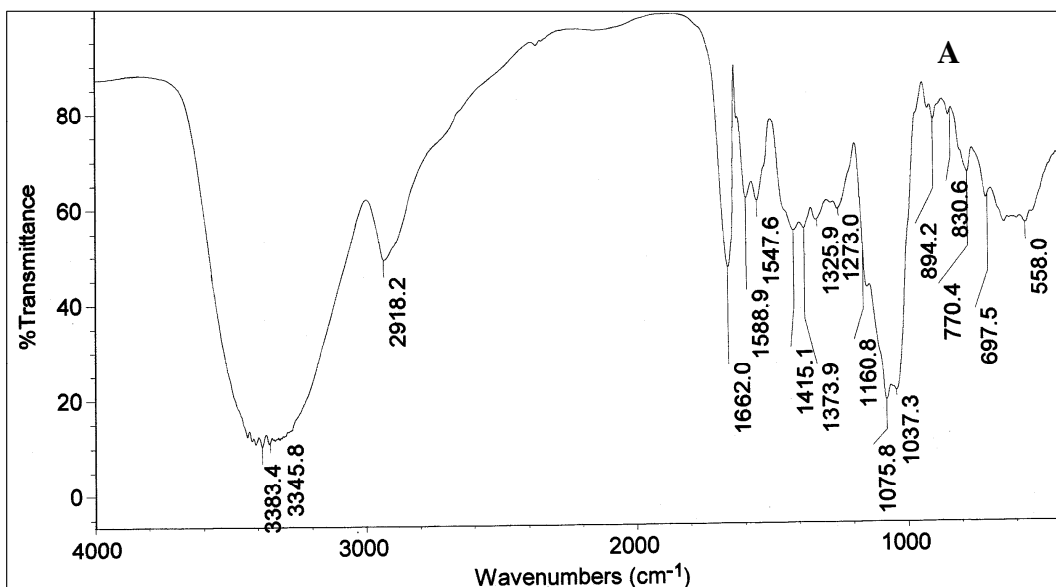


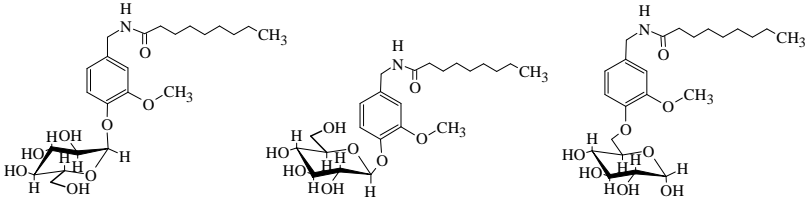
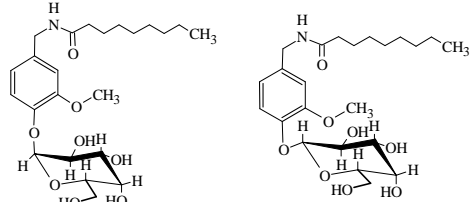
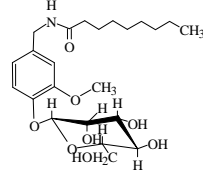
**Fig. 3.30** 4-*O*-( $\beta$ -D-Galactopyranosyl-(1'→4) $\beta$ -D-glucopyranosyl)N-vanillyl-nonanamide **29** (A) IR spectrum and (B) 2D-HSQC spectrum showing the C1-C6' region. Some of the assignments are interchangeable.

### 3.2.4 Discussion

Syntheses of N-vanillyl-nonanamide glycosides with carbohydrates were attempted under optimum conditions. The spectral characterization on the products formed (Section 3.2.3) and the yields are shown in Table 3.11. The following carbohydrates were glycosylated: D-glucose **6**, D-galactose **7**, D-mannose **8**, D-ribose **11**, maltose **12**, lactose **14**. The reaction did not occur without the use of both the glucosidases employed. Of these, amyloglucosidase catalysis gave rise to the following four glycosides: 4-*O*-(D-glucopyranosyl)N-vanillyl-nonanamide **24a,b**, 4-*O*-(D-galactopyranosyl)N-vanillyl-nonanamide **25a,b**, 4-*O*-(D-ribofuranosyl)N-vanillyl-nonanamide **27a,b** and 4-*O*-( $\alpha$ -D-glucopyranosyl-(1'→4)D-glucopyranosyl)N-vanillyl-nonanamide **28a-c**.  $\beta$ -Glucosidase catalysis gave rise to the following six glycosides: 4-*O*-( $\beta$ -D-glucopyranosyl)N-vanillyl-nonanamide **24c**, 4-*O*-( $\beta$ -D-galactopyranosyl)N-vanillyl-nonanamide **25b**, 4-*O*-( $\beta$ -D-mannopyranosyl)N-vanillyl-nonanamide **26**, 4-*O*-(D-ribofuranosyl)N-vanillyl-nonanamide **27a,b**, 4-*O*-( $\alpha$ -D-glucopyranosyl-(1'→4) $\beta$ -D-glucopyranosyl)N-vanillyl-nonanamide **28d** and 4-*O*-( $\beta$ -D-galactopyranosyl-(1'→4) $\beta$ -D-glucopyranosyl)N-vanillyl-nonanamide **29**. All these glycosides were soluble in water to different degrees and also less pungent. They could hence be used in pharmaceutical applications.

Both amyloglucosidase and  $\beta$ -glucosidase did not catalyse the reaction with D-fructose **9**, D-arabinose **10**, sucrose **13**, D-sorbitol **15** and D-mannitol **16**. Also, while  $\beta$ -glucosidase catalysed reaction with lactose **14**, amyloglucosidase did not. N-Vanillyl-nonanamide **2** could bind to these enzymes more strongly than the above carbohydrate molecules to the nucleophilic phenolic OH of N-vanillyl-nonanamide **2**.

Table 3.11 Syntheses of N-vanillyl-nonanamide glycosides<sup>a</sup>.

Glycosides	Amyloglucosidase catalysis		$\beta$ -Glucosidase catalysis	
	Product (% proportion) <sup>b</sup>	Yields (%) <sup>c</sup>	Product (% proportion) <sup>b</sup>	Yields (%) <sup>c</sup>
 <p><b>24a</b> 4-<i>O</i>-(<math>\alpha</math>-D-Glucopyranosyl)N-vanillyl-nonanamide  <b>24b</b> 4-<i>O</i>-(6-D-Glucopyranosyl)N-vanillyl-nonanamide  <b>24c</b> 4-<i>O</i>-(<math>\beta</math>-D-Glucopyranosyl)N-vanillyl-nonanamide</p>	C1 $\alpha$ glucoside (70), C6- <i>O</i> -arylated (30)	56	C1 $\beta$ glucoside	35
 <p><b>25a</b> 4-<i>O</i>-(<math>\alpha</math>-D-Galactopyranosyl)N-vanillyl-nonanamide  <b>25b</b> 4-<i>O</i>-(<math>\beta</math>-D-Galactopyranosyl)N-vanillyl-nonanamide</p>	C1 $\alpha$ galactoside (42), C1 $\beta$ galactosides (58)	14	C1 $\beta$ galactoside	26
 <p><b>26</b> 4-<i>O</i>-(<math>\beta</math>-D-Mannopyranosyl)N-vanillyl-nonanamide</p>	-	-	C1 $\beta$ mannoside	24

	C1 $\alpha$ riboside (33), C1 $\beta$ riboside (67)	9	C1 $\alpha$ riboside (30), C1 $\beta$ riboside (70)	10
<p><b>27a</b> 4-<i>O</i>-(<math>\alpha</math>-D-Ribofuranosyl)N-vanillyl-nonanamide  <b>27b</b> 4-<i>O</i>-(<math>\beta</math>-D-Ribofuranosyl)N-vanillyl-nonanamide</p>				
	C1 $\alpha$ maltoside (11), C6- <i>O</i> -arylated (40), C6'- <i>O</i> -arylated (49)	15	C1 $\beta$ maltoside	9
<p><b>28a</b> 4-<i>O</i>-(<math>\alpha</math>-D-Glucopyranosyl-(1'→4)<math>\alpha</math>-D-glucopyranosyl)N-vanillyl-nonanamide  <b>28b</b> 4-<i>O</i>-(<math>\alpha</math>-D-Glucopyranosyl-(1'→4)6-D-glucopyranosyl)N-vanillyl-nonanamide  <b>28c</b> 4-<i>O</i>-(<math>\alpha</math>-D-Glucopyranosyl-(1'→4)6'-D-glucopyranosyl)N-vanillyl-nonanamide  <b>28d</b> 4-<i>O</i>-(<math>\alpha</math>-D-Glucopyranosyl-(1'→4)<math>\beta</math>-D-glucopyranosyl)N-vanillyl-nonanamide</p>				
	-	-	C1 $\beta$ lactoside	28
<p><b>29</b> 4-<i>O</i>-(<math>\beta</math>-D-Galactopyranosyl-(1'→4)<math>\beta</math>-D-glucopyranosyl)N-vanillyl-nonanamide</p>				

<sup>a</sup> N-Vanillyl-nonanamide and carbohydrate – 0.5 mmol each; enzyme concentration 40% w/w of carbohydrate; solvent – di-isopropyl ether; buffer – 0.2 mM (2 mL) pH 7 phosphate buffer; incubation period – 72 h. <sup>b</sup>The product proportions were determined from the area of respective <sup>1</sup>H/<sup>13</sup>C signals. <sup>c</sup>Conversion yields were from HPLC with respect to free carbohydrate. Error in yield measurements is  $\pm$  10%.

Amyloglucosidase clearly exhibited its 'inverting' potentiality in the glycosylation giving rise to the  $\alpha$ -D-glucoside - 70% of the  $\alpha$ -glucoside without the  $\beta$  component compared to the 40:60  $\alpha$ :  $\beta$  anomeric composition of D-glucose employed,  $\alpha$ -D-galactoside - 42%  $\alpha$  and 58%  $\beta$  compared to the 92:8  $\alpha$ :  $\beta$  anomeric composition of D-galactose employed and  $\alpha$ -D-riboside - 33%  $\alpha$  and 67%  $\beta$  compared to the 34:66  $\alpha$ :  $\beta$  anomeric composition of D-ribose employed. Both the glucosidases gave low conversions with D-ribose and maltose ( $\leq 10\%$ ). Amyloglucosidase catalysis gave C1  $\alpha$  and  $\beta$  glycosides (D-glucose gave exclusively  $\alpha$ -D-glucoside only) along with C6-O- aryl derivatives (Table 3.11). However,  $\beta$ -glucosidase catalysis gave exclusively C1 $\beta$  glycosides with the exception of D-ribose, indicating its capability to exhibit excellent regioselectivity in this glycosylation with the carbohydrate molecules D-glucose **6**, D-galactose **7**, D-mannose **8**, maltose **12** and lactose **14** (Table 3.11).

Even the presence of hydrophobic bulky alkyl side chain in N-vanillyl-nonanamide did not pose much of a steric hindrance when the carbohydrate molecules were transferred to its phenolic OH group. About 13 individual glycosides were synthesized enzymatically using both the glucosidases, of which 10 are being reported for the first time. The new glycosides reported are: 4-O-(D-galactopyranosyl)N-vanillyl-nonanamide **25a,b**, 4-O-( $\beta$ -D-mannopyranosyl)N-vanillyl-nonanamide **26**, 4-O-(D-ribofuranosyl)N-vanillyl-nonanamide **27a,b**, 4-O-( $\alpha$ -D-glucopyranosyl-(1'→4)D-glucopyranosyl)N-vanillyl-nonanamide **28a-d** and 4-O-( $\beta$ -D-galactopyranosyl-(1'→4) $\beta$ -D-glucopyranosyl)N-vanillyl-nonanamide **29**.

### 3.3 Syntheses of curcuminyl-bis-glycosides

Curcumin [1E,6E-1,7-di(4-hydroxy-3-methoxy-phenyl)-1,6-heptadiene-3,5-dione], a yellow pigment of turmeric (the dried rhizome of *Curcuma longa* belonging to Zingiberaceae) is not only used primarily as a food colorant but also as a

pharmacologically-active principle of turmeric in folk medicine with potent anti-oxidative, anti-inflammatory and anti-leishmanial (Gomes *et al.* 2002) activities. It is highly lipophilic and insoluble in water, which limits its further pharmacological exploitation and practical application. Currently, very few reports are available on the synthesis of curcuminyl glycosides (Hergenbahn *et al.* 2002; Kaminaga *et al.* 2003; Mohri *et al.* 2003). Curcumin could be glycosylated enzymatically using amyloglucosidase from *Rhizopus* mold at both the phenolic hydroxyl groups which gave a bis-glycosylated products (Vijayakumar and Divakar 2005; Vijayakumar *et al.* 2006).

Since the bis-glycosides formed were water soluble the present investigation was undertaken to use  $\beta$ -glucosidase isolated from sweet almond for the preparation of the glycosides (Scheme 3.3).

The reaction conditions employed were: 0.2-2 mmol curcumin, 1 mmol D-glucose, 10-75% (w/w D-glucose)  $\beta$ -glucosidase, 0.04-0.2 mM (0.4-2 mL of 0.01 M buffer in 100 mL of reaction mixture), pH 4-8 buffer in di-isopropyl ether solvent and 3 to 120 h reflux (Scheme 3.3). After the reaction the solvent was distilled off and held in a boiling water bath for 5-10 min to denature the enzyme. Then the reaction mixture was dissolved in 20-30 mL of water and filtered through Whatmann filter paper No. 1 to remove unreacted curcumin **3** and the filtrate was evaporated to dryness. The reaction mixture was monitored by HPLC on an aminopropyl column (250 mm  $\times$  4.6 mm), using acetonitrile:water (70:30 v/v) as a mobile phase and a refractive index detector (Fig. 3.31). The other procedures are as described on page 74. HPLC analysis showed the following retention times: D-glucose-7.2 min, 1,7-*O*-(bis- $\beta$ -D-glucopyranosyl)curcumin-10.3 min, D-galactose-7.1 min, 1,7-*O*-(bis-D-galactopyranosyl)curcumin-10.1 min, D-mannose-6.7 min, 1,7-*O*-(bis-D-mannopyranosyl)curcumin-9.9 min, lactose-9.3 min and 1,7-*O*-(bis- $\beta$ -D-galactopyranosyl-(1' $\rightarrow$ 4)-D-glucopyranosyl)curcumin-14.1 min.

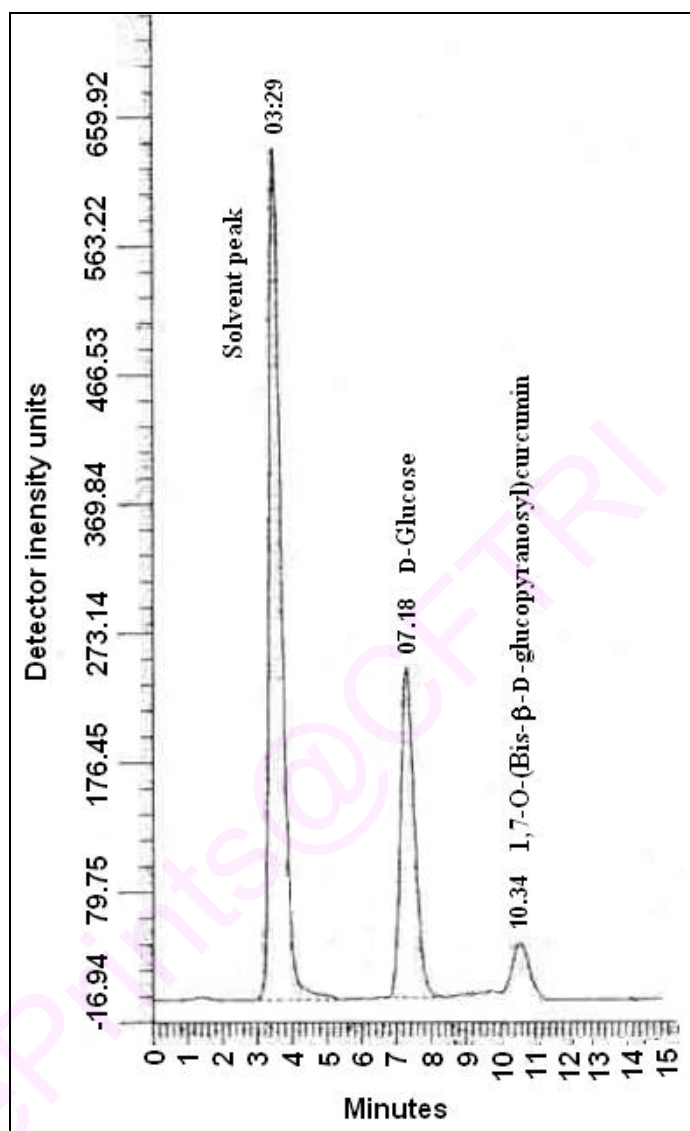
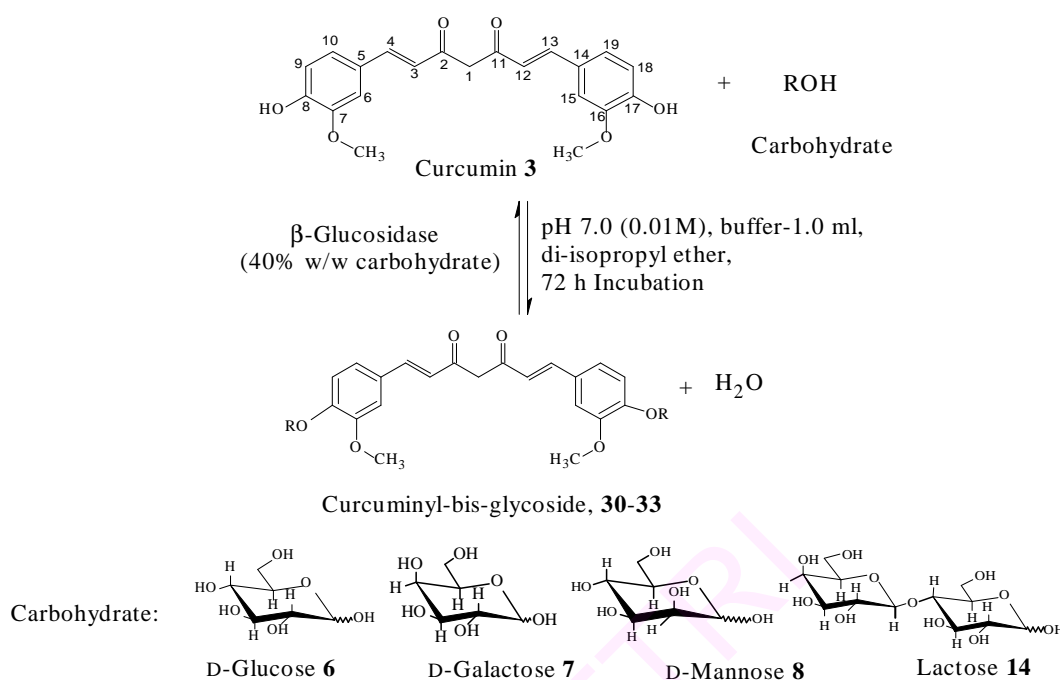


**Fig. 3.31** HPLC chromatogram for the reaction mixture of D-glucose and 1,7-*O*-(bis-β-D-glucopyranosyl)curcumin. HPLC conditions: Aminopropyl column (10 μm, 250 mm × 4.6 mm), solvent-CH<sub>3</sub>CN: H<sub>2</sub>O (70:30 v/v), Flow rate-1 mL/min, RI detector. Retention times: D-glucose-7.2 min and 1,7-*O*-(bis-β-D-glucopyranosyl)curcumin -10.3 min.



**Scheme 3.3** Syntheses of curcuminyl-bis-glycosides

### 3.3.1 Synthesis of 1,7-*O*-(bis-β-D-glucopyranosyl)curcumin using β-glucosidase

In the present work, synthesis of 1,7-*O*-(bis-β-D-glucopyranosyl)curcumin using β-glucosidase from sweet almond was optimized in terms of incubation period, pH, buffer, enzyme and curcumin concentration in di-isopropyl ether solvent.

#### 3.3.1.1 Effect of incubation period

In presence of 0.1 mM (1 mL), pH 7 buffer and 40% (w/w D-glucose) β-glucosidase, a reaction mixture of curcumin 0.5 mmol and D-glucose 1 mmol did not show any significant change in conversion upto 12 h (3-12 h, yield-18%). Further increase in incubation period increased the glucosylation upto 72 h and thereafter the yield decreased (120 h, yield-17%, Fig. 3.32A, Table 3.12).

#### 3.3.1.2 Effect of pH

The added buffer pH was varied from pH 4 to 8 with 0.1 mM (1 mL) of buffer concentration and the conversion yield showed that pH 7 gave the maximum conversion



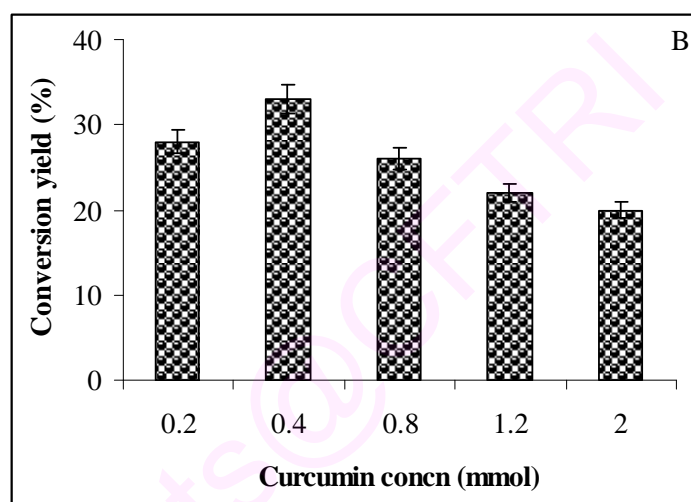
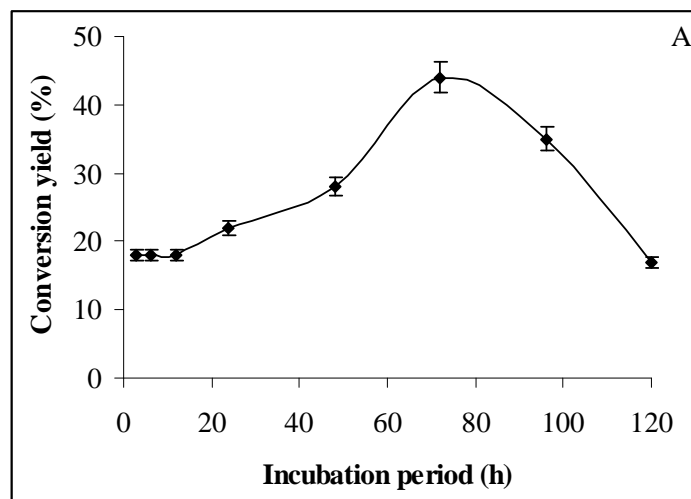


**Fig. 3.32** (A) Reaction profile for 1,7-*O*-(bis- $\beta$ -D-glucopyranosyl) curcumin synthesis by the reflux method. Conversion yields were from HPLC with respect to 1 mmol of D-glucose. Reaction conditions: curcumin-0.5 mmol, D-glucose-1 mmol,  $\beta$ -glucosidase-40% (w/w D-glucose), 0.1 mM (1 mL), pH 7 phosphate buffer, solvent-di-isopropyl ether and temperature-68 °C and (B) Effect of curcumin concentration for 1,7-*O*-(bis- $\beta$ -D-glucopyranosyl) curcumin synthesis. Reaction conditions: D-glucose-1 mmol,  $\beta$ -glucosidase-40% (w/w D-glucose), 0.1 mM (1 mL), pH 7 phosphate buffer, solvent-di-isopropyl ether, temperature-68 °C and incubation period – 72 h

of 44% (Table 3.12). There was no conversion at pH 4 and the yields were low at other pH values.

### 3.3.1.3 Effect of buffer concentration

Effect of buffer concentration at pH 7, showed that conversion yield increased with increase in buffer concentration from 0.04 to 0.08 mM (0.4 to 0.8 mL) with the maximum yield of 44% at 0.08 mM (0.8 mL). Increase in water activity at higher buffer concentrations (0.08 mM), increased the conversion more, besides solubilising D-glucose (Table 3.12).

### 3.3.1.4 Effect of $\beta$ -glucosidase concentration

Effect of increasing  $\beta$ -glucosidase concentration from 10 to 75% (w/w D-glucose) showed that 40% (w/w D-glucose) enzyme was required to reach a maximum glucosylation of 44% (Table 3.12). Still, further increase in enzyme concentrations decreased the conversion yield (75% enzyme-19% yield)

### 3.3.1.5 Effect of curcumin concentration

At the above-mentioned optimum conditions, curcumin concentration was varied from 0.2 mmol - 2 mmol (Fig. 3.32B, Table 3.12). Higher concentration of curcumin showed its inhibitory nature to the enzyme (2 mmol-yield 20%). A 0.4 mmol of curcumin gave the highest conversion of 33% and conversion yield decreased from 0.8 mmol curcumin (yield-26%) to 2 mmol (yield-20%).

### 3.3.1.6 Solubility of 1,7-*O*-(bis- $\beta$ -D-glucopyranosyl)curcumin

Determination of the water solubility of 1,7-*O*-(bis- $\beta$ -D-glucopyranosyl)curcumin showed that it is soluble to the extent of 14 g/L (Section 3.7.5) with good lanting color. Since, curcumin itself was not water soluble the enzymatic method was quite effective in yielding water soluble 1,7-*O*-(bis- $\beta$ -D-glucopyranosyl)curcumin.

**Table 3.12** Optimization of reaction conditions for the synthesis of 1,7-*O*-(bis- $\beta$ -D-glucopyranosyl)curcumin using  $\beta$ -glucosidase

Reaction conditions	Variable parameter <sup>b</sup>	Yields (%) <sup>c</sup>
	Incubation period (h)	
Curcumin – 0.5 mmol	3	18
D-Glucose – 1 mmol	6	18
pH – 7	12	18
Buffer concentration – 0.1 mM (1 mL)	24	22
$\beta$ -Glucosidase – 40 % w/w D-glucose	48	28
	72	44
	96	35
	120	17
		pH (0.01M)
Curcumin– 0.5 mmol <sup>a</sup>	4	No yield
D-Glucose – 1 mmol	5	15
$\beta$ -Glucosidase – 40 % w/w D-glucose	6	23
Buffer concentration – 0.1 mM (1 mL)	7	44
Incubation period – 72 h	8	18
	Buffer concentration (mM)	
Curcumin – 0.5 mmol	0.04	25
D-Glucose – 1 mmol	0.08	44
$\beta$ -Glucosidase – 40 % w/w D-glucose	0.12	20
pH – 7	0.16	15
Incubation period – 72 h	0.2	14
	$\beta$ -Glucosidase concentration (% w/w D-glucose)	
Curcumin – 0.5 mmol	10	9
D-Glucose – 1 mmol	20	10
pH – 7	30	14
Buffer concentration – 0.1 mM (1 mL)	40	44
Incubation period – 72 h	50	23
	75	19
	Curcumin (mmol)	
pH – 7	0.2	28
Buffer concentration – 0.1 mM (1 mL)	0.4	33
D-Glucose – 1 mmol	0.8	26
$\beta$ -Glucosidase – 40 % w/w D-glucose	1.2	22
Incubation period – 72 h	2	20

<sup>a</sup>Initial reaction conditions. <sup>b</sup>Other variables are the same as under reaction conditions, except the specified ones. <sup>c</sup>HPLC yields expressed with respect to 1 mmol D-glucose employed.

### 3.3.2 Syntheses of curcuminyl-bis-glycosides of other carbohydrates using $\beta$ -glucosidase

Under the above optimized conditions, curcuminyl-bis-glycosides were synthesized with other carbohydrates (D-glucose **6**, D-galactose **7**, D-mannose **8** and lactose **14**, 1 mmol). Optimum conditions employed were: curcumin **3** (0.5 mmol) with carbohydrates (1 mmol),  $\beta$ -glucosidase (40% w/w of carbohydrate) and 0.1 mM (1 mL) of 0.01 M pH 7 buffer for an incubation period of 72 h in 100 mL di-isopropyl ether. The work up and isolation procedure was as described on pages 74 and 121.

### 3.3.3 Spectral characterization

The isolated curcuminyl-bis-glycosides besides measuring melting point and optical rotation were also characterized by recording UV, IR, Mass and 2D-HSQCT spectra, which provided good information on the nature and proportions of the products formed.

**Curcumin 3:** Solid; mp 178 °C, UV (Ethanol,  $\lambda_{\max}$ ): 201.5 nm ( $\sigma \rightarrow \sigma^*$ ,  $\epsilon_{201.5} - 25829 \text{ M}^{-1}$ ), 224 nm ( $\sigma \rightarrow \pi^*$ ,  $\epsilon_{224} - 10845 \text{ M}^{-1}$ ), 256 nm ( $\pi \rightarrow \pi^*$ ,  $\epsilon_{256} - 12987 \text{ M}^{-1}$ ), 427.5 nm ( $n \rightarrow \pi^*$  extended conjugation,  $\epsilon_{427.5} - 56536 \text{ M}^{-1}$ ), IR (stretching frequency,  $\text{cm}^{-1}$ ): 1628 (CO), 3340 (OH), 1602 (aromatic C=C);  $^1\text{H}$  NMR  $\delta_{\text{ppm}}$  (500.13 MHz): 3.84 (6H, s, 2-OCH<sub>3</sub>), 6.05 (1H, s, H-1), 6.76 (2H, d, J = 15.8 Hz, H-3,12), 7.57 (2H, d, J = 15.8 Hz, H-4,13), 7.32 (2H, s, H-6,15), 6.82 (2H, d, J = 8.2 Hz, H-9,18), 7.15 (2 H, dd, J = 1.45 Hz, H-10,19) (Venkateshwaralu *et al.* 2005). Ultraviolet-visible spectra is shown in Fig. 3.33A.

**3.3.3.1 1,7-O-(Bis- $\beta$ -D-glucopyranosyl)curcumin 30:** Solid; mp 148 °C, UV (H<sub>2</sub>O,  $\lambda_{\max}$ ): 204 nm ( $\sigma \rightarrow \sigma^*$ ,  $\epsilon_{204} - 1450 \text{ M}^{-1}$ ), 225 nm ( $\sigma \rightarrow \pi^*$ ,  $\epsilon_{225} - 912 \text{ M}^{-1}$ ), 277 nm ( $\pi \rightarrow \pi^*$ ,  $\epsilon_{277} - 759 \text{ M}^{-1}$ ), 421 nm ( $n \rightarrow \pi^*$  extended conjugation,  $\epsilon_{421} - 147 \text{ M}^{-1}$ ); IR (stretching frequency,  $\text{cm}^{-1}$ ): 1657 (CO), 1029 (aryl alkyl C-O-C symmetrical), 1225 (glycosidic aryl

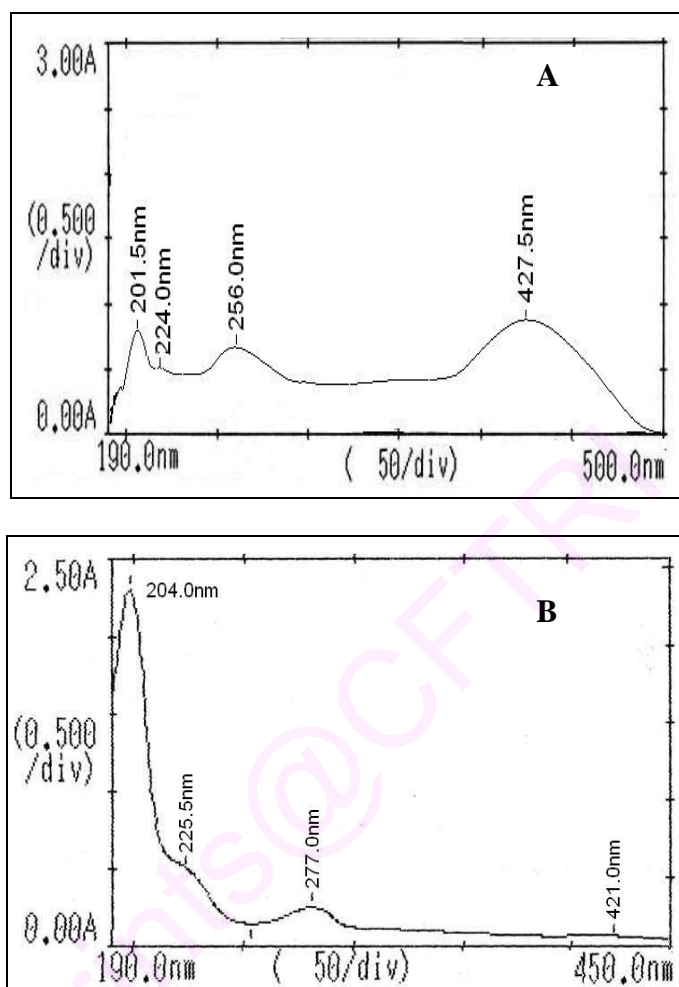


**Fig. 3.33** Ultraviolet-visible spectra of (A) Curcumin 3 and (B) 1,7-*O*-(Bis-β-D-glucopyranosyl)curcumin 30

alkyl C-O-C asymmetrical), 1598 (C=C), 3348 (OH), optical rotation  $[\alpha]_D^{25} = -13.3^\circ$  ( $c$  1, H<sub>2</sub>O), MS ( $m/z$ ) - 691 [M-1]<sup>+</sup>, 2D-HSQCT (DMSO-*d*<sub>6</sub>) <sup>1</sup>H NMR  $\delta_{\text{ppm}}$  (500.13 MHz) **Glu**: 4.16 (H-1 $\beta$ , d,  $J$  = 7.8 Hz), 3.28 (H-2 $\beta$ ), 3.03 (H-3 $\beta$ ), 3.75 (H-4 $\beta$ ), 3.10 (H-5 $\beta$ ), 3.60 (H-6a), **Cur**: 3.82 (6H, s, 2-OCH<sub>3</sub>), 6.10 (1H, s, H-1), 6.53 (2H, d,  $J$  = 15.8 Hz, H-3,12), 6.81 (2H, d,  $J$  = 8.2 Hz, H-9,18), <sup>13</sup>C NMR  $\delta_{\text{ppm}}$  (125 MHz) **Glu**: 103.2 (C1 $\beta$ ), 76 (C2 $\beta$ ), 79 (C3 $\beta$ ), 70.5 (C4 $\beta$ ), 79 (C5 $\beta$ ), 62.1 (C6 $\beta$ ), **Cur**: 56 (OCH<sub>3</sub>), 102 (C1), 183 (C2,C11), 121.3 (C3,C12), 148.4 (C7,C16), 150 (C8,C17), 116.4 (C9,C18).

Ultraviolet-visible, IR and 2D-HSQCT NMR spectra for 1,7-*O*-(bis- $\beta$ -D-glucopyranosyl)curcumin **30** are shown in Figures 3.33B, 3.34A and 3.34B respectively.

**3.3.3.2 1,7-*O*-(Bis-D-galactopyranosyl)curcumin 31a,b**: Solid; UV (H<sub>2</sub>O,  $\lambda_{\text{max}}$ ): 193.5 nm ( $\sigma \rightarrow \sigma^*$ ,  $\epsilon_{193.5} = 10956 \text{ M}^{-1}$ ), 226.5 nm ( $\sigma \rightarrow \pi^*$ ,  $\epsilon_{226.5} = 3126 \text{ M}^{-1}$ ), 263.5 nm ( $\pi \rightarrow \pi^*$ ,  $\epsilon_{263.5} = 1987 \text{ M}^{-1}$ ), 410 nm ( $n \rightarrow \pi^*$ , extended conjugation,  $\epsilon_{410} = 298 \text{ M}^{-1}$ ), IR (stretching frequency, cm<sup>-1</sup>): 1634 (CO), 1033 (glycosidic aryl alkyl C-O-C symmetrical), 1230 (glycosidic aryl alkyl C-O-C asymmetrical), 1612 (C=C), 3285 (OH), MS ( $m/z$ ) - 693 [M+1]<sup>+</sup>, 2D-HSQCT (DMSO-*d*<sub>6</sub>) **Bis-C1 $\alpha$ -galactoside 31a**: <sup>1</sup>H NMR  $\delta_{\text{ppm}}$  (500.13 MHz) **Gal**: 4.99 (H-1 $\alpha$ , d,  $J$  = 3.5 Hz), 3.68 (H-2 $\alpha$ ), 3.72 (H-3 $\alpha$ ), 3.75 (H-4 $\alpha$ ), 3.58 (H-5 $\alpha$ ), 3.38 (H-6a), **Cur**: 3.46 (6H, s, 2-OCH<sub>3</sub>), 6.10 (H-1), 7.20 (H-6,15), <sup>13</sup>C NMR  $\delta_{\text{ppm}}$  (125 MHz) **Gal**: 95.7 (C1 $\alpha$ ), 68 (C2 $\alpha$ ), 70.5 (C3 $\alpha$ ), 69.5 (C4 $\alpha$ ), 69.5 (C5 $\alpha$ ), 62.9 (C6 $\alpha$ ), **Cur**: 53 (OCH<sub>3</sub>), 103.7 (C1), 169.5 (C2,C11), 126.4 (C3,C12), 109 (C6,C15), **Bis-C1 $\beta$ -galactoside 31b**: <sup>1</sup>H NMR  $\delta_{\text{ppm}}$  **Gal**: 4.93 (H-1 $\beta$ , d,  $J$  = 6.2 Hz), 3.36 (H-3 $\beta$ ), 3.34 (H-4 $\beta$ ), 3.30 (H-5 $\beta$ ), 3.39 (H-6a), <sup>13</sup>C NMR  $\delta_{\text{ppm}}$  **Gal**: 102.1 (C1 $\beta$ ), 74.5 (C3 $\beta$ ), 73 (C4 $\beta$ ), 72.5 (C5 $\beta$ ), 63.2 (C6 $\beta$ ).

Infra-red and 2D-HSQCT NMR spectra for 1,7-*O*-(bis-D-galactopyranosyl)curcumin **31a,b** are shown in Figures 3.35A and 3.35B respectively.

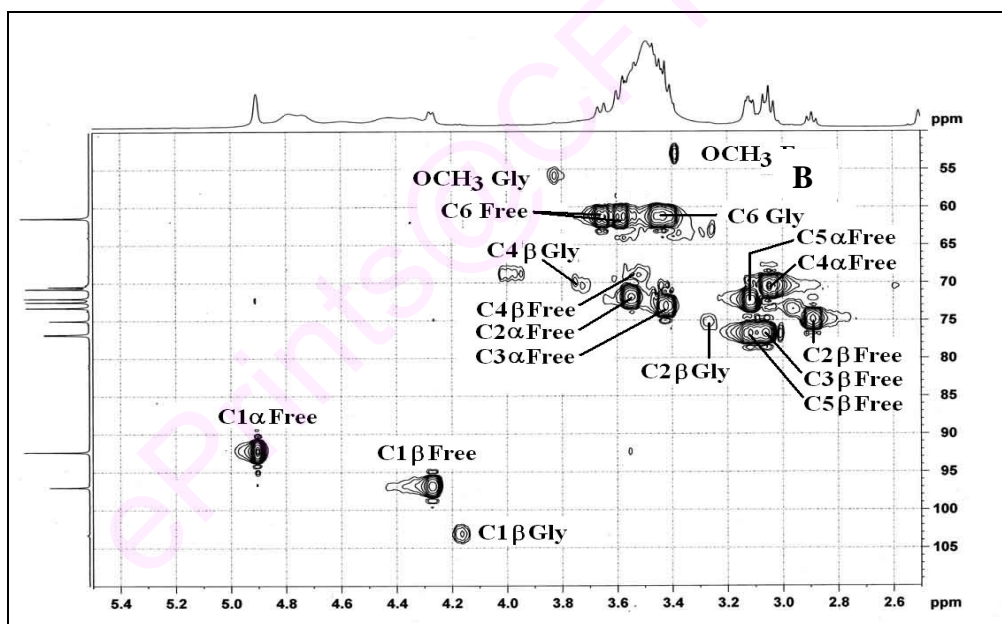
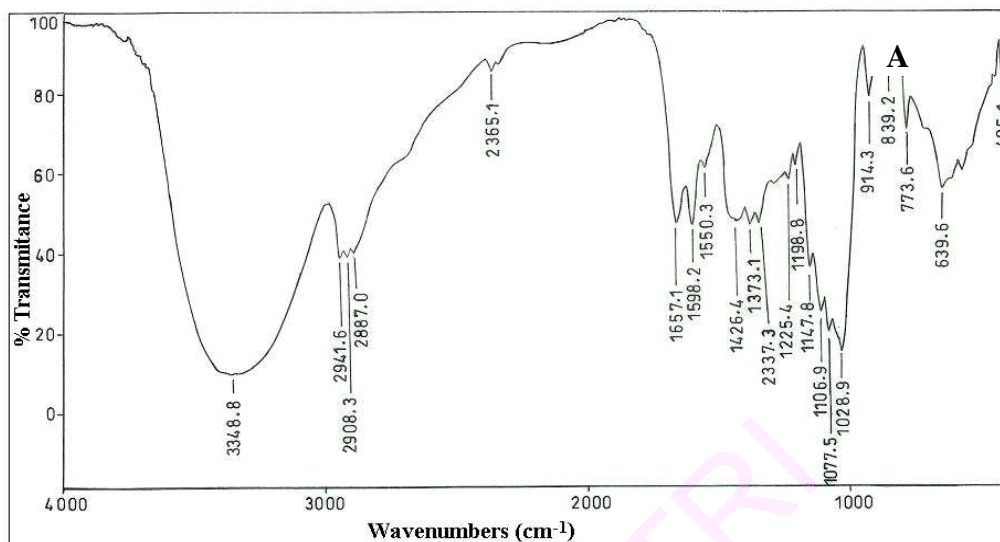


**Fig. 3.34** 1,7-*O*-(Bis- $\beta$ -D-glucopyranosyl)curcumin **30** (A) IR spectrum and (B) 2D-HSQC spectrum showing the C1-C6 region. Some of the assignments are interchangeable.

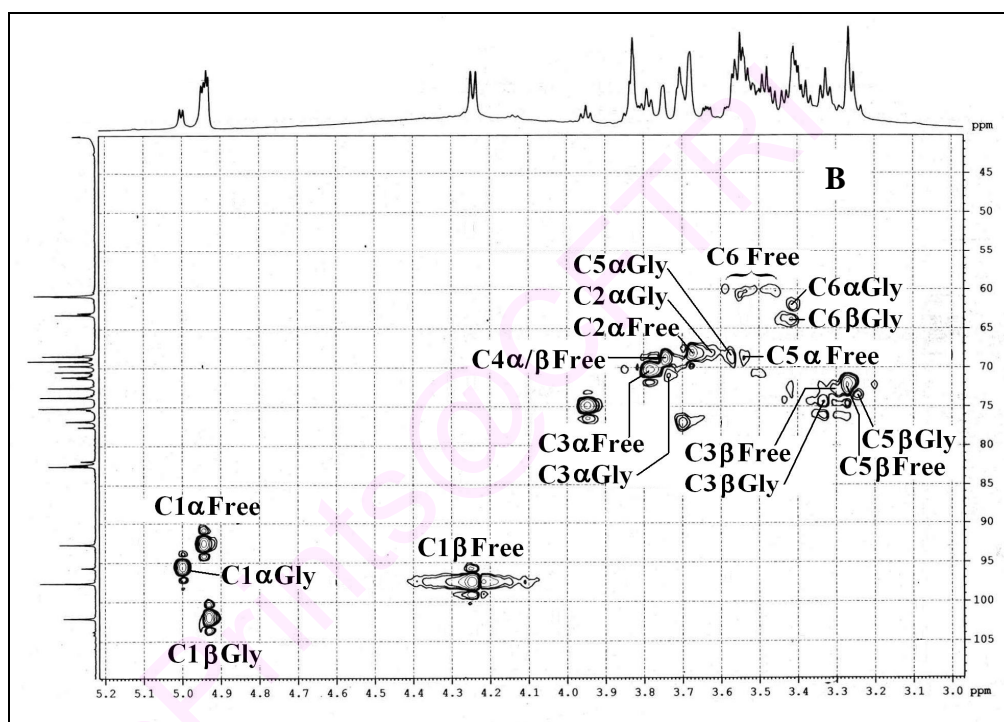
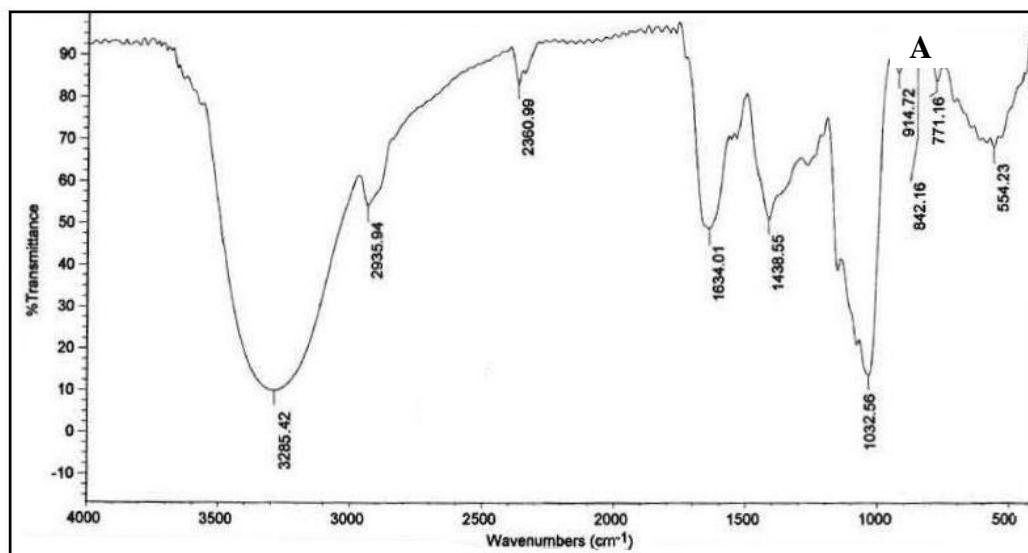


**Fig. 3.35** 1,7-*O*-(Bis-D-galactopyranosyl)curcumin **31a,b** (A) IR spectrum and (B) 2D-HSQC spectrum showing the C1-C6 region. Some of the assignments are interchangeable.



**3.3.3.3 1,7-*O*-(Bis-*D*-mannopyranosyl)curcumin 32a,b:** Solid; UV (H<sub>2</sub>O,  $\lambda_{\max}$ ): 192 nm ( $\sigma \rightarrow \sigma^*$ ,  $\epsilon_{192} = 11258 \text{ M}^{-1}$ ), 224.5 nm ( $\sigma \rightarrow \pi^*$ ,  $\epsilon_{224.5} = 4378 \text{ M}^{-1}$ ), 269 nm ( $\pi \rightarrow \pi^*$ ,  $\epsilon_{269} = 2219 \text{ M}^{-1}$ ), 411.5 nm ( $n \rightarrow \pi^*$ , extended conjugation,  $\epsilon_{411.5} = 321 \text{ M}^{-1}$ ), IR (stretching frequency,  $\text{cm}^{-1}$ ): 1680 (CO), 1073 (glycosidic aryl alkyl C-O-C symmetrical), 1245 (glycosidic aryl alkyl C-O-C asymmetrical), 1595 (C=C), MS ( $m/z$ ) - 692 [M]<sup>+</sup>, 2D-HSQCT (DMSO-*d*<sub>6</sub>) **Bis-C1 $\alpha$ -mannoside 32a:** <sup>1</sup>H NMR  $\delta_{\text{ppm}}$  (500.13 MHz) **Man:** 5.01 (H-1 $\alpha$ , d,  $J = 1.9 \text{ Hz}$ ), 3.62 (H-2 $\alpha$ ), 4.52 (H-3 $\alpha$ ), 3.55 (H-4 $\alpha$ ), 3.72 (H-5 $\alpha$ ), 3.42 (H-6a), **Cur:** 3.45 (6H, s, 2-OCH<sub>3</sub>), 6.10 (1H, s, H-1); <sup>13</sup>C NMR  $\delta_{\text{ppm}}$  (125 MHz) **Man:** 100 (C1 $\alpha$ ), 71.5 (C2 $\alpha$ ), 73.3 (C3 $\alpha$ ), 68 (C4 $\alpha$ ), 71.5 (C5 $\alpha$ ), 62 (C6 $\alpha$ ), **Cur:** 53 (OCH<sub>3</sub>), 101.8 (C1), 109 (C6,C15), **Bis-C1 $\beta$ -mannoside 32b:** <sup>1</sup>H NMR  $\delta_{\text{ppm}}$  **Man:** 4.90 (H-1 $\beta$ , d,  $J = 3.4 \text{ Hz}$ ), 3.42 (H-2 $\beta$ ), 3.41 (H-4 $\beta$ ), 3.11 (H-5 $\beta$ ), 3.52 (H-6a); <sup>13</sup>C NMR  $\delta_{\text{ppm}}$  **Man:** 102 (C1 $\beta$ ), 71.5 (C2 $\beta$ ), 67.5 (C4 $\beta$ ), 77 (C5 $\beta$ ), 62.5 (C6 $\beta$ ).

Figure 3.36A shows mass spectrum and Figures 3.36B and 3.36C show 2D-HSQCT NMR spectrum for 1,7-*O*-(bis-*D*-mannopyranosyl)curcumin **32a,b**.

**3.3.3.4 1,7-*O*-(Bis- $\alpha$ -*D*-galactopyranosyl-(1'  $\rightarrow$  4)*D*-glucopyranosyl)curcumin 33a,b:** Solid; UV (H<sub>2</sub>O,  $\lambda_{\max}$ ): 195 nm ( $\sigma \rightarrow \sigma^*$ ,  $\epsilon_{195} = 4975 \text{ M}^{-1}$ ), 226 nm ( $\sigma \rightarrow \pi^*$ ,  $\epsilon_{226} = 1469 \text{ M}^{-1}$ ), 275.5 nm ( $\pi \rightarrow \pi^*$ ,  $\epsilon_{275.5} = 684 \text{ M}^{-1}$ ), 410.5 nm ( $n \rightarrow \pi^*$ , extended conjugation,  $\epsilon_{410.5} = 168 \text{ M}^{-1}$ ), IR (stretching frequency,  $\text{cm}^{-1}$ ): 1032 (glycosidic aryl alkyl C-O-C symmetrical), 1236 (glycosidic aryl alkyl C-O-C asymmetrical), 3416 (OH), MS ( $m/z$ ) - 1016 [M]<sup>+</sup>, 2D-HSQCT (DMSO-*d*<sub>6</sub>) **Bis-C1 $\alpha$ -lactoside 33a:** <sup>1</sup>H NMR  $\delta_{\text{ppm}}$  (500.13 MHz) **Lact:** 5.02 (H-1 $\alpha$ , d,  $J = 2.3 \text{ Hz}$ ), 3.58 (H-3 $\alpha$ ), 3.75 (H-4 $\alpha$ ), 3.55 (H-5 $\alpha$ ), 3.68 (H-6a), 4.15 (H-1' $\alpha$ ), 3.18 (H-2'), 3.72 (H-4'), 3.52 (H-6'), **Cur:** 3.81 (6H, s, 2-OCH<sub>3</sub>), 6.68 (2H, H-3,12), 7.35 (2H, H-4,13), 6.90 (2H, H-9,18); <sup>13</sup>C NMR  $\delta_{\text{ppm}}$  (125 MHz) **Lact:** 95.5 (C1 $\alpha$ ), 69 (C3 $\alpha$ ), 70.2 (C4 $\alpha$ ), 73 (C5 $\alpha$ ), 61 (C6 $\alpha$ ), 103.5 (C1' $\alpha$ ), 70.5 (C2'), 69

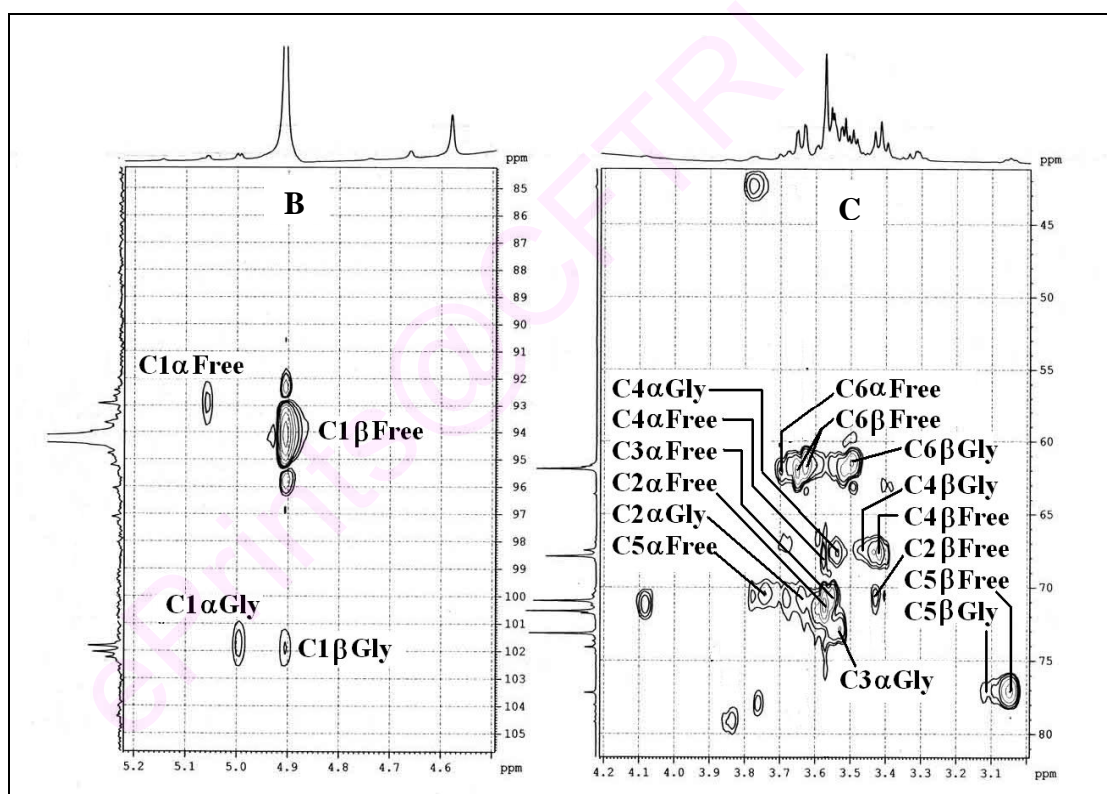
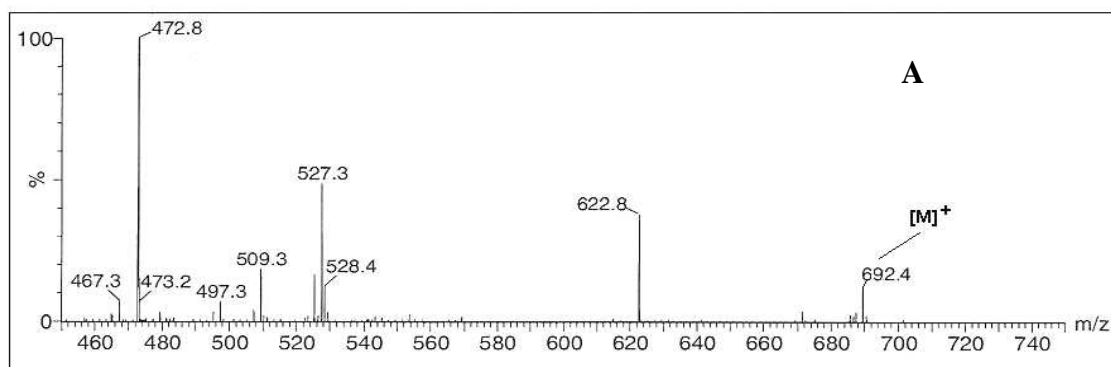


**Fig. 3.36** 1,7-*O*-(Bis-D-mannopyranosyl)curcumin **32a,b** (A) Mass spectrum, (B) 2D-HSQC spectrum (anomeric region) and (C) 2D-HSQC spectrum showing the C2-C6 region. Some of the assignments are interchangeable

(C4'), 62.5 (C6'), **Cur**: 53.1 (OCH<sub>3</sub>), 126 (C3,C12), 115.3 (C9,C18), 128 (C10,C19), **Bis-C1 $\beta$ -lactoside 33b**: <sup>1</sup>H NMR  $\delta_{\text{ppm}}$  **Lact**: 4.92 (H-1 $\beta$ , d, J = Hz), 3.30 (H-2 $\beta$ ), 3.45 (H-3 $\beta$ ), 3.18 (H-5 $\beta$ ), 3.68 (H-6a), 4.15 (H-1' $\beta$ ), 3.66 (H-3'), 3.31 (H-4'), 3.40 (H-6'a), <sup>13</sup>C NMR  $\delta_{\text{ppm}}$  **Lact**: 102 (C1 $\beta$ ), 74.2 (C2 $\beta$ ), 73.1 (C3 $\beta$ ), 73 (C5 $\beta$ ), 67 (C6 $\beta$ ), 103.5 (C1' $\beta$ ), 72.1 (C3'), 70.8 (C4'), 63 (C6').

Mass and 2D-HSQCT NMR spectra for 1,7-*O*-(bis- $\beta$ -D-galactopyranosyl-(1' $\rightarrow$ 4)D-glucopyranosyl)curcumin **33a,b** are shown in Figures 3.37A and 3.37B respectively.

UV spectra of curcuminyl-bis-glycosides, showed shifts of  $\sigma \rightarrow \sigma^*$  band in the 192 – 204 nm (201.5 nm for free curcumin) range,  $\sigma \rightarrow \pi^*$  band in the 224.5 – 226.5 nm (224 nm for free curcumin) range,  $\pi \rightarrow \pi^*$  band in the 263.5 – 277 nm (256 nm for free curcumin) range and  $n \rightarrow \pi^*$  extended conjugation band in the 410 – 421 nm (427.5 nm for free curcumin) range, IR C-O-C symmetrical stretching frequencies in the 1028 - 1073 cm<sup>-1</sup> range and asymmetrical stretching frequencies in the 1225 - 1245 cm<sup>-1</sup> range indicating that curcumin had undergone glycosylation. From 2D HSQCT spectra of the curcuminyl-bis-glycosides, the following glycoside formation were confirmed from their respective chemical shift values: from D-glucose **6** C1 $\beta$  glucoside **30** to C1 $\beta$  at 103.2 ppm and H-1 $\beta$  at 4.16 ppm; from D-galactose **7** C1 $\alpha$  galactoside **31a** to C1 $\alpha$  at 95.7 ppm and H-1 $\alpha$  at 4.99 ppm and C1 $\beta$  galactoside **31b** to C1 $\beta$  at 102.1 ppm and H-1 $\beta$  at 4.93 ppm; from D-mannose **8** C1 $\alpha$  mannoside **32a** to C1 $\alpha$  at 100 ppm and H-1 $\alpha$  at 5.01 ppm and C1 $\beta$  mannoside **32b** to C1 $\beta$  at 102 ppm and H-1 $\beta$  at 4.90 ppm; from lactose **14** C1 $\alpha$  lactoside **33a** to C1 $\alpha$  at 95.5 ppm and H-1 $\alpha$  at 5.02 ppm and C1 $\beta$  lactoside **33b** to C1 $\beta$  at 102 ppm and H-1 $\beta$  at 4.92 ppm. Mass spectra also confirmed the formation of the above mentioned glycosides.

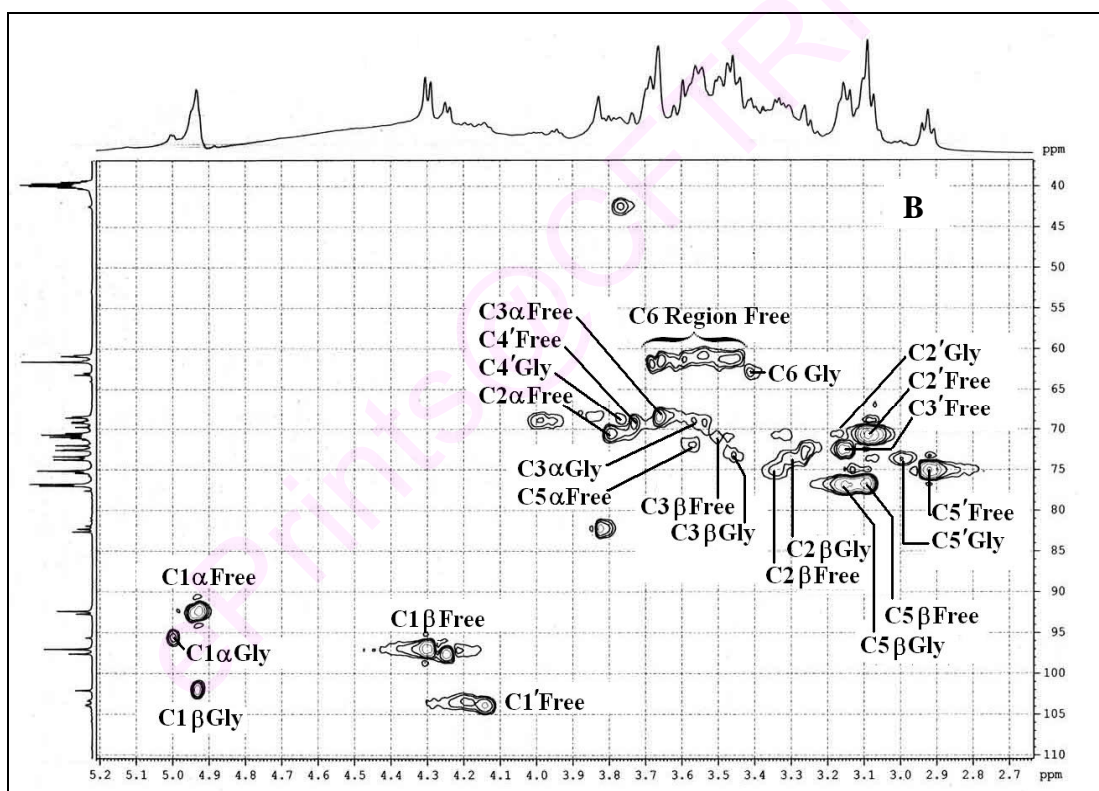
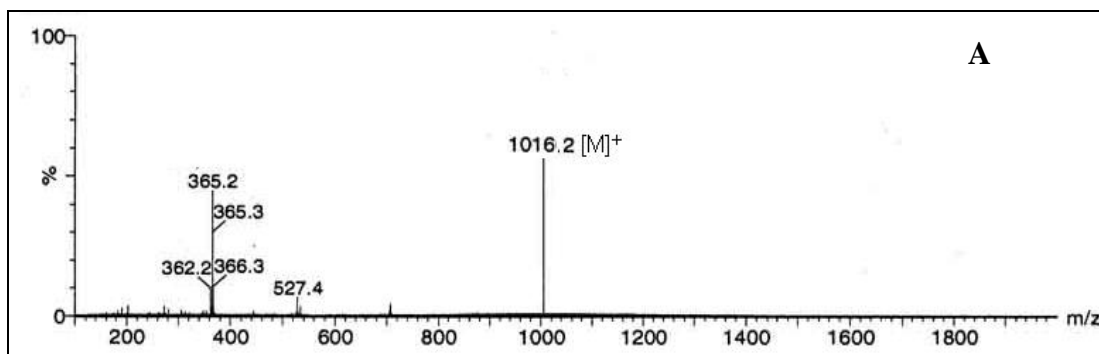


**Fig. 3.37** 1,7-*O*-(Bis- $\beta$ -D-galactopyranosyl-(1'→4)D-glucopyranosyl)curcumin **33a,b**  
 (A) Mass spectrum and (B) 2D-HSQC spectrum showing the C1-C6' region. Some of the assignments are interchangeable.

### 3.3.4 Discussion

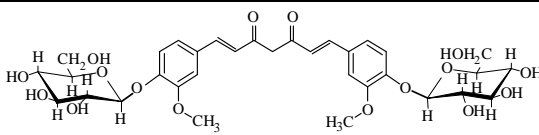
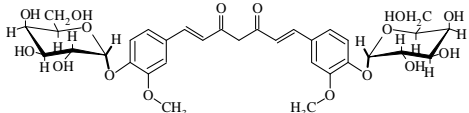
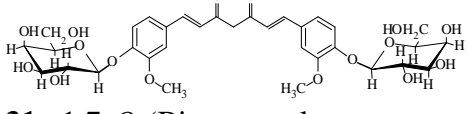
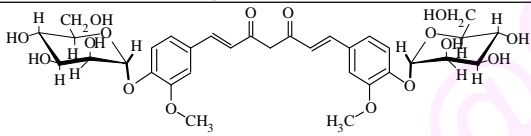
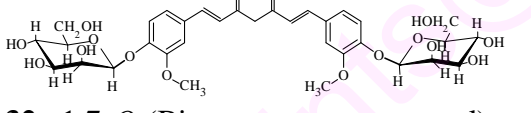
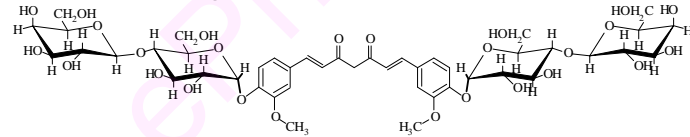
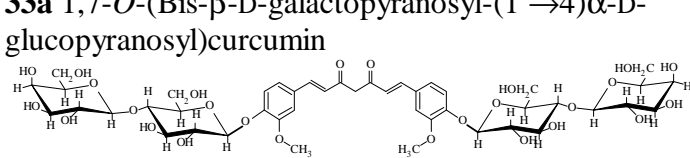
Curcuminyl-bis-glycosides were synthesized with carbohydrates with the optimized conditions (Section 3.3.1). The yields are shown in Table 3.13. The products formed are confirmed spectroscopically (Section 3.3.3) as follows: 1,7-*O*-(bis- $\beta$ -D-glucopyranosyl) curcumin **30**, 1,7-*O*-(bis- $\alpha$ -D-galactopyranosyl)curcumin **31a**, 1,7-*O*-(bis- $\beta$ -D-galactopyranosyl)curcumin **31b**, 1,7-*O*-(bis- $\alpha$ -D-mannopyranosyl)curcumin **32a**, 1,7-*O*-(bis- $\beta$ -D-mannopyranosyl)curcumin **32b**, 1,7-*O*-(bis- $\beta$ -D-galactopyranosyl-(1'→4) $\alpha$ -D-glucopyranosyl)curcumin **33a**, 1,7-*O*-(bis- $\beta$ -D-galactopyranosyl-(1'→4) $\beta$ -D-glucopyranosyl)curcumin **33b**.

Among the carbohydrates employed, D-glucose **6** gave rise to C1 $\beta$  glucosylated product, which shows the regioselectivity of  $\beta$ -glucosidase. A maximum conversion of 44% was obtained for 1,7-*O*-(bis- $\beta$ -D-glucopyranosyl)curcumin **30**. Although,  $\beta$ -glucosidase catalysis do not exhibit an inversion, it had significantly altered the  $\alpha$ ,  $\beta$  composition - D-galactose- 39%  $\alpha$ -D-galactoside and 61%  $\beta$ -D-galactoside (compared to 92:8  $\alpha$ : $\beta$  for free D-galactose) and D-mannose - 35%  $\alpha$ -D-mannoside and 65%  $\beta$ -D-mannoside (compared to 27:73  $\alpha$ : $\beta$  for free D-mannose). Also, curcumin **3**, showed bis-glycosylated products with the carbohydrates with which it reacted.

Among the carbohydrates employed D-fructose **9**, D-arabinose **10**, D-ribose **11**, maltose **12**, sucrose **13**, D-sorbitol **15** and D-mannitol **16** did not react with curcumin during  $\beta$ -glucosidase catalyses. Stronger binding of curcumin **3** to  $\beta$ -glucosidase compared to the above mentioned carbohydrate molecules could block the facile transfer of carbohydrate molecules to the phenolic OH of curcumin **3**. D-Galactose **7** and D-mannose **8** gave very low conversions ( $\leq 12\%$ ). Hence, they could function as efficient

inhibitors of the  $\beta$ -glucosidase or could possess very low binding potentiality (low binding constant value) to the enzyme.

**Table 3.13** Syntheses of curcuminyl-bis-glycosides using  $\beta$ -glucosidase<sup>a</sup>

Glycosides	$\beta$ -Glucosidase catalysis	
	Product (% proportion) <sup>b</sup>	Yields (%) <sup>c</sup>
 <p><b>30</b> 1,7-<i>O</i>-(Bis-<math>\beta</math>-D-glucopyranosyl)curcumin</p>	C1 $\beta$ glucoside	44
 <p><b>31a</b> 1,7-<i>O</i>-(Bis-<math>\alpha</math>-D-galactopyranosyl)curcumin</p>	C1 $\alpha$ galactoside (39), C1 $\beta$ galactosides (61)	12
 <p><b>31b</b> 1,7-<i>O</i>-(Bis-<math>\beta</math>-D-galactopyranosyl)curcumin</p>		
 <p><b>32a</b> 1,7-<i>O</i>-(Bis-<math>\alpha</math>-D-mannopyranosyl)curcumin</p>	C1 $\alpha$ mannoside (35), C1 $\beta$ mannoside (65)	10
 <p><b>32b</b> 1,7-<i>O</i>-(Bis-<math>\beta</math>-D-mannopyranosyl)curcumin</p>		
 <p><b>33a</b> 1,7-<i>O</i>-(Bis-<math>\beta</math>-D-galactopyranosyl-(1' <math>\rightarrow</math> 4)<math>\alpha</math>-D-glucopyranosyl)curcumin</p>	C1 $\alpha$ lactoside (48), C1 $\beta$ lactoside (52)	17
 <p><b>33b</b> 1,7-<i>O</i>-(Bis-<math>\beta</math>-D-galactopyranosyl-(1' <math>\rightarrow</math> 4)<math>\beta</math>-D-glucopyranosyl)curcumin</p>		

<sup>a</sup>Curcumin – 0.5 mmol and carbohydrate – 1 mmol; enzyme concentration 40% w/w of carbohydrate; solvent – di-isopropyl ether; buffer – 0.1 mM (1 mL) pH 7 phosphate buffer; incubation period – 72 h.

<sup>b</sup>Conversion yields were from HPLC with errors in yield measurements  $\pm$  5-10%. <sup>c</sup>The product proportions were determined from the area of respective <sup>1</sup>H/<sup>13</sup>C signals.

$\beta$ -Glucosidase, besides effecting glycosylation reactions, also facilitated the hydrolysis of the disaccharide like lactose **14** during the course of the reaction and the resultant monosaccharides (D-glucose and D-galactose) did not show any transglycosylated product. Presence of hydrophobic propanoid group *para* to the phenolic OH bestows good nucleophilicity in these molecules promoting reaction with quite diverse carbohydrates.

About 7 individual glycosides were synthesized enzymatically using both the glucosidases, of which 4 are being reported for the first time. The new glycosides reported are: 1,7-*O*-(bis- $\beta$ -D-galactopyranosyl)curcumin **31b**, 1,7-*O*-(bis- $\beta$ -D-manno pyranosyl)curcumin **32b**, 1,7-*O*-(bis- $\beta$ -D-galactopyranosyl-(1'→4) $\alpha$ -D-glucopyranosyl) curcumin **33a,b**.

### 3.4 Syntheses of DL-dopa glycosides

DL-Dopa (DL-3,4-dihydroxy phenylalanine), an aromatic amino acid precursor of dopamine is the most effective drug for Parkinson's disease (Yar 1993). Parkinson's disease is characterized by a severe and progressive degeneration of nigrostriatal dopamine (DA) neurons (Angerlacenci 2007) associated with the deficiency of catecholamine and dopamine (Shetty *et al.* 2002). It is generally accepted that after administration, L-dopa in Parkinson's disease is converted into dopamine by aromatic L-amino acid decarboxylase (AADC) within the serotonergic (5-HT) fibers in the striatum and *substantia nigra pars reticulata* (Yamada *et al.* 2007). Glucose is the brain source of energy and this as well as other hexoses are also transferred across the blood brain barrier (BBB) by the glucose carrier GLUT1 (Mueckler 1994). Such a transport will be facilitated if L-dopa is converted into the glycoside as the L-dopa converted product glucosyl dopamine is able to interact with the glucose transporter (GLUT1) and absorbed into the central nervous system (CNS) from the blood stream (Dalpiaz *et al.* 2007).



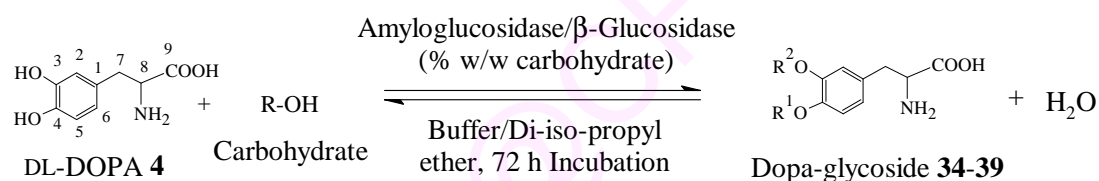
During chronic treatment with L-dopa, a variety of transport problems like involuntary movements occur which can be overcome by the employment of glucosyl derivatives (Pardridge 2002; Madrid *et al.* 1991). Side effects of the drugs can be reduced and drug stability can be increased by modification of the aglycon molecule. For example, L-dopa and new dopaminergics can be modified to improve bioactivity properties (Pras *et al.* 1995; Giri *et al.* 2001).

L-Dopa was first isolated from *Vicia faba* (Guggenheim 1913; Vered *et al.* 1994) as a  $\beta$ -anomer (Nagasawa *et al.* 1961; Andrews and Pridham 1965). *Vicia faba* has been incorporated into dietary strategies to manage Parkinsonian motor oscillations (Kempster *et al.* 1993). A crude extract from the petals of *Mirabilis jalapa* was mixed with *cyclo*-Dopa and UDP-glucose to give *cyclo*-Dopa-5-*O*-glucoside by the action of glucosyl transferases (Sasaki *et al.* 2004; Wyler *et al.* 2004). However, no chemical or enzymatic methods have been reported yet for the synthesis of DL-dopa glycosides. Enzymatic method could be the alternative one which does not require protection and deprotection process (Fernandez *et al.* 2003; Roode *et al.* 2003) and provide milder reaction conditions, easy workup, less pollution, higher yields and selectivity. It can also give rise to stable dopa derivatives with enhanced stability and pharmacological activity (Suzuki *et al.* 1996; Vijayakumar and Divakar 2007). The present work has been undertaken to synthesize DL-dopa glycosides using amyloglucosidase from *Rhizopus* mold and  $\beta$ -glucosidase from sweet almond in organic media (Scheme 3.4).

Synthesis of DL-dopa-D-glucoside involved refluxing DL-dopa **4** (0.2-2 mmol) with 1 mmol D-glucose **6**, in 100 mL di-isopropyl ether in presence of amyloglucosidase (10-75 % w/w D-glucose) and 0.03 mM – 0.22 mM (0.3-2.2 mL) of 0.01 M pH 4-8 buffer for an incubation period of 72 h at 68 °C (Scheme 3.4). The solvent was evaporated and the enzyme denatured at 100 °C by holding in boiling water bath for 5-10 min. The



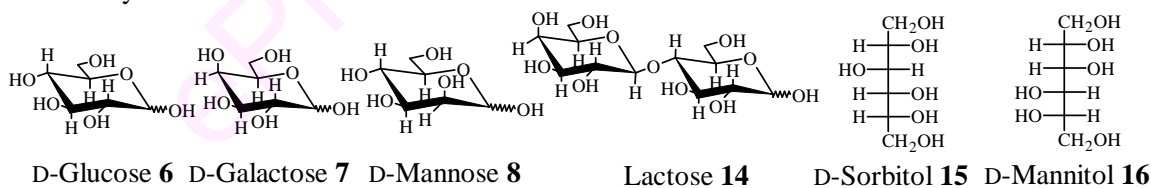
residue containing unreacted DL-dopa **4**, D-glucose **6**, along with the product glucosides were dissolved in 15-20 mL of water and evaporated to dryness. The dried residue was subjected to HPLC (Fig. 3.38) analysis to determine the extent of conversion. Other methods of estimation and isolation are as described on page 74. HPLC retention times for the substrates and products are: DL-dopa-8.5 min, D-glucose-6.2 min, DL-dopa-D-glucoside-13 min, D-galactose-7.1 min, DL-dopa-D-galactoside-11.9 min, D-mannose-6.7 min, DL-3-hydroxy-4-*O*-( $\beta$ -D-mannopyranosyl) phenylalanine-11.7 min, lactose-9.3 min, DL-3-hydroxy-4-*O*-( $\beta$ -D-galactopyranosyl-(1'→4) $\beta$ -D-glucopyranosyl)phenylalanine-1.9 min, D-sorbitol-6.7 min, DL-3-hydroxy-4-*O*-(6-D-sorbitol)phenylalanine-7.9 min, D-mannitol-6.8 min and DL-dopa-D-mannitol-7.8 min.



4-*O*-C1-gly/C1-C6-arylated : R<sup>1</sup> = Carbohydrate, R<sup>2</sup> = H

3-*O*-C1-gly : R<sup>1</sup> = H, R<sup>2</sup> = Carbohydrate

Carbohydrate:



**Scheme 3.4** Syntheses of DL-dopa glycosides

### 3.4.1 Synthesis of DL-dopa-D-glucoside using amyloglucosidase

Glucosylation reaction between DL-dopa **4** and D-glucose **6** catalysed by amyloglucosidase from *Rhizopus* mold was optimized in terms of incubation period, pH, buffer, enzyme and DL-dopa concentration.

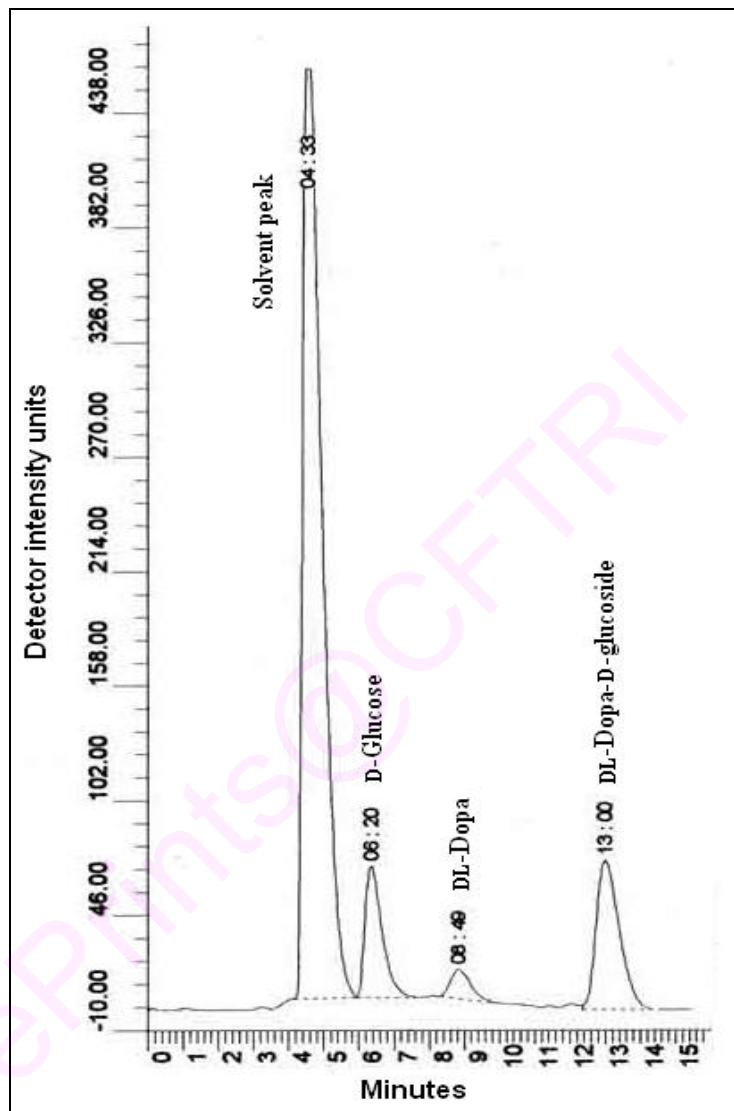


**Fig. 3.38** HPLC chromatogram for the reaction mixture of D-glucose and DL-dopa-D-glucoside. HPLC conditions: Aminopropyl column (10  $\mu\text{m}$ , 250 mm  $\times$  4.6 mm), solvent- $\text{CH}_3\text{CN}:\text{H}_2\text{O}$  (70:30 v/v), Flow rate-1 mL/min, RI detector. Retention times: D-glucose-6.2 min, DL-dopa-8.5 min and DL-dopa-D-glucoside -13 min.

#### **3.4.1.1 Effect of incubation period**

Effect of incubation period for the synthesis of DL-dopa-D-glucoside showed that there was no significant change in glucosylation between 12 h to 72 h (yield 58-62%). Even lesser incubation showed significant glucosylation at 3 h - 42% yield and 6 h - 48% yield. Beyond 72 h the conversion yield decreased gradually (120 h - 49% yield, Fig. 3.39A, Table 3.14).

#### **3.4.1.2 Effect of pH**

At a constant buffer concentration of 0.1 mM (1 mL), the pH was varied from 4 to 8. The glucosylation yield increased upto pH 6 and thereafter decreased (Fig. 3.39B, Table 3.14). The conversion yields were 16% (pH 4), 38% (pH 5), 62% (pH 6), 48% (pH 7) and 22% (pH 8).

#### **3.4.1.3 Effect of buffer concentration**

Since pH 6 gave the highest glucosylation yield, the effect of variation in buffer concentration from 0.03-0.22 mM (0.3-2.2 mL) was studied (Table 3.14). Between 0.06-0.14 mM (0.6-1.4 mL) the conversion yield did not show any significant change (62% to 59% respectively). Beyond 0.14 mM (1.4 mL) the conversion yield decreased to 0.22 mM (47%).

#### **3.4.1.4 Effect of amyloglucosidase concentration**

In presence of 0.5 mmol DL-dopa and 1 mmol D-glucose, amyloglucosidase was varied from 10-75% (w/w D-glucose). Upto 40% (w/w D-glucose) enzyme, the conversion yield more or less remained the same (yields 59%, 65%, 62% and 59% for 10%, 20%, 30% and 40% w/w D-glucose enzyme respectively). Further increase in enzyme concentrations led to a decrease (75% enzyme-45% yield) in the conversion yield (Table 3.14).

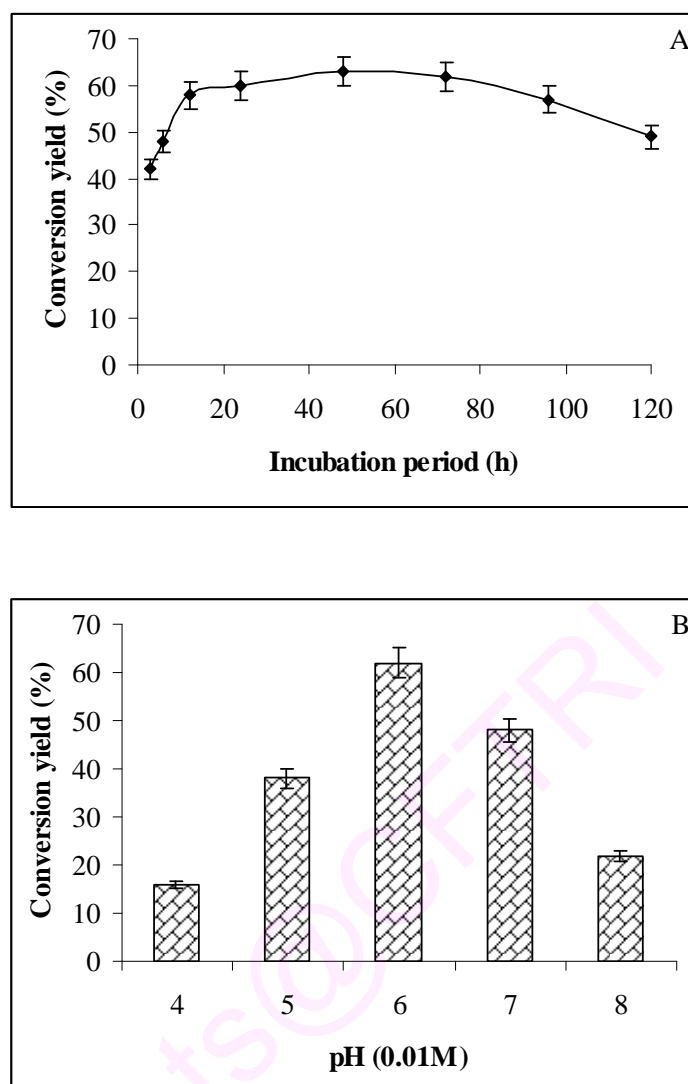


**Fig. 3.39** (A) Reaction profile for DL-dopa-D-glucoside synthesis by the reflux method. Conversion yields were from HPLC with respect to 1 mmol of D-glucose. Reaction conditions: DL-dopa-0.5 mmol, D-glucose-1 mmol, amyloglucosidase-10% (w/w D-glucose), 0.1 mM (1 mL), pH 6 phosphate buffer, solvent-di-isopropyl ether and temperature-68 °C and (B) Effect of pH for DL-dopa-D-glucoside synthesis. Reaction conditions: DL-dopa-0.5 mmol, D-glucose-1 mmol, amyloglucosidase-30% (w/w D-glucose), 0.1 mM (1 mL) - buffer, solvent-di-isopropyl ether, temperature-68 °C and incubation period – 72 h.

**Table 3.14** Optimization of reaction conditions for the synthesis of DL-dopa-D-glucoside using amyloglucosidase

Reaction conditions	Variable parameter <sup>b</sup>	Conversion Yields (%) <sup>c</sup>
Incubation period (h)		
DL-Dopa – 0.5 mmol	3	42
D-Glucose – 1 mmol	6	48
pH – 6	12	58
Buffer concentration – 0.1 mM (1 mL)	24	60
Amyloglucosidase – 10 % w/w D-glucose	48	63
	72	62
	96	57
	120	49
pH (0.01M)		
DL-Dopa – 0.5 mmol <sup>a</sup>	4	16
D-Glucose – 1 mmol	5	38
Amyloglucosidase – 30 % w/w D-glucose	6	62
Buffer concentration – 0.1 mM (1 mL)	7	48
Incubation period – 72 h	8	22
Buffer concentration (mM)		
DL-Dopa – 0.5 mmol	0.03	51
D-Glucose – 1 mmol	0.06	62
Amyloglucosidase – 30 % w/w D-glucose	0.1	63
pH – 6	0.14	59
Incubation period – 72 h	0.18	52
	0.22	47
Amyloglucosidase (% w/w D-glucose)		
DL-Dopa – 0.5 mmol	10	59
D-Glucose – 1 mmol	20	65
pH – 6	30	62
Buffer concentration – 0.1 mM (1 mL)	40	59
Incubation period – 72 h	50	47
	75	45
DL-Dopa (mmol)		
pH – 6	0.2	22
Buffer concentration – 0.1 mM (1 mL)	0.4	41
D-Glucose – 1 mmol	0.5	62
Amyloglucosidase – 10 % w/w D-glucose	0.8	53
Incubation period – 72 h	1.2	56
	1.6	55
	2	54

<sup>a</sup>Initial reaction conditions. <sup>b</sup>Other variables are the same as under reaction conditions, except the specified ones. <sup>c</sup>HPLC yields expressed with respect to 1 mmol D-glucose employed.

#### 3.4.1.5 Effect of DL-dopa concentration

Under the above determined optimum conditions, DL-dopa was varied from 0.2 mmol to 2 mmol. Glucosylation yield did not show any significant change in conversion at higher concentration of DL-dopa (2 mmol-54% yield). A maximum conversion of 62% was obtained at 0.5 mmol DL-dopa (Table 3.14).

#### 3.4.2 Syntheses of DL-dopa glycosides of other carbohydrates using amyloglucosidase

Syntheses of DL-dopa glycosides using amyloglucosidase involved refluxing DL-dopa **4** (0.5 mmol) with carbohydrates (D-glucose **6**, D-galactose **7**, D-mannose **8**, D-sorbitol **15** and D-mannitol **16**, 1 mmol) in 100 mL di-isopropyl ether in presence of amyloglucosidase (10% w/w of carbohydrate) and 0.1 mM (1 mL) of 0.01 M pH 6 buffer for an incubation period of 72 h (Scheme 3.4). The solvent was evaporated, the enzyme denatured at 100 °C for 5-10 min and the residue containing unreacted carbohydrate along with the product glycosides were dissolved in 20-30 mL water, filtered through Whatmann filter paper No. 1. The filtrate containing unreacted DL-dopa **4**, carbohydrate and the product glycosides was evaporated to dryness. Other procedures are as described on page 74.

#### 3.4.3 Syntheses of DL-dopa glycosides of other carbohydrates using $\beta$ -glucosidase

Syntheses of DL-dopa glycosides using  $\beta$ -glucosidase involved refluxing DL-dopa **4** (0.5 mmol) with carbohydrates (D-glucose **6**, D-galactose **7**, D-mannose **8** and lactose **14**, 1 mmol) in 100 mL di-isopropyl ether in presence of 10% w/w of carbohydrate  $\beta$ -glucosidase and 0.1 mM (1 mL) of 0.01 M pH 6 buffer for an incubation period of 72 h (Scheme 3.4) and further as described in Section 3.4.2.

### 3.4.4 Spectral characterization

DL-Dopa glycosides were characterized by UV, IR, Mass, melting point, optical rotation and 2D HSQCT, which provided good information on the nature and proportions of the products formed.

**DL-3,4-Dihydroxyphenylalanine 4:** Solid, decomposed at 270 °C, UV (H<sub>2</sub>O,  $\lambda_{\max}$ ): 199.5 nm ( $\sigma \rightarrow \sigma^*$ ,  $\epsilon_{199.5} - 42716 \text{ M}^{-1}$ ), 221 nm ( $\sigma \rightarrow \pi^*$ ,  $\epsilon_{221} - 7535 \text{ M}^{-1}$ ), 280 nm ( $\pi \rightarrow \pi^*$ ,  $\epsilon_{280} - 3234 \text{ M}^{-1}$ ), IR (stretching frequency,  $\text{cm}^{-1}$ ): 3422 (OH), 1523 (C=C), 1633 (CO), 2961 (CH), MS ( $m/z$ ) – 197.2 [ $\text{M}]^+$ , 2D-HSQCT (DMSO- $d_6$ ): <sup>1</sup>H NMR  $\delta_{\text{ppm}}$ : 6.69 (H-2), 6.51 (H-5), 6.64 (H-6), 2.98 ( $\beta\text{CH}_{2a-7}$ ), 2.70 ( $\beta\text{CH}_{2b-7}$ ), 3.36 ( $\alpha\text{CH-8}$ ); <sup>13</sup>C NMR  $\delta_{\text{ppm}}$  (125 MHz): 128.5 (C1), 117 (C2), 145.4 (C3), 144.2 (C4), 120.1 (C5), 115.8 (C6), 37 (C7), 56 (C8), 170.8 (C9). Ultraviolet-visible spectra is shown in Fig. 3.40A.

**3.4.4.1 DL-Dopa-D-glucoside 34a-d:** Solid, UV (H<sub>2</sub>O,  $\lambda_{\max}$ ): 192 nm ( $\sigma \rightarrow \sigma^*$ ,  $\epsilon_{192} - 3319 \text{ M}^{-1}$ ), 226 nm ( $\sigma \rightarrow \pi^*$ ,  $\epsilon_{226} - 959 \text{ M}^{-1}$ ), 295.5 nm ( $n \rightarrow \pi^*$ ,  $\epsilon_{295.5} - 571 \text{ M}^{-1}$ ), IR (stretching frequency,  $\text{cm}^{-1}$ ): 3358 (OH), 1328 (glycosidic aryl alkyl C-O-C asymmetrical), 1038 (glycosidic aryl alkyl C-O-C symmetrical), 1663 (CO), MS ( $m/z$ ) – 359.1 [ $\text{M}]^+$ , 2D-HSQCT (DMSO- $d_6$ ) **DL-3-Hydroxy-4-O-(D-glucopyranosyl)phenyl alanine: 4-O-C1 $\alpha$ -glucoside 34a:** <sup>1</sup>H NMR  $\delta_{\text{ppm}}$  (500.13) **Glu:** 5.04 (H-1 $\alpha$ , d, J = 3.4 Hz), 3.21 (H-2 $\alpha$ ), 3.47 (H-3 $\alpha$ ), 3.05 (H-4 $\alpha$ ), 3.58 (H-5 $\alpha$ ), 3.44 (H-6 $\alpha$ ), **DL-Dopa:** 6.81 (H-2), 6.80 (H-6), 3.02 ( $\beta\text{CH}_{2a-7}$ ), 2.70 ( $\beta\text{CH}_{2b-7}$ ), 3.48 ( $\alpha\text{CH-8}$ ), <sup>13</sup>C NMR  $\delta_{\text{ppm}}$  (125 MHz) **Glu:** 96.1 (C1 $\alpha$ ), 72 (C2 $\alpha$ ), 71.5 (C3 $\alpha$ ), 70.5 (C4 $\alpha$ ), 72 (C5 $\alpha$ ), 61.1 (C6 $\alpha$ ), **DL-Dopa:** 130.2 (C1), 110 (C2), 116 (C6), 57.4 (C8), 172.1 (C9); **4-O-C1 $\beta$ -glucoside 34b:** Solid, UV (H<sub>2</sub>O,  $\lambda_{\max}$ ): 192.5 nm ( $\sigma \rightarrow \sigma^*$ ,  $\epsilon_{192.5} - 3012 \text{ M}^{-1}$ ), 225 nm ( $\sigma \rightarrow \pi^*$ ,  $\epsilon_{225} - 842 \text{ M}^{-1}$ ), 291.5 nm ( $n \rightarrow \pi^*$ ,  $\epsilon_{291.5} - 356 \text{ M}^{-1}$ ), IR (stretching frequency,  $\text{cm}^{-1}$ ): 3325 (OH), 1330 (glycosidic aryl alkyl C-O-C asymmetrical), 1026 (glycosidic aryl alkyl C-O-C symmetrical), 1650 (CO), MS

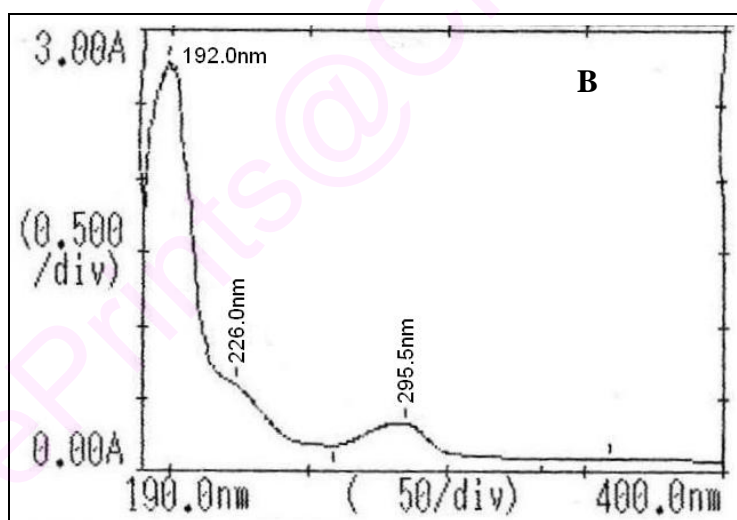
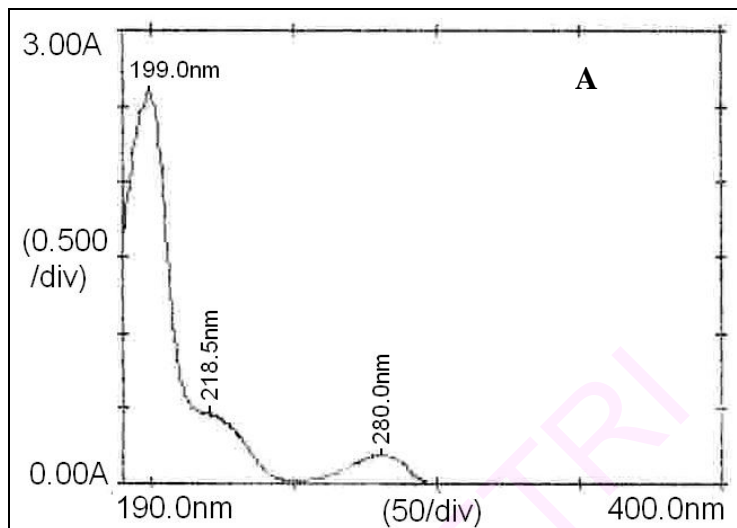


**Fig. 3.40** Ultraviolet-visible spectra of (A) DL-Dopa **4** and (B) DL-Dopa-D-glucoside **34a-d**



( $m/z$ ) – 360.2 [M+1]<sup>+</sup>, <sup>1</sup>H NMR **Glu**: 4.20 (H-1β, d, J = 6.3 Hz), 2.94 (H-2β), 3.13 (H-3β), 3.68 (H-4β), 3.37 (H-5β), 3.55 (H-6a), **DL-Dopa**: 6.71 (H-2), 6.40 (H-5), 6.60 (H-6), 3.02 (βCH<sub>2a</sub>-7), 2.70 (βCH<sub>2b</sub>-7), 3.47 (αCH-8), <sup>13</sup>C NMR δ<sub>ppm</sub> **Glu**: 103.4 (C1β), 73.5 (C2β), 77 (C3β), 72 (C4β), 62.8 (C6β), **DL-Dopa**: 127.9 (C1), 116.9 (C2), 145.2 (C3), 144.1 (C4), 120.2 (C5), 115.8 (C6), 36.6 (C7), 55.9 (C8), 172 (C9); **4-O-C6-O-arylated 34c**: <sup>1</sup>H NMR **Glu**: 3.51 (H-6a), **DL-Dopa**: 3.55 (αCH-8), <sup>13</sup>C NMR **Glu**: 66.9 (C6α), **DL-Dopa**: 55.9 (C8), **DL-4-Hydroxy-3-O-(β-D-glucopyranosyl)phenylalanine 34c**: <sup>1</sup>H NMR **Glu**: 4.55 (H-1β, d, J = 5.9 Hz), **DL-Dopa**: 3.58 (αCH-8), <sup>13</sup>C NMR **Glu**: 98.5 (C1β), **DL-Dopa**: 52.4 (C8).

Ultraviolet-visible, IR, mass and 2D-HSQCT NMR spectra for DL-dopa-D-glucoside **34a-d** synthesised using amyloglucosidase are shown in Figures 3.40B, 3.41A, 3.41B and 3.41C respectively. Mass and 2D-HSQCT NMR spectra for DL-3-Hydroxy-4-O-(D-glucopyranosyl)phenylalanine **34b,c** synthesized using β-glucosidase are shown in Figures 3.42A and 3.42B respectively.

**3.4.4.2 DL-Dopa-D-galactoside 35a-e**: Solid, UV (H<sub>2</sub>O, λ<sub>max</sub>): 191.5 nm (σ→σ\*, ε<sub>191.5</sub> – 2810 M<sup>-1</sup>), 225.5 nm (σ→π\*, ε<sub>225.5</sub> – 876 M<sup>-1</sup>), 296 nm (n→π\*, ε<sub>296</sub> – 624 M<sup>-1</sup>), IR (stretching frequency, cm<sup>-1</sup>): 3422 (OH), 1307 (glycosidic aryl alkyl C-O-C asymmetrical), 1039 (glycosidic aryl alkyl C-O-C symmetrical), 1407 (C=C), 1641 (CO), 2940 (CH), MS ( $m/z$ ) – 360.2 [M+1]<sup>+</sup>, 2D-HSQCT (DMSO-*d*<sub>6</sub>) **DL-3-Hydroxy-4-O-(D-galactopyranosyl)phenylalanine: 4-O-C1α-galactoside 35a**: <sup>1</sup>H NMR δ<sub>ppm</sub> (500.13) **Gal**: 4.98 (H-1α, d, J = 3.9 Hz), 3.55 (H-2α), 3.57 (H-3α), 3.67 (H-4α), 3.35 (H-5α), 3.44 (H-6a), **DL-Dopa**: 6.76 (H-2), 6.66 (H-6), 2.90 (βCH<sub>2a</sub>-7), 2.65 (βCH<sub>2b</sub>-7), 3.35 (αCH-8), <sup>13</sup>C NMR δ<sub>ppm</sub> (125 MHz): **Gal**: 96.3 (C1α), 64 (C2α), 68.5 (C3α), 68 (C4α), 70.7 (C5α), 63 (C6α), **DL-Dopa**: 124.4 (C1), 114.5 (C2), 145.4 (C3), 144.4 (C4), 122.3

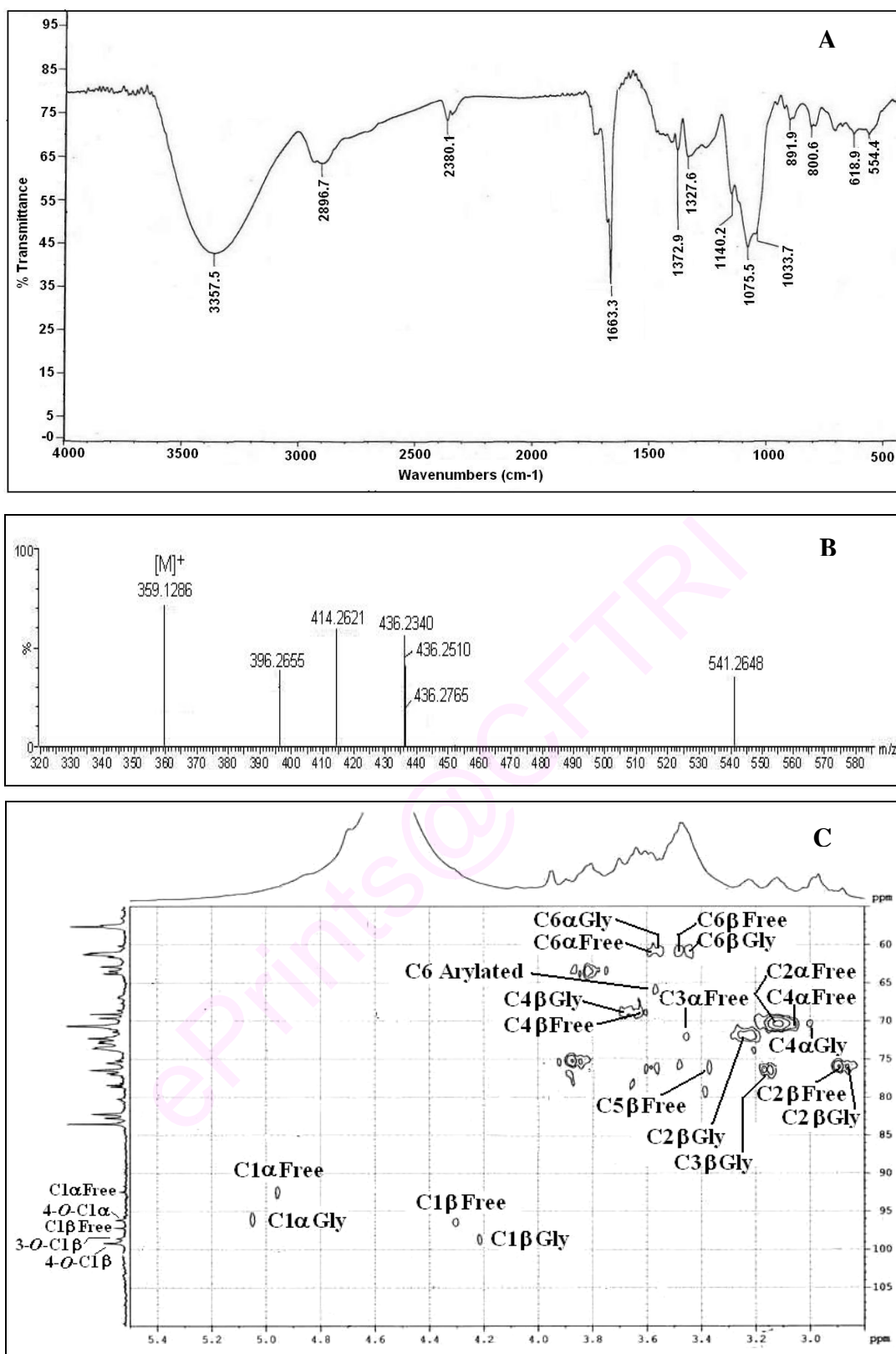


**Fig. 3.41** DL-Dopa-D-glucoside **34a-d** (A) IR spectrum, (B) Mass spectrum and (C) 2D-HSQC spectrum showing the C1-C6 region. Some of the assignments are interchangeable.

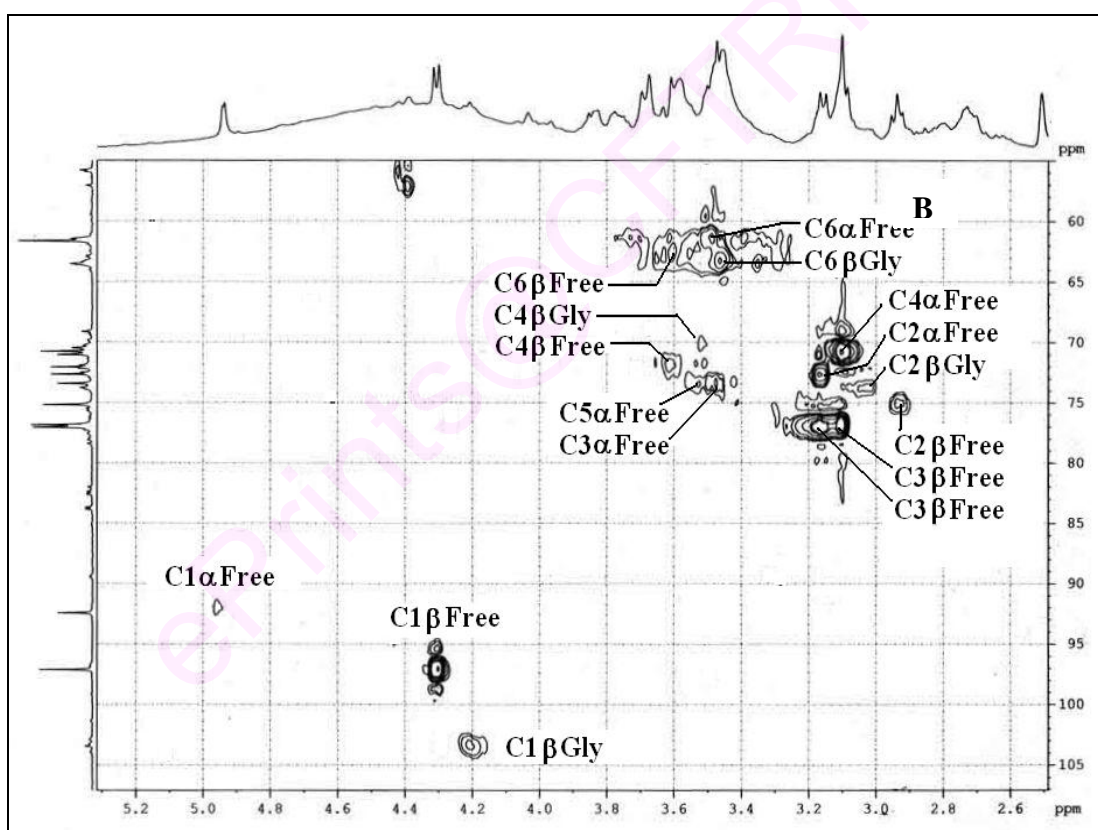
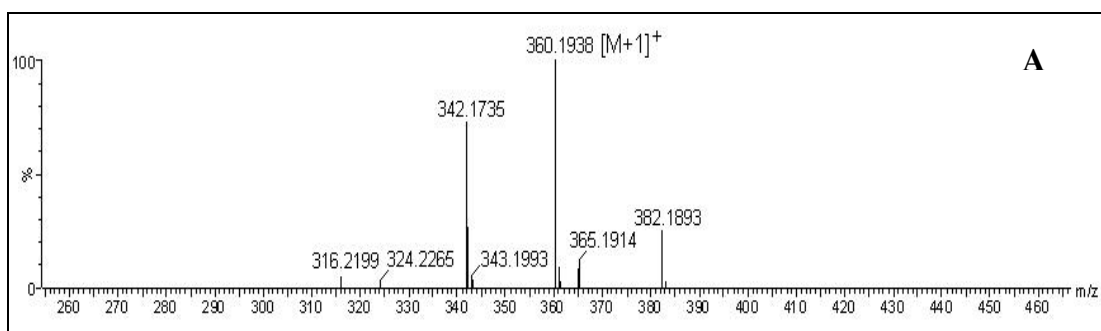


**Fig. 3.42** DL-3-Hydroxy-4-*O*-(D-glucopyranosyl)phenylalanine **34b,c** (A) Mass spectrum and (B) 2D-HSQC spectrum showing the C1-C6 region. Some of the assignments are interchangeable

(C5), 116.8 (C6), 36.8 (C7), 57.1 (C8), 173 (C9); **4-O-C1 $\beta$ -galactoside 35b**:  $^1\text{H}$  NMR **Gal**: 4.90 (H-1 $\beta$ , d,  $J = 7.1$  Hz), 3.56 (H-3 $\beta$ ), 3.04 (H-4 $\beta$ ), 3.28 (H-5 $\beta$ ), 3.46 (H-6a), **DL-Dopa**: 6.72 (H-2), 2.68 ( $\beta\text{CH}_{2b-7}$ ), 3.45 ( $\alpha\text{CH-8}$ ),  $^{13}\text{C}$  NMR  $\delta_{\text{ppm}}$  **Gal**: 102.1 (C1 $\beta$ ), 69.7 (C3 $\beta$ ), 72.6 (C4 $\beta$ ), 74.2 (C5 $\beta$ ), 63.5 (C6 $\beta$ ), **DL-Dopa**: 115.6 (C2), 144.8 (C4), 36.6 (C7), 53.2 (C8); **4-O-C6-O-arylated 35c**:  $^1\text{H}$  NMR **Gal**: 3.68 (H-6a),  $^{13}\text{C}$  NMR **Gal**: 66.5 (C6 $\alpha$ ), **DL-4-Hydroxy-3-O-(D-galactopyranosyl) phenylalanine: 3-O-C1 $\alpha$ -galactoside 35d**:  $^1\text{H}$  NMR **Gal**: 5.07 (H-1 $\alpha$ , d,  $J = 3.7$  Hz), 3.46 (H-6a), **DL-Dopa**: 6.80 (H-2), 6.70 (H-6), 2.70 ( $\beta\text{CH}_{2b-7}$ ), 3.45 ( $\alpha\text{CH-8}$ ),  $^{13}\text{C}$  NMR **Gal**: 95.7 (C1 $\alpha$ ), 63.2 (C6 $\alpha$ ), **DL-Dopa**: 125.5 (C1), 114.9 (C2), 117 (C6), 29.3 (C7), 56.2 (C8); **3-O-C1 $\beta$ -galactoside 35e**:  $^1\text{H}$  NMR **Gal**: 4.65 (H-1 $\beta$ , d,  $J = 6.1$  Hz),  $^{13}\text{C}$  NMR  $\delta_{\text{ppm}}$  **Gal**: 103.5 (C1 $\beta$ ).

Mass and 2D-HSQCT NMR spectra for DL-dopa-D-galactoside **35a-e** are shown in Figures 3.43A and 3.43B respectively.

**3.4.4.3 DL-3-Hydroxy-4-O-( $\beta$ -D-mannopyranosyl)phenylalanine 36**: Solid, mp: 108 °C; UV ( $\text{H}_2\text{O}$ ,  $\lambda_{\text{max}}$ ): 192 nm ( $\sigma \rightarrow \sigma^*$ ,  $\epsilon_{192} = 2433 \text{ M}^{-1}$ ), 224.5 nm ( $\sigma \rightarrow \pi^*$ ,  $\epsilon_{224.5} = 931 \text{ M}^{-1}$ ), 295.5 nm ( $n \rightarrow \pi^*$ ,  $\epsilon_{295.5} = 583 \text{ M}^{-1}$ ), IR (stretching frequency,  $\text{cm}^{-1}$ ): 3385 (OH), 1304 (glycosidic aryl alkyl C-O-C asymmetrical), 1040 (glycosidic aryl alkyl C-O-C symmetrical), 1406 (C=C), 1641 (CO), 2946 (CH), optical rotation ( $c$  0.5,  $\text{H}_2\text{O}$ ):  $[\alpha]_{\text{D}}$  at 25 °C = -29.7, MS ( $m/z$ ) - 360.2  $[\text{M}+1]^+$ , 2D-HSQCT ( $\text{DMSO-}d_6$ ) **4-O-C1 $\beta$ -mannoside**:  $^1\text{H}$  NMR **Man**: 4.69 (H-1 $\beta$ , d,  $J = 3.4$  Hz), 3.40 (H-2 $\beta$ ), 3.50 (H-3 $\beta$ ), 3.55 (H-4 $\beta$ ), 3.05 (H-5 $\beta$ ), 3.45 (H-6a), **DL-Dopa**: 6.77 (H-2), 6.40 (H-5), 6.57 (H-6), 2.95 ( $\beta\text{CH}_{2a-7}$ ), 2.60 ( $\beta\text{CH}_{2b-7}$ ), 3.44 ( $\alpha\text{CH-8}$ ),  $^{13}\text{C}$  NMR  $\delta_{\text{ppm}}$  **Man**: 102.8 (C1 $\beta$ ), 70.5 (C2 $\beta$ ), 73.1 (C3 $\beta$ ), 67 (C4 $\beta$ ), 73.1 (C5 $\beta$ ), 63.9 (C6 $\beta$ ), **DL-Dopa**: 128.7 (C1), 115.5 (C2), 145 (C3), 144 (C4), 120.2 (C5), 116.8 (C6), 36.4 (C7), 56 (C8), 172 (C9).

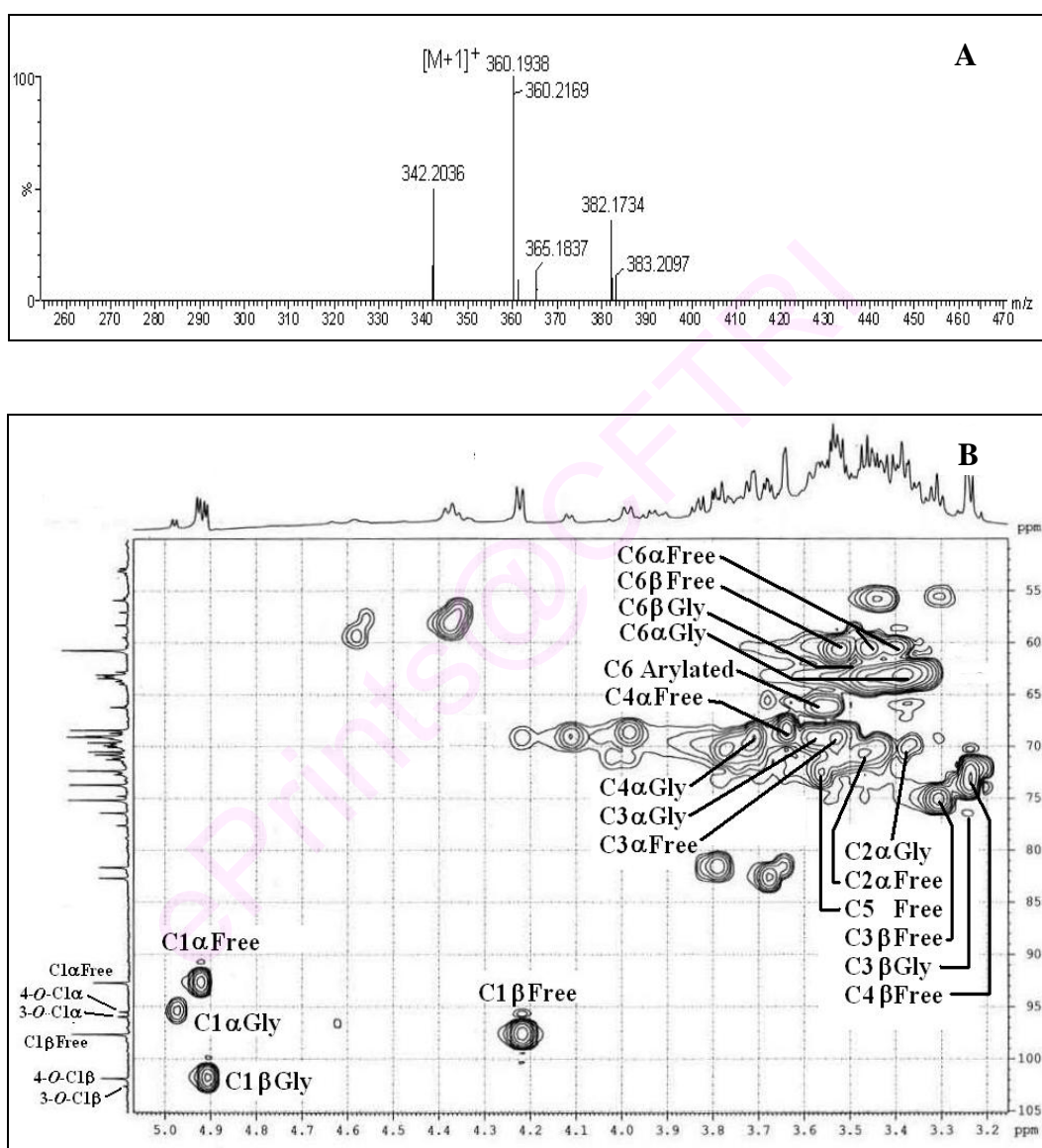


**Fig. 3.43** DL-Dopa-D-galactoside **35a-e** (A) Mass spectrum and (B) 2D-HSQC spectrum showing the C1-C6 region. Some of the assignments are interchangeable.

Infra-red and 2D-HSQCT NMR spectra for DL-3-hydroxy-4-*O*-( $\beta$ -D-mannopyranosyl)phenylalanine **36** are shown in Figures 3.44A and 3.44B respectively.

**3.4.4.4 DL-3-Hydroxy-4-*O*-( $\beta$ -D-galactopyranosyl-(1'→4) $\beta$ -D-glucopyranosyl)phenyl alanine 37:** Solid, mp: 140 °C, UV (H<sub>2</sub>O,  $\lambda_{\max}$ ): 198.5 nm ( $\sigma \rightarrow \sigma^*$ ,  $\epsilon_{198.5} - 4437 \text{ M}^{-1}$ ), 221.5 nm ( $\sigma \rightarrow \pi^*$ ,  $\epsilon_{221.5} - 1208 \text{ M}^{-1}$ ), 279.5 nm ( $\pi \rightarrow \pi^*$ ,  $\epsilon_{279.5} - 562 \text{ M}^{-1}$ ); IR (stretching frequency,  $\text{cm}^{-1}$ ): 3385 (OH), 1311 (glycosidic aryl alkyl C-O-C asymmetrical), 1039 (glycosidic aryl alkyl C-O-C symmetrical), 1372 (C=C), 1659 (CO), 2895 (CH), optical rotation (*c* 0.5, H<sub>2</sub>O):  $[\alpha]_{\text{D}}$  at 25 °C = +32.1, MS (*m/z*) – 522.3  $[\text{M}+1]^+$ , 2D-HSQCT (DMSO-*d*<sub>6</sub>) **4-*O*-C1 $\beta$ -lactoside:** <sup>1</sup>H NMR **Lact:** 4.92 (H-1 $\beta$ , d, *J* = 7.2 Hz), 3.28 (H-2 $\beta$ ), 3.55 (H-3 $\beta$ ), 3.38 (H-5 $\beta$ ), 3.52 (H-6a), 4.21 (H-1' $\beta$ ), 3.40 (H-2'), 3.22 (H-3'), 3.62 (H-4'), 2.82 (H-5'), 3.52 (H-6'a), **DL-Dopa:** 6.64 (H-2), 6.45 (H-5), 6.50 (H-6), 2.90 ( $\beta\text{CH}_{2\text{a}}-7$ ), 2.60 ( $\beta\text{CH}_{2\text{b}}-7$ ), 3.43 ( $\alpha\text{CH}-8$ ), <sup>13</sup>C NMR  $\delta_{\text{ppm}}$  **Lact:** 102 (C1 $\beta$ ), 76 (C2 $\beta$ ), 75 (C3 $\beta$ ), 76.5 (C5 $\beta$ ), 61.4 (C6 $\beta$ ), 103.9 (C1' $\beta$ ), 70.5 (C2'), 73 (C3'), 64 (C4'), 73 (C5'), 61 (C6'), **DL-Dopa:** 115.7 (C2), 144.3 (C4), 120.2 (C5), 116.9 (C6), 36.2 (C7), 55.9 (C8), 172 (C9).

Infra-red and 2D-HSQCT NMR spectra for DL-3-hydroxy-4-*O*-( $\beta$ -D-galactopyranosyl-(1'→4) $\beta$ -D-glucopyranosyl)phenylalanine **37** are shown in Figures 3.45A and 3.45B respectively.

**3.4.4.5 DL-3-Hydroxy-4-*O*-(6-D-sorbitol)phenylalanine 38:** Solid, mp: 88 °C, UV (H<sub>2</sub>O,  $\lambda_{\max}$ ): 192.5 nm ( $\sigma \rightarrow \sigma^*$ ,  $\epsilon_{192.5} - 1204 \text{ M}^{-1}$ ), 224 nm ( $\sigma \rightarrow \pi^*$ ,  $\epsilon_{224} - 358 \text{ M}^{-1}$ ), 295 nm ( $n \rightarrow \pi^*$ ,  $\epsilon_{295} - 158 \text{ M}^{-1}$ ), IR (stretching frequency,  $\text{cm}^{-1}$ ): 3050 (OH), 1301 (glycosidic aryl alkyl C-O-C asymmetrical), 1034 (glycosidic aryl alkyl C-O-C symmetrical), 1406 (C=C), 1644 (CO), 2946 (CH), optical rotation (*c* 0.5, H<sub>2</sub>O):  $[\alpha]_{\text{D}}$  at 25 °C = -2.6, MS (*m/z*) – 360.2  $[\text{M}-1]^+$ , 2D-HSQCT (DMSO-*d*<sub>6</sub>) **4-*O*-C6-*O*-sorbitol:** <sup>1</sup>H NMR **Sorb:** 3.48 (H-1), 3.62 (H-2), 3.62 (H-5), 3.72 (H-6), **DL-Dopa:** 6.70 (H-2), 6.52 (H-5), 6.54 (H-6),



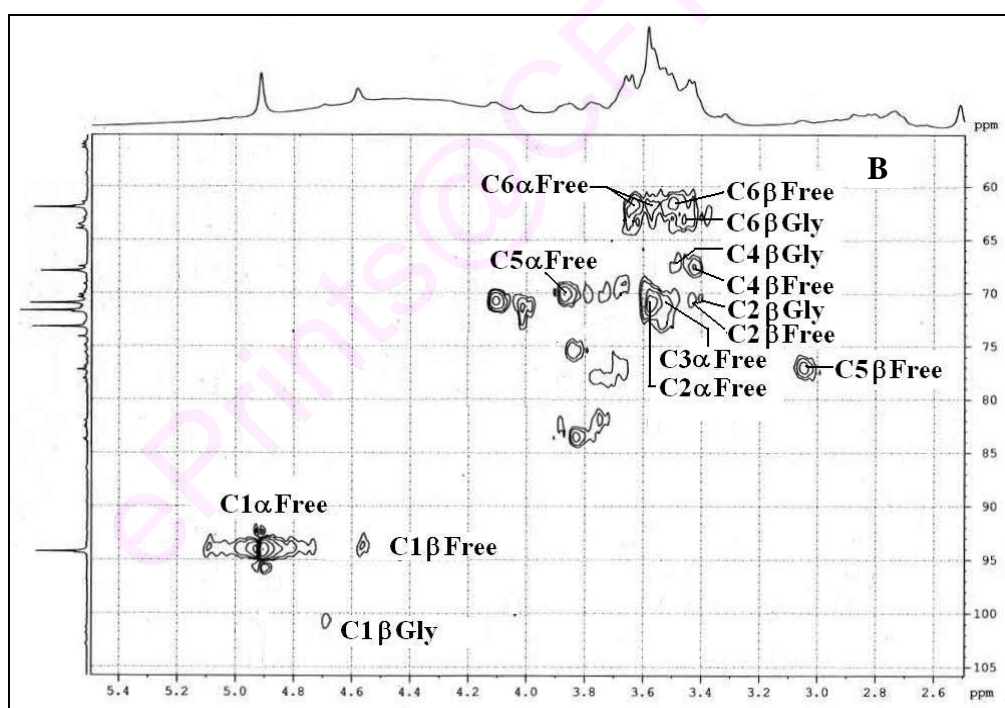
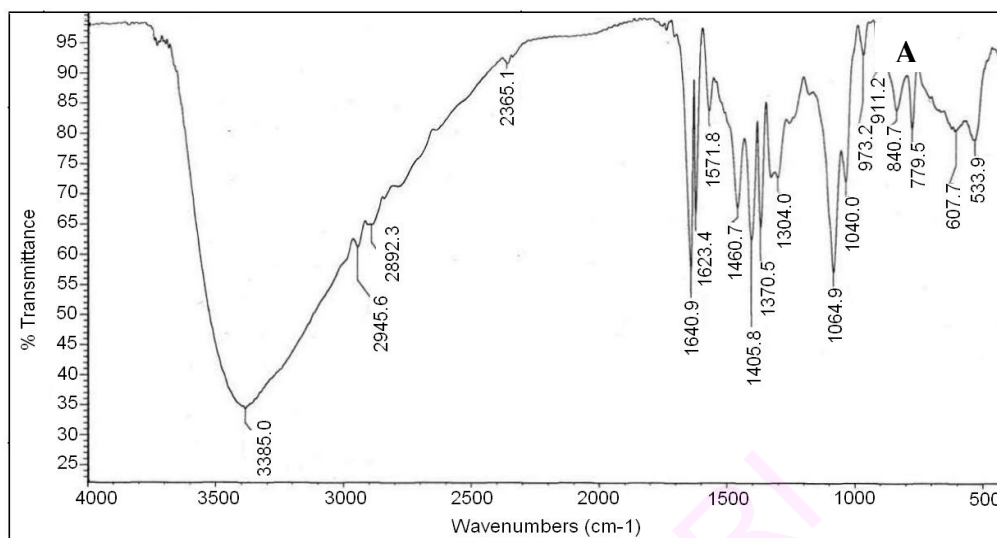


**Fig. 3.44** DL-3-Hydroxy-4-*O*-( $\beta$ -D-mannopyranosyl)phenylalanine **36** (A) IR spectrum and (B) 2D-HSQC spectrum showing the C1-C6 region. Some of the assignments are interchangeable.

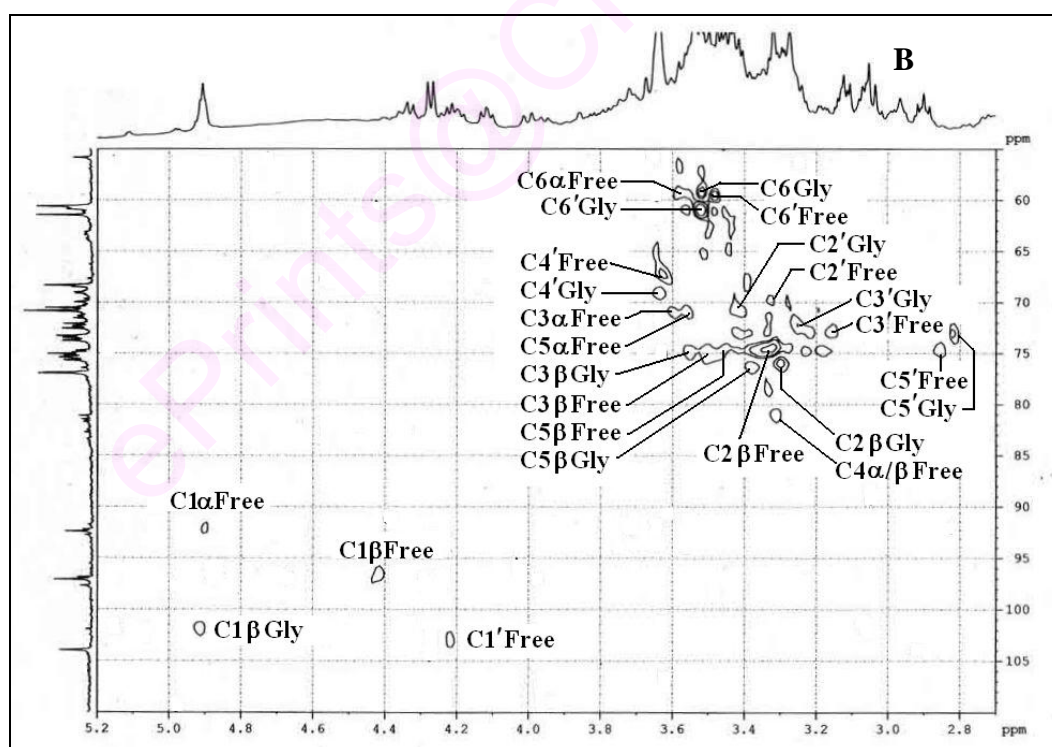
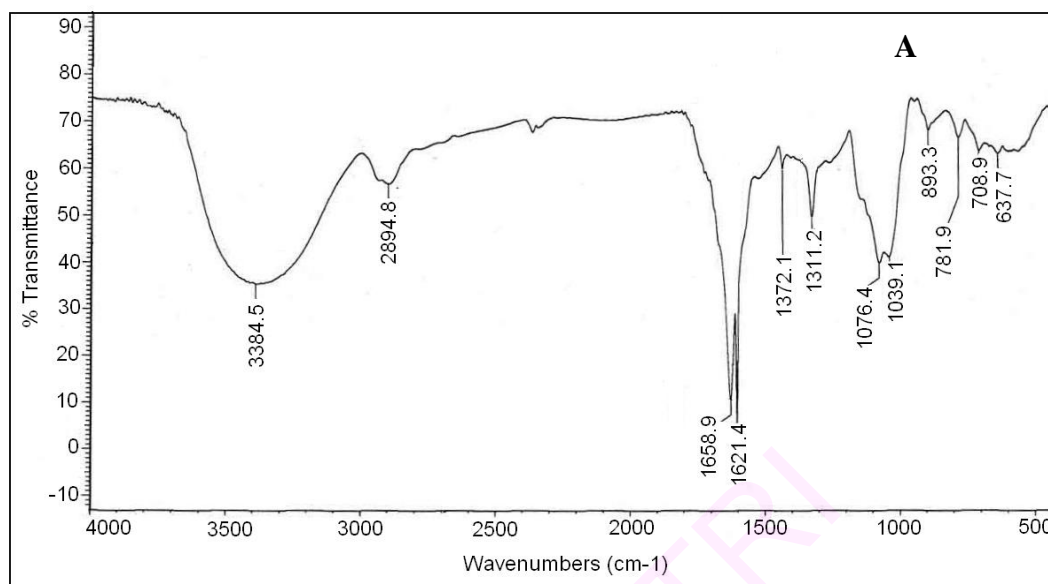


**Fig. 3.45** DL-3-Hydroxy-4-*O*-( $\beta$ -D-galactopyranosyl-(1'→4) $\beta$ -D-glucopyranosyl) phenylalanine **37** (A) IR spectrum and (B) 2D-HSQC spectrum showing the C1-C6' region. Some of the assignments are interchangeable.



2.51 ( $\beta\text{CH}_{2\text{b-7}}$ ), 3.46 ( $\alpha\text{CH-8}$ ),  $^{13}\text{C}$  NMR  $\delta_{\text{ppm}}$  **Sorb**: 63.5 (C1), 72.5 (C2), 72 (C5), 63.5 (C6), **DL-Dopa**: 128 (C1), 115.9 (C2), 144.3 (C4), 120.2 (C5), 116 (C6), 29 (C7).

Mass and 2D-HSQCT NMR spectra for DL-3-hydroxy-4-*O*-(6-D-sorbitol)phenylalanine **38** are shown in Figures 3.46A and 3.46B respectively.

**3.4.4.6 DL-3-Hydroxy-4-*O*-(1-D-mannitol)phenylalanine 39a,b**: Solid, UV ( $\text{H}_2\text{O}$ ,  $\lambda_{\text{max}}$ ): 198.5 nm ( $\sigma \rightarrow \sigma^*$ ,  $\epsilon_{198.5} - 6420 \text{ M}^{-1}$ ), 221.5 nm ( $\sigma \rightarrow \pi^*$ ,  $\epsilon_{221.5} - 1484 \text{ M}^{-1}$ ), 297.5 nm ( $n \rightarrow \pi^*$ ,  $\epsilon_{297.5} - 368 \text{ M}^{-1}$ ), IR (stretching frequency,  $\text{cm}^{-1}$ ): 3281 (OH), 1320 (glycosidic aryl alkyl C-O-C asymmetrical), 1020 (glycosidic aryl alkyl C-O-C symmetrical), 1459 (C=C), 1644 (CO), 2939 (CH), MS ( $m/z$ ) - 360.2  $[\text{M}-1]^+$ , 2D-HSQCT ( $\text{DMSO}-d_6$ ) **4-*O*-C1-*O*-mannitol 39a**:  $^1\text{H}$  NMR **Mann**: 3.52 (H-1), 3.48 (H-2), 3.61 (H-3), 3.61 (H-4), 3.48 (H-5), 3.60 (H-6), **DL-Dopa**: 6.71 (H-2), 6.64 (H-5), 6.51 (H-6), 3.01 ( $\beta\text{CH}_{2\text{a-7}}$ ), 2.71 ( $\beta\text{CH}_{2\text{a-7}}$ ), 3.45 ( $\alpha\text{CH-8}$ ),  $^{13}\text{C}$  NMR  $\delta_{\text{ppm}}$  **Mann**: 65 (C1), 70.5 (C2), 72 (C3), 72 (C4), 70.5 (C5), 64.5 (C6), **DL-Dopa**: 118 (C2), 144.3 (C4), 121 (C5), 115 (C6), 36.5 (C7), **1,6-*O*-(Bis DL-3-hydroxy-4-*O*-phenylalanine) D-mannitol 39b**:  $^1\text{H}$  NMR **Mann**: 3.52 (H-1), 3.63 (H-6),  $^{13}\text{C}$  NMR  $\delta_{\text{ppm}}$  **Mann**: 65 (C1), 64.5 (C6).

Infra-red and 2D-HSQCT NMR spectra for DL-dopa-D-mannitol **39a,b** are shown in Figures 3.47A and 3.47B respectively.

UV spectra of DL-dopa glycosides, showed  $\sigma \rightarrow \sigma^*$  band ranging from 191.5 to 198.5 nm (199.5 nm for DL-dopa),  $\sigma \rightarrow \pi^*$  band ranging from 221.5 to 226 nm (221 nm for DL-dopa) and  $n \rightarrow \pi^*$  band from 295 nm to 297.5 nm (280 nm for DL-dopa). IR spectra showed 1019-1040  $\text{cm}^{-1}$  band for the glycosidic C-O-C aryl alkyl symmetrical stretching and 1307-1320  $\text{cm}^{-1}$  band for the asymmetrical stretching frequencies. In 2D HSQCT spectra, the respective chemical shift values showed glycoside formation: from D-glucose **6 4-*O*-C1 $\alpha$  glucoside 34a** to C1 $\alpha$  at 96.1 ppm and H-1 $\alpha$  at 5.14 ppm, 4-*O*-C1 $\beta$  glucoside **34b** to C1 $\beta$  at 103.4 ppm and H-1 $\beta$  at 4.20 ppm, 4-*O*-C6-*O*-arylated **34c** to C6

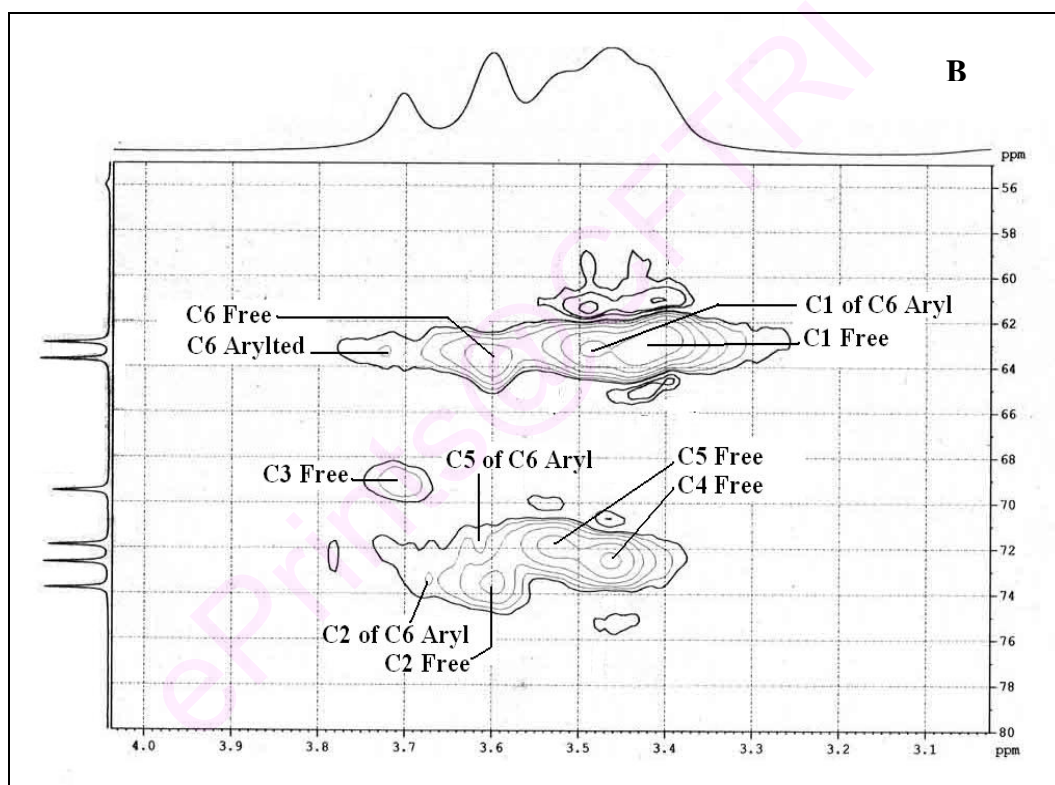
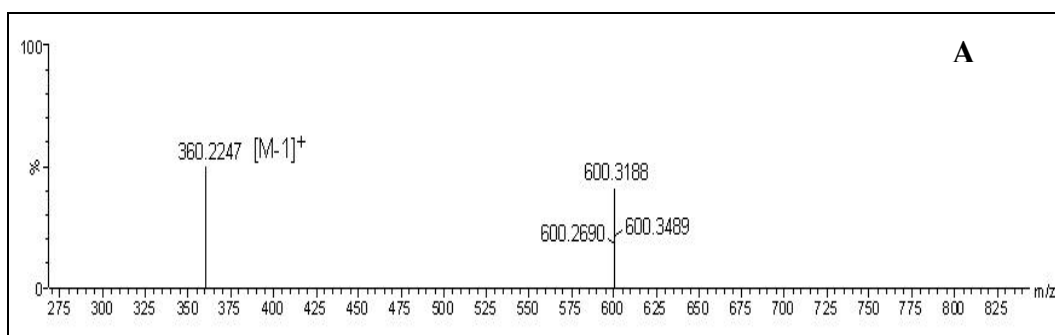


**Fig. 3.46** DL-3-Hydroxy-4-*O*-(6-D-sorbitol)phenylalanine **38** (A) Mass spectrum and (B) 2D-HSQC spectrum showing the C1-C6 region. Some of the assignments are interchangeable.

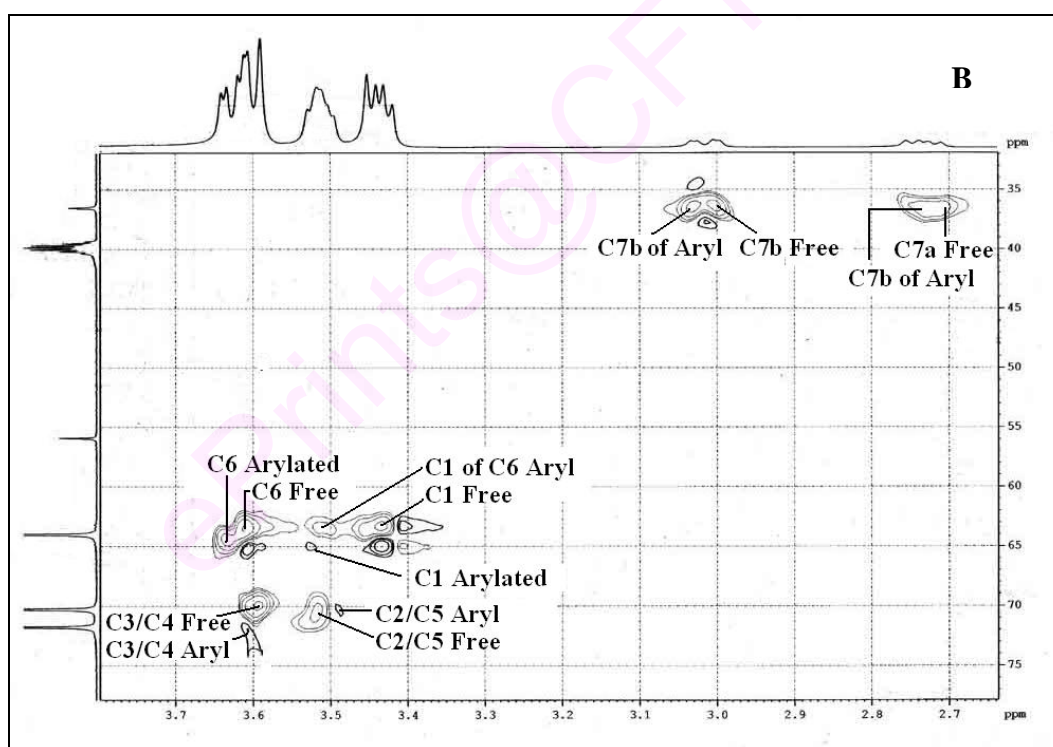
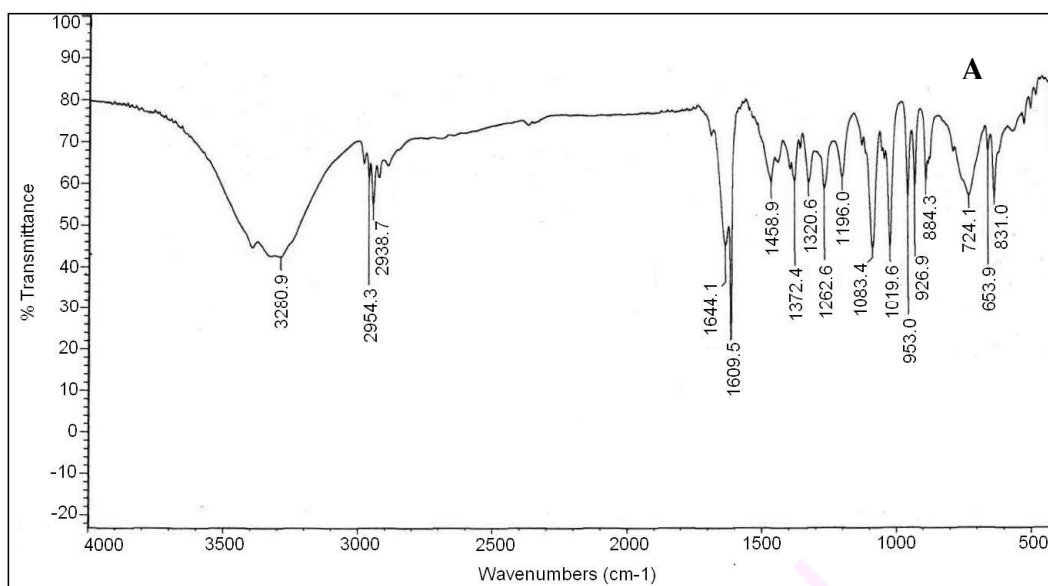


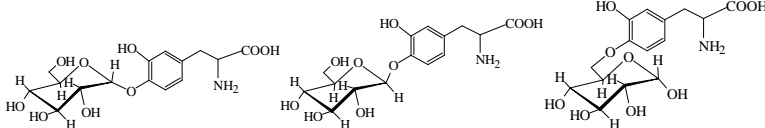
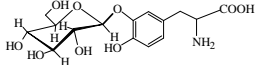
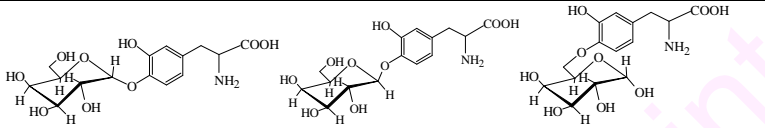
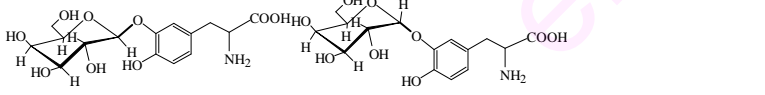
**Fig. 3.47** DL-Dopa-D-mannitol **39a,b** (A) IR spectrum and (B) 2D-HSQC spectrum showing the C1-C6 region. Some of the assignments are interchangeable

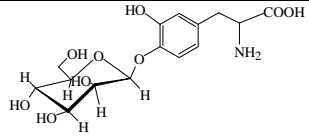
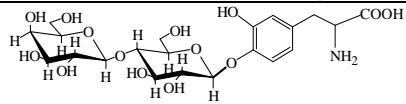
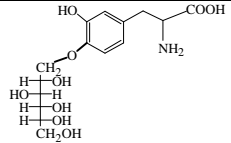
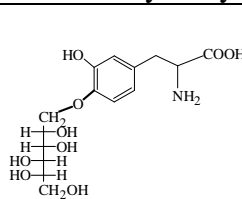
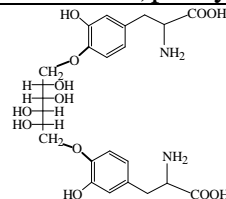
at 66.9 ppm and H-6a at 3.51 ppm and 3-*O*-C1 $\beta$  glucoside **34d** to C1 $\beta$  at 98.5 ppm and H-1 $\beta$  at 4.55 ppm; from D-galactose **7** 4-*O*-C1 $\alpha$  galactoside **35a** to C1 $\alpha$  at 96.3 ppm and H-1 $\alpha$  at 5.01 ppm, 4-*O*-C1 $\beta$  galactoside **35b** to C1 $\beta$  at 102.1 ppm and H-1 $\beta$  at 4.66 ppm, 4-*O*-C6-*O*-arylated **35c** to C6 at 66.5 ppm and H-6a at 3.68 ppm, 3-*O*-C1 $\alpha$  galactoside **35d** to C1 $\alpha$  at 95.7 ppm and H-1 $\alpha$  at 5.07 ppm and 3-*O*-C1 $\beta$  galactoside **35e** to C1 $\beta$  at 103.5 ppm and H-1 $\beta$  at 4.65 ppm; from D-mannose **8** 4-*O*-C1 $\beta$  mannoside **36** to C1 $\beta$  at 102.8 ppm and H-1 $\beta$  at 4.69 ppm; from lactose **14** 4-*O*-C1 $\beta$  lactoside **37** to C1 $\beta$  at 102 ppm and H-1 $\beta$  at 4.26 ppm; from D-sorbitol **15** 4-*O*-C6-*O*-sorbitol **38** to C6 at 63.5 ppm and H-6a at 3.72 ppm, from D-mannitol **16** 4-*O*-C1-*O*-mannitol **39a** to C1 at 65 ppm and H-6a at 3.52 ppm and bis-4-*O*-1,6-di-*O*-arylated **39b** to C1 at 65 ppm and H-1 at 3.52 ppm and C6 at 64.5 ppm and H-6 at 3.63 ppm. Mass spectral data also confirmed product formation.

### 3.4.5 Discussion

DL-Dopa glycosides were synthesized with carbohydrates by employing the optimized conditions (Section 3.4.1). The yields are shown in Table 3.15. The products formed are confirmed spectroscopically (Section 3.4.4). Amyloglucosidase catalyses gave rise to five glycosides: DL-dopa-D-glucoside **34a-d**, DL-dopa-D-galactoside **35a-e**, DL-3-hydroxy-4-*O*-( $\beta$ -D-mannopyranosyl) phenylalanine **36**, DL-3-hydroxy-4-*O*-(6-D-sorbitol)phenylalanine **38** and DL-dopa-D-mannitol **39a,b**.  $\beta$ -glucosidase catalyses gave rise to four glycosides: DL-dopa-D-glucoside **34b,c**, DL-dopa-D-galactoside **35a-e**, DL-3-hydroxy-4-*O*-( $\beta$ -D-mannopyranosyl)phenylalanine **36**, DL-3-hydroxy-4-*O*-( $\beta$ -D-galactopyranosyl-(1'→4) $\beta$ -D-glucopyranosyl)phenylalanine **37**.

**Table 3.15** Syntheses of DL-3,4-dihydroxyphenylalanine (DL-dopa) glycosides using amyloglucosidase and  $\beta$ -glucosidase<sup>a</sup>.

Glycosides	Amyloglucosidase catalysis		$\beta$ -Glucosidase catalysis	
	Product (% proportion) <sup>b</sup>	Yields (%) <sup>c</sup>	Product (% proportion) <sup>b</sup>	Yields (%) <sup>c</sup>
 <p><b>34a</b> DL-3-Hydroxy-4-<i>O</i>-(<math>\alpha</math>-D-glucopyranosyl)phenylalanine  <b>34b</b> DL-3-Hydroxy-4-<i>O</i>-(<math>\beta</math>-D-glucopyranosyl)phenylalanine  <b>34c</b> DL-3-Hydroxy-4-<i>O</i>-(6-D-glucopyranosyl)phenylalanine</p>	4- <i>O</i> -C1 $\alpha$ (24), 4- <i>O</i> -C1 $\beta$ (48), 4- <i>O</i> -C6- <i>O</i> -arylated (6), 3- <i>O</i> -C1 $\beta$ (22)	62	4- <i>O</i> -C1 $\beta$ (28), 4- <i>O</i> -C6- <i>O</i> -arylated (72)	33
 <p><b>34d</b> DL-4-Hydroxy-3-<i>O</i>-(<math>\beta</math>-D-glucopyranosyl)phenylalanine</p>				
 <p><b>35a</b> DL-3-Hydroxy-4-<i>O</i>-(<math>\alpha</math>-D-galactopyranosyl)phenylalanine  <b>35b</b> DL-3-Hydroxy-4-<i>O</i>-(<math>\beta</math>-D-galactopyranosyl)phenylalanine  <b>35c</b> DL-3-Hydroxy-4-<i>O</i>-(6-D-galactopyranosyl)phenylalanine</p>	4- <i>O</i> -C1 $\alpha$ (27), 4- <i>O</i> -C1 $\beta$ (25), 4- <i>O</i> -C6- <i>O</i> -arylated (29), 3- <i>O</i> -C1 $\alpha$ (10), 3- <i>O</i> -C1 $\beta$ (9)	46	4- <i>O</i> -C1 $\alpha$ (17), 4- <i>O</i> -C1 $\beta$ (35), 4- <i>O</i> -C6- <i>O</i> -arylated (23), 3- <i>O</i> -C1 $\alpha$ (21), 3- <i>O</i> -C1 $\beta$ (4)	31
 <p><b>35d</b> DL-4-Hydroxy-3-<i>O</i>-(<math>\alpha</math>-D-galactopyranosyl)phenylalanine  <b>35e</b> DL-4-Hydroxy-3-<i>O</i>-(<math>\beta</math>-D-galactopyranosyl)phenylalanine</p>				

	4- <i>O</i> -C1 $\beta$	61	4- <i>O</i> -C1 $\beta$	32
<b>36</b> DL-3-Hydroxy-4- <i>O</i> -( $\beta$ -D-mannopyranosyl)phenylalanine				
	-	-	4- <i>O</i> -C1 $\beta$	17
<b>37</b> DL-3-Hydroxy-4- <i>O</i> -( $\beta$ -D-galactopyranosyl-(1' $\rightarrow$ 4) $\beta$ -D-glucopyranosyl)phenylalanine				
	4- <i>O</i> -C6- <i>O</i> -arylated	12	-	-
<b>38</b> DL-3-Hydroxy-4- <i>O</i> -(6-D-sorbitol)phenylalanine				
	4- <i>O</i> -C1- <i>O</i> -arylated (70), Bis 4- <i>O</i> -C1,6-di- <i>O</i> - arylated (30)	20	-	-
				
<b>39a</b> DL-3-Hydroxy-4- <i>O</i> -(1-D-mannitol)phenylalanine				
<b>39b</b> 1,6- <i>O</i> -(Bis DL-3-hydroxy-4- <i>O</i> -phenylalanine)D-mannitol				

<sup>a</sup> DL-3,4-Dihydroxyphenylalanine - 0.5 mmol and carbohydrate - 1 mmol; enzyme concentration 10% w/w of carbohydrate; solvent – di-isopropyl ether; buffer – 0.1 mM (1mL) pH 6 phosphate buffer; incubation period – 72 h. <sup>b</sup>The product proportions were determined from the area of respective <sup>1</sup>H/<sup>13</sup>C signals. <sup>c</sup>Conversion yields were from HPLC with respect to free carbohydrate. Error in yield measurements is  $\pm$  10%.

Under the reaction conditions employed, DL-dopa **4** gave a mixture of 3-*O*- and 4-*O*- glycosylated/arylated products with many of the carbohydrates employed. The carbohydrates reacted were: glucose **6**, D-galactose **7**, D-mannose **8**, lactose **14**, D-sorbitol **15** and D-mannitol **16**. Amyloglucosidase catalysed the reaction with D-glucose **6**, D-galactose **7**, D-mannose **8**, D-sorbitol **15** and D-mannitol **16**.  $\beta$ -Glucosidase catalysed the reaction with D-glucose **6**, D-galactose **7**, D-mannose **8** and lactose **14**.

However, only mono glycosylated/arylated products were formed. No bis products with both the OH groups at 3<sup>rd</sup> and 4<sup>th</sup> positions glycosylated/arylated were detected. This indicated that steric effects are responsible for the formation of only monoglycosylated products. Amyloglucosidase gave selectivity with D-mannose **8** to give 4-*O*-C1 $\beta$  and D-sorbitol **15** to give 4-*O*-C6-*O*-arylated product.  $\beta$ -Glucosidase gave selectivity with D-mannose **8** to give 4-*O*-C1 $\beta$  and lactose **14** to give 4-*O*-C1 $\beta$  product. Glycosylated/arylated products at 3-*O*- and 4-*O*- positions were detected from D-glucose **6** and D-galactose **7** in the catalysis with both the enzymes. No other reacted carbohydrate molecule has formed products at the 3<sup>rd</sup> OH position. Hydrolysis of lactose **14** was observed during the course of reaction and the resultant carbohydrate did not show any transglycosylated product.

Glucosidases employed did not catalyse the reaction with D-fructose **9**, D-arabinose **10**, D-ribose **11**, maltose **12** and sucrose **13** which could be due to stronger binding of DL-dopa **4** to the enzymes compared to these carbohydrate molecules, thereby preventing their facile transfer to the nucleophilic phenolic OH of DL-dopa **4**. Amyloglucosidase exhibited 'invertin' potentiality in reacting with D-galactose **7**. D-Galactose **7** showed 66%  $\alpha$  and 34%  $\beta$  compared to the 92:8  $\alpha$ :  $\beta$  anomeric composition of free D-galactose employed.

About 14 individual glycosides were synthesized enzymatically using both the glucosidases, of which 10 are being reported for the first time. The new glycosides reported are: DL-dopa-D-galactoside **35a-e**, DL-3-hydroxy-4-*O*-( $\beta$ -D-mannopyranosyl) phenylalanine **36**, DL-3-hydroxy-4-*O*-( $\beta$ -D-galactopyranosyl-(1'→4) $\beta$ -D-glucopyranosyl) phenylalanine **37**, DL-3-hydroxy-4-*O*-(6-D-sorbitol)phenylalanine **38** and DL-dopa-D-mannitol **39a,b**

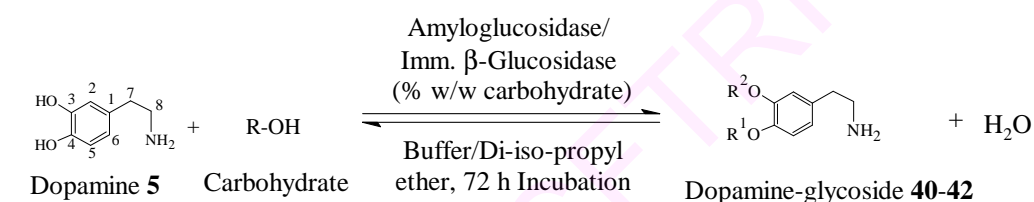
### 3.5 Syntheses of dopamine glycosides

Parkinson's disease is a neurodegenerative disease characterized by bradykinesia, tremors, rigidity and difficulty in walking (Geng *et al.* 2007; Geng *et al.* 2004). The usual treatment for this disorder is the use of L-dopa, which enters the central nervous system (CNS) through active transport and is enzymatically cleaved in the brain to release dopamine. To overcome the drawbacks of L-dopa treatment in transport problems across blood brain barrier (BBB), new derivatives of dopamine able to penetrate the BBB, by making use of specific transport systems (Pardridge 2002; Audus *et al.* 1992; Madrid *et al.* 1991) are employed. Glucose is the brain's source of energy and other hexoses are transported across the BBB by the glucose carrier GLUT1 (Mueckler 1994). Glycosyl dopamine derivatives bearing the sugar moiety linked to either the amino group or the catechol ring of dopamine through amide, ester or glycosidic bonds were synthesised chemically with potent anti-Parkinsonian properties (Fernandez *et al.* 2000). The glucosyl dopamine derivative is able to interact with the glucose transporter (GLUT1) and absorbed into the CNS from the blood stream (Dalpiaz *et al.* 2007). Glycosylated form of dopamine is stable in the periphery and after reaching the brain through GLUT1 carrier, gets hydrolyzed by the action of brain enzymes to release dopamine (Fernandez *et al.* 2003). Employing chemical methods for the synthesis of dopamine glycosides require protection and deprotection steps (Fernandez *et al.* 2003). Enzymatic method is



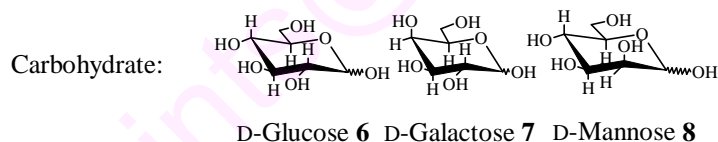
the alternative one which provides milder reaction conditions, easy workup, less pollution, higher yields and selectivity (Suzuki *et al.* 1996; Vic *et al.* 1992; Vijayakumar and Divakar 2007).

It is in this context, that the present work has been undertaken where dopamine is glycosylated using amyloglucosidase from *Rhizopus* mold and immobilized  $\beta$ -glucosidase in organic media to prepare dopamine glycosides.  $\beta$ -Glucosidase isolated from sweet almond was immobilized onto calcium alginate beads and used for the preparation (Section 2.2.4).



4-*O*-C1-gly/C6-arylated : R<sup>1</sup> = Carbohydrate, R<sup>2</sup> = H

3-*O*-C1-gly : R<sup>1</sup> = H, R<sup>2</sup> = Carbohydrate



### Scheme 3.5 Syntheses of dopamine glycosides

Synthesis of dopamine-D-glucosides involved refluxing dopamine **5** (0.25-2 mmol) with 1 mmol D-glucose **6** in 100 mL di-isopropyl ether in presence of amyloglucosidase (10-75 % w/w D-glucose) and 0.03 mM to 0.2 mM (0.3-2.5 mL) of 0.01 M pH 4-8 buffer for an incubation period of 72 h at 68 °C (Scheme 3.5). After the reaction, solvent was evaporated and the enzyme denatured at 100 °C by holding in boiling water bath for 5-10 min. The residue containing unreacted dopamine **5** and D-glucose **6** along with the product glucosides were dissolved in 15-20 mL of water and evaporated to dryness. The products were monitored by HPLC on an aminopropyl column (250 mm × 4.6 mm) using acetonitrile: water (70:30 v/v) as a mobile phase and

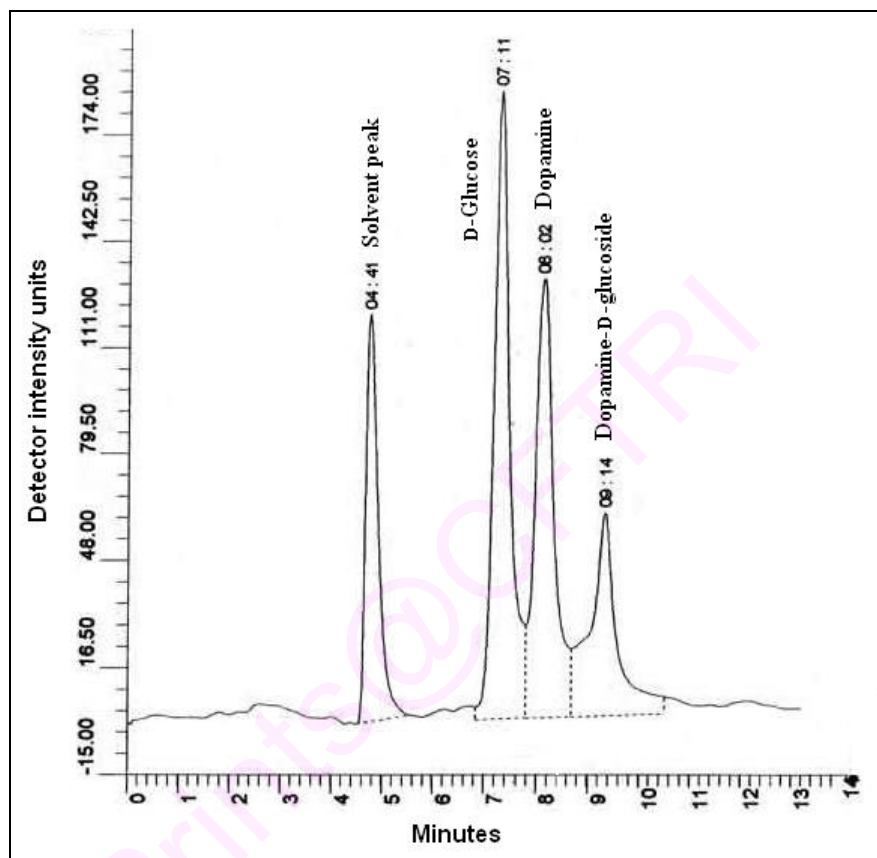


**Fig. 3.48** HPLC chromatogram for the reaction mixture of D-glucose and dopamine-D-glucoside. HPLC conditions: Aminopropyl column (10  $\mu\text{m}$ , 250 mm  $\times$  4.6 mm), solvent- $\text{CH}_3\text{CN}$ :  $\text{H}_2\text{O}$  (70:30 v/v), Flow rate-1 mL/min, RI detector. Retention times: D-glucose-7.1 min, dopamine-8 min and dopamine-D-glucoside-9.1 min

refractive index detector (Fig. 3.48). Other procedures are as described on page 74. HPLC retention times for the substrates and products are: dopamine-8.0 min, D-glucose-7.1 min, dopamine-D-glucoside-9.1 min, D-galactose-7.1 min, dopamine-D-galactoside-9.1 min, D-mannose-6.7 min and dopamine-D-mannoside-9.1 min.

### **3.5.1 Amyloglucosidase catalysed glucosylation of dopamine**

Enzymatic glucosylation between dopamine **5** and D-glucose **6** was optimized in terms of incubation period, pH, buffer, enzyme and dopamine concentrations using both amyloglucosidase (Section 3.5.1) and immobilized  $\beta$ -glucosidase (Section 3.5.2).

#### **3.5.1.1 Effect of incubation period**

The effect of incubation period was studied from 3 h to 120 h. Amyloglucosidase catalysis showed the highest conversion yield of 58% at 24 h incubation (Table 3.16). Further increase in incubation period resulted in a marginal drop in conversion between 48 - 96 h (Fig. 3.49A).

#### **3.5.1.2 Effect of pH**

For amyloglucosidase catalysis, the highest glucosylation yield of 35% was obtained at pH 6. No reaction was observed at pH 4 (Table 3.16).

#### **3.5.1.3 Effect of buffer concentration**

At pH 6, varying the buffer concentration from 0.03 mM to 0.25 mM (0.3 mL to 2.5 mL), resulted in a maximum conversion of 39% at 0.06 mM (0.6 mL) buffer concentration (Fig. 3.49B, Table 3.16).

#### **3.5.1.4 Effect of enzyme concentration**

Amyloglucosidase was varied from 10-75% (w/w D-glucose) at 1 mmol of D-glucose and 0.5 mmol dopamine. A 40 % (w/w D-glucose) amyloglucosidase showed the highest yield of 45% (Table 3.16) with 0.06 mM (0.6 mL) pH 6 phosphate buffer and 72 h of incubation.

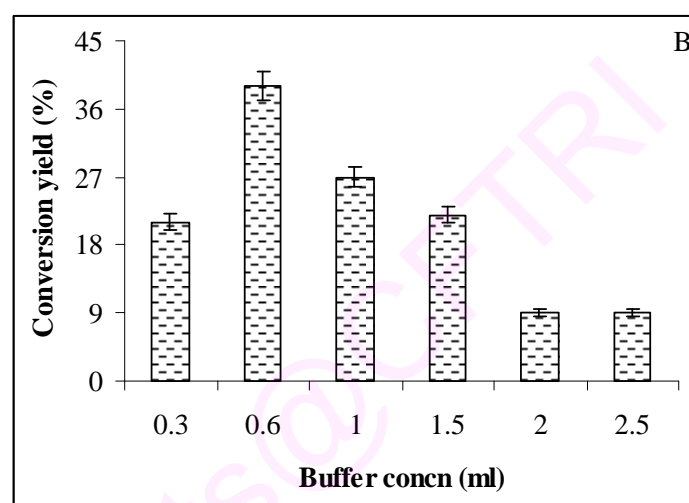
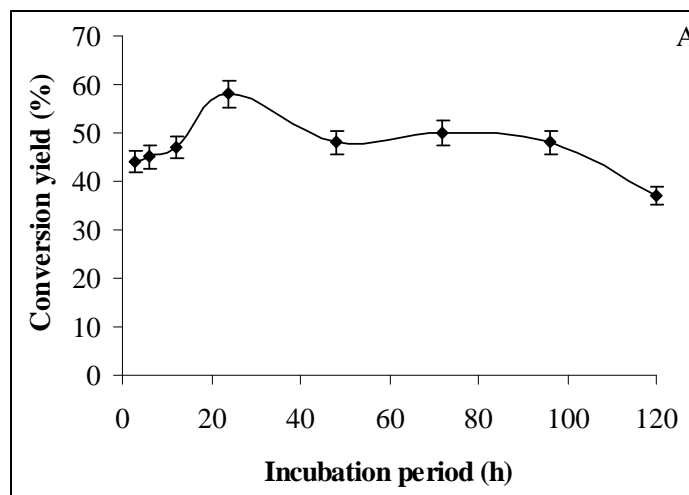


**Fig. 3.49 (A)** Reaction profile for dopamine-D-glucoside synthesis by the reflux method. Conversion yields were from HPLC with respect to 1 mmol of D-glucose. Reaction conditions: Dopamine-0.5 mmol, D-glucose-1 mmol, amyloglucosidase-40% (w/w D-glucose), 0.06 mM (0.6 mL), pH 6 phosphate buffer, solvent-di-isopropyl ether and temperature-68 °C and **(B)** Effect of buffer concentration for dopamine-D-glucoside synthesis. Reaction conditions: Dopamine-0.5 mmol, D-glucose-1 mmol, amyloglucosidase-30% (w/w D-glucose), pH 6 phosphate buffer, solvent-di-isopropyl ether, temperature-68 °C and incubation period – 72 h

**Table 3.16** Optimization of reaction conditions for the synthesis of dopamine-D-glucoside using amyloglucosidase

Reaction conditions	Variable parameter <sup>b</sup>	Conversion Yields (%) <sup>c</sup>
Incubation period (h)		
Dopamine – 0.5 mmol	3	44
D-Glucose – 1 mmol	6	45
pH – 6	12	47
Buffer concentration – 0.06 mM (0.6 mL)	24	58
Amyloglucosidase – 40 % w/w D-glucose	48	48
	72	52
	96	48
	120	37
pH (0.01M)		
Dopamine – 0.5 mmol <sup>a</sup>	4	No yield
D-Glucose – 1 mmol	5	16
Amyloglucosidase – 30 % w/w D-glucose	6	35
Buffer concentration – 1 mL (0.1 mM)	7	29
Incubation period – 72 h	8	23
Buffer concentration (mM)		
Dopamine – 0.5 mmol	0.03	21
D-Glucose – 1 mmol	0.06	39
Amyloglucosidase – 30 % w/w D-glucose	0.1	27
pH – 6	0.15	22
Incubation period – 72 h	0.2	9
	0.25	9
Amyloglucosidase (% w/w D-glucose)		
Dopamine – 0.5 mmol	10	13
D-Glucose – 1 mmol	20	26
pH – 6	30	34
Buffer concentration – 0.06 mM (0.6 mL)	40	45
Incubation period – 72 h	50	19
	75	21
Dopamine (mmol)		
pH – 6	0.25	33
Buffer concentration – 0.06 mM (0.6 mL)	0.5	50
D-Glucose – 1 mmol	0.75	48
Amyloglucosidase – 40 % w/w D-glucose	1	31
Incubation period – 72 h	1.5	25
	2	16

<sup>a</sup>Initial reaction conditions. <sup>b</sup>Other variables are the same as under reaction conditions, except the specified ones. <sup>c</sup>HPLC yields expressed with respect to 1 mmol D-glucose employed.

### 3.5.1.5 Effect of dopamine concentration

Dopamine concentration was varied from 0.25 mmol to 2 mmol at a fixed D-glucose concentration of 1 mmol. A 0.5 mmol of dopamine gave the maximum yield of

50%. Beyond 0.75 mmol increasing dopamine concentration led to drop in the yield (Table 3.16).

### 3.5.2 Immobilized $\beta$ -glucosidase catalysed glucosylation of dopamine

Optimum conditions for the glucosylation of dopamine using immobilized  $\beta$ -glucosidase was worked out. Synthesis of 3-hydroxy-4-*O*-( $\beta$ -D-glucopyranosyl)phenylethylamine involved refluxing dopamine **5** (0.25-2 mmol) with 1 mmol D-glucose **6** in 100 mL di-isopropyl ether in presence of imm.  $\beta$ -glucosidase (10-75 % w/w D-glucose) and 0.04 mM to 0.25 mM (0.4-2.5 mL) of 0.01 M pH 4-8 buffer for an incubation period of 3-120 h at 68 °C (Scheme 3.5). All other procedures are as described in Section 3.5.

Here also, immobilized  $\beta$ -glucosidase catalysed synthesis of 3-hydroxy-4-*O*-( $\beta$ -D-glucopyranosyl)phenylethylamine was optimized in terms of incubation period, pH, buffer, enzyme and dopamine concentrations.

#### 3.5.2.1 Effect of incubation period

Glucosylation yield increased gradually upto 72 h exhibiting the maximum conversion of 58% (Table 3.17, Fig. 3.50A). Imm.  $\beta$ -glucosidase showed that conversion yields increased with increasing incubation periods upto 72 h (yield-58%) and decreased beyond 96 h of incubation period (yield-35%).

#### 3.5.2.2 Effect of pH

In case of imm.  $\beta$ -glucosidase, the conversion yield was more or less same between pH 4 to pH 6 (yield-62%, 64% and 60% for pH 4, pH 5 and pH 6 respectively) and maximum glucosylation of 64% was observed at pH 5 (Table 3.17).

#### 3.5.2.3 Effect of buffer concentration

At pH 5, varying the buffer concentration from 0.04 mM to 0.25 mM (0.4 mL to 2.5 mL) yielded the maximum conversion of 65% at 0.04 mM (0.4 mL) buffer concentration (Table 3.17).

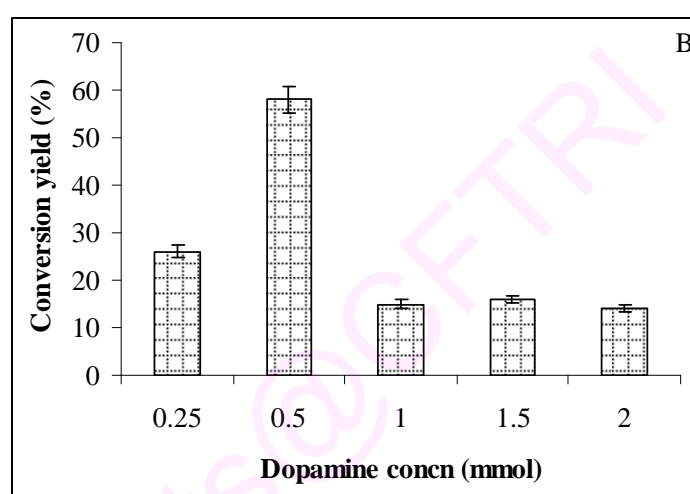
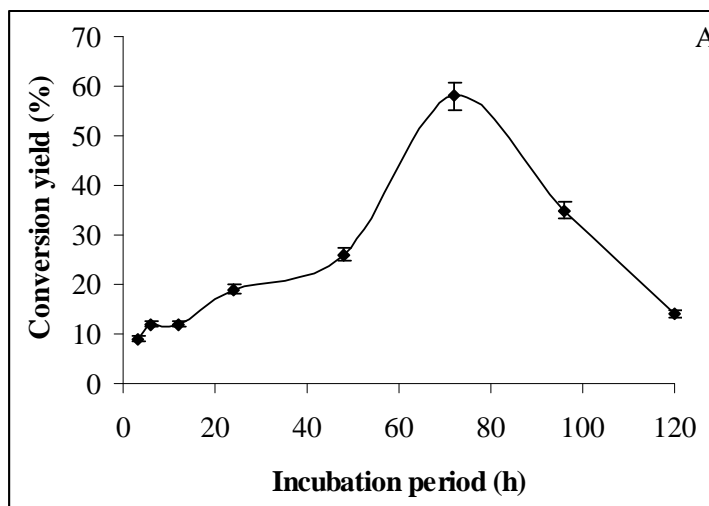


**Fig. 3.50** (A) Reaction profile for 3-hydroxy-4-*O*-( $\beta$ -D-glucopyranosyl)phenylethylamine synthesis by the reflux method. Conversion yields were from HPLC with respect to 1 mmol of D-glucose. Reaction conditions: Dopamine-0.5 mmol, D-glucose-1 mmol, imm.  $\beta$ -glucosidase-25% (w/w D-glucose), 0.04 mM (0.4 mL), pH 5 phosphate buffer, solvent-di-isopropyl ether and temperature-68 °C and (B) Effect of buffer concentration for 3-hydroxy-4-*O*-( $\beta$ -D-glucopyranosyl) phenylethylamine synthesis. Reaction conditions: D-glucose-1 mmol, imm.  $\beta$ -glucosidase-25% (w/w D-glucose), 0.04 mM - 0.4 mL, pH 5 phosphate buffer, solvent-di-isopropyl ether, temperature-68 °C and incubation period – 72 h.

**Table 3.17** Optimization of reaction conditions for the synthesis of 3-hydroxy-4-*O*-( $\beta$ -D-glucopyranosyl)phenylethylamine using imm.  $\beta$ -glucosidase

Reaction conditions	Variable parameter <sup>b</sup>	Conversion Yields (%) <sup>c</sup>
	Incubation period (h)	
Dopamine – 0.5 mmol	3	9
D-Glucose – 1 mmol	6	12
pH – 5	12	12
Buffer concentration – 0.04 mM (0.4 mL)	24	19
Imm. $\beta$ -Glucosidase – 25 % w/w D-glucose	48	26
	72	58
	96	35
	120	14
	pH (0.01M)	
Dopamine – 0.5 mmol <sup>a</sup>	4	62
D-Glucose – 1 mmol	5	64
Imm. $\beta$ -Glucosidase – 50 % w/w D-glucose	6	60
Buffer concentration – 0.1 mM (1 mL)	7	48
Incubation period – 72 h	8	42
	Buffer concentration (mM)	
Dopamine – 0.5 mmol	0.04	65
D-Glucose – 1 mmol	0.08	57
Imm. $\beta$ -Glucosidase – 50 % w/w D-glucose	0.12	56
pH – 5	0.18	35
Incubation period – 72 h	0.25	27
	Imm. $\beta$ -glucosidase concentration (% w/w D-glucose)	
Dopamine – 0.5 mmol	10	56
D-Glucose – 1 mmol	25	58
pH – 5	40	59
Buffer concentration – 0.04 mM (0.4 mL)	50	65
Incubation period – 72 h	75	21
	Dopamine (mmol)	
pH – 5	0.25	26
Buffer concentration – 0.04 mM (0.4 mL)	0.5	58
D-Glucose – 1 mmol	1	15
Imm. $\beta$ -Glucosidase – 25 % w/w D-glucose	1.5	16
Incubation period – 72 h	2	14

<sup>a</sup>Initial reaction conditions. <sup>b</sup>Other variables are the same as under reaction conditions, except the specified ones. <sup>c</sup>HPLC yields expressed with respect to 1 mmol D-glucose employed.

#### 3.5.2.4 Effect of enzyme concentration

Effect of imm.  $\beta$ -glucosidase concentration was studied by varying the enzyme concentration from 10-75% (w/w D-glucose) at 1 mmol of D-glucose and 0.5 mmol dopamine. Upto 50% (w/w D-glucose) imm.  $\beta$ -glucosidase the conversion yield did not



vary much between 56-65%. A maximum yield of 65% was observed with 50% (w/w D-glucose) imm.  $\beta$ -glucosidase (Table 3.17).

### 3.5.2.5 Effect of dopamine concentration

Dopamine concentration was varied from 0.25 mmol to 2 mmol at a fixed D-glucose concentration of 1 mmol. At the optimized conditions of pH 5, 0.04 mM (0.4 mL) buffer concentration and 25 % (w/w D-glucose), the highest conversion yield of 58% at 0.5 mmol dopamine was obtained. Beyond 0.5 mmol of dopamine, the conversion decreased and there was no significant change between 1 mmol and 2 mmol dopamine (Fig. 3.50B, Table 3.17).

### 3.5.3 Syntheses of dopamine glycosides of various carbohydrates using amyloglucosidase

Syntheses of the other dopamine glycosides were carried out under optimized conditions mentioned in Section 3.5.1, with dopamine **5** and carbohydrates: D-glucose **6**, D-galactose **7** and D-mannose **8**. The conditions employed for the amyloglucosidase catalysis are: dopamine **5** (0.5 mmol) and carbohydrate **6-8** (1 mmol), amyloglucosidase 40 % (w/w carbohydrate), 0.06 mM (0.6 mL) pH 6 phosphate buffer and 24 h of incubation period in di-isopropyl ether solvent (Scheme 3.5). Other procedures are described on pages 74 and 147.

### 3.5.4 Syntheses of dopamine glycosides of various carbohydrates using imm. $\beta$ -glucosidase

Syntheses of the other dopamine glycosides were carried out under optimized conditions mentioned in Section 3.5.2, with dopamine **5** and carbohydrates: D-glucose **6**, D-galactose **7**, D-mannose **8**. The conditions employed for the imm.  $\beta$ -glucosidase are: dopamine **5** (0.5 mmol) and carbohydrate **6-8** (1 mmol), imm.  $\beta$ -glucosidase 25 % (w/w carbohydrate), 0.04 mM (0.4 mL) pH 5 acetate buffer and 72 h of incubation period in di-

isopropyl ether solvent (Scheme 3.5). The other procedures are described on pages 74 and 147.

### 3.5.5 Spectral characterization

Isolated glycosides besides measuring melting point and optical rotation were also characterized by recording UV, IR, Mass and 2D-HSQCT spectra which provided good information about the nature and type of products.

**3,4-Dihydroxyphenylethylamine 5 (Dopamine):** Solid, decomposed at 241 °C, UV (H<sub>2</sub>O,  $\lambda_{\max}$ ): 199 nm ( $\sigma \rightarrow \sigma^*$ ,  $\epsilon_{199} - 41488 \text{ M}^{-1}$ ), 218.5 nm ( $\sigma \rightarrow \pi^*$ ,  $\epsilon_{218.5} - 7954 \text{ M}^{-1}$ ), 280 nm ( $n \rightarrow \pi^*$ ,  $\epsilon_{280} - 3515 \text{ M}^{-1}$ ) IR (stretching frequency,  $\text{cm}^{-1}$ ): 3368 (OH), 1498 (C=C), 1614 (CO), 2948 (CH), MS ( $m/z$ ) - 153.1 [M]<sup>+</sup>, 2D-HSQCT (DMSO-*d*<sub>6</sub>): <sup>1</sup>H NMR  $\delta_{\text{ppm}}$ : 6.69 (H-2), 6.47 (H-5), 6.63 (H-6), 2.70 (H-7), 2.91 (H-8); <sup>13</sup>C NMR  $\delta_{\text{ppm}}$  (125 MHz): 128.1 (C1), 115.9 (C2), 145.4 (C3), 144.2 (C4), 119.3 (C5), 116.2 (C6), 32.4 (C7), 40.4 (C8). Ultraviolet-visible spectra is shown in Fig. 3.51A.

**3.5.5.1 Dopamine-D-glucoside 40a-c:** Solid, UV ( $\lambda_{\max}$ ): 191.5 nm ( $\sigma \rightarrow \sigma^*$ ,  $\epsilon_{191.5} - 858 \text{ M}^{-1}$ ), 217 nm ( $\sigma \rightarrow \pi^*$ ,  $\epsilon_{217} - 184 \text{ M}^{-1}$ ), 276 nm ( $\pi \rightarrow \pi^*$ ,  $\epsilon_{276} - 84 \text{ M}^{-1}$ ), IR (stretching frequency,  $\text{cm}^{-1}$ ): 3348 (OH), 1196 (glycosidic aryl alkyl C-O-C asymmetrical), 1028 (glycosidic aryl alkyl C-O-C symmetrical), 1400 (C=C), 1652 (CO), 2944 (CH), MS ( $m/z$ ) - 316.2 [M+1]<sup>+</sup>, 2D-HSQCT (DMSO-*d*<sub>6</sub>) **3-Hydroxy-4-O-(D-glucopyranosyl) phenylethylamine: 4-O-C1 $\alpha$ -glucoside 40a** <sup>1</sup>H NMR  $\delta_{\text{ppm}}$  (500.13) **Glu:** 4.65 (H-1 $\alpha$ , d, J = 3.9 Hz), 3.18 (H-2 $\alpha$ ), 3.56 (H-5 $\alpha$ ), 3.42 (H-6 $\alpha$ ), **Dopamine:** 6.68 (H-2), 6.20 (H-5), 6.45 (H-6), 2.62 (H-7), 3.05 (H-8); <sup>13</sup>C NMR  $\delta_{\text{ppm}}$  (125 MHz) **Glu:** 95.9 (C1 $\alpha$ ), 70.5 (C2 $\alpha$ ), 70.5 (C5 $\alpha$ ), 62.6 (C6 $\alpha$ ), **Dopamine:** 115.3 (C2), 145.2 (C4), 115.9 (C6), 30.9 (C7), 49.4 (C8); **4-O-C1 $\beta$ -glucoside 40b:** Solid; mp: 133 °C, UV ( $\lambda_{\max}$ ): 192 nm ( $\sigma \rightarrow \sigma^*$ ,  $\epsilon_{192} - 3521 \text{ M}^{-1}$ ), 225.5 nm ( $\sigma \rightarrow \pi^*$ ,  $\epsilon_{225.5} - 1423 \text{ M}^{-1}$ ), 276.5 nm ( $\pi \rightarrow \pi^*$ ,  $\epsilon_{276.5} - 523 \text{ M}^{-1}$ ),

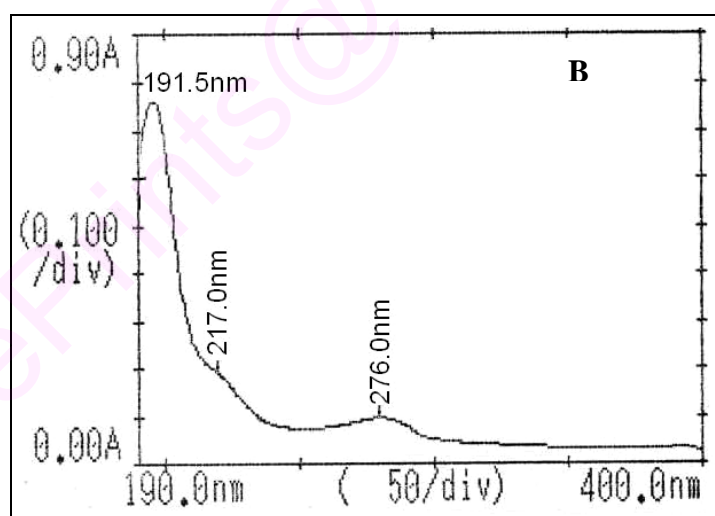
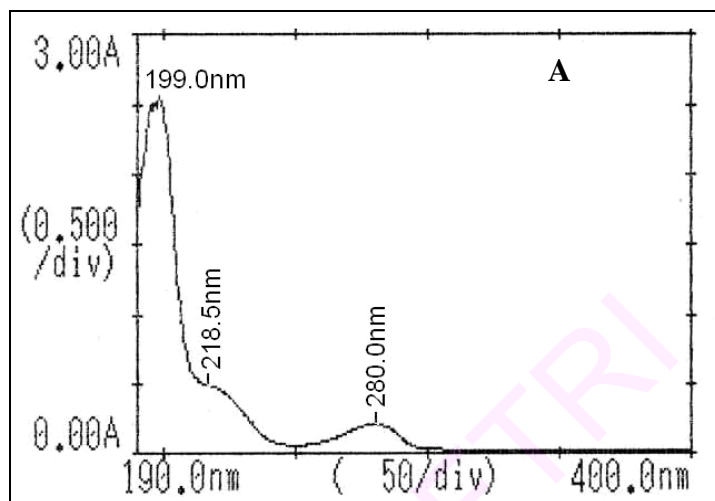


**Fig. 3.51** Ultraviolet-visible spectra of (A) Dopamine and (B) Dopamine-D-glucoside **40a-c**

<sup>1</sup>), IR (stretching frequency, cm<sup>-1</sup>): 3351 (OH), 1201 (glycosidic aryl alkyl C-O-C asymmetrical), 1031 (glycosidic aryl alkyl C-O-C symmetrical), 1412 (C=C), 1634 (CO), 2945 (CH), Optical rotation (*c* 0.5 H<sub>2</sub>O): [α]<sub>D</sub> at 25 °C = +12.6, MS (*m/z*) – 317.2 [M+2]<sup>+</sup>, 2D-HSQCT (DMSO-*d*<sub>6</sub>) <sup>1</sup>H NMR δ<sub>ppm</sub> (500.13 MHz) **Glu**: 4.98 (H-1β, d, J = 6.5 Hz), 2.91 (H-2β), 3.14 (H-3β), 3.62 (H-4β), 3.42 (H-5β), 3.55 (H-6a), **Dopamine**: 6.68 (H-2), 6.58 (H-5), 6.47 (H-6), 2.70 (H-7), 2.90 (H-8); <sup>13</sup>C NMR δ<sub>ppm</sub> (125 MHz) **Glu**: 101.8 (C1β), 74.8 (C2β), 77.6 (C3β), 72 (C4β), 77 (C5β), 63.9 (C6β), **Dopamine**: 128.1 (C1), 115.9 (C2), 145.4 (C3), 144.2 (C4), 118.7 (C5), 120 (C6), 40.5 (C7), 52.8 (C8); **4-Hydroxy-3-O-(β-D-glucopyranosyl)phenylethylamine 40c**: <sup>1</sup>H NMR **Glu**: 4.64 (H-1β, d, J = 7.8 Hz), 3.55 (H-6a), **Dopamine**: 6.20 (H-5), 3.54 (H-8), <sup>13</sup>C NMR **Glu**: 99 (C1β), 63.2 (C6β), **Dopamine**: 119.3 (C5), 52.4 (C8).

Ultraviolet-visible, IR, mass and 2D-HSQCT NMR spectra for dopamine-D-glucoside **40a-c** for amyloglucosidase catalysed products were shown in Figures 3.51B, 3.52A, 3.52B and 3.52C respectively. Infra-red and 2D-HSQCT NMR spectra for 3-Hydroxy-4-*O*-(β-D-glucopyranosyl) phenylethylamine **40b** for β-glucosidase catalysed product are shown in Figures 3.53A and 3.53B respectively.

**3.5.5.2 Dopamine-D-galactoside 41a-d**: Solid; UV (λ<sub>max</sub>): 193 nm (σ→σ\*, ε<sub>193</sub> – 1086 M<sup>-1</sup>), 219.5 nm (σ→π\*, ε<sub>219.5</sub> – 301 M<sup>-1</sup>), 284.5 nm (n→π\*, ε<sub>284.5</sub> – 110 M<sup>-1</sup>), IR (stretching frequency, cm<sup>-1</sup>): 3358 (OH), 1204 (glycosidic aryl alkyl C-O-C asymmetrical), 1078 (glycosidic aryl alkyl C-O-C symmetrical), 1407 (C=C), 1608 (CO), 2940 (CH), MS (*m/z*)-316.1 [M+1]<sup>+</sup>, 2D-HSQCT (DMSO-*d*<sub>6</sub>) **3-Hydroxy-4-O-(D-galactopyranosyl) phenylethylamine 4-O-C1α-galactoside 41a** <sup>1</sup>H NMR δ<sub>ppm</sub> (500.13 MHz) **Gal**: 4.98 (H-1α, d, J = 2.5 Hz), 3.56 (H-2α), 3.60 (H-3α), 3.70 (H-4α), 3.38 (H-5α), 3.38 (H-6a), **Dopamine**: 6.68 (H-2), 6.46 (H-5), 6.57 (H-6), 2.70 (H-7), 3.25 (H-8);

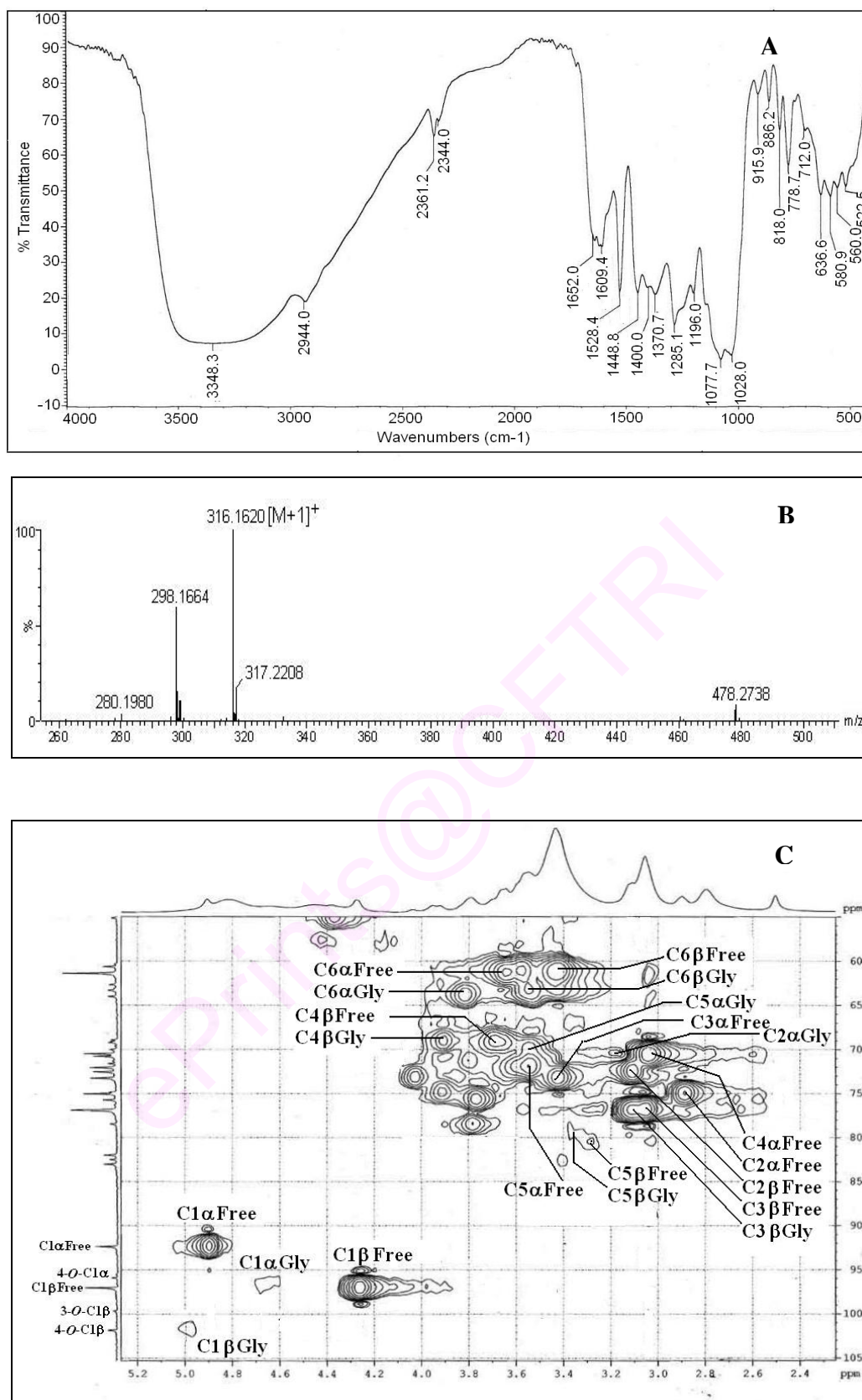


**Fig. 3.52** Dopamine-D-glucoside **40a-c** (A) IR spectrum, (B) Mass spectrum and (C) 2D-HSQC spectrum showing the C1-C6 region. Some of the assignments are interchangeable.

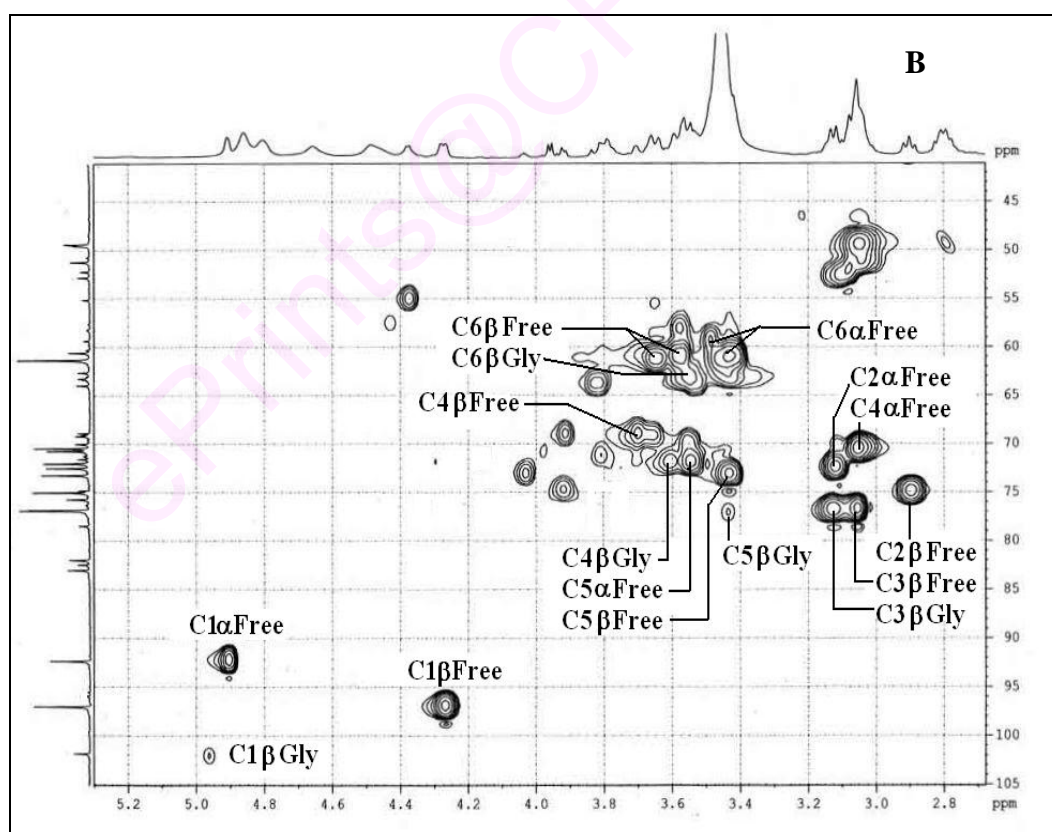
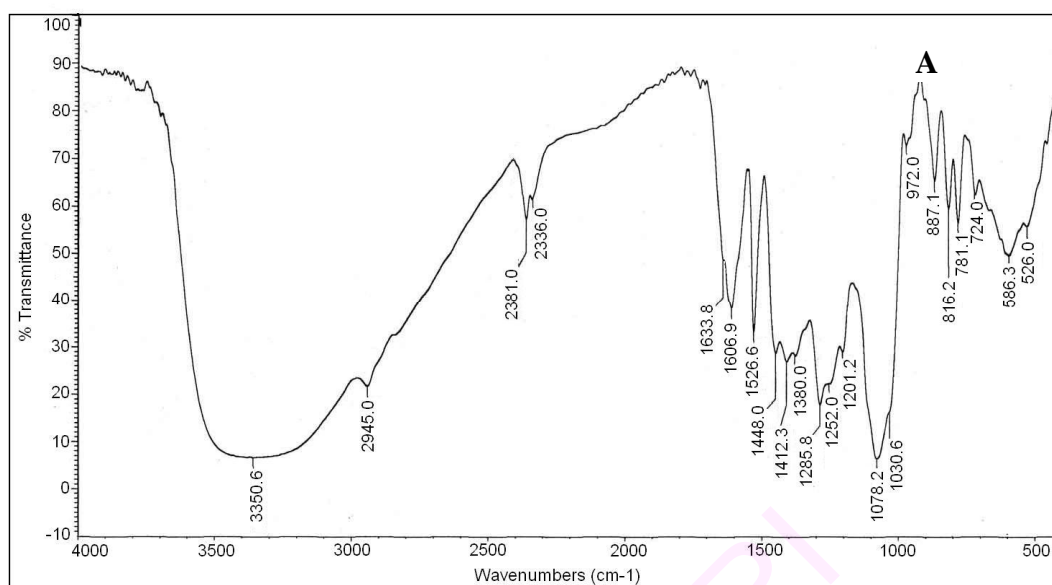


**Fig. 3.53** 3-Hydroxy-4-*O*-( $\beta$ -D-glucopyranosyl)phenylethylamine **40b** (A) IR spectrum and (B) 2D-HSQC spectrum showing the C1-C6 region. Some of the assignments are interchangeable

$^{13}\text{C}$  NMR  $\delta_{\text{ppm}}$  (125 MHz) **Gal**: 95.5 (C1 $\alpha$ ), 69 (C2 $\alpha$ ), 70.5 (C3 $\alpha$ ), 68.5 (C4 $\alpha$ ), 70.5 (C5 $\alpha$ ), 62.7 (C6 $\alpha$ ), **Dopamine**: 128 (C1), 115 (C2), 145.5 (C3), 144.5 (C4), 119.9 (C5), 116.1 (C6), 37.6 (C7), 49.4 (C8); **4-O-C1 $\alpha$ -galactoside 41b**  $^1\text{H}$  NMR  $\delta_{\text{ppm}}$  **Gal**: 4.90 (H-1 $\beta$ , d,  $J = 7.7$  Hz), 3.12 (H-2 $\beta$ ), 3.60 (H-3 $\beta$ ), 3.10 (H-4 $\beta$ ), 3.24 (H-5 $\beta$ ), 3.62 (H-6a); **Dopamine**: 6.74 (H-2), 6.45 (H-5), 2.80 (H-7), 3.08 (H-8);  $^{13}\text{C}$  NMR  $\delta_{\text{ppm}}$  **Gal**: 101.9 (C1 $\beta$ ), 72 (C2 $\beta$ ), 73 (C3 $\beta$ ), 70 (C4 $\beta$ ), 77 (C5 $\beta$ ), 63 (C6 $\beta$ ), **Dopamine**: 115.9 (C2), 123 (C5), 36 (C7), 52.3 (C8); **4-O-C6-O-arylated 41c**  $^1\text{H}$  NMR  $\delta_{\text{ppm}}$  **Gal**: 3.62 (H-6a);  $^{13}\text{C}$  NMR  $\delta_{\text{ppm}}$  **Gal**: 66.1 (C6 $\beta$ ), **4-Hydroxy-3-O-( $\alpha$ -D-galactopyranosyl)phenylethylamine 41d**  $^1\text{H}$  NMR  $\delta_{\text{ppm}}$  **Gal**: 4.64 (H-1 $\alpha$ , d,  $J = 2.6$  Hz), 3.55 (H-6a), **Dopamine**: 6.61 (H-2), 6.57 (H-5), 2.72 (H-7), 3.53 (H-8);  $^{13}\text{C}$  NMR  $\delta_{\text{ppm}}$  **Gal**: 95.8 (C1 $\alpha$ ), 63.2 (C6 $\alpha$ ), **Dopamine**: 128.1 (C1), 115.6 (C2), 120.6 (C5), 32.5 (C7), 52.4 (C8).

Mass and 2D-HSQCT NMR spectra for dopamine-D-galactoside **41a-d** are shown in Figures 3.54A and 3.54B respectively.

**3.5.5.3 Dopamine-D-mannoside 42a-c**: Solid, UV ( $\lambda_{\text{max}}$ ): 201 nm ( $\sigma \rightarrow \sigma^*$ ,  $\epsilon_{201} = 12868 \text{ M}^{-1}$ ), 222 nm ( $\sigma \rightarrow \pi^*$ ,  $\epsilon_{222} = 3376 \text{ M}^{-1}$ ), 286 nm ( $n \rightarrow \pi^*$ ,  $\epsilon_{286} = 1621 \text{ M}^{-1}$ ), IR (stretching frequency,  $\text{cm}^{-1}$ ): 3331 (OH), 1200 (glycosidic aryl alkyl C-O-C asymmetrical), 1079 (glycosidic aryl alkyl C-O-C symmetrical), 1448 (C=C), 1607 (CO), 2944 (CH), MS ( $m/z$ ) – 316.1  $[\text{M}+1]^+$ , 2D-HSQCT (DMSO- $d_6$ ) **3-Hydroxy-4-O-(D-mannopyranosyl)phenylethylamine: 4-O-C1 $\alpha$ -mannoside 42a**  $^1\text{H}$  NMR  $\delta_{\text{ppm}}$  (500.13) **Man**: 4.27 (H-1 $\alpha$ , d,  $J = 1.9$  Hz), 3.70 (H-2 $\alpha$ ), 3.70 (H-3 $\alpha$ ), 3.50 (H-4 $\alpha$ ), 3.39 (H-5 $\alpha$ ), 3.65 (H-6a), **Dopamine**: 6.66 (H-2), 6.47 (H-5), 6.55 (H-6), 2.72 (H-7), 2.92 (H-8),  $^{13}\text{C}$  NMR  $\delta_{\text{ppm}}$  (125 MHz) **Man**: 95.9 (C1 $\alpha$ ), 69 (C2 $\alpha$ ), 69.5 (C3 $\alpha$ ), 68 (C4 $\alpha$ ), 73 (C5 $\alpha$ ), 63.9 (C6 $\alpha$ ), **Dopamine**: 128.1 (C1), 115.3 (C2), 145.4 (C3), 144.5 (C4), 121.9 (C5), 119.3 (C6), 35.9 (C7), 51.2 (C8); **4-O-C1 $\beta$ -mannoside 42b**  $^1\text{H}$  NMR **Man**: 4.97 (H-1 $\beta$ , d,  $J = 3.9$



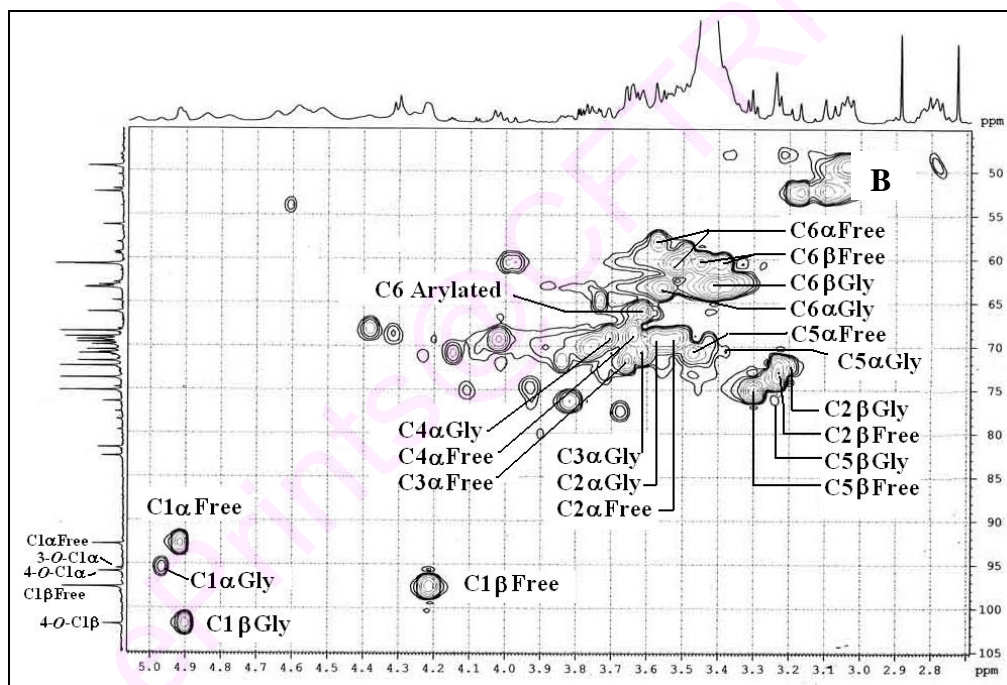
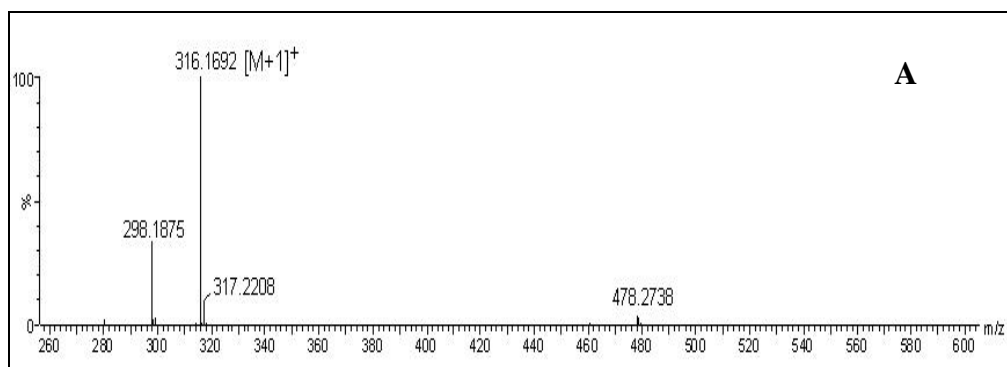


**Fig. 3.54** Dopamine-D-galactoside **41a-d** (A) Mass spectrum and (B) 2D-HSQC spectrum showing the C1-C6 region. Some of the assignments are interchangeable.



Hz), 3.18 (H-3 $\beta$ ), 3.39 (H-4 $\beta$ ), 3.12 (H-5 $\beta$ ), 3.55 (H-6a), **Dopamine**: 6.68 (H-2), 3.11 (H-8),  $^{13}\text{C}$  NMR  $\delta_{\text{ppm}}$  **Man**: 101.8 (C1 $\beta$ ), 71.5 (C3 $\beta$ ), 70 (C4 $\beta$ ), 76.5 (C5 $\beta$ ), 62.6 (C6 $\beta$ ), **Dopamine**: 129.4 (C1), 116.2 (C2), 52.8 (C8); **4-Hydroxy-3-O-( $\alpha$ -D-mannopyranosyl)phenylethylamine 42c**:  $^1\text{H}$  NMR **Man**: 4.58 (H-1 $\alpha$ , d, J = 3.9 Hz), 3.65 (H-6a), **Dopamine**: 6.80 (H-2), 2.68 (H-7), 2.85 (H-8),  $^{13}\text{C}$  NMR **Man**: 94.8 (C1 $\alpha$ ), 63.3 (C6 $\alpha$ ), **Dopamine**: 115.9 (C2), 41.1 (C7), 52.2 (C8).

Infra-red and 2D-HSQCT NMR spectra for dopamine-D-mannoside **42a-c** are shown in Figures 3.55A and 3.55B respectively.

Ultraviolet-visible spectra of dopamine glycosides, showed  $\sigma \rightarrow \sigma^*$  band ranging from 191.5 to 201 nm (199 nm for dopamine),  $\sigma \rightarrow \pi^*$  band ranging from 217 to 225.5 nm (218.5 nm for dopamine) and  $\pi \rightarrow \pi^*$  and  $n \rightarrow \pi^*$  band from 276 nm to 286 nm (280 nm for dopamine). IR spectra showed 1028-1079  $\text{cm}^{-1}$  band for the glycosidic C-O-C aryl alkyl symmetrical stretching and 1196-1204  $\text{cm}^{-1}$  band for the asymmetrical stretching frequencies. In 2D Heteronuclear Single Quantum Coherence Transfer (HSQCT) spectra, the respective chemical shift values showed glycoside formation: from D-glucose **6** 4-O-C1 $\alpha$  glucoside **40a** to C1 $\alpha$  at 95.9 ppm and H-1 $\alpha$  at 4.65 ppm, 4-O-C1 $\beta$  glucoside **40b** to C1 $\beta$  at 101.8 ppm and H-1 $\beta$  at 4.85 ppm and 3-O-C1 $\beta$  glucoside **40c** to C1 $\beta$  at 99 ppm and H-1 $\beta$  at 4.64 ppm; from D-galactose **7** 4-O-C1 $\alpha$  galactoside **41a** to C1 $\alpha$  at 95.5 ppm and H-1 $\alpha$  at 4.98 ppm, 4-O-C1 $\beta$  galactoside **41b** to C1 $\beta$  at 101.9 ppm and H-1 $\beta$  at 4.90 ppm, 4-O-C6-O-arylated **41c** to C6 at 66.1 ppm and H-6a at 3.62 ppm and 3-O-C1 $\alpha$  galactoside **41d** to C1 $\alpha$  at 95.8 ppm and H-1 $\alpha$  at 4.64 ppm; from D-mannose **8** 4-O-C1 $\alpha$  mannoside **42a** to C1 $\alpha$  at 95.9 ppm and H-1 $\alpha$  at 4.97 ppm, 4-O-C1 $\beta$  mannoside **42b** to C1 $\beta$  at 101.8 ppm and H-1 $\beta$  at 4.27 ppm and 3-O-C1 $\alpha$

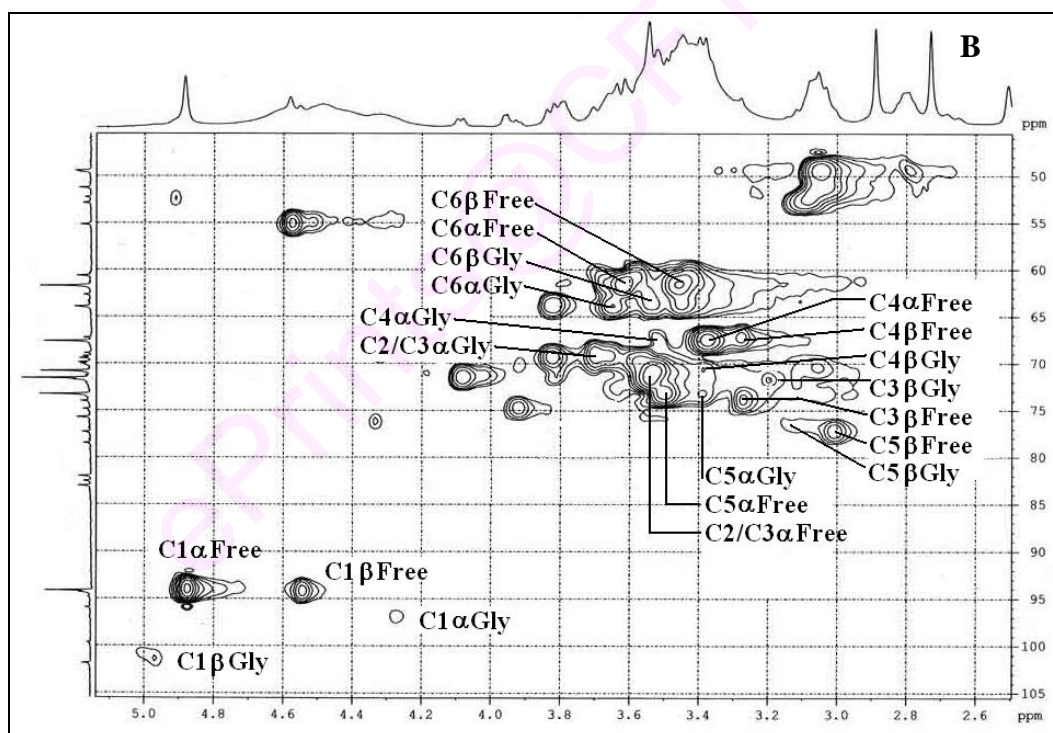
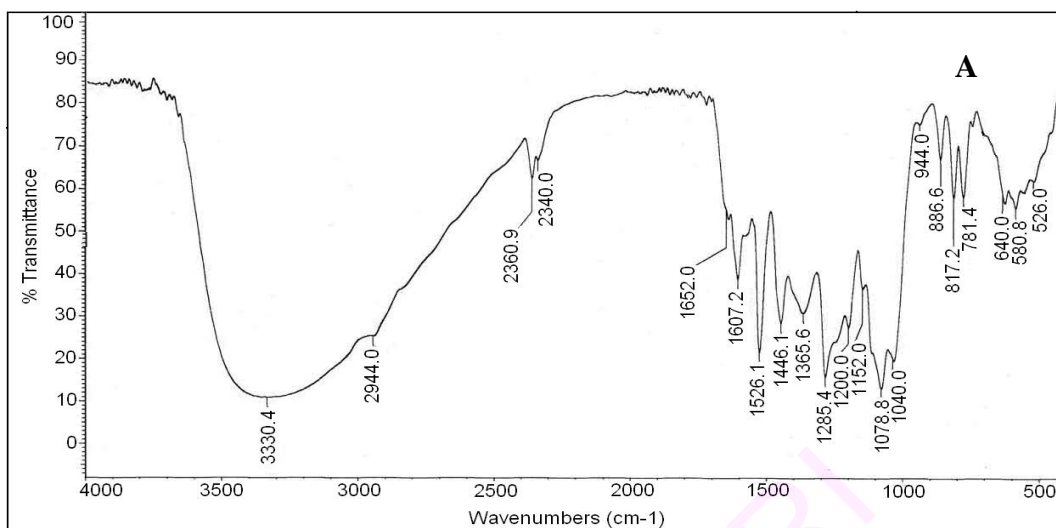


**Fig. 3.55** Dopamine-D-mannoside **42a-c** (A) IR spectrum and (B) 2D-HSQC spectrum showing the C1-C6 region. Some of the assignments are interchangeable.

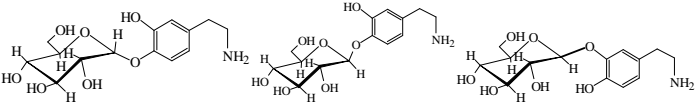
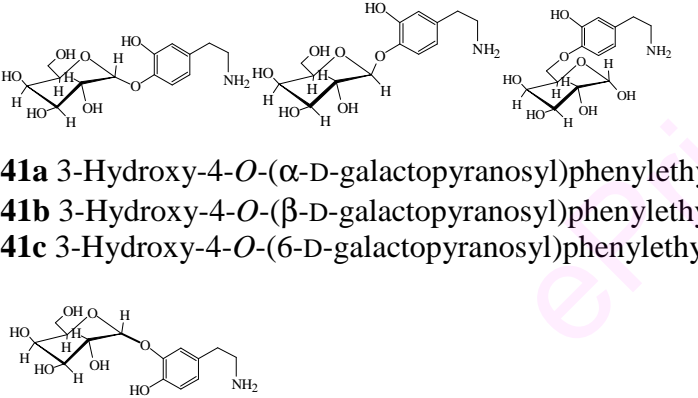
mannoside **42c** to C1 $\alpha$  at 94.8 ppm and H-1 $\alpha$  at 4.58 ppm. Mass spectral data also confirmed product formation.

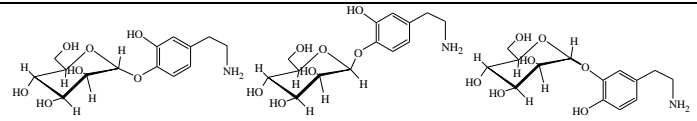
### 3.5.6 Discussion

Dopamine glycosides were synthesized with carbohydrates employing the optimized conditions. The products formed (Section 3.5.5) and the yields are shown in Table 3.18. Amyloglucosidase catalysis gave rise to 3-hydroxy-4-*O*-( $\alpha$ -D-glucopyranosyl)phenylethylamine **40a**, 3-hydroxy-4-*O*-( $\beta$ -D-glucopyranosyl)phenylethylamine **40b**, 4-hydroxy-3-*O*-( $\beta$ -D-glucopyranosyl)phenylethylamine **40c**, 3-hydroxy-4-*O*-( $\alpha$ -D-galactopyranosyl)phenylethylamine **41a**, 3-hydroxy-4-*O*-( $\beta$ -D-galactopyranosyl)phenylethylamine **41b**, 3-hydroxy-4-*O*-( $\beta$ -D-galactopyranosyl)phenylethylamine **41c**, 4-hydroxy-3-*O*-( $\alpha$ -D-galactopyranosyl)phenylethylamine **41d**, 3-hydroxy-4-*O*-( $\alpha$ -D-mannopyranosyl)phenylethylamine **42a**, 3-hydroxy-4-*O*-( $\beta$ -D-mannopyranosyl)phenylethylamine **42b** and 4-hydroxy-3-*O*-( $\alpha$ -D-mannopyranosyl)phenylethylamine **42c** (Table 3.18). Also, imm.  $\beta$ -glucosidase gave the above mentioned glycosides besides 3-hydroxy-4-*O*-( $\alpha$ -D-glucopyranosyl)phenylethylamine **40a** and 4-hydroxy-3-*O*-( $\beta$ -D-glucopyranosyl)phenylethylamine **40c** (Table 3.18).

Only monoglycosides were detected. Bis glycosides involving both the 4-OH and 3-OH phenolic groups simultaneously were not detected. Among the carbohydrates employed, both amyloglucosidase and immobilized  $\beta$ -glucosidase showed glycosylation with D-glucose **6**, D-galactose **7** and D-mannose **8**. Under the reaction conditions employed, immobilized  $\beta$ -glucosidase showed selectivity with D-glucose **6** to give rise to the 4-*O*-C1 $\beta$  product. Dopamine **5** gave a mixture of 3-*O*- and 4-*O*- glycosylated products with D-galactose **7** and D-mannose **8** with both the enzymes and 4-*O*-C6-*O*-arylated product detected only with D-galactose **7**.

**Table 3. 18** Syntheses of dopamine glycosides using amyloglucosidase and imm.  $\beta$ -glucosidase

Glycosides	Amyloglucosidase catalysis <sup>a</sup>		Imm. $\beta$ -Glucosidase catalysis <sup>b</sup>	
	Product (% proportions) <sup>c</sup>	Yields (%) <sup>d</sup>	Product (% proportions) <sup>c</sup>	Yields (%) <sup>d</sup>
 <b>40a</b> 3-Hydroxy-4- <i>O</i> -( $\alpha$ -D-glucopyranosyl)phenylethylamine <b>40b</b> 3-Hydroxy-4- <i>O</i> -( $\beta$ -D-glucopyranosyl)phenylethylamine <b>40c</b> 4-Hydroxy-3- <i>O</i> -( $\beta$ -D-glucopyranosyl)phenylethylamine	4- <i>O</i> -C1 $\alpha$ (57), 4- <i>O</i> -C1 $\beta$ (29), 3- <i>O</i> -C1 $\beta$ (14)	58	4- <i>O</i> -C1 $\beta$	65
 <b>41a</b> 3-Hydroxy-4- <i>O</i> -( $\alpha$ -D-galactopyranosyl)phenylethylamine <b>41b</b> 3-Hydroxy-4- <i>O</i> -( $\beta$ -D-galactopyranosyl)phenylethylamine <b>41c</b> 3-Hydroxy-4- <i>O</i> -(6-D-galactopyranosyl)phenylethylamine <b>41d</b> 4-Hydroxy-3- <i>O</i> -( $\alpha$ -D-galactopyranosyl)phenylethylamine	4- <i>O</i> -C1 $\alpha$ (21), 4- <i>O</i> -C1 $\beta$ (32), 4- <i>O</i> -C6- <i>O</i> -arylated (36), 3- <i>O</i> -C1 $\alpha$ (11)	32	4- <i>O</i> -C1 $\alpha$ (31), 4- <i>O</i> -C1 $\beta$ (26), 4- <i>O</i> -C6- <i>O</i> -arylated (33), 3- <i>O</i> -C1 $\alpha$ (10)	29

				
<b>42a</b> 3-Hydroxy-4- <i>O</i> -( $\alpha$ -D-mannopyranosyl)phenylethylamine	4- <i>O</i> -C1 $\alpha$ (29),		4- <i>O</i> -C1 $\alpha$ (29),	
<b>42b</b> 3-Hydroxy-4- <i>O</i> -( $\beta$ -D-mannopyranosyl)phenylethylamine	4- <i>O</i> -C1 $\beta$ (57),	40	4- <i>O</i> -C1 $\beta$ (55),	28
<b>42c</b> 4-Hydroxy-3- <i>O</i> -( $\alpha$ -D-mannopyranosyl)phenylethylamine	3- <i>O</i> -C1 $\alpha$ (14)		3- <i>O</i> -C1 $\alpha$ (16)	

<sup>a</sup>3,4-Dihydroxyphenylethylamine – 0.5 mmol and carbohydrate - 1 mmol; amyloglucosidase concentration 40% w/w of carbohydrate; solvent – di-isopropyl ether; buffer – 0.06 mM (0.6 mL) pH 6 phosphate buffer; incubation period – 24 h. <sup>b</sup>3,4-Dihydroxyphenylethylamine 0.5 mmol and carbohydrate – 1 mmol each; imm.  $\beta$ -Glucosidase concentration 25% w/w of carbohydrate; solvent – di-isopropyl ether; buffer – 0.04 mM (0.4mL) pH 5 acetate buffer; incubation period – 72 h. <sup>c</sup>The product proportions were determined from the area of respective <sup>1</sup>H/<sup>13</sup>C signals. <sup>d</sup>Conversion yields were from HPLC with respect to free carbohydrate. Error in yield measurements is  $\pm$  10%.

Amyloglucosidase exhibited its 'inverting' potentiality in the glycosylation of D-galactose **7** giving rise to 64% 4-*O*-products and 36% exclusively 3-*O*-C1 $\beta$  product compared to the 92:8  $\alpha$ :  $\beta$  anomeric composition of the D-galactose employed. Both amyloglucosidase and immobilized  $\beta$ -glucosidase did not catalyse the reaction with D-fructose **9**, D-arabinose **10**, D-ribose **11**, maltose **12**, sucrose **13**, lactose **14**, D-sorbitol **15** and D-mannitol **16** under the conditions employed. Dopamine **5** could be a better inhibitor to these enzymes compared to the carbohydrate molecules, thereby blocking the transfer of the carbohydrate molecules to the phenolic OH group of dopamine **5**.

About 10 glycosides were synthesized enzymatically using both the glucosidases, of which 7 are being reported for the first time. The new glycosides reported are: 3-hydroxy-4-*O*-( $\alpha$ -D-galactopyranosyl)phenylethylamine **41a**, 3-hydroxy-4-*O*-( $\beta$ -D-galactopyranosyl)phenylethylamine **41b**, 4-hydroxy-3-*O*-( $\alpha$ -D-galactopyranosyl)phenylethylamine **41c**, 3-hydroxy-4-*O*-( $\beta$ -D-galactopyranosyl)phenylethylamine **41d**, 3-hydroxy-4-*O*-( $\alpha$ -D-mannopyranosyl)phenylethylamine **42a**, 3-hydroxy-4-*O*-( $\beta$ -D-mannopyranosyl)phenylethylamine **42b** and 4-hydroxy-3-*O*-( $\alpha$ -D-mannopyranosyl)phenylethylamine **42c**.

### 3.6 General discussion

In the present work, optimized reaction conditions were worked out for the syntheses of glycosides of vanillin, N-vanillyl-nonanamide, curcumin, DL-dopa and dopamine. Optimum conditions were determined for these glycosylation reactions by studying the effect of various parameters like incubation period, pH, buffer concentrations, enzyme and substrate concentrations. In most of the glycosylation reactions, the conversion yields increased upto certain range and thereafter remained as such or decreased significantly. This complex glycosylation reaction is not controlled by kinetic factors or thermodynamic factors or water activity alone but by a interplay of more than one of these factors.

Effect of incubation period showed that the yield increased upto a time period of 72 h and then showed a remarkable drop at still higher incubation periods, which could be due to partial hydrolysis of the glycosides formed after 72 h. Since the enzymes could not be recovered, they were not reused again. Hence, the activity of the enzyme after the reaction could not be determined. Refluxing di-isopropyl ether for a specified incubation period did not produce any peroxides in these glycosylation reactions.

Glycosylation described in the present work did not occur without the use of enzyme. Glycosidase reactions occur only in presence of certain amount of water (Ljunger *et al.* 1994; Vic and Crout 1995; Vijayakumar *et al.* 2007), whose presence in the reaction mixture could be regulated carefully to get a good glycosylation yield. Besides imparting 'pH memory', added water is essential for the integrity of the three-dimensional structure of the enzyme molecule and therefore its activity (Dordick 1989) in a non polar solvent like di-isopropyl ether (Vijayakumar and Divakar 2005). Water has been added in the form of 10 mM buffer. When buffer concentration (buffer volume) was varied, the lower and higher buffer concentrations (buffer volume) resulted in lesser conversion yields. A lower buffer concentration may not be sufficient to keep the active conformation of the enzyme and a higher buffer concentrations could result in hydrolysis of the product.

Beyond a critical water concentration, glycosylation decreased due to the size of the water layer formed around the enzyme retarding the transfer of the glycosyl donor to the active site of the enzyme (Humeau *et al.* 1998; Camacho *et al.* 2003) besides renders water layer surrounding the enzymes more flexible by forming multiple H-bonds and interacting with organic solvent causing denaturation (Valiveti *et al.* 1991). The protonation of the ionizable groups during the addition of buffer on the enzyme could be controlled by the type and availability of the counter ions as well as hydrogen ions

resulting in 'pH memory' and the increase in ionic strength could play a favourable role in glycosylation (Patridge *et al.* 2001). The carbohydrate molecule could also reduce the water content of the reaction mixture. Adachi and Kobayashi (2005) have reported that the hexose, which is more hydrated, decreased the water activity in the system and shifts the equilibrium towards synthesis. The effect of pH showed that pH 4 for vanillin **1** and curcumin **3**, pH 7 for N-vanillyl-nanamide **2**, pH 6 for DL-dopa **4** and pH 5, 6 for dopamine **5** are the best for obtaining maximum conversion. The three dimensional structure of the enzyme upto pH 7 may still retain a highly active conformation. However, pH 8 was not the optimum one for any of the phenols employed.

At lesser enzyme concentrations, for a given amount of substrates (enzyme/substrate ratio low), rapid exchange between bound and unbound forms of both the substrates (carbohydrates and the aglycon) with the enzyme (on a weighted average based on binding constant values of both the substrates) leaves substantial number of unbound substrate molecules at the start of the reaction which decrease progressively as conversion takes place (Romero *et al.* 2003; Marty *et al.* 1992). This becomes more so, if one of them binds more firmly to the enzyme than the other (higher binding constant value) as the respective enzyme/substrate ratios keep changing (during the course of the reaction) unevenly till the conversion stops due to complete binding (inhibition) of the predominant substrate. At intermediary enzyme concentrations, such a competitive binding results in favourable proportions of bound and unbound substrates to effect quite a good conversion. At higher enzyme concentrations, most of the substrates would be in the bound form leading to inhibition and lesser conversion (higher enzyme/substrate ratios). Also, the glycosylation reaction requires larger amount of enzyme compared to hydrolysis. Effect of enzyme concentration at a fixed D-glucose concentration, showed a maximum conversion at around 40 % (w/w D-glucose) in many cases. At higher



concentrations of both glucosidases, conversion yields decreased probably due to inhibition of the enzyme by the phenols employed. While this leads to lesser selectivity, they also give rise to varying bound and unbound substrate concentrations till the conversion ends. For a given amount of enzyme and substrates there is no increase in conversion beyond 72 h to 120 h. Longer incubation periods of especially lesser enzyme concentrations could also result in partial enzyme inactivation. However, not all the enzyme is inactivated before the end of the reaction.

Phenols employed in the present work increased the conversions upto certain concentration which thereafter decreased or remained as such. This could be due to competitive binding between the substrates (Phenol/D-glucose) the active site (binding site) of glucosidases, where the more efficiently bound phenol displaces the bound D-glucose leading to the formation of the dead-end phenol-enzyme complex. This may not happen at lower concentrations of phenols employed.

Both amyloglucosidase and  $\beta$ -glucosidase (native/immobilized) did not catalyse the reaction with D-fructose **9** and D-arabinose **10** with any of the phenols employed. Also, while  $\beta$ -glucosidase (native/immobilized) catalysed reaction with lactose **14**, amyloglucosidase did not. Hence, D-fructose **9** and D-arabinose **10** could not result in not-so-facile formation of the required oxo-carbenium ion intermediate (Chiba 1997) during the catalytic action of the enzyme, which is an essential requirement for glycosylation. Since the carbohydrate molecules not reacting with the five phenols studied varied with the phenol employed, it could be concluded that the phenols are better inhibitor of these enzymes compared to the specific unreactive carbohydrate molecules. During hydrolysis of amylose, the  $\alpha$ -1,4 linked glucose units gets hydrolysed which give rise to  $\beta$ -D-glucose by amyloglucosidase. This clearly showed that amyloglucosidase possess 'invertin' potentiality. The same behavior was observed in

the glycosylation reaction also. In general amyloglucosidase catalyses gave C1  $\alpha$  and  $\beta$  glycosides along with C6-*O*-aryl derivatives. However,  $\beta$ -glucosidase (native/immobilized) catalyses gave exclusively C1 $\beta$  glycosides in several cases, indicating its capability to exhibit excellent regioselectivity in this glycosylation with the carbohydrate molecules.

In curcumin **3**, the phenolic OH group present at both phenolic ring which underwent glycosylation gave rise to bis-glycosylated products. Even presence of an hydrophobic bulky alkyl side chain as in case of *N*-vanillyl-nonanamide **2** and curcumin **3** did not pose much of a steric hindrance when the carbohydrate molecules were transferred to its phenolic OH group. Among the phenols employed, vanillin **1** and *N*-vanillyl-nonanamide **2** showed glycosylation with many of the carbohydrates employed. None of the secondary hydroxyl group of the carbohydrates reacted with the phenols. Only primary hydroxyl group and the C1 OH reacted, the former in some cases and the latter in many carbohydrate molecules.

All the phenols employed invariably reacted with aldohexoses (D-glucose **6**, D-galactose **7** and D-mannose **8**) employed to yield respective glycosides except in the reaction between *N*-vanillyl-nonanamide **2** and D-mannose **8**. Dopamine **5** showed exclusively glycosylation only with aldohexoses.

Hydrolysis of the disaccharides maltose **12**, sucrose **13** and lactose **14** during the course of the reaction has been observed and only in case of sucrose **13** the resultant glucose formed, underwent transglycosylation to give rise to C1 $\beta$  glucosylated and C6-*O*-arylated products with vanillin **1**. Other phenols employed did not show any such reaction with hydrolysed carbohydrate molecules. In general, glucosylated products were formed in higher proportions compared to other carbohydrates molecules. The loss of regioselectivity in many of the glycosylation reactions could be due to the employment

of large amount of the enzymes. This is inevitable, as the reversible reaction required such large concentrations of enzyme to be employed.

About 61 individual glycosides were synthesized enzymatically using both the glucosidases, of which 45 are being reported for the first time. New glycosides reported are: 4-*O*-(D-galactopyranosyl)vanillin **18a,b**, 4-*O*-(D-mannopyranosyl)vanillin **19a,b**, 4-*O*-( $\alpha$ -D-glucopyranosyl-(1'→4)D-glucopyranosyl)vanillin **20a-d**, 4-*O*-(D-fructofuranosyl-(2→1')  $\alpha$ -D-glucopyranosyl)vanillin **21a,b**, 4-*O*-( $\beta$ -D-galactopyranosyl-(1'→4) $\beta$ -D-glucopyranosyl)vanillin **22**, 4-*O*-(D-sorbitol)vanillin **23a-c**, 4-*O*-(D-galactopyranosyl)N-vanillyl-nonanamide **25a,b**, 4-*O*-( $\beta$ -D-mannopyranosyl)N-vanillyl-nonanamide **26**, 4-*O*-(D-ribofuranosyl)N-vanillyl-nonanamide **27a,b**, 4-*O*-( $\alpha$ -D-glucopyranosyl-(1'→4)D-glucopyranosyl)N-vanillyl-nonanamide **28a-d**, 4-*O*-( $\beta$ -D-galactopyranosyl-(1'→4) $\beta$ -D-glucopyranosyl)N-vanillyl-nonanamide **29**, 1,7-*O*-(bis- $\beta$ -D-galactopyranosyl)curcumin **31b**, 1,7-*O*-(bis- $\beta$ -D-mannopyranosyl)curcumin **32b**, 1,7-*O*-(bis- $\beta$ -D-galactopyranosyl-(1'→4) $\alpha$ -D-glucopyranosyl)curcumin **33a,b**, DL-dopa-D-galactoside **35a-e**, DL-3-hydroxy-4-*O*-( $\beta$ -D-mannopyranosyl)phenylalanine **36**, DL-3-hydroxy-4-*O*-( $\beta$ -D-galactopyranosyl-(1'→4) $\beta$ -D-glucopyranosyl)phenylalanine **37**, DL-3-hydroxy-4-*O*-(6-D-sorbitol)phenylalanine **38**, DL-dopa-D-mannitol **39a,b**, dopamine-D-galactoside **41a-d** and dopamine-D-mannoside **42a-c**.

All the phenols employed in this study possesses one or two phenolic groups – one invariably at the 4<sup>th</sup> position and another as such DL-dopa **4**, dopamine **5** or modified to a OCH<sub>3</sub> group (vanillin **1**, N-vanillyl-nonanamide **2** and curcumin **3**). However, both the OH groups have reacted giving monoglycosides and arylated products but no bis derivatives in case of DL-dopa **4** and dopamine **5** were observed. In curcumin **3** both the phenolic OH groups on either side reacted to give a bis products. Hence, the presence of bulky groups *para* to 4-OH did not hinder formation of glycoside. Thus, this study shows

that selected phenolic glycosides, could be synthesized enzymatically using amyloglucosidase from *Rhizopus* mold and  $\beta$ -glucosidase (isolated from sweet almond and immobilized) to produce more water soluble and stable derivatives with diverse carbohydrate molecules. A reasonable extent of selectivity exhibits by these enzyme have been utilized for the preparation of the glycosides, thereby eliminating the need for elaborate protective and de-protective strategies (Roode *et al.* 2003).

### **3.7 Experimental**

#### **3.7.1 Glycosylation procedures**

Procedure for the syntheses of vanillyl glycosides, N-vanillyl-nonanamide glycosides, curcuminyl-bis-glycosides, DL-dopa glycosides and dopamine glycosides are described in their respective Sections (3.1, 3.2, 3.3, 3.4 and 3.5).

#### **3.7.2 Response surface methodology**

A Central Composite Rotatable Design (CCRD) was employed for response surface methodology study with five variable at five levels. The five variables employed were vanillin concentration, glucosidase concentration, buffer volume, pH and incubation period, in case of both the glucosidases. The experimental design included 32 experiments of five variables at five levels (-2, -1, 0, +1, +2). The variables employed range of vanillin **1** - 0.5-2.5 mmol, maltose **12** - 0.5 mmol and amyloglucosidase/ $\beta$ -glucosidase - 10 to 50% w/w maltose. These were refluxed in a 150 mL two necked flat bottomed flask containing 100 mL of di-isopropyl ether solvent and 0.04 mM – 0.2 mM (0.4 mL - 2 mL) of 10 mM pH 4 to 8 buffer with stirring for specified incubation periods of 24 to 120 h.

#### **3.7.3 High Performance Liquid Chromatography**

HPLC analysis on a Shimadzu SLC 6A, Kyoto, Japan, was employed for HPLC. Two measurements amino propyl columns - LiChrosorb 100 Å, 5  $\mu$ m, 300 mm  $\times$  3.9 mm

and Phenomenex 100 Å, 5 µm, 250 mm × 4.6 mm were employed. They were equilibrated and eluted with acetonitrile:water 70:30 at a flow rate of 1mL/min and detected using Refractive Index Detector.

### 3.7.4 Size exclusion chromatography

Glycosides were separated using a Sephadex G25 (100 cm × 1 cm) column, eluting with water at a flow rate of 1 mL/h. The fractions were pooled by performing thin layer chromatography by spotting individual fractions on silica plate. Silica plates were prepared by dissolving 8 g of silica gel (mesh 60-120) in 20 mL of water spreaded uniformly over a 20 × 20 cm glass plate. Air and oven dried plates were used for separation of the compounds by using *n*-butanol: acetic acid: water (v/v/v 70:20:10) as mobile phase. The spots were identified by spraying sugar spray and kept in hot air oven at 100 °C for 20 minutes to obtain colored spots. Sugar spray was prepared by dissolving 1.46 g of α-naphthol in 41 mL of ethanol to which was added 3.4 mL of water and 5.6 mL of concentrated sulfuric acid. The fractions containing product glycoside were evaporated on a water bath and subjected to spectral characterization.

### 3.7.5 Solubility

A known amount of glycoside was saturated with a measured amount of water at 25 °C. After the saturation, the undissolved glycoside was removed by filtration from the solution and dried. The dried residue was weighed from which the amount of the dissolved glycoside was determined.

### 3.7.6 Spectral characterization

#### 3.7.6.1 UV-visible spectroscopy

Ultraviolet-visible spectra were recorded on a Shimadzu UV-1601, Kyoto, Japan spectrophotometer. Known concentrations of the samples in the range 5-10 mg dissolved respective solvents (indicated in spectral data) were used for recording the spectra.

### 3.7.6.2 IR spectroscopy

Infra-red spectra were recorded on a Nicolet-FTIR, Madison, USA spectrophotometer. Isolated solid glycoside samples (5-8 mg) were prepared as KBr pellets and employed for recording the IR spectra. Phenol standards were employed as such between KBr plates to obtain IR spectra.

### 3.7.6.3 Mass spectroscopy

Mass spectra of the isolated glycosides were recorded using a Q-TOF Waters Ultima, instrument (No.Q-Tof GAA 082, Waters Corporation, Manchester, UK) fitted with an electron spray ionization (ESI) source. Known concentration of the samples were dissolved in water and injected for recording the mass.

### 3.7.6.4 Polarimetry

Specific rotation of the isolated glycosides was measured at 25 °C using Perkin-Elmer 243, West Germany, polarimeter with a 0.5 % aqueous solution.

### 3.7.6.5 Melting point

Melting point of the glycosides was determined by the capillary method. A capillary tube containing the sample was stuck to a thermometer and suspended in the paraffin liquid in a beaker. The paraffin liquid was heated slowly and evenly with the help of a Bunsen burner. The temperature range over which the sample was observed to melt was taken as the melting point.

### 3.7.6.6 <sup>1</sup>H NMR

<sup>1</sup>H NMR spectra were recorded on a Brüker DRX 500 MHz NMR, Fallanden, Switzerland, spectrometer (500.13MHz). Proton pulse width was 12.25 μs. Sample concentration of about 40 mg of the sample dissolved in DMSO-*d*<sub>6</sub> was used for recording the spectra at 35 °C. About 100-200 scans were accumulated to get a good spectrum. The region between 0-10 ppm was recorded for all the samples. Chemical

shift values were expressed in ppm relative to internal tetra-methyl silane (TMS) as the standard.

### 3.7.6.7 $^{13}\text{C}$ NMR

$^{13}\text{C}$  NMR spectra were recorded on a Bruker DRX 500 MHz NMR, Fallanden, Switzerland, spectrometer (125MHz). Carbon  $90^\circ$  pulse width was 10.5  $\mu\text{s}$ . Sample concentration of about 40 mg dissolved in  $\text{DMSO-}d_6$  was used for recording the spectra at 35  $^\circ\text{C}$ . About 500 to 2000 scans were accumulated for each spectrum. A region from 0-200 ppm was scanned. Chemical shift values were expressed in ppm relative to internal tetramethyl silane (TMS) as the standard.

### 3.7.6.8 2D HSQCT NMR

Two-dimensional Heteronuclear Single Quantum Coherence Transfer Spectra (2-D HSQCT) were recorded on a Bruker DRX 500 MHz NMR, Fallanden, Switzerland, spectrometer (500.13 MHz for  $^1\text{H}$  and 125 MHz for  $^{13}\text{C}$ ). A sample concentration of about 40 mg in  $\text{DMSO-}d_6$  was used for recording the spectra. Other parameters employed were described in Section 2.2.9.6.

ePrints@CFTRI

**Chapter 4**

***Enzymatic syntheses of riboflavin, ergocalciferol  
and  $\alpha$ -tocopherol glycosides***



## Introduction

Vitamins are organic compounds that are required in small amounts for the normal functioning of the body and maintenance of metabolic integrity. As with many other biologically active compounds, glycoside derivatives of vitamins have been identified and their properties investigated. The formation of glycosylated derivatives of vitamins-whether naturally in plants, animals, or microorganisms or by intentional chemical modifications-represents a process that may cause dramatic changes in chemical, nutritional and metabolic properties. Vitamins, like riboflavin (vitamin B2) is a water-soluble one belonging to the B-complex group that is important for optimal body growth, erythrocyte production and helps in releasing energy from carbohydrates (LeBlane *et al.* 2005; Bates 1993). Ergocalciferol (vitamin D2) is not only a nutrient, but also a precursor of a steroid hormone with a range of activities that include roles in calcium metabolism and cell differentiation. Its derivatives can be useful agents for treatment of several forms of cancer. Their differentiating and antiproliferative activities are undergoing intense scrutiny currently (Smith *et al.* 1999; James *et al.* 1999; Peehl *et al.* 2003; Wieder *et al.* 2003 and Chen *et al.* 2003).  $\alpha$ -Tocopherol (vitamin E) has been shown to be a very important component of biological membranes, where it acts mainly as a potent antioxidant and radical scavenger (Burton *et al.* 1983) and contribute to membrane stabilization (Witkowski 1998). Some vitamins are prone to degradation and some have very less bio-availability in the human system like fat-soluble vitamins. In order to overcome such type of problems the present work attempts to develop their glycosylated forms.

This chapter describes the glycosylation of vitamins. Glycosylation of both fat soluble and less water soluble vitamins renders them more water soluble, thereby aiding in bioavailability, stability and accessibility to biological systems. Hence, glycosylation

of riboflavin (vitamin B2), ergocalciferol (vitamin D2) and  $\alpha$ -tocopherol (vitamin E) are investigated in the present work. All these vitamins possess OH groups present in their structure in the form of ribitol OH in riboflavin, acyclic OH in ergocalciferol and phenolic OH in  $\alpha$ -tocopherol. Glycosylating efficiency of amyloglucosidase from *Rhizopus* mold and  $\beta$ -glucosidase isolated from sweet almond has been investigated in detail. These results are presented below.

### Present work

The present chapter describes optimization and syntheses of selected vitamin glycosides of riboflavin (vitamin B2) **43**, ergocalciferol (vitamin D2) **44** and  $\alpha$ -tocopherol (vitamin E) **45** by reflux method using amyloglucosidase from *Rhizopus* mold and  $\beta$ -glucosidase from sweet almond in di-isopropyl ether solvent. The carbohydrate molecules employed for the glycoside preparations are: aldohexoses - D-glucose **6**, D-galactose **7**, D-mannose **8**, ketohexose - D-fructose **9**, aldopentoses - D-arabinose **10**, D-ribose **11**, disaccharides - maltose **12**, sucrose **13**, lactose **14** and sugar alcohols - D-sorbitol **15** and D-mannitol **16**. Glycosylation reaction was conducted as described in the previous Section in the presence of 0.01 M buffer employing acetate buffer for pH 4 and pH 5, phosphate buffer for pH 6 and pH 7 and borate buffer for pH 8. The reactions were investigated in terms of incubation period, pH, buffer, enzyme and substrate concentrations, regio and stereo selectivity. All the experiments were performed in duplicate. Unless otherwise stated, the glycosides prepared were analyzed by HPLC on an aminopropyl column (250 mm  $\times$  4.6 mm) eluted with 70:30 (v/v) acetonitrile:water at a flow rate of 1 mL/h and monitored using a RI detector. Conversion yields were determined from HPLC peak areas of the glycoside and free carbohydrate and expressed with respect to free carbohydrate concentration. Error based on HPLC measurements are

of the order of  $\pm 10\%$ . Glycosides were subjected to column chromatography using Sephadex G25/G15/G10 columns ( $100 \times 1$  cm), eluting with water at 1 mL/h rate. Although the glycosides were separated from unreacted carbohydrates by these procedures, individual glycosides could not be isolated in pure forms due to similar polarity of these molecules.

The isolated glycosides were subjected to measurement of melting point and optical rotation and were also characterized by recording UV, IR, Mass and 2D-HSQC spectra. Unless otherwise mentioned, in 2D NMR data of the present work, only resolvable signals are shown. Some of the assignments are interchangeable. Non-reducing end carbohydrate units are primed. Glycosides are surfactant molecules, which form micelles above certain critical micellar concentrations (CMC). Since the concentrations employed for 2D Heteronuclear Single Quantum Coherence Transfer (2D-HSQC) spectral measurements are very much higher than their respective CMCs, the proton NMR signals were unusually broad such that, in spite of recording the spectra at 35 °C, the individual coupling constant values could not be determined precisely.

#### 4.1 Syntheses of riboflavinyl glycosides

Riboflavin [1-deoxy-1-(3,4-dihydro-7,8-dimethyl-2,4-dioxobenzo{g}pteridine-10(2H)-yl)-D-ribitol], vitamin B<sub>2</sub>, is a constituent member of the vitamin B complex (LeBlane *et al.* 2005). Riboflavin is a necessary growth factor important for erythrocyte production (Bates 1993). As a prosthetic group of oxido-reductive flavoenzymes, it functions as a flavin nucleotide in the process of electron transport leading to oxidative degradation of pyruvate, fatty acids and amino acids (Werner *et al.* 2005). Riboflavin is a potent antioxidant, protective against many diseases including cancer (Sengodan *et al.* 2003). Also it degrades nicotin into a pharmacologically inactive substance (Dickerson *et*

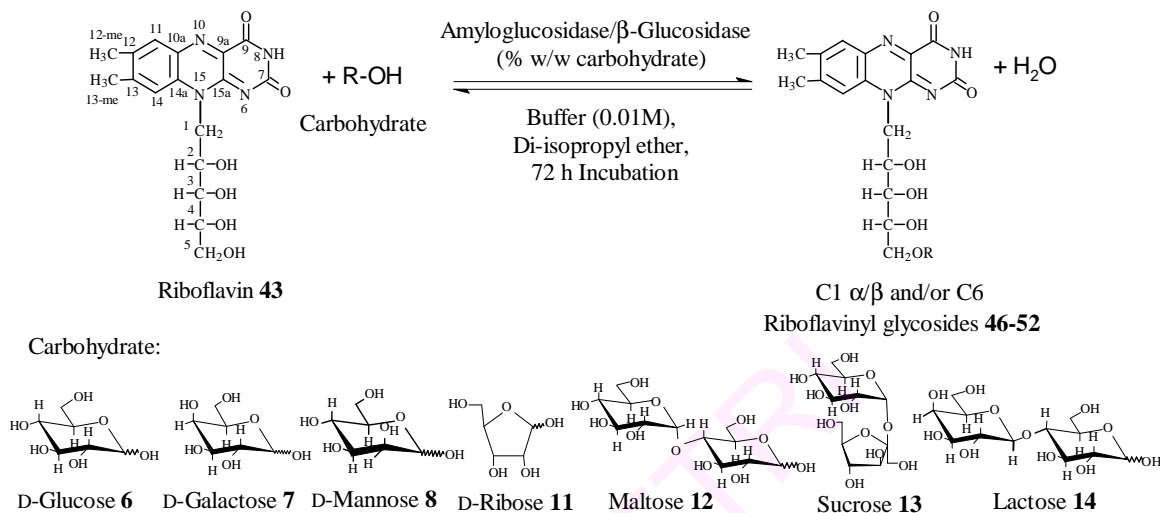
*al.* 2004). Recent researches focus on the role of plasma riboflavin in determining the homocysteine concentration, which is a risk factor in cardiovascular diseases (Powers 2003). Because of its limited gastrointestinal absorption, large doses of riboflavin remain unabsorbed.

Riboflavin is synthesized in plants and few microorganisms (Bacher *et al.* 2000). It is also obtained from animal source (Whitby 1971). As early as 1952, Whitby reported 5'-D-riboflavinyl-D-glucopyranoside from riboflavin by using homogenates of rat liver. Enzymes from different microorganisms have also been employed (Suzuki and Uchida 1969) for the preparation of 5'-D-riboflavinyl- $\alpha$ -D-glucopyranoside. Uchida and Suzuki (1968; Suzuki and Uchida 1983) have reported preparation of riboflavin glucoside in growing cultures of *Ashbya gossypii*, *Eremothecium ashbyii* and in germinating barley seeds. Tachibana (1955) has reported preparation of riboflavinyl- $\beta$ -D-galactoside in cell suspension cultures of *Aspergillus oryzae*. In 1971, Tachibana again showed riboflavin glucoside and other oligosaccharides from *Escherichia coli*, *Clostridium acetobutyricum*, *Leuconostoc mesentroides* and cotyledons of *Pumpkin curcurbita pepo* and of sugar beet *Beta vulgaris*. However, no systematic work on exclusive enzymatic synthesis of riboflavinyl glycosides were carried out so far.

It has been established that glycosides are more water soluble than their respective aglycons (Suzuki *et al.* 1996). Only 0.2 mg/mL of riboflavin can be dissolved in water at room temperature (Whitby 1954). Glycosylation improves the pharmacokinetic properties of water insoluble aglycons, like facile cell permeability and accessibility (Kren and Martinkova 2001). Attaching a glycosidic moiety into riboflavin increases its hydrophilicity and stability (Joseph and McCormick 1995).

Chemical methods of glycosylation involve protection and deprotection steps

which are tedious (Roode *et al.* 2003). The present work deals with enzymatic syntheses of riboflavinyl glycosides using amyloglucosidase from *Rhizopus* mold and  $\beta$ -glucosidase from sweet almond in di-isopropyl ether non-polar medium.



**Scheme 4.1** Syntheses of riboflavinyl glycosides

Synthesis of 5-*O*-(D-glucopyranosyl)riboflavin was studied in detail. A typical synthesis involved reacting riboflavin **43** (0.25-2 mmol) and D-glucose **6** (1 mmol) in reflux with stirring in 100 mL of di-isopropyl ether in the presence of 10-75% (w/w D-glucose) enzyme and 0.03-0.25 mM (0.3-2.5 mL) of 10 mM of pH 4-8 buffer for a period of 72 h (Scheme 4.1). Workup involved distilling off the solvent and the enzyme denatured at 100 °C by holding in boiling water bath for 5-10 min. The residue containing unreacted riboflavin **43** and D-glucose **6** along with the product glucosides was dissolved in 40-50 mL of water, filtered through Whatman filter paper No.1 to remove unreacted riboflavin **43** and the aqueous layer containing unreacted D-glucose **6** and the product glucosides was evaporated to dryness. The dried residue was subjected to HPLC (Fig. 4.1) and the conversion yields were determined from HPLC peak areas. Other procedures are as described on page 171.

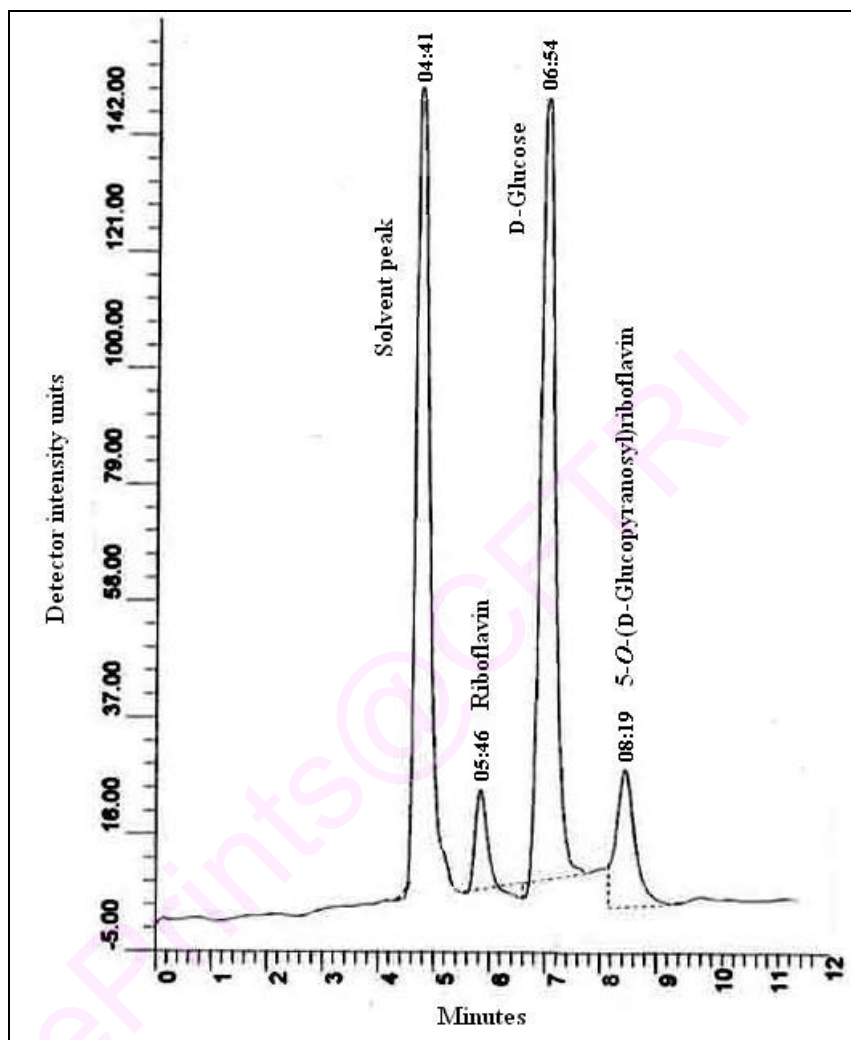


**Fig. 4.1** HPLC chromatogram for the reaction mixture of 5-*O*-(D-glucopyranosyl)riboflavin. HPLC conditions: Aminopropyl column (10  $\mu$ m, 300 mm  $\times$  3.9 mm), solvent-CH<sub>3</sub>CN: H<sub>2</sub>O (70:30 v/v), Flow rate-1 mL/min, RI detector. Peak retention times: solvent peak-4.4 min, riboflavin-5.5 min, D-glucose-6.5 min and 5-*O*-(D-glucopyranosyl)riboflavin-8.2 min.

HPLC retention times for the substrates and products are: riboflavin-5.5 min, D-glucose-6.5 min, 5-*O*-(D-glucopyranosyl)riboflavin-8.2 min, D-galactose-7.1 min, 5-*O*-(D-galactopyranosyl)riboflavin-12.4 min, D-mannose-6.7 min, 5-*O*-(D-mannopyranosyl)riboflavin-13.4 min, D-ribose-7.4 min, 5-*O*-(D-ribofuranosyl)riboflavin-9.1 min, maltose-11.5 min, 5-*O*-( $\alpha$ -D-glucopyranosyl-(1'→4)D-glucopyranosyl)riboflavin-17.2 min, sucrose-9.6 min, 5-*O*-(1-D-fructofuranosyl-(2→1') $\alpha$ -D-glucopyranosyl)riboflavin-16.1 min, lactose-9.3 min and 5-*O*-( $\beta$ -D-galactopyranosyl-(1'→4) $\beta$ -D-glucopyranosyl)riboflavin-15.1 min.

#### 4.1.1 Synthesis of 5-*O*-(D-glucopyranosyl)riboflavin using amyloglucosidase

Optimum conditions for the synthesis of 5-*O*-(D-glucopyranosyl)riboflavin using amyloglucosidase from *Rhizopus* mold was studied in detail in terms of incubation period, pH, buffer, enzyme and riboflavin concentrations.

##### 4.1.1.1 Effect of incubation period

Synthesis of 5-*O*-(D-glucopyranosyl)riboflavin was studied at various incubation periods of 3, 6, 12, 24, 48, 72 and 96 h. Amyloglucosidase catalysis gave a maximum yield of 25% between 12 to 72 h (Table 4.1, Fig. 4.2A). The yields decreased at longer incubation periods which could be due to inactivation of the enzymes at longer incubation periods.

##### 4.1.1.2 Effect of pH

Effect of pH on the extent of glucosylation was studied by varying pH from 4 to 8 at a fixed buffer concentration of 0.1 mM (1 mL). At pH 7, amyloglucosidase catalysis showed the highest conversion of 17%. The yield increased gradually from pH 4 to 7 and dropped to 14% at pH 8 (Table 4.1).

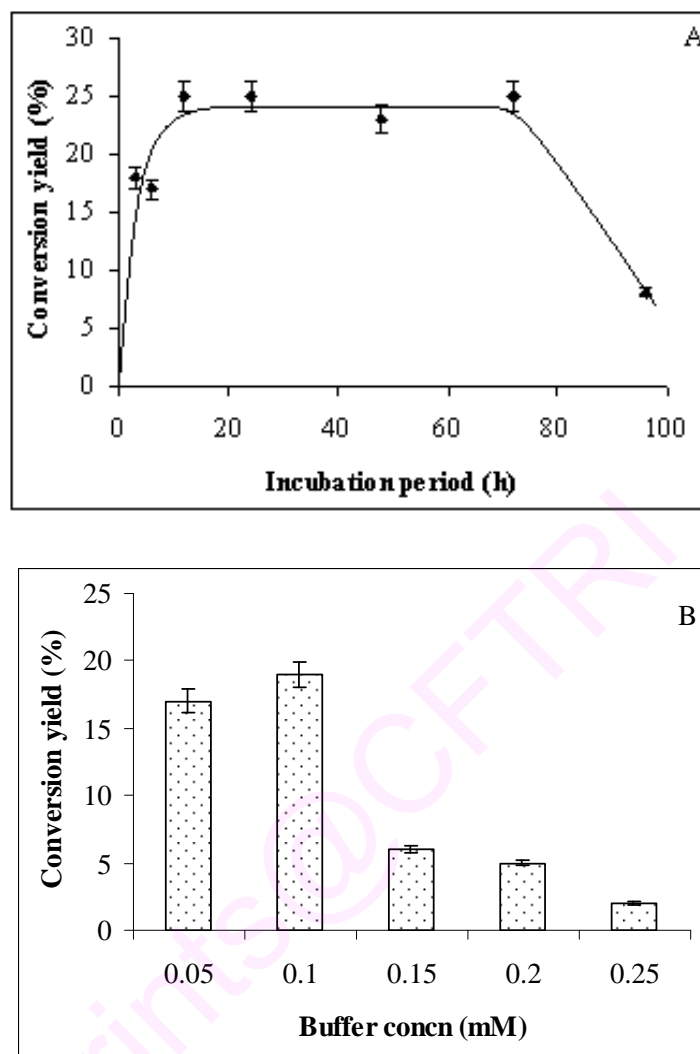


**Fig. 4.2 (A)** Reaction profile for 5-*O*-(D-glucopyranosyl)riboflavin synthesis by the reflux method. Conversion yields were from HPLC with respect to 1 mmol of D-glucose. Reaction conditions: D-glucose-1 mmol, riboflavin-0.5 mmol, amyloglucosidase-50% (w/w D-glucose), 0.1 mM (1 mL) pH 7 phosphate buffer, solvent-di-isopropyl ether and temperature-68 °C. **(B)** Effect of buffer concentration for 5-*O*-(D-glucopyranosyl)riboflavin synthesis. Reaction conditions: D-glucose-1 mmol, riboflavin-0.5 mmol, amyloglucosidase-40% (w/w D-glucose), pH 7 phosphate buffer, solvent-di-isopropyl ether, temperature-68 °C and incubation period – 72 h.



**Table 4.1** Optimization of reaction conditions for the synthesis of 5-*O*-(D-glucopyranosyl)riboflavin using amyloglucosidase

Reaction conditions	Variable parameter <sup>b</sup>	Yield (%) <sup>c</sup>
	Incubation period (h)	
Riboflavin – 0.5 mmol	3	18
D-glucose – 1 mmol	6	17
pH – 7	12	25
Buffer concentration – 0.1 mM (1 mL)	24	25
Amyloglucosidase – 50% w/w D-glucose	48	23
	72	25
	96	8
	pH (0.01M)	
Riboflavin – 0.5 mmol <sup>a</sup>	4	11
D-glucose – 1 mmol	5	14
Amyloglucosidase – 40% w/w D-glucose	6	15
Buffer concentration – 0.1 mM (1 mL)	7	17
Incubation period – 72 h	8	14
	Buffer concentration (mM)	
Riboflavin – 0.5 mmol	0.05	17
D-glucose – 1 mmol	0.1	19
Amyloglucosidase – 40% w/w D-glucose	0.15	6
pH – 7	0.2	5
Incubation period – 72 h	0.25	2
	Amyloglucosidase concentration (% w/w D-glucose)	
Riboflavin – 0.5 mmol	10	18
D-glucose – 1 mmol	20	19
pH – 7	30	23
Buffer concentration – 0.1 mM (1 mL)	40	24
Incubation period – 72 h	50	25
	75	21
	Riboflavin (mmol)	
pH – 7	0.25	19
Buffer concentration – 0.1 mM (1 mL)	0.5	25
D-glucose – 1 mmol	1	31
Amyloglucosidase – 50% w/w D-glucose	1.5	25
Incubation period – 72 h	2	25

<sup>a</sup>Initial reaction conditions. <sup>b</sup>Other variables are the same as under reaction conditions, except the specified ones. <sup>c</sup>HPLC yields expressed with respect to 1 mmol D-glucose employed.

#### 4.1.1.3 Effect of buffer concentration

About 0.05 mM to 0.25 mM (0.5 mL to 2.5 mL) of buffer concentration at pH 7 for amyloglucosidase was employed. A maximum yield of 19% was obtained at 0.1 mM

(1 mL) buffer concentration. Thereafter the yields showed considerable reduction at higher buffer concentrations (Table 4.1, Figure 4.2B).

#### 4.1.1.4 Effect of enzyme concentration

Under the above mentioned optimum conditions of pH and buffer concentrations, amyloglucosidase concentration was varied from 10% to 75% (w/w of D-glucose) to study the effect of enzyme on glucosylation. When amyloglucosidase was varied from 10% to 50% (w/w of D-glucose), the yields increased steadily (Table 4.1) exhibiting a maximum yield of 25% at 50% (w/w D-glucose) amyloglucosidase. At higher enzyme concentrations, the conversion yield decreased which could be due to larger concentrations of enzymes being available for fixed substrate (riboflavin and D-glucose) concentrations and as substrates bind differentially to the enzyme to varying degree of firmness, the tightly bound riboflavin (compared to D-glucose) could be unavailable for facile transfer to D-glucose molecule.

#### 4.1.1.5 Effect of substrate concentration

Effect of riboflavin concentrations on the conversion yield was studied between 0.25 to 2 mmol. Amyloglucosidase gave the lowest yield of 19% at 0.25 mmol riboflavin which increased steadily upto a maximum of 31% at 1 mmol (Table 4.1).

#### 4.1.2 Synthesis of 5-*O*-( $\beta$ -D-glucopyranosyl)riboflavin using $\beta$ -glucosidase

Optimum conditions for the synthesis of 5-*O*-( $\beta$ -D-glucopyranosyl)riboflavin using  $\beta$ -glucosidase isolated from sweet almond was also studied in detail in terms of incubation period, pH, buffer, enzyme and riboflavin concentrations (Scheme 4.1).

##### 4.1.2.1 Effect of incubation period

Synthesis of 5-*O*-( $\beta$ -D-glucopyranosyl)riboflavin was studied at various incubation periods of 3, 6, 12, 24, 48, 72 and 96 h.  $\beta$ -Glucosidase catalysis gave a

maximum yield of 22% at 72 h (Table 4.2, Figure 4.3A). The yields decreased here also as in amyloglucosidase at longer incubation periods which could be due to inactivation of the enzyme at longer incubation periods.

#### **4.1.2.2 Effect of pH**

Variation in pH did not affect the yield much in  $\beta$ -glucosidase catalysis (Table 4.2), where invariably very low yields of 6-8% were obtained irrespective of the pH employed.

#### **4.1.2.3 Effect of buffer concentration**

In case of  $\beta$ -glucosidase catalysis, at pH 6, buffer concentration was varied from 0.03 mM to 0.25 mM (0.3 mL to 2.5 mL). Conversion yields decreased drastically to zero beyond 0.1 mM (Table 4.2). The yields decreased at buffer concentration beyond 0.1 mM indicating the onset of hydrolysis (backward reaction).

#### **4.1.2.4 Effect of enzyme concentration**

Under the above mentioned optimum reaction conditions of pH and buffer concentrations,  $\beta$ -glucosidase concentrations was varied from 10% to 75% (w/w of D-glucose) to study the effect of enzyme on the glucosylation.  $\beta$ -Glucosidase at 30% (w/w D-glucose) enzyme, showed the highest conversion yield at 23% (Table 4.2). At higher enzyme concentrations, the conversion yield decreased.

#### **4.1.2.5 Effect of substrate concentration**

Effect of riboflavin concentrations on the conversion yield was studied by varying riboflavin concentration from 0.25 to 2 mmol.  $\beta$ -Glucosidase showed the maximum conversion yield 24% at 0.5 mmol riboflavin (Table 4.2, Fig. 4.3B).

### **4.1.3 Solubility of 5-O-(D-glucopyranosyl)riboflavin**

Determination of water solubility of 5-O-(D-glucopyranosyl)riboflavin showed

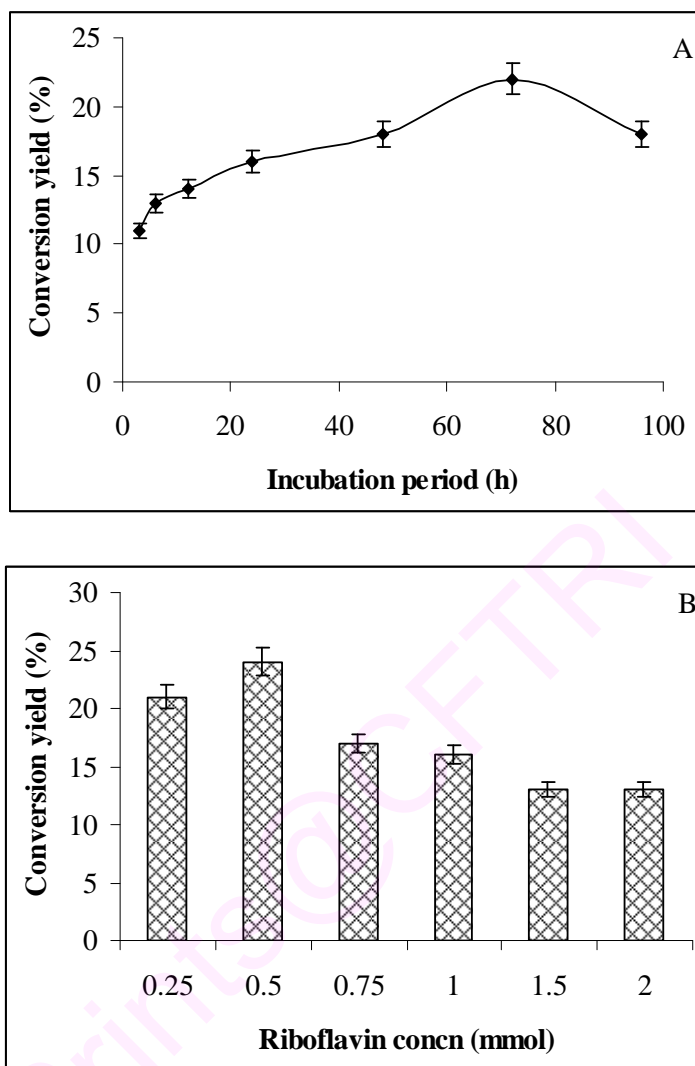


**Fig. 4.3 (A)** Reaction profile for 5-*O*-(β-D-glucopyranosyl)riboflavin synthesis by the reflux method. Conversion yields were from HPLC with respect to 1 mmol of D-glucose. Reaction conditions: D-glucose-1 mmol, riboflavin-0.5 mmol, β-glucosidase-30% (w/w D-glucose), 0.1 mM (1 mL), pH 6 phosphate buffer, solvent-di-isopropyl ether and temperature-68 °C. **(B)** Effect of riboflavin concentration for 5-*O*-(β-D-glucopyranosyl)riboflavin synthesis. Reaction conditions: D-glucose-1 mmol, β-glucosidase-30% (w/w D-glucose), 0.1 mM (1 mL) pH 6 phosphate buffer, solvent-di-isopropyl ether, temperature-68 °C and incubation period – 72 h.

that it is soluble to the extent of 8.2 g/L (Section 4.5.1) at room temperature (25 °C). Hence, 5-*O*-(D-glucopyranosyl)riboflavin was found to be more soluble than riboflavin itself (0.2 g/L at 25 °C) in water under identical conditions.

**Table 4.2** Optimization of reaction conditions for the synthesis of 5-*O*-( $\beta$ -D-glucopyranosyl)riboflavin using  $\beta$ -glucosidase

Reaction conditions	Variable parameter <sup>b</sup>	Yield (%) <sup>c</sup>
	Incubation period (h)	
Riboflavin – 0.5 mmol <sup>a</sup>	3	11
D-glucose – 1 mmol	6	13
pH – 6	12	14
Buffer concentration – 0.1 mM (1 mL)	24	16
$\beta$ -Glucosidase – 30% w/w D-glucose	48	18
	72	22
	96	18
	pH (0.01M)	
Riboflavin – 0.5 mmol	4	6
D-glucose – 1 mmol	5	7
$\beta$ -Glucosidase – 50% w/w D-glucose	6	8
Buffer concentration – 0.1 mM (1 mL)	7	8
Incubation period – 72 h	8	7
	Buffer concentration (mM)	
Riboflavin – 0.5 mmol	0.03	8
D-glucose – 1 mmol	0.06	11
$\beta$ -Glucosidase – 50% w/w D-glucose	0.1	18
pH – 6	0.14	8
Incubation period – 72 h	0.2	No yield
	0.25	No yield
	$\beta$ -Glucosidase concentration (% w/w D-glucose)	
Riboflavin – 0.5 mmol	10	5
D-glucose – 1 mmol	20	12
pH – 6	30	23
Buffer concentration – 0.1 mM (1 mL)	40	20
Incubation period – 72 h	50	17
	75	10
	Riboflavin (mmol)	
pH – 6	0.25	21
Buffer concentration – 0.1 mM (1 mL)	0.5	24
D-glucose – 1 mmol	0.75	17
$\beta$ -Glucosidase – 30% w/w D-glucose	1	16
Incubation period – 72 h	1.5	13
	2	13

<sup>a</sup>Initial reaction conditions. <sup>b</sup>Other variables are the same as under reaction conditions, except the specified ones. <sup>c</sup>HPLC yields expressed with respect to 1 mmol D-glucose employed.

#### 4.1.4 Syntheses of riboflavinyl glycosides of other carbohydrates using amyloglucosidase

Syntheses of riboflavinyl glycosides with other carbohydrates (D-glucose **6**, D-galactose **7**, D-mannose **8**, D-ribose **11**, maltose **12** and sucrose **13**) were attempted under the above determined optimum conditions (Scheme 4.1). Thus the optimum conditions determined for amyloglucosidase catalysed synthesis of 5-*O*-(D-glucopyranosyl)riboflavin (Table 4.1) were: riboflavin – 0.5 mmol, carbohydrate – 1 mmol, pH 7 of 0.1 mM (1 mL) buffer in 100 mL of di-isopropyl ether solvent, 50% (w/w D-glucose) amyloglucosidase concentration and 72 h incubation period. Other procedural condition described on page 174 was followed for work up, isolation and characterization of the glycosides.

#### 4.1.5 Syntheses of riboflavinyl glycosides of other carbohydrates using $\beta$ -glucosidase

Syntheses of riboflavinyl glycosides using  $\beta$ -glucosidase was carried out. The optimum conditions employed for the  $\beta$ -glucosidase catalysed synthesis of 5-*O*-( $\beta$ -D-glucopyranosyl)riboflavin (Table 4.2) were: riboflavin – 0.5 mmol, carbohydrate – (D-glucose **6**, D-galactose **7**, D-mannose **8** and lactose **14**, 1 mmol), pH 6 of 0.1 mM (1 mL) buffer in 100 mL of di-isopropyl ether solvent, 30% (w/w D-glucose)  $\beta$ -glucosidase concentration and 72 h incubation period. Other procedural condition described on page 174 was followed for work up, isolation and characterization of the glycosides.

#### 4.1.6 Spectral characterization

Riboflavinyl glycosides besides measuring melting point and optical rotation were also characterized by recording UV, IR, Mass and 2D-HSQCT, which provided good information on the nature and proportions of the products formed.

**Riboflavin 43 (Ribo):** Solid; decomposed at 279 °C; UV ( $\lambda_{\max}$ ): 191 nm ( $\sigma \rightarrow \sigma^*$ ,  $\epsilon_{191} - 15423 \text{ M}^{-1}$ ), 224 nm ( $\sigma \rightarrow \pi^*$ ,  $\epsilon_{224} - 21864 \text{ M}^{-1}$ ), 266 nm ( $\pi \rightarrow \pi^*$ ,  $\epsilon_{266} - 22102 \text{ M}^{-1}$ ), 373 nm ( $n \rightarrow \pi^*$ ,  $\epsilon_{373} - 8382 \text{ M}^{-1}$ ), 444.5 nm ( $n \rightarrow \pi^*$ , extended conjugation,  $\epsilon_{444.5} - 9794 \text{ M}^{-1}$ ), IR (stretching frequency,  $\text{cm}^{-1}$ ): 3496 (OH), 3333 (NH), 1580 (C=C), 1649 (CO), 3037 (CH), Optical rotation  $[\alpha]_{\text{D}}^{25} = -120.2^\circ$  ( $c$  0.5,  $\text{H}_2\text{O}$ ), 2D HSQCT NMR ( $\text{DMSO-}d_6$ ):  $^1\text{H}$  NMR  $\delta_{\text{ppm}}$ : 4.06 (H-1a), 4.24 (H-1b), 3.43 (H-2), 3.40 (H-3) 3.26 (H-4), 3.70 (H-5a), 4.15 (H-5b), 6.62 (H-11), 7.55 (H-14), 2.17 (12- $\text{CH}_3$ ), 2.07 (13- $\text{CH}_3$ ),  $^{13}\text{C}$  NMR  $\delta_{\text{ppm}}$ : 47.3 (C-1), 68.8 (C-2), 73.6 (C-3), 72.8 (C-4), 63.4 (C-5), 155.5 (C-7), 159.9 (C-9), 136.8 (C-9a), 134 (C-10a), 130.7 (C-11), 135.7 (C-12), 18.8 (C-12- $\text{CH}_3$ ), 146 (C-13), 20.8 (C-13- $\text{CH}_3$ ), 117.4 (C-14), 132.1 (C-14a), 150.8 (C-15a). Ultraviolet-visible spectra is shown in Fig. 4.4A.

**4.1.6.1 5-O-(D-Glucopyranosyl)riboflavin 46a-c:** Solid; UV ( $\lambda_{\max}$ ): 193.5 nm ( $\sigma \rightarrow \sigma^*$ ,  $\epsilon_{193.5} - 6461 \text{ M}^{-1}$ ), 230.5 nm ( $\sigma \rightarrow \pi^*$ ,  $\epsilon_{230.5} - 1090 \text{ M}^{-1}$ ), 253.5 nm ( $\pi \rightarrow \pi^*$ ,  $\epsilon_{253.5} - 752 \text{ M}^{-1}$ ), 270.5 nm ( $\pi \rightarrow \pi^*$ ,  $\epsilon_{270.5} - 660 \text{ M}^{-1}$ ), 283.5 nm ( $n \rightarrow \pi^*$ ,  $\epsilon_{283.5} - 658 \text{ M}^{-1}$ ), IR (stretching frequency,  $\text{cm}^{-1}$ ): 3381 (OH), 1031 (glycosidic alkyl-alkyl C-O-C symmetrical), 1262 (glycosidic alkyl-alkyl C-O-C asymmetrical), 1582 (C=C), 1647 (CO), 2929 (CH), MS ( $m/z$ ) - 538.2  $[\text{M}]^+$ , 2D HSQCT ( $\text{DMSO-}d_6$ ): **C1 $\alpha$ -glucoside 46a:**  $^1\text{H}$  NMR  $\delta_{\text{ppm}}$  **Glu:** 4.67 (H-1 $\alpha$ , d,  $J = 3.8 \text{ Hz}$ ), 3.30 (H-2 $\alpha$ ), 3.43 (H-3 $\alpha$ ), 3.65 (H-4 $\alpha$ ), 3.61 (H-5 $\alpha$ ), 3.45 (H-6a) 3.48 (H-6b), **Ribo:** 4.26 (H-1b), 3.42 (H-2), 3.64 (H-3) 3.29 (H-4), 3.68 (H-5a), 6.17 (H-11), 6.60 (H-14), 2.39 (12- $\text{CH}_3$ ), 1.90 (13- $\text{CH}_3$ );  $^{13}\text{C}$  NMR  $\delta_{\text{ppm}}$  **Glu:** 98.3 (C-1 $\alpha$ ), 70.5 (C-2 $\alpha$ ), 73.7 (C-3 $\alpha$ ), 70.3 (C-4 $\alpha$ ), 72.5 (C-5 $\alpha$ ), 61.5 (C-6 $\alpha$ ), **Ribo:** 47.6 (C1), 69.9 (C2), 73.5 (C3), 70.6 (C4), 66.5 (C5), 156 (C7), 136.7 (C10a), 131 (C11), 134.2 (C12), 18.9 (C12- $\text{CH}_3$ ), 146.5 (C13), 20.1 (C13- $\text{CH}_3$ ), 117.8 (C14), 131.3 (C14a); **C1 $\beta$ -glucoside 46b:** Solid; mp 143 °C, UV ( $\lambda_{\max}$ ): 194 nm ( $\sigma \rightarrow \sigma^*$ ,  $\epsilon_{194} - 198 \text{ M}^{-1}$ ), 264.5 nm

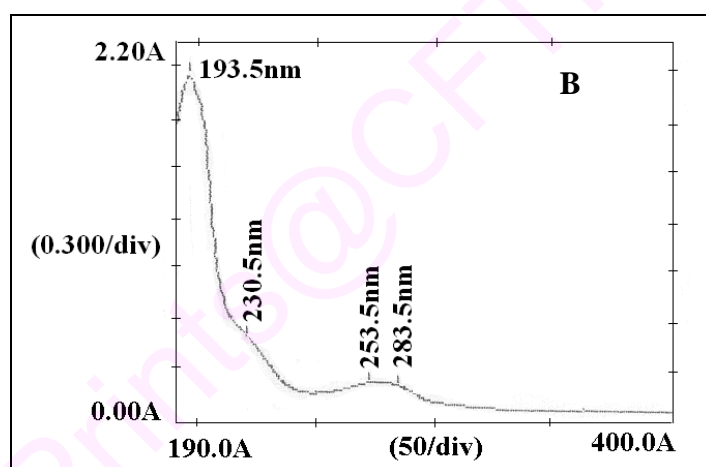
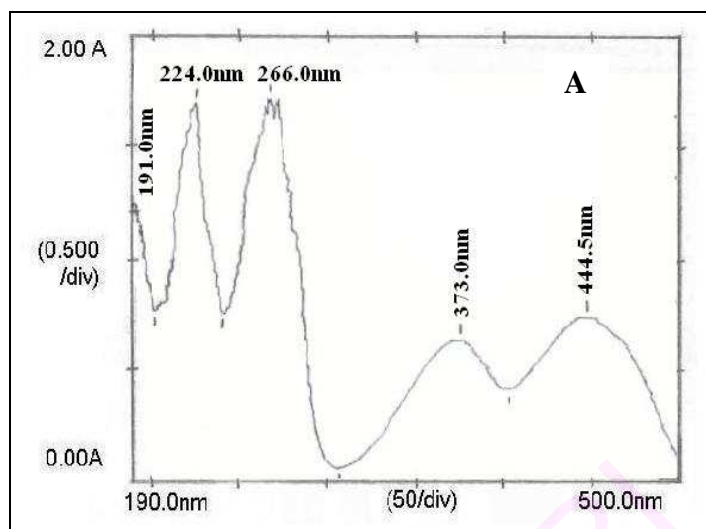


**Fig. 4.4** Ultraviolet-visible spectra of (A) Riboflavin **43** and (B) 5-*O*-(D-Glucopyranosyl)riboflavin **46a-c**



( $\pi \rightarrow \pi^*$ ,  $\epsilon_{264.5} - 12 \text{ M}^{-1}$ ), IR (stretching frequency,  $\text{cm}^{-1}$ ): 3316 (OH), 1039 (glycosidic alkyl-alkyl C-O-C symmetrical), 1148 (glycosidic alkyl-alkyl C-O-C asymmetrical), 1603 (C=C), 1630 (CO), 2931 (CH), Optical rotation  $[\alpha]_{\text{D}}^{25} = -40.7^\circ$  ( $c$  0.5,  $\text{H}_2\text{O}$ ), MS ( $m/z$ ) – 537.2  $[\text{M}-1]^+$ , 2D HSQCT ( $\text{DMSO}-d_6$ ):  $^1\text{H}$  NMR  $\delta_{\text{ppm}}$  **Glu**: 4.21 (H-1 $\beta$ , d,  $J = 7.5$  Hz), 3.30 (H-2 $\beta$ ), 3.45 (H-3 $\beta$ ), 3.68 (H-4 $\beta$ ), 3.62 (H-5 $\beta$ ), 3.46 (H-6a) 3.49 (H-6b), **Ribo**: 4.28 (H-1b), 3.43 (H-2), 3.66 (H-3) 3.30 (H-4), 3.66 (H-5a), 6.65 (H-14), 2.41 (12-CH<sub>3</sub>), 1.95 (13-CH<sub>3</sub>);  $^{13}\text{C}$  NMR  $\delta_{\text{ppm}}$  **Glu**: 103.2 (C1 $\beta$ ), 70.5 (C2 $\beta$ ), 73.6 (C3 $\beta$ ), 70.2 (C4 $\beta$ ), 72.6 (C5 $\beta$ ), 61.6 (C6 $\beta$ ), **Ribo**: 45.6 (C1), 69.2 (C2), 73.4 (C3), 70.7 (C4), 63.9 (C5), 157.2 (C7), 136.8 (C10a), 130.9 (C11), 18.9 (C12-CH<sub>3</sub>), 145.5 (C13), 20.1 (C13-CH<sub>3</sub>), 117.5 (C14), 130.1 (C14a); **C6-O-arylated 46c**:  $^1\text{H}$  NMR  $\delta_{\text{ppm}}$  **Glu**: 3.50 (H-6a), 3.55 (H-6b),  $^{13}\text{C}$  NMR  $\delta_{\text{ppm}}$  **Glu**: 66.3 (C6 $\beta$ ).

Ultraviolet-visible, IR, mass and 2D-HSQCT NMR spectra for 5-*O*-(D-glucopyranosyl)riboflavin **46a-c** for amyloglucosidase catalyzed product are shown in Figures 4.4B, 4.5A, 4.5B and 4.5C respectively. Infra-red and 2D-HSQCT NMR spectra for 5-*O*-(D-glucopyranosyl)riboflavin **46b** for  $\beta$ -glucosidase catalyzed product are shown in Figures 4.6A and 4.6B respectively.

**4.1.6.2 5-*O*-(D-Galactopyranosyl)riboflavin 47a,b**: Solid; UV ( $\lambda_{\text{max}}$ ): 193.5 nm ( $\sigma \rightarrow \sigma^*$ ,  $\epsilon_{193.5} - 4186 \text{ M}^{-1}$ ), 230.5 nm ( $\sigma \rightarrow \pi^*$ ,  $\epsilon_{230.5} - 1029 \text{ M}^{-1}$ ), 253.5 nm ( $\pi \rightarrow \pi^*$ ,  $\epsilon_{253.5} - 767 \text{ M}^{-1}$ ), 270.5 nm ( $\pi \rightarrow \pi^*$ ,  $\epsilon_{270.5} - 709 \text{ M}^{-1}$ ), 283.5 nm ( $n \rightarrow \pi^*$ ,  $\epsilon_{283.5} - 713 \text{ M}^{-1}$ ), IR (stretching frequency,  $\text{cm}^{-1}$ ): 3421 (OH), 1071 (glycosidic alkyl-alkyl C-O-C symmetrical), 1298 (glycosidic alkyl-alkyl C-O-C asymmetrical), 1548 (C=C), 1647 (CO), 2966 (CH), MS ( $m/z$ ) – 537.2  $[\text{M}-1]^+$ , 2D HSQCT ( $\text{DMSO}-d_6$ ): **C1 $\alpha$ -galactoside 47a**:  $^1\text{H}$  NMR  $\delta_{\text{ppm}}$  **Gal**: 4.98 (H-1 $\alpha$ , d,  $J = 2.2$  Hz), 3.56 (H-2 $\alpha$ ), 3.53 (H-3 $\alpha$ ), 3.66 (H-

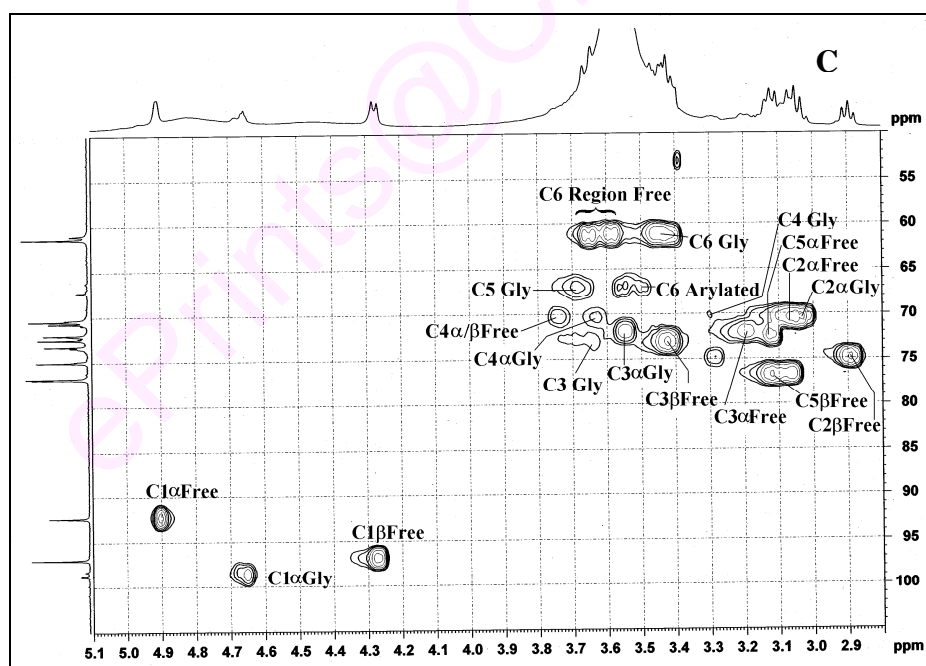
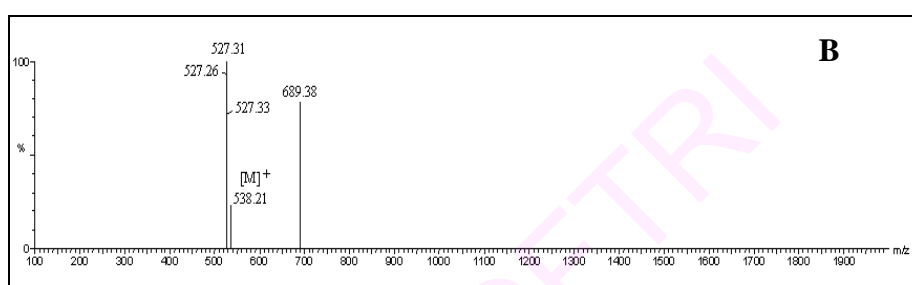
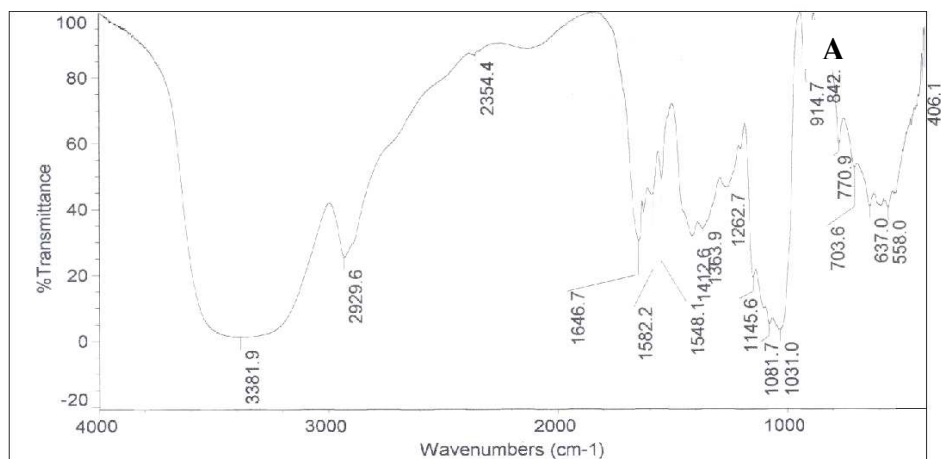


**Fig. 4.5** 5-*O*-(D-Glucopyranosyl)riboflavin **46a-c**: (A) IR spectrum, (B) Mass spectrum and (C) 2D-HSQC spectrum showing the C1-C6 region. Some of the NMR assignments are interchangeable.

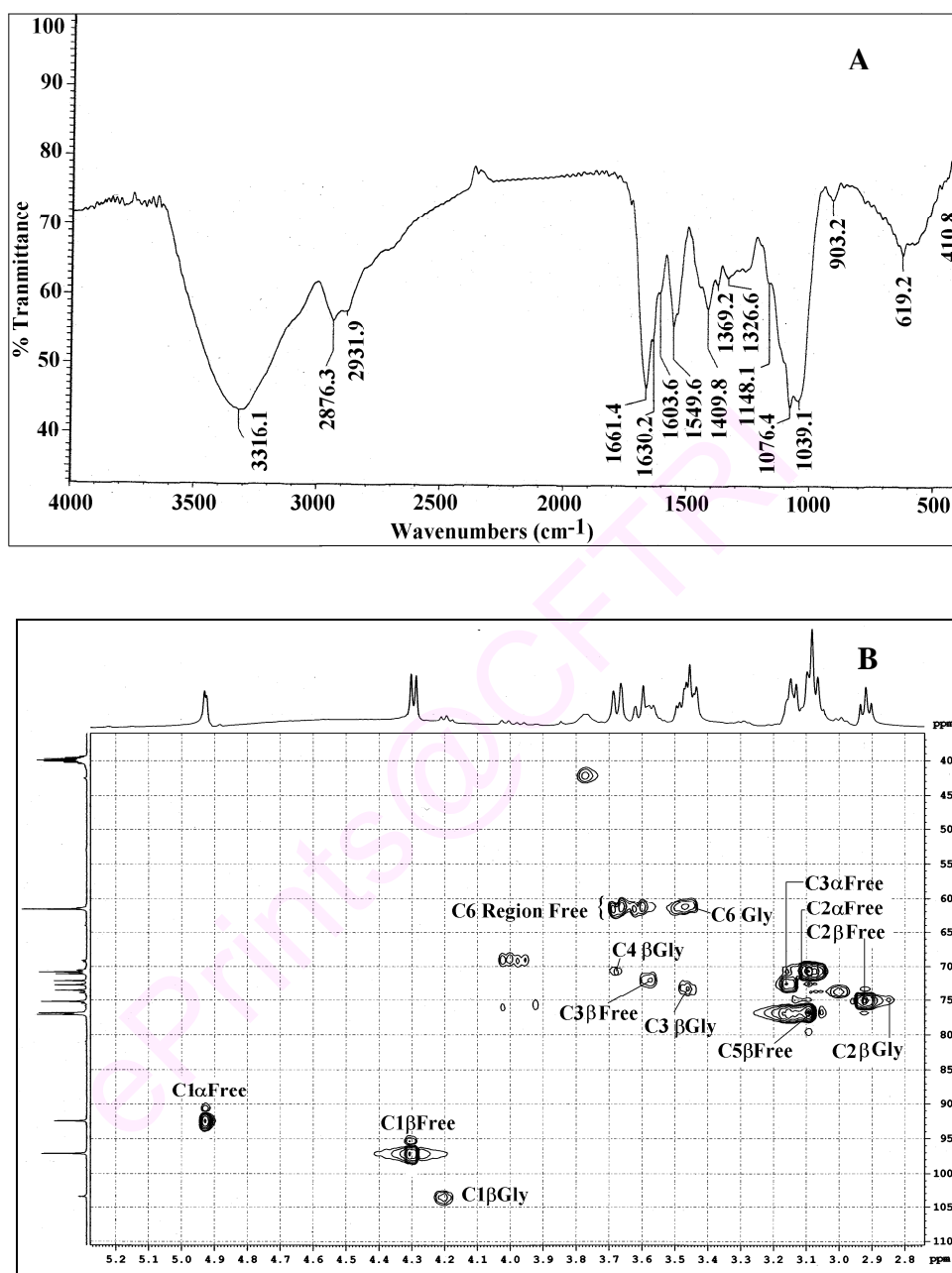
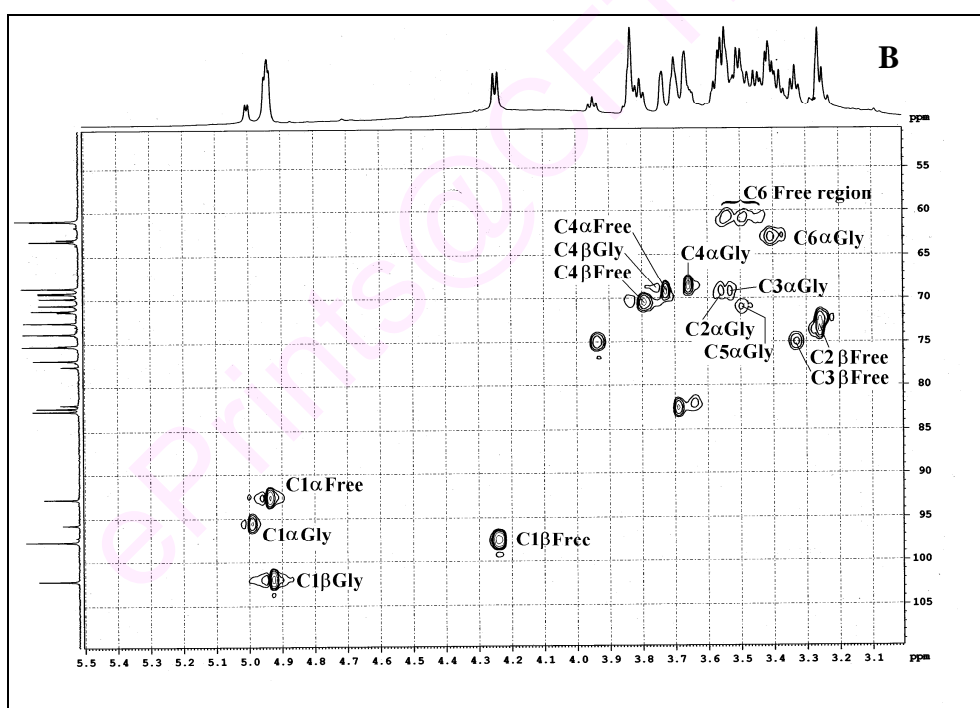
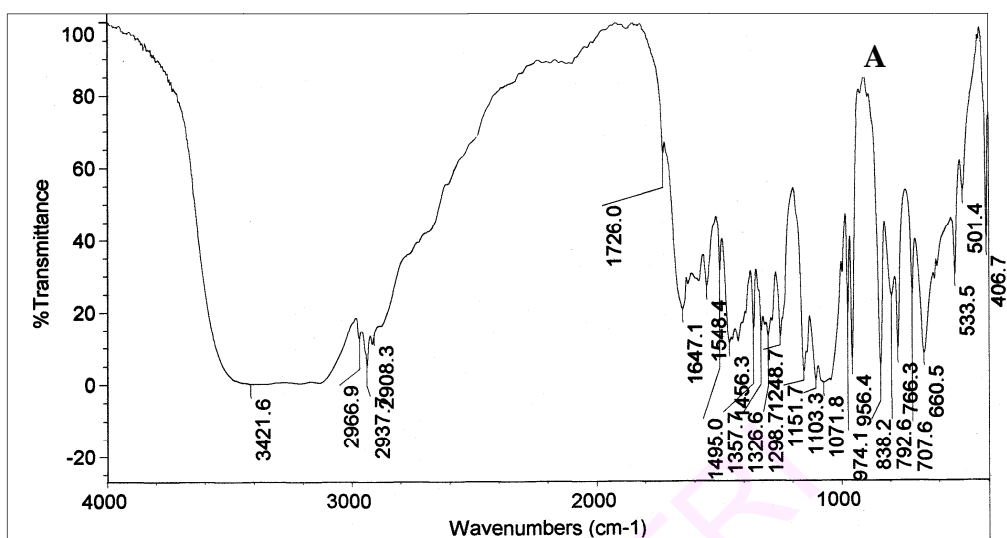


**Fig. 4.6** 5-*O*-(β-D-Glucopyranosyl)riboflavin **46b**: (A) IR spectrum and (B) 2D-HSQC spectrum showing the C1-C6 region. Some of the NMR assignments are interchangeable.

4 $\alpha$ ), 3.48 (H-5 $\alpha$ ), 3.38 (H-6a) 3.43 (H-6b), **Ribo**: 4.22 (H-1b), 3.42 (H-2), 3.68 (H-3) 3.28 (H-4), 3.70 (H-5a), 6.15 (H-11), 7.05 (H-14), 2.41 (12-CH<sub>3</sub>), 1.35 (13-CH<sub>3</sub>); <sup>13</sup>C NMR  $\delta_{\text{ppm}}$  **Gal**: 97.1 (C1 $\alpha$ ), 69.5 (C2 $\alpha$ ), 70.5 (C3 $\alpha$ ), 68.6 (C4 $\alpha$ ), 71.1 (C5 $\alpha$ ), 62.5 (C6 $\alpha$ ), **Ribo**: 47.5 (C1), 69.7 (C2), 76.5 (C3), 70.7 (C4), 66.5 (C5), 136.8 (C10a), 131.2 (C11), 134.5 (C12), 19.1 (C12-CH<sub>3</sub>), 146.5 (C13), 21 (C13-CH<sub>3</sub>), 117.6 (C14), 132.2 (C14a); **C1 $\beta$ -galactoside 47b**: <sup>1</sup>H NMR  $\delta_{\text{ppm}}$  **Gal**: 4.93 (H-1 $\beta$ , d, J = 7.9 Hz), 3.75 (H-4 $\beta$ ), 3.55 (H-6a), <sup>13</sup>C NMR  $\delta_{\text{ppm}}$  **Gal**: 102.1 (C1 $\beta$ ), 68.5 (C4 $\beta$ ), 61.6 (C6 $\beta$ ).

Infra-red and 2D-HSQCT NMR spectra for 5-*O*-(D-galactopyranosyl)riboflavin **47a,b** are shown in Figures 4.7A and 4.7B respectively.

**4.1.6.3 5-*O*-(D-Mannopyranosyl)riboflavin 48a,b**: Solid; mp 137 °C, UV ( $\lambda_{\text{max}}$ ): 193.5 nm ( $\sigma \rightarrow \sigma^*$ ,  $\epsilon_{193.5} - 6840 \text{ M}^{-1}$ ), 230.5 nm ( $\sigma \rightarrow \pi^*$ ,  $\epsilon_{230.5} - 2218 \text{ M}^{-1}$ ), 254 nm ( $\pi \rightarrow \pi^*$ ,  $\epsilon_{254} - 1615 \text{ M}^{-1}$ ), 270.5 nm ( $\pi \rightarrow \pi^*$ ,  $\epsilon_{270.5} - 1520 \text{ M}^{-1}$ ), 283.5 nm ( $n \rightarrow \pi^*$ ,  $\epsilon_{283.5} - 1450 \text{ M}^{-1}$ ); IR (stretching frequency,  $\text{cm}^{-1}$ ): 3378 (OH), 1069 (glycosidic alkyl-alkyl C-O-C symmetrical), 1254 (glycosidic alkyl-alkyl C-O-C asymmetrical), 1547 (C=C), 1647 (CO), 2935 (CH), Optical rotation  $[\alpha]_{\text{D}}^{25} = +12.5^\circ$  (*c* 0.5, H<sub>2</sub>O), MS (*m/z*) – 538.3 [M]<sup>+</sup>, 2D HSQCT (DMSO-*d*<sub>6</sub>): **C1 $\alpha$ -mannoside 48a**: <sup>1</sup>H NMR  $\delta_{\text{ppm}}$  **Man**: 4.98 (H-1 $\alpha$ , d, J = 1.8 Hz), 3.55 (H-2 $\alpha$ ), 3.56 (H-3 $\alpha$ ), 3.47 (H-5 $\alpha$ ), 3.49 (H-6b), **Ribo**: 4.20 (H-1b), 3.44 (H-2), 3.63 (H-3) 3.12 (H-4), 3.62 (H-5a), 6.15 (H-11), 6.60 (H-14), 2.36 (12-CH<sub>3</sub>), 1.90 (13-CH<sub>3</sub>); <sup>13</sup>C NMR  $\delta_{\text{ppm}}$  **Man**: 97.1 (C1 $\alpha$ ), 70.8 (C2 $\alpha$ ), 70.5 (C3 $\alpha$ ), 73 (C5 $\alpha$ ), 62.5 (C6 $\alpha$ ), **Ribo**: 43.5 (C1), 67.9 (C2), 72.8 (C3), 70.5 (C4), 67.4 (C5), 156.5 (C7), 130.9 (C11), 19 (C12-CH<sub>3</sub>), 146 (C13), 21 (C13-CH<sub>3</sub>), 118 (C14), 130.2 (C14a); **C1 $\beta$ -mannoside 48b**: <sup>1</sup>H NMR  $\delta_{\text{ppm}}$  **Man**: 4.91 (H-1 $\beta$ , d, J = 3.9 Hz), 3.41 (H-2 $\beta$ ), 3.38 (H-4 $\beta$ ), 3.45 (H-6a), <sup>13</sup>C NMR  $\delta_{\text{ppm}}$  **Man**: 102.2 (C1 $\beta$ ), 71 (C2 $\beta$ ), 67.2 (C4 $\beta$ ), 61.9 (C6 $\beta$ ).



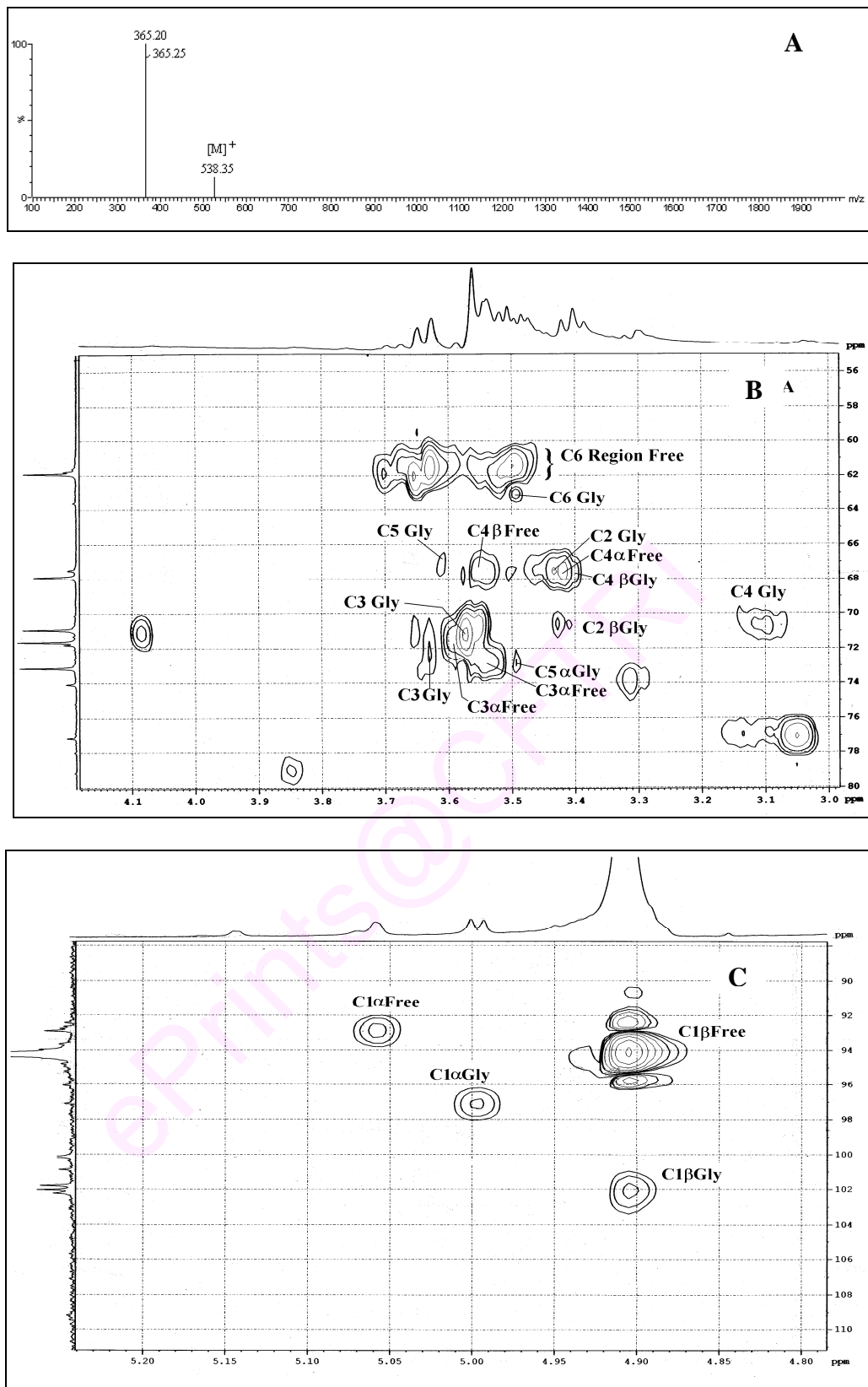
**Fig. 4.7** 5-*O*-(D-Galactopyranosyl)riboflavin **47a,b**: (A) IR spectrum and (B) 2D-HSQC spectrum showing the C1-C6 region. Some of the NMR assignments are interchangeable.

Figure 4.8A shows mass spectra and Figures 4.8B and 4.8C show 2D-HSQCT NMR spectra of 5-*O*-(D-mannopyranosyl)riboflavin **48a,b**.

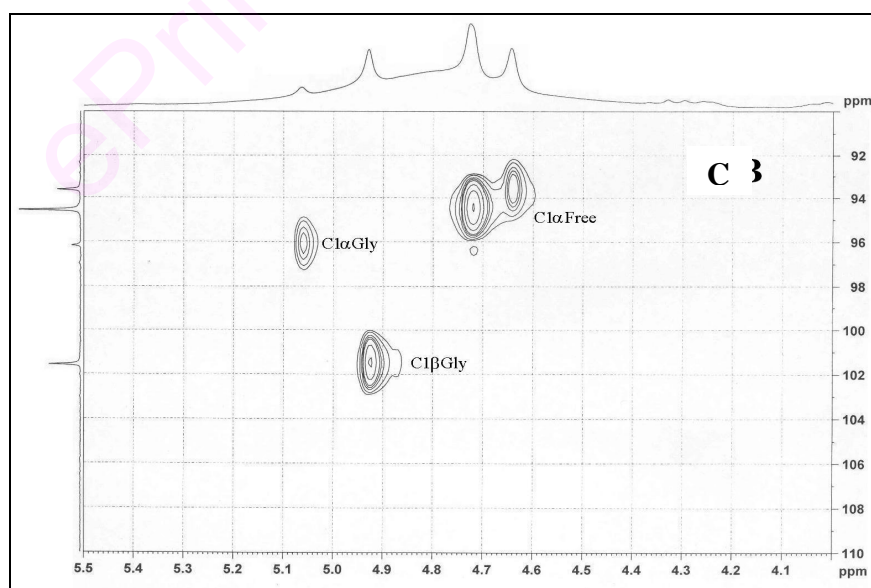
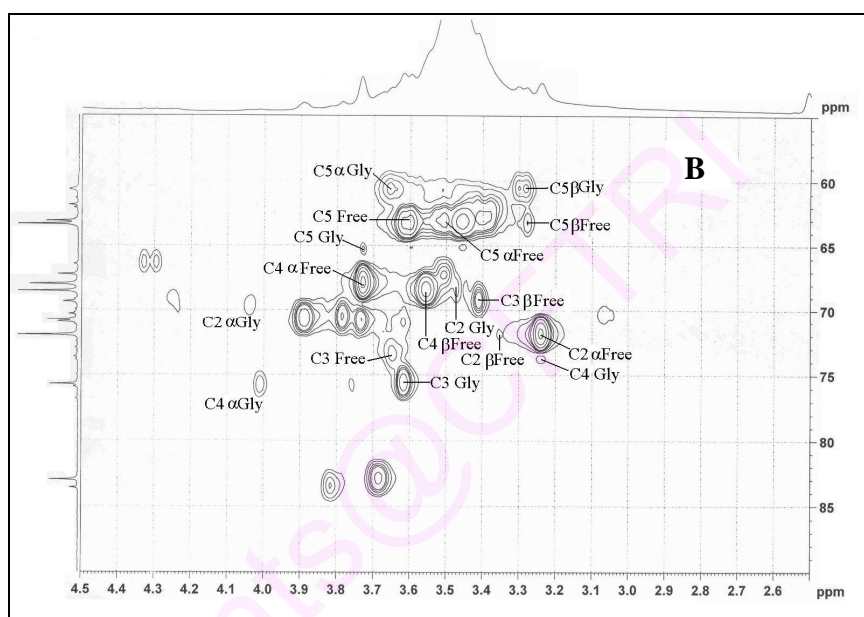
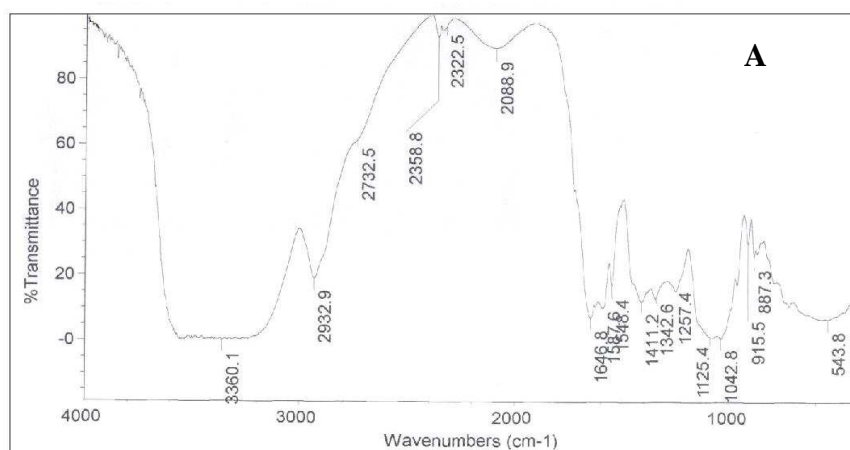
**4.1.6.4 5-*O*-(D-Ribofuranosyl)riboflavin 49a,b:** Solid; UV ( $\lambda_{\max}$ ): 193 nm ( $\sigma \rightarrow \sigma^*$ ,  $\epsilon_{193} - 7877 \text{ M}^{-1}$ ), 230.5 nm ( $\sigma \rightarrow \pi^*$ ,  $\epsilon_{230.5} - 2688 \text{ M}^{-1}$ ), 253.5 nm ( $\pi \rightarrow \pi^*$ ,  $\epsilon_{253.5} - 1918 \text{ M}^{-1}$ ), 270.5 nm ( $\pi \rightarrow \pi^*$ ,  $\epsilon_{270.5} - 1864 \text{ M}^{-1}$ ), 283.5 nm ( $n \rightarrow \pi^*$ ,  $\epsilon_{283.5} - 1772 \text{ M}^{-1}$ ); IR (stretching frequency,  $\text{cm}^{-1}$ ): 3360 (OH), 1042 (glycosidic alkyl-alkyl C-O-C symmetrical), 1257 (glycosidic alkyl-alkyl C-O-C asymmetrical), 1587 (C=C), 1646 (CO), 2932 (CH), MS ( $m/z$ ) - 506.1  $[\text{M}-2]^+$ , 2D HSQCT (DMSO- $d_6$ ): **C1 $\alpha$ -riboside 49a:**  $^1\text{H}$  NMR  $\delta_{\text{ppm}}$  **Ribose:** 5.06 (H-1 $\alpha$ , d,  $J = 3.5 \text{ Hz}$ ), 4.03 (H-2 $\alpha$ ), 4.64 (H-3 $\alpha$ ), 3.61 (H-5a), 3.78 (H-5b), **Ribo:** 4.06 (H-1a), 4.26 (H-1b), 3.42 (H-2), 3.67 (H-3), 3.28 (H-4), 3.73 (H-5a), 3.89 (H-5b), 6.15 (H-11), 7.06 (H-14), 2.35 (12-CH $_3$ ), 1.85 (13-CH $_3$ ),  $^{13}\text{C}$  NMR  $\delta_{\text{ppm}}$  **Ribose:** 96.9 (C1 $\alpha$ ), 70 (C2 $\alpha$ ), 75.7 (C3 $\alpha$ ), 60.7 (C5 $\alpha$ ), **Ribo:** 47.6 (C1), 69.9 (C2), 74.5 (C3), 72.4 (C4), 65 (C5), 155.8 (C7), 160.2 (C9), 136.7 (C10a), 130.1 (C11), 134.2 (C12), 18.8 (C12-CH $_3$ ), 146.4 (C13), 20.5 (C13-CH $_3$ ), 117.6 (C14), 132.3 (C14a), 150.9 (C15a); **C1 $\beta$ -riboside 49b:**  $^1\text{H}$  NMR  $\delta_{\text{ppm}}$  **Ribose:** 4.93 (H-1 $\beta$ , d,  $J = 6.1 \text{ Hz}$ ), 4.03 (H-4 $\beta$ ),  $^{13}\text{C}$  NMR  $\delta_{\text{ppm}}$  **Ribose:** 101.6 (C1 $\beta$ ), 75.1 (C4 $\beta$ ).

Figure 4.9A shows IR spectra and Figures 4.9B and 4.9C shows 2D-HSQCT NMR spectra of 5-*O*-(D-ribofuranosyl)riboflavin **49a,b**.

**4.1.6.5 5-*O*-( $\alpha$ -D-Glucopyranosyl-(1' $\rightarrow$ 4)D-glucopyranosyl)riboflavin 50a-c:** Solid; UV ( $\lambda_{\max}$ ): 194 nm ( $\sigma \rightarrow \sigma^*$ ,  $\epsilon_{194} - 9982 \text{ M}^{-1}$ ), 230.5 nm ( $\sigma \rightarrow \pi^*$ ,  $\epsilon_{230.5} - 1553 \text{ M}^{-1}$ ), 253.5 nm ( $\pi \rightarrow \pi^*$ ,  $\epsilon_{253.5} - 976 \text{ M}^{-1}$ ), 270.5 nm ( $\pi \rightarrow \pi^*$ ,  $\epsilon_{270.5} - 899 \text{ M}^{-1}$ ), 283.5 nm ( $n \rightarrow \pi^*$ ,  $\epsilon_{283.5} - 935 \text{ M}^{-1}$ ), IR (stretching frequency,  $\text{cm}^{-1}$ ): 3223 (OH), 1046 (glycosidic alkyl-alkyl C-O-C symmetrical), 1263 (glycosidic alkyl-alkyl C-O-C asymmetrical), 1548 (C=C), 1647 (CO), 2929 (CH), MS ( $m/z$ ) - 701.2  $[\text{M}+1]^+$ , 2D HSQCT (DMSO- $d_6$ ): **C1 $\alpha$ -maltoside**



**Fig. 4.8** 5-O-(D-Mannopyranosyl)riboflavin **48a,b**: (A) Mass spectrum, (B) 2D-HSQC spectrum showing the C2-C6 region and (C) Anomeric region of the same compound. Some of the NMR assignments are interchangeable.



**Fig. 4.9** 5-*O*-(D-Ribofuranosyl)riboflavin **49a,b**: (A) IR spectrum, (B) 2D-HSQC spectrum showing the C2-C5 region and (C) Anomeric region of the same compound. Some of the NMR assignments are interchangeable.



**50a:**  $^1\text{H}$  NMR  $\delta_{\text{ppm}}$  **Malt:** 4.67 (H-1 $\alpha$ , d,  $J = 3.3$  Hz), 3.25 (H-2 $\alpha$ ), 3.48 (H-3 $\alpha$ ), 3.58 (H-4 $\alpha$ ), 3.61 (H-5 $\alpha$ ), 3.48 (H-6a) 3.48 (H-6b), 4.96 (H-1' $\alpha$ ), 3.10 (H-3'), 3.03 (H-4'), 3.45 (H-6'a), **Ribo:** 4.02 (H-1a), 4.28 (H-1b), 3.43 (H-2), 3.66 (H-3) 3.29 (H-4), 3.68 (H-5a), 6.15 (H-11), 6.90 (H-14), 2.40 (12-CH<sub>3</sub>), 2.10 (13-CH<sub>3</sub>),  $^{13}\text{C}$  NMR  $\delta_{\text{ppm}}$  **Malt:** 98.5 (C1 $\alpha$ ), 70.6 (C2 $\alpha$ ), 73.5 (C3 $\alpha$ ), 71.8 (C4 $\alpha$ ), 72.4 (C5 $\alpha$ ), 61.5 (C6 $\alpha$ ), 98.9 (C1' $\alpha$ ), 72.8 (C3'), 71 (C4'), 61.5 (C6'), **Ribo:** 47.5 (C1), 69.9 (C2), 73.4 (C3), 70.7 (C4), 66.7 (C5), 155.5 (C7), 137 (C10a), 131 (C11), 134.5 (C12), 19 (C12-CH<sub>3</sub>), 146 (C13), 21 (C13-CH<sub>3</sub>), 118 (C14), 130.5 (C14a); **C6-O-arylated 50b:**  $^1\text{H}$  NMR  $\delta_{\text{ppm}}$  **Glu:** 3.71 (H-6a),  $^{13}\text{C}$  NMR  $\delta_{\text{ppm}}$  **Glu:** 67.4 (C6); **C6'-O-arylated 50c:**  $^1\text{H}$  NMR  $\delta_{\text{ppm}}$  **Glu:** 3.62 (H-6'a),  $^{13}\text{C}$  NMR  $\delta_{\text{ppm}}$  **Glu:** 67.6 (C6').

Infra-red and 2D-HSQCT NMR spectra for 5-*O*-( $\alpha$ -D-glucopyranosyl-(1'→4)-D-glucopyranosyl)riboflavin **50a-c** are shown in Figures 4.10A and 4.10B respectively.

**4.1.6.6 5-O-(1-D-Fructofuranosyl-(2→1')-D-glucopyranosyl)riboflavin 51:** Solid; mp 145 °C, UV ( $\lambda_{\text{max}}$ ): 194 nm ( $\sigma \rightarrow \sigma^*$ ,  $\epsilon_{194} = 8481 \text{ M}^{-1}$ ), 230.5 nm ( $\sigma \rightarrow \pi^*$ ,  $\epsilon_{230.5} = 1785 \text{ M}^{-1}$ ), 254 nm ( $\pi \rightarrow \pi^*$ ,  $\epsilon_{254} = 1244 \text{ M}^{-1}$ ), 270.5 nm ( $\pi \rightarrow \pi^*$ ,  $\epsilon_{270.5} = 1187 \text{ M}^{-1}$ ), 283.5 nm ( $n \rightarrow \pi^*$ ,  $\epsilon_{283.5} = 1218 \text{ M}^{-1}$ ), IR (stretching frequency,  $\text{cm}^{-1}$ ): 3233 (OH), 1052 (glycosidic alkyl-alkyl C-O-C symmetrical), 1259 (glycosidic alkyl-alkyl C-O-C asymmetrical), 1550 (C=C), 1643 (CO), 2934 (CH), Optical rotation  $[\alpha]_{\text{D}}^{25} = +33.3^\circ$  ( $c$  0.5, H<sub>2</sub>O), MS ( $m/z$ ) – 723.1  $[\text{M}+\text{Na}]^+$ , 2D HSQCT (DMSO- $d_6$ ): **C1-O-arylated:**  $^1\text{H}$  NMR  $\delta_{\text{ppm}}$  **Suc:** 3.69 (H-1), 3.78 (H-3), 3.86 (H-4), 3.55 (H-5); 3.51 (H-6a), 5.22 (H-1' $\alpha$ ), 3.71 (H-2'), 3.18 (H-3'), 3.12 (H-4'), 3.48 (H-5'), 3.61 (H-6'a) 3.64 (H-6'b), **Ribo:** 4.05 (H-1a), 4.29 (H-1b), 3.48 (H-2), 3.62 (H-3) 3.28 (H-4), 3.78 (H-5a), 3.83 (H-5b), 6.20 (H-11), 7.10 (H-14), 2.40 (12-CH<sub>3</sub>), 2.15 (13-CH<sub>3</sub>),  $^{13}\text{C}$  NMR  $\delta_{\text{ppm}}$  **Suc:** 66.8 (C1), 104.3 (C2), 76.5

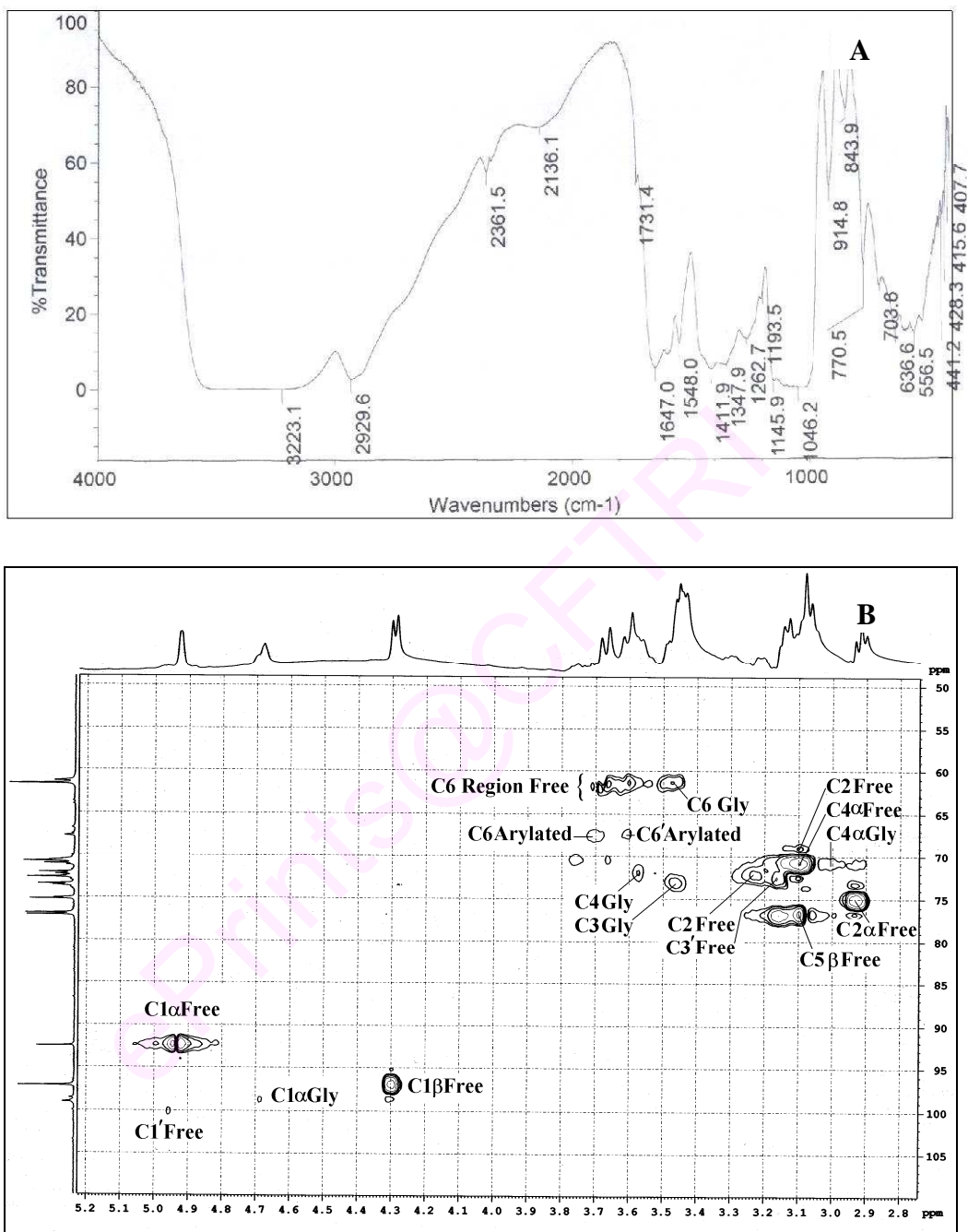


**Fig. 4.10** 5-*O*-( $\alpha$ -D-Glucopyranosyl-(1'→4)D-glucopyranosyl)riboflavin **50a-c**: (A) IR spectrum and (B) 2D-HSQC spectrum showing the C1-C6' region. Some of the NMR assignments are interchangeable

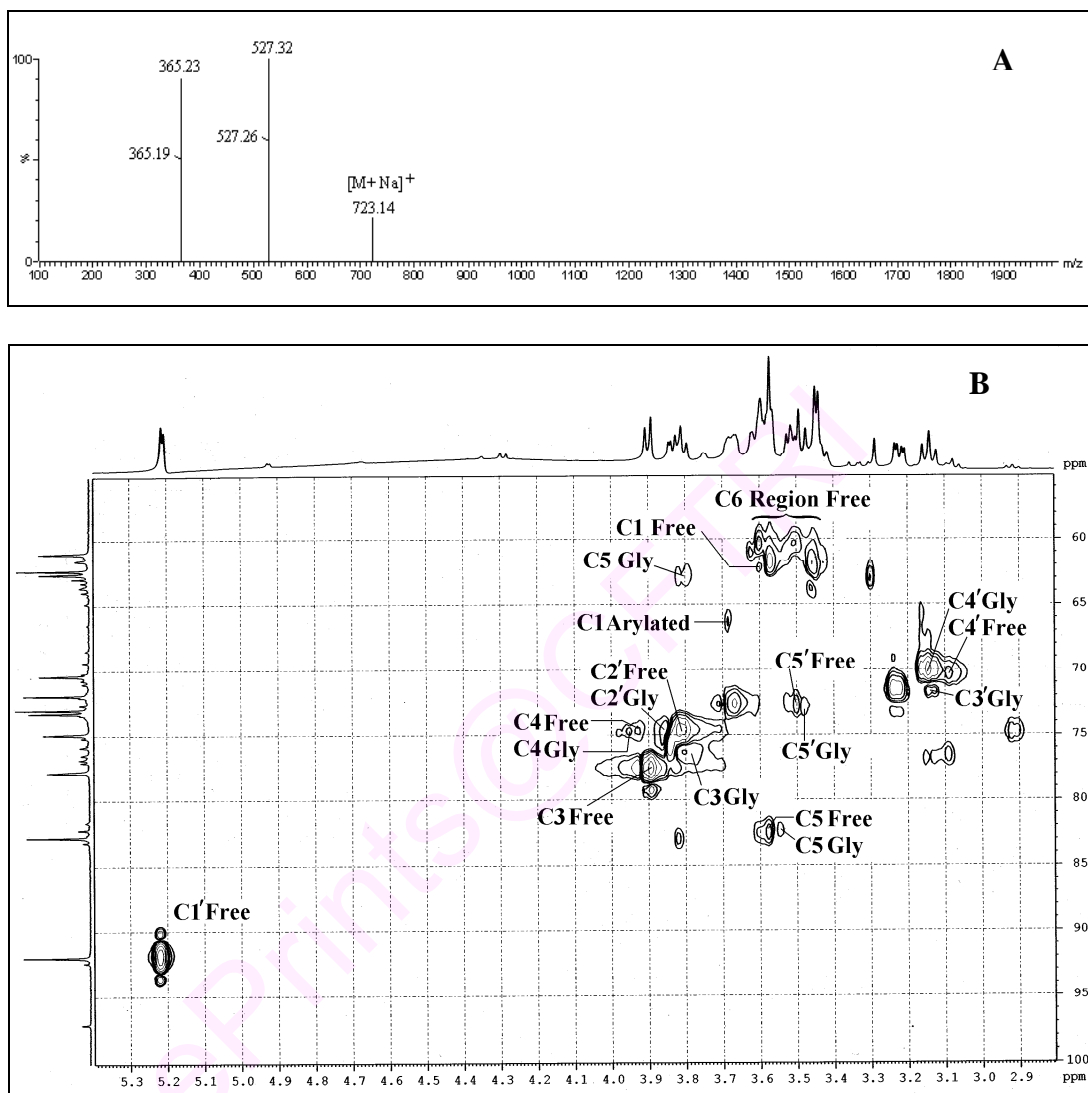
(C3), 74.5 (C4), 82.2 (C5), 62.5 (C6); 92.2 (C1'α), 72.6 (C2'), 71.8 (C3'), 70.5 (C4'), 73 (C5'), 61 (C6'), **Ribo**: 47.3 (C1), 70.5 (C2), 72.5 (C3), 71.5 (C4), 63.9 (C5), 155.5 (C7), 136.8 (C10a), 130.1 (C11), 135.9 (C12), 18.8 (C12-CH<sub>3</sub>), 20.8 (C13-CH<sub>3</sub>), 117.5 (C14).

Mass and 2D-HSQCT NMR spectra for 5-*O*-(1-D-fructofuranosyl-(2→1')α-D-glucopyranosyl)riboflavin **51** are shown in Figures 4.11A and 4.11B respectively.

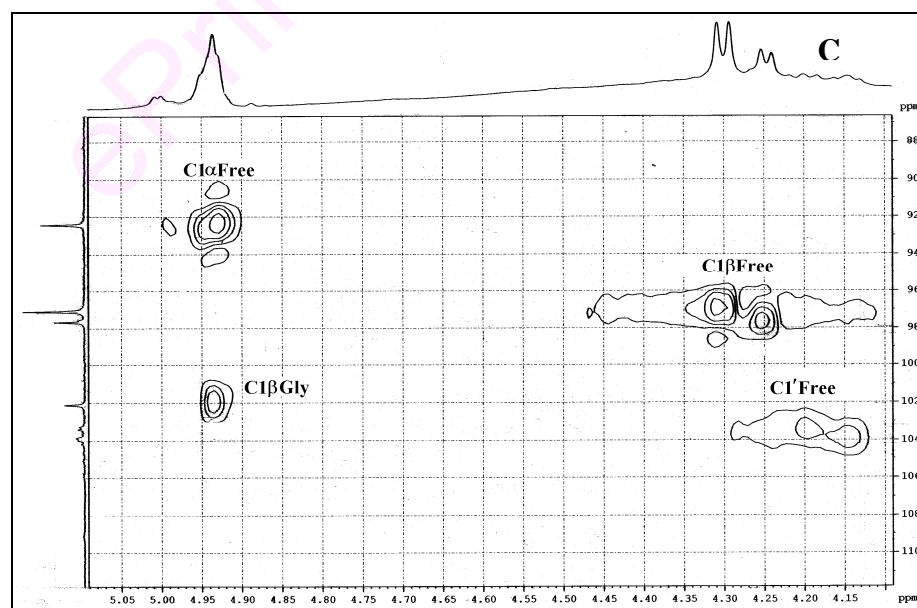
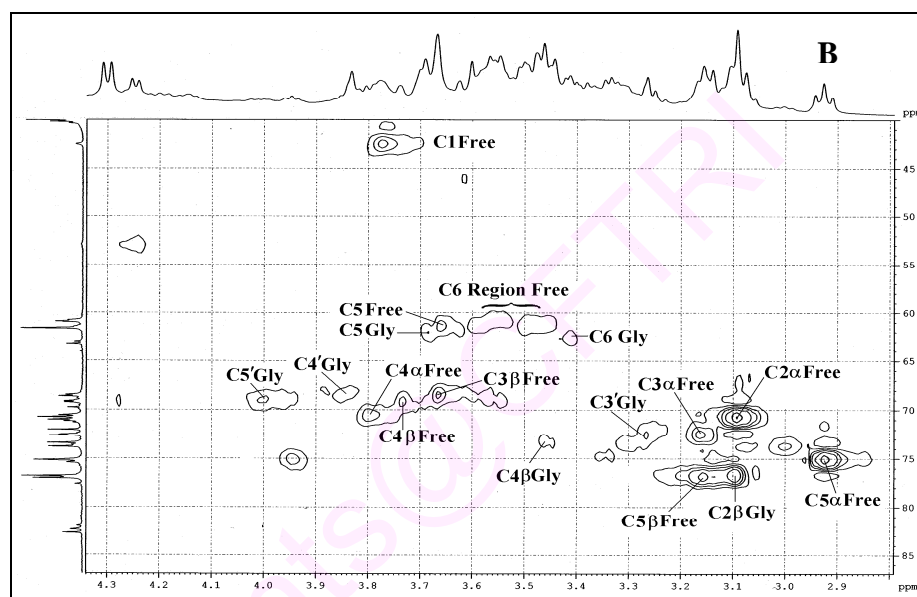
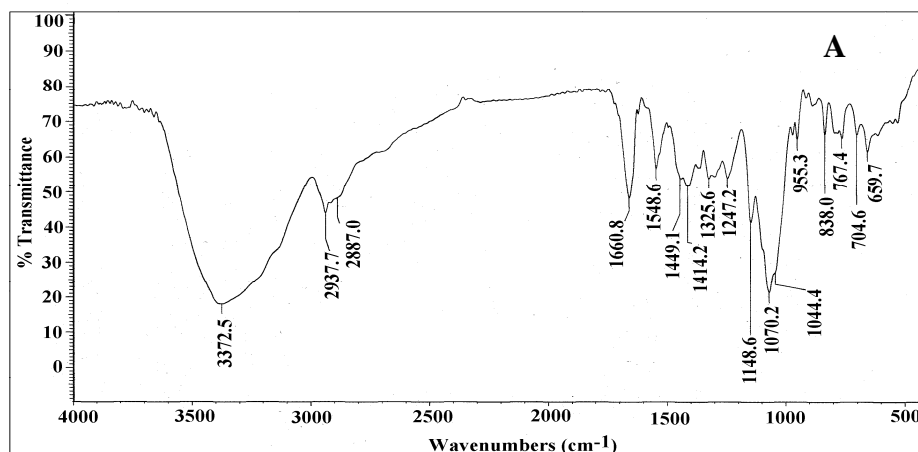
**4.1.6.7 5-*O*-(β-D-Galactopyranosyl-(1'→4)β-D-glucopyranosyl)riboflavin 52**: Solid; mp 153 °C, UV ( $\lambda_{\max}$ ): 196.5 nm ( $\sigma \rightarrow \sigma^*$ ,  $\epsilon_{196.5} = 10678 \text{ M}^{-1}$ ), 223 nm ( $\sigma \rightarrow \pi^*$ ,  $\epsilon_{223} = 1924 \text{ M}^{-1}$ ), 255 nm ( $\pi \rightarrow \pi^*$ ,  $\epsilon_{255} = 612 \text{ M}^{-1}$ ), 278.5 nm ( $\pi \rightarrow \pi^*$ ,  $\epsilon_{278.5} = 506 \text{ M}^{-1}$ ); IR (stretching frequency,  $\text{cm}^{-1}$ ): 3372 (OH), 1044 (glycosidic alkyl-alkyl C-O-C symmetrical), 1247 (glycosidic alkyl-alkyl C-O-C asymmetrical), 1548 (C=C), 1660 (CO), 2937 (CH), Optical rotation  $[\alpha]_{\text{D}}^{25} = -7.35^\circ$  ( $c$  0.5, H<sub>2</sub>O), MS ( $m/z$ ) – 698.1 [ $\text{M}-2$ ]<sup>+</sup>, 2D HSQCT (DMSO-*d*<sub>6</sub>): **C1β-lactoside**: <sup>1</sup>H NMR  $\delta_{\text{ppm}}$  **Lact**: 4.92 (H-1β, d,  $J = 7.6 \text{ Hz}$ ), 3.16 (H-2β), 3.48 (H-3β), 3.47 (H-4β), 3.60 (H-5β), 3.50 (H-6a) 3.47 (H-6b), 4.16 (H-1'β), 3.25 (H-3'), 3.83 (H-4'), 3.94 (H-5'), 3.42 (H-6'a), **Ribo**: 3.96 (H-1a), 4.29 (H-1b), 3.44 (H-2), 3.69 (H-3) 3.28 (H-4), 3.73 (H-5a), 6.15 (H-11), 6.92 (H-14), 2.42 (12-CH<sub>3</sub>), 2.15 (13-CH<sub>3</sub>), <sup>13</sup>C NMR  $\delta_{\text{ppm}}$  **Lact**: 102.1 (C1β), 76.9 (C2β), 75.4 (C3β), 71 (C4β), 76.9 (C5β), 61.6 (C6β), 103.3 (C1'β), 72.9 (C3'), 68.4 (C4'), 73.6 (C5'), 62.9 (C6'), **Ribo**: 43.5 (C1), 68.8 (C2), 73.6 (C3), 71 (C4), 63.9 (C5), 155.5 (C7), 130.9 (C11), 19 (C12-CH<sub>3</sub>), 22 (C13-CH<sub>3</sub>), 117.5 (C14), 130.1 (C14a).

Figure 4.12A shows IR spectra and Figures 4.12B and 4.12C shows 2D-HSQCT NMR spectra of 5-*O*-(β-D-galactopyranosyl-(1'→4)β-D-glucopyranosyl)riboflavin **52**.

Ultraviolet-visible spectra of riboflavinyl glycosides, showed shifts in  $\sigma \rightarrow \sigma^*$  band in the 193 – 196.5 nm (191 nm for free riboflavin) range,  $\sigma \rightarrow \pi^*$  band in the 223 – 230.5 nm (224 nm for free riboflavin) range and  $\pi \rightarrow \pi^*$  band in the 253.5 – 283.5 nm (266 nm



**Fig. 4.11** 5-*O*-(1-D-Fructofuranosyl-(2→1') $\alpha$ -D-glucopyranosyl)riboflavin **51**: (A) Mass spectrum and (B) 2D-HSQCT spectrum showing the C1-C6' region. Some of the assignments are interchangeable.



**Fig. 4.12** 5-*O*-( $\beta$ -D-Galactopyranosyl-(1'→4) $\beta$ -D-glucopyranosyl)riboflavin **52**: (A) IR spectrum, (B) 2D-HSQC spectrum showing the C2-C6' region and (C) Anomeric region of the same compound. Some of the NMR assignments are interchangeable.

for free riboflavin) range and IR glycosidic C-O-C symmetrical stretching frequencies in the 1031-1071  $\text{cm}^{-1}$  range and glycosidic C-O-C asymmetrical stretching frequencies in the 1148-1298  $\text{cm}^{-1}$  range indicating that riboflavin had undergone glycosylation. From the 2D HSQCT spectra of the riboflavinyl glycosides, the following glycoside formation were confirmed from their respective chemical shift values: from D-glucose **6** C1 $\alpha$  glucoside **46a** to C1 $\alpha$  at 98.3 ppm and H-1 $\alpha$  at 4.67 ppm, C1 $\beta$  glucoside **46b** to C1 $\beta$  at 103.2 ppm and H-1 $\beta$  at 4.21 ppm and C6-*O*-arylated **46c** to C6 at 66.3 ppm and H-6a at 3.50 ppm, H-6b at 3.55 ppm; from D-galactose **7** C1 $\alpha$  galactoside **47a** to C1 $\alpha$  at 97.1 ppm and H-1 $\alpha$  at 4.98 ppm and C1 $\beta$  galactoside **47b** to C1 $\beta$  at 102.1 ppm and H-1 $\beta$  at 4.93 ppm; from D-mannose **8** C1 $\alpha$  mannoside **48a** to C1 $\alpha$  at 97.1 ppm and H-1 $\alpha$  at 4.98 ppm and C1 $\beta$  mannoside **48b** to C1 $\beta$  at 102.2 ppm and H-1 $\beta$  at 4.91 ppm; from D-ribose **11** C1 $\alpha$  riboside **49a** to C1 $\alpha$  at 96.9 ppm and H-1 $\alpha$  at 5.06 ppm and C1 $\beta$  riboside **49b** to C1 $\beta$  at 101.6 ppm and H-1 $\beta$  at 4.93 ppm; from maltose **12** C1 $\alpha$  maltoside **50a** to C1 $\alpha$  at 98.5 ppm and H-1 $\alpha$  at 4.67 ppm, C6-*O*-arylated **50b** to C6 at 67.4 ppm and H-6a at 3.71 ppm and C6'-*O*-arylated **50c** to C6' at 67.6 ppm and H-6'a at 3.62 ppm; from sucrose **13** C1-*O*-arylated **51** to C1 at 66.8 ppm and H-1 at 3.69 ppm and from lactose **14** C1 $\beta$  lactoside **52** to C1 $\beta$  at 102.1 ppm and H-1 $\beta$  at 4.92 ppm. Mass spectra also confirmed the formation of the above mentioned glycosides. Two-Dimensional HSQCT data clearly indicated that the glycosylation has occurred at the 5-CH<sub>2</sub>OH of ribitol moiety of riboflavin.

#### 4.1.7 Discussion

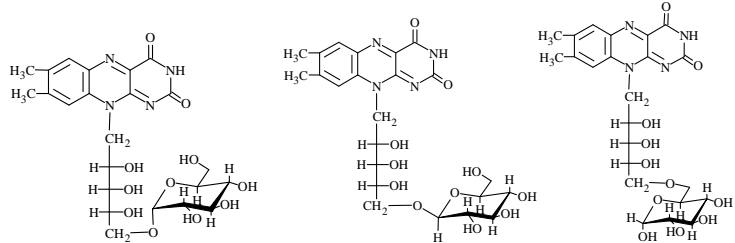
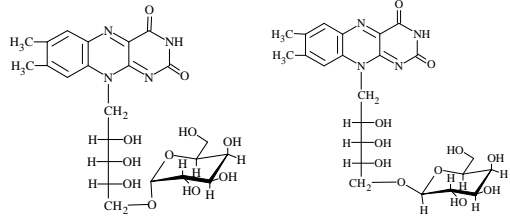
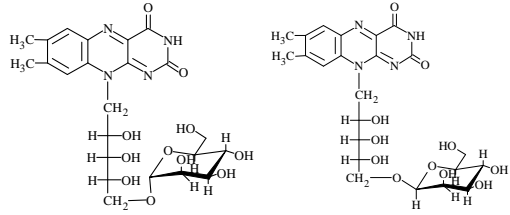
Riboflavinyl glycosides have been formed from many of the carbohydrates employed. The yields are shown in Table 4.3. Of these, amyloglucosidase catalysis gave rise to six glycosides: 5-*O*-(D-glucopyranosyl)riboflavin **46a-c**, 5-*O*-(D-galactopyranosyl)

riboflavin **47a,b**, 5-*O*-( $\alpha$ -D-mannopyranosyl)riboflavin **48a**, 5-*O*-(D-ribofuranosyl)riboflavin **49a,b**, 5-*O*-( $\alpha$ -D-glucopyranosyl-(1'→4)D-glucopyranosyl)riboflavin **50a-c** and 5-*O*-(1-D-fructofuranosyl-(2→1') $\alpha$ -D-glucopyranosyl)riboflavin **51**.  $\beta$ -Glucosidase catalysis gave rise to the following four glycosides: 5-*O*-( $\beta$ -D-glucopyranosyl)riboflavin **46b**, 5-*O*-(D-galactopyranosyl)riboflavin **47a,b**, 5-*O*-(D-mannopyranosyl)riboflavin **48a,b** and 5-*O*-( $\beta$ -D-galactopyranosyl-(1'→4) $\beta$ -D-glucopyranosyl)riboflavin **52**. All these glycosides were soluble in water to higher extents than riboflavin itself. They could hence be used in pharmaceutical applications.

Out of 13 glycosides prepared, eleven glycosides are reported for the first time. New glycosides are: 5-*O*-(D-galactopyranosyl)riboflavin **47a,b**, 5-*O*-(D-mannopyranosyl)riboflavin **48a,b**, 5-*O*-(D-ribofuranosyl)riboflavin **49a,b**, 5-*O*-( $\alpha$ -D-glucopyranosyl-(1'→4)D-glucopyranosyl)riboflavin **50a-c**, 5-*O*-(1-D-fructofuranosyl-(2→1') $\alpha$ -D-glucopyranosyl)riboflavin **51** and 5-*O*-( $\beta$ -D-galactopyranosyl-(1'→4) $\beta$ -D-glucopyranosyl)riboflavin **52**.

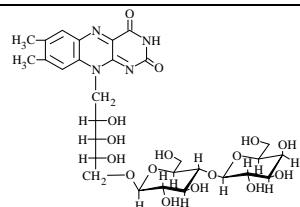
In spite of possessing a ribitol group, riboflavin **43** is soluble to the extent of only 0.2 g/L (Whitby 1954), which is due to the strong non-polar nature of the aglycon molecule. However, attachment of a monosaccharide unit to ribitol improved the water solubility of riboflavin to 8.2 g/L. This shows that glycosylation is capable of counteracting the non-polar aglycon characteristics to a great extent.

**Table 4.3** Syntheses of riboflavinyl glycosides using amyloglucosidase and  $\beta$ -glucosidase.

Glycosides	Amyloglucosidase catalysis <sup>a</sup>		$\beta$ -Glucosidase catalysis <sup>b</sup>	
	Product (% proportion) <sup>c</sup>	Yields (%) <sup>d</sup>	Product (% proportion) <sup>c</sup>	Yields (%) <sup>d</sup>
 <p><b>46a</b> 5-<i>O</i>-(<math>\alpha</math>-D-Glucopyranosyl)riboflavin  <b>46b</b> 5-<i>O</i>-(<math>\beta</math>-D-Glucopyranosyl)riboflavin  <b>46c</b> 5-<i>O</i>-(6-D-Glucopyranosyl)riboflavin</p>	C1 $\alpha$ glucosides (43), C1 $\beta$ glucosides (22), C6- <i>O</i> -arylated (35)	25	C1 $\beta$ glucoside	24
 <p><b>47a</b> 5-<i>O</i>-(<math>\alpha</math>-D-Galactopyranosyl)riboflavin  <b>47b</b> 5-<i>O</i>-(<math>\beta</math>-D-Galactopyranosyl)riboflavin</p>	C1 $\alpha$ galactosides (52), C1 $\beta$ galactosides (48)	14	C1 $\alpha$ galactosides (47), C1 $\beta$ galactosides (53)	9
 <p><b>48a</b> 5-<i>O</i>-(<math>\alpha</math>-D-Mannopyranosyl)riboflavin  <b>48b</b> 5-<i>O</i>-(<math>\beta</math>-D-Mannopyranosyl)riboflavin</p>	C1 $\alpha$ mannoside	11	C1 $\alpha$ mannoside (59) C1 $\beta$ mannoside (41)	7



	C1 $\alpha$ riboside (23), C1 $\beta$ riboside (77)	40	-	-
<p><b>49a</b> 5-<i>O</i>-(<math>\alpha</math>-D-Ribofuranosyl)riboflavin <b>49b</b> 5-<i>O</i>-(<math>\beta</math>-D-Ribofuranosyl)riboflavin</p>				
	C1 $\alpha$ maltoside (35), C6- <i>O</i> -arylated (48), C6'- <i>O</i> -arylated (17)	5	-	-
<p><b>50a</b> 5-<i>O</i>-(<math>\alpha</math>-D-Glucopyranosyl-(1'→4)<math>\alpha</math>-D-glucopyranosyl)riboflavin <b>50b</b> 5-<i>O</i>-(<math>\alpha</math>-D-Glucopyranosyl-(1'→4)6-D-glucopyranosyl)riboflavin <b>50c</b> 5-<i>O</i>-(<math>\alpha</math>-D-Glucopyranosyl-(1'→4)6'-D-glucopyranosyl)riboflavin</p>				
	C1- <i>O</i> -arylated	12	-	-
<p><b>51</b> 5-<i>O</i>-(1-D-Fructofuranosyl-(2→1')<math>\alpha</math>-D-glucopyranosyl)riboflavin</p>				



- - C1β lactoside 9

### 52 5-O-(β-D-Galactopyranosyl-(1'→4)β-D-glucopyranosyl)riboflavin

<sup>a</sup>Riboflavin – 0.5 mmol; carbohydrate – 1 mmol; amyloglucosidase concentration 50% w/w of carbohydrate; solvent – di-isopropyl ether; buffer – 0.1 mM (1 mL) pH 7 phosphate buffer; incubation period – 72 h. <sup>b</sup>Riboflavin – 0.5 mmol; carbohydrate – 1 mmol; β-glucosidase concentration 30% w/w of carbohydrate; solvent – di-isopropyl ether; buffer – 0.1 mM (1 mL) pH 6 phosphate buffer; incubation period – 72 h. <sup>c</sup>Conversion yields were from HPLC with respect to free carbohydrate. Error in yield measurements is ± 5-10%. <sup>d</sup>The product proportions were determined from the area of respective <sup>1</sup>H/<sup>13</sup>C signals.

Amyloglucosidase catalysed the reactions with D-glucose **6**, D-galactose **7**, D-mannose **8**, D-ribose **11**, maltose **12** and sucrose **13**. It did not catalyse the reaction with D-fructose **9**, D-arabinose **10**, lactose **14**, D-sorbitol **15** and D-mannitol **16**. Similarly,  $\beta$ -glucosidase catalysed the reactions with D-glucose **6**, D-galactose **7**, D-mannose **8** and lactose **14**. It did not catalyse reactions with D-fructose **9**, D-arabinose **10**, D-ribose **11**, maltose **12**, sucrose **13**, D-sorbitol **15** and D-mannitol **16** under the conditions employed. In both glucosidases catalyzed reactions riboflavin **43** could bind strongly to active site of enzyme than the above mentioned non-reactive carbohydrate molecules, thereby preventing the facile transfer of these carbohydrate molecules to the nucleophilic primary OH of riboflavin **43**. In case of amyloglucosidase catalysis, 5-*O*-(D-ribofuranosyl)riboflavin **49a,b** was found to give the highest yield (40%) and 5-*O*-( $\alpha$ -D-glucopyranosyl-(1'→4)D-glucopyranosyl)riboflavin **50a-c** gave the lowest yield of 5% (Table 4.3). This clearly showed that D-ribose being a smaller carbohydrate molecule acts as a better acceptor than the bulkier maltose.  $\beta$ -Glucosidase gave the highest yield of 24% for 5-*O*-( $\beta$ -D-glucopyranosyl)riboflavin **46b** and the lowest yield of 7% for 5-*O*-(D-mannopyranosyl)riboflavin **48a,b**. Also, while  $\beta$ -glucosidase favoured lactoside formation, amyloglucosidase did not.

Amyloglucosidase gave the following  $\alpha$ : $\beta$  proportions: D-glucose **6** - 66% of  $\alpha$ -D-glucoside and 44%  $\beta$ -D-glucoside compared to the 40:60  $\alpha$ : $\beta$  anomeric composition of free D-glucose **6**, D-galactose **7** - 52%  $\alpha$ -D-galactoside and 48%  $\beta$ -D-galactoside compared to the 92:8  $\alpha$ : $\beta$  of free D-galactose **7** and D-ribose **11** - 23%  $\alpha$ -D-riboside and 77%  $\beta$ -D-riboside compared to the 34:66  $\alpha$ : $\beta$  of free D-ribose **11**. Although,  $\beta$ -glucosidase in general do not exhibit inversion, had significantly altered the  $\alpha$ - $\beta$  composition: D-galactose **7** - 47%  $\alpha$ -D-galactoside and 53%  $\beta$ -D-galactoside and D-

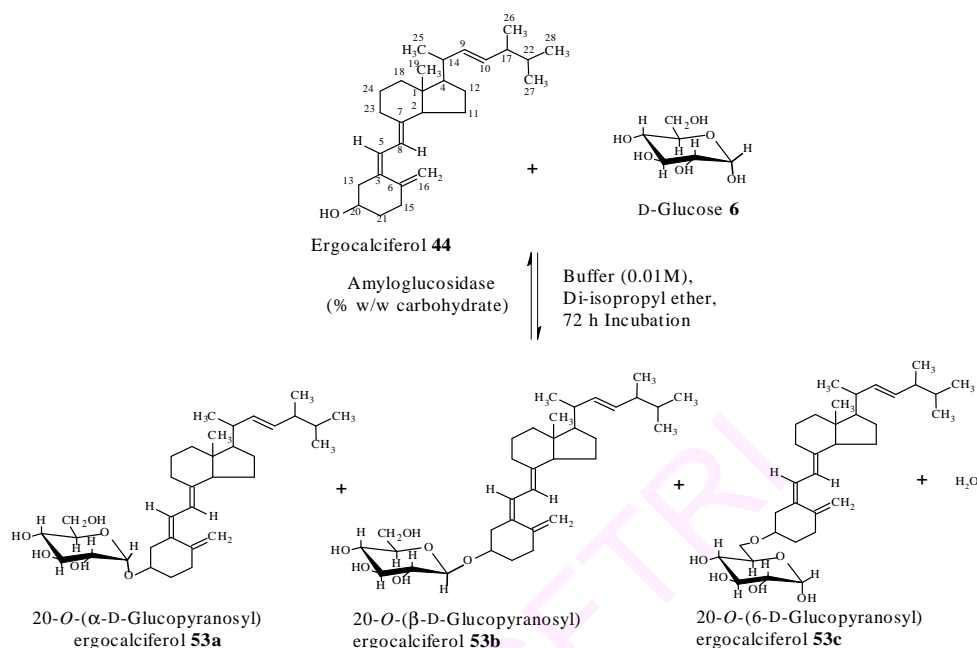
mannose **8** - 59%  $\alpha$ -D-mannoside and 41%  $\beta$ -D-mannoside comparable to 27:73  $\alpha$ : $\beta$  of free D-mannose.

Amyloglucosidase catalysis showed selectivity in case of D-mannose **8** by yielding the C1 $\alpha$ -D-mannoside and with sucrose **13** yielding C1-*O*-arylated product. It gave C1 $\alpha$  and  $\beta$  glycosides in case of D-glucose **6**, D-galactose **7** and D-ribose **11**. With D-glucose **6** and maltose **12**, C6-*O*-arylated products were also formed.  $\beta$ -Glucosidase showed selectivity with D-glucose **6** yielding C1 $\beta$ -D-glucoside and with lactose **14** yielding C1 $\beta$ -lactoside. However it gave a mixture of C1 $\alpha$  and  $\beta$  glycosides in case of D-galactose **7** and D-mannose **8**.

#### 4.2 Syntheses of ergocalciferol glycosides

Ergocalciferol (vitamin D<sub>2</sub>) is a plant sterol, derived from ergosterol which is the most common dietary source (Mello 2003). Vitamin D is not only a nutrient, but also a precursor of a steroid hormone with a wide range of activities that include an important role in calcium metabolism and cell differentiation. Vitamin D derivatives can be useful in treatment of several forms of cancer and their mode of action are currently under scrutiny (Smith *et al.* 1999; James *et al.* 1999; Peehl *et al.* 2003; Wieder *et al.* 2003 and Chen *et al.* 2003). Ergocalciferol prevents infantile rickets, capable of healing adult osteomalacia and osteonecrosis during renal transplantation (Houghton and Vieth 2006; Scholze *et al.* 1983). Active metabolite of vitamin D<sub>3</sub> is 1 $\alpha$ , 25-dihydroxyvitamin D<sub>3</sub> which regulates a wide variety of biological activities like intestinal calcium absorption, bone resorption and mineralization (Feldman *et al.* 2000). 1,25-Dihydroxyvitamin D<sub>3</sub>-glycoside has been identified in the plant. For example *Solanum malacoxylon* possess a vitamin D-like calcinogenic principle, which is water-soluble (Hausser *et al.* 1976). However, no reports are available on the syntheses of ergocalciferol (D<sub>2</sub>) glycosides. Therefore the present work deals with enzymatic syntheses of ergocalciferol (vitamin

D2) glycosides using amyloglucosidase from *Rhizopus* mold in di-isopropyl ether non-polar medium.



**Scheme 4.2** Synthesis of 20-*O*-(D-glucopyranosyl)ergocalciferol

Synthesis of 20-*O*-(D-glucopyranosyl)ergocalciferol was studied in detail. A typical synthesis involved refluxing ergocalciferol **44** (0.5 mmol) and D-glucose **6** (1 mmol) with stirring in a amber coloured 150 mL round bottomed flask fitted with a amber coloured condenser containing 100 mL of di-isopropyl ether in the presence of 10-75% (w/w D-glucose) amyloglucosidase and 0.04-0.2 mM (0.4-2 mL) of 10 mM of pH 4-8 buffer for a period of 72 h (Scheme 4.2). The reactions were carried out under a nitrogen atmosphere. Workup involved distilling off the solvent and denaturing the enzyme at 100 °C by holding in boiling water bath for 5-10 min. The residue containing unreacted ergocalciferol **44** and D-glucose **6** along with the product glucosides was extracted with hexane to remove unreacted ergocalciferol **44** and the aqueous layer containing unreacted D-glucose **6** and the product glucosides was evaporated to dryness. Workup and isolation of the compound was carried out in dark as ergocalciferol is a light sensitive compound. The glycoside was also stored in dark. The dried residue was

subjected to HPLC and the conversion yields were determined from HPLC peak areas (Fig. 4.13). Other procedures are as described on page 171. HPLC retention times for the substrates and products are: ergocalciferol-4.5 min, D-glucose-6.5 min, 20-*O*-(D-glucopyranosyl)ergocalciferol-9.3 min. An attempt was made to synthesize the ergocalciferyl glycosides using various other earlier mentioned carbohydrates **6-16** also but no other carbohydrate except D-glucose **6** underwent glycosylation with ergocalciferol.

#### **4.2.1 Synthesis of 20-*O*-(D-glucopyranosyl)ergocalciferol using amyloglucosidase**

Optimization conditions for the synthesis of 20-*O*-(D-glucopyranosyl) ergocalciferol using amyloglucosidase was studied in detail in terms of pH, buffer and enzyme concentrations.

##### **4.2.1.1 Effect of pH**

Buffers of different pH ranging from 4 to 8, 0.1 mM (1 mL) of buffer were added to 100 mL of di-isopropyl ether solvent and reactions performed (Table 4.4). Maximum glucosylation of 32% yield was obtained at pH 6 (phosphate buffer) and the conversion yield decreased beyond this pH values (Fig 4.14A).

##### **4.2.1.2 Effect of buffer concentration**

At pH 6, buffer concentration was varied from 0.04 to 0.2 mM (0.4 to 2 mL of 10 mM acetate buffer). With increase in buffer concentration, conversion yield increased from 30% for 0.04 mM (0.4 mL) buffer to 43% for 0.12 mM (1.2 mL) buffer. Beyond 0.12 mM (1.2 mL) concentration, the conversion yield decreased significantly.

##### **4.2.1.3 Effect of amyloglucosidase concentration**

Between 10 to 75% (w/w D-glucose) of enzyme concentration, 40% enzyme was found to give the best conversion yield of 42%, but all the other enzyme concentrations gave lesser conversion yields (Table 4.4, Fig 4.14B). Further increase in enzyme

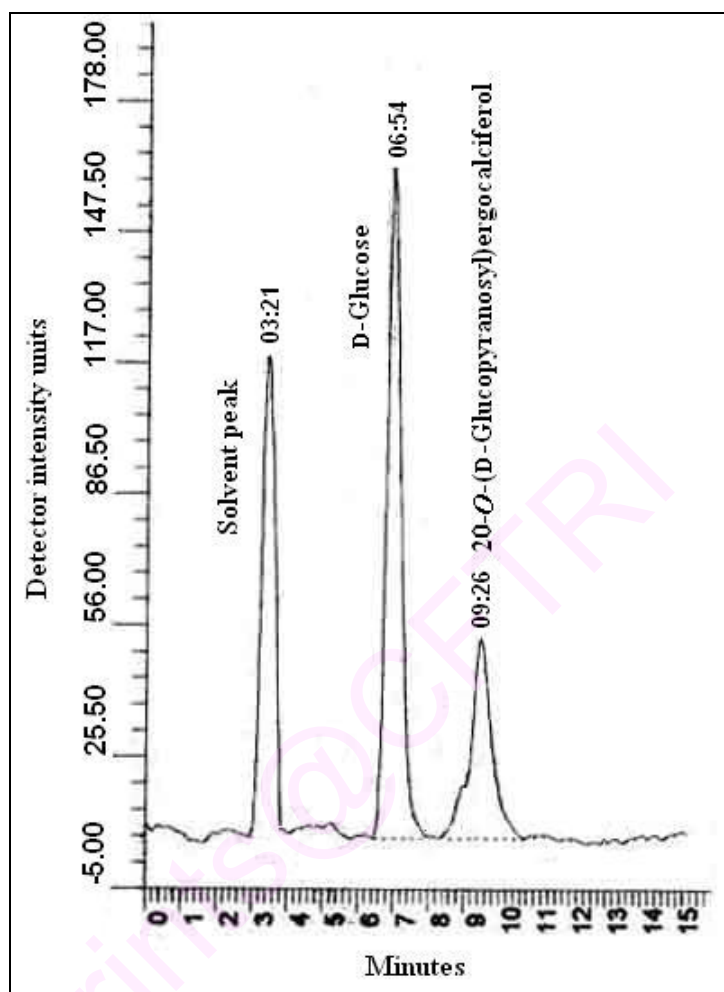


**Fig. 4.13** HPLC chromatogram for the reaction mixture of 20-*O*-(D-glucopyranosyl)ergocalciferol. HPLC conditions: Aminopropyl column (10  $\mu$ m, 300 mm  $\times$  3.9 mm), solvent-CH<sub>3</sub>CN: H<sub>2</sub>O (70:30 v/v), Flow rate-1 mL/min, RI detector. Peak retention times: solvent peak-3.2 min, D-glucose-6.5 min and 20-*O*-(D-glucopyranosyl)ergocalciferol-9.3 min.

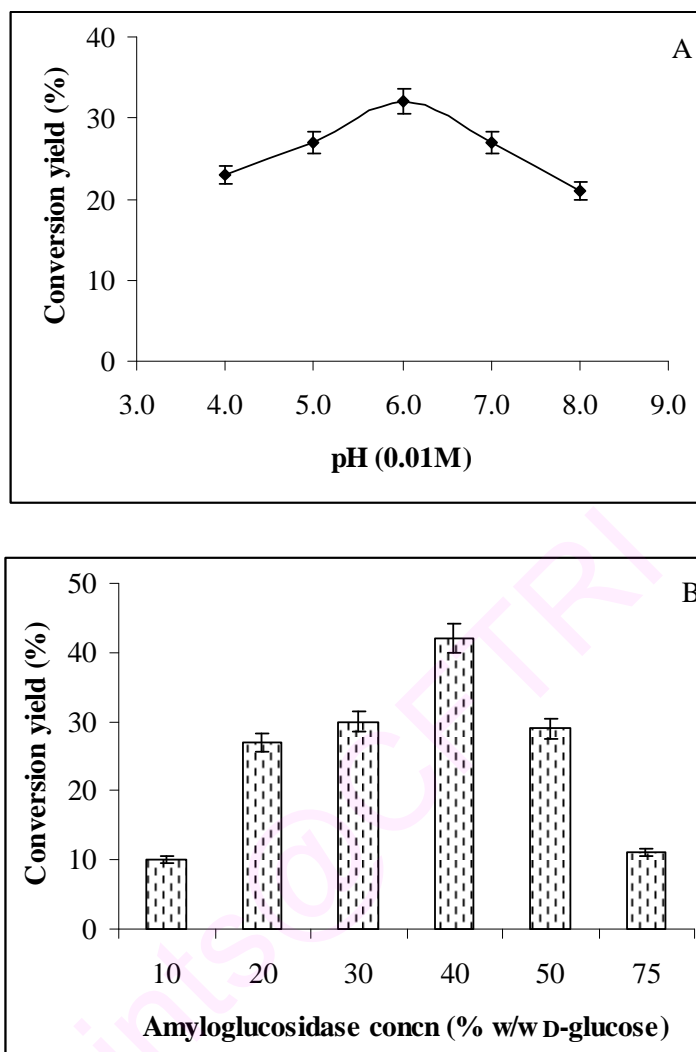


**Fig. 4.14 (A)** Effect of pH for 20-*O*-(D-glucopyranosyl)ergocalciferol synthesis by the reflux method. Conversion yields were from HPLC with respect to 1 mmol of D-glucose. Reaction conditions: D-glucose-1 mmol, ergocalciferol-0.5 mmol, amyloglucosidase-40% (w/w D-glucose), 0.1 mM (1 mL) solvent-di-isopropyl ether, temperature-68 °C and incubation period – 48 h. **(B)** Effect of enzyme concentration for 20-*O*-(D-glucopyranosyl) ergocalciferol synthesis. Reaction conditions: D-glucose-1 mmol, ergocalciferol-0.5 mmol, 0.12 mM (1.2 mL) pH 6 phosphate buffer, solvent-di-isopropyl ether, temperature-68 °C and incubation period – 48 h.



concentration beyond 40% w/w D-glucose decreased the conversion yield to 29% at 50% enzyme and 11% yield at 75% enzyme concentration.

**Table 4.4** Optimization of reaction conditions for the synthesis of 20-*O*-(D-glucopyranosyl)ergocalciferol using amyloglucosidase

Reaction conditions	Variable parameter <sup>b</sup>	Yield (%) <sup>c</sup>
	pH (0.01M)	
Ergocalciferol – 0.5 mmol <sup>a</sup>	4	23
D-glucose – 1 mmol	5	27
Amyloglucosidase – 40% w/w D-glucose	6	32
Buffer concentration – 0.1 mM (1 mL)	7	27
Incubation period – 48 h	8	21
	Buffer concentration (mM)	
Ergocalciferol – 0.5 mmol	0.04	30
D-glucose – 1 mmol	0.08	37
Amyloglucosidase – 40% w/w D-glucose	0.12	43
pH – 6	0.16	30
Incubation period – 48 h	0.2	8
	Amyloglucosidase concentration (% w/w D-glucose)	
Ergocalciferol – 0.5 mmol	10	10
D-glucose – 1 mmol	20	27
pH – 6	30	30
Buffer concentration – 0.12 mM (1.2 mL)	40	42
Incubation period – 48 h	50	29
	75	11

<sup>a</sup>Initial reaction conditions. <sup>b</sup>Other variables are the same as under reaction conditions, except the specified ones. <sup>c</sup>HPLC yields expressed with respect to 1 mmol D-glucose employed

#### 4.2.2 Solubility of 20-*O*-(D-glucopyranosyl)ergocalciferol

Determination of water solubility of 20-*O*-(D-glucopyranosyl)ergocalciferol showed that it is soluble to the extent of 6.4 g/L (Section 4.5.1). Hence, 20-*O*-(D-glucopyranosyl)ergocalciferol was found to be soluble than the water insoluble ergocalciferol.

#### 4.2.3 Spectral characterization

20-*O*-(D-Glucopyranosyl)ergocalciferol was characterized by recording UV, IR, Mass and 2D-HSQCT, which provided good information on the nature and proportions of the products formed.

**Ergocalciferol (Ergo) 44:** Solid; mp. 114 °C, UV (DMSO,  $\lambda_{\max}$ ): 194 nm ( $\sigma \rightarrow \sigma^*$ ,  $\epsilon_{194} - 406 \text{ M}^{-1}$ ), 216.5 nm ( $\sigma \rightarrow \pi^*$ ,  $\epsilon_{216.5} - 2140 \text{ M}^{-1}$ ), 265.5 nm ( $\pi \rightarrow \pi^*$ ,  $\epsilon_{265.5} - 3091 \text{ M}^{-1}$ ), IR (stretching frequency,  $\text{cm}^{-1}$ ) 3285 (OH), 1641 (aromatic C=C), 2D-HSQCT (DMSO- $d_6$ )  $^1\text{H}$  NMR  $\delta_{\text{ppm}}$  (500.13 MHz): 1.71 (H-4), 6.58 (H-5), 5.87 (H-6), 5.85 (H-8), 5.02 (H-9), 5.02 (H-10), 1.82 (H-11), 2.02 (H-12), 1.94 (H-13), 1.75 (H-14), 2.33 (H-15), 4.83 (H-16a), 5.07 (H-16b), 1.88 (H-17), 0.64 (H-19), 3.54 (H-20), 1.60 (H-21), 1.77 (H-22), 2.05 (H-23), 1.62 (H-24), 0.95 (H-26), 0.95 (H-27), 0.81 (H-28),  $^{13}\text{C}$  NMR  $\delta_{\text{ppm}}$  (125 MHz): 43.4 (C1), 135.9 (C3), 56.7 (C4), 130.2 (C5), 143.2 (C6), 116.6 (C8), 136 (C9), 132.5 (C10), 24.2 (C11), 28.3 (C12), 40.8 (C13), 40.2 (C14), 30.7 (C15), 110.9 (C16), 43.1 (C17), 11.9 (C19), 71.3 (C20), 30.5 (C21), 32.5 (C22), 17.6 (C26), 20.4 (C27), 20.4 (C28). Ultraviolet-visible spectra is shown in Fig. 4.15A.

**4.2.3.1 20-O-(D-Glucopyranosyl)ergocalciferol 53a-c:** Solid; UV ( $\text{H}_2\text{O}$ ,  $\lambda_{\max}$ ): 193 nm ( $\sigma \rightarrow \sigma^*$ ,  $\epsilon_{193} - 204 \text{ M}^{-1}$ ), 216 nm ( $\sigma \rightarrow \pi^*$ ,  $\epsilon_{216} - 95 \text{ M}^{-1}$ ), 265 nm ( $\pi \rightarrow \pi^*$ ,  $\epsilon_{265} - 10 \text{ M}^{-1}$ ), IR (stretching frequency,  $\text{cm}^{-1}$ ) 1033 (C-O-C aryl alkyl symmetrical), 1258 (C-O-C aryl alkyl asymmetrical), 3360 (OH), 1620 (aromatic C=C), MS ( $m/z$ ) - 557.31  $[\text{M}-1]^+$ , 2D-HSQCT (DMSO- $d_6$ ) **C1 $\alpha$ -glucoside 53a:**  $^1\text{H}$  NMR  $\delta_{\text{ppm}}$  (500.13 MHz) **Glu:** 5.21 (H-1 $\alpha$ , d,  $J = 3.7 \text{ Hz}$ ), 3.30 (H-2 $\alpha$ ), 3.44 (H-3 $\alpha$ ), 3.67 (H-4 $\alpha$ ), 3.63 (H-5 $\alpha$ ), 3.46 (H-6a), **Ergo:** 1.85 (H-4), 6.50 (H-5), 5.87 (H-8), 5 (H-9), 5 (H-10), 1.90 (H-11), 2.02 (H-12), 1.93 (H-13), 1.85 (H-14), 2.30 (H-15), 4.83 (H-16a), 5.06 (H-16b), 1.97 (H-17), 0.50 (H-19), 3.50 (H-20), 1.62 (H-21), 1.90 (H-22), 2.10 (H-23), 1.56 (H-24), 0.88 (H-26), 0.99 (H-27), 0.81 (H-28),  $^{13}\text{C}$  NMR  $\delta_{\text{ppm}}$  (125 MHz) **Glu:** 96.5 (C1 $\alpha$ ), 70.7 (C2 $\alpha$ ), 73.5 (C3 $\alpha$ ), 69.9 (C4 $\alpha$ ), 72.6 (C5 $\alpha$ ), 61.6 (C6), **Ergo:** 136.9 (C3), 53.7 (C4), 125.7 (C5), 144.7 (C6), 117.5 (C8), 136 (C9), 136.6 (C10), 24.5 (C11), 28.1 (C12), 40.7 (C13), 40.3 (C14), 30.7 (C15), 110.8 (C16), 43.3 (C17), 11.5 (C19), 72.3 (C20), 29.9 (C21), 31.5 (C22), 17.4 (C26), 21 (C27), 20.7 (C28), **C1 $\beta$ -glucoside 53b:**  $^1\text{H}$  NMR  $\delta_{\text{ppm}}$  **Glu:** 4.85 (H-1 $\beta$ , d,  $J =$

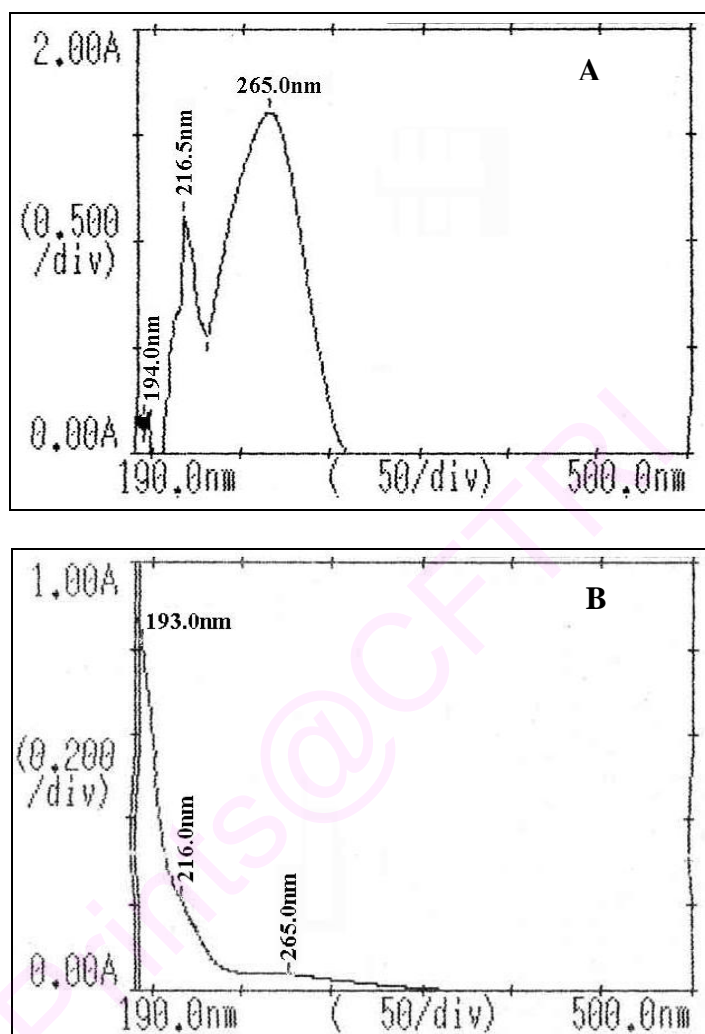


**Fig. 4.15** Ultraviolet-visible spectra of **(A)** Ergocalciferol **44** and **(B)** 20-O-(D-Glucopyranosyl) ergocalciferol **53a-c**.

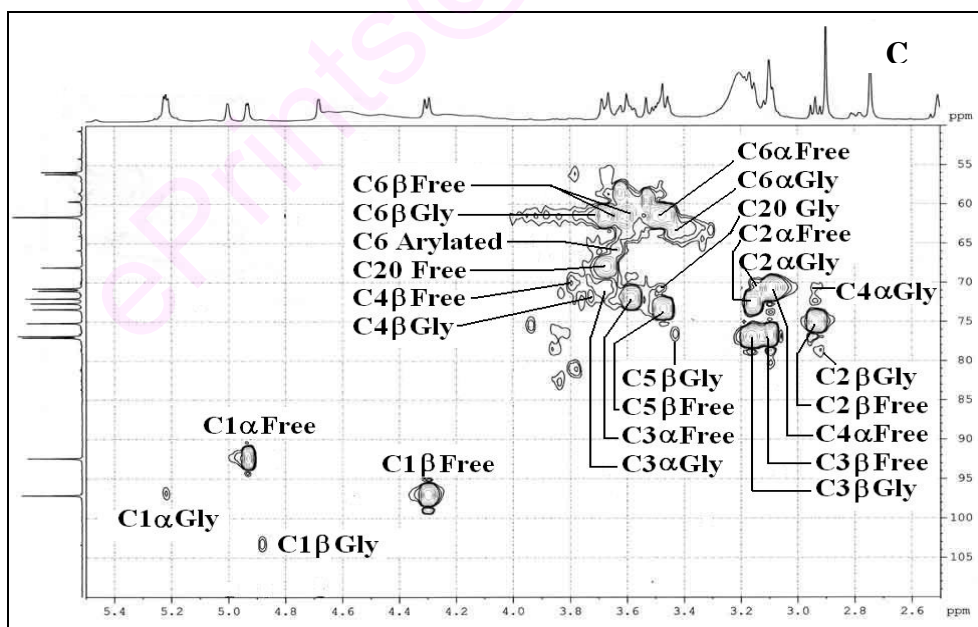
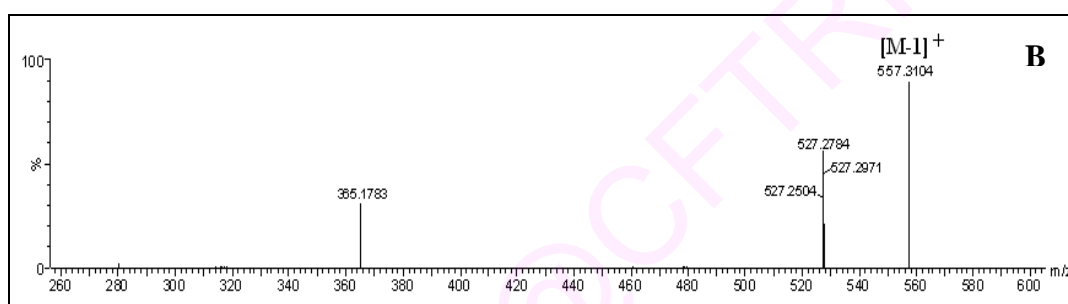
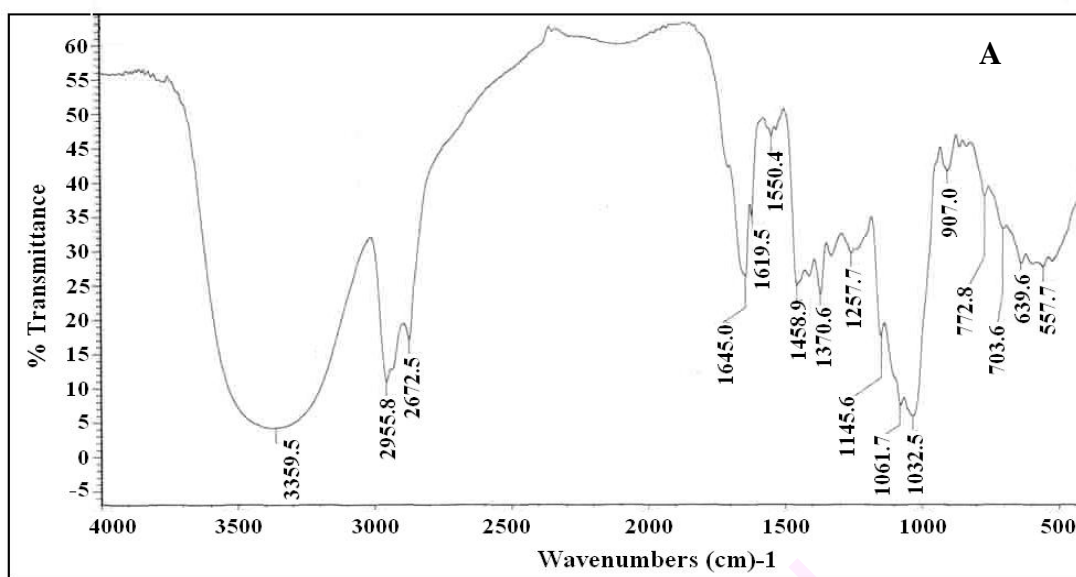
7.1 Hz), 2.94 (H-2 $\beta$ ), 3.17 (H-3 $\beta$ ), 3.68 (H-4 $\beta$ ), 3.46 (H-5 $\beta$ ), 3.46 (H-6a),  $^{13}\text{C}$  NMR  $\delta_{\text{ppm}}$  **Glu**: 103 (C1 $\beta$ ), 76.5 (C2 $\beta$ ), 76.4 (C3 $\beta$ ), 71.5 (C4 $\beta$ ), 76.6 (C5 $\beta$ ), 61.6 (C6), **C6-O-arylated 53c**:  $^1\text{H}$  NMR  $\delta_{\text{ppm}}$  **Glu**: 3.62 (H-6a),  $^{13}\text{C}$  NMR  $\delta_{\text{ppm}}$  **Glu**: 66.7 (C6).

Ultraviolet-visible, IR, mass and 2D-HSQCT NMR spectra for 20-*O*-(D-glucopyranosyl)ergocalciferol **53a-c** are shown in Figures 4.15B, 4.16A, 4.16B and 4.16C respectively.

Ultraviolet-visible spectra of 20-*O*-(D-glucopyranosyl)ergocalciferol, showed shifts in  $\sigma \rightarrow \sigma^*$  band at 193 nm (194 nm for free ergocalciferol),  $\sigma \rightarrow \pi^*$  band at 216 nm (216.5 nm for free ergocalciferol) and  $\pi \rightarrow \pi^*$  band in the 265 nm (265.5 nm for free riboflavin), IR glycosidic C-O-C symmetrical stretching frequency at 1033  $\text{cm}^{-1}$  and glycosidic C-O-C asymmetrical stretching frequency at 1258  $\text{cm}^{-1}$  indicating that ergocalciferol had undergone glycosylation. From 2D HSQCT spectra of 20-*O*-(D-glucopyranosyl)ergocalciferol, the following glucoside formation was confirmed the respective chemical shift values - C1 $\alpha$  glucoside **53a** to C1 $\alpha$  at 96.5 ppm and H-1 $\alpha$  at 5.21 ppm, C1 $\beta$  glucoside **53b** to C1 $\beta$  at 103 ppm and H-1 $\beta$  at 4.85 ppm and C6-*O*-arylated **53c** to C6 at 66.7 ppm and H-6a at 3.62 ppm. Mass spectra also confirmed the formation of the above mentioned glucosides. Two-dimensional HSQCT data clearly indicated that glycosylation has occurred at the acyclic OH of 20<sup>th</sup> position of ergocalciferol.

#### 4.2.4 Discussion

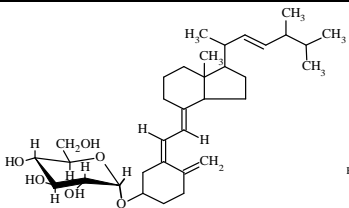
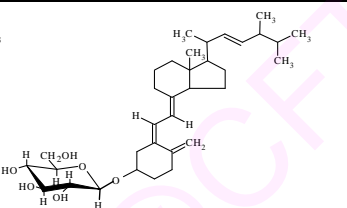
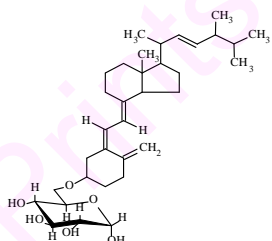
Ergocalciferol-D-glucosides **53a-c** [20-*O*-( $\alpha$ -D-glucopyranosyl)ergocalciferol **53a**, 20-*O*-( $\beta$ -D-glucopyranosyl)ergocalciferol **53b** and 20-*O*-(6-D-glucopyranosyl)ergocalciferol **53c**] were detected in the reaction when amyloglucosidase was employed (Table 4.5). However, amyloglucosidase did not show much regioselectivity in this reaction. Amyloglucosidase did not catalyze the reaction with the other carbohydrate



**Fig. 4.16** 20-*O*-(D-Glucopyranosyl)ergocalciferol **53a-c**: (A) IR spectrum, (B) Mass spectrum and (C) 2D-HSQC spectrum showing the C1-C6 region. Some of the NMR assignments are interchangeable.

molecules. This could be due to either steric hindrance caused by the bulkier hydrophobic vitamin D<sub>3</sub> molecule when the carbohydrate molecules were transferred to its acyclic OH group or due to the stronger binding of vitamin D<sub>2</sub> compared to the other carbohydrate molecules employed. The maximum conversion was found to 42% for 20-*O*-(D-glucopyranosyl)ergocalciferol **53a-c**. Being ‘inverting’ in nature, amyloglucosidase gave the following  $\alpha$ : $\beta$  proportions - 48% of  $\alpha$ -D-glucoside and 52%  $\beta$ -glucoside compared to the 40:60  $\alpha$ : $\beta$  anomeric composition of the D-glucose employed.

**Table 4.5** Synthesis of 20-*O*-(D-glucopyranosyl)ergocalciferol using amyloglucosidase

Glycosides	Amyloglucosidase catalysis <sup>a</sup>	
	Product (% proportion) <sup>b</sup>	Yields (%) <sup>c</sup>
 <p><b>53a</b> 20-<i>O</i>-(<math>\alpha</math>-D-Glucopyranosyl)ergocalciferol</p>	C1 $\alpha$ glucoside (22), C1 $\beta$ glucoside (52), C6- <i>O</i> -arylated (26)	42
 <p><b>53b</b> 20-<i>O</i>-(<math>\beta</math>-D-Glucopyranosyl)ergocalciferol</p>		
 <p><b>53c</b> 20-<i>O</i>-(6-D-Glucopyranosyl)ergocalciferol</p>		

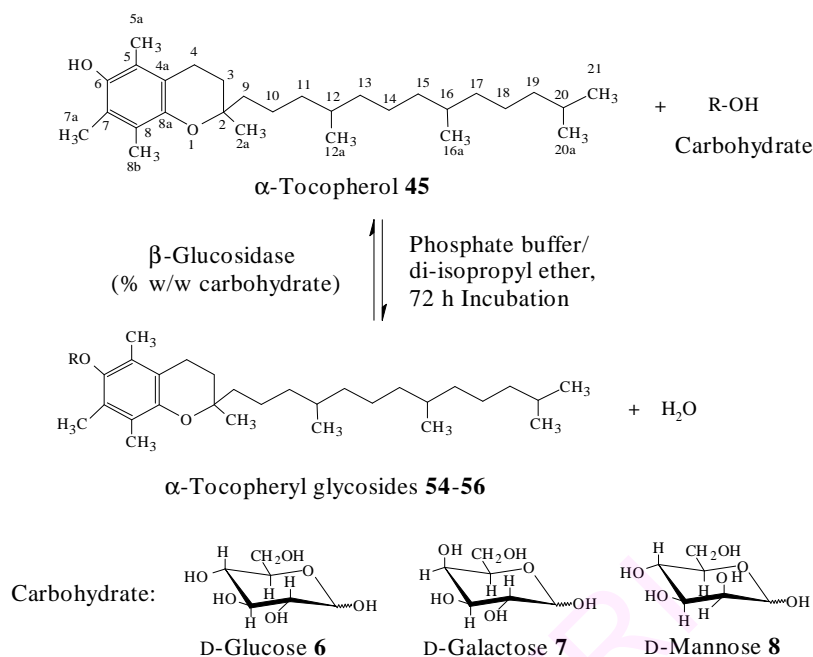
<sup>a</sup> Ergocalciferol – 0.5 mmol; D-glucose – 1 mmol; amyloglucosidase – 40% (w/w D-glucose); solvent – diisopropyl ether; buffer – 0.12 mM (1.2 mL) pH 6 phosphate buffer; incubation period – 48 h. <sup>b</sup>The product proportions were determined from the area of respective <sup>1</sup>H/<sup>13</sup>C signals. <sup>c</sup>Conversion yields were from HPLC with respect to free D-glucose. Error in yield measurements is  $\pm$  5-10%.

### 4.3 Syntheses of $\alpha$ -tocopheryl glycosides

$\alpha$ -Tocopherol [2,5,7,8-tetramethyl-2-(4',8',12'-trimethyltridecyl)-6-chromanol, vitamin E], an oil soluble vitamin, is a very important component of biological membranes (Witkowski *et al.* 1998), stabilizing them by acting as a potent antioxidant and free radical scavenger (Burton *et al.* 1983). Vitamin E, has been frequently used

since 1970 to treat various diseases (Sato *et al.* 2001), which includes treatment against gynecological internal secretion, control against sterility, heart circulation, liver diseases, peripheral blood circulation, thrombosis, drug poisoning, radiation damage, aging and carcinogenesis. Vitamin E is also used as a therapeutic agent against acute lung and aspirin induced gastric mucosal injuries (Ochiai *et al.* 2002; Isozaki *et al.* 2005; Ichikawa *et al.* 2003).

Vitamin E has been reported to exhibit poor water solubility, stability and absorbtivity. Glycosylation improves the pharmacological property by increasing the water solubility of vitamin E. Attachment of  $\beta$ -glucosyl,  $\beta$ -maltosyl and  $\beta$ -oligomaltosyl units via 6-OH group of  $\alpha$ -tocopherol (Trolox) was achieved by Lahman and Thiem (1997). One-step enzymatic glycosylation is useful for the preparation of glycosides rather than chemical glycosylation, which requires large number of protection-deprotection steps. Water soluble  $\alpha$ -tocopherol derivatives 2,5,7,8-tetramethyl-2-(4-methylpentyl)chroman-6-yl- $\beta$ -D-glucopyranoside and 2,5,7,8-tetramethyl-2-(4methyl pentyl)chroman-6-yl-6-O- $\beta$ -D-glucopyranosyl- $\beta$ -D-glucopyranoside using cultured plant cells of *Phytolacca americana* and *Catheranthus roseus* (Hamada *et al.* 2002; Kondo *et al.* 2006; Shimoda *et al.* 2006) were prepared. Enzymatic glycosylation of vitamin E using a  $\alpha$ -glucosidase from *Saccharomyces* sp. (Murase *et al.* 1997) showed that the glycosylated product is water-soluble (>1 gm/mL) and its free radical scavenging activity is similar to that of  $\alpha$ -tocopherol. However, a detailed study on exclusive enzymatic glycosylation of  $\alpha$ -tocopherol has not been reported. Hence, the present study is attempted to prepare water soluble  $\alpha$ -tocopheryl glycosides enzymatically using  $\beta$ -glucosidase isolated from sweet almond in di-isopropyl ether non polar medium.



### Scheme 4.3 Syntheses of $\alpha$ -tocopheryl glycosides

Syntheses of  $\alpha$ -tocopherol glycosides involved refluxing  $\alpha$ -tocopherol **45** (0.25-2.5 mmol) with 0.5 mmol carbohydrates (D-glucose **6**, D-galactose **7** and D-mannose **8**) in a 150 mL amber coloured round bottomed flask fitted with a amber coloured condenser containing 100 mL di-isopropyl ether in presence of  $\beta$ -glucosidase 10-75% (w/w D-glucose) and 0.05 – 0.25 mM (0.5 – 2.5 mL) of 0.01 M pH 4-8 buffer for an incubation period of 72 h at 68 °C (Scheme 4.3). The reactions were carried out under nitrogen atmosphere. The solvent was evaporated and the enzyme denatured at 100 °C by holding in boiling water bath for 5-10 min. The residue containing  $\alpha$ -tocopherol **45**, D-glucose **6**, along with the product glycosides were dissolved in 15-20 mL of water and the reaction mixture after extraction with hexane to remove  $\alpha$ -tocopherol **45** was evaporated to dryness. Workup and isolation of the glycosides were carried out in dark as  $\alpha$ -tocopherol is a light sensitive compound. The glycosides were also stored at dark. The dried residue was subjected to HPLC analysis to determine the extent of conversion (Fig. 4.17). Other procedures are as described on page 172. HPLC retention times for the



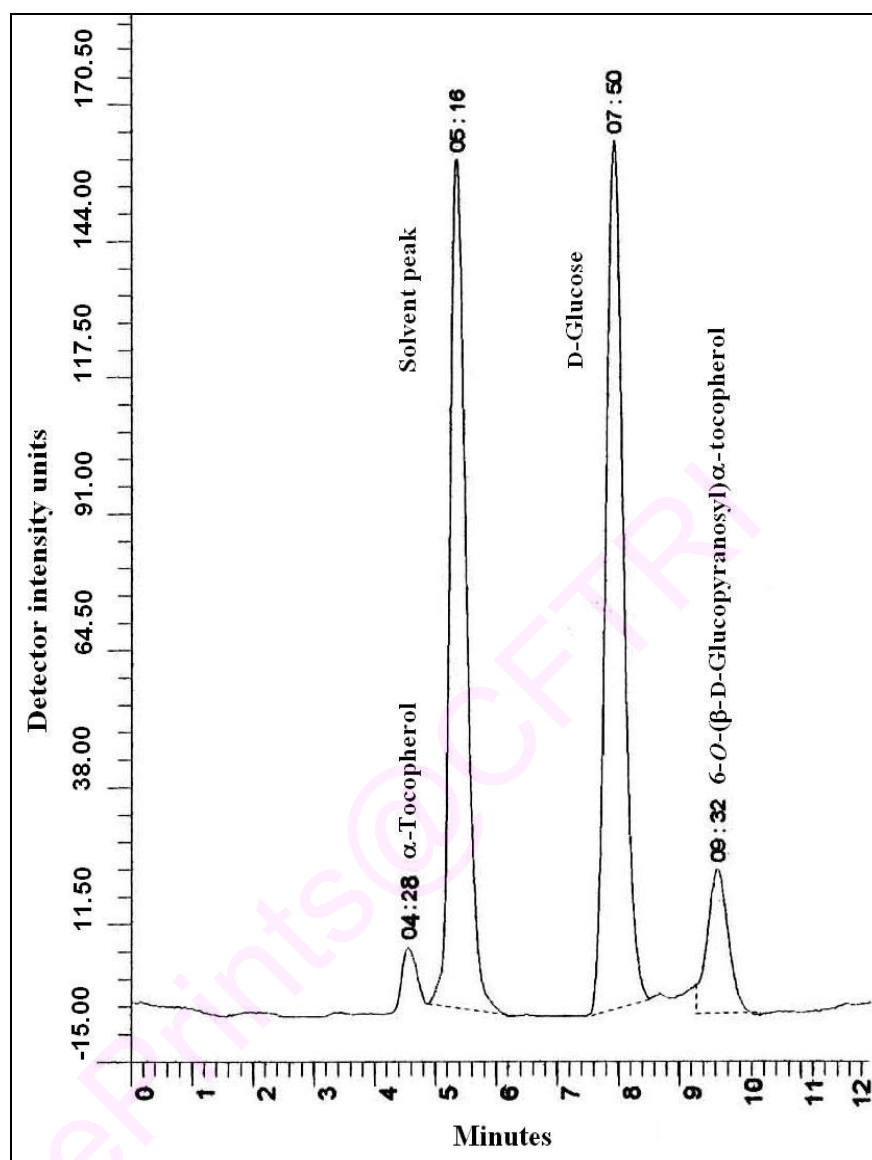


**Fig. 4.17** HPLC chromatogram for the reaction mixture of 6-O-( $\beta$ -D-glucopyranosyl) $\alpha$ -tocopherol. HPLC conditions: Aminopropyl column (10  $\mu$ m, 300 mm  $\times$  3.9 mm), solvent-CH<sub>3</sub>CN: H<sub>2</sub>O (70:30 v/v), Flow rate-1 mL/min, RI detector. Peak retention times:  $\alpha$ -tocopherol-4.3 min, solvent peak-5.2 min, D-glucose-7.5 min and 6-O-( $\beta$ -D-glucopyranosyl) $\alpha$ -tocopherol-9.3 min.

substrates and products are:  $\alpha$ -tocopherol-4.3 min, D-glucose-7.5 min, D-galactose-7.1 min and D-mannose-6.7 min, 6-*O*-(D-glucopyranosyl)  $\alpha$ -tocopherol-9.3 min, 6-*O*-(D-galactopyranosyl) $\alpha$ -tocopherol-10.1 min and 6-*O*-(D-mannopyranosyl) $\alpha$ -tocopherol-9.1 min.

#### 4.3.1 Synthesis of 6-*O*-( $\beta$ -D-glucopyranosyl) $\alpha$ -tocopherol using $\beta$ -glucosidase

$\beta$ -Glucosidase isolated from sweet almond catalyzed synthesis of 6-*O*-(D-glucopyranosyl) $\alpha$ -tocopherol was optimized in terms of incubation period, pH, buffer, enzyme and  $\alpha$ -tocopherol concentrations (Scheme 4.3).

##### 4.3.1.1 Effect of incubation period

Effect of incubation period studied from 3 h to 96 h showed that the highest yield was achieved at 72 h incubation period. The conversion yields increased with increasing incubation periods from 3 h to 72 h and decreased at 96 h of incubation period (Table 4.6, Fig. 4.18A). Incubation period resulted in attaining maximum equilibrium conversion at 72-96 h, which decreased due to prolonged incubation at 68 °C, the boiling temperature of di-isopropyl ether solvent.

##### 4.3.1.2 Effect of pH

At a fixed buffer concentration of 0.1 mM (1 mL) the conversion yield was the highest at pH 6, being 24% (Table 4.6). At higher pH values (above pH 6) the conversion yield decreased.

##### 4.3.1.3 Effect of buffer concentration

Glucosylation occurred in presence of a very small amount of buffer. Since the highest conversion yield for  $\beta$ -glucosidase was obtained at pH 6, varying concentration of pH 6 buffer from 0.05 mM to 0.25 mM (0.5 mL to 2.5 mL) resulted in a maximum yield of 23% at 0.1 mM (1 mL) buffer concentration (Table 4.6, Fig. 4.18B).

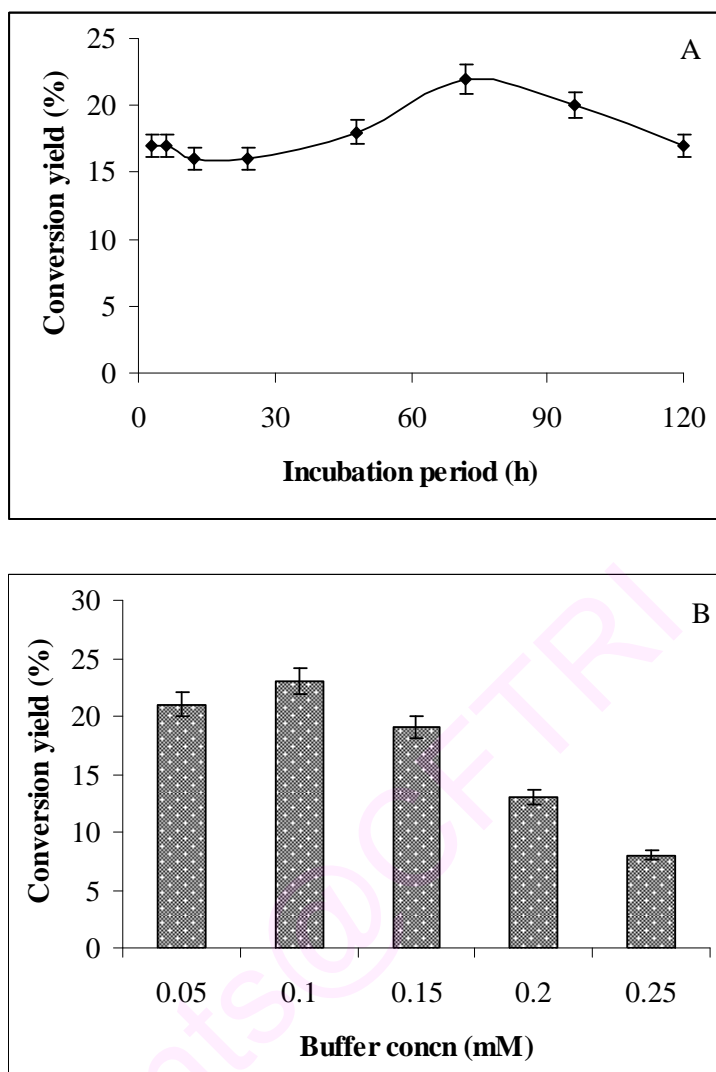


**Fig. 4.18** (A) Reaction profile for 6-*O*-(β-D-glucopyranosyl)α-tocopherol synthesis by the reflux method. Conversion yields were from HPLC with respect to 0.5 mmol of D-glucose. Reaction conditions: D-glucose-0.5 mmol, α-tocopherol-0.5 mmol, β-glucosidase-40% (w/w D-glucose), 0.1 mM (1 mL) pH 6 phosphate buffer, solvent-di-isopropyl ether and temperature-68 °C. (B) Effect of buffer concentration for 6-*O*-(β-D-glucopyranosyl)α-tocopherol synthesis. Reaction conditions: D-glucose-0.5 mmol, α-tocopherol-0.5 mmol, β-glucosidase-40% (w/w D-glucose), pH 6 phosphate buffer, solvent-di-isopropyl ether, temperature-68 °C and incubation period – 72 h.

**Table 4.6** Optimization of reaction conditions for the synthesis of 6-*O*-( $\beta$ -D-glucopyranosyl) $\alpha$ -tocopherol using  $\beta$ -glucosidase

Reaction conditions	Variable parameter <sup>b</sup>	Conversion Yields (%) <sup>c</sup>
	Incubation period (h)	
$\alpha$ -Tocopherol – 0.5 mmol <sup>a</sup>	3	17
D-Glucose – 0.5 mmol	6	17
pH – 6	12	16
Buffer concentration – 0.1 mM (1 mL)	24	16
$\beta$ -Glucosidase – 40% w/w D-glucose	48	18
	72	22
	96	20
	120	17
	pH (0.01M)	
$\alpha$ -Tocopherol – 0.5 mmol	4	18
D-Glucose – 0.5 mmol	5	20
$\beta$ -Glucosidase – 40% w/w D-glucose	6	24
Buffer concentration – 0.1 mM (1 mL)	7	20
Incubation period – 72 h	8	17
	Buffer concentration (mM)	
$\alpha$ -Tocopherol – 0.5 mmol	0.05	21
D-Glucose – 0.5 mmol	0.1	23
$\beta$ -Glucosidase – 40% w/w D-glucose	0.15	19
pH – 6	0.2	13
Incubation period – 72 h	0.25	8
	$\beta$ -Glucosidase concentration (% w/w D-glucose)	
$\alpha$ -Tocopherol – 0.5 mmol	10	10
D-Glucose – 0.5 mmol	20	18
pH – 6	30	17
Buffer concentration – 0.1 mM (1 mL)	40	23
Incubation period – 72 h	50	8
	75	7
	$\alpha$ -Tocopherol (mmol)	
pH – 6	0.25	18
Buffer concentration – 0.1 mM (1 mL)	0.5	21
D-Glucose – 0.5 mmol	0.75	17
$\beta$ -Glucosidase – 40% w/w D-glucose	1	15
Incubation period – 72 h	1.5	15
	2	15
	2.5	16

<sup>a</sup>Initial reaction conditions. <sup>b</sup>Other variables are the same as under reaction conditions, except the specified ones. <sup>c</sup>HPLC yields expressed with respect to 0.5 mmol D-glucose employed.

#### 4.3.1.4 Effect of enzyme concentration

Effect of increasing enzyme concentration was studied by varying  $\beta$ -glucosidase concentrations from 10 to 75% (w/w D-glucose) at 0.5 mmol of D-glucose and  $\alpha$ -tocopherol. A 40% (w/w D-glucose)  $\beta$ -glucosidase at 0.1mM (1 mL) pH 6 buffer gave the maximum conversion yield of 23% (Table 4.6).

#### 4.3.1.5 Effect of $\alpha$ -tocopherol concentration

$\alpha$ -Tocopherol concentration was varied from 0.5 mmol to 2.5 mmol at a fixed D-glucose concentration of 0.5 mmol. The above optimized conditions of pH 6, 0.1mM (1 mL) buffer concentration and 40% (w/w D-glucose)  $\beta$ -glucosidase, gave the highest conversion yield of 21% at 0.5 mmol  $\alpha$ -tocopherol. There was no significant conversion beyond 0.5 mmol of  $\alpha$ -tocopherol, which remained more or less constant at higher concentrations of  $\alpha$ -tocopherol (Table 4.6).

#### 4.3.2 Solubility of 6-*O*-(D-glucopyranosyl) $\alpha$ -tocopherol

Determination of water solubility of 6-*O*-(D-glucopyranosyl) $\alpha$ -tocopherol showed that it is soluble to the extent of 25.9 g/L (Section 4.5.1). Hence, a water soluble 6-*O*-(D-glucopyranosyl) $\alpha$ -tocopherol was prepared in the present work from water insoluble  $\alpha$ -tocopherol.

#### 4.3.3 Syntheses of $\alpha$ -tocopheryl glycosides of other carbohydrates using $\beta$ -glucosidase

Syntheses of the other  $\alpha$ -tocopheryl glycosides were carried out at the above determined optimized conditions, with  $\alpha$ -tocopherol **45** and carbohydrates: D-glucose **6**, D-galactose **7** and D-mannose **8**. The conditions employed for  $\beta$ -glucosidase catalysis are:  $\alpha$ -tocopherol **45** (0.5 mmol) and carbohydrate (0.5 mmol),  $\beta$ -glucosidase 40% (w/w

carbohydrate), 0.1 mM (1 mL) pH 6 phosphate buffer and 72h of incubation period (Scheme 4.3). Other procedures are as described on page 201.

#### 4.3.4 Spectral characterization

$\alpha$ -Tocopheryl glycosides besides measuring melting point and optical rotation were also characterized by recording UV, IR, Mass and 2D-HSQCT, which provided good information on the nature and proportions of the products formed.

**$\alpha$ -Tocopherol ( $\alpha$ -Toco) 45:** Viscous liquid; bp 220 °C, UV (DMSO,  $\lambda_{\max}$ ): 199 nm ( $\sigma \rightarrow \sigma^*$ ,  $\epsilon_{199} - 730 \text{ M}^{-1}$ ), 228 nm ( $\sigma \rightarrow \pi^*$ ,  $\epsilon_{228} - 4330 \text{ M}^{-1}$ ), 292 nm ( $n \rightarrow \pi^*$ ,  $\epsilon_{292} - 2580 \text{ M}^{-1}$ ), IR (stretching frequency,  $\text{cm}^{-1}$ ): 3472 (OH), 1616 (aromatic C=C), 2D-HSQCT (DMSO- $d_6$ )  $^1\text{H NMR } \delta_{\text{ppm}}$ : 1.22 (H-2a), 1.71 (H-3), 2.45 (H-4), 1.96 (H-5a), 1.98 (H-7a), 2.05 (H-8b), 1.35 (H-9), 1.36 (H-10), 1.22 (H-11), 1.35 (H-12), 0.78 (H-12a), 1.05 (H-13), 1.15 (H-14), 1.22 (H-15), 1.23 (H-16), 0.85 (H-16a), 1.22 (H-17), 0.80 (H-18), 1.42 (H-19), 1.48 (H-20), 0.85 (H-20a), 0.80 (H-21);  $^{13}\text{C NMR } \delta_{\text{ppm}}$  (125 MHz): 73.9 (C2), 23.8 (C2a), 31.4 (C3), 20.5 (C4), 116.8 (C4a), 120.3 (C5), 11.7 (C5a), 144.6 (C6), 122.6 (C7), 12.8 (C-a), 121 (C8), 145.2 (C8a), 11.8 (C8b), 38.9 (C9), 23.7 (C10), 37 (C11), 32.1 (C12), 19.7 (C12a), 36.8 (C13), 24.2 (C14), 37 (C15), 32 (C16), 19.6 (C16a), 37 (C17), 24.2 (C18), 39.1 (C19), 27.5 (C20), 22.6 (C20a), 22.5 (C21). Ultraviolet-visible spectra is shown in Fig. 4.19A.

**4.3.4.1 6-O-( $\beta$ -D-Glucopyranosyl) $\alpha$ -tocopherol 54:** Semi solid; mp. 104°C, UV ( $\text{H}_2\text{O}$ ,  $\lambda_{\max}$ ): 195 nm ( $\sigma \rightarrow \sigma^*$ ,  $\epsilon_{195} - 2542 \text{ M}^{-1}$ ), 223 nm ( $\sigma \rightarrow \pi^*$ ,  $\epsilon_{223} - 753 \text{ M}^{-1}$ ), 270.5 nm ( $\pi \rightarrow \pi^*$ ,  $\epsilon_{270.5} - 348 \text{ M}^{-1}$ ), IR (stretching frequency,  $\text{cm}^{-1}$ ): 1028 (glycosidic C-O-C aryl alkyl symmetrical), 1259 (glycosidic C-O-C aryl alkyl asymmetrical), 3346 (OH), 1603 (aromatic C=C),  $[\alpha]_{\text{D}}^{25} = -5.7^\circ$  ( $c$  1,  $\text{H}_2\text{O}$ ), MS ( $m/z$ ) - 615  $[\text{M}+\text{Na}]^+$ , 2D-HSQCT (DMSO- $d_6$ )  $^1\text{H NMR } \delta_{\text{ppm}}$  **Glu**: 4.20 (H-1 $\beta$ , d,  $J = 7.8 \text{ Hz}$ ), 2.98 (H-2 $\beta$ ), 3.18 (H-3 $\beta$ ), 3.76 (H-4 $\beta$ ), 3.02 (H-5 $\beta$ ), 3.43 (H-6a), 3.48 (H-6b),  **$\alpha$ -Toco**: 1.22 (H-2a), 2.5 (H-4), 1.92

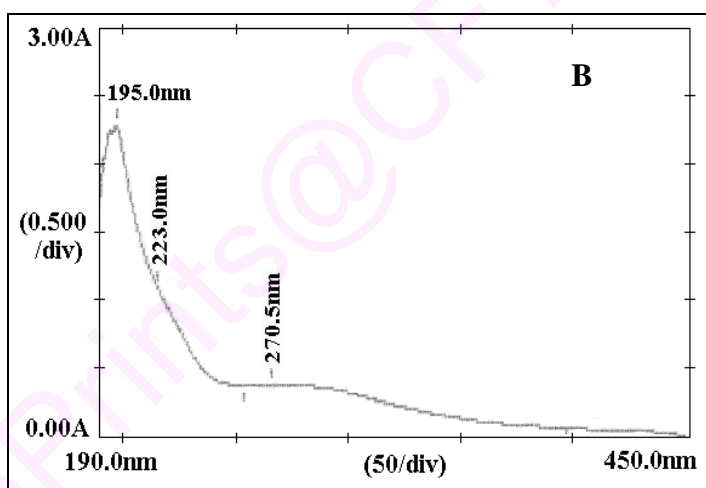
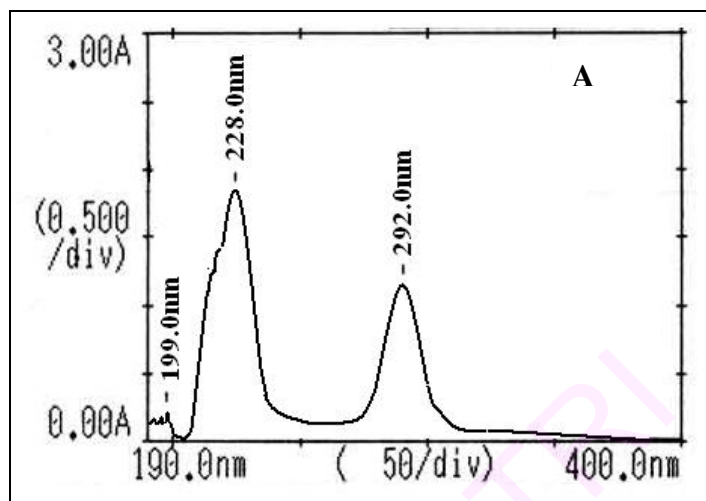


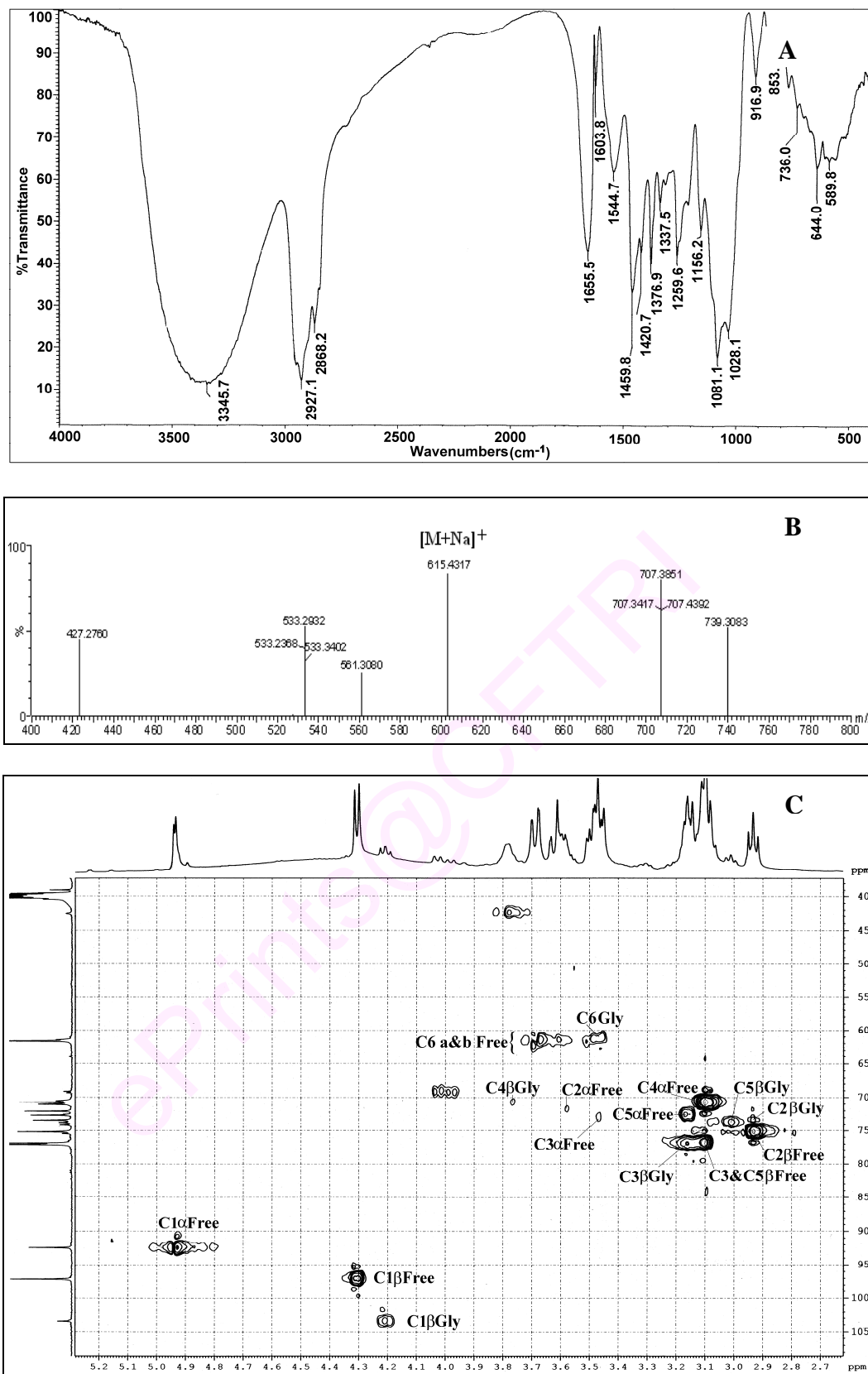
**Fig. 4.19** Ultraviolet-visible spectra of (A)  $\alpha$ -Tocopherol **45** and (B) 6-O-( $\beta$ -D-Glucopyranosyl) $\alpha$ -tocopherol **54**.

(H-5a), 1.96 (H-7a), 1.99 (H-8b), 0.90 – 1.32 (H-9 – H-20), 0.70 (H-12a), 0.81 (H-16a), 0.82 (H-20a), 0.70 (H-21),  $^{13}\text{C}$  NMR  $\delta_{\text{ppm}}$  **Glu**: 103.2 (C1 $\beta$ ), 73 (C2 $\beta$ ), 76 (C3 $\beta$ ), 70.3 (C4 $\beta$ ), 73.5 (C5 $\beta$ ), 61.2 (C6 $\beta$ ),  **$\alpha$ -Toco**: 23.6 (C2a), 20.5 (C4), 120.4 (C4a), 121 (C5), 14 (C5a), 150 (C6), 123 (C7), 11.5 (C7a), 116.8 (C8), 145.2 (C8a), 11.5 (C8b), 37.1 (C9), 20.2 (C10), 37 (C11), 32 (C12), 19.4 (C12a) 39 (C13), 24 (C14), 37.9 (C15), 32.2 (C16), 19.4 (C16a), 23 (C18), 39 (C19), 27.2 (C20), 22.5 (C20a, C21).

Ultraviolet-visible, IR, mass and 2D-HSQCT NMR spectra for 6-*O*-( $\beta$ -D-glucopyranosyl) $\alpha$ -tocopherol **54** are shown in Figures 4.19B, 4.20A, 4.20B and 4.20C respectively.

**4.3.4.2 6-*O*-(D-Galactopyranosyl) $\alpha$ -tocopherol 55a,b**: Semi solid; UV ( $\text{H}_2\text{O}$ ,  $\lambda_{\text{max}}$ ): 193 nm ( $\sigma \rightarrow \sigma^*$ ,  $\epsilon_{193} - 4717 \text{ M}^{-1}$ ), 224.5 nm ( $\sigma \rightarrow \pi^*$ ,  $\epsilon_{224.5} - 1001 \text{ M}^{-1}$ ), 273.5 nm ( $\pi \rightarrow \pi^*$ ,  $\epsilon_{273.5} - 407 \text{ M}^{-1}$ ), IR (stretching frequency,  $\text{cm}^{-1}$ ): 1083 (glycosidic C-O-C aryl alkyl symmetrical), 1260 (glycosidic C-O-C aryl alkyl asymmetrical), 3404 (OH), 1624 (aromatic C=C), MS ( $m/z$ ) – 592 [ $\text{M}]^+$ , 2D-HSQCT (DMSO- $d_6$ ) **C1 $\alpha$ -galactoside 55a**:  $^1\text{H}$  NMR  $\delta_{\text{ppm}}$  **Gal**: 5.03 (H-1 $\alpha$ , d,  $J = 3.8 \text{ Hz}$ ), 3.72 (H-2 $\alpha$ ), 3.57 (H-3 $\alpha$ ), 3.74 (H-4 $\alpha$ ), 3.71 (H-5 $\alpha$ ), 3.37 (H-6a),  **$\alpha$ -Toco**: 1.68 (H-3), 2.50 (H-4), 1.98 (H-5a), 2.02 (H-7a), 2.18 (H-8b), 0.90 – 1.41 (H-9 – H-20), 0.81 (H-12a), 0.86 (H-16a), 0.92 (H-20a), 0.83 (H-21),  $^{13}\text{C}$  NMR  $\delta_{\text{ppm}}$  **Gal**: 95.7 (C1 $\alpha$ ), 68.6 (C2 $\alpha$ ), 69.2 (C3 $\alpha$ ), 69.5 (C4 $\alpha$ ), 70.8 (C5 $\alpha$ ), 62.9 (C6 $\alpha$ ),  **$\alpha$ -Toco**: 73.8 (C2), 32 (C3), 20.3 (C4), 120.4 (C5), 12.5 (C5a), 145.3 (C6), 12.5 (C7a), 121.1 (C8), 11.7 (C8b), 40.2 (C9), 36.8 (C11), 21.5 (C12a), 37.2 (C13), 21.5 (C16a), 22.7 (C20a), 23.7 (C21), **C1 $\beta$ -galactoside 55b**:  $^1\text{H}$  NMR  $\delta_{\text{ppm}}$  **Gal**: 4.94 (H-1 $\beta$ , d,  $J = 6.7 \text{ Hz}$ ), 3.36 (H-3 $\beta$ ), 3.34 (H-4 $\beta$ ), 3.30 (H-5 $\beta$ ), 3.39 (H-6a),  $^{13}\text{C}$  NMR  $\delta_{\text{ppm}}$  **Gal**: 102.1 (C1 $\beta$ ), 69.2 (C2 $\beta$ ), 73.2 (C4 $\beta$ ), 72.5 (C5 $\beta$ ), 63.2 (C6 $\beta$ ).





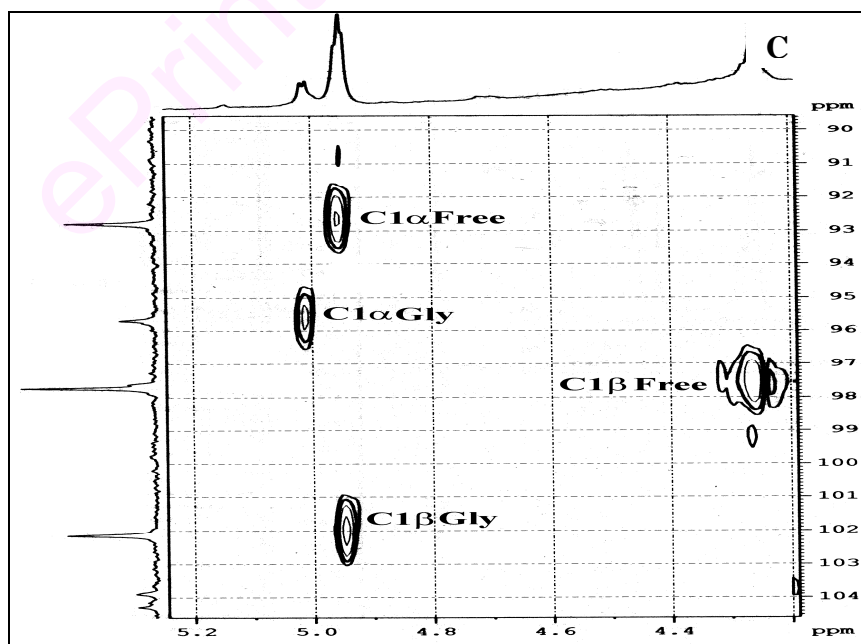
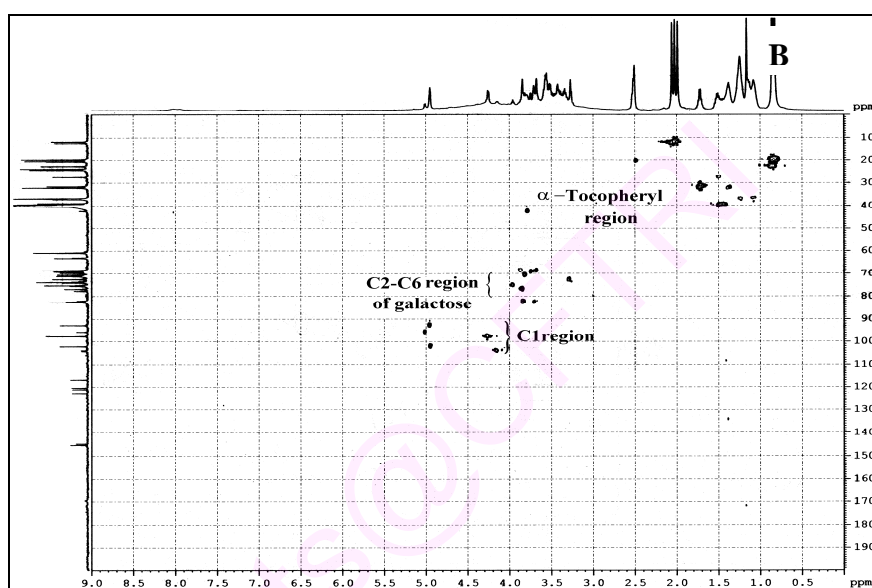
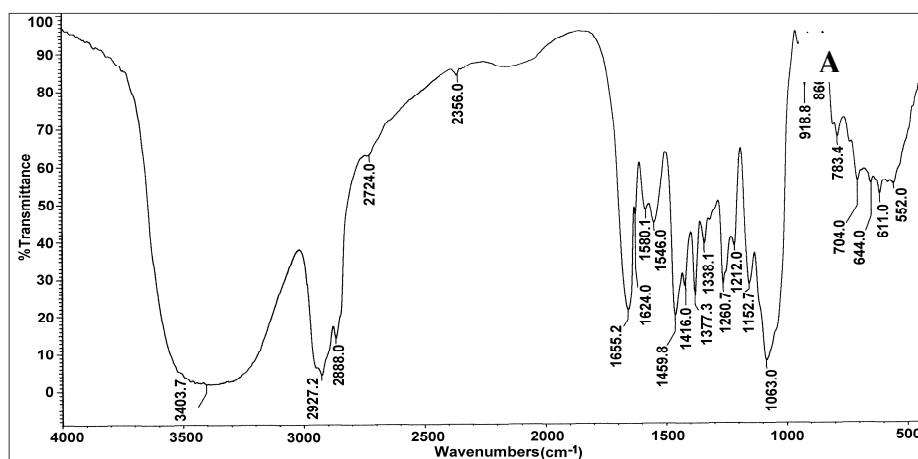
**Fig. 4.20** 6-*O*-( $\beta$ -D-Glucopyranosyl) $\alpha$ -tocopherol **54**: (A) IR spectrum, (B) Mass spectrum and (C) 2D-HSQC spectrum showing the C1-C6 region. Some of the NMR assignments are interchangeable.

Figure 4.21A shows IR spectra and Figures 4.21B and 4.21C shows 2D-HSQCT NMR spectra for 6-*O*-(D-galactopyranosyl) $\alpha$ -tocopherol **55a,b**.

**4.3.4.3 6-*O*-(D-Mannopyranosyl) $\alpha$ -tocopherol 56a,b:** Semi solid; UV (H<sub>2</sub>O,  $\lambda_{\max}$ ): 194.5 nm ( $\sigma \rightarrow \sigma^*$ ,  $\epsilon_{194.5} - 8779 \text{ M}^{-1}$ ), 223.5 nm ( $\sigma \rightarrow \pi^*$ ,  $\epsilon_{223.5} - 1837 \text{ M}^{-1}$ ), 272 nm ( $\pi \rightarrow \pi^*$ ,  $\epsilon_{272} - 570 \text{ M}^{-1}$ ), IR (stretching frequency,  $\text{cm}^{-1}$ ): 1084 (glycosidic C-O-C aryl alkyl symmetrical), 1260 (glycosidic C-O-C aryl alkyl asymmetrical), 3354 (OH), 1624 (aromatic C=C), MS ( $m/z$ ) - 615 [M+Na]<sup>+</sup>, 2D-HSQCT (DMSO-*d*<sub>6</sub>) **C1 $\alpha$ -mannoside 56a:** <sup>1</sup>H NMR  $\delta_{\text{ppm}}$  **Man:** 4.87 (H-1 $\alpha$ , d,  $J = 1.8 \text{ Hz}$ ), 3.65 (H-2 $\alpha$ ), 3.55 (H-3 $\alpha$ ), 3.18 (H-4 $\alpha$ ), 3.51 (H-5 $\alpha$ ), 3.61 (H-6 $\alpha$ ),  **$\alpha$ -Toco:** 2.38 (H-4), 1.96 (H-5 $\alpha$ ), 1.98 (H-7 $\alpha$ ), 0.86 – 1.41 (H-9 – H-20), 0.68 (H-12 $\alpha$ ), 0.94 (H-16 $\alpha$ ), 0.94 (H-20 $\alpha$ ), 0.68 (H-21), <sup>13</sup>C NMR  $\delta_{\text{ppm}}$  **Man:** 102 (C1 $\alpha$ ), 71 (C2 $\alpha$ ), 69.5 (C3 $\alpha$ ), 67 (C4 $\alpha$ ), 75 (C5 $\alpha$ ), 63.5 (C6 $\alpha$ ),  **$\alpha$ -Toco:** 20.3 (C4), 120.3 (C5), 13.5 (C5 $\alpha$ ), 145.2 (C6), 121 (C8), 13.5 (C8 $\beta$ ), 36.8 (C9), 20.5 (C10), 33.5 (C12), 19.6 (C12 $\alpha$ ), 38 (C13), 23.8 (C14), 19.6 (C16 $\alpha$ ), 24.5 (C18), 22.8 (C20 $\alpha$ ), 22.5 (C21), **C1 $\beta$ -mannoside 56b:** <sup>1</sup>H NMR  $\delta_{\text{ppm}}$  **Man:** 4.62 (H-1 $\beta$ , d,  $J = 3.8 \text{ Hz}$ ), 3.40 (H-2 $\beta$ ), 3.38 (H-4 $\beta$ ), 3.17 (H-5 $\beta$ ), 3.47 (H-6 $\alpha$ ), <sup>13</sup>C NMR  $\delta_{\text{ppm}}$  **Man:** 100.1 (C1 $\beta$ ), 72 (C2 $\beta$ ), 68.5 (C4 $\beta$ ), 75 (C5 $\beta$ ), 63.5 (C6 $\beta$ ).

Infra-red and 2D-HSQCT NMR spectra for 6-*O*-(D-mannopyranosyl) $\alpha$ -tocopherol **56a,b** are shown in Figures 4.22A and 4.22B respectively.

Ultraviolet-visible spectra of  $\alpha$ -tocopheryl glycosides, showed in  $\sigma \rightarrow \sigma^*$  band in the 193 to 198.5 nm (199 nm for  $\alpha$ -tocopherol) range,  $\sigma \rightarrow \pi^*$  band in the 223 to 224.5 nm (228 nm for  $\alpha$ -tocopherol) range and  $\pi \rightarrow \pi^*$  band in the 270.5 to 273.5 nm (292 nm for  $\alpha$ -tocopherol) range, IR spectra showed 1028-1084  $\text{cm}^{-1}$  range band for the glycosidic C-O-C aryl alkyl symmetrical stretching and 1259-1260  $\text{cm}^{-1}$  range band for the asymmetrical stretching frequencies indicating that  $\alpha$ -tocopherol had undergone



**Fig. 4.21** 6-*O*-(D-Galactopyranosyl) $\alpha$ -tocopherol **55a,b**: (A) IR spectrum, (B) 2D-HSQC full spectrum and (C) Anomeric region of the same compound. Some of the NMR assignments are interchangeable.

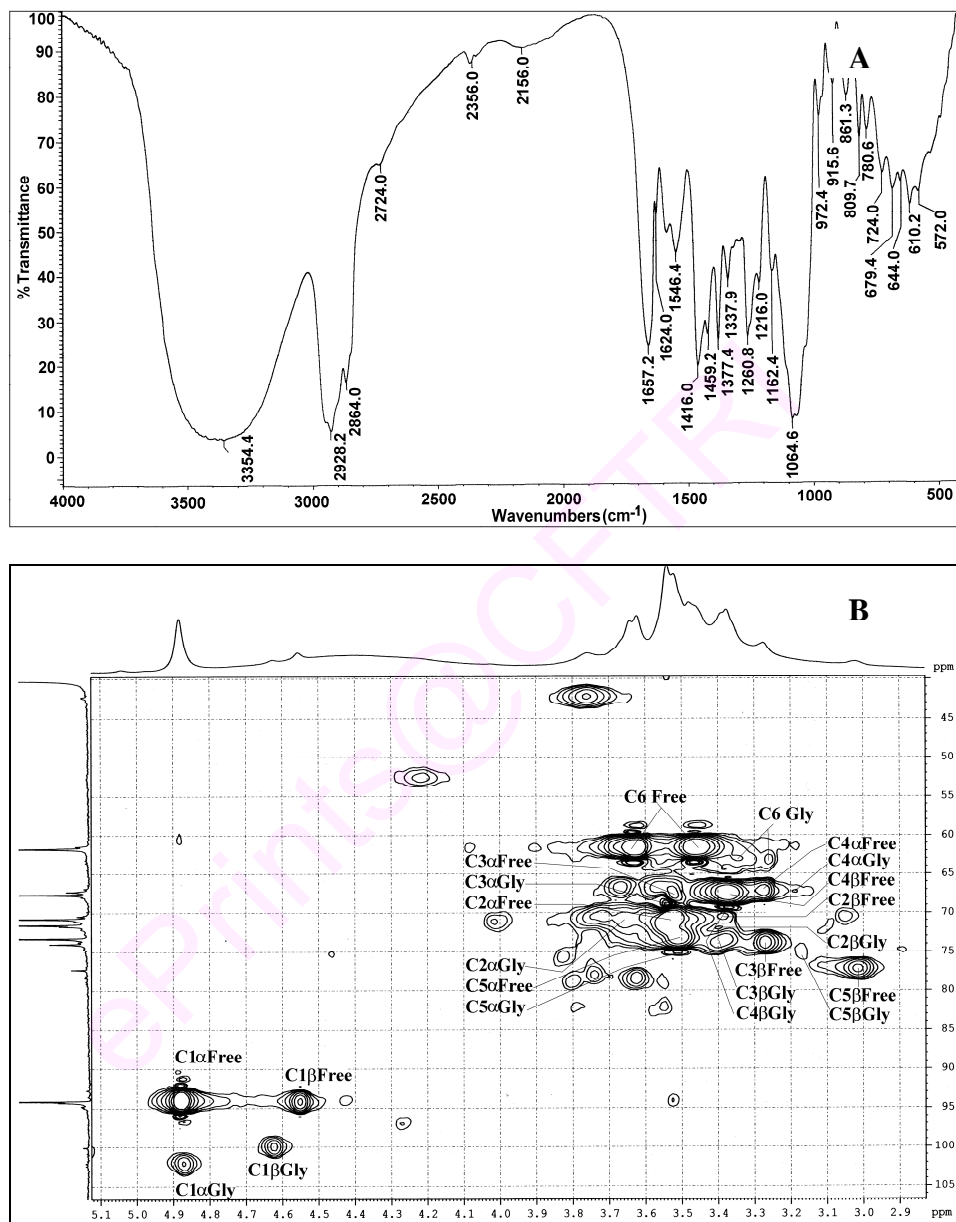


**Fig. 4.22** 6-*O*-(D-Mannopyranosyl) $\alpha$ -tocopherol **56a,b**: (A) IR spectrum and (B) 2D-HSQC spectrum showing the C1-C6 region. Some of the NMR assignments are interchangeable.

glycosylation. In 2D HSQCT spectra, the respective chemical shift values showed glycoside formation: from D-glucose **6** C1 $\beta$  glucoside **54** to C1 $\beta$  at 103.2 ppm and H-1 $\beta$  at 4.20 ppm; from D-galactose **7** C1 $\alpha$  galactoside **55a** to C1 $\alpha$  at 95.7 ppm and H-1 $\alpha$  at 5.03 ppm and C1 $\beta$  galactoside **55b** to C1 $\beta$  at 102.1 ppm and H-1 $\beta$  at 4.94 ppm; from D-mannose **8** C1 $\alpha$  mannoside **56a** to C1 $\alpha$  at 102 ppm and H-1 $\alpha$  at 4.87 ppm and C1 $\beta$  mannoside **56b** to C1 $\beta$  at 100.1 ppm and H-1 $\beta$  at 4.62 ppm. The phenolic carbon chemical shift value at 150.5 ppm (145.4 ppm for free  $\alpha$ -tocopherol) indicated that glucosylation occurred at the phenolic OH group of  $\alpha$ -tocopherol. Mass spectral data also confirmed product formation.

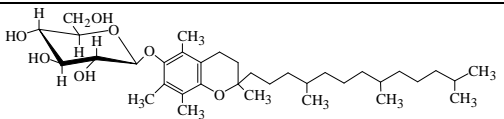
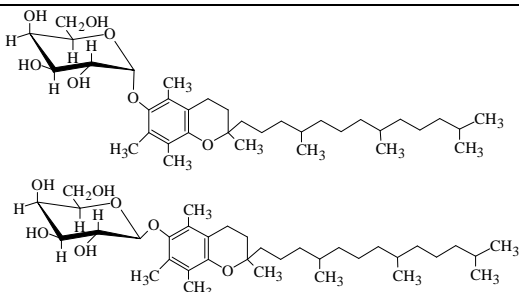
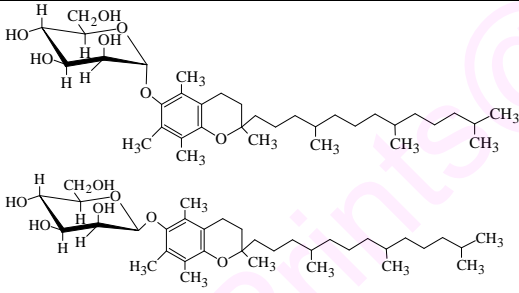
#### 4.3.5 Discussion

$\alpha$ -Tocopheryl glycosides have been synthesized using  $\beta$ -glucosidase. The yields and product proportions are shown in Table 4.7.  $\beta$ -Glucosidase 40% (w/w D-glucose) gave a maximum conversion yield of 23% for 6-*O*-( $\beta$ -D-glucopyranosyl) $\alpha$ -tocopherol **54** at 0.1mM (1 mL) of pH 6 phosphate buffer, indicated excellent regioselectivity.

The  $\alpha$  and  $\beta$  form of glycosides were determined based on the  $^1\text{H}$  and  $^{13}\text{C}$  chemical shift values of the anomeric proton and carbon signals respectively. Besides, the coupling constant values of the anomeric  $^1\text{H}$  protons were also useful in arriving at the anomeric configuration. In an  $\alpha$  configuration, the anomeric carbon exhibited chemical shift values between 92-94 ppm. In a  $\beta$  configuration, such values are between 96-104 ppm. In an  $\alpha$  configuration, the coupling between the anomeric and C2 proton is equatorial-axial corresponding to coupling constant values of 2-4 Hz. In case of a  $\beta$  configuration, the coupling between the anomeric and C2 proton is axial-axial corresponding to a value of 6-8 Hz. However, in D-mannose, since the OH at C2 position

is axial, the coupling for the C2 and the anomeric protons are equatorial-equatorial (1-2 Hz) for the  $\alpha$  configuration and axial-equatorial (2-4 Hz) for the  $\beta$  configuration.

**Table 4.7** Syntheses of  $\alpha$ -tocopheryl glycosides using  $\beta$ -glucosidase

Glycosides	$\beta$ -Glucosidase catalysis <sup>a</sup>	
	Product (% proportion) <sup>b</sup>	Yields (%) <sup>c</sup>
	C1 $\beta$ glucoside	23
<b>54</b> 6- <i>O</i> -( $\beta$ -D-Glucopyranosyl) $\alpha$ -tocopherol		
	C1 $\alpha$ galactosides (41), C1 $\beta$ galactosides (59)	11
<b>55a</b> 6- <i>O</i> -( $\alpha$ -D-Galactopyranosyl) $\alpha$ -tocopherol		
<b>55b</b> 6- <i>O</i> -( $\beta$ -D-Galactopyranosyl) $\alpha$ -tocopherol		
	C1 $\alpha$ mannoside (46), C1 $\beta$ mannoside (54)	18
<b>56a</b> 6- <i>O</i> -( $\alpha$ -D-Mannopyranosyl) $\alpha$ -tocopherol		
<b>56b</b> 6- <i>O</i> -( $\beta$ -D-Mannopyranosyl) $\alpha$ -tocopherol		

<sup>a</sup> $\alpha$ -Tocopherol – 0.5 mmol; carbohydrate – 0.5 mmol;  $\beta$ -glucosidase concentration 40% (w/w D-glucose); solvent – di-isopropyl ether; buffer – 0.1 mM (1 mL) pH 6 phosphate buffer; incubation period – 72 h. <sup>b</sup>The product proportions were determined from the area of respective  $^1\text{H}/^{13}\text{C}$  signals. <sup>c</sup>Conversion yields were from HPLC with respect to free carbohydrate. Error in yield measurements is  $\pm$  5-10%.

Under the reaction conditions, 11% 6-*O*-( $\alpha$ -D-galactopyranosyl) $\alpha$ -tocopherol **55a** and 6-*O*-( $\beta$ -D-galactopyranosyl) $\alpha$ -tocopherol **55b** and 18% 6-*O*-( $\alpha$ -D-mannopyranosyl) $\alpha$ -tocopherol **56a** and 6-*O*-( $\beta$ -D-mannopyranosyl) $\alpha$ -tocopherol **56b** were also obtained with  $\beta$ -glucosidase (Table 4.7). In case of D-galactose **7**, the  $\alpha/\beta$  proportions were found to be 41:59 ( $\alpha/\beta$ ) with respect to  $\alpha/\beta$  proportions of 92:8, for the

free D-galactose, thus favouring a slight excess of  $\beta$ -D-galactoside formation. However,  $\beta$ -glucosidase only marginally favoured  $\alpha$ -D-mannoside formation as evidenced from the  $\alpha/\beta$  proportions of 46:54 ( $\alpha:\beta$ ) for the glycosides compared to an  $\alpha/\beta$  proportion of 27:73 for free D-mannose.

Out of five glycosides prepared, four of them are reported for the first time. They are: 6-*O*-( $\alpha$ -D-galactopyranosyl) $\alpha$ -tocopherol **55a** and 6-*O*-( $\beta$ -D-galactopyranosyl) $\alpha$ -tocopherol **55b**, 6-*O*-( $\alpha$ -D-mannopyranosyl) $\alpha$ -tocopherol **56a** and 6-*O*-( $\beta$ -D-mannopyranosyl) $\alpha$ -tocopherol **56b**.

Syntheses of the other  $\alpha$ -tocopheryl glycosides with carbohydrate molecules showed that except for the three aldohexoses employed, D-fructose **9**, D-arabinose **10**, D-ribose **11**, maltose **12**, sucrose **13**, lactose **14**, D-sorbitol **15** and D-mannitol **16** did not undergo glycosylation under the conditions employed.  $\alpha$ -Tocopherol **45** could bind strongly to the enzyme than the above mentioned carbohydrate molecules which did not react, thereby preventing the facile transfer of these carbohydrate molecules to the nucleophilic phenolic OH of  $\alpha$ -tocopherol **45**.  $\beta$ -Glucosidase is not an inverting enzyme. In the present work,  $\beta$ -glucosidase gave  $\beta$ -glucoside and  $\alpha/\beta$  anomeric mixture of glycosides with D-galactose and D-mannose. In the oxo-carbenium ion mechanism (Chiba 1997), a planar carbenium ion center formed with D-galactose **7** and D-mannose **8** could be available for attack by the nucleophilic  $\alpha$ -tocopherol phenol from both above and below the plane giving rise to a mixture of  $\alpha/\beta$  anomeric products. With D-glucose **6**,  $\beta$ -glucosidase gave its natural  $\beta$ -glucoside. Since D-galactose **7** and D-mannose **8** are not natural products of  $\beta$ -glucosidase, the same selectivity could not be achieved by this enzyme.

This could be the first report for the enzyme mediated glycosylation of  $\alpha$ -tocopherol by the reverse hydrolytic method. Earlier reports using plant cell culture (Hamada *et al.* 2002; Kondo *et al.* 2006; Shimoda *et al.* 2006) have shown only very low yields. The selectivity of these enzymes have been utilized for the preparation of the glycosides, thereby eliminating the need for elaborate protective and de-protective strategies (Roode *et al.* 2003). Thus, the results show that a lipophilic molecule like  $\alpha$ -tocopherol could be glycosylated under the reaction conditions employed to produce pharmacologically and therapeutically active water soluble  $\alpha$ -tocopheryl glycosides.

#### 4.4 General discussion

In the present work, optimized reaction conditions were worked out for the syntheses of glucosides of riboflavin (vitamin B<sub>2</sub>), ergocalciferol (vitamin D<sub>2</sub>) and  $\alpha$ -tocopherol (vitamin E) by studying the effect of various parameters like incubation period, pH, buffer concentrations, enzyme and substrate concentrations. In most of the glycosylation reactions, the conversion yields increased upto certain range and thereafter remained as such or decreased significantly.

Out of 21 individual glycosides prepared, 15 glycosides are reported for the first time. The new glycosides are: 5-*O*-( $\alpha$ -D-galactopyranosyl)riboflavin **47a**, 5-*O*-( $\beta$ -D-galactopyranosyl)riboflavin **47b**, 5-*O*-( $\alpha$ -D-mannopyranosyl)riboflavin **48a**, 5-*O*-( $\beta$ -D-mannopyranosyl)riboflavin **48b**, 5-*O*-( $\alpha$ -D-ribofuranosyl)riboflavin **49a**, 5-*O*-( $\beta$ -D-ribofuranosyl)riboflavin **49b**, 5-*O*-( $\alpha$ -D-glucopyranosyl-(1'→4) $\alpha$ -D-glucopyranosyl)riboflavin **50a**, 5-*O*-( $\alpha$ -D-glucopyranosyl-(1'→4) $\beta$ -D-glucopyranosyl)riboflavin **50b**, 5-*O*-( $\alpha$ -D-glucopyranosyl-(1'→4) $\beta'$ -D-glucopyranosyl)riboflavin **50c**, 5-*O*-(1-D-fructofuranosyl-(2→1') $\alpha$ -D-glucopyranosyl)riboflavin **51**, 5-*O*-( $\beta$ -D-galactopyranosyl-(1'→4) $\beta$ -D-glucopyranosyl)riboflavin **52**, 6-*O*-( $\alpha$ -D-galactopyranosyl) $\alpha$ -tocopherol **55a**, 6-*O*-



( $\beta$ -D-galactopyranosyl) $\alpha$ -tocopherol **55b**, 6-*O*-( $\alpha$ -D-mannopyranosyl) $\alpha$ -tocopherol **56a** and 6-*O*-( $\beta$ -D-mannopyranosyl) $\alpha$ -tocopherol **56b**.

Both amyloglucosidase and  $\beta$ -glucosidase did not catalyze the reaction with D-fructose **9** and D-arabinose **10** for any of the vitamins employed. This could be probably due to not-so-facile formation of the required oxo-carbenium ion intermediate (Chiba 1997) by these carbohydrate molecules, which is an essential requirement for glycosylation during the catalytic action of the enzyme. Amyloglucosidase catalyze the hydrolysis of  $\alpha$ -1,4 and  $\alpha$ -1,6 glycosidic linkages from the non-reducing ends of starch and related oligosaccharides (Meages 1989; Jafari-Aghdam *et al.* 2005) with the inversion of the anomeric configuration to produce  $\beta$ -D-glucose (Norouzian 2006; Thorsen 2006). In these glycosylation reactions also, amyloglucosidase clearly exhibited its 'inverting' potentiality giving rise to more of the  $\beta$ -D-glucoside.  $\beta$ -Glucosidase catalyses gave only  $\beta$ -D-glucoside with D-glucose **6** indicated its regioselectivity with the carbohydrate molecules. Amyloglucosidase catalyses gave C1  $\alpha$  and  $\beta$  glycosides along with C6-*O*- aryl derivatives in most of the aldohexoses employed.

Riboflavin **43** showed glycosylation with many of the carbohydrates compared to the other vitamins employed (ergocalciferol **44** and  $\alpha$ -tocopherol **45**) in spite of the bulky acceptor molecule. This could be due to the presence of primary OH present at the ribitol moiety in riboflavin **43**, nucleophilic enough to serve as an efficient acceptor towards certain carbohydrate molecules which get glycosylated.

Among the carbohydrates employed disaccharides maltose **12**, sucrose **13** and lactose **14** showed glycosylation only with riboflavin **43**. Other than C1 and C6 hydroxyl group of the carbohydrates, none of the secondary hydroxyl groups were found to react. Hydrolysis of the disaccharides maltose **12**, sucrose **13** and lactose **14** has been observed during the course of the reaction and the resultant transglycosylation reaction did not

occur with the respective vitamins. Riboflavin **43** and  $\alpha$ -tocopherol **45** showed glycosylation with all the aldohexoses employed, whereas ergocalciferol **44** showed glycosylation only with D-glucose **6**. The highest conversion of 40% for 5-*O*-(D-ribofuranosyl)riboflavin **49a,b** and 42% for 20-*O*-(D-glucopyranosyl)ergocalciferol **53a-c** were observed for the amyloglucosidase catalyses.  $\beta$ -Glucosidase on the other hand showed 24% for 5-*O*-( $\beta$ -D-glucopyranosyl)riboflavin **46b** and 23% for 6-*O*-( $\beta$ -D-glucopyranosyl) $\alpha$ -tocopherol **54** were obtained. In general, the yields were low for  $\beta$ -glucosidase catalyses and the selectivity was marginally higher than amyloglucosidase catalyses.

Thus, this study shows that selected vitamin glycosides, could be synthesized enzymatically using amyloglucosidase from *Rhizopus* mold and  $\beta$ -glucosidase isolated from sweet almond to produce more water soluble and stable vitamin derivatives with diverse carbohydrate molecules. This could be the first report on glycosylation of riboflavin (vitamin B2), ergocalciferol (vitamin D2) and  $\alpha$ -tocopherol (vitamin E) using enzymes in a non-polar media.

## 4.5 Experimental

### 4.5.1 Glycosylation procedures

Syntheses of riboflavinyl glycosides, ergocalciferol glycosides and  $\alpha$ -tocopherol glycosides are described in their respective Sections of 4.1, 4.2 and 4.3.

High Performance Liquid Chromatography (HPLC), size exclusion chromatography, solubility and spectral characterization were the same as earlier described in Chapter 3 Sections 3.7.3-3.7.6 and Chapter 2 Sections 2.2.7-2.2.9.

ePrints@CFTRI

*Chapter 5*

*Competitive inhibition of amyloglucosidase by  
vanillin in the glucosylation of vanillin*

## Introduction

Kinetic studies on few enzymatic hydrolytic reactions are known (Hiromi *et al.* 1983; Tanaka *et al.* 1983; Ohinishi and Hiromi 1989; Goto *et al.* 1994). However, kinetic studies on the glycosylation reaction especially those involving a carbohydrate and aglycon molecules are practically nil. Among the kinetic reports available on the hydrolytic enzymes in reverse reactions, those on lipases, show that lipases follow Ping-Pong Bi-Bi mechanism in several esterification reactions (Kiran and Divakar 2002; Janssen *et al.* 1999; Marty *et al.* 1992; Yadav and Lathi 2004). This mechanism involves binding of acid and alcohol in successive steps releasing water and the product ester again in succession. However, no such mechanism has been reported in glycosylation reactions.

Glucoamylases possess  $(\alpha/\alpha)_6$  barrel fold structure which is different from the  $(\beta/\alpha)_8$  barrel fold structure of  $\alpha$ -amylase,  $\beta$ -amylase and  $\alpha$ -glucosidase (Chiba 1997; Svensson *et al.* 1990; Aleshin *et al.* 1992). In the catalytic domain, two glutamic acids Glu314 and Glu544 in *Rhizopus oryzae* (Aleshin *et al.* 1992; Ashikari *et al.* 1986) are reported to be the catalytic amino acid residues directly involved as acid base catalysts in the hydrolytic reaction (Chiba 1997; Sierks *et al.* 1990). It has also been shown that oxocarbenium ion mechanism is the most suitable in the hydrolytic reaction for both “retaining” and “inverting” enzymes. Although, no decisive mechanism has been proposed so far for the glycosylation reactions, it is generally believed that the oxocarbenium ion mechanism could be the most probable one.

In this chapter an attempt has been made to carry out a detailed kinetic investigation on the glucosylation reaction between vanillin **1** and D-glucose **6** involving an amyloglucosidase from *Rhizopus* mold leading to the synthesis of 4-*O*-(D-glucopyranosyl)vanillin **17a-c**. The results from these investigations are described below.

## Present work

To graphically evaluate the apparent values of the kinetic parameters  $V_{\max}$ ,  $K_i$ ,  $K_m$  vanillin and  $K_m$  D-glucose, initial rates (specific reaction rate) were evaluated by measuring of 4-*O*-(D-glucopyranosyl)vanillin formation at different incubation periods. A typical time course of amyloglucosidase catalyzed reaction is shown in Fig. 5.1. For each concentration of vanillin **1** (5 mM to 0.1 M) and D-glucose **6** (5 mM to 0.1 M) individual experiments were performed for incubation periods of 3 h, 6 h, 12 h and 24 h (30  $\times$  4 for each system). The experiments were performed in duplicate. Initial rates ( $v$ ) were determined from the initial slope values of the plots of the amount of the glucoside (M) formed versus incubation period (h).  $R^2$  values obtained from least square analysis for the initial velocities in both the cases were found to be around 0.95. Effect of external mass transfer phenomenon involving internal and external diffusion (Marty *et al.* 1992), if any, were not tested in the present work. The plots shown in this work were constructed from all the experimentally determined and few computer generated initial rate values.

### 5.1 Kinetic experiments on amyloglucosidase catalyzed synthesis of 4-*O*-(D-glucopyranosyl)vanillin

Kinetic experiments were conducted by refluxing vanillin **1** and D-glucose **6** in the concentration range 5 mM to 0.1 M along with 90 mg amyloglucosidase (corresponding protein content-54.5 mg) in 100 mL di-isopropyl ether solvent containing 0.1 mM (1 mL) of 0.01 M pH 4 acetate buffer. Kinetic experiments were carried out at the refluxing temperature of di-isopropyl ether at 68 °C. After work up as described on page 74. The reaction mixture was subjected to HPLC analysis to determine the extent of product formation.

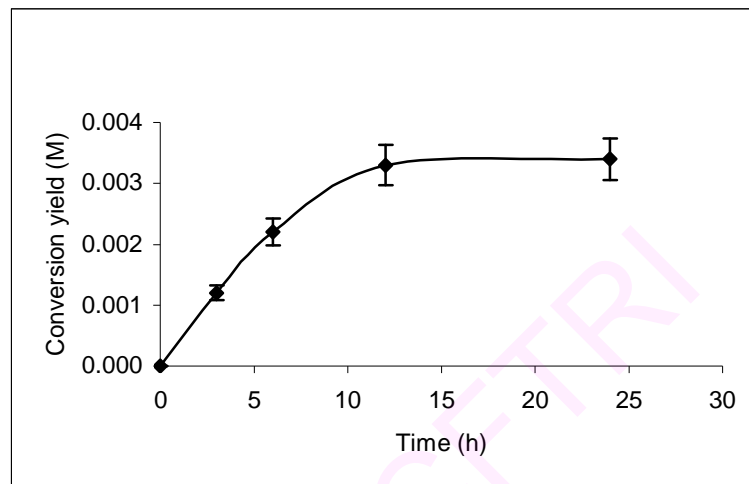


**Fig. 5.1** Initial rate ( $v$ ) plot: D-glucose 10 mM, vanillin 5 mM, amyloglucosidase 90 mg and 0.1 mM (1 mL) of 0.01 M, pH 4 acetate buffer.

Amyloglucosidase exhibited good activity only in the presence of water present as buffer. The water of reaction also contributed to the water activity essential for the enzymatic action. Only vanillin **1** dissolved in di-isopropyl ether and the reaction mixture remained largely heterogenous due to insolubility of the enzyme and D-glucose **6**. Experiments were conducted by maintaining the concentration of one of the substrate constant and varying the concentration of the other and *vice versa*. Since a constant amount of enzyme was employed for all the reactions, the enzyme/substrate ratio varied with varying substrate concentrations. The enzyme lost only 10% of its activity after incubation for 24 h.

A typical rate plot for vanillin glucosidic reactions is shown in Fig. 5.1 and the initial velocities ( $v$ ) were found to be in the range 0.17 to  $10.5 \times 10^{-5}$  M/h.mg protein. At initial periods of incubation, the reaction is relatively fast and slows down at longer incubation periods beyond 24 h which could indicate attainment of steady state equilibrium conditions.

Double reciprocal plot was constructed by plotting  $1/v$  versus  $1/[\text{vanillin}]$ . The plot is shown in Fig. 5.2, which shows a series of curves obtained for different fixed concentrations of D-glucose **6** at varying vanillin **1** concentrations, where slight increase in initial rates at lower vanillin concentrations is observed and at higher concentrations of vanillin **1** the rates reduce drastically. Also, increase in D-glucose **6** increased the initial rate at all vanillin concentrations. Figure 5.3 shows a series of lines obtained for different fixed concentrations of vanillin **1** at varying D-glucose **6** concentrations where at fixed lower vanillin **1** concentrations, the lines were parallel and at fixed higher vanillin concentrations, lines with different slopes were observed. The plots in Figs. 5.2 and 5.3 showed that the kinetics could be best described by (Segel 1993) Ping-Pong Bi-Bi model (Scheme 5.1) with competitive substrate inhibition leading to dead-end inhibition.

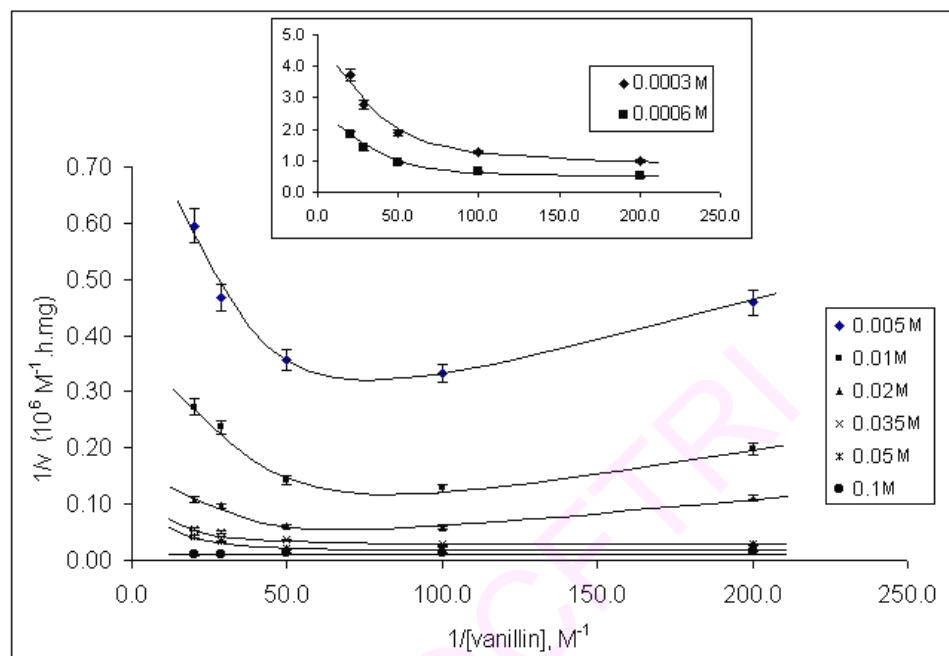


**Fig. 5.2** Double reciprocal plot:  $1/v$  versus  $1/[\text{vanillin}]$ . Series of plots from experimentally measured initial rate values showing the effect of varying vanillin concentrations at different fixed concentrations of D-glucose in the 5 mM to 0.1 M range. Insets show plots obtained from the computer simulation procedure for 0.3 mM and 0.6 mM concentrations of D-glucose.



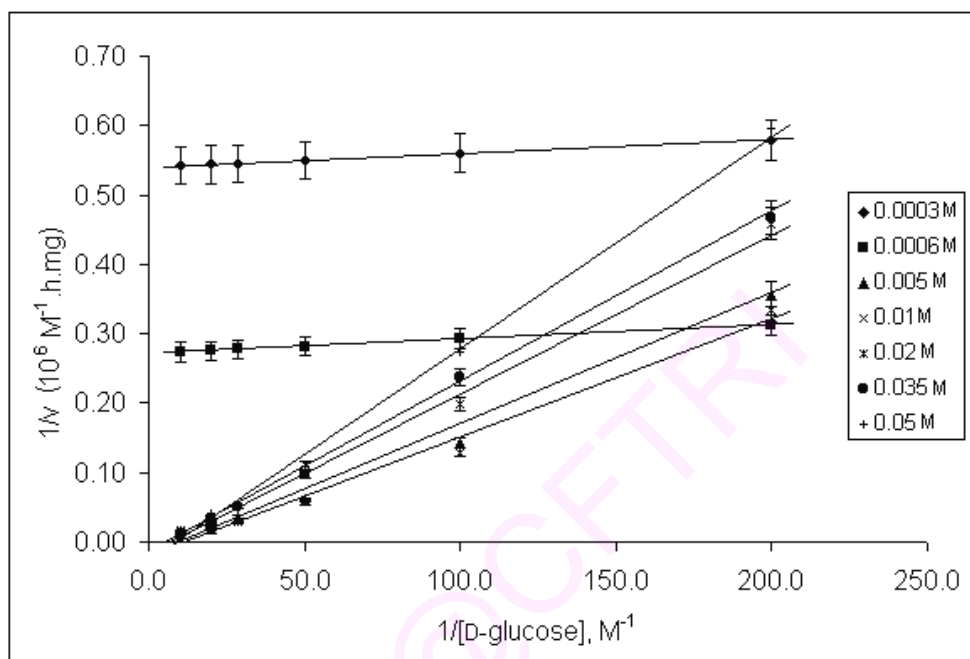
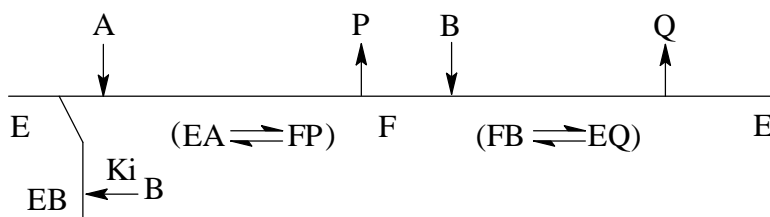


**Fig 5.3** Double reciprocal plot:  $1/v$  versus  $1/[D\text{-glucose}]$ . Series of plots from experimentally measured initial rate values showing the effect of varying D-glucose concentrations at different fixed concentrations of vanillin in the 5 mM to 0.05 M range. The plots shown for 0.3 mM and 0.6 mM concentrations of vanillin are from the computer simulation procedure.



**Scheme 5.1** Ping-Pong Bi-Bi model with competitive substrate inhibition

Where, A = D-glucose, P = H<sub>2</sub>O, B = vanillin, F = glucosyl-amyloglucosidase complex, E = amyloglucosidase, EA = amyloglucosidase-glucose complex, FP = glucosyl-amyloglucosidase-water complex, EB = amyloglucosidase-vanillin complex, K<sub>i</sub> = dissociation constant of amyloglucosidase-inhibitor complex, FB = glucosyl-amyloglucosidase-vanillin complex, EQ = amyloglucosidase-glucoside complex, Q = 4-*O*-(D-glucopyranosyl)vanillin.

This model could be described by the following rate equation,

$$\frac{v}{V_{\max}} = \frac{[A][B]}{K_{mA}[B](1 + [B]/K_i) + K_{mB}[A] + [A][B]} \quad (1)$$

where,  $v$  = initial rate,  $V_{\max}$  = maximum velocity, A = D-glucose concentration, B = vanillin concentrations,  $K_{mA}$  = Michelis-Menten constant for the amyloglucosidase-D-glucose complex,  $K_i$  = dissociation constant of the amyloglucosidase-inhibitor (vanillin) complex,  $K_{mB}$  = Michelis-Menten constant for the amyloglucosidase-vanillin complex. Since the initial rates are in M/h.mg of the protein,  $V_{\max}$  is expressed as  $k_{\text{cat}}$  as  $k_{\text{cat}} = V_{\max}/\text{enzyme concentration}$ .

The four important kinetic parameters  $K_i$  vanillin,  $K_m$  D-glucose,  $K_m$  vanillin and  $k_{\text{cat}}$  vanillin were evaluated graphically. Intercept of the positive slope of Fig. 5.2 on the Y-axis, especially, at the highest concentration of D-glucose (0.1 M) employed, gave  $1/k_{\text{cat}}$  for vanillin (Table 5.1).

**Table 5.1** Kinetic parameters for the synthesis of 4-*O*-(D-glucopyranosyl)vanillin

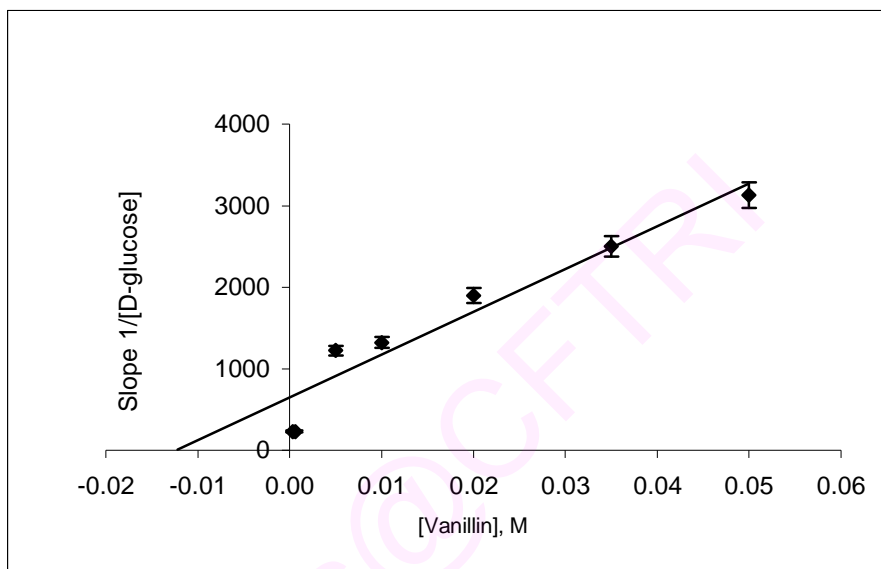
	$k_{\text{cat}} 10^{-5} \text{ M/h. mg}$	$K_{\text{m D-glucose}} \text{ (mM)}$	$K_{\text{m vanillin}} \text{ (mM)}$	$K_i \text{ (mM)}$
Graphical method	$10.0 \pm 1$	$65.0 \pm 6.7$	$45.6 \pm 4.4$	$12.5 \pm 1.3$
Computer simulated values	$35.0 \pm 3.2$	$60.0 \pm 6.2$	$50.0 \pm 4.8$	$10.5 \pm 1.1$

Figure 5.4 shows the replot of slope of Fig. 5.3 ( $1/[\text{D-glucose}]$  versus  $[\text{vanillin}]$  plot) from which slope =  $K_{\text{m D-glucose}}/(k_{\text{cat}} K_i)$ , Y intercept =  $K_{\text{m D-glucose}}/k_{\text{cat}}$  and X intercept =  $-K_i$ , where  $K_i$  represents dissociation constant for the amyloglucosidase-vanillin complex.  $K_{\text{m vanillin}}$  was obtained from equation 2 generated by rearranging equation 1,

$$K_{mB} = \frac{k_{\text{cat}} [\text{B}]}{v} - \frac{K_{mA} [\text{B}]}{[\text{A}]} - \frac{K_{mA} [\text{B}]^2}{[\text{A}] K_i} - [\text{B}] \quad (2)$$

where,  $K_{mB}$  = Michelis-Menten constant for the amyloglucosidase-vanillin complex.

The values of the four important kinetic parameters,  $k_{\text{cat}}$ ,  $K_i$ ,  $K_{mA}$  and  $K_{mB}$ , were also estimated mathematically through computer simulation. The range of values tested for these parameters and the constraints employed for the iteration procedure is as follows:  $k_{\text{cat vanillin}} < 0.01 \text{ M/h.mg}$ ,  $K_i \text{ vanillin} < K_{\text{m vanillin}}$ ,  $K_{\text{m vanillin}} < K_{\text{m D-glucose}}$  and  $K_{\text{m D-glucose}} < 0.1 \text{ M}$ . The iteration procedure involved determination of initial velocities ( $v_{\text{pred}}$ ) by incrementing the above mentioned four kinetic parameters in eq. 1 from their lowest approximations (bound by the above mentioned constraints) and subjecting the  $v_{\text{pred}}$  (obtained for all the concentrations of D-glucose and vanillin) to non-linear optimization, by minimizing the sum of squares of deviation between  $v_{\text{pred}}$  and  $v_{\text{exptl}}$ . The set of four kinetic parameters which resulted from minimum sum of squares of deviation between  $v_{\text{pred}}$  and  $v_{\text{exptl}}$  were considered to be the best set and they are shown in Table 5.1 which lists graphical as well as the computer simulated values for comparison. Table 5.2 shows the comparison between experimental and predictive initial rate values obtained under



**Fig 5.4** Replot of Slope (from Fig. 5.3):  $1/[\text{D-glucose}]$  versus [vanillin]

different reaction conditions. Computer simulation showed  $v_{\text{pred}}$  values with  $R^2$  values of 0.85 for vanillin reaction emphasizing that this model is reasonably good in explaining the kinetics of this reaction.

**Table 5.2** Experimental and predicted initial rate values for the synthesis of 4-*O*-(D-glucopyranosyl)vanillin

D-Glucose (M)	Vanillin (M)	$v_{\text{experimental}}$ $10^{-5} \text{ M.h}^{-1}.\text{mg}^{-1}$	$v_{\text{predictive}}$ $10^{-5} \text{ M h}^{-1}.\text{mg}^{-1}$
0.005	0.005	0.218	1.219
0.005	0.01	0.300	1.189
0.005	0.02	0.280	0.913
0.005	0.035	0.214	0.643
0.005	0.05	0.168	0.492
0.01	0.005	0.506	1.763
0.01	0.01	0.774	1.976
0.01	0.02	0.702	1.672
0.01	0.035	0.422	1.231
0.01	0.05	0.366	0.957
0.02	0.005	1.003	2.269
0.02	0.01	1.746	2.952
0.02	0.02	1.666	2.866
0.02	0.035	1.033	2.269
0.02	0.05	0.917	1.815
0.035	0.005	2.069	2.587
0.035	0.01	4.128	3.745
0.035	0.02	2.757	4.128
0.035	0.035	1.987	3.551
0.035	0.05	1.774	2.947
0.05	0.005	3.475	2.741
0.05	0.01	1.618	4.195
0.05	0.02	4.968	5.010
0.05	0.035	3.027	4.588
0.05	0.05	2.401	3.926
0.1	0.005	6.110	2.945
0.1	0.01	7.340	4.881
0.1	0.02	7.510	6.676
0.1	0.035	9.170	6.961
0.1	0.05	10.480	6.414

## 5.2 Discussion

This kinetic data clearly shows the inhibitory nature of vanillin **1** towards amyloglucosidase from *Rhizopus* mold. With increasing concentrations of D-glucose (Fig. 5.2), the rate increases at lower concentrations of vanillin. At higher concentrations of vanillin corresponding to minimum  $1/v$ , the rate decreases, the plots tend to become

closer to  $1/v$  axis. Figure 5.3 also reflect the same behaviour, where at lower concentrations of vanillin, the lines appear parallel probably so for as  $K_i > K_{mB}$ . However at higher fixed concentrations of vanillin, the slopes vary drastically where  $K_i < K_{mB}$ . Thus the kinetic data clearly shows the inhibitory nature of vanillin **1** in this reaction. Competition between D-glucose and vanillin for the active site (binding site) of amyloglucosidase could result in predominant vanillin binding at higher concentrations, displacing D-glucose, leading to the formation of the dead-end amyloglucosidase-vanillin complex.

In this reaction  $K_{m \text{ D-glucose}}$  ( $60.0 \pm 6.2$  mM, Table 5.1) is always higher than  $K_{mB}$  ( $50.0 \pm 4.8$  mM) which shows that while glucose binding could lead to product formation, vanillin binding to the active site could result in inhibition of the amyloglucosidase activity.

Catalysis occurs mainly between subsites 1 and 2 of glucoamylase. Active site of glucoamylase from *Rhizopus mold* could be identical to that of *Rhizopus oryzae* (Stoffer *et al.* 1995). Carbohydrate OH groups are held firmly in the active site subsites 1 and 2 of *Rhizopus oryzae* through hydrogen bonds with Arg191, Asp192, Leu312, Trp313, Glu314, Glu315 and Arg443 (Aleshin *et al.* 1992; Ashikari *et al.* 1986). The above mentioned residues can also stabilize planar vanillin bound to the active site through hydrogen bonds. Also, vanillin phenolic hydroxyl and aldehyde carbonyl could form effective hydrogen bonds with Arg191, Asp192, Trp313, Glu315 and Arg443. Hence, higher concentrations of vanillin are capable of displacing the glucose-oxo-carbenium ion from the active site and occupy its position instead, leading thereby to dead end inhibition. This may not happen at lower concentrations of vanillin.

Several lipase catalyzed esterification reactions have been described to follow Ping-Pong Bi-Bi mechanism, which deals with two substrates (acid and alcohol) and two

products (water and ester). So far, enzyme mediated glycosylation, especially the one involving a carbohydrate molecule and a aglycon molecule has not been reported to follow Ping-Ping Bi-Bi model. This could be the first report of its kind.

### 5.3 Experimental

#### 5.3.1 Kinetic experiments

Kinetic experiments were carried out by refluxing 5 mM to 0.1 M of vanillin **1** and 5 mM to 0.1 M of D-glucose **6** along with 90 mg amyloglucosidase in 100 mL diisopropyl ether solvent containing 0.1 mM (1 mL) of 0.01 M, pH 4 acetate buffer for an incubation period of 3-24 h. Workup involved distilling off the solvent and maintaining the reaction mixture at boiling water temperature for 5-10 min to denature the enzyme. The residue was repeatedly extracted with chloroform to remove unreacted vanillin **1**, the dried residue consisting of 4-*O*-(D-glucopyranosyl)vanillin and unreacted D-glucose **6**, was subjected to HPLC analysis on an aminopropyl column (300 mm × 3.9 mm) eluted with 80:20 (v/v) acetonitrile:water at a flow rate of 1 mL/h and monitored using a RI detector. Conversion yields were determined from HPLC peak area of the glucoside and free carbohydrate and expressed with respect to free D-glucose concentration. Error based on HPLC measurements are of the order of ± 10%. Overall uncertainty in kinetic rate constant measurements will be of the order of ± 15%.

For each concentration of vanillin **1** (5 mM to 0.1 M) and D-glucose **6** (5 mM to 0.1 M) individual experiments were performed for incubation periods of 3 h, 6 h, 12 h and 24 h (30 × 4 for each system). The experiments were performed in duplicate. Initial rates ( $v$ ) were determined from the initial slope values of the plots of the amount of the glucoside ( $M$ ) formed versus incubation period ( $h$ ). The plots shown in this work were constructed from all the experimentally determined and few computer generated initial rate values.

ePrints@CFTRI

## **Chapter 6**

***Evaluation of antioxidant and angiotensin converting enzyme inhibition activity of the synthesized phenolic and vitamin glycosides***



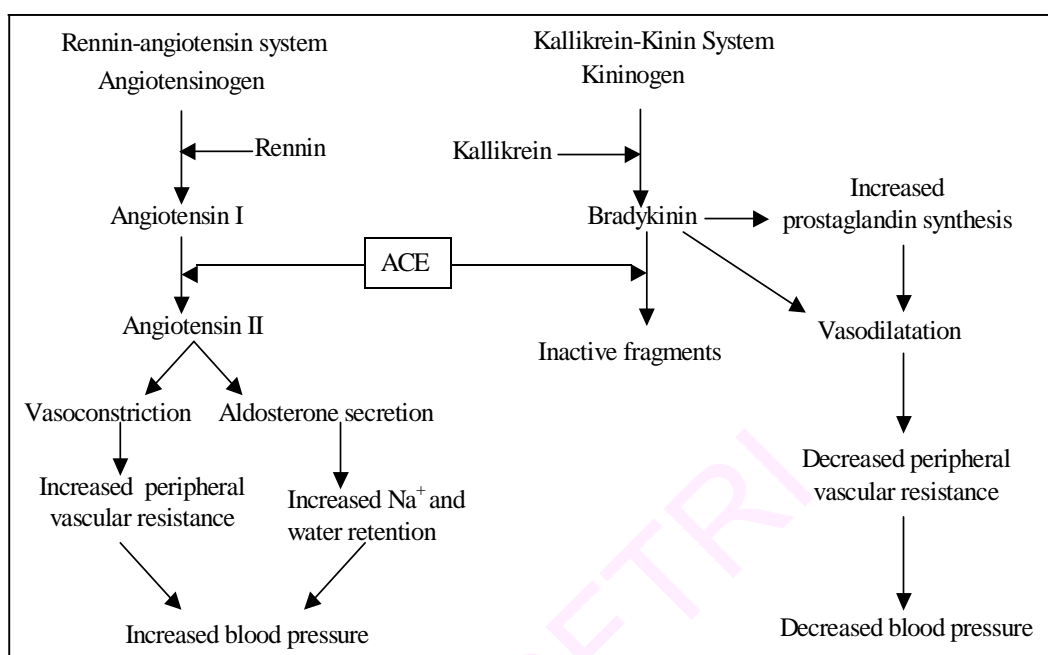
## Introduction

Phenolic glycosides found in a variety of fruits and vegetables have been studied extensively for their antioxidant properties (Moon *et al.* 2007). Antioxidative action is reported to protect living organisms from oxidative damages, resulting in the prevention of various diseases such as cancer, cardiovascular diseases, diabetes and aging (Azuma *et al.* 1999). Flavonols and their glycosides protect red blood cells against free radical-induced oxidative hemolysis (Dai *et al.* 2006). The key role of phenols as antioxidants stem from the presence of hydroxyl groups attached to their aromatic rings, which enable them to scavenge free radicals (Kefalas *et al.* 2003; Villano *et al.* 2007).

Angiotensin converting enzyme (dipeptidyl carboxypeptidase, EC 3.4.15.1) is a zinc containing nonspecific dipeptidyl carboxypeptidase widely distributed in mammalian tissues (Li *et al.* 2004). Angiotensin converting enzyme (ACE) regulates the blood pressure by modulating renin-angiotensin system as shown in Scheme 6.1 (Vermeirssen *et al.* 2002). This enzyme increases the blood pressure by converting the decapeptide angiotensin I into the potent vaso-constricting octapeptide, angiotensin II. Angiotensin II brings about several central effects, all leading to a further increase in blood pressure. ACE is a multifunctional enzyme that also catalyses the degradation of bradykinin (blood pressure-lowering nanopeptide) and therefore inhibition of ACE results in an overall antihypertensive effect (Li *et al.* 2004; Johnston 1992).

Several synthetic drugs and bio-molecules are available for ACE inhibition. One such drug is enalapril a successful synthetic anti-hypertensive drug. Similar such molecules captopril, perindopril, ceranopril, ramipril, quinapril and fosinopril also show ACE inhibitory activities (Hyuncheol *et al.* 2003; Dae-Gill *et al.* 2003; Chong-Qian *et al.* 2004). Hypothetical representation of inhibitors, namely hydrolyzed products of peptides like glycine, valine and leucine at the carboxyl terminus of the peptide inhibitor are

considered the potent inhibitors (De-Lima 1999; Wu and Ding 2002; Kim *et al.* 2001) of ACE.



**Scheme 6.1** Role of angiotensin converting enzyme (ACE) in regulating blood pressure

Some naturally occurring 'biologically active peptides' also act as ACE inhibitors. Deloffre *et al.* (2004) reported that a neuro-peptide from leach brain showed ACE inhibition with an  $IC_{50}$  value of  $19.8 \mu\text{M}$ . The N-terminal dipeptide (Tyr-Leu) of  $\beta$ -lactorphin was found to be the most potent inhibitor (Mullally *et al.* 1996). Many peptide inhibitors are derived from different food proteins like Asp-Leu-Pro and Asp-Gly from soy protein hydrolysis (Wu and Ding 2002) and Gly-Pro-Leu and Gly-Pro-Val from bovine skin gelatin hydrolysis (Kim *et al.* 2001). Glycosides from the leaves of *Abeliophyllum distichum* like acteoside, isoacteoside, rutin and hirsutin moderately inhibited the angiotensin I converting enzyme activity (Hyuncheol *et al.* 2003). Glycosides like 3-O-methyl crenatoside from *Microtoena prainiana* also showed more than 30% ACE inhibitory activity (Chong-Qian *et al.* 2004). Phenyl propanoid glycosides from *Clerodendron trichotomum* such as acteoside, leucosceptoside A,

martynoside, acetoside isomer and isomartynoside also showed ACE inhibitory effect (Dae-Gill *et al.* 2003).

Several bioactive water insoluble phenolic molecules have been converted in to their respective glycosides through glycosylation (Lohith *et al.* 2006; Vijayakumar and Divakar 2007), thereby enhancing their pharmaceutical applications. Similarly, glycosylation is also reported to improve the bioactivity of several vitamins (Kren and Martinkova 2001). Although few glycosides of such phenols and vitamins prepared chemically and enzymatically were reported earlier (Kren and Martinkova 2001; Vijayakumar and Divakar 2005; Badman *et al.* 1990), reports on their biological activities are scanty. The present work describes the ACE inhibition and antioxidant activities of the synthesized glycosides, reported in Chapter 3 and 4 in detail.

### **Present work**

Totally 39 glycosides were tested for antioxidant activity and 48 glycosides tested for angiotensin converting enzyme (ACE) inhibitory activities. ACE was isolated from pig lung. The enzymatic reactions were carried out under optimized conditions worked out for these reactions. Thus, the present work deals with investigation of antioxidant and ACE inhibitions activities of phenolic and vitamin glycosides synthesized using amyloglucosidase from *Rhizopus mold* and  $\beta$ -glucosidase (native/immobilized) isolated from sweet almond in organic media. Phenols and vitamins subjected to this study are vanillin **1**, N-vanillyl nonanamide **2**, curcumin **3**, DL-3,4-dihydroxyphenylalanine **4** (DL-dopa), 3,4-dihydroxyphenylethylamine **5** (dopamine), riboflavin **43** (vitamin B2), ergocalciferol **44** (vitamin D2) and  $\alpha$ -tocopherol **45** (vitamin E). Of these many phenols and vitamins are either less soluble in water (vanillin **1** 2 g/L, riboflavin **43** 0.2 g/L) or insoluble in water at all (N-vanillyl-nonanamide **2**, curcumin **3**, ergocalciferol **44** and  $\alpha$ -tocopherol **45**) or susceptible to heat, light and oxidation (DL-dopa **4**, dopamine **5**).

DPPH (2,2-diphenyl-1-picrylhydrazyl) was employed to evaluate the free radical scavenging effectiveness of the phenolic and vitamin glycosides (Chu *et al.* 2000). The absorbance of DPPH decreases when the odd electron of nitrogen in DPPH is paired off and therefore DPPH can be used as a substrate for studying free radical scavenging activity (Lee *et al.* 2003). ACE inhibition activity of the above mentioned glycosides were determined by the Cushman and Cheung method (1971). Since hippuryl-L-histidyl-L-leucine (HHL) mimics the carboxyl dipeptide of angiotensin I, it has been used as the substrate for screening ACE inhibitors.

### 6.1 Antioxidant activity

DPPH (2,2-diphenyl-1-picrylhydrazyl) is a highly colored commercially available radical source, widely used for rough estimation of the ability of antioxidants to trap potentially damaging one-electron oxidants *i.e.* the number of DPPH molecules reduced by one molecule of an antioxidant (Potier *et al.* 1999). Many methods to evaluate the antioxidative activity of specific compounds have been described, but the most widely documented one deals with DPPH radical (Portes *et al.* 2007; Roche *et al.* 2005). The radical scavenging efficiency of phenolic and vitamin glycosides tested in this investigation is listed in Table 6.1.

**Table 6.1** Antioxidant and angiotensin converting enzyme inhibitory activities of various phenolic and vitamin glycosides<sup>a</sup>

Compounds	Antioxidant activity IC <sub>50</sub> Value (mM) <sup>b</sup>	ACE Inhibition IC <sub>50</sub> Value (mM) <sup>c</sup>
Butylated Hydroxy Anisole (BHA)	0.046 ± 0.002	-
Enalapril	-	0.071 ± 0.004
Vanillin <b>1</b>	1.65 ± 0.08	1.87 ± 0.09
4- <i>O</i> -(D-Glucopyranosyl)vanillin <b>17a-c</b>	2.66 ± 0.13	1.11 ± 0.06
4- <i>O</i> -(β-D-Glucopyranosyl)vanillin <b>17b</b>	0.9 ± 0.45	0.61 ± 0.03
4- <i>O</i> -(α-D-Galactopyranosyl)vanillin <b>18a</b>	1.62 ± 0.08	1.12 ± 0.06
4- <i>O</i> -(D-Galactopyranosyl)vanillin <b>18a,b</b>	1.18 ± 0.06	0.61 ± 0.03

4- <i>O</i> -( $\alpha$ -D-Mannopyranosyl)vanillin <b>19a</b>	1.55 $\pm$ 0.08	1.02 $\pm$ 0.05
4- <i>O</i> -(D-Mannopyranosyl)vanillin <b>19a,b</b>	1.08 $\pm$ 0.05	2.3 $\pm$ 0.1
4- <i>O</i> -( $\alpha$ -D-Glucopyranosyl-(1'→4)D-glucopyranosyl)vanillin <b>20a,c,d</b>	1.17 $\pm$ 0.06	1.63 $\pm$ 0.08
4- <i>O</i> -( $\alpha$ -D-Glucopyranosyl-(1'→4) $\beta$ -D-glucopyranosyl)vanillin <b>20b</b>	2.64 $\pm$ 0.13	1.89 $\pm$ 0.09
4- <i>O</i> -(D-Fructofuranosyl-(2→1') $\alpha$ -D-glucopyranosyl)vanillin <b>21a,b</b>	1.23 $\pm$ 0.06	15.7 $\pm$ 0.79
4- <i>O</i> -( $\beta$ -D-Galactopyranosyl-(1'→4) $\beta$ -D-glucopyranosyl)vanillin <b>22</b>	0.8 $\pm$ 0.04	0.92 $\pm$ 0.05
4- <i>O</i> -(D-Sorbitol)vanillin <b>23a-c</b>	1.24 $\pm$ 0.06	0.81 $\pm$ 0.04
N-Vanillyl-nonanamide <b>2</b>	0.054 $\pm$ 0.003	1.53 $\pm$ 0.08
4- <i>O</i> -(D-Glucopyranosyl)N-vanillyl-nonanamide <b>24a,b</b>	1.18 $\pm$ 0.06	1.33 $\pm$ 0.07
4- <i>O</i> -( $\beta$ -D-Glucopyranosyl)N-vanillyl-nonanamide <b>24c</b>	1.4 $\pm$ 0.07	3.33 $\pm$ 0.17
4- <i>O</i> -(D-Galactopyranosyl)N-vanillyl-nonanamide <b>25a,b</b>	2.9 $\pm$ 0.15	2.05 $\pm$ 0.1
4- <i>O</i> -( $\beta$ -D-Galactopyranosyl)N-vanillyl-nonanamide <b>25b</b>	0.94 $\pm$ 0.05	2 $\pm$ 0.1
4- <i>O</i> -( $\beta$ -D-Mannopyranosyl)N-vanillyl-nonanamide <b>26</b>	1.14 $\pm$ 0.06	2.57 $\pm$ 0.13
4- <i>O</i> -( $\alpha$ -D-Ribofuranosyl)N-vanillyl-nonanamide <b>27a,b</b>	0.98 $\pm$ 0.05	1 $\pm$ 0.05
4- <i>O</i> -( $\alpha$ -D-Glucopyranosyl-(1'→4)D-glucopyranosyl)N-vanillyl-nonanamide <b>28a-c</b>	0.8 $\pm$ 0.04	2.41 $\pm$ 0.12
4- <i>O</i> -( $\alpha$ -D-Glucopyranosyl-(1'→4) $\beta$ -D-glucopyranosyl)N-vanillyl-nonanamide <b>28d</b>	0.75 $\pm$ 0.04	0.8 $\pm$ 0.04
4- <i>O</i> -( $\beta$ -D-Galactopyranosyl-(1'→4) $\beta$ -D-glucopyranosyl)N-vanillyl-nonanamide <b>29</b>	1.04 $\pm$ 0.05	1.82 $\pm$ 0.09
Curcumin <b>3</b>	0.053 $\pm$ 0.003	0.83 $\pm$ 0.04
1,7- <i>O</i> -(Bis- $\beta$ -D-glucopyranosyl)curcumin <b>30</b>	0.8 $\pm$ 0.04	1.09 $\pm$ 0.05
1,7- <i>O</i> -(Bis-D-galactopyranosyl)curcumin <b>31a,b</b>	0.92 $\pm$ 0.05	0.88 $\pm$ 0.04
1,7- <i>O</i> -(Bis-D-mannopyranosyl)curcumin <b>32a,b</b>	0.75 $\pm$ 0.04	1.9 $\pm$ 0.1
1,7- <i>O</i> -(Bis- $\beta$ -D-galactopyranosyl-(1'→4)D-glucopyranosyl)curcumin <b>33a,b</b>	0.95 $\pm$ 0.05	0.67 $\pm$ 0.03
DL-Dopa <b>4</b>	0.045 $\pm$ 0.002	0.6 $\pm$ 0.03
DL-3-Hydroxy-4- <i>O</i> -(D-glucopyranosyl)phenylalanine <b>34a-d</b>	1.11 $\pm$ 0.06	1.2 $\pm$ 0.06
DL-3-Hydroxy-4- <i>O</i> -(D-glucopyranosyl)phenylalanine <b>34b,c</b>	0.98 $\pm$ 0.05	1.26 $\pm$ 0.06
DL-3-Hydroxy-4- <i>O</i> -(D-galactopyranosyl)phenylalanine <b>35a-e</b>	2.26 $\pm$ 0.11	1.71 $\pm$ 0.08
DL-3-Hydroxy-4- <i>O</i> -( $\beta$ -D-mannopyranosyl)phenylalanine <b>36</b>	1.13 $\pm$ 0.06	1.87 $\pm$ 0.09
DL-3-Hydroxy-4- <i>O</i> -( $\beta$ -D-galactopyranosyl-(1'→4) $\beta$ -D-glucopyranosyl)phenylalanine <b>37</b>	0.9 $\pm$ 0.05	3.33 $\pm$ 0.17
DL-3-Hydroxy-4- <i>O</i> -(6-D-sorbitol)phenylalanine <b>38</b>	1.86 $\pm$ 0.09	0.56 $\pm$ 0.03
DL-Dopa-D-mannitol <b>39a,b</b>	1.9 $\pm$ 0.09	1.58 $\pm$ 0.08
Dopamine <b>5</b>	0.04 $\pm$ 0.002	1.93 $\pm$ 0.1

3-Hydroxy-4- <i>O</i> -(D-glucopyranosyl)phenylethylamine <b>40a-c</b>	1.45 ± 0.07	1.27 ± 0.06
3-Hydroxy-4- <i>O</i> -(β-D-glucopyranosyl)phenylethylamine <b>40b</b>	0.98 ± 0.05	2.38 ± 0.12
3-Hydroxy-4- <i>O</i> -(D-galactopyranosyl)phenylethylamine <b>41a-d</b>	0.93 ± 0.05	2.38 ± 0.12
3-Hydroxy-4- <i>O</i> -(D-mannopyranosyl)phenylethylamine <b>42a-c</b>	1.8 ± 0.09	1.93 ± 0.1
Riboflavin <b>43</b>	-	1.08 ± 0.05
5- <i>O</i> -(D-Glucopyranosyl)riboflavin <b>46a-c</b>	-	1.27 ± 0.06
5- <i>O</i> -(β-D-Glucopyranosyl)riboflavin <b>46b</b>	-	1.75 ± 0.09
5- <i>O</i> -(D-Galactopyranosyl)riboflavin <b>47a,b</b>	-	0.83 ± 0.04
5- <i>O</i> -(α-D-Mannopyranosyl)riboflavin <b>48a</b>	-	2.08 ± 0.1
5- <i>O</i> -(D-Mannopyranosyl)riboflavin <b>48a,b</b>	-	1.92 ± 0.1
5- <i>O</i> -(D-Ribofuranosyl)riboflavin <b>49a,b</b>	-	1.11 ± 0.06
5- <i>O</i> -(α-D-Glucopyranosyl-(1'→4)D-glucopyranosyl)riboflavin <b>50a-c</b>	-	0.8 ± 0.04
5- <i>O</i> -(1-D-Fructofuranosyl-(2→1')α-D-glucopyranosyl)riboflavin <b>51</b>	-	1.03 ± 0.05
5- <i>O</i> -(β-D-Galactopyranosyl-(1'→4)β-D-glucopyranosyl)riboflavin <b>52</b>	-	1.09 ± 0.05
Ergocalciferol <b>44</b>	-	1.2 ± 0.06
20- <i>O</i> -(D-Glucopyranosyl)ergocalciferol <b>53a-c</b>	0.9 ± 0.05	1.17 ± 0.06
α-Tocopherol <b>45</b>	0.054 ± 0.003	1.07 ± 0.05
6- <i>O</i> -(β-D-Glucopyranosyl)α-tocopherol <b>54</b>	1.2 ± 0.06	1.33 ± 0.07
6- <i>O</i> -(D-Galactopyranosyl)α-tocopherol <b>55a,b</b>	0.72 ± 0.04	2.59 ± 0.13
6- <i>O</i> -(D-Mannopyranosyl)α-tocopherol <b>56a,b</b>	0.5 ± 0.03	1.8 ± 0.09

<sup>a</sup>Glucosidases catalyzed synthesis of phenolic glycosides of vanillin-Table 3.3, *N*-vanillyl-nonanamide-Table 3.11, curcumin-Table 3.13, DL-dopa-Table 3.15, dopamine-Table 3.18 and vitamin glycosides of riboflavin-Table 4.3, ergocalciferol-Table 4.5 and α-tocopherol-Table 4.7 where the conversion yields and product proportions are shown. Carbohydrates did not show any antioxidant and ACE inhibition activity. Error in measurements is ± 5%.

<sup>b</sup>Antioxidant activity values determined by DPPH radical scavenging method (Moon and Tearo 1998). <sup>c</sup>ACE activity determined by Cushman and Cheung method (1971).

Butylated hydroxy anisole (BHA) was used as a control. The plot obtained is shown in Fig. 6.1. Plots for the antioxidant activity of a few selected glycosides, 4-*O*-(β-D-glucopyranosyl)vanillin **17b** (Fig. 6.2A), 4-*O*-(β-D-galactopyranosyl-(1'→4)β-D-glucopyranosyl)vanillin **22** (Fig. 6.2B), 4-*O*-(β-D-galactopyranosyl)*N*-vanillyl-nonanamide **25b** (Fig. 6.2C), 4-*O*-(α-D-glucopyranosyl-(1'→4)β-D-glucopyranosyl)*N*-vanillyl-nonanamide **28d** (Fig. 6.2 D), 1,7-*O*-(bis-β-D-glucopyranosyl)curcumin **30** (Fig. 6.2E), 1,7-*O*-(bis-D-mannopyranosyl)curcumin **32a,b** (Fig. 6.2F), DL-3-hydroxy-4-*O*-(D-glucopyranosyl)phenylethylamine **40a-c** (Fig. 6.2G), 3-hydroxy-4-*O*-(β-D-glucopyranosyl)phenylethylamine **40b** (Fig. 6.2H), 3-hydroxy-4-*O*-(D-galactopyranosyl)phenylethylamine **41a-d** (Fig. 6.2I), 3-hydroxy-4-*O*-(D-mannopyranosyl)phenylethylamine **42a-c** (Fig. 6.2J), riboflavin **43** (Fig. 6.2K), 5-*O*-(D-Glucopyranosyl)riboflavin **46a-c** (Fig. 6.2L), 5-*O*-(β-D-Glucopyranosyl)riboflavin **46b** (Fig. 6.2M), 5-*O*-(D-Galactopyranosyl)riboflavin **47a,b** (Fig. 6.2N), 5-*O*-(α-D-Mannopyranosyl)riboflavin **48a** (Fig. 6.2O), 5-*O*-(D-Mannopyranosyl)riboflavin **48a,b** (Fig. 6.2P), 5-*O*-(D-Ribofuranosyl)riboflavin **49a,b** (Fig. 6.2Q), 5-*O*-(α-D-Glucopyranosyl-(1'→4)D-glucopyranosyl)riboflavin **50a-c** (Fig. 6.2R), 5-*O*-(1-D-Fructofuranosyl-(2→1')α-D-glucopyranosyl)riboflavin **51** (Fig. 6.2S), 5-*O*-(β-D-Galactopyranosyl-(1'→4)β-D-glucopyranosyl)riboflavin **52** (Fig. 6.2T), ergocalciferol **44** (Fig. 6.2U), 20-*O*-(D-Glucopyranosyl)ergocalciferol **53a-c** (Fig. 6.2V), α-tocopherol **45** (Fig. 6.2W), 6-*O*-(β-D-Glucopyranosyl)α-tocopherol **54** (Fig. 6.2X), 6-*O*-(D-Galactopyranosyl)α-tocopherol **55a,b** (Fig. 6.2Y), 6-*O*-(D-Mannopyranosyl)α-tocopherol **56a,b** (Fig. 6.2Z).

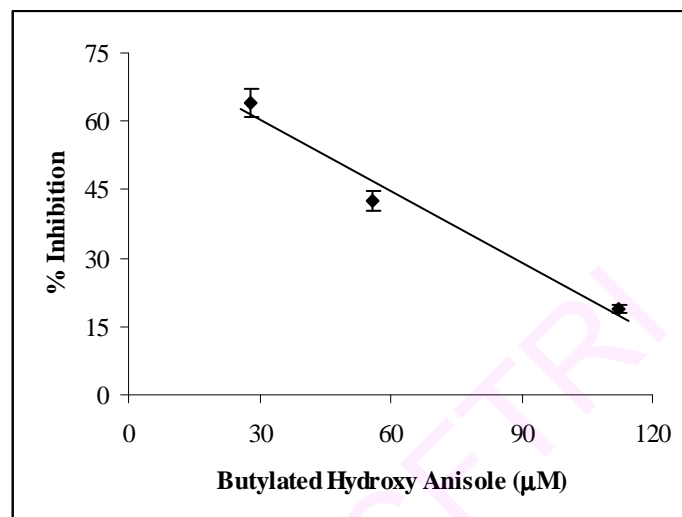


**Fig. 6.1** Antioxidant inhibition plot for Butylated Hydroxy Anisole (BHA). Concentration range – 0-120  $\mu\text{M}$ , DPPH - 1 mL (3.6 mM), Buffer – 0.1 M Tris-HCl (pH 7.4), Incubation period – 20 min and temperature - 37 °C.  $\text{IC}_{50}$  value -  $0.046 \pm 0.002$  mM.

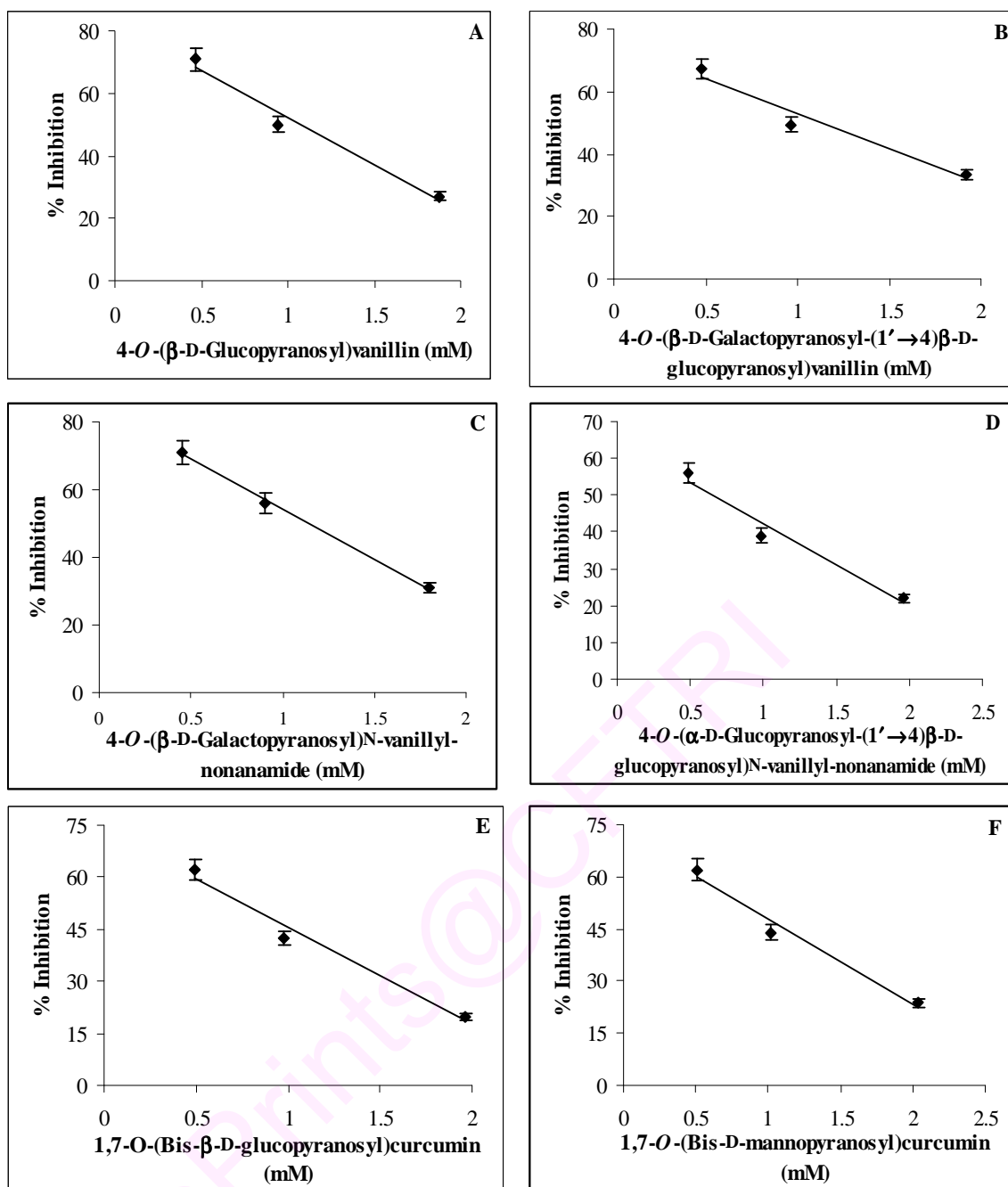


**Fig. 6.2** Antioxidant activity plot for phenolic glycosides. DPPH – 1 mL (3.6 mM), glycoside concentration range – 5-10 mM, Buffer – 0.1 M Tris-HCl (pH 7.4), Incubation period – 20 min and temperature – 37 °C. IC<sub>50</sub> value for the antioxidant activity was obtained as the concentration of the glycoside corresponding to 50% decrease in DPPH absorbance from these plots. (A) 4-O-(β-D-glucopyranosyl)vanillin **17b**, (B) 4-O-(β-D-galactopyranosyl-(1'→4)β-D-glucopyranosyl)vanillin **22**, (C) 4-O-(β-D-galactopyranosyl)N-vanillyl-nonanamide **25b**, (D) 4-O-(α-D-glucopyranosyl-(1'→4)β-D-glucopyranosyl)N-vanillyl-nonanamide **28d**, (E) 1,7-O-(bis-β-D-glucopyranosyl)curcumin **30** and (F) 1,7-O-(bis-D-mannopyranosyl)curcumin **32a,b**.



pyranosyl)phenylalanine **34b,c** (Fig. 6.3A), DL-3-hydroxy-4-*O*-( $\beta$ -D-galactopyranosyl-(1'→4) $\beta$ -D-glucopyranosyl)phenylalanine **37** (Fig. 6.3B), 3-hydroxy-4-*O*-( $\beta$ -D-glucopyranosyl)phenylethylamine **40b** (Fig. 6.3C), 3-hydroxy-4-*O*-(D-galactopyranosyl)phenylethylamine **41a-d** (Fig. 6.3D), 20-*O*-(D-glucopyranosyl) ergocalciferol **53a-c** (Fig. 6.3E) and 6-*O*-(D-mannopyranosyl) $\alpha$ -tocopherol **56a,b** (Fig. 6.3F) are shown.

## 6.2 Angiotensin converting enzyme inhibitory activity

ACE was isolated from pig lung. The isolated ACE tested for lipase and protease activity (Table 6.2), showed a small extent of protease activity (13.3%) compared to ACE activity but no lipase activity. In presence of glycosides prepared, the isolated ACE showed 8.2% protease activity (Table 6.2) compared to the ACE activity. This confirmed that the ACE inhibition observed in the presence of glycosides prepared is more due to ACE inhibition rather than protease inhibition.

**Table 6.2** Inhibition of protease in ACE by glycoside<sup>a</sup>

System	Protease activity Unit min <sup>-1</sup> mg <sup>-1</sup> enzyme protein <sup>b</sup>	Percentage of protease activity with respect to ACE activity <sup>c</sup>
Control: ACE- 0.5 mL + 0.5 ml of 0.6% hemoglobin + 0.5 mL Buffer	0.044	13.3
Glycoside: 0.5 mL glycoside + ACE - 0.5 mL + 0.5 mL of 0.6% hemoglobin	0.029	8.2

<sup>a</sup>Conditions: ACE – 0.5 mL (0.5mg), All the solutions were prepared in 0.1 M pH 7.5 Tris-HCl, incubation period – 30 min, temperature – 37 °C, 0.5 mL of 10% trichloroacetic acid added to arrest the reaction; Blank performed without enzyme and glycoside; Absorbance measured at 440 nm; glycoside – 0.5 mL of 0.8 mM; <sup>b</sup>Average absorbance values from three individual experiments; <sup>c</sup>Percentage protease activity with respect to an ACE activity of 0.33  $\mu$ mol/min.mg protein.

Table 6.1 shows the glycosides tested for their ACE inhibitory activities. ACE inhibition plot for enalapril, a known synthetic drug, used as a control is shown in Fig. 6.4. Typical ACE inhibition plots for few representative glycosides 4-*O*-(D-galactopyranosyl)vanillin **18a,b** (Fig. 6.5A), 4-*O*-(D-sorbitol)vanillin **23a-c** (Fig. 6.5B), 4-*O*-( $\alpha$ -D-ribofuranosyl)N-vanillyl-nonanamide **27a,b** (Fig. 6.5C), 4-*O*-( $\alpha$ -D-glucopyranosyl)N-vanillyl-nonanamide **27a,b** (Fig. 6.5D), 4-*O*-( $\alpha$ -D-glucopyranosyl)N-vanillyl-nonanamide **27a,b** (Fig. 6.5E), 4-*O*-( $\alpha$ -D-glucopyranosyl)N-vanillyl-nonanamide **27a,b** (Fig. 6.5F), 4-*O*-( $\alpha$ -D-glucopyranosyl)N-vanillyl-nonanamide **27a,b** (Fig. 6.5G), 4-*O*-( $\alpha$ -D-glucopyranosyl)N-vanillyl-nonanamide **27a,b** (Fig. 6.5H), 4-*O*-( $\alpha$ -D-glucopyranosyl)N-vanillyl-nonanamide **27a,b** (Fig. 6.5I), 4-*O*-( $\alpha$ -D-glucopyranosyl)N-vanillyl-nonanamide **27a,b** (Fig. 6.5J), 4-*O*-( $\alpha$ -D-glucopyranosyl)N-vanillyl-nonanamide **27a,b** (Fig. 6.5K), 4-*O*-( $\alpha$ -D-glucopyranosyl)N-vanillyl-nonanamide **27a,b** (Fig. 6.5L), 4-*O*-( $\alpha$ -D-glucopyranosyl)N-vanillyl-nonanamide **27a,b** (Fig. 6.5M), 4-*O*-( $\alpha$ -D-glucopyranosyl)N-vanillyl-nonanamide **27a,b** (Fig. 6.5N), 4-*O*-( $\alpha$ -D-glucopyranosyl)N-vanillyl-nonanamide **27a,b** (Fig. 6.5O), 4-*O*-( $\alpha$ -D-glucopyranosyl)N-vanillyl-nonanamide **27a,b** (Fig. 6.5P), 4-*O*-( $\alpha$ -D-glucopyranosyl)N-vanillyl-nonanamide **27a,b** (Fig. 6.5Q), 4-*O*-( $\alpha$ -D-glucopyranosyl)N-vanillyl-nonanamide **27a,b** (Fig. 6.5R), 4-*O*-( $\alpha$ -D-glucopyranosyl)N-vanillyl-nonanamide **27a,b** (Fig. 6.5S), 4-*O*-( $\alpha$ -D-glucopyranosyl)N-vanillyl-nonanamide **27a,b** (Fig. 6.5T), 4-*O*-( $\alpha$ -D-glucopyranosyl)N-vanillyl-nonanamide **27a,b** (Fig. 6.5U), 4-*O*-( $\alpha$ -D-glucopyranosyl)N-vanillyl-nonanamide **27a,b** (Fig. 6.5V), 4-*O*-( $\alpha$ -D-glucopyranosyl)N-vanillyl-nonanamide **27a,b** (Fig. 6.5W), 4-*O*-( $\alpha$ -D-glucopyranosyl)N-vanillyl-nonanamide **27a,b** (Fig. 6.5X), 4-*O*-( $\alpha$ -D-glucopyranosyl)N-vanillyl-nonanamide **27a,b** (Fig. 6.5Y), 4-*O*-( $\alpha$ -D-glucopyranosyl)N-vanillyl-nonanamide **27a,b** (Fig. 6.5Z).

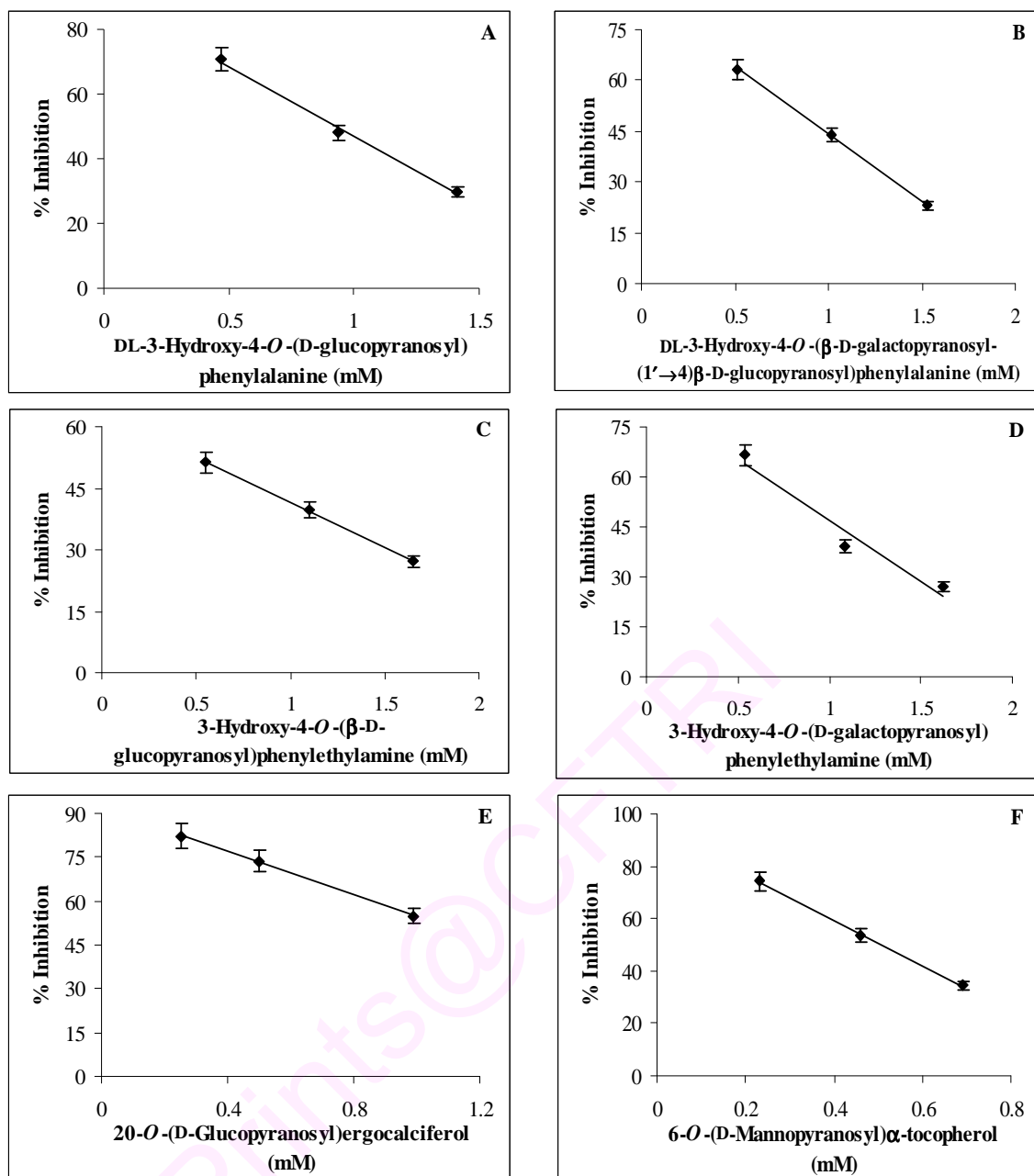


**Fig. 6.3** Antioxidant activity plot for phenolic and vitamin glycosides. DPPH – 1 mL (3.6 mM), glycoside concentration range – 5-10 mM, Buffer – 0.1 M Tris-HCl (pH 7.4), Incubation period – 20 min and temperature – 37 °C. IC<sub>50</sub> value for the antioxidant activity was obtained as the concentration of the glycoside corresponding to 50% decrease in DPPH absorbance from these plots. (A) DL-3-hydroxy-4-O-(D-glucopyranosyl)phenylalanine **34b,c**, (B) DL-3-hydroxy-4-O-(β-D-galactopyranosyl-(1'→4)β-D-glucopyranosyl)phenylalanine **37**, (C) 3-hydroxy-4-O-(β-D-glucopyranosyl)phenylethylamine **40b**, (D) 3-hydroxy-4-O-(D-galactopyranosyl)phenylethylamine **41a-d**, (E) 20-O-(D-glucopyranosyl)ergocalciferol **53a-c** and (F) 6-O-(D-mannopyranosyl)α-tocopherol **56a,b**.

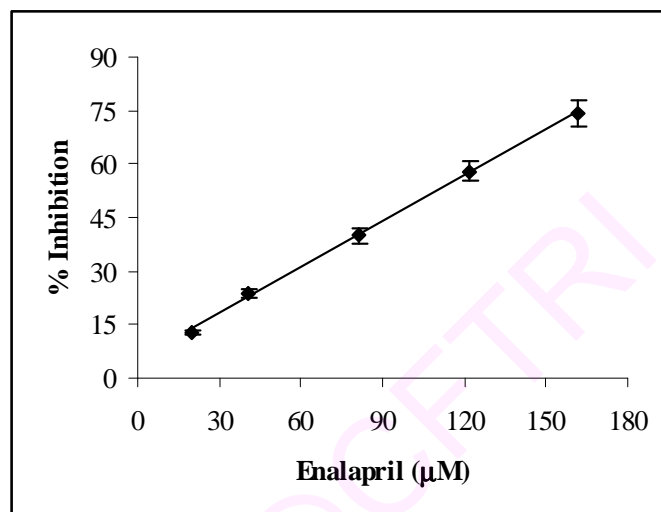


**Fig. 6.4** ACE inhibition plot for enalapril. Concentration range – 0-180  $\mu\text{M}$ , substrate – 0.1 mL hippuryl-L-histidyl-L-leucine (5 mM), buffer – 100 mM phosphate buffer (pH 8.3) containing 0.3 M NaCl, incubation period – 30 min and temperature – 37  $^{\circ}\text{C}$ .  $\text{IC}_{50}$  value -  $0.071 \pm 0.004$  mM.

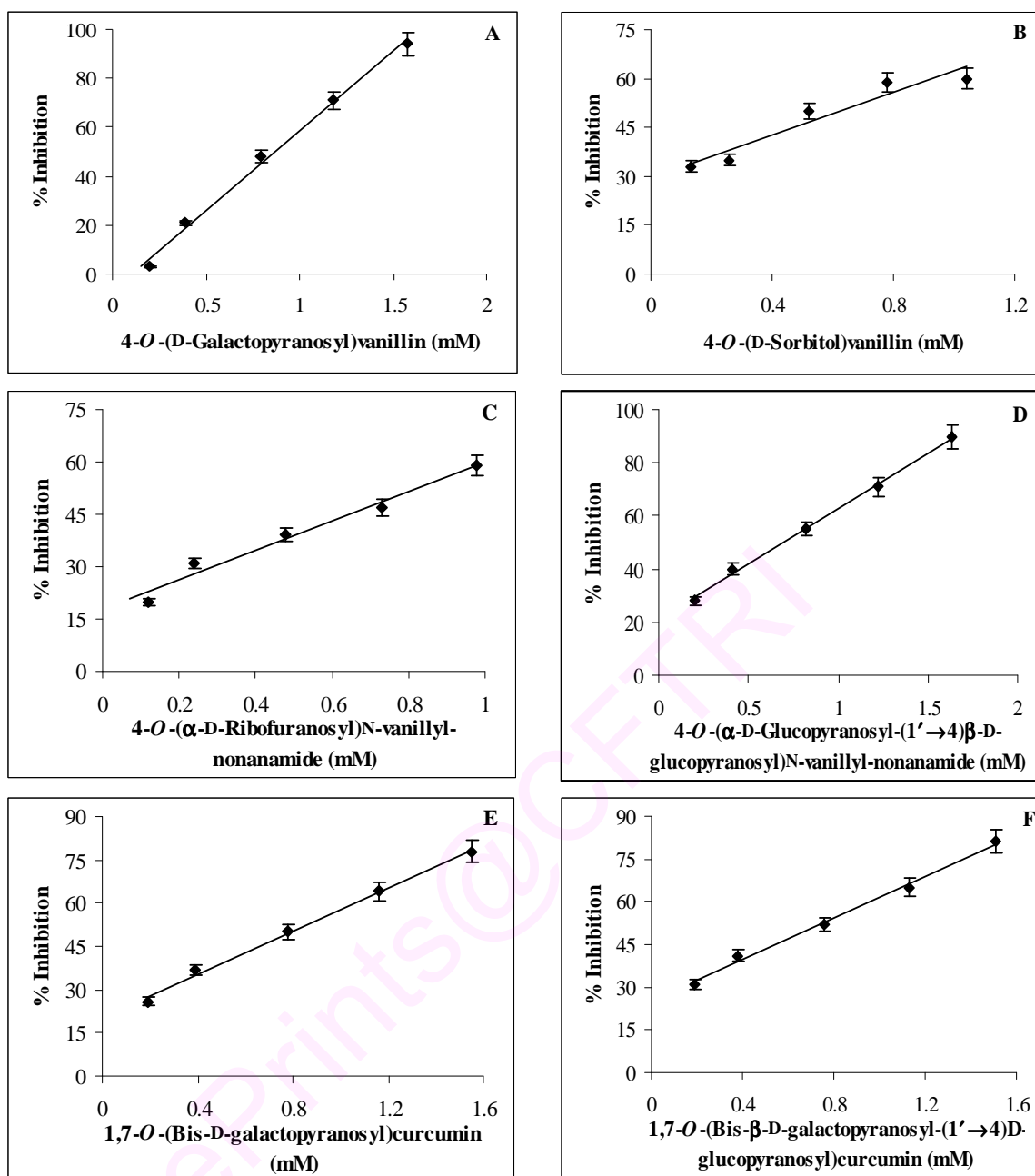


**Fig. 6.5** ACE inhibition plots for phenolic glycosides: ACE – 0.1 mL (10 mg in 25 mL stock solution), glycoside concentration range – 0.2-1.8 mM, substrate – 0.1 mL hippuryl-L-histidyl-L-leucine (5 mM), buffer – 100 mM phosphate buffer pH 8.3 containing 0.3 M sodium chloride, incubation period – 30 min and temperature – 37 °C (A) 4-O-(D-galactopyranosyl)vanillin **18a,b**, (B) 4-O-(D-sorbitol)vanillin **23a-c**, (C) 4-O-(α-D-ribofuranosyl)N-vanillyl-nonanamide **27a,b**, (D) 4-O-(α-D-glucopyranosyl-(1'→4)β-D-glucopyranosyl)N-vanillyl-nonanamide **28d**, (E) 1,7-O-(bis-D-galactopyranosyl)curcumin **31a,b** and (F) 1,7-O-(bis-β-D-galactopyranosyl-(1'→4)D-glucopyranosyl)curcumin **33a,b**.

pyranosyl-(1'→4)β-D-glucopyranosyl)N-vanillyl-nonanamide **28d** (Fig. 6.5D), 1,7-*O*-(bis-D-galactopyranosyl)curcumin **31a,b** (Fig. 6.5E), 1,7-*O*-(bis-β-D-galactopyranosyl-(1'→4)D-glucopyranosyl)curcumin **33a,b** (Fig. 6.5F), DL-3-hydroxy-4-*O*-(D-glucopyranosyl)phenylalanine **34a-d** (Fig. 6.6A), DL-3-hydroxy-4-*O*-(6-D-sorbitol) phenylalanine **38** (Fig. 6.6B), 3-hydroxy-4-*O*-(D-glucopyranosyl)phenylethylamine **40a-c** (Fig. 6.6C), 3-hydroxy-4-*O*-(D-mannopyranosyl)phenylethylamine **42a-c** (Fig. 6.6D), 5-*O*-(D-galactopyranosyl)riboflavin **47a,b** (Fig. 6.6E), 5-*O*-(α-D-glucopyranosyl-(1'→4)D-glucopyranosyl)riboflavin **50a-c** (Fig. 6.6F), 20-*O*-(D-glucopyranosyl) ergocalciferol **53a-c** (Fig. 6.7A), 6-*O*-(β-D-glucopyranosyl)α-tocopherol **54** (Fig. 6.7B) and 6-*O*-(D-mannopyranosyl)α-tocopherol **56a,b** (Fig. 6.7C) are shown.

### 6.3 Discussion

About 39 glycosides were tested for antioxidant activity and 48 glycosides for angiotensin converting enzyme (ACE) inhibitory activities. Enzymatic glycosylation produced only monoglycosides and no diglycosides were detected except curcumin, which showed bis glycosylation. In spite of possessing OH groups at 3<sup>rd</sup> and 4<sup>th</sup> positions, DL-dopa and dopamine gave a mixture of 4-OH, 3-OH and 4-*O*-C6-arylated compounds (Table 6.1) but no bis glycosides. With many phenols and vitamins, C1α and/or C1β glycosides were formed and in some case C6-*O*-arylated products were also formed.

The aglycon phenols and free vitamins were also subjected to measurement of antioxidant activity and ACE inhibition as controls. Antioxidant activities were determined (Table 6.1) for phenols and also vitamins possessing phenolic OH group and alicyclic OH group like ergocalciferol (vitamin D2). Antioxidant activities of the phenolic and vitamin glycosides were in the 0.5 ± 0.03 mM to 2.66 ± 0.13 mM range when compared to the free aglycons whose values were much higher (0.053 ± 0.003 mM

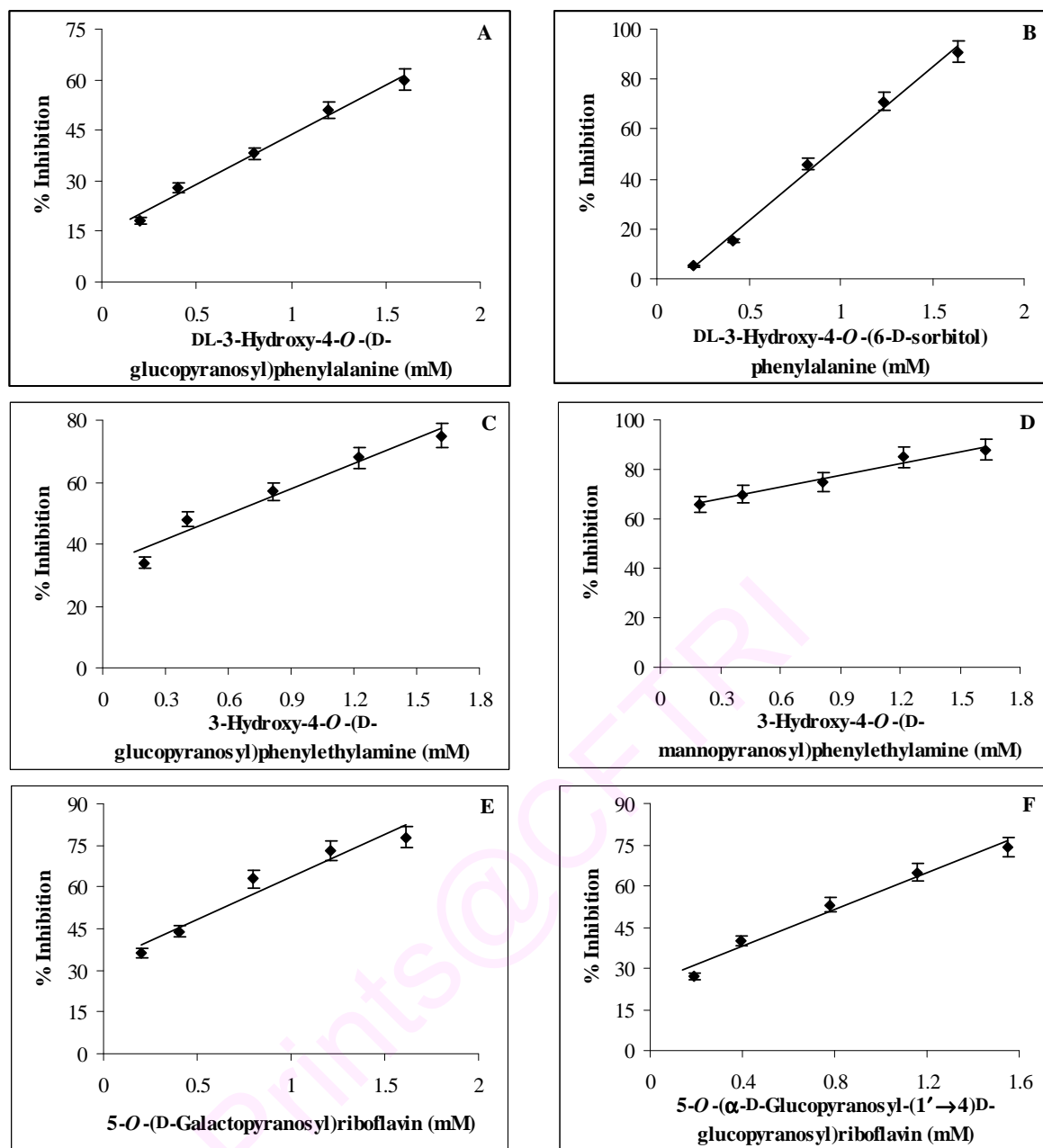


**Fig. 6.6** ACE inhibition plots for phenolic and vitamin glycosides: ACE – 0.1 mL (10 mg in 25 mL stock solution), glycoside concentration range – 0.2-1.8 mM, substrate – 0.1 mL hippuryl-L-histidyl-L-leucine (5 mM), buffer – 100 mM phosphate buffer pH 8.3 containing 0.3 M sodium chloride, incubation period – 30 min and temperature – 37 °C (A) DL-3-hydroxy-4-O-(D-glucopyranosyl)phenylalanine **34a-d**, (B) DL-3-hydroxy-4-O-(6-D-sorbitol)phenylalanine **38**, (C) 3-hydroxy-4-O-(D-glucopyranosyl)phenyl ethylamine **40a-c**, (D) 3-hydroxy-4-O-(D-mannopyranosyl)phenylethylamine **42a-c**, (E) 5-O-(D-galactopyranosyl)riboflavin **47a,b** and (F) 5-O-( $\alpha$ -D-glucopyranosyl-(1'→4)D-glucopyranosyl)riboflavin **50a-c**.

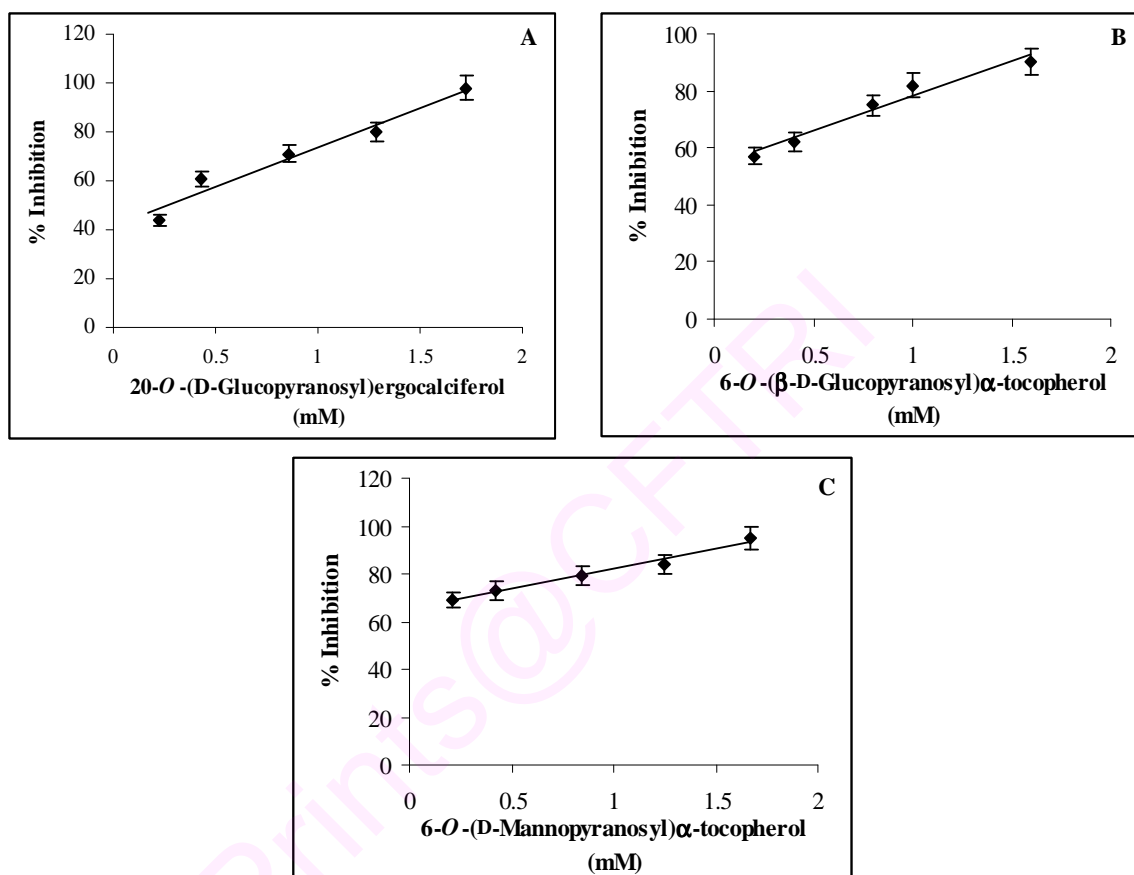


**Fig. 6.7** ACE inhibition plots for phenolic and vitamin glycosides: ACE – 0.1 mL (10 mg in 25 mL stock solution), glycoside concentration range – 0.2-1.8 mM, substrate – 0.1 mL hippuryl-L-histidyl-L-leucine (5 mM), buffer – 100 mM phosphate buffer pH 8.3 containing 0.3 M sodium chloride, incubation period – 30 min and temperature – 37 °C (A) 20-*O*-(*D*-glucopyranosyl)ergocalciferol **53a-c**, (B) 6-*O*-( $\beta$ -*D*-glucopyranosyl) $\alpha$ -tocopherol **54** and (C) 6-*O*-(*D*-mannopyranosyl) $\alpha$ -tocopherol **56a,b**.

to  $1.65 \pm 0.08$  mM). Butylated Hydroxy Anisole (BHA) showed the lowest  $IC_{50}$  value at  $0.046 \pm 0.002$  mM and no other glycosides could come closer to this value. Many of the glycosides showed lesser  $IC_{50}$  values of  $< 1$  mM (Table 6.1). The best  $IC_{50}$  values ( $\leq 0.75$  mM) observed are: 4-*O*-( $\alpha$ -D-glucopyranosyl-(1'→4) $\beta$ -D-glucopyranosyl)N-vanillyl-nonanamide **28d** -  $0.75 \pm 0.04$  mM, 1,7-*O*-(bis-D-mannopyranosyl)curcumin **32a,b** -  $0.75 \pm 0.04$  mM, 6-*O*-(D-galactopyranosyl) $\alpha$ -tocopherol **55a,b** -  $0.72 \pm 0.04$  mM and 6-*O*-(D-mannopyranosyl) $\alpha$ -tocopherol **56a,b** -  $0.5 \pm 0.03$  mM.

$IC_{50}$  values for ACE inhibition of glycosides range from  $0.56 \pm 0.03$  mM to  $3.33 \pm 0.17$  mM (Table 6.1). Enalapril, a known synthetic drug, showed an  $IC_{50}$  value of  $0.071 \pm 0.004$  mM but no other phenolic or vitamin glycosides could exhibit such a low value. However, the best ACE inhibitory activities for the glycosides ( $< 0.75$  mM) detected were: 4-*O*-( $\beta$ -D-glucopyranosyl)vanillin **17b** -  $0.61 \pm 0.03$  mM, 4-*O*-(D-galactopyranosyl)vanillin **18a,b** -  $0.61 \pm 0.03$  mM, 1,7-*O*-(bis- $\beta$ -D-galactopyranosyl-(1'→4)D-glucopyranosyl)curcumin **33a,b** -  $0.67 \pm 0.03$  mM and DL-3-hydroxy-4-*O*-(6-D-sorbitol)phenylalanine **38** -  $0.56 \pm 0.03$  mM. Among the glycosides tested, phenolic glycosides showed better ACE activities than the vitamin glycosides. Both phenolic and vitamin glycosides showed comparable  $IC_{50}$  values to aglycon units. Derivatization by the introduction of carbohydrate molecule to the phenolic/alcoholic OH had very little effect on the  $IC_{50}$  values compared to the control. Hence, it can be concluded that the presence of free phenolic or derivated OH groups are not essential for ACE inhibition. Many commercial inhibitors like enalapril are peptides containing the essential prolyl units. Among the carbohydrates employed, aglycons modified with D-glucose **6**, D-galactose **7** and D-sorbitol **15** showed less  $IC_{50}$  values ( $0.56 \pm 0.03$  mM to  $0.75 \pm 0.04$  mM) than those modified with the other carbohydrate molecules.



Among the phenols employed vanillin **1**, N-vanillyl-nonanamide **2**, curcumin **3**, DL-dopa **4** and dopamine **5** possess structural similarity by having hydroxyl group at the 4<sup>th</sup> position and hydroxyl or methoxy group at 3<sup>rd</sup> position besides having a CH= or CH<sub>2</sub> carbon *para* to the 4<sup>th</sup> OH position. Such a structural similarity is responsible for better antioxidant activities of the free phenols compared to their glycosides which also have not lost much of their activities even after glycosylation. However, these glycosides did not show high ACE inhibition activities. Some like vanillin and DL-dopa glycosides showed reasonable extent of ACE inhibition activities. Phenolic OH was found to be very essential for antioxidant activity. Although introduction of a carbohydrate molecule at the phenolic OH decreases the antioxidant activity, some of the glycosides still possess substantial amount of antioxidant activities. Presence of free OH group in case of DL-dopa **4** and dopamine **5** did not show good antioxidant activity of the glycosides where one of the OH group is modified leaving the other free. Since riboflavin **43** did not contain a phenolic OH group, its antioxidant activities were not measured. However, introduction of the carbohydrate molecules at the phenolic OH did not alter the ACE inhibition activities much.

Since the reaction conditions employed were milder, no other side products were detected in the reaction. However, the phenolic and vitamin glycosides tested in the present work, showed that they could be accommodated in the hydrophobic S<sub>1</sub> and S<sub>2</sub> subsites of angiotensin I converting enzyme (Michaud *et al.* 1997). Carbohydrates in glycosides could also bind to the hydrophobic and/or hydrophilic subsites of angiotensin I converting enzyme, as they possess both hydrophobic and hydrophilic groups in their structure. ACE preparation of the present work from pig lung is ACE I (Sanchez *et al.* 2003) and it showed a low protease inhibitory activity but no lipase activity. This indicated that ACE is inhibited rather than protease as protease exists at a very low activity

which could not be construed to be ACE inhibition. These results suggest that both the phenolic and vitamin glycosides hold promising potential as antioxidants and ACE inhibitors although the IC<sub>50</sub> values are slightly on the higher side a drawback which could be corrected through suitable modifications.

## 6.4 Experimental

### 6.4.1 Glycosylation procedure

Glycosylation procedure has been described for vanillin **1**, N-vanillyl nonanamide **2**, curcumin **3**, DL-3,4-dihydroxyphenylalanine **4** (DL-dopa), 3,4-dihydroxyphenyl ethylamine **5** (dopamine), riboflavin **43** (vitamin B2), ergocalciferol **44** (vitamin D2) and  $\alpha$ -tocopherol **45** (vitamin E) in their respective Sections of 3.1, 3.2, 3.3, 3.4, 3.5, 4.1, 4.2 and 4.3.

### 6.4.2 Antioxidant activity by DPPH method

Antioxidant activity of the glycosides was evaluated by the DPPH (2,2-Diphenyl-1-picrylhydrazyl) radical scavenging method (Moon and Tearo 1998). Absorbance of a solution in duplicate, containing 0.1 mL of test sample (5-10 mM) and 1 mL of DPPH (0.36 mM in ethanol) was measured with the final volume made up to 2 mL with 0.1 M Tris-HCl buffer (pH 7.4). After incubation at room temperature for 20 minutes in dark, absorbance was measured at 517 nm on a UV-Visible spectrophotometer (Shimadzu, UV 1601). Decrease in absorbance compared to DPPH itself was a measure of the radical scavenging ability of the test sample. Butylated hydroxyanisole (BHA, 5.6 mM) was used as a positive control. Error in measurements will be  $\pm 5\%$ . IC<sub>50</sub> value was expressed as the amount of the glycoside required to bring down the absorbance of DPPH by 50%.

### 6.4.3 Extraction of ACE from pig lung

ACE was extracted from pig lung using the method described by Andujar-Sanchez *et al.* (2003). A 100 g of pig lung was minced and homogenized using a blender

with 10 mM HEPES buffer (pH 7) containing 0.4 M NaCl at a volume ratio of 5:1 (v/w of pig lung) at 4 °C. The homogenate was centrifuged at 9000 g for 60 min. The supernatant was discarded and the precipitate was washed twice with 200 ml of 10 mM HEPES buffer (pH 7) containing 0.4 M NaCl. The final precipitate was resuspended in 200 ml of 10 mM pH 7 HEPES buffer containing 0.4 M NaCl, 10 µM ZnCl<sub>2</sub>, 0.5 % (w/v) Triton-X-100 and stirred over night at 4 °C. The solution was centrifuged to remove the pellets. The supernatant was dialyzed against water and later lyophilized. The protein content of ACE determined by Lowry's method was found to be 8.3 %. The specific activity of the enzyme was found to be 0.24 µmol/min/mg of enzyme protein.

#### **6.4.4 Angiotensin converting enzyme (ACE) inhibition assay**

ACE inhibition assay for the glycosides prepared was performed by Cushman and Cheung (1971) method. Aliquots of glycoside solutions in the concentration range 0.2 to 1.8 mM (0.1 mL to 0.8 mL of 2 mM stock solution) were taken and to this 0.1 mL of ACE solution (0.1% in 0.1 M phosphate buffer, pH 8.3 containing 0.3 M NaCl) was added. To this solution a further 0.1 mL of 2.5 mM hippuryl-L-histidyl-L-leucine (HHL) was also added and the total volume made upto 1.25 mL with phosphate buffer (0.1 M pH 8.3 containing 0.3 M NaCl). The solution was incubated on a Heto-Holten shaking water bath for 30 min at 37 °C. Blanks were performed without the enzyme by taking only the glycoside solution (0.1 to 0.8 mL) along with 0.1 mL of 5 mM HHL. The total volume was made upto to 1.25 mL with the same buffer. The reaction was terminated by adding 0.25 mL of 1 M HCl. Hippuric acid formed in the reaction was extracted with 1.5 mL of ethyl acetate. One mL of ethyl acetate layer was evaporated to dryness and treated with equal amount of distilled water and the absorbance was measured at 228 nm for hippuric acid. The hippuric acid formed in 1.5 mL of ethyl acetate was determined from a calibration plot prepared using a standard 0-280 nmol hippuric acid solution in 1

mL of distilled water. Specific activity was expressed as  $\mu\text{mol}$  of hippuric acid formed per min per mg of enzyme protein.

$$\text{Specific activity} = \frac{A_{\text{ts}} - A_{\text{blank}}}{T \times S \times E}$$

$A_{\text{ts}}$  = absorbance of test solution,  $A_{\text{blank}}$  = absorbance of blank solution, T = incubation period in min, S = slope value of the calibration plot (0.011 Abs. units/nmol of hippuric acid), E = amount of the enzyme in mg protein.

Percentage inhibition was expressed as the ratio of specific activity of ACE in presence of the inhibitor to that in its absence, the latter being considered as 100%.  $\text{IC}_{50}$  value was expressed as the concentration of the inhibitor required for 50% reduction in ACE specific activity. Error in measurements will be  $\pm 5\%$ .

#### 6.4.5 Protease and lipase assay

Protease activity for the ACE inhibitor was determined by the method described by Dubey and Jagannadham (2003) and lipase activity by the tributyrin method (Vorderwulbecke *et al.* 1992) in presence of glycoside (0.8 mM in 0.1M Tris-HCl buffer, pH 7.5). Specific protease activity was expressed as the increase in absorbance at 440 nm per min per mg of the protein employed. Similarly specific lipase activity was determined as  $\mu\text{mol}$  of butyric acid formed per min per mg of the protein employed.

ePrints@CFTRI

***Conclusions***

**The important findings of the present investigation are:**

1. The present work is the first detailed study on the glycosylation of phenols like vanillin **1**, N-vanillyl-nonanamide **2**, curcumin **3**, DL-dopa **4** and dopamine **5** and vitamins like riboflavin (vitamin B2) **43**, ergocalciferol (vitamin D2) **44** and  $\alpha$ -tocopherol (vitamin E) **45** with the following carbohydrate molecules: aldohexoses - D-glucose **6**, D-galactose **7**, D-mannose **8**, ketohexose - D-fructose **9**, aldopentoses - D-arabinose **10**, D-ribose **11**, disaccharides - maltose **12**, sucrose **13**, lactose **14** and carbohydrate alcohols - D-sorbitol **15** and D-mannitol **16**. Phenols employed for the glycosylation possesses 3,4-dihydroxy phenyl derivatives, where a substituent *para* to the hydroxyl group at position 4 of the phenyl ring is substituted by -CHO or -CH=CH- or -CH<sub>2</sub> and the 3<sup>rd</sup> position substituted with -OCH<sub>3</sub> and -OH.
2. Amyloglucosidase from *Rhizopus* mold,  $\beta$ -glucosidase isolated from sweet almond and the same  $\beta$ -glucosidase immobilized onto calcium alginate beads were employed in the reverse hydrolytic/transglycosylation reaction in non-polar di-isopropyl ether solvent media.
3. A novel experimental setup was developed for even large-scale synthesis of glycosides using lesser enzymes and larger concentrations of substrates to give higher yields. This set up involved refluxing the reaction mixture containing the phenol/vitamin and carbohydrate with appropriate concentrations of amyloglucosidase and  $\beta$ -glucosidase (native/immobilized) in presence of specified pH and buffer concentrations in 100 mL of di-isopropyl ether solvent at 68 °C for a specified incubation period. This setup gave higher yields and selectivity than the conventional shake flask experiments.

4. Optimization of reaction parameters for the synthesis of above mentioned phenolic and vitamin glucosides were carried out in terms of incubation period, pH, buffer, enzyme and phenol/vitamin concentrations.
5. In most cases C1 glycosylated products were detected. Only few carbohydrate molecules showed C1-*O*-/C6-*O*-arylation. D-Sorbitol **15** and D-mannitol **16** gave arylated products by reacting only to the primary OH groups. No reaction occurred at the secondary hydroxyl groups of the carbohydrate molecules. Only mono glycosylated or mono arylated products were detected. No carbohydrate molecule gave bis products. Among the phenols employed only curcumin **3** showed bis glycosylated products by reacting at both the hydroxyl moieties of the feruloyl units. Even DL-dopa **4** and dopamine **5** did not give bis products.  $\beta$ -Glucosidase showed generally  $\beta$ -glycosides and in very few cases C1-*O*-/C6-*O*-arylated products. However, amyloglucosidase on the other hand showed both C1 $\alpha$  and C1 $\beta$ -glycosylated and/or C6 arylated products. Phenolic OH at the 4<sup>th</sup> position readily reacted with the carbohydrate molecules employed and wherever possible DL-dopa **4** and dopamine **5** underwent reaction at the 3<sup>rd</sup> phenolic OH also.
6. Totally hydrophobic acceptor molecules like curcumin **3**, ergocalciferol **44** and  $\alpha$ -tocopherol **45** reacts with only very few carbohydrate molecules like D-glucose **6**, D-galactose **7**, D-mannose **8** and lactose **14** where as the remaining hydrophilic phenols and vitamins employed vanillin **1**, N-vanillyl-nonanamide **2**, DL-dopa **4**, dopamine **5** and riboflavin **43** reacts with large number of carbohydrate molecules.
7. The glycosylation yields were better with phenols compared to those with the vitamins employed. Vitamins could not be better nucleophiles compared to the phenols employed.

8. Both amyloglucosidase and  $\beta$ -glucosidase did not catalyze the reaction with D-fructose **9** and D-arabinose **10**. This could be probably due to not-so-facile formation of the required oxo-carbenium ion intermediate by these carbohydrate molecules, which is an essential requirement for glycosylation during the catalytic action of the enzyme.
9. In both the glucosidases catalysed reactions, other than D-fructose **9** and D-arabinose **10** the remaining above mentioned carbohydrates underwent glycosylation/arylation with different phenols/vitamins to different extents. Such selective reactions could be due to stronger binding of the phenols/vitamins to the active site of enzymes than the respective unreacted carbohydrate molecules, thereby preventing facile transfer of the carbohydrate molecules to the nucleophilic phenolic OH of vanillin **1**, N-vanillyl-nonanamide **2**, curcumin **3**, DL-dopa **4**, dopamine **5**,  $\alpha$ -tocopherol **45**, primary OH of riboflavin **43** and acyclic OH of ergocalciferol **44**.
10. Amyloglucosidase from *Rhizopus* mold gave higher yield with lesser selectivity and  $\beta$ -glucosidase from sweet almond gave lesser yield and greater selectivity. In general, conversion yields ranging from 5% to 62% for amyloglucosidase catalyses and 7% to 65% for  $\beta$ -glucosidase (native/immobilized) catalyses were obtained for various phenols/vitamins. Invariably DL-dopa **4** and dopamine **5** gave high yields with less regioselectivity with both the glucosidases employed. Loss of regioselectivity in many of the glycosylation/arylation reactions could be due to the employment of large amount of the enzymes. This is inevitable, as the reversible reaction requires such large concentrations of enzymes for conversions.
11. Hydrolysis of disaccharides - maltose **12**, sucrose **13** and lactose **14** during the course of the reaction has been observed. Only in case of sucrose **13** the resultant



- glucose formed underwent trans-glycosylation with vanillin **1** in presence of amyloglucosidase to yield C1 $\beta$  glucosylated and C6-*O*-arylated product.
12. Thus water insoluble N-vanillyl-nonanamide **2**, curcumin **3**, ergocalciferol **44** and  $\alpha$ -tocopherol **45** and less water soluble vanillin **1** and riboflavin **43** were converted to more water soluble glycosides thereby improving their potential bioavailability and pharmacological properties.
13. Phenols/vitamins underwent glycosylation/arylation with the following respective carbohydrate molecules: vanillin **1** – D-glucose **6**, D-galactose **7**, D-mannose **8**, maltose **12**, sucrose **13**, lactose **14** and D-sorbitol **15**; N-vanillyl-nonanamide **2** – D-glucose **6**, D-galactose **7**, D-mannose **8**, D-ribose **11**, maltose **12** and lactose **14**; curcumin **3** – D-glucose **6**, D-galactose **7**, D-mannose **8** and lactose **14**; DL-dopa **4** – D-glucose **6**, D-galactose **7**, D-mannose **8**, D-sorbitol **15** and D-mannitol **16**; dopamine **5** – D-glucose **6**, D-galactose **7** and D-mannose **8**. riboflavin **43** – D-glucose **6**, D-galactose **7**, D-mannose **8**, D-ribose **11**, maltose **12**, sucrose **13** and lactose **14**; ergocalciferol **44** only with D-glucose **6** and  $\alpha$ -tocopherol **45** – D-glucose **6**, D-galactose **7** and D-mannose **8**.
14. Out of 82 individual phenolic and vitamin glycosides synthesized enzymatically using both the glucosidases, about 60 are being reported for the first time. New glycosides reported are: 4-*O*-(D-galactopyranosyl)vanillin **18a,b**, 4-*O*-(D-mannopyranosyl)vanillin **19a,b**, 4-*O*-( $\alpha$ -D-glucopyranosyl-(1'→4)D-glucopyranosyl)vanillin **20a-d**, 4-*O*-(D-fructofuranosyl-(2→1')  $\alpha$ -D-glucopyranosyl)vanillin **21a,b**, 4-*O*-( $\beta$ -D-galactopyranosyl-(1'→4) $\beta$ -D-glucopyranosyl)vanillin **22**, 4-*O*-(D-sorbitol)vanillin **23a-c**, 4-*O*-(D-galactopyranosyl)N-vanillyl-nonanamide **25a,b**, 4-*O*-( $\beta$ -D-mannopyranosyl)N-vanillyl-nonanamide **26**, 4-*O*-(D-ribofuranosyl)N-vanillyl-nonanamide **27a,b**, 4-*O*-( $\alpha$ -D-glucopyranosyl-(1'→4)D-glucopyranosyl)N-vanillyl-nona

namide **28a-d**, 4-*O*-( $\beta$ -D-galactopyranosyl-(1'→4) $\beta$ -D-glucopyranosyl)N-vanillyl-nonanamide **29**, 1,7-*O*-(bis- $\beta$ -D-galactopyranosyl)curcumin **31b**, 1,7-*O*-(bis- $\beta$ -D-mannopyranosyl)curcumin **32b**, 1,7-*O*-(bis- $\beta$ -D-galactopyranosyl-(1'→4) $\alpha$ -D-glucopyranosyl)curcumin **33a,b**, DL-dopa-D-galactoside **35a-e**, DL-3-hydroxy-4-*O*-( $\beta$ -D-mannopyranosyl)phenylalanine **36**, DL-3-hydroxy-4-*O*-( $\beta$ -D-galactopyranosyl-(1'→4) $\beta$ -D-glucopyranosyl)phenylalanine **37**, DL-3-hydroxy-4-*O*-(6-D-sorbitol)phenylalanine **38**, DL-dopa-D-mannitol **39a,b**, dopamine-D-galactoside **41a-d**, dopamine-D-mannoside **42a-c**, 5-*O*-( $\alpha$ -D-galactopyranosyl)riboflavin **47a**, 5-*O*-( $\beta$ -D-galactopyranosyl)riboflavin **47b**, 5-*O*-( $\alpha$ -D-mannopyranosyl)riboflavin **48a**, 5-*O*-( $\beta$ -D-mannopyranosyl)riboflavin **48b**, 5-*O*-( $\alpha$ -D-ribofuranosyl)riboflavin **49a**, 5-*O*-( $\beta$ -D-ribofuranosyl)riboflavin **49b**, 5-*O*-( $\alpha$ -D-glucopyranosyl-(1'→4) $\alpha$ -D-glucopyranosyl)riboflavin **50a**, 5-*O*-( $\alpha$ -D-glucopyranosyl-(1'→4)6-D-glucopyranosyl)riboflavin **50b**, 5-*O*-( $\alpha$ -D-glucopyranosyl-(1'→4)6'-D-glucopyranosyl)riboflavin **50c**, 5-*O*-(1-D-fructofuranosyl-(2→1') $\alpha$ -D-glucopyranosyl)riboflavin **51**, 5-*O*-( $\beta$ -D-galactopyranosyl-(1'→4) $\beta$ -D-glucopyranosyl)riboflavin **52**, 6-*O*-( $\alpha$ -D-galactopyranosyl) $\alpha$ -tocopherol **55a**, 6-*O*-( $\beta$ -D-galactopyranosyl) $\alpha$ -tocopherol **55b**, 6-*O*-( $\alpha$ -D-mannopyranosyl) $\alpha$ -tocopherol **56a** and 6-*O*-( $\beta$ -D-mannopyranosyl) $\alpha$ -tocopherol **56b**.

15. Response surface methodological study was employed for the optimization of 4-*O*-( $\alpha$ -D-glucopyranosyl-(1'→4) $\beta$ -D-glucopyranosyl)vanillin synthesis using amyloglucosidase and  $\beta$ -glucosidase. A Central Composite Rotatable Design (CCRD) involving vanillin, enzyme and buffer concentration, pH and incubation period as variables at five levels were employed to get optimized conditions for

- both the enzyme catalysed reactions. Predictive equations were developed to predict the maltosylation yields.
16. Kinetic studies of glucosylation between vanillin **1** and D-glucose **6** catalyzed by amyloglucosidase showed that the kinetics followed Ping-Pong Bi-Bi mechanism with competitive substrate inhibition by vanillin at higher concentrations leading to dead end amyloglucosidase-vanillin inhibitor complex formation. The values of four important kinetic parameters values evaluated through computer simulation are:  $k_{cat} = 35.0 \pm 3.2 \cdot 10^{-5}$  M/h.mg,  $K_i = 10.5 \pm 1.1$  mM,  $K_{m \text{ D-glucose}} = 60.0 \pm 6.2$  mM,  $K_{m \text{ vanillin}} = 50.0 \pm 4.8$  mM.
17. Totally 39 glycosides were tested for antioxidant activity by DPPH free radical scavenging method. Antioxidant activities of phenols were reduced due to glycosylation.  $IC_{50}$  values of the glycosides were in the  $0.5 \pm 0.03$  mM to  $2.66 \pm 0.13$  mM range. Best  $IC_{50}$  values ( $\leq 0.75$  mM) observed are for: 4-*O*-( $\alpha$ -D-glucopyranosyl-(1'→4) $\beta$ -D-glucopyranosyl)N-vanillyl-nonanamide **28d** -  $0.75 \pm 0.04$  mM, 1,7-*O*-(bis-D-mannopyranosyl)curcumin **32a,b** -  $0.75 \pm 0.04$  mM, 6-*O*-(D-galactopyranosyl) $\alpha$ -tocopherol **55a,b** -  $0.72 \pm 0.04$  mM and 6-*O*-(D-mannopyranosyl) $\alpha$ -tocopherol **56a,b** -  $0.5 \pm 0.03$  mM. Free phenols tested for antioxidant activity showed  $IC_{50}$  values ranging from  $0.053 \pm 0.003$  mM to  $1.65 \pm 0.08$  mM. Expectedly free phenols showed better antioxidant activities than the glycosides as the available phenyl groups were reduced due to glycosylation.
18. About 48 glycosides were tested for angiotensin converting enzyme (ACE) inhibition activities. Introduction of the carbohydrate molecules to the phenolic OH did not alter the ACE inhibition activities much. Free phenols/vitamins showed  $IC_{50}$  values ranging from  $0.6 \pm 0.03$  to  $1.93 \pm 0.1$  mM.  $IC_{50}$  values of the glycosides were in the  $0.56 \pm 0.03$  mM to  $3.33 \pm 0.17$  mM range. Best ACE inhibitory

activities for the glycosides (< 0.75 mM) detected were: 4-*O*-( $\beta$ -D-glucopyranosyl)vanillin **17b** -  $0.61 \pm 0.03$  mM, 4-*O*-(D-galactopyranosyl)vanillin **18a,b** -  $0.61 \pm 0.03$  mM, 1,7-*O*-(bis- $\beta$ -D-galactopyranosyl-(1'→4)D-glucopyranosyl)curcumin **33a,b** -  $0.67 \pm 0.03$  mM and DL-3-hydroxy-4-*O*-(6-D-sorbitol)phenylalanine **38** -  $0.56 \pm 0.03$  mM.

Thus the present work has brought out the multifaceted characteristics of amyloglucosidase from *Rhizopus* mold and  $\beta$ -glucosidase (native/immobilized) from sweet almond in the glycosylation of selected phenols and vitamins with structurally diverse carbohydrate molecules employed.

ePrints@CFTRI

*Summary*

In the present work amyloglucosidase from *Rhizopus* mold and  $\beta$ -glucosidase isolated from sweet almond were employed to synthesize few selected phenolic and vitamin glycosides. The phenols employed possess a hydroxyl group at the 4<sup>th</sup> position of phenyl ring along with another hydroxyl or -OCH<sub>3</sub> group at the 3<sup>rd</sup> position besides possessing a -CH=CH-, -CH<sub>2</sub> or -CHO group *para* to the 4<sup>th</sup> -OH like vanillin **1**, N-vanillyl-nonanamide **2**, curcumin **3**, DL-dopa **4** and dopamine **5**. The vitamins employed are riboflavin **43** (vitamin B2), ergocalciferol **44** (vitamin D2) and  $\alpha$ -tocopherol **45** (vitamin E). All these vitamins possess OH groups in their structure in the form of ribitol OH in riboflavin **43**, acyclic OH in ergocalciferol **44** and phenolic OH in  $\alpha$ -tocopherol **45**. The results from these investigations are presented in detail.

Chapter **THREE** describes amyloglucosidase from *Rhizopus* mold and  $\beta$ -glucosidase from sweet almond (native/immobilized) catalysed syntheses of selected phenolic glycosides of vanillin **1**, N-vanillyl-nonanamide **2**, curcumin **3**, DL-dopa **4** and dopamine **5** with D-glucose **6**, D-galactose **7**, D-mannose **8**, D-fructose **9**, D-arabinose **10**, D-ribose **11**, maltose **12**, sucrose **13**, lactose **14**, D-sorbitol **15** and D-mannitol **16** by reflux method in di-isopropyl ether solvent at 68 °C. Reaction parameters were optimized for the synthesis of respective glucosides. Conversion yields were in the range 10% to 65%. Solubility in water of 4-*O*-(D-glucopyranosyl)vanillin, 4-*O*-(D-glucopyranosyl)N-vanillyl-nonanamide and 1,7-*O*-(bis- $\beta$ -D-glucopyranosyl)curcumin were found to be 35.2 g/L, 7.7 g/L and 14 g/L respectively.

Under the optimized conditions determined, glycosides of vanillin **1**, N-vanillyl-nonanamide **2**, curcumin **3**, DL-dopa **4** and dopamine **5** were synthesized with various carbohydrates molecules. Product glycosides were isolated through column chromatography and characterized by measuring melting point and optical rotation besides subjecting them to a detailed spectroscopic investigation by UV, IR, Mass and

2D HSQCT NMR. Phenols underwent glycosylation mostly and in few cases arylation also with conversion yields were in the range 6% to 65%. About 61 individual glycosides were synthesized enzymatically using both the glucosidases, of which 45 are being reported for the first time. Two-Dimensional NMR studies confirmed the linking between phenolic OH of aglycon and C1 and/or C1-*O*-/C6-*O*- position of the carbohydrate molecules. Amyloglucosidase from *Rhizopus* mold and  $\beta$ -glucosidase from sweet almond, catalysed synthesis of 4-*O*-( $\alpha$ -D-glucopyranosyl-(1'→4)D-glucopyranosyl) vanillin was optimized using response surface methodology.

$\beta$ -Glucosidase exclusively yielded  $\beta$ -glycosides and in very few cases C6-*O*-arylated products. However, amyloglucosidase on the other hand showed both C1 $\alpha$  and C1 $\beta$ -glycosylated and/or C1-*O*-/C6-*O*-arylated products. In most cases C1 glycosylated products were detected. Only few carbohydrate molecules showed C1-*O*-/C6-*O*-arylation. D-Sorbitol **15** and D-mannitol **16** gave aryated products by reacting only to the primary OH groups. No reaction occurred at the secondary hydroxyl groups of the carbohydrate molecules. Also, only mono glycosylated or mono aryated products were detected. No carbohydrate molecule gave bis products. Both amyloglucosidase and  $\beta$ -glucosidase did not catalyze the reaction with D-fructose **9** and D-arabinose **10**. Among the phenols employed only curcumin **3** showed bis glycosylated products. Phenolic OH at the 4<sup>th</sup> position readily reacted with the carbohydrate molecules employed and wherever possible DL-dopa **4** and dopamine **5** underwent reaction at the 3<sup>rd</sup> phenolic OH also. Thus water insoluble N-vanillyl-nonanamide **2**, curcumin **3** and less water soluble vanillin **1** were converted to more water soluble glycosides.

Chapter **FOUR** describes amyloglucosidase and  $\beta$ -glucosidase catalysed syntheses of glycosides of riboflavin **43** (vitamin B2), ergocalciferol **44** (vitamin D2) and  $\alpha$ -tocopherol **45** (vitamin E). Since ergocalciferol **44** and  $\alpha$ -tocopherol **45** are light and

air sensitive, the reaction was carried out in an amber coloured 150 mL round bottomed flask under nitrogen atmosphere. Work-up and isolation of the compound was also carried out in dark. Reaction parameters were optimized for the syntheses of glucosides of riboflavin **43**, ergocalciferol **44** and  $\alpha$ -tocopherol **45**. Conversion yields were in the range 23% to 42%. Water solubility of 5-*O*-(D-glucopyranosyl)riboflavin, 20-*O*-(D-glucopyranosyl)ergocalciferol and 6-*O*-( $\beta$ -D-glucopyranosyl) $\alpha$ -tocopherol were determined to be 8.2 g/L, 6.4 g/L and 25.9 g/L respectively.

Under the optimized conditions, glycosides of riboflavin **43**, ergocalciferol **44** and  $\alpha$ -tocopherol **45** with various carbohydrates like D-glucose **6**, D-galactose **7**, D-mannose **8**, D-ribose **11**, maltose **12**, sucrose **13** and lactose **14** were synthesised. Vitamins underwent glycosylation/arylation with the conversion yields in the range 5% to 40%. Out of 21 individual glycosides prepared, 15 glycosides are reported for the first time. Here also the glycosides were isolated by column chromatography and characterized by measuring melting point and optical rotation and by recording UV, IR, Mass and 2D HSQCT spectra. Two-Dimensional NMR studies confirmed the linking between primary/acyclic/phenolic OH of the aglycon and the C1 and/or C1-*O*-/C6-*O*-position of the carbohydrate molecules.

$\beta$ -Glucosidase exclusively yielded  $\beta$ -glycosides only and no C6-*O*-arylated products were detected. However, amyloglucosidase on the other hand showed both C1 $\alpha$  and C1 $\beta$ -glycosylated and/or C1-*O*-/C6-*O*-arylated products. Here also, no reaction occurred at the secondary hydroxyl groups of the carbohydrate molecules and only mono glycosylated or mono arylated products were detected. Both amyloglucosidase and  $\beta$ -glucosidase did not catalyze the reaction with D-fructose **9**, D-arabinose **10**, D-Sorbitol **15** and D-mannitol **16**. Among the vitamins employed ergocalciferol **44** showed glycosylation/arylation only with D-glucose **6**. Thus the water insoluble ergocalciferol **44**



and  $\alpha$ -tocopherol **45** and less water soluble riboflavin **43** were converted to more water soluble glycosides thereby improving their potential bioavailability and pharmacological properties.

Chapter **FIVE** describes kinetic study of the glucosylation reaction between vanillin **1** and D-glucose **6** catalyzed by amyloglucosidase from *Rhizopus* mold leading to the synthesis of 4-*O*-(D-glucopyranosyl)vanillin **17a-c** in detail. Graphical double reciprocal plots showed that kinetics of the amyloglucosidase catalyzed reaction followed Ping-Pong Bi-Bi mechanism where competitive substrate inhibition by vanillin **1** led to dead-end amyloglucosidase-vanillin complexes at higher concentrations of vanillin **1**. An attempt to obtain best fit of this kinetic model through computer simulation yielded in good approximation, the values of four important kinetic parameters:  $k_{\text{cat}} = 35.0 \pm 3.2 \cdot 10^{-5} \text{ M/h.mg}$ ,  $K_i = 10.5 \pm 1.1 \text{ mM}$ ,  $K_{\text{m D-glucose}} = 60.0 \pm 6.2 \text{ mM}$ ,  $K_{\text{m vanillin}} = 50.0 \pm 4.8 \text{ mM}$ .

Chapter **SIX** describes evaluation of antioxidant and angiotensin converting enzyme inhibition activity of phenolic and vitamin glycosides. About 39 enzymatically prepared phenolic and vitamin glycosides were subjected to antioxidant activities and 48 glycosides were tested for angiotensin converting enzyme (ACE) inhibition activity. Introduction of a carbohydrate molecule to the phenolic OH decreased the antioxidant activity. Comparable ACE inhibition values only were observed between free phenol/vitamin and the respective glycosides. Among the glycosides tested, phenolic glycosides showed better antioxidant and ACE activities than the vitamin glycosides. Thus the present investigation has brought out clearly the glycosylation potentialities of amyloglucosidase from *Rhizopus* mold and  $\beta$ -glucosidase from sweet almond in the reaction between selected phenols/vitamins with structurally diverse carbohydrate molecules employed.

ePrints@CFTRI

## ***References***

- Abraham, T.E., Joseph, J.R., Bindu, L.B.V., Jayakumar, K.K., 2004. Cross linked enzyme crystals of glucoamylase as a potent catalyst for biotransformations. **Carbohydr. Res.** 339, 1099-1104.
- Adachi, S., Kobayashi, T., 2005. Synthesis of esters by immobilized lipase catalyzed condensation reaction of sugar and fatty acids in water-miscible organic solvent. **J. Biosci. Bioengg.** 99, 87-94.
- Aga, H., Yoneyama, M., Sakai, S., Yamamoto, I., 1991. Synthesis of 2-O- $\alpha$ -D-glucopyranosyl L-ascorbic acid by cyclomaltodextrin glucotransferase from *Bacillus stearothermophilus*. **Agric. Biol. Chem.** 55, 1751-1756.
- Aguilar, C.F., Sanderson, I., Moracci, M., Ciaramella, M., Nucci, R., Rossi, M., Pearl, L.H., 1997. Crystal structure of  $\beta$ -glucosidase from hyperthermophilic archeon *Sulfolobus sulfataricus*: Resilience as a key factor in thermostability. **J. Mol. Biol.** 271, 789-802.
- Akita, H., Kurashima, K., Nakamura, J., Kato, K., 1999. Chemoenzymatic synthesis of naturally occurring  $\beta$ -glucosidase. **Tetrahedron Assym.** 10, 2429-2439.
- Aleshin, A.E., Golubev, A., Firsov, L.M., Honzatko, R.B., 1992. Crystal structure of glucoamylase from *Aspergillus awamori* var X100 to 2.2-Å resolution. **J. Biol. Chem.** 267, 19291-19298.
- Aleshin, A.E., Firsov, L.M., Honzatko, R.B., 1994. Refined structure for the complex of acarbose with glucoamylases from *Aspergillus awamori* var. X100 to 2.4 Å resolution. **J. Biol. Chem.** 269, 15631-15639.
- Ali, S., Hossain, Z., 1991. Characteristics of glucoamylase from *Aspergillus terreus*. **J. Appl. Bacteriol.** 71, 144 -146.
- Allen, M.J., Fang, T.Y., Li, Y., Liu, H.L., Chen, H.M., Coutinho, P., Honzatko, R., Ford C., 2003. Engineering *Aspergillus awamori* glucoamylase variants for improved thermostability, reduced isomaltase formation and increased pH optimum. **US 6537792 B1** (CA 138:250712).
- Allison, D.D., Grande-Allen, K.J., 2006. Hyaluronan: A powerful tissue engineering tool. **Tissue Engg.** 12, 2131-2140.
- Almeida, J.C.B., Gomes, E., Franco, C.L., Silva, R.D., 2007. Thermostable saccharifying and dextransucrosylating amylases from a newly isolated *Bacillus* sp. 13.22. **J. Biotechnol.** 131(2), S 228.
- Ambati, P., Ayyanna, C., 2001. Optimization of medium constituents and fermentation conditions for citric acid production from palmyra jaggery using response surface method, **World J. Microbiol. Biotechnol.** 17, 331-335.
- Andersson, M., Adlercreutz, P., 2001. A kinetic study of almond- $\beta$ -glucosidase catalyzed synthesis of hexyl-glycosides in low aqueous media. Influence of glycosyl donor and water activity. **J. Mol. Catal. B: Enzym.** 14, 69-76.
- Andrews, R.S., Pridham, J.B., 1965. Structure of dopa glucoside from *Vicia faba*. **Nature.** 205, 1213-1214.
- Angerlacenci, M., 2007. Dopamine dysregulation of movement control in L-dopa induced dyskinesia. **Trends Neurosci.** 30(5), 236-243.

- Antonini, E., Carrea, G., Cremonesi, P., 1981. Enzyme catalyzed reactions in water-organic solvent two phase systems. **Enzyme Microb. Technol.** 3, 291-296.
- Arrigo, P.D., Fasoli, E., Fantoni, G.P., Rossi, C., Saraceno, C., Tessaro, D., Servi, S., 2007. A practical selective synthesis of mixed short/long chains glycerophosphocholines. **Chem. Phy. Lipids.** 147(2), 113-118.
- Ashikari, T., Nakamura, N., Tanaka, Y., Kiuchi, N., Shibano, Y., Tanaka, T., Amachi, T. and Yoshizumi, H., 1986. *Rhizopus* raw-starch-degrading glucoamylase: Its cloning and expression in yeast, **Agric. Biol. Chem.** 50, 957-964.
- Audus, K.L., Chikhale, P.J., Miller, W.D., Thompson, S.E., Borchardt, R.T., 1992. Brain uptake of drugs: The influence of chemicals and biological factors. **Adv. Drug Res.** 23, 1-64.
- Auge, C., Fernandez, R.F., Gautheron, C.M., 1990. The use of immobilized glycosyltransferases in the synthesis of sialyl oligosaccharides. **Carbohydr. Res.** 200, 257-268.
- Azuma, K., Nakayama, M., Koshioka, M., Ippoushi, K., Yamaguchi, Y., Kohata, K., Yamauchi, Y., Ito, H., Higashio, H.J., 1999. Phenolic antioxidants from the leaves of *Corchorus olitorius* L. **Agric. Food Chem.** 47, 3963-3966.
- Bacher, A., Eberhardt, S., Fischer, M., Kis, K., Richter, G., 2000. Biosynthesis of vitamin B<sub>2</sub> (riboflavin). **Annu. Rev. Nutr.** 20, 153-167.
- Badman, G.T., Green, D.V.S., Voyle, M.J., 1990. A novel synthesis of  $\beta$ -phenylglucuronides using the Mitsunobu reaction: An application of phenolic chromium tricarbonyl complexes. **Organomet. Chem.** 388, 117-121.
- Bahar, T., Celebi, S.S., 1998. Characterization of glucoamylase immobilized on magnetic poly (styrene) particles. **Enzyme Microb. Technol.** 23, 301-304.
- Balzar, D., 1991. Alkylglucosides, their physico-chemical properties and their uses. **Tenside Surf. Det.** 28, 419-427.
- Bandaru, V.V.R., Somalanka, S.R., Mendu, D.R., Madicherla, N.R., Chityala, A., 2006. Optimization of fermentation conditions for the production of ethanol from sago starch by co-immobilized amyloglucosidase and cells of *Zymomonas mobilis* using response surface methodology. **Enzyme Microb. Technol.** 38, 209-214.
- Bai, Y.X., Li, Y.F., Wang, M.T., 2006. Study on synthesis of a hydrophilic bead carrier containing epoxy groups and its properties for glucoamylase immobilization. **Enzyme Microb. Technol.** 39, 540-547.
- Barolini, M., Cavrini, V., Andrisano, V., 2004. Monolithic micro-immobilized enzyme reactor with human recombinant acetylcholinesterase for on line inhibition studies. **J. Chromatogr.** 1031, 27-34.
- Basso, A., Ducret, A., Gardossi, L., Lortie, R., 2002. Synthesis of octyl glucopyranoside by almond  $\beta$ -glucosidase adsorbed onto Celite R-640. **Tetrahedron Lett.** 43, 2005-2008.
- Bates, C., 1993. Riboflavin. **Int. J. Vitam. Nutr. Res.** 63, 274-277.
- Beckman, E.J., 2003. Green chemical processing using CO<sub>2</sub>. **Ind. Engg. Chem. Res.** 42, 1598-1602.

- Bender, H., 1981. A bacterial glucoamylase degrading cyclodextrins. **Eur. J. Biochem.** 115, 287-291.
- Berfoldo, C., Anthranikian, G., 2001. Amylolytic enzymes from hyperthermophiles. **Methods Enzymol.** 330, 269-289.
- Bestoldo, C., Duffner, F., Jorgensen, P.L., Antranikian, G., 1999. Pullulanase type I from *Fervidobacterium pennavorans* ven 5: Cloning, sequencing and expression of the gene and biochemical characterization of the recombinant enzyme. **Appl. Environ. Microbiol.** 65, 2084-2091.
- Bhabadeh, C., Somnath, M., Dehdas, B., De Amit, K., 1996. Capsaicin a unique antioxidant, antifungal, antiinflammatory analgesic compound with antifungal activity against dermatophytes. **Med. Sci. Res.** 24, 669-670.
- Bhatia, Y., Mishra, S., Bisaria, V.S., 2002. Microbial  $\beta$ -glucosidase: Cloning, properties, applications. **Crit. Rev. Biotechnol.** 22, 375-407.
- Bhatti, H.N., Rashid, M.H., Asghal, M., Nawaz, R., Khalid, A.M., Perveen, R., 2007a. Chemical modification results in hyper activation and thermo stabilization of *Fusarium solani* glucoamylase. **Can. J. Microbiol.** 53, 177-185.
- Bhatti, H.N., Rashid, M.H., Nawaz, R., Khalid, A.M., Asgher, M., Jabbar, M., 2007b. Effect of aniline coupling on kinetic and thermodynamic properties of *Fusarium solani* glucoamylase. **Appl. Microbiol. Biotechnol.** 73, 1290-1298.
- Biely, P., 2003. Xylanolytic enzymes. In: **Handbook of Food Enzymology**, Whitaker, P.R., Voragen, A.J.J., Wong, D.W.S. (Eds), Marcel Dekker, New York, 879-915.
- Bonina, F., Puglia, C., Rimoli, M.G., Melisi, D., Boatto, G., Nieddu, M., Calignano, A., La Rana, G., De Caprariis, P., 2003. Glycosyl derivatives of dopamine and L-dopa as anti-Parkinson prodrugs: Synthesis, pharmacological activity and *in vitro* stability studies. **J. Drug Target.** 11(1), 25-36.
- Book, K., Pedersen, C., 1983. Carbon 13 NMR spectroscopy of monosaccharides. In: **Adv. Carbohydr. Chem. Biochem.** Stuart-Tipson, R., Horton, D., (Eds), 41, 27-66.
- Book, K., Pedersen, C., Pedersen, H., 1983. Carbon 13 NMR data for oligosaccharides. In: **Adv. Carbohydr. Chem. Biochem.** Stuart-Tipson, R., Horton, D., (Eds), 42, 27-66.
- Brandle, J.E., Telmer, P.G., 2007. Steviol glycoside biosynthesis. **Phytochemistry.** 68, 1855-1863.
- Braun, H., Cogoli, A., Semenza, G., 1977. Carboxyl groups at the two active centers of sucrose-isomaltase from rabbit small intestine **Eur. J. Biochem.** 73, 437-442.
- Bravman, T., Zolotnitsky, G., Shulami, S., Belakhov, V., Solomon, D., Baasov, T., Shoham, G., Shoham, Y., 2001. Stereo chemistry of family 52 glycosyl hydrolases, a  $\beta$ -xylosidase from *Bacillus stearothermophilus* T-6 is a retaining enzyme. **FEBS Lett.** 495, 39-43.
- Bridiau, N., Taboubi, S., Marzouki, N., Legoy, M., Maugard, T., 2006.  $\beta$ -Galactosidase catalysed selective galactosylation of aromatic compounds. **Biotechnol Prog.** 22 (1), 326-330.

- Bringmann, G., Ochse, M., Wolf, K., Kraus, J., Peters, K., Peters, E.M., Herderich, Assi, L.A., Tayman, F.S.K., 1999. 4-Oxonicotinamide-1-(1'- $\beta$ -D-ribofuranoside) from *Rohmannia Longiflora* salisb (Rubiaceae). **Phytochemistry**. 51, 271-276.
- Brink, L.E.S., Tramper, J., 1985. Optimization of organic solvent in multiple biocatalysis. **Biotechnol. Bioengg.** 27, 1259-1269.
- Brown, J.R., Guther, M.L.S., Field, R.A., Ferguson, M.A.J., 1997. Hydrophobic mannosides act as acceptors for trypanosome  $\alpha$ -mannosyltransferases. **Glycobiology** 7, 549-558.
- Bryjak, J., Anilyte, J., Liesiene, J., 2007. Evaluation of mantailored cellulose-based carriers in glucoamylase immobilization. **Carbohydr. Res.** 342, 1105-1109.
- Burri, J., Graf, M., Lambelet, P., Loliger, J., 1989. Vanillin: More than a flavoring agent - A potential antioxidant. **J. Sci. Food Agric.** 48, 49-56.
- Burton, G.W., Joyce, A., Ingold, K.U., 1983. Is vitamin E the only lipid soluble, chain-breaking antioxidant in human blood plasma and erythrocyte membrane. **Arch. Biochem. Biophys.** 221, 281-290.
- Butler, L.G., 1979. Enzymes in non-aqueous solvents. **Enzyme Microb. Technol.** 1, 253-259.
- Cai, H-C., Fang, Y., Xia, Y-M., Cai, K., 2003. New catalytic technique: Microwave irradiation-enzyme coupling catalysis. **Youji Huaxue.** 23, 298-304 (Chinese).
- Camacho, P.B., Robles, M.A., Camacho, R.F., Gonzalez, M.P., Molina, G.E., 2003. Modeling the effect of free water on enzyme activity in immobilized lipase-catalyzed reactions in organic solvents. **Enzyme Microb. Technol.** 33, 845-853.
- Candussio, A., Schmid, G., Bock, A., 1990. Biochemical and genetic analysis of a maltopentaose-producing amylase from an alkaliphilic gram-positive bacterium. **Eur. J. Biochem.** 191, 177-185.
- Cantarella, M., Cantarella, L., Alfani, F., 1991. Hydrolytic reaction in two phase: Effect of water-immiscible organic solvents on stability on acid phosphatase,  $\beta$ -glucosidase and  $\beta$ -fructofuranosidase. **Enzyme Microb. Technol.** 13, 547-553.
- Cao, L., van Rantwijk, F., Sheldon, R.A., 2000. Cross-linked enzyme aggregates: A simple and effective method for the immobilization of penicillin acylase. **Org. Lett.** 2, 1361-1364.
- Carra, J.H., Privalov, P.L., 1996. Thermodynamics of denaturation of *Staphylococcal nuclease* mutants: An intermediate state in protein folding. **FASEB J.** 10, 67-74.
- Castillo, B., Pacheco, Y., Al.Azzam, A., Griebenow, K., Devi, M., Ferrer, A., Barletta, G., 2005. On the activity loss of hydrolases in organic solvents I. Rapid loss of activity of a variety of enzymes and formulations in a range of organic solvents. **J. Mol. Catal. B: Enzym.** 35, 147-153.
- Cereia, M., Guimarães, L., H.S., Peixoto-Nogueira, S.C., Jorge, J.A., Terenzi, H.F., Greene, L.J., Polizeli, T.M., 2006. Glucoamylase isoform (GAII) purified from a thermophilic fungus *Scytalidium thermophilum* 15.8 with biotechnological potential. **African J. Biotechnol.** 5(12), 1239-1245.
- Chaga, G., Porath, J., Illeni, T., 1993. Isolation and purification of amyloglucosidase from *Halobacterium sodomense*. **Biomed. Chromatogr.** 7, 256-261.

- Chahid, Z., Montet, D., Pina, M., Bonnot, F., Graille, J., 1994. Biocatalyzed octylglycoside synthesis from a disaccharide. **Biotechnology Lett.** 16, 795-800.
- Chahid, Z., Montet, D., Pina, M., Graille, J., 1992. Effect of water activity on enzymic synthesis of alkyl glycosides. **Biotechnology Lett.** 14, 281-284.
- Chang, M.Y., Juang, R.S., 2007. Use of chitosan clay composite as immobilization support for improved activity and stability of  $\beta$ -glucosidase. **Biochem. Engg. J.** 35, 93-98.
- Chang, M-Y., Juang, R-S., 2005. Activities, stabilities and reaction kinetics of three free and chitosan-clay composite immobilized enzymes. **Enzyme Microb. Technol.** 36, 75-82.
- Chen, C.W., Ou-Yang, C-C., Yeh, C-W., 2003. Synthesis of galactooligosaccharides and transgalactosylation modeling in reverse micelles. **Enzyme Microb. Technol.** 33, 497-507.
- Chen, H.C., Chang, C.C., Chen, C.X., 1997. Optimization of arachidonic acid production by *Mortierella alpina* Wuji-H4 isolate. **J. Am. Oil Chem. Soc.** 74, 569-578.
- Chen, I.J., Yang, J.M., Yeh, J.L., Wu, B.N., Lo, Y.C., Chen, S.J., 1992. Hypotensive and antinociceptive effects of ether linked and relatively non pungent analogs of N-nonanoyl-vanillylamide. **Eur. J. Med. Chem.** 27, 187-192.
- Chen, S-X., Wei, D-Z., Hu, Z-H., 2001. Synthesis of galacto-oligosaccharides in AOT/isooctane reverse micelles by  $\beta$ -galactosidase. **J. Mol. Catal. B: Enzym.** 16, 109-114.
- Chen, T.C., Holick, M.F., Lokeshwar, B.L., Burnstein, K.L., Schwartz, G.G, 2003. Evaluation of vitamin D analogs as therapeutic agents for prostate cancer. **Recent Results Cancer Res.** 164, 273-288.
- Chi, Z.M., Liu, J., Zhang, W., 2001. Trehalose accumulation from starch by *Saccharomycopsis fibuligera* sud. **Enzyme Microb. Technol.** 28, 240-245.
- Chiba, S., 1997. Molecular mechanism in  $\alpha$ -glucosidase and glucoamylase. **Biosci. Biotech. Biochem.** 61, 1233-1239.
- Chojceki, A., Blaschek, H.P., 1986. Effect of carbohydrate source on alpha-amylase and glucoamylase formation by *Clostridium acetobutylicum* SA-1. **Ind. Microbiol.** 1, 63-67.
- Chong-Qian, L., Bo-Gang, L., Hua-Yi, Q., Qi-Lin, L., Feng-Peng, W., Guo-Lin, Z., 2004. Three cyclooctapeptides and one glycoside from *Microtoena prainiana* J. **Nat. Prod.** 67, 978-982.
- Chu, Y.H., Chang, C.L., Hsu, H.F., 2000. Flavonoid content of several vegetables and their antioxidant activity. **J. Sci. Food Agric.** 80, 561-566.
- Clarks, A, J., Svensson, B., 1984. Identification of an essential tryptophanyl residue in the primary structure of glucoamylase G2 from *Aspergillus niger*. **Carlsberg. Res. Commun.** 49, 559-566.
- Collins, C.M., Murray, P.G., Denman, S., Morrissey, J.P., Byrnes, L., Teeri, T.T., Tuohy, M.G., 2007. Molecular cloning and expression analysis of two distinct  $\beta$ -glucosidase genes *bg1* and *aven1* with different biological roles from the



- thermophilic, saprophytic fungus *Talaromyces emersonii*. **Micol. Res.** 111(7), 840-849.
- Colowick, S.P., Kaplan, N.O., 1976. Immobilized enzymes. **Methods Enzymol.** Mosbach, K. (Ed.), 44, 101.
- Coulon, D., Ismail, A., Girardin, M., Rovel, B., Ghoul, M., 1996. Effect of different biochemical parameters on the enzymatic synthesis of fructose oleate. **J. Biotechnol.** 51, 115-121.
- Coutinho, P.M., Henrissat, B., 1999. Carbohydrate active enzymes server at <http://afmb.cnrs-mrs.fr/CAZY>.
- Coutinho, P.M., Reilly, P.J., 1997. Glucoamylase structural, functional and evolutionary relationships. **Protein.** 29, 334-347.
- Crout, D.H.G., Vic, G., 1998. Glycosidases and glycosyl transferases in glycoside and oligosaccharides synthesis. **Biocatal. Biotransform.** 2, 98-111.
- Cruz-Guerrero, A.E., Ruiz, L.G., Gonzalez, G.V., Barzana, E., Garibay, M.G., 2006. Influence of water activity in the synthesis of galactooligosaccharides produced by a hyperthermophilic  $\beta$ -glycosidase in an organic medium. **Biotechnol. Bioeng.** 93, 1123-1129.
- Cushman, D.W., Cheung, H.S., 1971. Spectrophotometric assay and properties of the Angiotensin-Converting Enzyme of rabbit lung. **Chem. Pharmacol.** 20, 1637-1638.
- Czjzek, M., Cicek, M., Zamboni, V., Bevan, D.R., Henrissat, B., Esen, A., 2000. The mechanism of substrate (aglicone) specificity in  $\beta$ -glucosidase –DIMBOA, –DIMBOA Glc and –dhurrin complexes. **Proc. Natl. Acad. Sci. USA**, 97, 13555-13560.
- Czjzek, M., Cicek, M., Zamboni, V., Burmeister, W.P., Beven, R.B., Henrissat, B., Esen, A., 2001. Crystal structure of a monocotyledon (maize ZmGlu1)  $\beta$ -glucosidase and a model of its complex with p-nitrophenyl  $\beta$ -D-thioglycoside. **Biochem. J.** 354, 37-46.
- Dae-Gill, K., Yong-Sup, L., Hyoung-Ja, K., Yun-Mi, L., Ho-Sub, L., 2003. Angiotensin converting enzyme inhibitory phenylpropanoid glycosides from *Clerodendron trichotomum*. **J. Ethanopharmacol.** 89, 151-154.
- Dai, F., Miao, Q., Zhou, B., Yang, L., Liu, Z.L., 2006. Protective effects of flavanols and their glycosides against free radical induced oxidative hemolysis of red blood cells. **Life Sci.** 78, 2488-2493.
- Dale, M., Kopfler, W.P., Chair, I., Byers, L.D., 1986.  $\beta$ -Glucosidase: Substrate, solvent and viscosity variation as probes of the rate-limiting steps. **Biochemistry.** 25, 2522-2529
- Dalpiazz, A., Filosa, R., de Caprariis, P., Conte, G., Bortolotti, F., Biondi, C., Scatturin, A., Prasad, P.D., Pavanc, B., 2007. Molecular mechanism involved in the transport of a prodrug dopamine glycosyl conjugate. **Int. J. Pharm.** 336, 133-139.
- Daubmann, T., Hennemann, H.G., Rosen, T.C., 2006. Enzymatische technologien zur synthese chiraler alcohol-derivate. **Chem. Ing. Tech.** 78, 249-255.



- David, H.G., Gabin, V., 1998. Glycosidases and glycosyl transferases in glycoside and oligosaccharide synthesis. **Curr. Opinion Chem. Biol.** 2, 98-111.
- Davis, B.G., Boyer, V., 2001. Biocatalysis and enzymes in organic synthesis. **Nat. Prod. Rep.** 18, 618-640.
- De Lima, D.P., 1999. Synthesis of angiotensin converting enzyme (ACE) inhibitors: An important class of anti-hypertensive drugs. **Quim. Nova.** 22, 375-381.
- De Oliveira, R.N., De Freitas, F.J.R., Srivastava, R.M., 2002. Microwave-induced synthesis of 2,3-unsaturated O-glycosides under solvent-free conditions. **Tetrahedron Lett.** 43, 2141-2143.
- De-Lima, D.P., 1999. Synthesis of Angiotensin-Converting Enzyme (ACE) inhibitors: An important class of antihypertensive drugs. **Quim Nova.** 22, 375-381.
- Deloffre, L., Sautiere, P.E., Huybrechts, R., Hens, K., Vieau, D., Salzet, M., 2004. Angiotensin-converting enzyme inhibition studies by natural leech inhibitors by capillary electrophoresis and competition assay. **Eur. J. Biochem.** 271, 2101-2106.
- DeSantis, G., Davis, B.G., 2006. The expanding roles of biocatalysis and biotransformations. **Curr. Opinion Chem. Biol.** 10, 139-140.
- DeSimone, J., 2002. Practical approaches to green solvents. **Science.** 297, 799-803.
- Dickerson, T.J., Yamamoto, N., Janda Kim, D., 2004. Antibody-catalysed oxidative degradation of nicotin using riboflavin. **Bio. Org. Med. Chem.** 12, 4981-4987.
- Dijkstra, Z.J., Doornbos, A.R., Weyten, H., Ernsting, J.M., Elsevier, C.J., Keurentjes, J.T.F., 2007. Formation of carbamic acid in organic solvents and in supercritical carbon dioxide. **J. Supercrit. Fluids.** 41(1), 109-114.
- Ding, S., Ge, W., Buswell, J.A., 2007. Molecular cloning and transcriptional expression analysis of an intracellular  $\beta$ -glucosidase, a family 3-glycosyl hydrolase from the edible straw mushroom, *Volvariella volvacea*. **FEMS Microbiol. Lett.** 267, 221-229.
- Donho, M., Kimura, T., Hara, H., 1996. Methods of producing geranyl  $\beta$ -D-galactopyranoside as flavoring material by enzymatic galactosylation of citronellol. **Jpn. Kokai Tokkyo Koho JP 8188589-8188591** (CA 125:222344).
- Dordick, J.S., 1989. Enzymatic catalysis in monophasic organic solvents. **Enzyme Microb. Technol.** 11, 194-211.
- Dubey, V.K. Jagannadham, M.B., 2003. Procerain, a stable cysteine protease from the latex of *Calotropis procera*. **Phytochemistry** 62, 1057-1071.
- Ducret, A., Carriere, J.F., Trani, M., Lortie, R., 2002a. Enzymatic synthesis of octyl glucoside catalysed by almond  $\beta$ -glucosidase in organic media. **Can. J. Chem.** 80, 653-656.
- Ducret, A., Troni, M., Larotie, R., 2002b. Screening of various glycosides for the synthesis of octyl glucoside. **Biotechnol. Bioeng.** 77, 752-757.
- Effenberger, F., Syed, J., 1998. Stereoselective synthesis of biologically active tetronic acids. **Tetrahedron.** 9, 817-825.

- Ekino, K., Hayashi, H., Moriyama, M., Matsuda, M., Goto, M., Yoshino, S., Furukawa, K., 2002. Engineering of polyploid *Saccharomyces cerevisiae* for secretion of large amounts of fungal glucoamylase. **Appl. Environ. Microbiol.** 68, 5693-5697.
- Eneyskaya, E.V., Brumer, H., Backinwsky, L.V., Ivanen, D.R., Kulminskaya, A.A., Shabalin, K.A., Neustroev, K.N., 2003. Enzymatic synthesis of  $\beta$ -xylanase, substrate transglycosylation reactions of the  $\beta$ -xylosidase from *Aspergillus* sp. **Carbohydr. Res.** 338, 313-325.
- Eriksson, S., Nylén, U., Rojas, S., Boutonnes, M., 2004. Preparation of catalysis from microemulsions and their applications in heterogeneous catalysis. **Appl. Catal. A: General.** 265, 207-219.
- Ermer, J., Rose, K., Huber, G., Schellenberger, A., 1993. Subsite affinities of *Aspergillus niger* glucoamylase II determined with *p*-nitrophenylmaltooligosaccharides. **Biol. Chem. Hoppe-Seyler.** 374, 123-128.
- Eupergit, C., 2000. A carrier for immobilization of enzymes of industrial potential. **J. Mol. Catal. B: Enzym.** 10, 157-176.
- Eveleigh, D.E., Perlin, A.S., 1969. A proton magnetic resonance study of the anomeric species produced by D-glucosidases. **Carbohydr. Res.** 10, 87-95.
- Faber, K., 2004. Enzymes in organic solvents, **Biotransform. Organic Chem**, 5th ed., Faber, K., (Ed.), Springer, Berlin.
- Fadnavis, N.W., Deshpande, A., 2002. Synthetic applications of enzymes entrapped in reverse micelles and organogels. **Cur. Org. Chem.** 6, 393-410.
- Fagerstrom, R., 1991. Subsite mapping of *Hormoconis resinae* glucoamylase and their inhibition by gluconolactone. **J. Gen. Microbiol.** 137, 1001-1008.
- Faijes, M., Planas, A., 2007. *In vitro* synthesis of artificial polysaccharides by glycosidases and glycosynthases. **Carbohydr. Res.** 342, 1581-1594.
- Faijes, M., Saura-Valls, M., Perez, X., Conti, M., Planas, A., 2006. Acceptor dependent Regioselectivity of glycosynthase reactions by *Streptomyces* E383A  $\beta$ -glucosidase. **Carbohydr. Res.** 341, 2055-2065.
- Feldman, D., Xiao-Yan, Z., Krishnan, A.V., 2000. Vitamin D and prostate cancer. **Endocrinology.** 141, 5-9.
- Fellunga, F., Forzato, C., Ghelfi, F., Nitti, P., Pitacco, G., Pagnoni, E.M., Roncaglia, F., 2007. Atom transfer radical cyclization (ATRC) applied to a chemoenzymatic synthesis of quercus lactone. **Tetrahedron Assym.** 18(4), 527-536.
- Fernandez, C., Nieto, O., Fontenla, J.A., Rivas, E., de Ceballos, M.L., Fernandez-Mayoralas, A., 2003. Synthesis of glycosyl derivatives as dopamine prodrugs: Interaction with glucose carrier GLUT-1. **Org. Biomol. Chem.** 1, 767-771.
- Fernandez, C., Nieto, O., Rivas, E., Montenegro, G., Fontenla, J.A., 2000. Fernandez-Mayoralas A. Synthesis and biological studies of glycosyl dopamine derivatives as potential antiparkinsonian agents. **Carbohydr. Res.** 327, 353-365.
- Fiorentino, A., DellaGreca, M., D'Abrosca, B., Golino, A., Pacifico, S., Izzo, A., Monaco, P., 2006. Unusual sesquiterpene glucosides from *Amaranthus retroflexus*. **Tetrahedron.** 62, 8952-8958.

- Fischer, E., 1894. Einfluss der konfiguration auf die wirkung der enzyme. **Ber. Chem. Ges.** 27, 2985-2993.
- Fitzgerald, D.J., Stratford, M., Gasson, M.J., Narbad, A., 2005. Structure function analysis of the vanillin molecule and its antifungal properties. **J. Agric. Food Chem.** 53, 1769-1775.
- Fitzpatrick, P.A., Steinmetz, A.C.U., Rine, D., Klibanov, A.M., 1993. Enzyme crystal structure in neat organic solvent. **Proc. Natl. Acad. Sci. USA**, 90, 8653-8657.
- Ford, C., 1999. Improving operating performance of glucoamylase by mutagenesis. **Curr. Opinion Biotechnol.** 10, 352-357.
- Fourage, L., Dion, M., Color, B., 2000. Kinetic study of a thermostable  $\beta$ -glucosidase of *thermos thermophilus*. Effects of temperature and glucose on hydrolysis and transglycosylation reactions. **Glycoconjugate J.** 17, 377-383.
- Frandsen, T.P., Dupont, C., Lehmbeck, J., Stoffer, B., Sierks, M.R., Honzatko, R.B., Svensson, B., 1994. Site-directed mutagenesis of the catalytic base Glutamic acid 400 in glucoamylase from *Aspergillus niger* and of Tyrosine 48 and Glutamine 401, both hydrogen bonded to the gamma-carboxylate group of Glutamic acid 400. **Biochemistry.** 33, 13808-13816.
- Fujimoto, H., Isomura, M., Ajisaka, K., 1997. Syntheses of alkyl  $\beta$ -D-mannopyranosides and  $\beta$ -1,4-linked oligosaccharides using  $\beta$ -mannosidase from *Rhizopus niveus*. **Biosci. Biotechnol. Biochem.** 61, 164-165.
- Ganghofner, D., Kellerman, J., Staudenbaver, W.L., Bronnenmier, K., 1998. Purification and properties of an amylopullulanase, a glucoamylase and an alpha-glucosidase in the amyolytic enzyme system of thermo anaerobacterium *Thermosaccharolyticum*. **Biosci. Biotechnol. Biochem.** 62, 302-308.
- Gannett, P.M., Nagel, D.L., Reilly, P.J., Lawson, T., Sharpe, J., Toth, B., 1988. The capsaicinoids: Their separation, synthesis and mutagenicity. **J. Org. Chem.** 53, 1064-1071.
- Gargouri, M., Smaali, I., Maugardb, T., Dominique, L.M., Marzouki, N., 2004. Fungus  $\beta$ -glycosidases: Immobilization and use in alkyl- $\beta$ -glycoside synthesis. **J. Mol. Catal. B: Enzym.** 29, 89-94.
- Gellissen, G., Janowicz, Z.A., Merckelbach, A., Piontek, M., Keup, P., Weydemann, U., Hollenberg, C.P., Srasser, A.W.M., 1991. Heterologus gene expression in *Hansenula polymorpha*: Efficient secretion of glucoamylase. **Biotechnology.** 9, 291-295.
- Gelo-Pujic, M., Guibe-Jampel, E., Loupy, A., Tricone, A., 1997. Enzymic glycosidation in dry media under microwave irradiation. **J. Chem. Soc. Perkin Trans.** 1, 1001-1002.
- Geng, X., Song, L., Pu, X., Tu, P., 2004. Neuroprotective effects of phenylethanoid glycosides from *Cistanches salsa* against 1-Methyl-4-phenyl-1,2,3,6-tetrahydropyridine (MPTP)-induced dopaminergic toxicity in C57 Mice. **Biol. Pharm. Bull.** 27(6), 797-801.
- Geng, X., Tian, X., Tu, P., Pu, X., 2007. Neuroprotective effects of echinacoside in the mouse MPTP model of Parkinson's disease. **Eur. J. Pharmacol.** 564, 66-74.

- Ghosh, A., Chatterjee, B.S., Das, A., 1990. Characterization of glucoamylase from *Aspergillus terreus* 4. **FEMS Microbiol. Lett.** 66, 345-349.
- Gill, R.K., Kaur, J., 2004. A thermostable glucoamylase from a thermophilic *Bacillus* sp. characterization and thermal stability. *J. Industrial Microbiol. Biotechnology.* 31, 540-543.
- Giri, A., Dhingra, V., Giri, C.C., Singh, A., Ward O.P., Narasu. M.L., 2001. Biotransformations using plant cells, organ cultures and enzyme systems: Current trends and future prospects. **Biotechnol. Adv.** 19, 175–199.
- Goldberg, K., Schroer, K., Lutz, S., Liese, A., 2007a. Biocatalytic ketone reduction: A powerful tool for the production chiral alcohols-Part I. Processes with isolated enzymes. **Appl. Microbiol. Biotechnol.** 76(2), 237-248.
- Goldberg, K., Schroer, K., Lutz, S., Liese, A., 2007b. Biocatalytic ketone reduction: A powerful tool for the production chiral alcohols-Part II. Processes with isolated enzymes. **Appl. Microbiol. Biotechnol.** 76(2), 249-255.
- Golik, J., Clardy, J., Dubay, G., Groenewold, G., Kawaguchi, H., Konishi, M., Krishnan, B., Ohkuma, H., Saitoh, K., Doby, T.W., 1987. Esperamicins, a novel class of potent antitumor antibiotics. 3. Structures of esperamicins A1, A2 and A1b. **J. Am. Chem. Soc.** 109, 3461-3464.
- Gomes, D.C.F., Alegrio, L.V., Leon, L.L., de Lima, M.E.F., 2002. Total synthesis and anti-leishmanial activity of some curcumin analogues. **Arzneim-Forsch.** 52, 695-698.
- Gorman, L.A.S., Dordick, J.S., 1992. Organic solvents strip water off enzymes. **Biotechnol. Bioengg.** 39, 392-397.
- Goto, M., Tanigawa, K., Kanlayakrit, W., Hayashida, S., 1994. The molecular mechanism of binding of glucoamylases I from *Aspergillus awamori* var. kawachi to cyclodextrin and raw starch, **Biosci. Biotech. Biochem.** 58, 49-54.
- Gregory, J.F., 1998. Nutritional properties and significance of vitamin glycosides. **Annu. Rev. Nutr.** 18, 277-96.
- Griegenow, K., Klivanov, A.M., 1995. Lyophilization induced reversible changes in the secondary structure of proteins. **Proc. Natl. Acad. Sci. USA,** 92, 10969-10976.
- Guggenheim, M., 1913. Dioxyphenylalanine neue Aminosauereaus *Vicia faba*. **Hoppe-Seylers's Zeitschr Physiol. Chem.** 88, 276-284.
- Guillemette, T., van Peij, N.N.A.E., Goosen, T., Lanthaler, K., Robson, G.D., van den Hondel, A.M.J.J., Stam, H., Arches, D.B., 2007. Genomic analysis of of the secretion stress response in the enzyme-producing cell factory *Aspergillus niger*. **BMC Genomics.** 8, 158-175.
- Gunata, Z., Vallier, M.J., Sapis, J.C., Baumes, R., Bayonove, C., 1994. Enzymic synthesis of monoterpeny  $\beta$ -D-glucosides by various  $\beta$ -glucosidases. **Enzyme Microb. Technol.** 16, 1055-1058.
- Gunawan, E.R., Basri, M., Abdul Rahman, M.B., Salleh, A.B., Abdul Rahman, R.N.Z., 2005. Study on response surface methodology (RSM) of lipase-catalysed synthesis palm-based wax ester. **Enzyme Microb. Technol.** 37, 739-744.

- Gunther, S., Heymann, H., 1998. Di and oligosaccharide substrate specificities and subsite binding energies of pig intestinal glucoamylase-maltase. **Arch. Biochem. Biophys.** 354, 111-116.
- Gupta, R., Gigras, P., Mohapatra, H., Goswami, V.K., Chauhan, B., 2003. Microbial  $\alpha$ -amylases: A biotechnological perspective. **Process Biochem.** 38, 1599-1616.
- Gygax, D., Spies, P., Winkler, T., Pfaar, U., 1991. Enzymatic synthesis of  $\beta$ -D-glucuronides with *in situ* regeneration of uridine 5'-diphosphoglucuronic acid. **Tetrahedron** 47, 5119-5122.
- Haasum, I., Ericksen, S.H., Jensen, B., Olsen, J., 1991. Growth and glucoamylase production by the thermophilic fungus *Thermophilus lanuginose* in a synthetic medium. **Appl. Microbiol. Biotechnol.** 34, 656-660.
- Haines, A.H., 1976. Relative reactivities of hydroxyl groups in carbohydrates. **Adv. Carbohydr. Chem. Biochem.** 33, 11-109.
- Hakulinen, N., Paavilainen, S., Korpela, T., Rouvinen, J., 2000. The crystal structure of  $\beta$ -glucosidase from *Bacillus circulans* sp. alkalophilus: Ability to form long polymeric assemblies. **J. Struct. Biol.** 129, 69-79.
- Hamada, H., Nishida, K., Furuya, T., Ishihara, K., Nakajima, N., 2001. Preparation of a new pepper: Chemoenzymatic synthesis of capsaicin oligosaccharide and 8-nordihydrocapsaicin. **J. Mol. Catal. B: Enzym.** 16, 115-119.
- Hamada, H., Ohiwa, S., Nishida, T., Katssuragi, H., Takeda, T., Hamada, H., Nakajima, N., Ishihara, K., 2003. One step glucosylation of capsaicinoids by cultured cells of *Phytolacca americana*. **Plant Biotechnol.** 20, 253-255.
- Hamada, H., Tomi, R., Asada, Y., Furuya, T., 2002. Phytoremediation of bisphenol A by cultured suspension cells of *Eucalyptus perriniana* regioselective hydroxylation and glycosylation. **Tetrahedron Lett.** 43, 4087-4089.
- Hang, H.T., 1995. Decolourization of anthocyanins by fungal enzymes. **Agric. Food Chem.** 3, 141-146.
- Hansson, T., Adlercreutz, P., 2002. Enzymatic synthesis of hexyl glycosides from lactose at low water activity and high temperature using hyperthermostable  $\beta$ -glucosidase. **Biocatal. Biotransform.** 20, 167-178.
- Hansson, T., Andersson, M., Wehtje, E., Aldercreutz, P., 2001. Influence of water activity on the competition between  $\beta$ -glycosidase catalysed transglycosylation and hydrolysis in aqueous hexanol. **Enzyme Microb. Technol.** 29, 527-534.
- Harris, E.M.S., Aleshin, A.E., Firsov, L.M., Honzatko, R.B., 1993. Refined structure of the complex of 1-deoxynojirimycin with glucoamylase from *Aspergillus awamori* var X100. **Biochemistry.** 32, 1618-1626.
- Hausser, M.R., Wasserman, R.H., McCaina, T.A., Peterlik, M., Bursaca, K.M., Hughes, M.R., 1976. 1,25-Dihydroxyvitamin D<sub>3</sub>-glycosides: Identification of a calcinogenic principle of *Solanum malacoxylon*. **Life Sci.** 18(10), 1049-1056.
- Hays, W.S., Jeniso, S.A., Yamada, T., Pastuszyn, A.P., Glew, R.H., 1996. Primary structure of the cytosolic  $\beta$ -glucosidase of guinea pig liver. **Biochem. J.** 319, 829-837.



- Hays, W.S., Vander Jagt, D.J., Bose, B., Serianni, A.S., Glew, R.H., 1998. Catalytic mechanism and specificity for hydrolysis and transglycosylation reactions of cytosolic  $\beta$ -glucosidase from guinea pig liver. **J. Biol. Chem.** 273, 34941-34948.
- He, S., Withers, S.G., 1997. Assignment of sweet almond  $\beta$ -glucosidase as a family 1 glycosidase and identification of its active site nucleophile. **J. Biol. Chem.** 272, 24864-24867.
- Helferich, B., Kleinschmidt, T., 1965. Data on sweet emulsion, **Z. Physiol. Chem.** 340, 31.
- Helting, T., Peterson, P.A., 1972. Galactosyl transfer in mouse mastocytoma: Synthesis of a galactose containing polar metabolite of retinoid. **Biochem. Biophys. Res. Commun.** 46, 429-433.
- Henry, C.J.K., Emery, B., 1986. Effects of spiced food on metabolic rate. **Hum. Nutr. Clin. Nutr.** 40C, 165-168.
- Hergenbahn, M., Bertram, B., Wiessler, M., Sorg, B.L., 2002. Saccharide containing curcumin derivatives with improved water solubility for pharmaceuticals. German Patent **WO 2001-DE 2337** (CA 136:90984).
- Hestrin, S., Feingold, D.S., Schramm, M., 1955.  $\beta$ -Glucosidase from sweet almond emulsin. **Methods Enzymol.** Colowick, S.P., Kaplan, N.O., (Eds), 1, 234-240.
- Heyes, Z., Szabo, A., Nemeth, J., Jakab, B., Pinter, E., Banvolgyl, A., Kereskai, L., Keri, G., Szolcsanyl, J., 2004. Antiinflammatory and analgesic effects of somatostatin released from chronic arthritis model in the rat. **Arthritis Rheum.** 50, 1677-1685.
- Hirofumi, S., Kenro, T., Akikaszu, A., Takaaki, F., Makoto, S., Yoshimichi, D., Tsunco, Y., 1991. Enzymatic synthesis of useful alkyl- $\beta$ -glucoside. **Agric. Biol. Chem.** 55, 1679-1681.
- Hiromi, K., 1970. Interpretation of dependency of rate parameters on the degree of polymerization of substrate in enzyme-catalyzed reactions. Evaluation of subsite affinities of exoenzyme. **Biochem. Biophys. Res. Commun.** 40, 1-6.
- Hiromi, K., Kawai, M., Ono, S., 1966a. Kinetic studies on glucoamylase IV. Hydrolysis of isomaltose. **J. Biochem.** 59, 476-480.
- Hiromi, K., Nitta, Y., Numata, C., Ono, S., 1973. Subsite affinities of glucoamylase examination of the validity of the subsite theory. **Biochim. Biophys. Acta.** 302, 362-375.
- Hiromi, K., Ohnishi, M., Tanaka, A., 1983. Subsite structure and ligand binding mechanism of glucoamylase, **Mol. Cell. Biochem.** 51, 79-95.
- Hiromi, K., Takahashi, K., Hamazu, Z., Ono, S., 1966b. Kinetic studies on glucoamylase III. The influence of pH on the rates of hydrolysis of maltose and panose. **J. Biochem.** 59, 469-475.
- Hofmann, R.W., Swinny, E.E., Bloor, S.J., Markham, K.R., Ryan, K.G., Campbell, B.D., Jordan, B.R., Fountain, D.W., 2000. Responses of nine *Trifolium repens* L. populations to ultraviolet-B radiation. Differential flavonol glycoside accumulation and biomass production. **Ann. Bot.** 86, 527-537.

- Honda, K., Ishige, T., Kataoka, M., Shimizu, S., 2006. Microbial and enzymatic processes for the production of chiral compounds. In: **Biocatal. Pharm. Biotechnol. Ind.**, Patel, R.N., (Ed.), Taylor and Francis, New York, 529-546.
- Hong, J., Tamaki, H., Kumagai, H., 2007. Cloning and functional expression of thermostable  $\beta$ -glucosidase gene from *Thermoascus aurantiacus*. **Appl. Microbiol. Biotechnol.** 73, 1331-1339.
- Horvathova, V., Janecek, S., Sturdik, E., 2001. Amylolytic enzymes: Molecular aspects of their properties. **General Physiol. Biophys.** 20, 7-32.
- Hostinova, E., Balanova, J., Gasperik, J., 1991. The nucleotide sequence of the glucoamylase gene GLA1 from *Saccharomyces fibuligera* KZ. **FEMS Microbiol. Lett.** 83(1), 103-108.
- Houghton, L.A., Vieth, R., 2006. The care against ergocalciferol (vitamin D<sub>2</sub>) as a vitamin supplement. **Am. J. Clin. Nutr.** 84, 694-697.
- Huang, K.H., Akoh, C.C., 1996. Optimization and scale up of enzymatic synthesis of structured lipids using RSM. **J. Food Sci.** 61,137-141.
- Hui-Lei, Y., Jian-He, X., Wen-Ya, L., Guo-Qiang, L., 2007. Identification, purification and characterization of  $\beta$ -glucosidase from apple seed as a novel catalyst for synthesis of O-glucosides. **Enzyme Microb. Technol.** 40, 354-361.
- Humeau, M., Girardin, B., Rovel, A.M., 1998. Effect of the thermodynamic water activity and the reaction medium hydrophobicity on the enzymatic synthesis of ascorbyl palmitate. **J. Biotechnol.** 63, 1-8.
- Huo, Y., Li, Y., Yuan, Z., Huang, J., 2004. Immobilization of glucoamylase onto novel porous polymer supports of vinylene carbonate and 2-hydroxy ethyl methacrylate. **Appl. Biochem. Biotechnol.** 119, 121-131.
- Hussein, S.A., Hashim, A.N., El-Sharawy, R.T., Seliem, M.A., Linscheid, M., Lindequist, U., Nawwar, M.A., 2007. Ericifolin: An eugenol 5-O-galloylglucoside and other phenolics from *Melaleuca ericifolia*. **Phytochemistry.** 68, 1464-1470.
- Hyun, H.H., Zeikus, J.G., 1985. General biochemical characterization of thermostable pullulanase and glucoamylase from *Clostridium thermohydrosulfuricum*. **Appl. Environ. Microbiol.** 49, 1168-1173.
- Hyuncheol, O., Dae-Gill, K., C., Hun-Taeg, L., Ho-Sub, L., 2003. Four glycosides from the leaves of *Abeliophyllum distichum* with inhibitory effects on angiotensin converting enzyme. **Phytotherapy Res.** 17, 811-813.
- Ichikawa, H., Yoshida, N., Takano, H., Ishikawa, T., Handa, O., Takagi, T., Nito, Y., Murase, H., Yoshikawa, T. 2003. A novel water-soluble vitamin E derivative (TMG) protects against gastric mucosal damage induced by ischemic and reperfusion in rats. **Dig. Dis. Sci.** 48(1), 54-58.
- Ichikawa, Y., Look, G.C., Wong, C.H., 1992. Enzyme-catalysed oligosaccharide synthesis. **Anal. Biochem.** 202, 215-238.
- Ida, J., Matsuyama, T., Yamamoto, H., 2000. Immobilisation of glucoamylase on ceramic membrane surfaces modified with a new method of treatment utilizing SPCP-CVD. **Biochem. Engg. J.** 5, 179-184.

- Igarashi, K., 1977. The Koenigs-Knorr reaction. **Adv. Carbohydr. Chem. Biochem.** 34, 243-283.
- Ikeda, D., Umezawa, S., 1999. Aminoglycoside antibiotics. In: **Naturally occurring glycosides**, Ikan, R., (Ed.), John Wiley & Sons, Ltd., England, pp 1-42.
- Ikeda, T., Yamauchi, K., Nakano, D., Nakanishi, K., Miyashita, H., Ito, S.H., Nohara, T., 2006. Chemical transglycosylation of bioactive glycolinkage: Synthesis of an  $\alpha$ -lycotetraosyl cholesterol. **Tetrahedron Lett.** 47, 4355-4359.
- Iorizzi, M., Lanzotti, V., De Marino, S., Zollo, F., Blanco-Molina, M., Macho, A., Munoz, E., 2001. New glycosides from *Capsicum annum* L. Var. *accuminatum*. Isolation, structure determination and biological activity. **J. Agric. Food Chem.** 49, 2022-2029.
- Ismail, A., Ghouli, M., 1996. Enzymatic synthesis of butyl glycosides by glycosidases. **Biotechnology Lett.** 18, 1199-1204.
- Ismail, A., Linder, M., Ghouli, M., 1999b. Optimization of butylgalactoside synthesis by  $\beta$ -galactosidase from *Aspergillus oryzae*. **Enzyme Microb. Technol.** 25, 208-213.
- Ismail, A., Soultani, S., Ghouli, M., 1998. Optimization of the enzymatic synthesis of butyl glucoside using response surface methodology. **Biotechnol. Prog.** 14, 874-878.
- Ismail, A., Soultani, S., Ghouli, M., 1999a. Enzymatic-catalyzed synthesis of alkylglycosides in monophasic and biphasic systems. I. The transglycosylation reaction. **J. Biotechnol.** 69, 135-143.
- Isozaki, Y., Yoshida, N., Ichikawa, H., Kuroda, M., Kokura, S., Naito, Y., Okanoue, T., Yoshikawa, T., 2005. A novel water-soluble vitamin E derivative protect against aspirin-induced gastric mucosal injury in rats. **Int. J. Mol. Med.** 16(6), 1035-1040.
- Itoh, T., Sakata, Y., Akada, R., Nimi, O., Yamashita, I., 1989. Construction and characterization of mutant glucoamylases from the yeast *Sacharomycopsis fibuligera*. **Agric. Biol. Chem.** 53, 3159-3168.
- Jacobson, R.H., Kuroki, R., Weaver, L.H., Zhang, X.-J., Matthews, B.W., 1995. Enzymatic degradation of insoluble carbohydrates, In: **ACS Symposium series**, Saddler, J.N., Penner, M.H., (Eds.), Washington, 618, 38-50.
- Jacobson, R.H., Zhang, X.-J., DuBose, R.F., Matthews, B.W., 1994. Three dimensional structure of  $\beta$ -galactosidase from *E. Coli*. **Nature.** 369, 761-766.
- Jafari-Aghdam, J., Khajek, K., Ranjbar, B., Nemat-Gorgani, M., 2005. Deglycosylation of glucoamylase from *Aspergillus niger*: Effects on structure, activity and stability. **Biochim. Biophys. Acta.** 1750, 61-68.
- James, J.A., Berger, J.L., Lee, B.H., 1997. Purification of glucoamylase from *Lactobacillus amylovorus* ATCC 33621. **Curr. Microbiol.** 34, 186-191.
- James, J.A., Lee, B.H., 1995. Cultural conditions for production of glucoamylase from *Lactobacillus amylovorus* ATCC 33621. **J. Appl. Bacteriol.** 79, 499-505.



- James, S.Y., Williams, M.A., Newland, A.C., Colston, K.W., 1999. Leukemia cell differentiation: Cellular and molecular interactions of retinoids and vitamin D, **Gen. Pharmacol.** 32, 143-154.
- Janssen, A.E.M., Sijnsnes, B.J., Vakurov, A.V., Halling, P.J., 1999. Kinetics of lipase-catalysed esterification in organic media: Correct model and solvent effects on parameters, **Enzyme Microb. Technol.** 24, 463-470.
- Jiang, Z., Zhu, Y., Li, Z., Yu, X., Kusakabe, I., Kitaoka, M., 2004. Transglycosylation reaction of xylanase B from the hyperthermophilic *Thermotoga maritima* with the ability of synthesis of tertiary alkyl  $\beta$ -D-xylobiosides and xylosides. **J. Biotechnol.** 114, 125-134.
- Jianping, Z., Weizhong, G., Jianqian, W., Hui, Y., 2003. Immobilization of glucoamylase on polyvinyl alcohol complex gel. **Weishengwuxue Tongbao** 30, 10-13 (Chinese).
- Johannes, T.W., Zhao, H., 2006. Directed evolution of enzymes and biosynthetic pathways, **Curr. Opin. Microbiol.** 9(3), 261-267.
- Johnston, I., 1992. Renin-angiotensin system: A dual tissue and hormonal system for cardiovascular control. **J. Hypertens.** 10, 13-26.
- Joseph, T., McCormick, D.B., 1995. Uptake and metabolism of riboflavin-5'- $\alpha$ -D-glucoside by rat and isolated liver cells. **J. Nutr.** 125, 2194-2198.
- Kadi, N., Crouzet, J., 2008. Transglycosylation reaction of endoxylanase from *Trichoderma longibrachiatum*. **Food Chem.** 106, 466-474.
- Kaljuzhin, O.V., Shkalev, M.V., 2000. Immunomodulator and pharmaceutical compositions with antitumor properties, and a food additive. Patent **EP1038532** (CA 129:335732).
- Kaminaga, Y., Nagatsu, A., Akiyama, T., Sugimoto, N., Yamazaki, T., Maitani, T., Mizukami, H., 2003. Production of unnatural glucosides of curcumin with drastically enhanced water solubility by cell suspension cultures of *Catharanthus roseus*. **FEBS Lett.** 555, 311-316.
- Kaper, T., Lebbink, J.H.G., Pouwels, J., Kopp, J., Schulz, G.E., Oost, J.V., Vos, W.M., 2000. Comparative structural analysis and substrate specificity engineering of the hyperthermostable  $\beta$ -glucosidase CelB from *Pyrococcus furiosus*. **Biochemistry.** 39, 4963-4970.
- Kara, A., Osman, B., Yavuz, H., Besirli, N., Denizli, A., 2005. Immobilisation of  $\alpha$ -amylase on  $\text{Cu}^{2+}$  chelated poly(ethylene glycol dimethacrylate-n-vinyl imidazole) matrix via adsorption. **React. Funct. Polym.** 62, 61-68.
- Karnchanat, A., Petsom, A., Sanganich, P., Piaphukiew, J., Whalley, A.J., Reynolds, C.D., Sihanonth, P., 2007. Purification and biochemical characterisation of an extracellular beta-glucosidase from the wood-decaying fungus *Daldinia eschscholzii* (Ehrenb. Fr.) Rehm. **FEMS Microbiol. Lett.** 270, 162-170.
- Katusumi, K., Mikio, F., Yoshiteru, I., Hiroyuki, A., 2004. Simple synthesis of  $\beta$ -D-glycopyranosides using  $\beta$ -glycosidase from almonds. **Chem. Pharm. Bull.** 52, 270-275.

- Kaur, P., Satyanarayana, T., 2004. Production of starch saccharification by a thermophilic mould *Thermomucor indicae-seudaticae*. **World J. Microbiol. Biotechnol.** 20, 419-425.
- Kawada, T., Watanabae, T., Takahashi, T., Tanaka, T., Iwai, K., 1986. Effects of capsaicin on lipid metabolism in rats fed a high fat diet. **J. Nutr.** 116, 1272-1278.
- Kawai, F., Yamada, H., Ogata, K., 1971a. Properties of pyridoxine glucoside. **J. Vitaminol.** 17, 121-124.
- Kawai, F., Yamada, H., Ogata, K., 1971b. Studies on transglycosidation to vitamin B<sub>6</sub> by microorganisms Part IV. Purification of a bacterial enzyme catalyzing pyridoxine glucoside synthesis. **Agric. Biol. Chem.** 35, 184-190.
- Kefalas, P., Kallithraka, S., Parejo, I., Makris, D.P., 2003. A Comparative Study on the in Vitro Antiradical Activity and Hydroxyl Free Radical Scavenging Activity in Aged Red Wines. **Food Sci. Technol. Int.** 9, 383-387.
- Kempster, P.A., Bogetic, Z., Secombe, J.W., Martin, H.D., Balazs, N.D.H., Wahlquist, M.C., 1993. Motor effect of broad beans *Vicia faba* in Parkinson's disease: Single dose studies. **Asia Pacific J. Clin. Nutr.** 2, 85-89.
- Ken, V., Cvak, L., 1999. Ergot genus *Claviceps*, medicinal and aromatic plants-industrial profiles, Harwood Publ. Ltd. Amsterdam, London.
- Kengen, S.W.M., Luesink, E.J., Stams, A.J.M., Zehnder, A.J.B., 1993. Purification and characterization of an extremely thermostable  $\beta$ -glucosidase from the hyperthermophilic archaeon *Pyrococcus furiosus*. **Eur. J. Biochem.** 213, 305-312.
- Kim, H.J., Park, H.S., Lee, I.S., 2006. Microbial transformation of silybin by *Trichoderma koningii*. **Bioorg. Med. Chem. Lett.** 16(4), 790-793.
- Kim, S.K., Byun, H.G., Park, P.J., Shahidi, F., 2001. Angiotensin I converting enzyme inhibitory peptides purified from bovine skin gelatin hydrolysate. **J. Agric. Food Chem.** 49, 2992-2997.
- Kim, W.D., Kaneko, S., Park, G.G., Tanaka, H., Kusakabe, I., Kobayashi, H., 2003. Purification and characterization of  $\alpha$ -galactosidase from sunflower seeds. **Biotechnol. Lett.** 25, 353-358.
- Kiran, K.R., Divakar, S., 2002. Enzyme inhibition by *p*-cresol and lactic acid in lipase-mediated synthesis of *p*-cresyl acetate and steroyl lactic acid: A kinetic study. **World J. Microb. Biotechnol.** 18, 707-712.
- Kleinman, M.J., Wilkinson, A.E., Wright, I.P., Evans, I.H., Bevan, E.A., 1988. Purification and properties of an extracellular glucoamylase from a diastatic strain of *Saccharomyces cerevisiae*. **Biochem. J.** 249, 163-170.
- Kobayashi, T., Adachi, S., Naknishi, K., Matsuno, R., 2000. Synthesis of alkyl glycosides through  $\beta$ -glucosidase catalysed condensation in an aqueous organic biphasic system and estimation of the equilibrium constants for their formation. **J. Mol. Catal. B: Enzym.** 11, 13-21.
- Kohda, H., Kasai, R., Yamasaki, K., Tanaka, O., 1976. New sweet diterpene glucosides from *Stevia rebaudiana*. **Phytochemistry.** 15, 981-983.

- Kometani, T., Nishimura, T., Nakae, T., Takii, H., Okada, S., 1996. Synthesis of neohesperidin glycosides and naringin glycosides by cyclodextrin glucanotransferase from an alkalophilic *Bacillus* species. **Biosci. Biotechnol. Biochem.** 60, 645-649.
- Kometani, T., Tanimoto, H., Nishimura, T., Kanbara, I., Okada, S., 1993a. Glucosylation of capsaicin by cell suspension cultures of *Coffea arabica*. **Biosci. Biotech. Biochem.** 57, 2192-2193.
- Kometani, T., Tanimoto, H., Nishimura, T., Okada, S., 1993b. Glucosylation of vanillin by cultured plant cells. **Biosci. Biotech. Biochem.** 57, 1290-1293.
- Kondo, Y., Shimoda, K., Takimura, J., Hamada, H., Hamada, H., 2006. Glycosylation of vitamin E homologue by cultured plant cells. **Chem. Lett.** 35, 324-326.
- Konstantinovic, S., Predojevic, J., Gojkovic, S., Ratkovic, Z., Mojsilovic, B., Pavlovic, V., 2001. Synthesis of C7-C16 alkyl 2,3 dideoxy glucosides from glucose and fatty acids. **Ind. J. Chem.** 40B, 1242-1244.
- Kosary, J., Stefanovits-Banyai, E., Boross, L., 1998. Reverse hydrolytic process for O-alkylation of glucose catalyzed by immobilized  $\alpha$ - and  $\beta$ -glucosidases. **J. Biotechnol.** 66, 83-86.
- Kouptsova, O.S., Klyachko, N.L., Levashov, A.V., 2001. Synthesis of alkyl glycosides catalyzed by  $\beta$ -glucosidases in a system of reverse micelles. **Russian J. Bioorg. Chem.** 27, 380-384.
- Krause, D.R., Wood, C.J., Mac Lean, D.J., 1991. Glucoamylase (exo-1,4- $\alpha$ -D-glucohydrolase, E.C. 3.2.1.3) is the major starch-degrading enzyme secreted by the phytopathogenic fungus *Colletotrichum gloeosporioides*. **J. Gen. Microbiol.** 137, 2463-2468.
- Kren, V., 2001. Chemical biology and biomedicine of glycosylated natural compounds. In: **Glycoscience Chemistry and Chemical Biology**, Fraser-Reid, B., Tatsuta, K., Thiem, J., (Eds.), Springer Berlin, 3, 2471-2529.
- Kren, V., Hunkova, Z., Halada, P., Suzuki, Y., 1998. Transglycosylation of thiamine by fungal  $\beta$ -N-Acetylhexosaminidases. **Biosci. Biotechnol. Biochem.** 62(12), 2415-2417.
- Kren, V., Martinkova, L., 2001. Glycosides in medicine: The role of glycosidic residue in biological activity. **Curr. Med. Chem.** 8, 1313-1338.
- Kumano, Y., Sakamoto, T., Egawa, M., Iwai, I., Tanaka, M., Yamamoto, I., 1998. *In vitro* and *in vivo* prolonged biological activities of novel vitamin C derivative, 2-O- $\alpha$ -D-glucopyranosyl-L-ascorbic acid (AA-2G), in cosmetic fields. **J. Nutr. Sci. Vitaminol.** 44, 345-359.
- Kumar, P., Satyanarayana, T., 2007a. Optimization of culture variable for improving glucoamylase production by alginate entrapped *Thermomucor indicae seudaticae* using statistical methods. **Biores. Technol.** 98(6), 1252-1259.
- Kumar, P., Satyanarayana, T., 2007b. Economical glucoamylase production by alginate immobilized *Thermomucor indicae seudaticae* in cane molasses medium. **Lett. Appl. Microbiol.** 45, 392-397.

- Kumar, S., Satyanarayana, T., 2005. Production of cell-bound phytase by *Pichia anomala* in an economical cane molasses medium: Optimization using statistical tools. **Process Biochem.** 40, 3095-3102.
- Kurashima, K., Fujii, M., Ida, Y., Akita, H., 2004. Simple synthesis of  $\beta$ -glycopyranosides using  $\beta$ -glycosidase from almonds. **Chem. Pharm. Bull.** 52, 270-275.
- Kvamer, G.F.H., Gunning, A.P., Morris, V.J., Belshaw, N.J., Williamson, G., 1993. Scanning tunneling microscopy of *Aspergillus niger* glucoamylase. **J. Chem. Soc. Faraday Trans.** 89, 2595-2602.
- La Cara, F., Scarfi, M.R., D'Auria, S., Massa, R., D'Ambrosio, G., Franceschetti, G., Rossi, M., De Rosa, M., 1999. Different effects of microwave energy and conventional heat on the activity of a thermophilic  $\beta$ -galactosidase from *Bacillus acidocaldarius*. **Bioelectromagnetics.** 20, 172-176.
- Laane, C., Boeren, S., Vos, K., Veeger, C., 1987. Rules for optimization of biocatalysis in organic solvents. **Biotechnol. Bioengg.** 30, 81-87.
- Ladero, M., Ruiz, G., Pessela, B.C.C., Vian, A., Santos, A., Ochoa, F.G., 2006. Thermal and pH inactivation of an immobilized thermostable  $\beta$ -galactosidase from *Thermus* sp. strain T2: Comparison to the free enzyme. **Biochem. Engg. J.** 31, 14-24.
- Lahmann, M., Thiem, J., 1997. Synthesis of  $\alpha$ -tocopheryl oligosaccharides. **Carbohydr. Res.** 299, 23-31.
- Lamelli, U.K., 1970. Cleavage of structural protein during the assembly of the head of bacteriophage T4. **Nature.** 227, 680-685.
- Lan, T., Dalip, R., Errol, M.Y., 2004. Isolation and purification of the hypoglycemic principle present in *Cap. Frutescens*. **Phytotherapy Res.** 18, 95-96.
- Laroute, V., Willemot, R.M., 1992a. Glucoside synthesis by glucoamylase or  $\beta$ -glucosidase in organic solvents. **Biotechnology Lett.** 14, 169-174.
- Laroute, V., Willemot, R.M., 1992b. Effect of organic solvents on stability of two glycosidases and on glucoamylase-catalyzed oligosaccharides synthesis. **Enzyme Microb. Technol.** 14, 528-534.
- Larsson, J., Svensson, D., Adlercreutz, P., 2005.  $\alpha$ -Amylase catalysed synthesis of alkyl glycosides. **J. Mol. Catal. B: Enzym.** 37, 84-87.
- LeBlane, J.G., Burgees, C., Sesma, F., de Giori, G.S., Van Sinderen, D., 2005. *Lactococcus lactis* is capable of improving the riboflavin status in deficient rats. **British J. Nutr.** 94, 262-267.
- Lee, H-J., Larue, J. N., Wilson, I. B., 1971. Angiotensin converting enzyme from guinea pig and hog lung. **Biochem. Biophys. Acta** 250, 549-557.
- Lee, M.D., Dunne, T.S., Chang, C.C., Ellestad, G.A., Siegel, M.M., Morton, G.O., McGahren, W.J., Borders, D.B., 1987. Calicheimicines, a novel family of antitumor antibiotics 2. Chemistry and structure of calicheimicin,  $\gamma^1$ . **J. Am. Chem. Soc.** 109, 3466-3468.
- Lee, S.E., Hwang, H.J., Ha, J.S., 2003. Screening of medicinal plant extracts for antioxidant activity. **Life Sci.** 73, 167-179.

- Lee, Y., Howard, L.R., Villalon, B., 1995. Flavonoids and antioxidant activity of fresh pepper (*C. annuum*) cultivars. **J. Food Sci.** 60, 473-476.
- Lerouxel, O., Cavalies, D.M., Liepman, A.H., Keegstra, K., 2006. Biosynthesis of plant cell wall polysaccharides: A complex process. **Curr. Opin Plant Biol.** 9, 621-630.
- Li, G.H., Le, G.W., Yong-Hui, S., Shrestha, S., 2004. Angiotensin I-converting enzyme inhibitory peptides derived from food proteins and their physiological and pharmacological effects. **Nutrition Res.** 24, 469-486.
- Li, H., Chi, Z., 2007. Purification and characterisation of extracellular amylase from the marine yeast *Aureobasidium pullulans* N13d and its raw potato starch digestion. **Enzyme Microb. Technol.** 40(5), 1006-1012.
- Limousin, C., Cleophax, J., Petit, A., Loupy, A., Lukacs, G., 1997. Solvent-free synthesis of decyl D-glycopyranosides under focused microwave irradiation. **J. Carbohydr. Chem.** 16, 327-342.
- Linder, M., Fanni, J., Parmentier, M., Sergent, M., Phan-Tan-Luu, R., 1995. Protein recovery from veal bones by enzymatic hydrolysis. **J. Food Sci.** 60, 949-952.
- Liu, H.L., Wang, W.C., 2003. Protein engineering to improve the thermostability of glucoamylase from *Aspergillus awmori* based on molecular dynamics simulations. **Protein Engg.** 16, 19-25.
- Liu, H-S., Cheng, Y-C., 2000. Stability enhancement of  $\alpha$ -amylase by supercritical carbon dioxide pretreatment. **Prog. Biotechnol.** 16, 149-154.
- Liu, Y.N., Lai, Y.T., Chou, W.I., Chang, M.D.T., Lyu, P.C., 2007. Solution structure of family 21 carbohydrate-binding module from *Rhizopus oryzae* glucoamylase. **Biochem. J.** 403, 21-30.
- Ljunger, G., Adlercreutz, P., Mattiasson, B., 1994. Enzymatic synthesis of octyl- $\beta$ -glucoside in octanol at controlled water activity. **Enzyme Microb. Technol.** 16, 751-755.
- Long, B.H., Golik, J., Forenza, S., Ward, B., Rehfuess, R., Onbeowiak, J.C., Catino, J.J., Musial, S.T., Brookshire, K.W., Doyle, T., 1989. Esperamicins, a class of potent antitumor antibiotics: Mechanism of action. **Proc. Natl. Acad. Sci. USA.** 86, 2-6.
- Lopez-Malo, A., Alzamora, S.M., Argaiz, A., 1998. Vanillin and pH synergistic effects on mold growth. **J. Food Sci.** 63, 143-146.
- Lowry, O.H., Rosenbrough, N.J., Farr, A.L., Randal, R.J., 1951. Protein measurement with Folin Phenol reagent. **J. Biol. Chem.** 193, 265-275.
- Luisi, P.L., Gimini, M., Pileni, M.P., Robinson, B.H., 1998. Reverse micelles as hosts for proteins and small molecules. **Biochim. Biophys. Acta** 947, 209-246.
- Lukowska, E., Plenkiewicz, J., 2007. Chemo-enzymatic preparation of optically active thiiranes. **Tetrahedron Assym.** 18(4), 493-499.
- Luther, H., Stehlin, A., Minklei, M., 1999. Sunscreen compositions. US Patent. 5980872.
- Luthi, P., Luisi, P.L., 1984. Enzymatic synthesis of hydrocarbon soluble peptide with reverse micelles. **J. Am. Chem. Soc.** 106, 7285-7286.



- Madrid, Y., Langer, L.F., Brem, H., Langer, R., 1991. New directions in the delivery of drugs and other substances to the central nervous system. **Adv. Pharmacol.** 22, 299-324.
- Maheswar Rao, J.L.U., Satayanarayana, T., 2007. Improving production of hyperthermostable and highmaltose forming alpha-amylase by an extreme thermophile *Geobacillus thermoleovorans* using response surface methodology and its applications. **Biores. Technol.** 98, 345-352.
- Malek, S.A.S., Hossain, Z., 1994. Purification and characterization of a thermostable glucoamylase from *Myrothecium* isolate. **J. Appl. Bacteriol.** 76, 210-215.
- Mamo, G., Gessesse, A., 1999. Production of raw starch digesting amyloglucosidase by *Aspergillus* sp. GP-21 in solid state fermentation. **J. Ind. Microbiol. Biotechnol.** 22, 622-626.
- Manohar, B., Divakar, S., 2002. Application of Central Composite Rotatable Design to lipase catalyzed synthesis of *m*-cresyl acetate. **World. J. Microbiol. Biotechnol.** 18, 745-751.
- Marana, S.R., 2006. Molecular basis of substrate specificity in family 1 glycoside hydrolases. **IUBMB Life.** 58, 63-73.
- Marana, S.R., Andrade, E.H., Ferreira, C., Terra, W.R., 2004. Investigation of the substrate specificity of a  $\beta$ -glycosidase from *Spodoptera frugiperda* using site-directed mutagenesis and bioenergetics analysis. **Eur. J. Biochem.** 271, 4169-4177.
- Marana, S.R., Jacobs-Lorena, M., Terra, W.R., Ferreira, C., 2001. Amino acid residues involved in substrate binding and catalysis in an insect digestive  $\beta$ -glycosidase. **Biochim. Biophys. Acta.** 1545, 41-52.
- Margolin, A.L., Tai, D.F., Klivanov, A.M., 1987. Incorporation of D-amino acids into peptides via enzymatic condensation of organic solvents. **J. Am. Chem. Soc.** 109, 7885-7887.
- Mariano, G.G., Agustin, L.M., Eduardo, B., 2000. Alcoholysis and reverse hydrolysis reactions in organic one-phase system with a hyperthermophilic  $\beta$ -glycosidase. **Biotechnol. Bioeng.** 69, 627-632.
- Marin-Zamorae, M.E., Melgarejo, F.R., Canovasb, F.G., Ruiz, P.A.G., 2006. Direct immobilization of tyrosinase enzyme from natural mushrooms (*Agaricus bisporus*) on D-sorbitolcinnamic ester. **J. Biotechnol.** 126, 295-303.
- Marlida, Y., Hassan, S.N., Radu, S.Z., Baker, J., 2000. Purification and characterization of sago starch degrading glucoamylase from *Acremonium* sp. endophytic fungus. **Food Chem.** 71, 221-227.
- Martinez, S.G., Alvira, E., Cordero, L.V., Ferrer, A., Clemente, I.M., Barletta, G., 2002. High initial activity but low storage stability observed for several preparations of subtilisin carsberg suspended in organic solvents. **Biotechnol. Prog.** 18, 1462-1466.
- Marty, A., Chulalaksananukul, W., Willemot R.M., Condoret, J.S., 1992. Kinetics of lipase-catalysed esterification in supercritical CO<sub>2</sub>. **Biotechnol. Bioeng.** 39, 273-280.

- Masumura, Y., Kasunoki, M., Harada, W., Kakudo, M., 1984. Structure and possible catalytic residues of taka amylase A. **J. Biochem.** 95, 697-702.
- Matsuda, T., Harada, T., Nakamura, K., 2002. Biotransformations in supercritical carbon dioxide. **Fain Kemikaru** 31, 40-49.
- Matsumura, S., Imai, K., Yoshikawa, S., Kawada, K., Uchibori, T., 1990. Surface activities, biodegradability and antimicrobial properties of n-alkyl glucosides, manosides and galactosides. **J. Am. Oil. Chem. Soc.** 67, 996-1001.
- Matsumura, S., Nakamura, T., Yao, E., Toshima, K., 1999. Biocatalytic one-step synthesis of n-Octyl  $\beta$ -D-xylotrioside and xylobioside from xylan and n-octanol in supercritical carbon dioxide. **Chem. Lett.** 7, 581-582.
- Maugard, T., Gaunt, D., Legoy, M.D., Besson, T., 2003. Microwave-assisted synthesis of galacto-oligosaccharides from lactose with immobilized  $\beta$ -galactosidase from *Kluyveromyces lactis*. **Biotechnology Lett.** 25, 623-629.
- Mc Carter, J., Withers, S.G., 1994. Mechanisms of enzymatic glycoside hydrolysis. **Curr. Opinion Struct. Biol.** 4, 885-892.
- Meages, M.M., Nikolov, Z.L., Reilly, P.J., 1989. Subsite mapping of *Aspergillus niger* glucoamylase I and II. **Biotechnol. Bioeng.** 34, 681-688.
- Mello, J.R.B., 2003. Calcinosis-calcinogenic plants. **Toxicol.** 41, 1-12.
- Miao, W., Yao, S., 1999. Study of  $\beta$ -1,4-glucosidase in water/PC/heptane-butanol reverse micelles. **Wuli Huaxue Xuebao.** 15, 930-937(Chinese).
- Michaud, A., Williams, T.A., Chauvet, M.T., Corvol, P., 1997. Substrate dependence of angiotensin I converting enzyme inhibition: Captopril displays a selectivity for inhibition of N-acetyl-seryl-aspartyl-lysyl-proline hydrolysis compares with that of angiotensin I. **Mol. Pharmacol.** 51, 1070-1076.
- Mislovicova, D., 2006. Modulation of biorecognition of glucoamylase with concanavalin A by glycosylation via recombinant expression. **Int. J. Biol. Macromol.** 39, 286-290.
- Mohri, K., Watanabe, Y., Yoshida, Y., Satoh, M., Isobe K., Sugimoto, N., Tsuda, Y., 2003. Synthesis of glycosylcurcuminoids. **Chem. Pharm. Bull.** 51, 1268-1272.
- Montgomery, D.C., 1991. Design and analysis of experiments. John Wiley and Sons, New York. pp 542-547.
- Moon, J.H., Terao, J., 1998. Antioxidant activity of caffeic acid and dihydrocaffeic acid in Lard and human low-density lipoprotein. **J. Agri. Food chem.** 46, 5062-5065.
- Moon, Y.H., Lee, J.H., Jhon, D.Y., Jun, W.J., Kang, S.S., Sim, J., Choi, H., Moon, J.H., Kim, D., 2007. Synthesis and characterization of novel quercetin- $\beta$ -D-glucopyranosides using glucansucrase from *Leuconostoc mesenteriods*. **Enzyme Microb. Technol.** 40, 1124-1129.
- Morales-Serna, J.A., Boutureira, O., Diaz, Y., Mathev, M.I., Castillon, S., 2007. Recent advances in the glycosylation of sphingosines and ceramides. **Carbohydr. Res.** 342, 1595-1612.
- Mori, T., Okahata, Y., 1998. Effective biocatalytic transgalactosylation in a supercritical fluid using a lipid-coated enzyme. **Chem. Commun.** 20, 2215-2216.

- Mori, T., Okahata, Y., 2000. Enzyme-catalyzed reactions in supercritical fluids. **Chorinkai Saishin Gijutsu**. 4, 36-40.
- Mori, T., Okahata, Y., 2002. Enzyme catalytic reactions in supercritical fluids. **Chorinkai Ryutaino Subete**. Arai, Y., Tekuno, S., (Eds.), Tokyo, Japan. pp 543-547.
- Mori, T., Okahata, Y., 2003. Control of enzymatic reactions by supercritical fluids. **Kagaku Kogyo**. 54, 93-97.
- Morre, D.J., Chueh, P.J., Morre, D.M., 1995. Capsaicin inhibits preferentially the NADH oxidase and growth of transformed cells in culture. **Proc. Natl. Acad. Sci. USA** 92, 1831-1835.
- Mueckler, M., 1994. Facilitative glucose transporters. **Eur. J. Biochem**. 219, 713-725.
- Mullally, M.M., Meisel, H., FitzGerald, R.J., 1996. Synthetic peptides corresponding to a lactalbumin and  $\beta$ -lactoglobulin sequences with angiotensin-I-converting enzyme inhibitory activity. **Biol. Chem**. 377, 259-260.
- Murase, H., Yamauchi, R., Kato, K., Kunieda, T., Terao, J., 1997. Synthesis of a novel vitamin E derivative, 2-( $\alpha$ -D-glucopyranosyl) methyl-2,5,7,8-tetramethyl chroma-6-ol transglycosylation. **Lipids**. 32, 73-78.
- Nagasawa, T., Takagi, H., Kawakami, K., Suzuki, T., Shahaghi, Y., 1961. The browning compounds of bean III isolation of dopa-O- $\beta$ -D-glucoside and the enzymic mechanism for the color change of broad bean. **Agric. Biol. Chem**. 25, 441-447.
- Nakamura, K., Matsuda, T., 2002. Enzyme catalysed reduction reactions. **Enzyme Catal. Org. Syn.** 2<sup>nd</sup> ed, Drauz, K., Waldmann, H., (Eds), Wiley-VCH, Weinheim, 1-3, 991-1047.
- Nakamura, T., Komori, C., Lee, Y.-Y., Hashimoto, F., Yohara, S., Nohara, T., Ejima, A., 1996. Cytotoxic activities of solanum steroidal glycosides. **Biol. Pharm. Bull**. 19, 546-566.
- Nakamura, T., Toshima, K., Matsumura, S., 2000. One-step synthesis of n-octyl  $\beta$ -D-xylotrioside, xylobioside and xyloside from xylan and n-octanol using acetone powder of *Aureobasidium pullulans* in supercritical fluids. **Biotechnology Lett**. 22, 1183-1189.
- Natarajan, S.K., Sierks, M.R., 1997. Minimizing nanoproductive substrate binding: A new look at glucoamylase substrate affinities. **Biochemistry**. 36, 14946-14955.
- Nath, K., Olson, J.A., 1967. Natural occurrence and biological activity of vitamin A derivatives in rat bile. **J. Nutr**. 93, 461-469.
- Neilsen, P.K., Bonsagar, B.C., Fukuda, K., Svensson, B., 2004. Barley  $\alpha$ -amylase/substilin inhibitor: Structure, biophysics and protein engineering. **Biochim. Biophys. Acta**. 1696, 157-164.
- Nielsen, B.R., Lehmbeck, J., Frandsen, T.P., 2002. Cloning heterologous expression and enzymatic characterization of a thermostable glucoamylase from *Talaromyces emersonii*. **Protein expres. purif**. 26, 1-8.
- Nijikken, Y., Tsukada, T., Igarashi, K., Samejima, M., Wakagi, T., Shoun, H., Fushinobu, S., 2007. Crystal structure of intracellular family 1  $\beta$ -glucosidase



- BGL1A from the *Basidiomycete phanerochaete chrysosporium*. **FEBS Lett.** 581, 1514-1520.
- Nolling, J., Breton, G., Omelchenko, M.V., Makarova, K.S., Zeng, Q., Gibson, R., Lee, H.M., Dubois, J.A., Qiu, D., Hiffi, J., 2001. Genome sequence and comparative analysis of the solvent producing bacterium *Clostridium acetobutylicum*. **J. Bacteriol.** 183, 4823-4838.
- Norouzian, D., Akbarzadek, A., Schärer, J.M., Young, M.M., 2006. Fungal glucoamylases. **Biotechnol. Adv.** 24, 80-85.
- Nuchter, M., Ondruschka, B., Lautenschlager, W., 2001. Microwave-assisted synthesis of alkyl glycosides. **Synthetic Commun.** 31, 1277-1283.
- Oakes, R.S., Clifford, A.A., Rayner, C.M., 2001. The use of supercritical fluids in synthetic organic chemistry. **J. Chem. Soc. Perkins Trans 1** 9, 917-941.
- Ochiai, J., Takano, H., Ichikawa, H., Naito, Y., Yoshida, N., Yanagisawa, R., Yoshino, S., Murase, H., Yoshikawa, T., 2002. A novel water-soluble vitamin E derivative, 2-( $\alpha$ -D-glucopyranosyl)methyl-2,5,7,8-tetramethylchroman-6-ol, protects against acute lung injury and mortality in endotoxemic rats. **Int. J. Mol. Med.** 18(6), 580-584.
- Odoux, E., Escoute, J., Verdeil, J.L., Brillouet, J.M., 2003. Localization of  $\beta$ -D-glucosidase activity and glucovanillin in vanilla bean (*Vanilla planifolia andrews*). **Ann. Botany.** 92, 437-444.
- Oh, J.T., Kim, J.H., 2000. Preparation and properties of immobilized amyloglucosidase on nonporous PS/PnaSS microspheres. **Enzyme Microb. Technol.** 27, 356-361.
- Ohinishi, H., Sakai, H., Ohta, T., 1991. Purification and some properties of a glucoamylase from *Clostridium sp. G0005*. **Agric. Biol. Chem.** 55, 1901-1902.
- Ohinishi, M., 1990. Subsite structure of *Rhizopus niveus* glucoamylase, estimated with the binding parameters for maltooligosaccharides. **Starch/Starke** 42, 311-313.
- Ohnishi, M., Hiromi, K., 1989. Binding of maltose to *Rhizopus niveus* glucoamylases in the pH range where the catalytic carboxyl groups are ionized. **Carbohydr. Res.** 195, 138-144.
- Ohnuki, K., Haramizu, S., Oki, K., Watanabe, T., Yazawa, S., Fushiki, T., 2001. Administration of capsiate, a non-pungent capsaicin analog, promotes energy metabolism and suppresses body fat accumulation in mice. **Biosci. Biotechnol. Biochem.** 65, 2735-2740.
- Okada, G., Unno, T., 1989. A glucodextranase accompanied by glucoamylase activity from *Arthrobacter globiformis* I 42. **Agric. Biol. Chem.** 53, 223-228.
- Oliveira, B.H., Packer, J.F., Chimelli, M., Jesus, D.A., 2007. Enzymatic modification of stevioside by cell-free extract of *Gibberella fujikuroi*. **J. Biotechnol.** 131(1), 92-96.
- Omori, A.T., Assis, L.F., Andrade, L.H., Comasseto, J.V., Porto, A.L.M., 2007. Enantiomerically pure organoseleno-1-arylethanol by enzymatic resolution with *Candida antarctica* lipase: Novozym 435. **Tetrahedron Assym.** 18(9), 1048-1053.

- Ooi, Y., Hashimoto, T., Mitsuo, N., Satoh, T., 1985. Enzymatic formation of  $\beta$ -galactosidase from *Aspergillus oryzae* and its application to the synthesis of chemically unstable cardiac glycosides. **Chem. Pharm. Bull.** 33, 1808-1814.
- Oosterom, M.W., Rantwijk, F., Sheldon, R.A., 1996. Regioselective acylation of disaccharides in tert-butyl alcohol catalyzed by *Candida antarctica* lipase. **Biotechnol. Bioeng.** 49, 328-333.
- Orihara, Y., Furuya, T., Hashimoto, N., Deguchi, Y., Tokoro, K., Kanisawa, T., 1992. Biotransformation of isoeugenol and eugenol by cultured cells of *Eucalyptus perriniana*. **Phytochemistry.** 31, 827-831.
- Orlich, B., Schomacker, R., 2002. Enzyme catalysis in reverse micelles. **Adv. Biochem. Engg. Biotechnol.** 75, 185-208.
- Ortega, N., Busto, M.D., Perez-Mateos, M., 2001. Kinetics of cellulose saccharification by *Trichoderma reesei* cellulases. **Int. Biodeter. Biodegrad.** 47, 7-14.
- Oshima, T., Sato, M., Shikaze, Y., Ohto, K., Inoue, K., Baba, Y., 2007. Enzymatic polymerization of O-phenylenediamine with cytochrome C activated by a calixarene derivative in organic media. **Biochem. Engg. J.** 35(1), 66-70.
- Osman, B., Kara, A., Uzun, L., Besirli, N., Denizli, A., 2005. Vinyl-imidazole carrying metal-chelated beads for reversible use in yeast invertase adsorption. **J. Mol. Catal. B: Enzym.** 37, 88-94.
- Ouyang, J., Wang, X.D., Zhao, B., Wang, Y.C., 2005. Enhanced production of phenyl ethanoid glycosides by precursor feeding to cell culture of *Cistanchedeserticola*. **Process Biochem.** 40, 3480-3484.
- Panday, A., Nigam, P., Soccol, C., Soccol, V.T., Singh, D., Mohan, R., 2000. Advances in microbial amylases. **Biotechnol. Appl. Biochem.** 31, 135-152.
- Pandey, A., 1995. Glucoamylase research an overview. **Starch/starke.** 47, 439-445.
- Panintrarux, C., Adachi, S., Araki, Y., Kimura, Y., Matsuno, R., 1995. Equilibrium yield of n-alkyl- $\beta$ -D-glucoside through condensation of glucose and n-octanol by  $\beta$ -galactosidase in a biphasic system. **Enzyme Microb. Technol.** 17, 32-40.
- Papanikolaou, S., 2001. Enzyme-catalyzed synthesis of alkyl- $\beta$ -glucosides in a water-alcohol two-phase system. **Biores. Technol.** 77, 157-161.
- Pardridge, W.M., 2002. Targeting neurotherapeutic agents through the blood-brain barrier. **Arch. Neurol.** 59, 35-40.
- Partridge, J., Harper, N., Moore, B., Halling, P.J., 2001. Enzymes in nonaqueous solvents methods and protocols. In: **Methods Biotechnol.** Rouse, A., Rischel, C., (Eds.), 227-234.
- Payen, A., Persoz, J.F., 1833. Mémoire sur la diastase, les principaux produits de ses reactions et leur applications aux arts industriels. **Annales de chimie et de physique.** 53,73-92.
- Pazur, J.H., Knull, H.R., Cepure, A., 1971. Glucoenzymes: Structure and properties of the two forms of glucoamylase from *Aspergillus niger*. **Carbohydr. Res.** 20, 83-96.
- Peehl, D.M., Krishnan, A.V., Feldman, D., 2003. Pathways mediating the growth-inhibitory actions of vitamin D in prostate cancer. **J. Nutr.** 133, 2461-2469.

- Perveen, R., Rashid, M.H., Saleem, M., Khalid, A.M., Rajoka, M.I., 2006. Kinetic and thermodynamic properties of an immobilized glucoamylase from a mesophilic fungus, *Arachniotus Citrinus*. **Protein Pept. Lett.** 13, 665-671.
- Peterson, P.A., Rask, L., Helting, T., Ostberg, L., Fernstedt, Y., 1976. Formation and properties of retinylphosphate galactose. **J. Biol. Chem.** 251(16), 4986-4995.
- Poon, D.K.Y., Ludwiczek, M.L., Schubert, M., Kwan, E.M., Withers, S.G., McIntosh, L.P., 2007. NMR Spectroscopic characterization of a  $\alpha$ -(1,4)-glycosidase along its reaction pathway: Stabilization upon formation of the glycosyl-enzyme intermediate. **Biochemistry.** 46, 1759-1770.
- Pornpong, S., Saovanee, D., Sitliwat, L., 2005. Effect of glycation on stability and kinetic parameters of thermostable glucoamylase from *Aspergillus niger*. **Proc. Biochem.** 40, 2821-2826.
- Portes, E., Gardrat, C., Castellan, A., 2007. A comparative study on the antioxidant properties of tetrahydrocurcuminoids and curcuminoids. **Tetrahedron.** 63, 9092-9099.
- Post, C.B., Karplus, M., 1986. Does lysozyme follow the lysozyme pathway? An alternative based on dynamic structural and stereoelectronic considerations. **J. Am. Chem. Soc.** 108, 1317-1319.
- Potier, P., Maccario, V., Giudicelli, M.B., Queneau, Y., Dangles, O., 1999. Gallic esters of sucrose as a new class of antioxidants. **Tetrahedron Lett.** 40, 3387-3390.
- Powers, H.J., 2003. Riboflavin and health. **Am. J. Clinical Nutr.** 77, 1352-1360.
- Prabakaran, M, Mano, J.F., 2006. Stimuli-responsive hydrogels based on polysaccharides incorporated with thermo-responsive polymers as novel biomaterials. **Macromol. Biosci.** 6, 991-1008.
- Pras, N., Woerdenbag, J., Van Uden, W., 1995. Bioconversion potential of plant enzymes for the production of pharmaceuticals. **Plant Cell, Tissue Org. Cult.** 43,117-121.
- Pretorius, I.S., Lambrechts, M.G., Marmur, J., 1991. The glucoamylase multigene family in *Saccharomyces cerevisiae* var. *diastaticus*: An overview. **CRC Crit. Rev. in Biochem. Mol. Biol.** 26, 53-76.
- Pugh, T.A., Shah, J.C., Magee, P.T., Clancy, M.J., 1989. Characterization and localization of the sporulation glucoamylase from *Saccharomyces cerevisiae*. **Biochim. Biophys. Acta.** 994, 200-209.
- Quintero, D., Velasco, Z., Gomez, E.H., Neira, J.L., Contreras, L.M., 2007. Isolation and characterization of a thermostable  $\beta$ -xylosidase in the thermophilic bacterium *Geobacillus pallidus*. **Biochim. Biophys. Acta.** 1774, 510-518.
- Ramasesh, N., Srekantiah, K.R., Murthy, V.S., 1982. Studies on the two forms of amyloglucosidase from *Aspergillus niger* van Tieghem. **Starch/Starke**, 34, 346-351.
- Rambeck, W.A., Weiser, H., Zucker, H., 1984. Biological activity of glycosides of vitamin D3 and 1 $\alpha$ -hydroxyvitamin D3. **Int. J. Vitam. Nutr. Res.** 54(1), 25-34.
- Rantwijk, F.V., Oosterom, M.W., Shedon, R.A., 1999. Glycosidase-catalyzed synthesis of alkyl glycosides. **J. Mol. Catal. B: Enzym.** 6, 511-532.

- Rao, V.B., Sastri, N.V.S., Rao, P.V.S., 1981. Purification and characterization of a thermostable glucoamylase from the thermophilic fungus *Thermomyces lanuginose*. **Biochem. J.** 193, 379-385.
- Rashid, M.H., Inoue, M., Kondo, S., Kawashima, T., Bakoshi, S., Ueda, H., 2003. Novel expression of vanilloid receptor I on capsaicin-insensitive fibres accounts for the analgesic effect of capsaicin in neuropathic pain. **J. Pharmacol. Exp. Ther.** 304, 940-948.
- Ratnam, B.V.V., Subba Rao, S., Damodar Rao, M., Narasimha Rao, M., Ayyanna, C., 2005. Optimization of medium constituents and fermentation conditions for the production of ethanol from palmyra jaggery using response surface methodology. **World J. Microbiol. Biotechnol.** 21, 399-404.
- Rebros, M., Rosenberg, M., Mlichova, Z., Kristofikova, L., Paluch, M., 2006. A simple entrapment of glucoamylase into lentikats as an efficient catalyst for maltodextrin hydrolysis. **Enzyme Microb. Technol.** 39, 800-804.
- Rehan, M., Younus, H., 2006. Effect of organic solvents on the conformation and interaction of catalase and anticatalase antibodies. **Int. J. Biol. Macromol.** 38(3-5), 289-295.
- Reichel, L., Sckickle, R., 1943. Synthesen neuer methoxylierter Chalkon-Flavanon-glucoside unter physiologischen Bedingungen. Chemie und Biochemie der Pflanzenstoffe, XII. Mitteilung **Plant Chem.** 76B, 1134-1137.
- Rezaci, K., Temelli, F., Jenab, E., 2007. Effect of pressure and temperature on enzymatic reactions in supercritical fluids. **Biotechnol. Adv.** 25(3), 272-280.
- Rhode, O., Witt, S., Hardacker, I., 1999. Method for preparation of alkyl-glycosides using microwave irradiation. German patent **DE 19730836 A1** (CA 130: 110555).
- Riaz, M., Perveen, P., Javel, M.R., Nadeen, H., Rashid, M.H., 2007. Kinetic and thermodynamic properties of novel glucoamylase from *Humicola* sp. **Enzyme Microb. Technol.** 41(5), 558-564.
- Roche, M., Dufour, C., Mora, N., Dangles, O., 2005. Antioxidant activity of olive phenols: Mechanistic investigation and characterization of oxidation products by mass spectrometry. **Org. Biomol. Chem.** 3, 423-429.
- Roig, M.G., Slade, A., Kennedy, J.F., Taylor, D.W., Garaita, M.G., 1995. Investigations of stabilities, pH, and temperature profiles and kinetic parameters of glucoamylase immobilized on plastic supports. **Appl. Biochem. Biotechnol.** 50, 11-33.
- Romero, M.D., Calvo, L., Alba, C., Daneshfar, A., Ghaziaskar, H.S. 2003. Enzymatic synthesis of isoamyl acetate with immobilized *Candida antarctica* lipase in n-hexane. **Enzyme Microb. Technol.** 37, 42-48.
- Roode, B.M., Franssen, M.C.R., van der Padt, A., Boom, R.M., 2003. Perspective for the industrial enzymatic production of glycosides. **Biotechnol. Prog.** 19, 1391-1402.
- Rubio, E., Fernandez M.A., Klivanov, A.M., 1991. Effect of the solvent on enzyme regio-selectivity. **J. Am. Chem. Soc.** 113, 695-696.
- Saha, B.C., Zeikus, J.G., 1989. Microbial glucoamylases: Biochemical and biotechnological features. **Starch/Starke**, 41, 57-64.

- Sakaki, H., Kaneno, H., Sumiya, Y., Tsushima, Y., Miki, W., Kishimoto, N., Fujita, T., Matsumoto, S., Komemushi, S., Sawabe, A., 2002. A new carotenoid glycosyl ester isolated from a marine microorganism *Fusarium strain* T-1. **J. Nat. Prod.** 65, 1683-1684.
- Sakata, I., Maruyama, I., Kobayashi, A., Yamamoto, I., 1998. Production of phenethyl alcohol glycoside. **Jpn. Kokai Tokkyo Konho**, Japan Patent **JP 10052297** (CA 128:229438).
- Sakurai, T., Margolin, A., Russell, A., Klibanov, A., 1988. Control of enzyme enantioselective by the reaction medium. **J. Am. Chem. Soc.** 110, 7236-7237.
- San-Aparicio, J., Hermoso, J.A., Martinz-Ripoll, M., Laquerica, J.L., Polaina, J., 1998. Crystal structure of  $\beta$ -glucosidase A from *Bacillus polymyxa*: In sights into the catalytic activity in family1 glycosyl hydrolases. **J. Mol. Biol.** 275, 491-502.
- Sanchez, M.A., Artigar, A.C., Perez, V.J., 2003. Purification of angiotensin I converting enzyme from pig lung using concanavalin-A sepharose chromatography. **J Chromatogr. B**, 783, 247-252.
- Sandler, J.S., Forsburg, S.L., Faulkner, D.J., 2005. Bioactive steroidal glycosides from the marine sponge *Erylus lendenfeldi*. **Tetrahedron**. 61, 1199-1206.
- Sanjay, G., Sugunan, S., 2005. Glucoamylase immobilized on montmorillonite: Synthesis, characterization and starch hydrolysis activity in a fixed bed reactor. **Catal. Commun.** 6, 525-530.
- Sari, M., Akgol, S., Karatas, M., Denizli, A., 2006. Reversible immobilization of catalase by metal chelate affinity interaction on magnetic beads. **Ind. Engg. Chem. Res.** 45, 3036-3043.
- Sasaki, N., Adachi, T., Koda, T., Ozeki, Y., 2004. Detection of UDP-glucose: Cyclo-dopa 5-O-glucosyltransferase activity in four O' clocks (*Mirabilis jalapa L.*). **FEBS Lett.** 568, 159-162.
- Sato, T., Takeuchi, H., Takahashi, K., Kurosu, J., Yoshida, K., Tsugane, T., Shimura, S., Kino, K., Kirimura, K., 2003. Selective  $\alpha$ -glucosylation of eugenol by  $\alpha$ -glucosyl transfer enzyme of *Xanthomonas campestris* WU-9701. **J. Biosci. Bioengg.** 96, 199-202.
- Satoh, T., Miyataka, H., Yamamoto, K., Hirano, K., 2001. Synthesis and physiological activity of novel tocopheryl glycosides. **Chem. Pharm. Bull.** 49(8), 948-953.
- Saver, J., Sigurskjold, B.W., Christensen, U., Frandsen, J.P., Mirgorodskaya, E., Harrison, M., Roepstorff, P., Svennson, B., 2000. Glucoamylase: Structure/function relationships and protein engineering. **Biochim. Biophys. Acta.** 1543, 275-293.
- Schoemaker, H.E., Mink, D., Wubbolts, M.G., 2003, Dispelling the myths-biocatalysis in industrial synthesis. **Science.** 299, 1694-1697.
- Scholz, D., Mebel, M., Topelmann, J., Grossmann, I., Scholze, J., Mrochen, H., 1983. Prevention of osteonecrosis following renal transplantation by using vitamin D2 (ergocalciferol). **Proc. Eur. Dial. Transplant Assoc.** 20, 331-337.
- Segel, I.H., 1993. Enzyme Kinetics-Behavior and analysis of rapid equilibrium and steady - state enzyme systems. A Wiley-interscience publication. pp 826-829.



- Sengodan, S., Palanivel, S., Panchanadham, S., 2003. Curative effect of riboflavin, niacin and ascorbic acid on tamoxifen mediated endometrial carcinoma bearing Sprague-Dawley rats with reference to lipid peroxidation and antioxidant status. **J. Clinical Biochem. Nutr.** 33, 39-45.
- Seung-Heon, Y., Fulton, B.D., Robyt, J.F., 2004. Enzymatic synthesis of two salicin analogues by reaction of salicyl alcohol with *Bacillus macerans* cyclomaltodextrin glucanyltransferase and *Leuconostoc mesenteroides* B-742CB dextransucrase. **Carbohydr. Res.** 339, 1517–1529.
- Shah, C., Sellappan, S., Madamwar, D., 2000. Entrapment of enzyme in water-restricted microenvironment -amyloglucosidase in reverse micelles. **Process Biochem.** 35, 971-975.
- Shetty, P., Atallah, M.T., Shetty, K., 2002. Effects of UV treatment on the proline-linked pentose phosphate pathway for phenolics and L-DOPA synthesis in dark germinated *Vicia faba*. **Process Biochem.** 37, 1285–1295.
- Shibata, H., Sonoke, S., Ochiai, H., Nishihashi, H., Yamada, M., 1991. Glucosylation of steviol and steviol glucosides in extracts from *Stevia rebaudiana Bertoni*. **Plant Physiol.** 95, 152-156.
- Shieh, C.J., Akoh, C.C., Koehler, P.E., 1995. Four-factor response surface optimization of the enzymatic modification of triolin to structured lipids. **J. Am. Oil Chem. Soc.** 72, 619-623.
- Shimoda, K., Konda, Y., Abe, K., Hamada, H., Hamada, H., 2006. Formation of water-soluble vitamin derivatives from lipophilic vitamins by cultured plant cells. **Tetrahedron Lett.** 47, 2695-2698.
- Shimoda, K., Kwon, S., Utsuki, A., Ohiwa, S., Katsuragi, H., Yonemoto, N., Hamada, H., Hamada, H., 2007. Glycosylation of capsaicin and 8-nordihydro capsaicin by cultured cells of *Catharanthus roseus*. **Phytochemistry.** 68, 1391-1396.
- Shin, H.K., Kong, J.Y., Lee, J.D., Lee, T.H., 2000. Synthesis of hydroxy benzyl- $\alpha$ -glucosides by amyloglucosidase-catalysed transglycosylation. **Biotechnology Lett.** 22, 321-325.
- Shoseyou, O., Bravdo, B.A., Siegel, D., Ikan, R., Goldman, A., Cohen, S., Shoseyov, L., 1990. Immobilised  $\beta$ -glucosidase enriches flavour of wine and passion fruit juice. **J. Agric. Food Chem.** 38, 1387-1390.
- Sierks, M.R., Ford, C., Reilly, P.J., Svensson, B., 1990. Catalytic mechanism of fungal glucoamylases as defined by mutagenesis of Asp 176, Glu179, and Glu180 in the enzyme from *Aspergillus awamori*, **Protein Engg.** 3, 193-198.
- Sills, A.M., Saunder, M.E., Stewart, G.G., 1984. Isolation and characterization of the amyolytic system of *Schwanniomyces castellii*. **J. Inst. Brew.** 90, 311-316.
- Simon, L.M., Kotorman, M., Szabo, A., Nemcsok, J., Laczko, I., 2007. The effect of organic solvent/water mixtures on the structure and catalytic activity of porcine pepsin. **Process Biochem.** 42, 909-912.
- Sinnot, M.L., 1990. Catalytic mechanism of glycosyl transfer. **Chem. Rev.** 90, 1171-1202.
- Smaali, I., Maugard, T., Limam, F., Legoy, M.D., Marzouki, N., 2007. Efficient synthesis of gluco-oligosaccharides and alkyl-glucosides by transglycosylation

- activity of *b*-glucosidase from *Sclerotinia sclerotiorum*. **World J. Microbiol. Biotechnol.** 23, 145-149.
- Smith, D.C., Johnson, C.S., Freeman, C.C., Muindi, J., Wilson, J.W., Trump, D.L., 1999. A phase I trial of calcitriol (1,25-dihydroxycholecalciferol) in patients with advanced malignancy. **Clin. Cancer Res.** 5, 1339-1345.
- Sommer, J., Schroeder, C., Stockigt, J., 1997. *In vivo* formation of vanillin glucoside. **Plant Cell Tiss. Org. Cult.** 50, 119-123.
- Soni, B.K., Kapp, C., Goma, G., Soucaille, P., 1992. Solvent production from starch: Effect of pH on  $\alpha$ -amylase and glucoamylase localization and synthesis in synthetic medium. **Appl. Microbiol. Biotechnol.** 37, 539-543.
- Sorimachi, K., Jacks, A.J., Gal-coeffet, M.F.L., Williamson, G., Archer, D.B., Williamson, M.P., 1996. Solution: Structure of the granular starch binding domain of glucoamylase from *Aspergillus niger* by nuclear magnetic resonance. **J. Mol. Biol.** 259, 970-987.
- Specka, U., Mayer, F., Antranikian, G., 1991. Purification and properties of thermoactive glucoamylase from *Clostridium thermosaccharolyticum*. **Appl. Environ. Microbiol.** 57, 2317-2323.
- Srivastava, A., Strasser, R.J., 2001. Biomolecules in reverse micelles. **Biophysical Processes in Living Systems**, Saradhi, P.P., (Ed.), Science Publishers, Enfield, N.H. pp 1-23.
- Srivastava, R.A.K., 1984. Studies on extracellular and intracellular purified amylases from a thermophilic *Bacillus stearothermophilus*. **Enzyme Microb. Technol.** 6, 422-426.
- Stanek, J., Cerny, M., Kocourek, J., Pacak, J., 1963. **The monosaccharides**. Everest, I., Hebky, J., (Eds). Academic Publishing Inc., New York.
- Stephan, D., Peter, K., 2003. Vanillins - a novel family of DNA-PK inhibitors. **Nucleic Acid Res.** 31, 5501-5512.
- Stevenson, D.E., Stanley, R.A., Furneaux, R.H., 1993. Optimization of alkyl  $\beta$ -D-galactopyranoside synthesis from lactose using commercially available  $\beta$ -galactosidase. **Biotechnol. Bioeng.** 42, 657-666.
- Stoffer, B., Aleshin, A.E., Firsov, L.M., Svensson, B., Honzatko, R.B., 1995. Refined structure for the complex of D-gluco-dihydroacarbose with glucoamylases from *Aspergillus awamori* var. X100 to 2.2 Å resolution: Dual conformation for extended inhibitors bound to the active site of glucoamylases, **FEBS Lett.** 358, 57-61.
- Stoffer, B., Frandsen, T., Busk, P., Schneider, P., Svendsen, I., Svensson, B., 1993. Production, purification and characterization of the catalytic domain of glucoamylase from *Aspergillus niger*. **Biochem. J.** 292, 197-202.
- Sumner, J.B., Sisler, E.B., 1944. A simple method for blood sugar. **Arch. Biochem.** 4, 333-336.
- Suntornsuk, W., Hang, Y.D., 1994. Strain improvement of *Rhizopus oryzae* for production of l(+)-lactic acid and glucoamylase. **Lett. Appl. Microbiol.** 19, 249-252.

- Suzuki, Y., Ki, Y.H., Uchida, K., Takami, M., 1996. Enzymatic synthesis of glucosylated and phosphatidylated biologically active compounds. **J. Appl. Glycosci.** 43, 273-282.
- Suzuki, Y., Uchida, K., 1969. Biosynthesis of riboflavin- $\alpha$ -glucoside by plant grains. **Arch. Biochem. Biophys.** 130(1), 683-684.
- Suzuki, Y., Uchida, K., 1983. Formation of glucosyl riboflavin in germinating barley seeds. **Nogaku Kenkyu.** 9, 285-292.
- Suzuki, Y., Uchida, K., 1994. Enzymatic formation of a new derivative of thiamin,  $\beta$ -galactosylthiamin. **Biosci. Biotech. Biochem.** 58, 1273-1276.
- Svensson, B., 1994. Protein engineering in the  $\alpha$ -amylase family: Catalytic mechanism, substrate specificity and stability. **Plant Mol. Biol.** 25, 141-157.
- Svensson, B., Clarke, A.J., Svendsen, I., Moller, H., 1990. Identification of carboxylic acid residues in glucoamylase G2 from *Aspergillus niger* that participate in the catalysis and substrate binding. **Eur. J. Biochem.** 18, 29-38.
- Svensson, B., Larsen, K., Svendsen, I., Boel, E., 1983. The complete amino acid sequence of the glycoprotein glucoamylase G1 from *Aspergillus niger*. **Carlsberg. Res. Commun.** 48, 529-544.
- Synowiecki, J., Wolosowska, S., 2006. Immobilization of  $\beta$ -glucosidase from *Sulfolobus shibatae* by cross-linking with transglutaminase. **Enzyme Microb. Technol.** 39, 1417-1422.
- Szymanski, W., Zwolinska, M., Ostaszewski, R., 2007. Studies and application of the Pesslerini reaction and enzymatic procedures to the synthesis of tripeptide mimetics. **Tetrahedron.** 63(32), 7647-7653.
- Tachibana, S., 1955. Sugar compounds of riboflavin II Biosynthesis of riboflavinyll galactoside by *Aspergillus oryzae*. **Vitamins.** 9, 119-124.
- Tachibana, S., 1971. Isolation of riboflavin glycosides. In Vitamin and Coenzymes. **Methods Enzymol.** McCormick, C.D.B., Wright, L.D. (Eds). Academic Press, New York. , 18B, 413-416
- Takahashi, T., Kato, K., Ikegami, Y., Irie, M., 1985. Different behavior towards raw starch of three forms of glucoamylase from a *Rhizopus* sp. **J. Biochem.** 98, 663-671.
- Takaishi, Y., Ohashi, T., Tomimatsu, T., 1989. Ergosta-7,22-dien-3 $\beta$ -O-L-glycosides from *Tylopilus neofelleus*. **Phytochemistry.** 28(3), 945-947.
- Takaishi, Y., Uda, M., Ohashi, T., Nakano, K., Murakami, K., Tomimatsu, T., 1991. Glycosides of ergosterol derivatives from *Hericum erinacens*. **Phytochemistry.** 30(12), 4117-4120.
- Takashima, S., Nakamura, A., Hidaka, M., Masaki, H., Uozumi, T., 1999. Molecular cloning and expression of the novel fungi  $\beta$ -glucosidase genes from *Humicola grisea* and *Trichoderma reesei*. **J. Biochem.** 125, 728-736.
- Takayama, S., McGarvey, G.J., Wong, C.H., 1997. Enzymes in organic synthesis: Recent developments in aldol reaction and glycosylation. **Chem. Soc. Rev.** 26, 407-415.



- Tanaka, A., Yamashita, T., Ohnishi, M., Hiromi, K., 1983. Steady-state and transient kinetic studies on the binding of maltooligosaccharides to glucoamylases, **J. Biochem.** 93, 1037-1043.
- Tanaka, Y., Ashikari, T., Nakamura, N., Kiuchi, N., Shibano, Y., Amachi, T., Yoshizumi, H., 1986. Comparison of amino acid sequences of three glucoamylases and their structure-function relationships. **Agric. Biol. Chem.** 50, 965-969.
- Tapavicza, S.V., Bell, D., Kopp-Holtwiesche, B., 2000. Plant growth enhancement against phytopathogenic fungi and /or soil borne pests. Patent **WO 0002451** (CA 132:60488).
- Tatsumi, H., Katano, H., 2005. Kinetics of the surface hydrolysis of raw starch by glucoamylase. **J. Agric. Food Chem.** 53, 8123-8127.
- Tatsumi, H., Katano, H., Ikeda, T., 2007. Kinetic analysis of starch granules from various botanical sources. **Biosci. Biotech. Biochem.** 71, 946-950.
- Taylor, P.M., Napier, E.J., Fleming, I.D., 1978. Some properties of a glucoamylase produced by the thermophilic fungus *Humicola lanuginosa*. **Carbohydr. Res.** 16, 301-308.
- Thanukrishnan, K., Loganathan, D., Bhatia, Y., Mishra, S., Bisaria, V.S., 2004. Transglycosylation catalyzed by almond  $\beta$ -glucosidase and cloned *Pichia etchellsii*  $\beta$ -glucosidase II using glycosylasparagine mimetics as novel acceptors, **Biocatal. Biotransform.** 22, 1-7.
- The Merck Index; An encyclopedia of chemicals, drugs and biologicals, 14<sup>th</sup> ed. Neil, M.J.O., (Ed.), Merck & Co., USA, 2006.
- Therisod, M., Klibanov, A.M., 1987. Facile enzymatic preparation of monoacetylated sugars in pyridine. **J. Am. Chem. Soc.** 109, 3977-3981.
- Thorsen, T.S., Johnsen, A.H., Josefsen, K., Jensen, B., 2006. Identification and characterization of glucoamylase from the fungus *Thermomyces lanuginosus*. **Biochim. Biophys. Acta.** 1764(4), 671-676.
- Tietze, L.F., Griesbach, U., Schuberth, I., Bothe, U., Marra, A., Dondoni, A., 2003. Novel carboranyl C-glycosides for the treatment of cancer by boron neutron capture therapy. **Chem. Eur. J.** 9, 1296-1302.
- Torres, R., Pessela, B.C., Mateo, C., Ortiz, C., Fuentes, M., Guisan, J.M., Fernandez-Lafuente, R., 2004. Reversible immobilization of glucoamylase by ionic adsorption on sephabeads coated with polyethyleneimine. **Biotechnol. Prog.** 20, 1297-300.
- Toyoda-Ono, Y., Maeda, M., Nakao, M., Yoshimura, M., Sugiura-Tomimori, N., Fukami, H., 2004. 2-O-( $\beta$ -D-glucopyranosyl)ascorbic acid, a novel ascorbic acid analogue isolated from *Lycium* fruit. **J. Agric. Food Chem.** 52, 2092-2096.
- Tramice, A., Pagnotta, E., Romano, I., Gambacorta, A., Trincone, A., 2007. Transglycosylation reactions using glycosyl hydrolases from *Thermotoga neapolitana*, a marine hydrogen-producing bacterium. **J. Mol. Catal. B: Enzym.** 47, 21-27.

- Trincone, A., Pagnotta, E., Giordano, A., Perugino, G., Rossi, M., Moracci M., 2003. Enzymatic synthesis of 2-deoxyglycosides using the  $\beta$ -glycosidase of the archaeon *Sulfolobus solfataricus*. **Biocatal. Biotransform.** 21, 17-24.
- Tripathi, P., Leggio, L.L., Mansfeld, J., Hofmann, R.U., Kayastha, A.M., 2007.  $\alpha$ -Amylase from mung beans *Vigna radiate*: Correlation of biochemical properties and tertiary structure by homology modeling. **Phytochemistry.** 68, 1623-1631.
- Tsuge, H., Maeno, M., Hayakawa, T., Suzuki, Y., 1996. Comparative study of pyridoxine- $\alpha,\beta$ -glucosides, and phosphopyridoxyl-lysine as a vitamin B<sub>6</sub> nutrient. **J. Nutr. Sci. Vitaminol.** 42, 377-386.
- Tsuruhama, K., Mori, S., Sakata, K., Amarume, S., Saruwatari, S., 2005. Efficient synthesis of primeverosides as aroma precursors by transglycosylation of diglycosidase from *Penicillium multicolor*. **J. Carbohydr. Chem.** 24, 849-863.
- Turner, P., Svensson, D., Adlercreutz, P., Karlsson, E.N., 2007. A novel variant of *Thermotoga neapolitana* beta-glucosidase B: Is an efficient catalyst for the synthesis of alkyl glucosides by transglycosylation. **J. Biotechnol.** 130, 67-74.
- Uchida, K., Suzuki, Y., 1968. Production of riboflavin glucoside in growing cultures of *Ashbya gossypii* and *Eremothecium ashbyii*. **Denpon Noge Kagaku Kaishi.** 42 (4), 233-237.
- Uchida, K., Suzuki, Y., 1974. Purification and properties of riboflavin- $\alpha$ -glucoside synthesising enzyme ( $\alpha$ -glucosidase) from pig liver. **Agric. Biol. Chem.** 38, 195-206.
- Uchida, K., Suzuki, Y., 1998. Enzymatic synthesis of a new derivative of thiamin, O- $\alpha$ -glucosylation. **Biosci. Biotechnol. Biochem.** 62, 221-224.
- Valivety, R.H., Halling, P.J., Macrae, A.R., 1992. *Rhizomucor mechei* remains highly active at water activity below 0.0001. **FEBS Lett.** 301, 258-260.
- Valivety, R.H., Johnston, G.A., Suckling, C.J., Halling, P.J., 1991. Solvent effect on Biocatalysis in organic systems: Equilibrium position and rates of lipase catalysed esterification. **Biotechnol. Bioeng.** 38, 1137-1143.
- Vallmitjana, M., Navarro, M.F., Planell, R., Abel, M., Ausin, C., Querol, E., Planas, A., Pons, J.A.P., 2001. Mechanism of the family 1  $\beta$ -glucosidase from *Streptomyces* sp. catalytic residues and kinetic studies. **Biochemistry.** 40, 5975-5982.
- Van der Maarel, J.E.C., Van der Veen, B., Vitdehaag, C.M.J., Leemhuis, H., Dijkhuizen, L., 2002. Properties and applications of starch converting enzyme of the  $\alpha$ -amylase family. **J. Biotechnol.** 94, 137-155.
- Vasella, A., Davies, G.J., Böhm, M., 2002. Glycosidase mechanisms. **Curr. Opinion Chem. Biol.** 6, 619-629
- Verdoucq, L., Czjzek, M., Moriniere, J., Beven, D.R., Esen, A., 2003. Mutational and structural analysis of aglycone specificity in maize and sorghum  $\beta$ -glucosidase. **J. Biol. Chem.** 278, 25055-25062.
- Vered, Y., Rabey, J.M., Paleveitch, D., Grosskopf, I., Harsat, A., Yanowski, A., Shabtai, H., Graff, E., 1994. Bioavailability of levodopa after consumption of *Vicia faba* seedlings by Parkinsonian patients and control subjects. **Clin. Neuropharmacol.** 17, 138-46.

- Vermeirssen, V., Van-Camp, J., Verstraete, W., 2002. Optimization and validation of an angiotensin-converting enzyme inhibition assay for the screening of bioactive peptides. **J. Biochem. Biophys. Methods**, 51, 75-87.
- Vic G., Hastings, J.J., Crout, D.H.G., 1996. Glycosidase catalyzed synthesis of glycosides by an improved procedure for reverse hydrolysis. Application to the chemoenzymatic synthesis of galactopyranosyl-(1→4)-O- $\alpha$ -galactopyranoside derivatives. **Tetrahedron Asym.** 7, 1973-1984.
- Vic, G., Biton, J., Beller, D.L., Michel, J.M., Thomas, D., 1995. Enzymatic glycosylation of hydrolytic alcohols in organic medium by the reverse hydrolysis reaction using almond  $\beta$ -D-glucosidase. **Biotechnol. Bioengg.** 46, 109-116.
- Vic, G., Crout, D.H.G., 1994. Synthesis of glucosidic derivatives with a spacer arm by reverse hydrolysis using almond  $\beta$ -D-glucosidase. **Tetrahedron Asym.** 5, 2513-2516.
- Vic, G., Crout, D.H.G., 1995. Synthesis of allyl and benzyl  $\beta$ -D-glucopyranosides and allyl  $\beta$ -D-galactopyranoside from D-glucose or D-galactose and the corresponding alcohol using almond  $\beta$ -D-glucosidase. **Carbohydr. Res.** 279, 315-319.
- Vic, G., Thomas, D., 1992. Enzyme-catalyzed synthesis of alkyl- $\beta$ -D-glucosides in organic media. **Tetrahedron Lett.** 33, 4567-4570.
- Vic, G., Thomas, D., Crout, D.H.G., 1997. Solvent effect on enzyme-catalyzed synthesis of  $\beta$ -D-glucosides using the reverse hydrolysis method: Application to the preparative-scale synthesis of 2-hydroxybenzyl and octyl  $\beta$ -D-glucopyranosides. **Enzyme Microb. Technol.** 20, 597-603.
- Vieille, C., Zeikus, G.J., 2001. Hyperthermophilic enzymes: Sources, uses and molecular mechanism for thermostability. **Microbiol. Mol. Biol. Rev.** 65, 1-43.
- Vihinen, M., Mantsala, P., 1989. Microbial amylolytic enzymes. **Crit. Rev. Biochem. Mol. Biol.** 24, 329-418.
- Vijayakumar, G.R., Divakar, S., 2005. Synthesis of guaiacol- $\alpha$ -D-glucoside and curcumin-bis- $\alpha$ -D-glucoside by an amyloglucosidase from *Rhizopus*. **Biotechnology Lett.** 27, 1411-1415.
- Vijayakumar, G.R., Divakar, S., 2007. Amyloglucosidase catalyzed synthesis of eugenyl and curcuminyl glycosides. **Biotechnology Lett.** 29, 575-584.
- Vijayakumar, G.R., George, C., Divakar, S., 2007. Synthesis of n-alkyl glucosides by amyloglucosidase. **Ind. J. Chem. B.** 46B, 314-319.
- Vijayakumar, G.R., Manohar, B., Divakar, S., 2005. Amyloglucosidase catalyzed synthesis of n-octyl-D-glucoside-Analysis using Response Surface Methodology. **Eur. Food Res. Technol.** 220, 272-277.
- Vijayakumar, G.R., Manohar, B., Divakar, S., 2006. Amyloglucosidase catalyzed synthesis of curcumin-bis- $\alpha$ -D-glucoside-A Response Surface Methodological study. **Eur. Food Res. Technol.** 223, 725-730.
- Villano, D., Fernandez-Pachon, M.S., Moy, M.L., Troncoso, A.M., Garca-Parrilla, M.C., 2007. Radical scavenging ability of polyphenolic compounds towards DPPH free radical. **Talanta.** 71, 230-235.

- Volpi, N., 2006. Therapeutic applications of glycosaminoglycans. **Curr. Med. Chem.** 13, 1799-1810.
- Voorhorst, W.G.B., Eggen, R.I.K., Luesink, E.J., De Vos, W.M., 1995. Characterization of the Cel B gene coding for  $\beta$ -glucosidase from the hyperthermophilic archaeon *Pyrococcus furiosus* and its expression and site directed mutation in *Escherichia coli*. **J. Bacteriol.** 177, 7105-7111.
- Vorderwulbecke, T., Kieslich, K., Erdmann, H., 1992. Comparison of lipases by different assays. **Enzyme Microb. Technol.** 14, 631-639.
- Vulfson, E.N., Patel, R., Beecher, J.E., Andrews, A.T., Law, B.A., 1990. Glycosidases in organic solvents: I. Alkyl- $\beta$ -glucoside synthesis in a water-organic two-phase system. **Enzyme Microb. Technol.** 12, 950-954.
- Walton, N.J., Mayer, M.J., Narbad, A., 2003. Vanillin. **Phytochemistry.** 63, 505-515.
- Wang, C., Eufemi, M., Turano, C., Giartosio, A., 1996. Influence of the carbohydrate moiety on the stability of glycoproteins. **Biochemistry.** 35, 7299-7307.
- Wang, F., Guo, C., Liu, H.Z., Liu, C.Z., 2007. Reversible immobilization of glucoamylase by metal affinity adsorption on magnetic chelator particles. **J. Mol. Catal. B: Enzym.** 48, 1-7.
- Wang, Q., Graham, R.W., Trimbur, D., Warren, R.A.J., Withers, S.G., 1994. Changing enzymatic reaction mechanisms by mutagenesis: Conversion of a retaining glucosidase to an inverting enzyme. **J. Am. Chem. Soc.** 116, 11594-11595.
- Wang, Q., Trimbur, D., Graham, R., Warren, R.A., Withers, S.G., 1995. Identification of the acid/base catalyst in *Agrobacterium faecalis*  $\beta$ -glucosidase by kinetic analysis of mutants. **Biochemistry.** 34, 14554-14562.
- Wang, X., He, X., Yang, S., An, X., Chang, W., Liang, D., 2003. Structural basis for thermostability of  $\beta$ -glycosidase from the thermophilic eubacterium *Thermus nonproteolyticus* HG102. **J. Bacteriol.** 185, 4248-4255.
- Wantanbe, N., Wantanbe, S., Nakajima, R., Moon, J. H., Shimokihara, K., Inagaki, J., Etoh, H., Asai, T., Sakata, K., Ina, K., 1993. Formation of flower fragrance compounds from their precursors by enzymic action during flower opening. **Biosci. Biotechnol. Biochem.** 57, 1101-1106.
- Wasserman, B.P., Burke, D., Jacobson, B.S., 1982. Immobilization of glucoamylase from *Aspergillus niger* on poly(ethylenimine)-coated non-porous glass beads. **Enzyme Microb. Technol.** 4, 107-109.
- Watanabae, T., Kawada, T., Kato, T., Harada, T., Iwai, K., 1994. Effects of capsaicin analogs on adrenalin catecholamine secretion in rats. **Life Sciences.** 54, 369-374.
- Weast, R.C., 1983. Handbook of Chemistry and Physics, 64<sup>th</sup> Edn, Weast, R.C., Astle, M.J., Beyer, W.H. Eds. CRC Press, Boca Raton. C-696.
- Wei, S., Semel, Y., Bravdo, B.A., Czosnek, H., Shoseyov, O., 2007. Expression of subcellular compartmentation of *Aspergillus niger*  $\beta$ -glucosidase in transgenic tobacco result in an increased insecticidal activity on whiteflies (*Bemisia tabaci*). **Plant Sci.** 172, 1175-1181.

- Werner, R., Manthey, K.C., Griffin, J.B., Zempleni, J., 2005. HepG2 cells develop signs of riboflavin deficiency within 4 days of culture in riboflavin-deficient medium. **J. Nutr. Biochem.** 16, 617-624.
- Whitby, L.G., 1952. Riboflavinyl glucoside: A new derivative of riboflavin. **Biochem. J.** 50, 433-438.
- Whitby, L.G., 1954 Transglucosidation reactions with flavins. **Biochem. J.** 57, 390-396.
- Whitby, L.G., 1971. Glycosides of riboflavin, In Vitamin and Coenzymes. McCormick, C.D.B., Wright, L.D. Eds. Methods in enzymology, Academic Press, New York, 18B, 404-413.
- Whitelock, J.M., Iozzo, R.V., 2005. Heparan sulfate: A complex polymer charged with biological activity. **Chem. Rev.** 105, 2745-2764.
- Wieder, R., Novick, S.C., Hollis, B. W., Bryan, M., Chanel, S. M., Owusu, K., Camastra, D., Saunders, T., Pliner, L., Harrison, J., Bonate, P., Williams, T., Soignet, S., 2003. Pharmacokinetics and safety of ILX23-7553, a non-calcemic-vitamin D<sub>3</sub> analogue, in a phase I study of patients with advanced malignancies. **Invest. New Drugs.** 21, 445-452.
- Wiesmann, C., Hengstenberg, W., Schulz, G.E., 1997. Crystal structures and mechanism of 6-phospho- $\beta$ -galactosidase from *Lactococcus lactis*. **J. Mol. Biol. Chem.** 269, 851-860.
- Williamson, G., Belshaw, N.J., Williamson, M.P., 1992. O-Glycosylation in *Aspergillus* glucoamylase. Confirmation and role in binding. **Biochem. J.** 282, 423-428.
- Withers, G.G., Warren, R.A.J., Street, I.P., Rupitz, K., Kempton, J.B., Abersold, R., 1990. Unequivocal demonstration of the involvement in the mechanism of a retaining glycosidase. **J. Am. Chem. Soc.** 112, 5887-5889.
- Withers, S.G., Street, I.P., 1988. Identification of a covalent  $\alpha$ -D-glucopyranosyl enzyme intermediate formed on a  $\beta$ -glucosidase. **J. Am. Chem. Soc.** 110, 8551-8553.
- Witkowski, S., Walejko, P., Wawer, I., 1998. <sup>13</sup>C CP MAS NMR study of 6-O-( $\beta$ -D-glucopyranosyl)-and 6-O-( $\beta$ -D-mannopyranosyl)-d- $\alpha$ -tocopherols. **Solid-State Nuclear Magn. Reson.** 10, 123-128.
- Won, K., Kim, S., Kim, K.J., Park, H.W., Moon, S.J., 2005. Optimization of lipase entrapment in Ca-alginate gel beads. **Process Biochem.** 40, 2149-2154.
- Woudenberg-van O.M., van Belle, H.J.A., van Rantwijk, F., Sheldon, R.A., 1998. Immobilized  $\beta$ -galactosidases and their use in galactoside synthesis. **J. Mol. Catal. A: Chem.** 134, 267-274.
- Wu, J., Ding, X., 2002. Characterization of inhibition and stability of soy-protein derived angiotensin I converting enzyme inhibitory peptides. **Food Res. Int.** 35, 367-375.
- Wyler, H., Meuer, U., Bauer, J., Stravs-Mombelli, L., 2004. Cyclodopa glucoside ((2S)-5-( $\beta$ -D-glucopyranosyloxy)-6-hydroxyindoline-2-carboxylic acid) and its occurrence in red beet (*Beta Vulgaris* Var. *rubra* L.). **Helvetica Chim. Acta.** 67(5), 1348-1355.
- Yadav, G.D., Lathi, P.S., 2004. Synthesis of citronellol laurate in organic media catalyzed by immobilized lipases: Kinetic studies, **J. Mol. Catal. B: Enzym.** 27, 113-119.



- Yamada, H., Aimi, Y., Nagatsu, I., Taki, K., Kudo, M., Arai, R., 2007. Immunohistochemical detection of L-dopa derived dopamine within serotonergic fibres in the striatum and the substantia nigra pars reticulata in Parkinsonian model rats. **Neuroscience Res.** 59, 1-7.
- Yang, L., Dordick, J.S., Garde, S., 2004. Hydration of enzymes in nonaqueous media is consistent with solvent dependence of its activity. **Biophys. J.** 87, 812-821.
- Yankov, D., Beschkov, V., Rouleau, D., 1997. Kinetics and modeling of the enzyme hydrolysis of maltose with free and immobilized glucoamylase. **Starch/Starke**, 49, 288-293.
- Yar, M.D., 1993. Parkinson's disease, the L-dopa era. **Adv. Neurobiol.** 60, 11-17.
- Yavuz, H., Bayrmoglu, G., Kacar, Y., Denizli, A., Arica, M.Y., 2002. Congo-Red attached monosize poly (HEMA-CO-MMA) microspheres for use in reversible enzyme immobilization. **Biochem. Engg. J.** 10(1), 1-8.
- Yip, G.W., Smollich, M., Gotte, M., 2006. Therapeutic values of glycosaminoglycans in cancer. **Mol. Cancer Ther.** 5, 2139-2148.
- Yoon, J.J., Igarashi, K., Kajisa, T., Samejima, M., 2006. Purification identification and molecular cloning of glycoside hydrolase family 15 glucoamylase from brown-rot *Basidiomycete fomitopsis palustris*. **FEMS Microbiol.** 259, 288-294.
- Yoon, S.H., Fulton, D.B., Robyt, J.F., 2004. Enzymatic synthesis of two salicin analogues by reaction of salicyl alcohol with *Bacillus macerans* cyclomaltodextrin glucanyltransferase and *Leuconostoc mesenteroides* B-742CB dexransucrase. **Carbohydr. Res.** 339, 1517-1529.
- Yu, R.C., Hang, Y.D., 1991. Purification and characterization of a glucoamylase from *Rhizopus oryzae*. **Food chem.** 40, 301-308.
- Yun, R.H., Anderson, A., Hermans, J., 1991. Proline in  $\alpha$ -helix, stability and conformation studied by dynamic stimulation. **Protein.** 10, 219-228.
- Zaks, A., Klibanov, A.M., 1985. Enzyme catalysed process in non aqueous solvents. **Proc. Natl. Acad. Sci. USA.** 82, 3192-3196.
- Zaks, A., Klibanov, A.M., 1984. The effect of water on enzyme reaction in organic media. **J. Biol. Chem.** 263, 8017-8021.
- Zaks, A., Klibanov, A.M., 1986. Substrate specificity of enzymes in organic solvents vs. water is reversed. **J. Am. Chem. Soc.** 108, 2767-2768.
- Zechel, D.L., Withers S.G., 2001. Dissection of nucleophilic and acid -base catalysis in glycosidases. **Curr. Opinion Chem. Biol.** 5, 643-649.
- Zhang, S., Liu, S., Zhang, L., 1998. Kinetics of saccharification of potato starch with glucoamylase. **Zhongguo Liangyou Xuebao.** 13, 21-25 (Chinese).
- Zheng, R.C., Zheng, Y.G., Shen, Y.C., 2007. A simple method to determine concentration of enantiomers in enzyme-catalyzed kinetic resolution. **Biotechnology Lett.** 29, 1087-1091.
- Zhou, J.H., 2000. Herbal sweetening and preservative composition comprising licorice extract and mogrosides obtained from plants belonging to cucurbitaceae and/or *Momordica*. Patent **US 6103240** (CA 133:168393).